Universität Rostock Traditio et Innovatio

Catalysis LIKAT Leibniz-Institut für Katalyse e.V.

Bio-inspired Sustainable Catalysis with Base-Metals and Visible Light

Cumulative Habilitation

for obtaining the academic degree
doctor rerum naturalium habilitatus (Dr. rer. nat. habil.)
at the Faculty of Mathematics and Natural Sciences
of the University of Rostock

Presented by

Dr. Osama El-Sepelgy

Born on February 10th, 1984,

Damietta, Egypt

Rostock, 2025

https://doi.org/10.18453/rosdok_id00005152

Erklärung

Ich versichere hiermit an Eides statt, dass ich die vorliegende Arbeit selbstständig angefertigt und ohne Hilfe verfasst habe, keine außer den von mir angegebenen Hilfsmitteln und Quellen dazu verwendet habe und die den benutzten Werken inhaltlich und wörtlich entnommenen Stellen als solche kenntlich gemacht habe.

Osama El-Sepelgy

Rostock, den 2.2025

Der Hauptteil der vorliegenden Arbeit wurde von Juli 2021 bis Januar 2025 am Leibniz-Institut für Katalyse e.V. an der Universität Rostock angefertigt.

1. Gutachter: Prof. Matthias Beller (Leibniz-Institut für Katalyse e.V.)

2. Gutachter: Prof. Lutz Ackermann (Georg-August-Universität Göttingen)

3. Gutachter: Prof. Armido Studer (Universität Münster)

Tag und Thema der Probevorlesung:

26. June 2025

Organische Chemie V - Organische Moleküle - Synthese und Nutzung

Tag und Thema des wissenschaftlichen Kolloquiums:

10. July 2025

Breaking Boundaries: Non-precious Metals in Modern Catalysis

Abstract

In traditional noble-metal homogeneous catalysis, supporting ligands act as spectators that do not interact directly with substrates. This thesis explores biomimetic catalytic systems inspired by metalloenzymes, leveraging ligand-to-metal charge transfer (LMCT) and metal-ligand cooperation (MLC) concepts to enable efficient 3d-metal catalysis. By employing earth-abundant base metals, these approaches mimic enzymatic mechanisms, where the ligand plays an active role beyond mere support, directly participating in catalytic transformations. This strategy enables sustainable and efficient reactions, aligning with the principles of green chemistry.

Under the LMCT concept inspired by the chemistry and enzymology of vitamin B_{12}, cobalt catalysis was harnessed for visible-light-induced radical desaturation of aliphatic compounds under mild conditions, showcasing its utility in the synthesis of valuable chemicals. In the MLC catalysis inspired by heterolytic activation of hydrogen using hydrogenases, manganese pincer complexes leveraged metal-ligand interactions to drive diverse redox transformations, including the hydrogenation of carbonates and alkynes, C- and N-alkylation using alcohols and acceptorless dehydrogenative synthesis of pyrroles.

This research is underpinned by comprehensive experimental and theoretical mechanistic studies, including UV-vis spectroscopy, electron paramagnetic resonance (EPR), and density functional theory (DFT). These investigations provided critical insights into reaction pathways and intermediates, enabling the rational optimization of catalytic systems and bridging fundamental concepts with practical advancements in sustainable catalysis.

Zusammenfassung

In der traditionellen homogenen Katalyse mit Edelmetallen fungieren unterstützende Liganden als Zuschauer, die nicht direkt mit den Substraten interagieren. Diese Dissertation untersucht biomimetische katalytische Systeme, die von Metalloenzymen inspiriert sind und die Konzepte des Ligand-zu-Metall-Ladungstransfers (LMCT) sowie der Metall-Ligand-Kooperation (MLC) nutzen, um eine effiziente 3d-Metall-Katalyse zu ermöglichen. Durch den Einsatz erdreicher Basismetalle ahmen diese Ansätze enzymatische Mechanismen nach, wobei der Ligand eine aktive Rolle übernimmt, die über reine Unterstützung hinausgeht, und direkt an katalytischen Umwandlungen beteiligt ist. Diese Strategie ermöglicht nachhaltige und effiziente Reaktionen im Einklang mit den Prinzipien der Grünen Chemie.

Im Rahmen des LMCT-Konzepts, das von der Chemie und Enzymologie von Vitamin B12 inspiriert ist, wurde die Kobalt-Katalyse für die sichtlichtinduzierte radikalische Desaturierung aliphatischer Verbindungen unter milden Bedingungen genutzt, wodurch ihr Potenzial für die Synthese wertvoller Chemikalien demonstriert wurde. In der MLC-Katalyse, die von der heterolytischen Aktivierung von Wasserstoff durch Hydrogenasen inspiriert ist, wurden Mangan-Pincer-Komplexe eingesetzt, um über Metall-Ligand-Wechselwirkungen verschiedene Redoxreaktionen zu steuern. Dazu gehören die Hydrierung von Carbonaten und Alkinen, die C- und N-Alkylierung mit Alkoholen sowie die akzeptorlose dehydrierende Synthese von Pyrrolen.

Diese Forschung wird durch umfassende experimentelle und theoretische mechanistische Studien gestützt, darunter UV-Vis-Spektroskopie, Elektronenspinresonanz (EPR) und Dichtefunktionaltheorie (DFT). Diese Untersuchungen lieferten entscheidende Einblicke in Reaktionswege und Zwischenprodukte, wodurch eine gezielte Optimierung katalytischer Systeme ermöglicht wurde und grundlegende Konzepte mit praktischen Fortschritten in der nachhaltigen Katalyse verknüpft werden konnten.

Acknowledgments

I would like to begin by expressing my heartfelt gratitude to Prof. Matthias Beller and the former and current members of the board of LIKAT Rostock for their unwavering support in helping me establish my independent research group. Their efforts in facilitating access to institutional resources and providing financial support through the institute have been instrumental to the success of my junior research group at LIKAT. I am also deeply thankful to the German Research Foundation (DFG) for funding my group, enabling the exploration of innovative ideas, and fostering the growth of my research endeavors. I would like also to thank the financing organizations that has supported my team members by scholarships; Chinese scholarship council (CSC), Rohan/DAAD graduate school and Erasmus Mundus programs ASC and SuCat.

I am profoundly grateful to my postdoc mentor at RWTH Aachen, Prof. Magnus Rueping, for offering me the opportunity and confidence to work independently at a very early stage of my career. His trust in my abilities laid the foundation for my academic journey and significantly shaped my approach to research leadership.

A special thank you goes to my current and former MSc and PhD students and posdocs, whose hard work, expertise, and dedication have been fundamental to the research presented in this thesis. Their efforts in the laboratory, commitment to excellence, and enthusiasm for science have been invaluable in achieving the goals of this project. It is a privilege to lead such a talented and motivated team.

I also extend my deepest gratitude to my collaborators, Dr. Luis Miguel Azofra (DFT calculations) and Dr. Jabor Rabeah (spectroscopy), whose valuable insights, constructive discussions, and significant contributions have greatly enriched this research. Their expertise and shared passion for advancing knowledge have been immensely appreciated.

My deepest, most sincere appreciation goes to my loving wife, Amira, whose unwavering support, patience, and encouragement have been my greatest source of strength. Through the journey of academia, she has stood by my side, offering not only motivation but also incredible patience in adapting to our frequent relocations. Her warmth and understanding have made every challenge more bearable, and without her love and support, this work would not have been possible.

Objectives and aim of the work

This habilitation thesis aims to develop innovative strategies in biomimetic catalysis, emphasizing sustainable and efficient transformations. Inspired by natural metalloenzymes, this research focuses on designing environmentally benign catalytic systems aligned with green chemistry principles. A key goal is replacing expensive noble metal catalysts with earth-abundant alternatives such as cobalt, iron, and manganese to enhance sustainability and cost-effectiveness. The study explores enzyme-inspired catalytic systems, particularly iron hydrogenase and vitamin B_{12} mimics, to facilitate selective and efficient organic transformations. By integrating biomimetic principles with modern synthetic methodologies, this work bridges biological and synthetic catalysis, offering sustainable solutions for chemical synthesis.

Building on the radical chemistry of vitamin B12, this research investigates ligand-to-metal charge transfer (LMCT) in selective radical desaturation. A major focus is the development of cobaloxime-based catalysis and photocatalysis, including the design and optimization of catalysts for radical-based transformations such as remote functionalization of aliphatic alcohols and amines. Photoinduced cobalt catalysis is explored to enable sustainable desaturation of amines and dehydrogenative functionalization of olefins under visible light.

Additionally, this work advances hydrogenation, dehydrogenation, and hydrogen borrowing catalysis using first-row transition metals, inspired by hydrogenase activity. Key objectives include selective hydrogenation of challenging substrates, the use of alcohols (including methanol) as alkylating reagents, and the development of air- and moisture-stable manganese catalysts for these transformations. Investigating metal-ligand cooperativity is essential for enhancing efficiency and selectivity.

Beyond mechanistic insights, this research emphasizes scalability and industrial relevance. It contributes to sustainable chemistry by minimizing waste, reducing reliance on rare metals, and improving energy efficiency. By merging biomimetic inspiration with synthetic innovation, this work aims to establish new catalytic paradigms for more sustainable and economically viable chemical transformations.

Contents

1 Literature review and work summary

1.1 Catalysis in organic synthesis

Catalysis is a cornerstone of modern chemistry, enhancing reaction rates and enabling essential transformations in various industries.[1] Introduced over 180 years ago by Jöns Jacob Berzelius,[2] catalysis now drives over 90% of all chemical processes, underpinning the production of countless commodities, from fuels to pharmaceuticals. Traditional catalysis predominantly relies on transition metals, especially precious metals such as palladium, platinum, and rhodium. These metals are valued for their exceptional stability, high catalytic activity, and selective transformations. However, as research delves deeper into sustainability, the field of catalysis faces a significant challenge: how to meet the world's growing chemical demands without depleting finite resources or harming the environment.

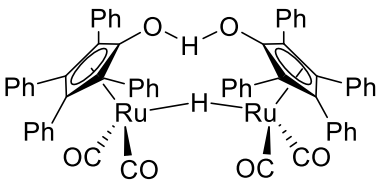

Shvo catalyst

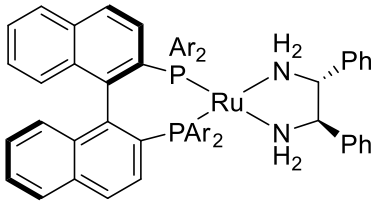

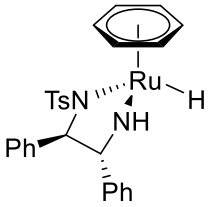

Noyori hydrogenation catalysts

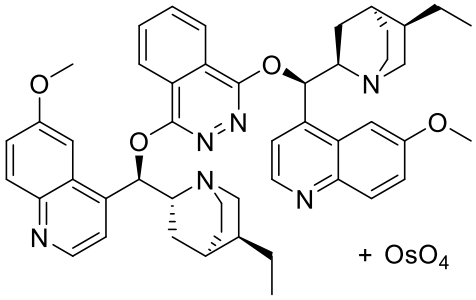

Sharpless dihydroxlation catalyst

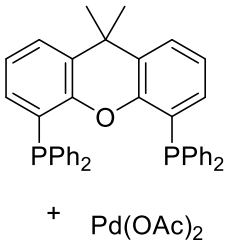

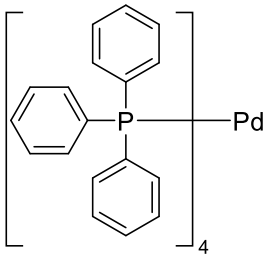

Palladium Cross-coupling catalysis

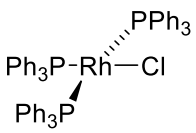

Wilkinson's catalyst

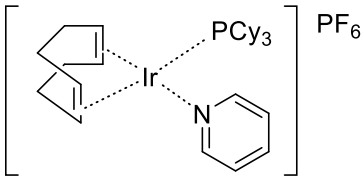

Crabtree catalyst

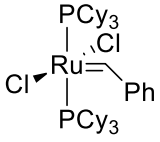

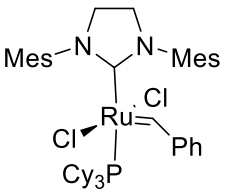

Grubbs metathesis catalysts

***Scheme 1**. Notable noble metal catalysts*

Noble metals catalysis, such as palladium and ruthenium, are highly valued in catalysis for their exceptional stability, reactivity, and selectivity.[3] These metals also undergo

classical two-electron redox processes, allowing precise control over reaction pathways and enabling selective synthesis of complex molecules, which has led to significant breakthroughs recognized by three Nobel Prizes in Chemistry: in 2001 for asymmetric catalytic hydrogenations and hydroxylation (ruthenium and osmium), in 2005 for olefin metathesis (mostly ruthenium),[4] and in 2010 for palladium-catalyzed cross-coupling reactions.[5] A selection of widely applied noble metal catalysis are shown in Scheme 1. Despite their transformative impact in industrial and academic chemistry, precious metals are economically and environmentally costly. They are scarce and concentrated in limited regions, making them vulnerable to supply fluctuations. Extraction and refinement of these metals are resource-intensive, requiring substantial fossil fuel consumption and generating high CO_2 emissions; for example, obtaining a single ounce of platinum may involve processing up to 40 tons of ore from deep mines. Moreover, precious metals are rarely recycled in industrial processes due to low economic feasibility, raising concerns over long-term availability and environmental impact.[6]

In the 21st century, homogeneous catalysis has experienced significant advancements through alternative approaches such as biocatalysis, organocatalysis, and base metal catalysis. Biocatalysis, particularly when combined with directed evolution,[7] has enabled the creation of engineered enzymes capable of catalyzing novel reactions with high selectivity and efficiency. Organocatalysis[8] has emerged as a vital area, with the development of small organic molecules as catalysts, facilitating various asymmetric transformations and expanding the scope of chemical synthesis (Scheme 2).

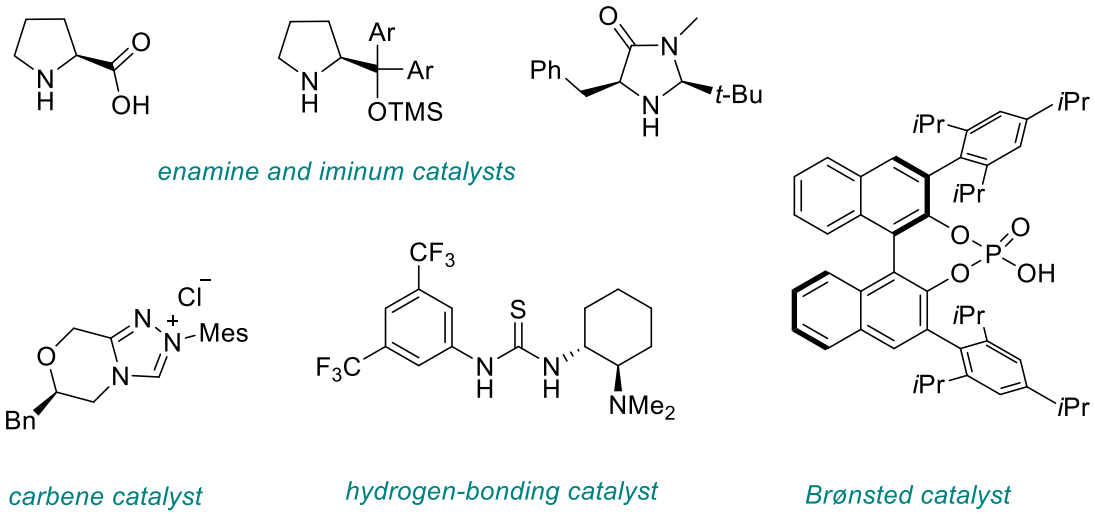

***Scheme 2**. Selected examples of widely applied Organocatalysis*

Base metal catalysis[9] has also gained attention as a sustainable alternative to precious metal catalysts, with significant developments in utilizing earth-abundant metals like copper and nickel for various organic transformations, thereby reducing costs and environmental impact. These advancements collectively contribute to more sustainable and efficient catalytic processes in modern chemistry.

1.2 Biomimetic Driven Sustainability

The pursuit of sustainable and efficient catalysis, as discussed in the previous section, has often drawn inspiration from nature's unparalleled ability to orchestrate chemical transformations. Concepts such as engineered biocatalysis, organocatalysis, and base metal catalysis are all, in essence, inspired by natural processes. Biocatalysis directly utilizes enzymes or modified enzymes, the products of billions of years of evolution, to achieve selective and efficient reactions. Organocatalysis leverages small organic molecules to mimic the roles of natural cofactors and catalytic intermediates. Similarly, base metal catalysis reflects the principles of natural metalloenzymes, which rely on earth-abundant metals like iron and copper for catalytic activity.

Building on these nature-inspired approaches, biomimetic catalysis specifically focuses on replicating the core principles of enzyme functionality—efficiency, selectivity, and sustainability—in synthetic systems.[10] Enzymes, nature's catalytic masterpieces, accelerate complex biochemical reactions under mild, environmentally benign conditions while displaying extraordinary specificity for their substrates. Biomimetic catalysis seeks to emulate these properties, not by merely copying biological systems, but by understanding and recreating the key principles that govern enzyme performance. These include substrate binding, transition-state stabilization, and precise control over reaction pathways.

One of the most promising aspects of biomimetic catalysis is its potential to address the limitations of traditional catalysis, particularly the reliance on precious metals. Drawing inspiration from metalloenzymes such as hydrogenases and vitamin B_{12}, synthetic catalysts based on abundant and non-toxic elements like iron, cobalt, and nickel have demonstrated remarkable capabilities in hydrogenation, oxidation, and radical reactions. By mimicking the coordination environments and mechanistic pathways of these natural systems, biomimetic catalysts offer a sustainable and versatile alternative to precious-metal-based catalysis.

The integration of biomimetic principles into catalysis not only advances the field scientifically but also aligns with the broader goals of green chemistry. By bridging the gap between biology and synthetic chemistry, biomimetic catalysis contributes to the development of transformative catalytic systems that meet the demands of modern chemical industries while minimizing environmental impact and conserving finite resources. In doing so, it represents a critical step forward in creating a more sustainable future, complementing the other nature-inspired approaches discussed in the previous section. The work of this thesis focuses on the inspiration from natural metalloenzymes.

1.2.1 Natural metalloenzymes

Natural metalloenzymes are proteins that incorporate metal ions as essential cofactors, enabling a wide array of biological reactions vital for life.[11] These enzymes harness the unique chemical properties of metals to facilitate processes such as electron transfer, substrate binding, and catalysis under physiological conditions.[12] Natural

metalloenzymes are central to life's chemistry, with diverse metal ions enabling a multitude of biochemical reactions. Their study not only enhances our understanding of biological processes but also drives innovations in medicine and industry.[13] Key metals involved in metalloenzymes include iron[14], copper[15], zinc[16], nickel, manganese[13], cobalt[17], magnesium[18], calcium[19], molybdenum[20], vanadium[21], and tungsten[22]. Selected examples are shown in Table 1.

Table 1. Selected examples of natural metalloenzymes.

Element	Role in Biological Systems	Examples of Enzymes Involved
Iron (Fe)	Facilitates oxygen transport and electron transfer; protects cells from oxidative damage by decomposing hydrogen peroxide.	Hemoglobin, Cytochromes, Catalase, Peroxidase
Copper (Cu)	Plays a role in electron transport and defense against reactive oxygen species.	Cytochrome c Oxidase, Superoxide Dismutase
Zinc (Zn)	Stabilizes protein structures; activates water molecules for nucleophilic attacks.	Carbonic Anhydrase, Alcohol Dehydrogenase
Nickel (Ni)	Participates in nitrogen metabolism and hydrogen gas processing.	Urease, Hydrogenase
Manganese (Mn)	Crucial for photosynthesis and protection against oxidative stress.	Photosystem II, Superoxide Dismutase
Cobalt (Co)	Vital for DNA synthesis and metabolic processes as a component of vitamin B12.	Vitamin B_{12}-dependent Enzymes
Magnesium (Mg)	Stabilizes nucleic acid structures; essential for ATP-dependent reactions and energy metabolism.	Numerous ATP-dependent Enzymes
Calcium (Ca)	Plays a structural role and acts as a secondary messenger in signal transduction.	Calmodulin, Troponin C
Molybdenum (Mo)	Involved in redox reactions, particularly in nitrogen and sulfur metabolism.	Nitrogenase, Sulfite Oxidase
Vanadium (V)	Found in certain haloperoxidases and nitrogenases.	Haloperoxidases, Nitrogenases
Tungsten (W)	Utilized by extremophilic microorganisms in redox enzymes.	Redox Enzymes (e.g., Aldehyde Oxidoreductase)

1.3 Natural Inspirations for Ligand-to-metal charge transfer catalysis

Ligand-to-metal charge transfer (LMCT) catalysis is often found in various metalloenzymes.[20, 23] LMCT involves the transfer of electrons from ligand orbitals to metal orbitals, resulting in characteristic absorption bands in the UV-visible spectrum and influencing biological functions. LMCT transitions are crucial for enzymatic functions, as they often play roles in electron transfer processes essential for various biological activities (Scheme 3). For example, ***blue copper proteins*** such as plastocyanin[24] and azurin[25] contain a copper ion coordinated by ligands including cysteine, histidine, and methionine. The strong interaction between the copper ion and the cysteine sulfur allows for electron density transfer from the ligand to the metal, leading to intense absorption bands around 600 nm, which impart a deep blue color to these proteins.[23b, 23d-f] In enzymes like **sulfite oxidase**,[26] the molybdenum center is coordinated by a cysteine ligand. Resonance Raman studies have identified an absorption band around 480 nm, attributed to an LMCT transition from the sulfur atom of cysteine to the molybdenum ion. This specific electron transfer is crucial for the enzyme's catalytic function, facilitating the oxidation of sulfite to sulfate. Similarly, in dimethyl sulfoxide (DMSO) reductase, the molybdenum center undergoes LMCT transitions that are essential for its catalytic mechanism. The enzyme facilitates the reduction of DMSO to dimethyl sulfide, a process involving the transfer of an oxygen atom from the substrate to the molybdenum center. This reaction is coupled with electron transfer processes, where LMCT plays a pivotal role in enabling the necessary redox changes at the active site. [20] While MLCT transitions have been characterized in xanthine oxidase, specific ligand-to-metal charge-transfer (LMCT) transitions have not been prominently reported in the literature. The enzyme's catalytic activity primarily involves electron transfer processes facilitated by the molybdenum center and its associated cofactors, with MLCT playing a significant role in these mechanisms.[23c]

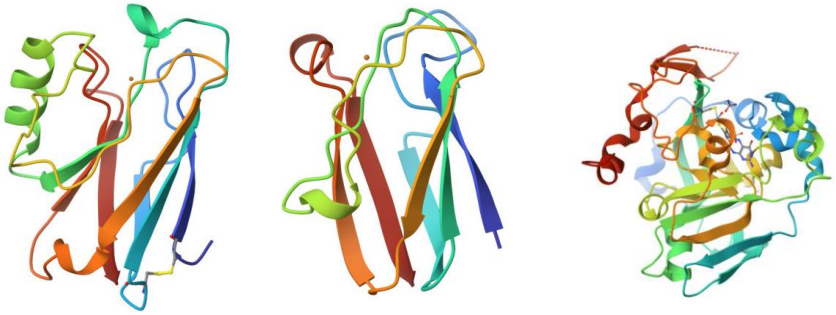

***Scheme 3**. Selected LMCT enzymes (protein data bank)*

Vanadium haloperoxidases (VHPOs) are enzymes that catalyze the oxidation of halides (such as chloride, bromide, and iodide) using hydrogen peroxide, resulting in the formation of hypohalous acids. These enzymes play significant roles in the biosynthesis of halogenated organic compounds in marine organisms. The active site of VHPOs contains a vanadium ion coordinated by oxygen and nitrogen ligands.

Studies have shown that the electronic interactions between vanadium and its ligands can result in ligand-to-metal charge transfer (LMCT) transitions. For instance, research on functional models of VHPOs has identified a peroxo-to-vanadium charge transfer band at approximately 450 nm in the UV-visible spectrum. This band is attributed to LMCT transitions from the peroxo ligand to the vanadium center.[23a]

The enzymatic functions of **vitamin B_{12}** derivatives, particularly coenzyme B_{12} (AdoCbl) and methylcobalamin (MeCbl), are driven by their organometallic chemistry.[27] These cofactors participate in radical-based and nucleophilic reactions essential for metabolic pathways. AdoCbl is crucial in enzymatic radical rearrangements. The Co–C bond in AdoCbl undergoes homolytic cleavage, generating a 5'-deoxyadenosyl radical and cob(II)alamin (B_{12}). This radical acts as a reactive intermediate in enzymatic transformations such as mutase-catalyzed rearrangements (Scheme 4). In methyl malonyl-CoA mutase, for example, the 5'-deoxyadenosyl radical abstracts a hydrogen atom from the substrate, initiating a 1,2-rearrangement before returning the hydrogen, regenerating the radical and completing the catalytic cycle. This mechanism enables difficult carbon-skeleton rearrangements essential for amino acid and fatty acid metabolism. The homolytic bond dissociation energy (BDE) of the Co–C bond (~30 kcal/mol) is ideal for facilitating radical chemistry, making AdoCbl uniquely suited for enzymatic radical reactions.[27d]

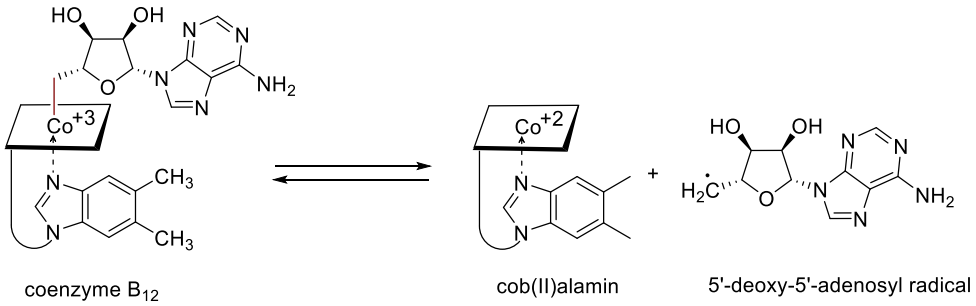

***Scheme 4**. Reversible radical trap enabled by Coenzyme B_{12}*

MeCbl, in contrast, plays a pivotal role in enzymatic methyl transfer reactions. It acts as a methyl donor in processes like methionine biosynthesis, where methionine synthase catalyzes the transfer of the methyl group from MeCbl to homocysteine, forming methionine (Scheme 5).[28] This reaction regenerates cob(I)alamin (B_{12}), a highly nucleophilic species that is rapidly remethylated using methyl donors such as methyl tetrahydrofolate. This continuous regeneration of MeCbl ensures the catalytic cycle persists efficiently. The stability of MeCbl's Co–C bond in aqueous environments prevents unwanted degradation, while its ability to donate methyl groups selectively under enzymatic control ensures precise biological methylation. Beyond nucleophilic methyl transfer, recent evidence suggests that MeCbl also participates in radical-mediated methylations. Enzymatic systems have been observed to facilitate methyl transfer to radicals, expanding the mechanistic repertoire of MeCbl beyond simple nucleophilic pathways. This suggests a broader role for B_{12} cofactors in radical-based enzymatic transformations.[27d]

Both AdoCbl and MeCbl resist proteolytic degradation within enzymes, ensuring their longevity as cofactors. However, the methyl group of MeCbl can be abstracted by electrophilic species, radicals, or transition metals under enzymatic conditions, which can regulate its reactivity in vivo. The nucleotide moiety of complete cobalamins stabilizes MeCbl, increasing its resistance to non-enzymatic degradation and ensuring efficient catalytic performance. Thus, B_{12}-dependent enzymatic reactions rely on finely tuned organometallic transformations, with AdoCbl facilitating radical-based rearrangements and MeCbl driving methylation processes. Their unique Co–C bond chemistry enables challenging biochemical transformations fundamental to metabolism.

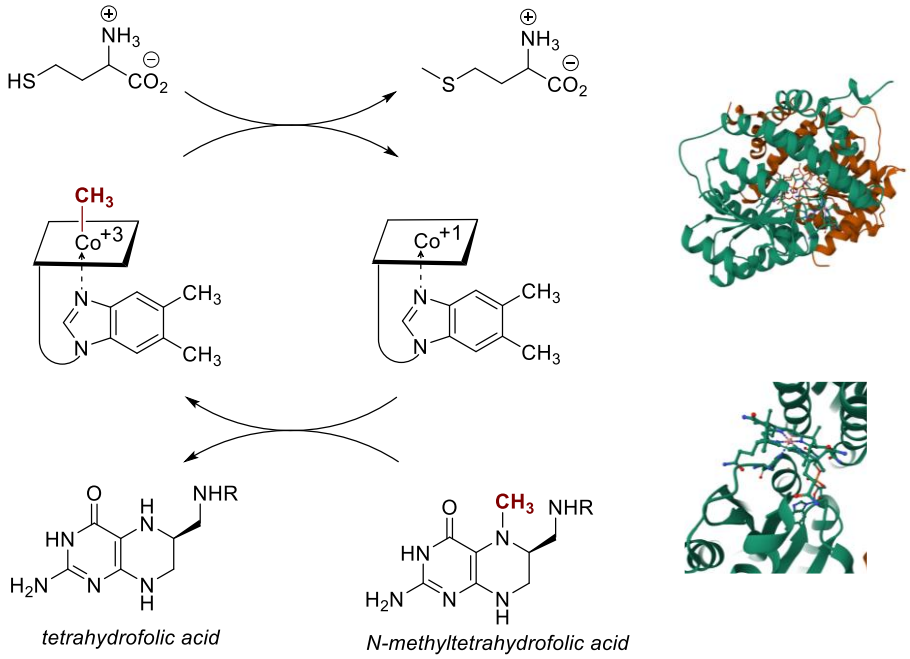

***Scheme 5**. Methyl transfer enabled by Methionine synthase*

1.3.1 Merger of light and enzymatic LMCT catalysis

Nature has evolved to utilize inexpensive 3d transition metals to facilitate complex enzymatic transformations under mild conditions.[29] Remarkably, when additional energy is required, nature harnesses visible light—an abundant and renewable energy source.[30] The interaction between light and first-row transition metal complexes is fundamental to numerous life-sustaining processes. A prime example is photosynthesis, where a series of photochemical reactions convert light into chemical energy. This process relies on 3d-metalloproteins such as ferredoxin (Fe) for electron transfer, manganese-containing water oxidation cofactors for oxygen evolution, and the Rieske protein (Fe) for redox regulation.[31]

Over the past decade, outer-sphere photoredox catalysis has gained immense popularity, primarily due to its versatility in redox-driven transformations.[32] This approach relies on excited-state photocatalysts (PC*) engaging in bimolecular single-electron transfer (SET) with a substrate, provided that the redox potentials are well-matched. However, its application is inherently constrained by the need for long-lived

excited states and strong oxidative or reductive potentials, which has necessitated the widespread use of noble-metal photocatalysts such as iridium(III) and ruthenium(II) complexes.[33]

In contrast, the recent surge of interest in ligand-to-metal charge transfer (LMCT) catalysis has opened new avenues by enabling base-metal photocatalysis in a biomimetic fashion. Unlike outer-sphere SET, LMCT operates through an inner-sphere mechanism, where the substrate is pre-coordinated to a metal center prior to light absorption. Upon excitation, direct charge transfer from the ligand to the metal occurs, resulting in radical formation or selective bond homolysis. Because LMCT catalysis does not require long-lived excited states, it allows even short-lived photogenerated species (<1 ns) to drive efficient transformations. This feature is particularly valuable for enabling photochemical reactivity with earth-abundant 3d metals such as iron, copper, and cobalt, making LMCT a more sustainable and cost-effective alternative.

Beyond expanding the accessibility of base metals, LMCT catalysis has unlocked reactivities that are not feasible under traditional outer-sphere photoredox conditions. For example, it enables the oxidation of high-potential substrates, such as halides (e.g., $Cl^- \rightarrow Cl\bullet$), with relatively weakly oxidizing metal complexes. This capability arises because LMCT activation bypasses the redox potential constraints that typically limit outer-sphere SET reactions. Additionally, LMCT-driven radical generation often involves reversible bond homolysis, which can be strategically leveraged to stabilize reactive intermediates or modulate selectivity, as demonstrated in recent Cu(II)-catalyzed decarboxylation reactions.[34]

Moreover, LMCT catalysis streamlines photoredox processes by integrating radical generation and functionalization within a single catalytic system. Unlike metallaphotoredox strategies that require a separate transition metal catalyst for substrate activation, LMCT directly couples light absorption with metal-catalyzed transformations, reducing the reliance on dual catalytic manifolds. This direct metal-ligand interaction introduces mechanistic flexibility and enables novel synthetic pathways beyond those accessible via traditional photoredox catalysis. The growing interest in LMCT catalysis reflects a broader movement toward biomimetic and sustainable photochemical strategies. By harnessing base metals and overcoming the limitations of outer-sphere photoredox catalysis, LMCT provides a complementary and, in many cases, superior approach to radical-based transformations.

1.3.2 Evolution of Cobaloxime Catalysis in Organic Synthesis[35]

The catalytic potential of cobaloximes in organic transformations was first reported in the 1980s by research groups such as Tada, Pattenden, Branchaud, and Giese.[36] Over the years, numerous studies have demonstrated that cobaloxime catalysis can be achieved under reductive conditions, employing electrochemical approaches or chemical reductants like zinc, sodium borohydride, or Grignard reagents. A significant breakthrough was reported in 2011 by Carreira and co-workers, who demonstrated that cobaloxime catalysis can proceed with turnover using simple organic bases.[37]

Another milestone was reached in 2015 when researchers successfully merged cobaloxime catalysis with photoredox catalysis, expanding its synthetic utility.[38]

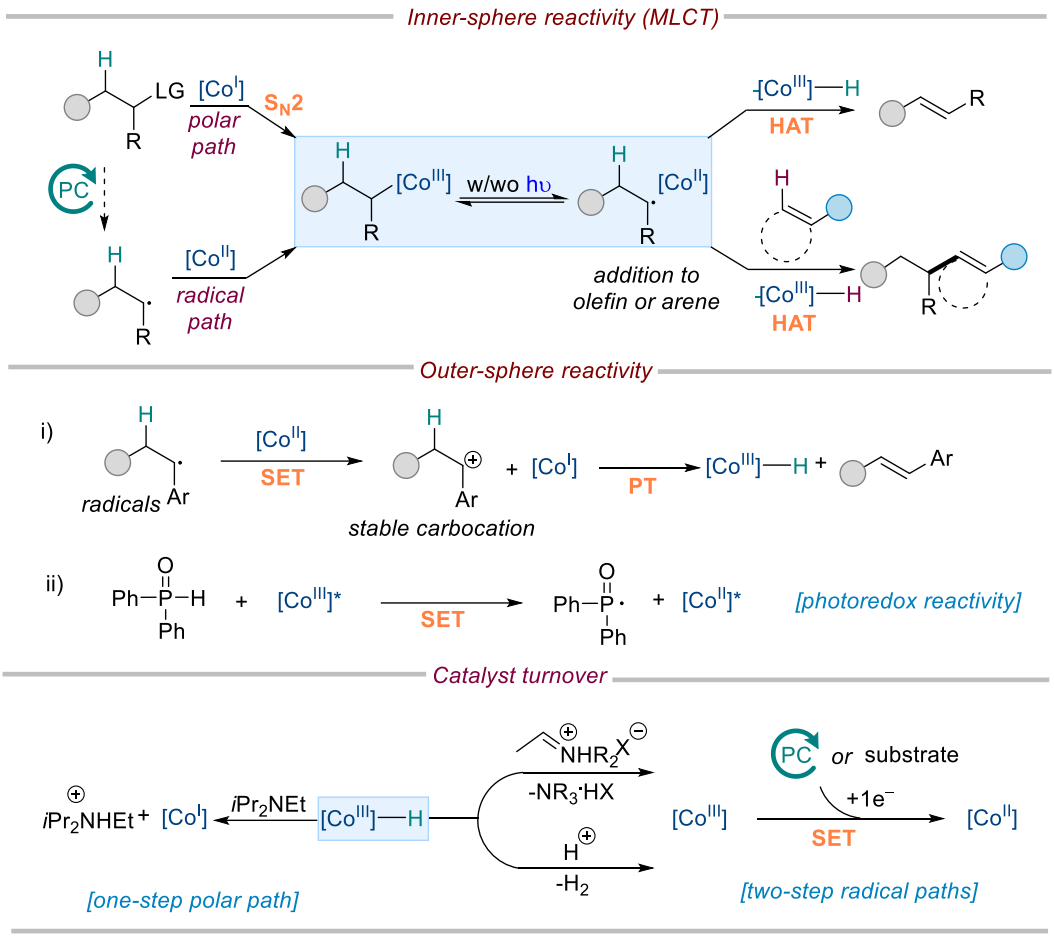

***Scheme 6**. Concepts of cobaloxime catalysis in organic synthesis*

Cobaloxime exhibits diverse catalytic features, enabling both inner-sphere and outer-sphere reactivity in organic transformations. Through inner-sphere mechanisms, cobaloximes facilitate direct interactions with substrates, forming [Co^{III}]–alkyl complexes via nucleophilic substitution or radical capture. Upon activation, these complexes undergo Co–C bond homolysis, generating reactive radicals that can either eliminate β-hydrogen to form olefins or participate in radical addition reactions, leading to functionalized products (Scheme 6). In outer-sphere reactivity, cobaloximes operate via single-electron transfer (SET). Ground-state [Co^{II}] species can oxidize organic radicals to carbocations, which subsequently undergo proton transfer, yielding [Co^{III}]–H and unsaturated products. Photoinduced SET further extends cobaloxime's catalytic versatility, where excited-state [Co^{III}] species act as photoredox catalysts, exemplified by the oxidation of H-phosphines to generate P-radicals. Catalyst regeneration occurs through multiple pathways. In the polar pathway, deprotonation of [Co^{III}]–H by an organic base enables the regeneration of [Co^{I}], sustaining the catalytic cycle. In the radical pathway, [Co^{III}]–H reacts with protons to release H2 and reform [Co^{III}], a step accelerated by proton shuttles or protic acids. Electron-deficient [Co^{III}] species can also be reduced to [Co^{II}] via substrates or co-catalysts, ensuring continuous turnover. With

applications ranging from proton reduction and water splitting to radical transformations, cobaloxime catalysis continues to evolve, offering unique mechanistic flexibility and expanding the scope of sustainable and selective synthetic methodologies.

1.3.3 Remote functionalization of aliphatic alcohols and amines

The first paper of the thesis presents a novel method for the catalytic desaturation of aliphatic amides and imides, using a photoexcited cobalt complex as the catalyst under visible-light irradiation.[39] The process achieves selective C(sp^3)–H bond functionalization at room temperature, producing highly valuable cyclic and acyclic enamides and enimides. This method is notable for its mild conditions, oxidant-free operation, and the use of an earth-abundant cobalt catalyst, making it an environmentally friendly alternative to conventional systems reliant on noble metals (Scheme 7). The study demonstrates the broad applicability of the cobalt catalyst across various substrates, including cyclic and linear amides, as well as commercially available drugs and natural products. Cyclic amides, such as piperidine derivatives, and imides like acetimides, underwent efficient desaturation, with excellent yields and regioselectivity. Mechanistic studies revealed that the reaction proceeds through a photoinduced 1,5-hydrogen atom transfer (HAT) mechanism, followed by radical type β-hydride elimination, facilitated by the cobalt complex.

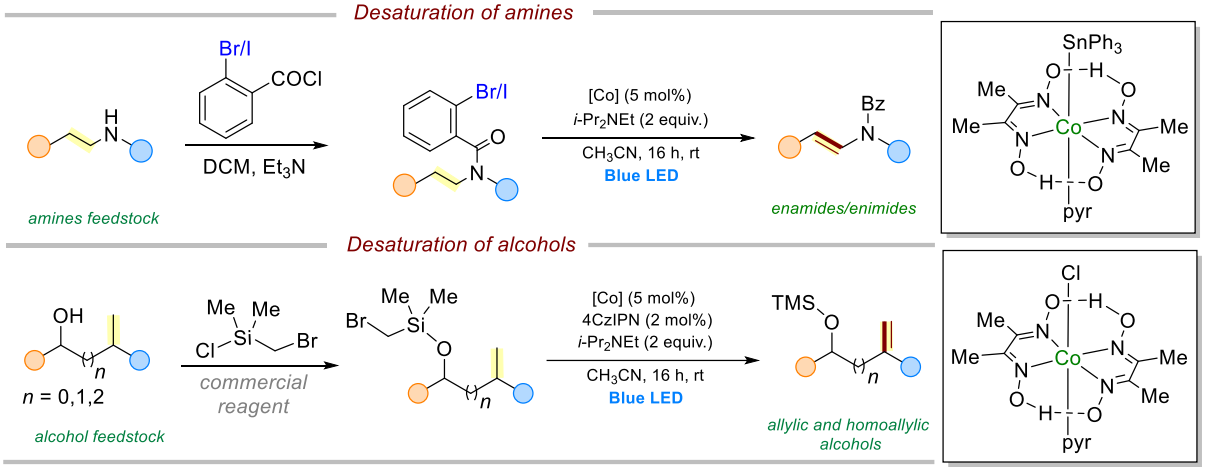

***Scheme 7**. Remote desaturation of alcohols and amines*

The process was successfully scaled up using continuous flow photoreactor technology, addressing light penetration limitations observed in batch systems. This advancement highlights the potential for industrial application, with significant improvements in yield and reaction efficiency. Additionally, density functional theory (DFT) and experimental studies provided insights into the reaction mechanism, including the role of the photoexcited cobalt and triphenyl tin species in enabling these transformations.

Next paper involves a related photoinduced cobaloxime-catalyzed remote desaturation of aliphatic alcohols, offering a sustainable and efficient alternative for synthesizing cyclic and acyclic allylic and homoallylic alcohols from saturated aliphatic alcohols.

This method operates under mild conditions, avoiding the need for external oxidants, noble metals, or phosphine ligands (Scheme 7).[40]

This work addresses the challenge of remote desaturation of alcohols, a transformation that remains difficult due to the inertness of C–H bonds and the intrinsic stability of aliphatic chains. Previous methods involving palladium catalysts and silicon auxiliaries achieved some success but were limited by high catalyst loadings and the need to handle sensitive reagents. Inspired by prior research, the team employed cobaloxime catalysis—a system that mimics vitamin B12—to facilitate alcohol desaturation via radical chemistry.[41] Mechanistic studies, including UV–Vis spectroscopy and density functional theory (DFT) calculations, revealed a preference for a 1,6-hydrogen atom transfer (HAT) pathway over alternative pathways.

1.3.4 Dehydrofunctionalization of amines

This work introduces a biomimetic approach for the catalytic deamination of primary amines to produce olefins, using visible light and a combination of acridinium salt and cobaloxime catalysts (Scheme 8).[42] This method mimics enzymatic processes like those of phenylalanine ammonia lyase, offering an environmentally friendly and efficient alternative for the synthesis of alkenes from non-fossil-based chemicals.
The process involves photoexcitation of the acridinium catalyst, generation of α-amino radicals, and subsequent cobalt-catalyzed desaturation to yield olefins. This dual-catalysis strategy enables high regioselectivity, operating under mild conditions without the need for harsh reagents or conditions. It shows broad applicability across diverse substrates, including amino acids, natural products, and pharmaceuticals.

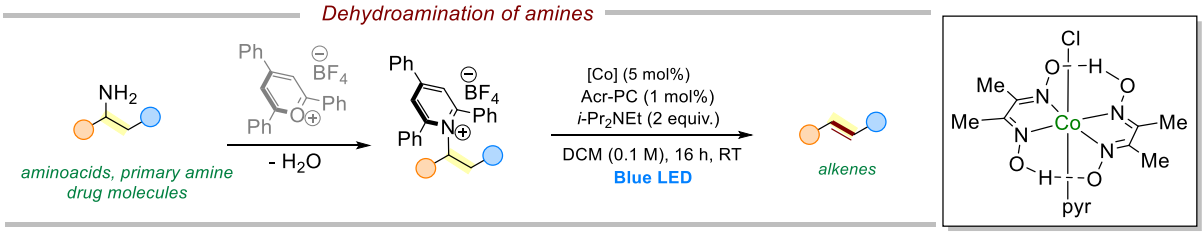

Scheme 8. *Dehydroamination of primary amines*

Mechanistic studies using fluorescence quenching, EPR spectroscopy, and DFT calculations provided insights into the catalytic cycle, confirming the synergistic role of photoredox and cobalt catalysis. The method demonstrates significant functional group tolerance and allows for late-stage functionalization of complex molecules, highlighting its potential for applications in sustainable chemistry. This innovative protocol advances the field of organic synthesis, addressing limitations of traditional methods such as Hofmann and Cope eliminations, and presents a practical, scalable solution for the transformation of amines into valuable olefin derivatives.

1.3.5 Alkyl Heck reaction

The article presents a new photoexcited cobalt-catalyzed endo-selective alkyl Heck reaction (Scheme 9).[43] This reaction transforms iodomethylsilyl ethers of phenols and

alkenols into seven- and eight-membered siloxycycles with excellent yields. These siloxycycles can be oxidized further to produce allylic alcohols, demonstrating potential for selective hydroxymethylation of *o*-hydroxystyrenes and alkenols. Unlike traditional palladium-catalyzed methods requiring costly ligands and harsh conditions, this approach employs cobalt catalysis under visible light, avoiding photoredox catalysts or strong reductive conditions.[44]

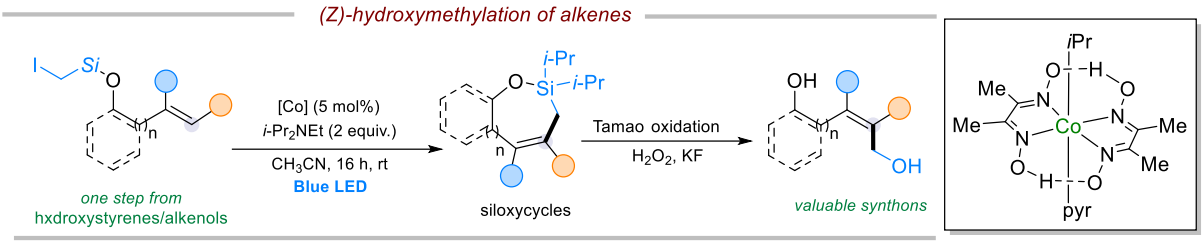

***Scheme 9**. endo-selective alkyl Heck reaction.*

Mechanistic studies, including EPR and UV-Vis spectroscopy, support a cobalt-based radical pathway, involving single-electron transfer and concerted β-hydrogen elimination in the triplet state. Density functional theory (DFT) calculations elucidate the proposed reaction mechanism.

1.4 Natural Inspirations for Metal–Ligand Cooperative Catalysis

Nature provides a remarkable model for efficient hydrogen activation and transfer reactions, particularly through metalloenzymes. Enzymatic systems, such as hydrogenases, lactate racemase, and alcohol dehydrogenase, demonstrate how nature leverages coordinated interactions between metal centers and ligand environments for efficient catalysis. These biological systems utilize cooperative metal-ligand interactions to challenging catalysis under mild conditions, inspiring the development of small-molecule catalysts that mimic their function.[45]

Cooperative Catalysis in [FeFe]- and [NiFe]-Hydrogenases highlights the role of metal–ligand cooperation (MLC) in hydrogenases, specifically in the heterolytic cleavage of H_2 are shown in Scheme 10a and b. In [FeFe]-hydrogenase, the active site consists of a binuclear Fe cluster, where a pendant amine functions as a proton relay, deprotonating coordinated H_2 at the Fe(II) center.[46] This cooperative effect is crucial for efficient hydrogen activation and is a common feature in biomimetic catalyst design. Similarly, in [NiFe]-hydrogenase, an arginine (Arg509) residue in the second coordination sphere assists in H_2 cleavage by acting as a general base. This structural arrangement facilitates proton transfer and stabilizes key catalytic intermediates.[47] These findings have inspired synthetic catalysts that incorporate pendant amines or similar functional groups to enhance their efficiency in hydrogenation and dehydrogenation reactions.

The heterolytic activation of hydrogen (H_2) in [Fe]-hydrogenase occurs through a cooperative mechanism involving the Fe center, the Fe-guanylylpyridinol (FeGP) cofactor, and the substrate methenyl-H_4MPT$^+$. The process begins with H_2 binding to the Fe(II) active site, which features an open coordination site stabilized by the FeGP

cofactor, modulating the electronic properties of the metal center. Heterolytic cleavage of H_2 then takes place through a three-component system, where the pyridonate oxygen of the FeGP cofactor, the Fe(II) center, and the carbocation-like substrate methenyl-H_4MPT$^+$ work in concert. The Fe(II) center acts as a Lewis acid, stabilizing the negative charge that develops during H_2 cleavage, while the pyridonate oxygen functions as a proton acceptor, abstracting H^+ from H_2. Simultaneously, methenyl-H_4MPT$^+$ serves as a hydride (H^-) acceptor, receiving the second hydrogen atom. As a result, the extracted H^+ remains within the enzyme for potential proton transfer reactions, while the H^- is stereospecifically transferred to the pro-R face of methenyl-H_4MPT$^+$, forming methylenetetrahydromethanopterin (methylene-H_4MPT), a crucial intermediate in the methanogenesis pathway of hydrogenotrophic archaea.

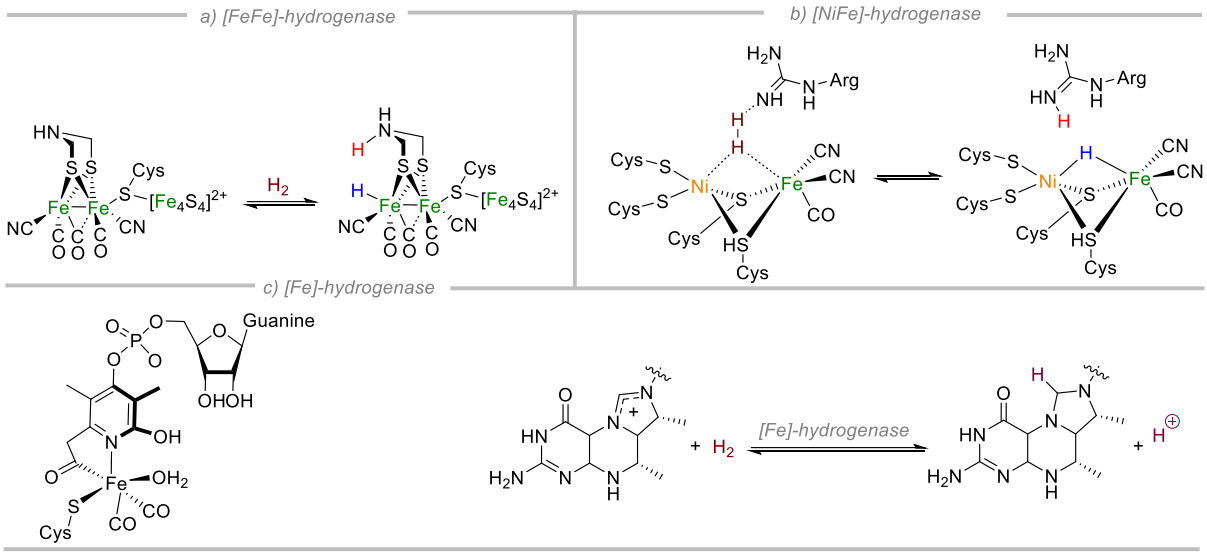

***Scheme 10**. Heterolytic hydrogen activation enabled by MLC enzymes*

1.4.2 Evolution of 3d metal-ligand catalysis

Traditionally, hydrogenation and dehydrogenation reactions have relied on noble-metal catalysts, such as ruthenium and iridium complexes. However, recent efforts have focused on replacing these precious metals with more earth-abundant and sustainable alternatives, particularly iron, cobalt, and manganese. These 3d transition metals have demonstrated significant potential in catalyzing heterolytic hydrogen activation, enabling a variety of transformations, including hydrogenation, dehydrogenation, and hydrogen borrowing.[48] This section highlights key developments in these catalytic systems and their underlying bioinspired principles. See Scheme 11 for selected 3d-metal pincer complexes. These bioinspired catalysts exhibit broad applicability, enabling hydrogenation and dehydrogenation processes, as well as hydrogen borrowing strategies. Their ability to activate hydrogen under mild conditions, combined with their straightforward synthesis from inexpensive materials, underscores their potential for sustainable catalysis. By closely emulating the function of hydrogenase enzymes, these iron complexes represent an important step toward efficient and cost-effective catalytic systems.

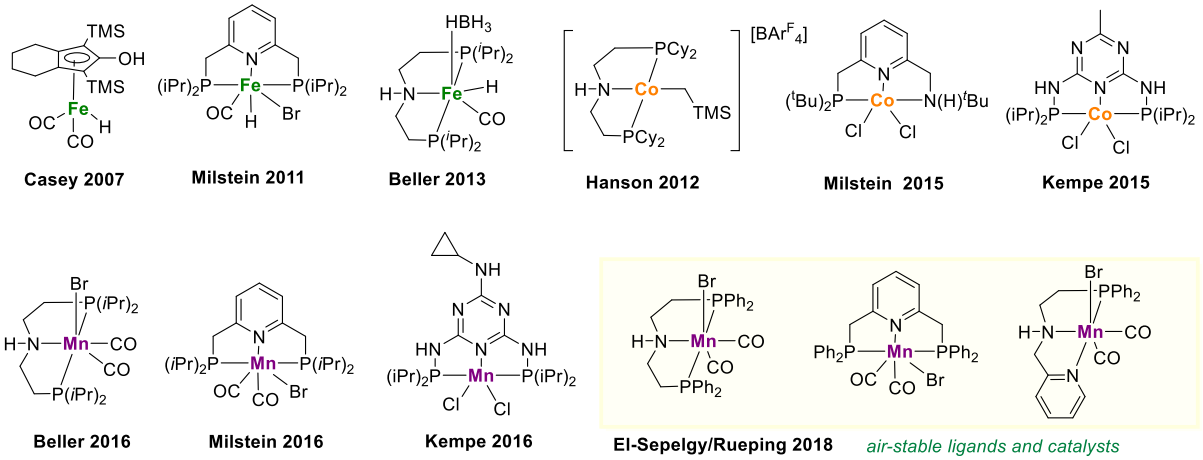

***Scheme 11**. Selected man-made 3d-metal-ligand catalysts*

Iron catalysis: Inspired by these enzymatic systems, Casey and co-workers reported in 2007 that an iron-hydride hydroxycyclopentadienyl complex could facilitate heterolytic hydrogen activation.[49] Subsequent studies demonstrated that bifunctional iron(II) hydride species could be generated in situ using air- and moisture-stable iron(0) cyclopentadienone complexes, These air stable inexpensive phosphine free catalysts undergo activation via the selective removal of a carbonyl ligand, which can be achieved using trimethylamine N-oxide, inorganic bases, or light irradiation (Figure 3a).[50] However, iron cyclopentadienone complexes suffer from the low activity towards the hydrogenation of demanding carbonyl compounds such as esters, amides as well as the acceptorless dehydrogenation catalysts. In this regards several groups including Beller and Milstein have developed iron pincer complexes that could efficiently reduce demanding substrates including ester hydrogenation and methanol dehydrogenation.[51] However, these complexes are relatively difficult to synthetized and must be handled in anaerobic conditions.

Cobalt catalysis: Cobalt-based cooperative metal-ligand complexes have also demonstrated notable hydrogen activation capabilities. Hanson and coworkers have developed the first example cobalt pincer hydrogenation catalysis.[52] A more accessible and air stable alternative was reported be Kempe in 2015.[53] In general, cobalt pincer complexes are much less explored than iron and manganese counterparts. However, simple mixture of cobalt salts and polydentate phosphine ligands such as Tris(diphenylphosphinomethyl)ethane (Triphos) have shown great utility in hydrogenation, dehydrogenation, and hydrogen borrowing transformations through a classical monohydride pathway.[54]

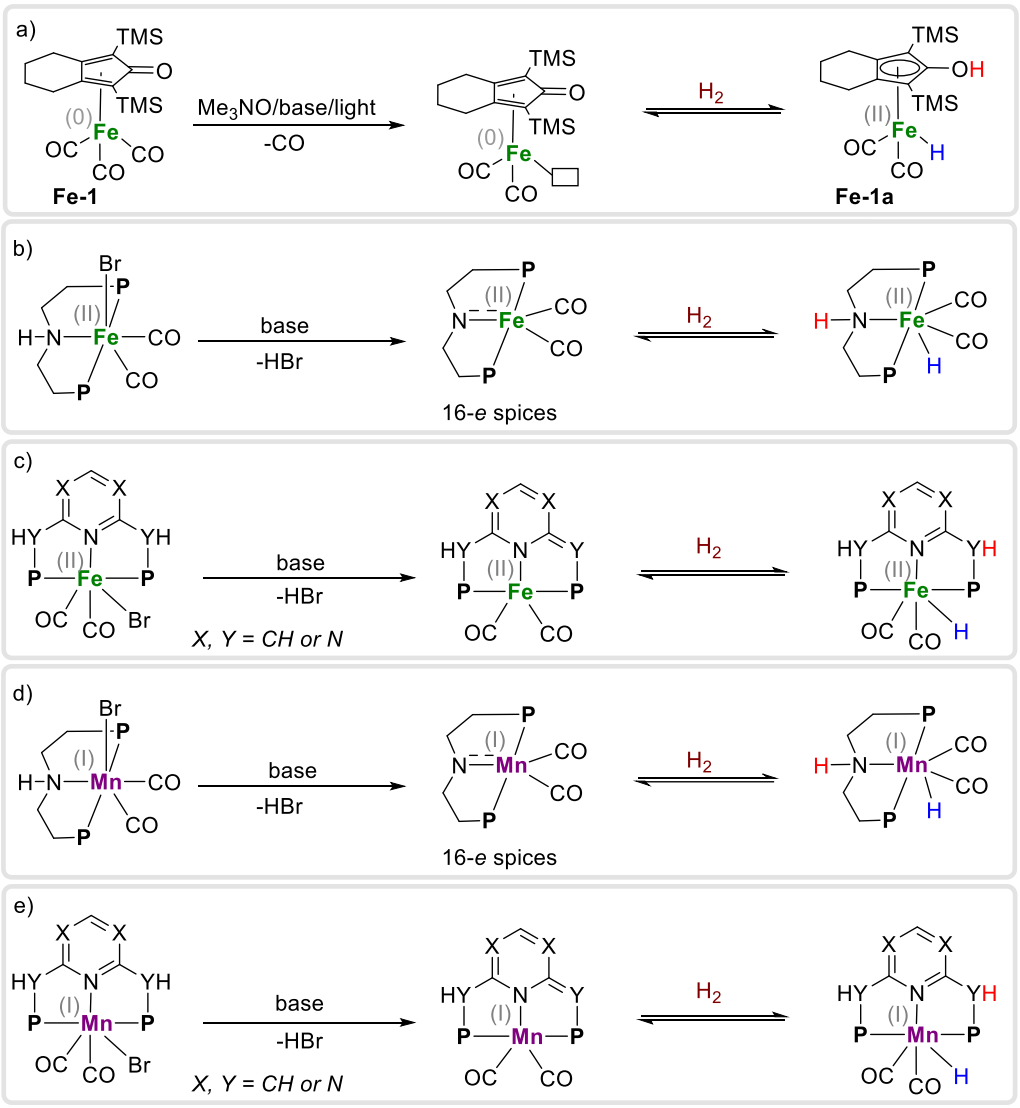

***Scheme 12**. Activation 3d-complexes enables heterolysis of H_2*

Manganese catalysis: manganese has recently gained attention as a promising alternative to noble metals for hydrogen activation processes, inspired by biological hydrogenase and dehydrogenase enzymes. The groundbreaking research by Beller and Milstein in 2016 sparked widespread interest in manganese-based catalysis,[55] positioning it as a key contributor to (de)hydrogenation and hydrogen borrowing reactions. Unlike iron and most cobalt pincer complexes, manganese pincer complexes are easy to synthesize and offer exceptional stability in both air and moisture. Moreover, manganese pincer complexes exhibit superior catalytic activity compared to other base-metal alternatives, making them a viable substitute for noble metal catalysis. In 2018, we developed a series of catalytically active manganese complexes utilizing air-stable phosphine ligands, a feature not achievable with iron and cobalt (Scheme 11).[56]

For iron cyclopentadienone complexes, the pre-catalyst activation involves the removal of one carbonyl ligand via trimethylamine N-oxide, near-UV light, or a base. Upon exposure to hydrogen, the Fe(0) pre-catalyst undergoes transformation into an Fe(II) species, featuring a hydride at the metal center and a proton on the non-innocent ligand

(Figure 12a). In the case of manganese and iron pincer complexes, the pincer ligands can adopt aliphatic motifs such as PN(H)P or PN(H)N. Treatment with bases like carbonates or butoxides leads to the elimination of hydrogen bromide, yielding a 16-electron imido complex of iron or manganese (Figure 12b, d). Beyond aminopincer systems, pyridine-based pincer ligands (PNPyP, PNPyN, PN3P), as well as the triazine-derived PN5P ligand, have been widely employed. In these systems, catalyst activation occurs via an aromatization–dearomatization pathway (Figure 12c, e).[51a]

1.4.2. Manganese catalyzed hydrogenation

We have reported manganese-catalyzed method for the hydrogenation of CO_2-derived cyclic organic carbonates (COCs) and polycarbonates into methanol and diols.[56a] The catalytic system, based on a Mn-PNN complex, operates under mild conditions and achieves high yields, with up to 99% of diols and 92% of methanol produced. The manganese system addresses the challenge of hydrogenating carbonic acid derivatives, which are typically stabilized by resonance effects that reduce their reactivity. The study explores the catalytic mechanism, highlighting the importance of metal-ligand cooperation. Experiments and density functional theory (DFT) calculations reveal that the process involves three catalytic cycles, each driven by the synergistic action of manganese and the ligand's N–H functionality. Modifications to the ligand structure demonstrate the critical role of this cooperative interaction in achieving high catalytic efficiency. Experimental results demonstrate the broad substrate scope of the system, with a variety of substituted five- and six-membered cyclic carbonates successfully converted to diols and methanol. Additionally, polycarbonate recycling was achieved, producing methanol and diols in high yields, thus addressing the pressing issue of plastic waste. For the best of our knowledge, this represents the first example of base metal catalyzed hydrogenolysis of poly carbonates. The use of low catalyst loadings (as little as 0.25 mol%) further underscores the system's efficiency and scalability.

The second hydrogenation study describes a novel manganese-catalyzed method for the highly chemo- and stereoselective transfer semihydrogenation of internal alkynes to (*Z*)-alkenes (Scheme 13).[57] Using ammonia borane as an environmentally benign hydrogen donor, this process is catalyzed by a stable manganese(II) complex in the absence of additives, bases, or super hydrides. The reaction is efficient under mild conditions, offering a sustainable alternative to traditional noble metal-based systems such as palladium and rhodium catalysts. The manganese pincer complex, based on a pyridyl-based PNP ligand, demonstrates exceptional performance, achieving up to 98% yield and >99:1 (*Z*):(*E*) selectivity. This system is effective across a broad range of substrates, including aromatic alkynes with various functional groups and alkyl-substituted alkynes. Sensitive groups, such as nitriles, esters, and heterocycles, are well tolerated. Importantly, the system enables purification of alkenes from alkyne impurities without causing alkene isomerization, making it valuable for industrial applications. Mechanistic studies using density functional theory (DFT) reveal that the reaction occurs through a triplet spin state, involving two competing catalytic cycles: a reduction cycle that converts alkynes to (*Z*)-alkenes and an isomerization cycle that

can convert (*Z*)- to (*E*)-alkenes. The manganese hydride species is stabilized by complexation with the alkyne substrate, which plays a crucial role in maintaining the high stereoselectivity. The alkyne coordination step is thermodynamically favored, effectively suppressing the isomerization pathway and ensuring the formation of (*Z*)-alkenes.

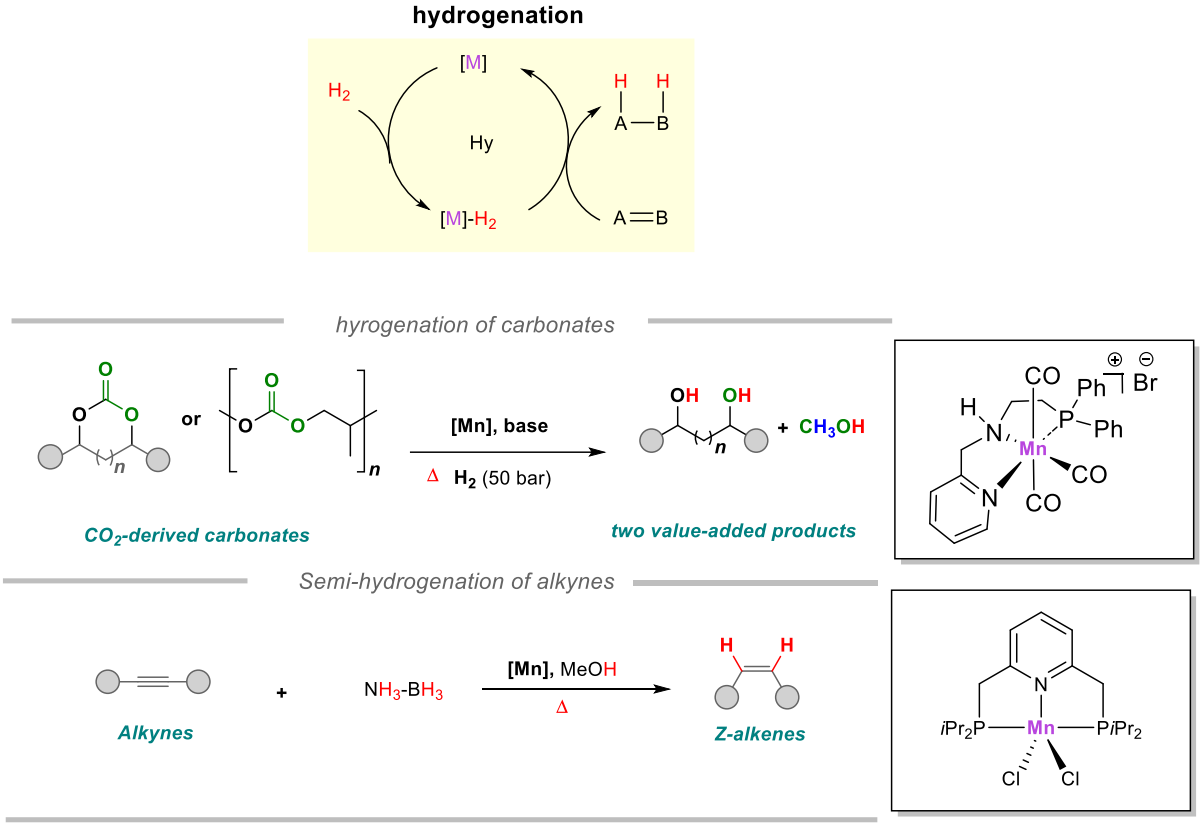

***Scheme 13**. Hydrogenation of carbonates and polycarbonates.*

1.4.3 Manganese catalyzed hydrogen autotransfer

The thesis includes a series of hydrogen borrowing papers catalyzed my pincer manganese complex (scheme 14). The first study describes the development of a manganese-catalyzed methylation process for carbonyl compounds using methanol and its isotopically labeled variants.[56c] This method is highly sustainable, generating water as the sole byproduct under mild conditions. The work highlights the significance of isotope labeling in life sciences, particularly for stable carbon-deuterium bonds that enhance metabolic stability in pharmaceuticals. This work addresses challenges in methanol's high dehydrogenation stability and intermediate side reactions by optimizing manganese-based catalysis for chemoselective and efficient transformations. Using methanol as a C1 building block, the study demonstrates the successful alkylation of diverse ketones, including aromatic, aliphatic, and heteroaromatic derivatives. It also achieves selective isotope labeling, producing deuterated and ^{13}C-labeled products. The process shows versatility, efficiency, and environmental compatibility, offering potential for bioactive molecule synthesis. This approach presents a cost-effective and practical alternative to traditional labeling methods reliant on toxic or expensive reagents.

Similarly, we have also outlined a sustainable method for β-alkylation of secondary alcohols using primary alcohols. The process employs a well-defined manganese PNN pincer complex as the catalyst, along with a catalytic base, to facilitate a double hydrogen autotransfer reaction.[58] This environmentally friendly strategy eliminates the need for harmful alkyl halides and noble metal catalysts, generating water as the sole byproduct. The method involves the dehydrogenation of both alcohols, base-catalyzed aldol condensation to form α,β-unsaturated ketones, and selective hydrogenation to yield β-alkylated alcohols. It offers high chemoselectivity and a wide substrate scope, accommodating both aromatic and aliphatic alcohols. The catalyst performs efficiently under mild conditions, with excellent yields and selectivity.

We have also reported manganese-catalyzed C-alkylation of unactivated esters and amides using alcohols through a hydrogen autotransfer strategy. This approach enables the sustainable transformation of renewable alcohol and carboxylic acid derivative feedstocks into valuable esters and amides while producing water as the only byproduct. The catalytic system, based on a bench-stable manganese complex with a PNN ligand, efficiently alkylates a broad range of substrates, including aliphatic, benzylic, and heterocyclic alcohols, eliminating the need for toxic alkyl halides. Mechanistic studies suggest a monohydride transfer process involving metal-ligand cooperation.[59]

Next paper reports an efficient method for the alkylation of nitriles using a manganese-based catalyst.[60] This approach leverages the hydrogen autotransfer mechanism, where alcohols act as benign alkylating agents, and water is the only byproduct. The system circumvents the use of toxic alkyl halides and eliminates waste, making it highly sustainable. Key features include its broad substrate scope, allowing the alkylation of various nitriles and alcohols, including challenging methylation reactions with methanol as a C1 source. Mechanistic investigations reveal the manganese catalyst's dual role in activating alcohols through dehydrogenation and facilitating nitrile C−H functionalization. The reaction proceeds via in situ generation of aldehyde and alkenyl nitrile intermediates, followed by hydrogenation to yield the desired cyanoalkylated products with excellent chemoselectivity.

The last hydrogen borrowing paper introduces a manganese-catalyzed method for synthesizing chiral amine precursors from racemic alcohols.[61] This redox-neutral reaction employs Ellman’s sulfinamide as an ammonia surrogate and achieves high stereoselectivity through a dynamic kinetic resolution mechanism. The process involves the dehydrogenation of secondary alcohols to ketones, condensation with sulfinamide to form imines, and their stereoselective hydrogenation to yield optically active amines. Mechanistic studies using DFT reveal that stereocontrol arises from the unique dynamic interaction between the catalyst and imine intermediate, where only one catalyst enantiomer participates in the stereoselective step while the other racemizes. This method tolerates a broad range of substrates, including benzylic, aliphatic, and heterocyclic alcohols, and delivers high yields and enantioselectivities. The resulting chiral amines are valuable intermediates for pharmaceuticals such as

carpropamid and rivastigmine. The use of a non-precious manganese catalyst and the operational simplicity underscore its potential for scalable applications in sustainable synthesis of optically pure compounds.

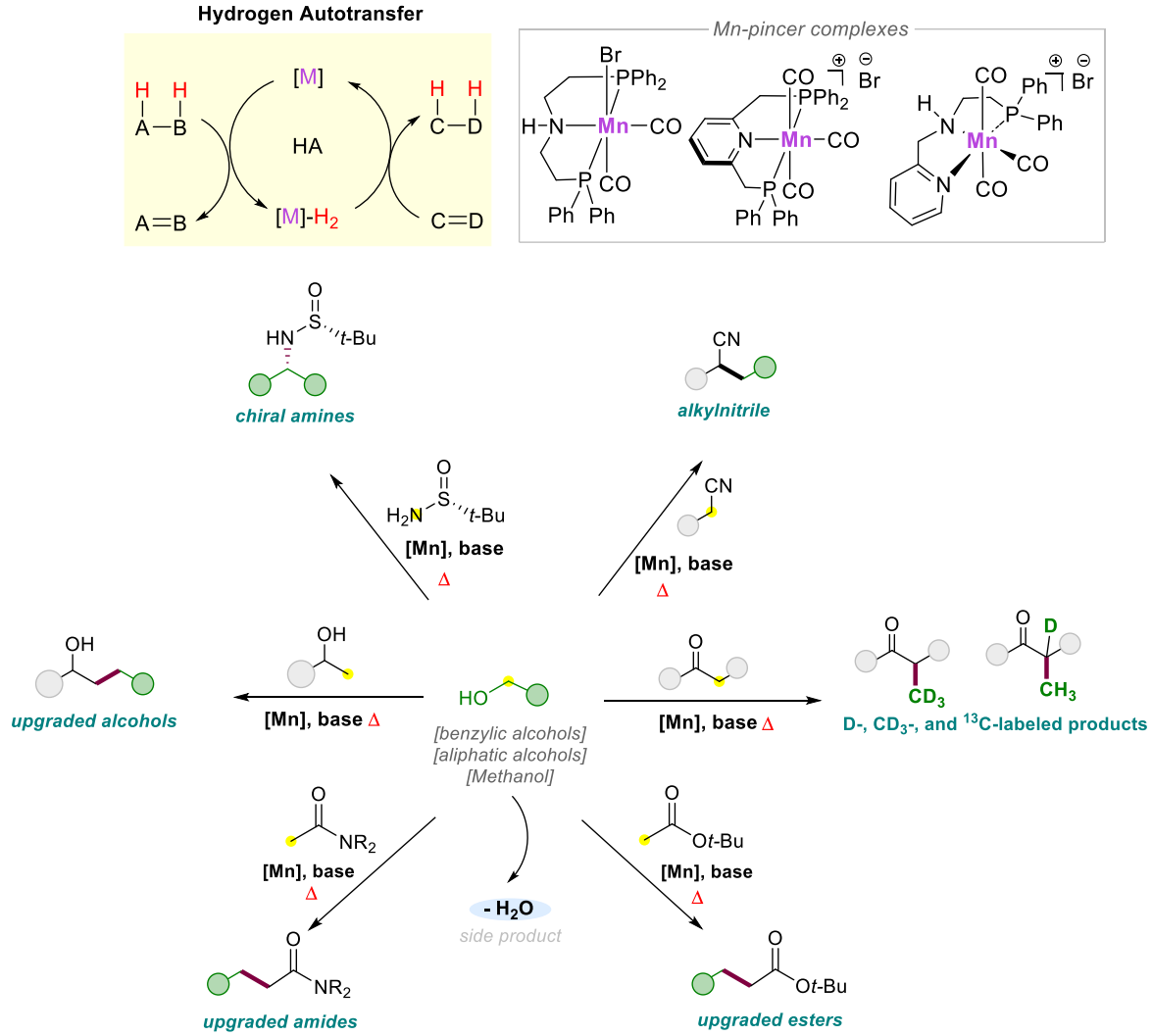

***Scheme 14**. Manganese catalyzed alkylation with alcohols*

1.4.4 Manganese catalyzed acceptorless dehydrogenation

In the first study, a novel method for synthesizing 2,5-unsubstituted pyrroles was developed using a manganese PNP pincer catalyst under solvent-free conditions (Scheme 15).[56b] The reaction couples biomass-derived 1,4-diols with primary amines, producing water and hydrogen gas as the only byproducts, making the approach highly sustainable. This method exhibits excellent chemoselectivity, avoiding side products such as pyrrolidines and imides, and achieves high yields with diverse substrates, including aromatic, aliphatic, and heterocyclic amines. Mechanistically, the manganese catalyst facilitates the dehydrogenation of 1,4-diols into intermediate dialdehydes, which then condense with amines to yield pyrroles. The study also highlights the

scalability and practicality of the method, offering a green synthetic route for pyrroles—key intermediates in pharmaceuticals and materials science.

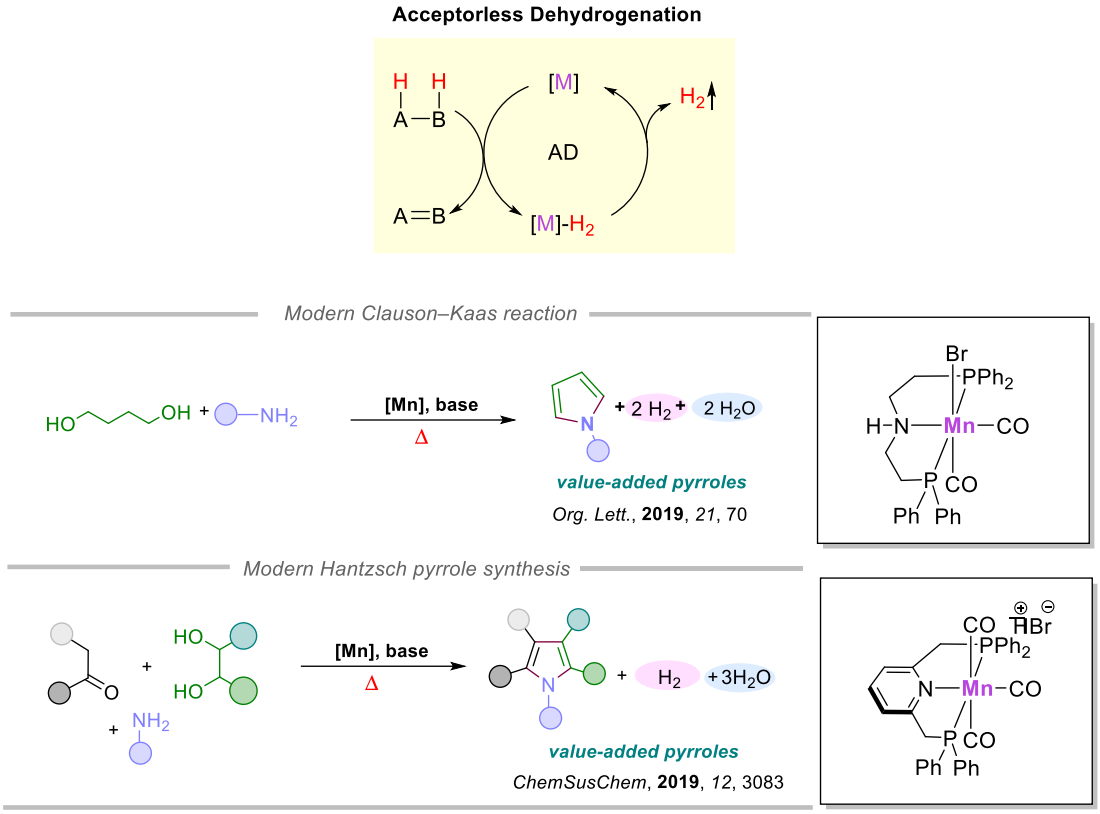

***Scheme 15**. Manganese catalyzed dehydrogenative synthesis of heterocycles*

In the second study, a manganese-based catalytic system was developed for synthesizing pyrroles, employing acceptorless dehydrogenation (AD) and hydrogen autotransfer (HA) mechanisms (Scheme 15).[62] This approach replaces toxic α-haloketones with 1,2-diols and enables pyrrole synthesis in a single pot using ketones, primary amines, and diols, with water and hydrogen gas as the only byproducts. Mechanistic insights reveal that the AD process dehydrogenates diols into aldehydes, which condense with amines and ketones, while the HA step shuttles hydrogen to form imines and pyrroles. The method demonstrates broad substrate scope and scalability, yielding substituted pyrroles, including heteroatom-containing and sterically hindered derivatives. Computational studies confirm the manganese complex's dual role in the AD and HA steps, emphasizing its sustainability and efficiency as a green alternative for pyrrole synthesis. Together, these studies showcase the versatility of manganese PNP pincer complexes in sustainable pyrrole synthesis. Both methods emphasize environmentally friendly practices, exceptional substrate tolerance, and practical scalability, offering valuable contributions to green chemistry and the production of pharmaceutical and material science intermediates.

1.5 References

[1] G. Rothenberg, *Catalysis: concepts and green applications*, John Wiley & Sons, **2017**.

[2] J. Berzelius, *Jahres-Bericht* **1835**, *14*, 237.

[3] B. Cornils, W. A. Herrmann, M. Beller, R. Paciello, *Applied homogeneous catalysis with organometallic compounds: a comprehensive handbook in four volumes, Vol. 4*, John Wiley & Sons, **2017**.

[4] aY. Chauvin, *Angew. Chem. Int. Ed.* **2006**, *45*, 3740-3747; bR. R. Schrock, *Angew. Chem. Int. Ed.* **2006**, *45*, 3748-3759; cR. H. Grubbs, *Angew. Chem. Int. Ed.* **2006**, *45*, 3760-3765.

[5] aE.-i. Negishi, *Angew. Chem. Int. Ed.* **2011**, *50*, 6738-6764; bA. Suzuki, *Angew. Chem. Int. Ed.* **2011**, *50*, 6722-6737.

[6] C. Hagelüken, in *Factor X: Re-source - Designing the Recycling Society* (Eds.: M. Angrick, A. Burger, H. Lehmann), Springer Netherlands, Dordrecht, **2013**, pp. 221-241.

[7] F. H. Arnold, *Angew. Chem. Int. Ed.* **2019**, *58*, 14420-14426.

[8] aB. List, *Science of Synthesis: Asymmetric Organocatalysis Vol. 1: Lewis Base and Acid Catalysts*, Thieme, **2014**; bK. Maruoka, *Science of Synthesis: Asymmetric Organocatalysis Vol. 2: Bronsted Base and Acid Catalysts, and Additional Topics*, Georg Thieme Verlag, **2014**.

[9] R. J. K. Gebbink, M.-E. Moret, *Non-Noble Metal Catalysis: Molecular Approaches and Reactions*, John Wiley & Sons, **2019**.

[10] E. Poupon, B. Nay, *Biomimetic organic synthesis*, John Wiley & Sons, **2011**.

[11] R. Buller, S. Lutz, R. J. Kazlauskas, R. Snajdrova, J. C. Moore, U. T. Bornscheuer, *Science (New York, N.Y.)* **2023**, *382*, eadh8615.

[12] E. L. Bell, W. Finnigan, S. P. France, A. P. Green, M. A. Hayes, L. J. Hepworth, S. L. Lovelock, H. Niikura, S. Osuna, E. Romero, K. S. Ryan, N. J. Turner, S. L. Flitsch, *Nat. Rev. Methods Primers* **2021**, *1*, 46.

[13] L. Li, X. Yang, *Oxid. Med. Cell. Longev.* **2018**, *2018*, 7580707.

[14] *Iron-Containing Enzymes: Versatile Catalysts of Hydroxylation Reactions in Nature*, The Royal Society of Chemistry, **2011**.

[15] A. Messerschmidt, in *Comprehensive Natural Products II* (Eds.: H.-W. Liu, L. Mander), Elsevier, Oxford, **2010**, pp. 489-545.

[16] K. A. McCall, C.-c. Huang, C. A. Fierke, *J. Nutr.* **2000**, *130*, 1437S-1446S.

[17] aP. A. Frey, in *Comprehensive Natural Products II* (Eds.: H.-W. Liu, L. Mander), Elsevier, Oxford, **2010**, pp. 501-546; bK. Halczuk, J. Kaźmierczak-Barańska, B. T. Karwowski, A. Karmańska, M. Cieślak, *Nutrients* **2023**, *15*.

[18] J. A. Cowan, *Biometals* **2002**, *15*, 225-235.

[19] aH. Schulman, in *Integrative Aspects of Calcium Signalling* (Eds.: A. Verkhratsky, E. C. Toescu), Springer US, Boston, MA, **1998**, pp. 35-57; bF. C. Stevens, *Can. J. Biochem. Cell Biol.* **1983**, *61*, 906-910.

[20] M. L. Kirk, R. Hille, *Molecules* **2022**, *27*, 4802.

[21] D. Tripathi, V. Mani, R. P. Pal, *Biol. Trace Elem. Res* **2018**, *186*, 52-67.

[22] A. Kletzin, M. W. W. Adams, *FEMS Microbiology Reviews* **1996**, *18*, 5-63.
[23] aG. J. Colpas, B. J. Hamstra, J. W. Kampf, V. L. Pecoraro, *J. Am. Chem. Soc.* **1996**, *118*, 3469-3478; bF. De Rienzo, R. R. Gabdoulline, M. C. Menziani, R. C. Wade, *Protein Sci.* **2000**, *9*, 1439-1454; cC. Dong, J. Yang, S. Leimkühler, M. L. Kirk, *Inorg. Chem.* **2014**, *53*, 7077-7079; dS. A. Pérez-Henarejos, L. A. Alcaraz, A. Donaire, *Arch. Biochem. Biophys.* **2015**, *584*, 134-148; eE. I. Solomon, R. G. Hadt, *Coord. Chem. Rev.* **2011**, *255*, 774-789; fE. I. Solomon, R. K. Szilagyi, S. DeBeer George, L. Basumallick, *Chem. Rev.* **2004**, *104*, 419-458.
[24] T. Inoue, H. Sugawara, S. Hamanaka, H. Tsukui, E. Suzuki, T. Kohzuma, Y. Kai, *Biochemistry* **1999**, *38*, 6063-6069.
[25] C. Hammann, A. Messerschmidt, R. Huber, H. Nar, G. Gilardi, G. W. Canters, *J. Mol. Biol.* **1996**, *255*, 362-366.
[26] L. Loschi, S. J. Brokx, T. L. Hills, G. Zhang, M. G. Bertero, A. L. Lovering, J. H. Weiner, N. C. J. Strynadka, *J. Biol. Chem.* **2004**, *279*, 50391-50400.
[27] aW. Buckel, B. T. Golding, in *Wiley Encyclopedia of Chemical Biology*, pp. 1-9; bK. L. Brown, *Chem. Rev.* **2005**, *105*, 2075-2150; cM. Giedyk, K. Goliszewska, D. Gryko, *Chem. Soc. Rev.* **2015**, *44*, 3391-3404; dK. Gruber, B. Puffer, B. Kräutler, *Chem. Soc. Rev.* **2011**, *40*, 4346-4363; eA. J. Moser, B. E. Funk, J. G. West, *ChemCatChem*, *n/a*, e202301231; fG. N. Schrauzer, *Acc. Chem. Res.* **1968**, *1*, 97-103; gK. Tahara, L. Pan, T. Ono, Y. Hisaeda, *Beilstein J. Org. Chem.* **2018**, *14*, 2553-2567.
[28] aR. G. Matthews, *Acc. Chem. Res.* **2001**, *34*, 681-689; bH. Mosimann, B. Kräutler, *Angew. Chem. Int. Ed.* **2000**, *39*, 393-395.
[29] F. Juliá, *ChemCatChem* **2022**, *14*, e202200916.
[30] A. Taylor, D. J. Heyes, N. S. Scrutton, *Curr. Opin. Struct. Biol.* **2022**, *77*, 102491.
[31] J. Barber, *Chem. Soc. Rev.* **2009**, *38*, 185-196.
[32] A. H. Proppe, Y. C. Li, A. Aspuru-Guzik, C. P. Berlinguette, C. J. Chang, R. Cogdell, A. G. Doyle, J. Flick, N. M. Gabor, R. van Grondelle, S. Hammes-Schiffer, S. A. Jaffer, S. O. Kelley, M. Leclerc, K. Leo, T. E. Mallouk, P. Narang, G. S. Schlau-Cohen, G. D. Scholes, A. Vojvodic, V. W.-W. Yam, J. Y. Yang, E. H. Sargent, *Nat. Rev. Mater.* **2020**, *5*, 828-846.
[33] aF. Strieth-Kalthoff, F. Glorius, *Chem* **2020**, *6*, 1888-1903; bL. Capaldo, D. Ravelli, M. Fagnoni, *Chem. Rev.* **2022**, *122*, 1875-1924; cA. Y. Chan, I. B. Perry, N. B. Bissonnette, B. F. Buksh, G. A. Edwards, L. I. Frye, O. L. Garry, M. N. Lavagnino, B. X. Li, Y. Liang, E. Mao, A. Millet, J. V. Oakley, N. L. Reed, H. A. Sakai, C. P. Seath, D. W. C. MacMillan, *Chem. Rev.* **2022**, *122*, 1485-1542; dS. Dutta, J. E. Erchinger, F. Strieth-Kalthoff, R. Kleinmans, F. Glorius, *Chem. Soc. Rev.* **2024**; eF. Strieth-Kalthoff, M. J. James, M. Teders, L. Pitzer, F. Glorius, *Chem. Soc. Rev.* **2018**, *47*, 7190-7202.
[34] aW. Su, P. Xu, T. Ritter, *Angew. Chem. Int. Ed.* **2021**, *60*, 24012-24017; bP. Xu, P. López-Rojas, T. Ritter, *J. Am. Chem. Soc.* **2021**, *143*, 5349-5354; cT. Q. Chen, P. S. Pedersen, N. W. Dow, R. Fayad, C. E. Hauke, M. C. Rosko, E. O. Danilov, D. C. Blakemore, A.-M. Dechert-Schmitt, T. Knauber, *J. Am. Chem. Soc.* **2022**, *144*, 8296-8305; dN. W. Dow, P. S. Pedersen, T. Q. Chen, D. C. Blakemore, A.-

M. Dechert-Schmitt, T. Knauber, D. W. MacMillan, *J. Am. Chem. Soc.* **2022**, *144*, 6163-6172.
[35] P. Dam, K. Zuo, L. M. Azofra, O. El-Sepelgy, *Angew. Chem. Int. Ed.* **2024**, *63*, e202405775.
[36] aH. Bhandal, G. Pattenden, J. J. Russell, *Tetrahedron Lett.* **1986**, *27*, 2299-2302; bB. P. Branchaud, M. S. Meier, Y. Choi, *Tetrahedron Lett.* **1988**, *29*, 167-170; cA. Ghosez, T. Göbel, B. Giese, *Chemische Berichte* **1988**, *121*, 1807-1811; dB. Giese, J. Hartung, J. He, O. Hüter, A. Koch, *Angew. Chem. Int. Ed.* **1989**, *28*, 325-327.
[37] M. E. Weiss, L. M. Kreis, A. Lauber, E. M. Carreira, *Angew. Chem. Int. Ed.* **2011**, *50*, 11125-11128.
[38] aG. Zhang, C. Liu, H. Yi, Q. Meng, C. Bian, H. Chen, J.-X. Jian, L.-Z. Wu, A. Lei, *J. Am. Chem. Soc.* **2015**, *137*, 9273-9280; bJ. G. West, D. Huang, E. J. Sorensen, *Nat. Commun.* **2015**, *6*, 10093.
[39] C. Wang, L. M. Azofra, P. Dam, M. Sebek, N. Steinfeldt, J. Rabeah, O. El-Sepelgy, *ACS Catal.* **2022**, *12*, 8868-8876.
[40] K. Zuo, J. Zhu, F. Akhtar, P. Dam, L. M. Azofra, O. El-Sepelgy, *Org. Lett.* **2025**, *27*, 30-35.
[41] aP. Chuentragool, M. Parasram, Y. Shi, V. Gevorgyan, *J. Am. Chem. Soc.* **2018**, *140*, 2465-2468; bM. Parasram, P. Chuentragool, Y. Wang, Y. Shi, V. Gevorgyan, *J. Am. Chem. Soc.* **2017**, *139*, 14857-14860.
[42] C. Wang, P. Dam, M. Elghobashy, A. Brückner, J. Rabeah, L. M. Azofra, O. El-Sepelgy, *ACS Catal.* **2023**, *13*, 14205-14212.
[43] C. Wang, L. M. Azofra, P. Dam, E. J. Espinoza-Suarez, H. T. Do, J. Rabeah, A. Brückner, O. El-Sepelgy, *Chem. Commun.* **2023**, *59*, 3862-3865.
[44] M. Parasram, V. O. Iaroshenko, V. Gevorgyan, *J. Am. Chem. Soc.* **2014**, *136*, 17926-17929.
[45] M. D. Wodrich, X. Hu, *Nat. Rev. Chem.* **2017**, *2*, 0099.
[46] aG. Zampella, C. Greco, P. Fantucci, L. De Gioia, *Inorg. Chem.* **2006**, *45*, 4109-4118; bT. B. Rauchfuss, *Acc. Chem. Res.* **2015**, *48*, 2107-2116.
[47] aR. M. Evans, E. J. Brooke, S. A. M. Wehlin, E. Nomerotskaia, F. Sargent, S. B. Carr, S. E. V. Phillips, F. A. Armstrong, *Nat. Chem. Bio.* **2016**, *12*, 46-50; bD. Schilter, J. M. Camara, M. T. Huynh, S. Hammes-Schiffer, T. B. Rauchfuss, *Chem. Rev.* **2016**, *116*, 8693-8749.
[48] aT. Irrgang, R. Kempe, *Chem. Rev.* **2019**, *119*, 2524-2549; bA. Corma, J. Navas, M. J. Sabater, *Chem. Rev.* **2018**, *118*, 1410-1459.
[49] C. P. Casey, H. Guan, *J. Am. Chem. Soc.* **2007**, *129*, 5816-5817.
[50] aS. Fleischer, S. Zhou, K. Junge, M. Beller, *Angew. Chem. Int. Ed.* **2013**, *52*, 5120-5124; bA. Pagnoux-Ozherelyeva, N. Pannetier, M. D. Mbaye, S. Gaillard, J.-L. Renaud, *Angew. Chem. Int. Ed.* **2012**, *51*, 4976-4980; cA. Quintard, J. Rodriguez, *Angew. Chem. Int. Ed.* **2014**, *53*, 4044-4055.
[51] aT. Zell, D. Milstein, *Acc. Chem. Res.* **2015**, *48*, 1979-1994; bE. Alberico, P. Sponholz, C. Cordes, M. Nielsen, H.-J. Drexler, W. Baumann, H. Junge, M.

Beller, *Angew. Chem. Int. Ed.* **2013**, *52*, 14162-14166; cR. Langer, G. Leitus, Y. Ben-David, D. Milstein, *Angew. Chem. Int. Ed.* **2011**, *50*, 2120-2124.

[52] G. Zhang, K. V. Vasudevan, B. L. Scott, S. K. Hanson, *J. Am. Chem. Soc.* **2013**, *135*, 8668-8681.

[53] S. Rösler, J. Obenauf, R. Kempe, *J. Am. Chem. Soc.* **2015**, *137*, 7998-8001.

[54] aW. Liu, B. Sahoo, K. Junge, M. Beller, *Acc. Chem. Res.* **2018**, *51*, 1858-1869; bT. J. Korstanje, J. Ivar van der Vlugt, C. J. Elsevier, B. de Bruin, *Science (New York, N.Y.)* **2015**, *350*, 298-302.

[55] aA. Mukherjee, A. Nerush, G. Leitus, L. J. W. Shimon, Y. Ben David, N. A. Espinosa Jalapa, D. Milstein, *J. Am. Chem. Soc.* **2016**, *138*, 4298-4301; bS. Elangovan, C. Topf, S. Fischer, H. Jiao, A. Spannenberg, W. Baumann, R. Ludwig, K. Junge, M. Beller, *Journal of the American Chemical Society* **2016**, *138*, 8809-8814.

[56] aV. Zubar, Y. Lebedev, L. M. Azofra, L. Cavallo, O. El-Sepelgy, M. Rueping, *Angew. Chem. Int. Ed.* **2018**, *57*, 13439-13443; bJ. C. Borghs, Y. Lebedev, M. Rueping, O. El-Sepelgy, *Org. Lett.* **2019**, *21*, 70-74; cJ. Sklyaruk, J. C. Borghs, O. El-Sepelgy, M. Rueping, *Angew. Chem. Int. Ed.* **2019**, *58*, 775-779.

[57] A. Brzozowska, L. M. Azofra, V. Zubar, I. Atodiresei, L. Cavallo, M. Rueping, O. El-Sepelgy, *ACS Catal.* **2018**, *8*, 4103-4109.

[58] O. El-Sepelgy, E. Matador, A. Brzozowska, M. Rueping, *Chemsuschem* **2019**, *12*, 3099.

[59] Y. K. Jang, T. Krückel, M. Rueping, O. El-Sepelgy, *Org. Lett.* **2018**, 7779-7783.

[60] J. C. Borghs, M. A. Tran, J. Sklyaruk, M. Rueping, O. El-Sepelgy, *J. Org. Chem.* **2019**, *84*, 7927-7935.

[61] L. M. Azofra, M. A. Tran, V. Zubar, L. Cavallo, M. Rueping, O. El-Sepelgy, *Chem. Commun.* **2020**, *56*, 9094-9097.

[62] J. C. Borghs, L. M. Azofra, T. Biberger, O. Linnenberg, L. Cavallo, M. Rueping, O. El-Sepelgy, *Chemsuschem* **2019**, *12*, 3083.

1.6 Published Reviews

Review 1: Dam, P.; Zuo, K.; Azofra, L. M.; El-Sepelgy, O.* Biomimetic Photoexcited Cobaloxime Catalysis in Organic Synthesis. *Angew. Chem. Int. Ed.* **2024**, *63*, e202405775.

Review 2: Wang, C.; El-Sepelgy, O.* Reductive depolymerization of plastics catalyzed with transition metal complexes. *Curr. Opin. Green Sustain. Chem* **2021**, *32*, 100547.

Review 3: Elghobashy, M.; El-Sepelgy, O.* Catalytic Methylation Using Methanol as C1 Source. In *Dehydrogenation Reactions with 3d Metals*, Sundararaju, B. Ed.; Springer Nature Switzerland, **2024**; pp 173-197.

Authors Contributions

O.E.-S. conceptualized the topics and structure of the reviews. K.Z., P.D., M.E., C.W., and L.A.M. prepared 90% of the schemes and figures and contributed approximately 20% of the text. O.E.-S. wrote 80% of the text, reviewed, and edited the manuscripts before submission.

Review 1:

Cobaloxime catalysis in organic Synthesis

Dam, P.; Zuo, K.; Azofra, L. M.; El-Sepelgy, O.*

Angew. Chem. Int. Ed. **2024**, *63*, e202405775.

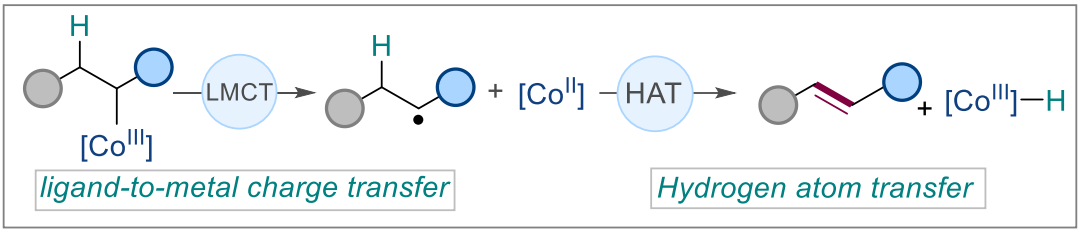

How to cite: *Angew. Chem. Int. Ed.* **2024**, *63*, e202405775
doi.org/10.1002/anie.202405775

Photoredox Catalysis

Biomimetic Photoexcited Cobaloxime Catalysis in Organic Synthesis

*Phong Dam, Kaiming Zuo, Luis Miguel Azofra, and Osama El-Sepelgy**

Abstract: Drawing inspiration from nature has long been a cornerstone of chemical innovation, with natural systems offering a wealth of untapped potential for discovery. In this minireview, we delve into the burgeoning field of cobaloxime catalysis in organic synthesis, which mimics the catalytic activity of the natural organometallic alkylcobalamine enzymes. Our focus lies on elucidating the latest advancements in this area, as well as delineating the primary mechanistic pathways at play. By describing, and comparing these mechanisms, we provide a comprehensive overview of the current state-of-the-art, while also shedding light on the key unresolved challenges that await further exploration.

1. Introduction

Biomimetic catalysis, which emulates the highly efficient biological transformations, offers a potent approach for the deliberate design of artificial small molecule catalysts.[1] Methylcobalamin (MeCbl or MeB_{12}) and Adenosylcobalamin (AdoCbl), two forms of Vitamin B_{12}, serve as rare examples of natural organometallic compounds that contains metal-alkyl bonds (Scheme 1).[2] The formation and cleavage of the Co–C bond within these molecules is pivotal in their enzymatic functions.[3] For example, methylcobalamin acts as a reversible free radical carrier that effectively stabilizes highly reactive methyl radicals via the formation of weak carbon–cobalt bonds.[4] These weak Co–C bond (bond dissociation energy (BDE) ≈ 14–42 kcal/mol) can undergo facile cleavage via thermolysis or photolysis.[5]

Simple cobaloxime complexes have been initially synthesized to mimic the structure of natural alkylcobalamines and to study the mechanism of its enzymatic function.[6] These octahedral cobalt(III) complexes are featuring dioximate ligands interconnected via hydrogen bonding or BF_2 bridges. Typically, the two axial ligands are nitrogen-containing ligands like pyridine and halogens (Scheme 1). Cobaloximes are well-known as proton reduction catalysis for water splitting processes.[7] However, the extensive use of these complexes in organic synthesis has only gained attention recently. Several excellent reviews have already sparked excitement; however, they predominantly concentrate on the merger of photoredox and cobalt catalysis, rather than delving deeply into the concepts of cobaloxime catalysis.[8] This minireview comprehensively summarizes, critically discusses, and reclassifies the chemistry of cobaloxime catalysis in organic synthesis.

The seminal stoichiometric reactivity of cobaloxime in organic synthesis was reported in the 1980s by the groups of Tada, Pattenden, Branchaud, and Giese.[9] Additionally, several groups have reported the catalytic turnover of cobaloxime under reductive conditions, such as electrochemistry or stoichiometric amounts of reductants like Zn, sodium borohydride, or Grignard reagents.[10] An important milestone in the cobaloxime catalysis is from the group of Carriera in 2011. The authors have outlined the possibility of cobaloxime turnover using simple organic base base.[11] Another milestone is the merger of cobaloxime catalysis with photoredox catalysis in 2015.[12] To aid comprehension for readers unacquainted with this chemistry, we furnished a concise summary in this section elucidating the principal catalytic concepts of cobaloxime complexes.

The catalytic activity of cobaloxime catalysis can be categorized into two general types: inner-sphere and outer-sphere reactivities, which may occur in either the excited or ground state (Scheme 1). Inner-sphere reactivity or ligand-to-metal charge transfer (LMCT)[13] involves the direct association of the catalyst and the reactant, resembling enzymatic processes closely. In this scenario, [Co^{III}]-alkyl complexes can be formed through S_N2-type reactions of highly nucleophilic [Co^{I}] species with alkyl electrophiles (polar path), or by capturing organic radicals with persistent [Co^{II}] radicals (radical path). The Co–C bond within this complex can be reversibly homolyzed into a radical pair under thermal conditions or irradiation. This radical pair could undergo radical-type β-hydrogen elimination, resulting in the formation of [Co^{III}]–H via hydrogen atom transfer (HAT) and an olefin or aromatic compound. Alternatively, the organic radical may escape from the radical pair and engage in free radical transformations, primarily radical addition to olefin or arene, leading to the formation of a new radical intermediate. This intermediate could then be trapped again by the metalloradical [Co^{II}] species, yielding [Co^{III}]–H and a new olefin or functionalized aromatic compound.

On the other hand, outer-sphere reactivity is also proposed in cobaloxime catalysis (Scheme 1). For instance, ground-state [Co^{II}] metalloradicals could induce outer-sphere single electron transfer (SET) oxidation of organic radicals, resulting in the formation of carbocations and [Co^{I}] species. These intermediates could further undergo a proton transfer (PT) process to produce [Co^{III}]–H and unsaturated compounds. Given the low reductive potential of [Co^{II}] species ($E_{p/2}(Co^{II}/Co^{I}) = -1.13$ V *vs* SCE), this approach is likely suitable for radical intermediates that can be readily oxidized, such as benzylic and dibenzylic radicals, to form stable carbocations ($E_{ox} < 0$ V vs SCE).[14] Another outer-sphere reactivity of cobalt complexes involves photoinduced SET (photoredox activity). In this respect, excited-state [Co^{III}] complexes function as photoredox catalyst for the

[*] P. Dam, K. Zuo, Dr. O. El-Sepelgy
Leibniz Institute for Catalysis e.V.
Albert-Einstein-Str. 29a, 18059 Rostock, Germany
E-mail: Osama.Elsepelgy@Catalysis.de
Dr. L. M. Azofra
Instituto de Estudios Ambientales y Recursos Naturales (i-UNAT)
Universidad de Las Palmas de Gran Canaria (ULPGC),
Campus de Tafira, 35017 Las Palmas de Gran Canaria, Spain

oxidation of H-phosphines, leading to the formation of P-radical and [Co^{II}] species.

The turnover of [Co^{III}]–H can be facilitated by a one-step polar pathway through simple deprotonation with an organic base such as iPr_2NEt to produce the Co(I) species (Scheme 1). Alternatively, two-steps radical pathway can occur, [Co^{III}]–H can react with another proton to release H_2 and form [Co^{III}] species, a process that could be accelerated in the presence of proton shuttle such as pyridine or protic acid such as acetic acid. The [Co^{III}] species could also form upon the reaction of the [Co^{III}]–H with an imine salt intermediate. The electron-deficient [Co^{III}] species could be readily reduced to [Co^{II}] species directly by a substrate such as H-phosphine or by a co-catalyst ($E_{p/2}(Co^{III}/Co^{II}) = -0.68$ V *vs* SCE).

2. Alkyl Heck-Type Reaction

Palladium catalyzed Mizoroki-Heck reaction represents one of the most versatile synthetic methods to form C–C bonds. However, the reaction generally cannot be performed on alkyl halide substrates due to the slow oxidative addition and the facile competing β-hydrogen elimination.[15]

2.1. Polar Alkyl Heck-Type Reaction

In 2011, Carreira and co-workers reported the use of the simple **Co-1** complex together with under visible light conditions for the intramolecular *exo*-selective Heck reaction of primary alkyl iodides (Scheme 2).[11] The key to success is the formal reduction of [Co^{III}]–H to an anionic Co(I) species via deprotonation using a simple organic base (iPr_2NEt). The authors have proposed the formation of the alkylcobalt intermediates via nucleophilic substitution with the catalytically active Co(I) species. It is worth noting that, secondary alkyl iodide (only one example) remained unreactive under these conditions with **Co-1** catalyst but showed reactivity when using stannyl cobaloxime complex (**Co-2**). In 2023, El-Sepelgy group have outlined that the bifunctional Co–Sn complex (**Co-2**) operates via a different radical pathway, elucidating the disparate reactivity of **Co-1** and **Co-2** catalysts in the seminal work of Carreira.[16] Recently, El-Sepelgy and co-workers have reported intramolecular *endo*-selective Heck reaction of iodo- and bromomethylsilyl ethers of phenols and alkenols using the **Co-1** catalyst (Scheme 2).[17] The method could be used for the formal hydroxymethylation of allylic alcohols and *o*-hydroxystyrenes, eliminating the need for the use of palladium salts and expensive phosphine ligand.[18] In 2016, the Morandi group demonstrated the use of epoxides and aziridines as electrophiles and intramolecular coupling with alkenes catalyzed by **Co-1**.[19]

The cobalt-catalyzed polar alkyl Heck-type reaction starts with the visible light homolysis of the **Co-1** complex to produce [Co^{III}]–H and propene. After deprotonation with a base such as iPr_2NEt or methoxide, the super nucleophile [Co^{I}] species is in situ generated. A key mechanistic step involves the S_N2-type reaction between the [Co^{I}] species and the primary alkyl electrophiles (**2.1**) to give the corresponding alkyl-[Co^{III}] intermediate (**2.2**). This Co–C bond is cleaved under irradiation to produce [Co^{II}] species and an alkyl radical intermediate (**2.3**). DFT calculated location of a

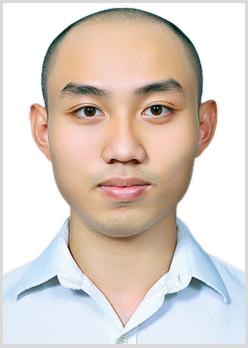

Phong Dam earned his B.Sc. from Hanoi University of Science and Technology (HUST). Afterwards, he pursued M.Sc. studies under the guidance of Prof. Thanh Huyen Pham at HUST, Hanoi, and Prof. Angelika Brückner at LIKAT Rostock. He is currently pursuing his doctoral studies in the group of Dr. Osama El-Sepelgy at LIKAT Rostock. His research interests revolve around photoexcited cobalt catalysis and operando spectroscopic mechanistic studies.

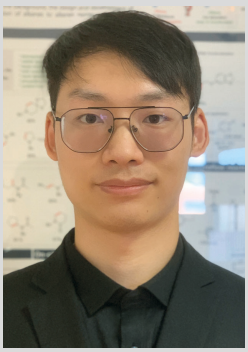

Kaiming Zuo was born in Sichuan, China. He studied chemical engeneering at Hainan University (master thesis in material science with Prof. Yanan Gao). Currently he is a Ph.D student at the Leibniz Institute for Catalysis (LIKAT Rostock) under the guidance of Dr. Osama El-Sepelgy. His research focouses on photoexcied base-metal catalyzed C-H functionalization transformations.

Luis Miguel Azofra received his M.Sc. and Ph.D. degrees from Universidad Autónoma de Madrid. Following this, he pursued postdoctoral studies at Monash University and King Abdullah University of Science and Technology. Later, he moved to Universidad de Las Palmas de Gran Canaria. Since 2023, he has served as a Ramón y Cajal research leader and lecturer at the same institution. His primary research focus revolves around utilizing quantum mechanics to model catalytic processes.

Osama El-Sepelgy completed his Ph.D. studies with Prof. Jacek Mlynarski at Jagiellonian University in Krakow and Prof. Christoph Schneider at the University of Leipzig in 2014. Then, he pursued two years of postdoctoral studies at RWTH Aachen University with Prof. Magnus Rueping. Subsequently, he led a sub-group at the same institution. In July 2021, Osama started his independent career at the Leibniz Institute of Catalysis (LIKAT Rostock). His group focuses on dicovery of new sustainable catalytic methods employing base metal catalysis and harnessing visible light.

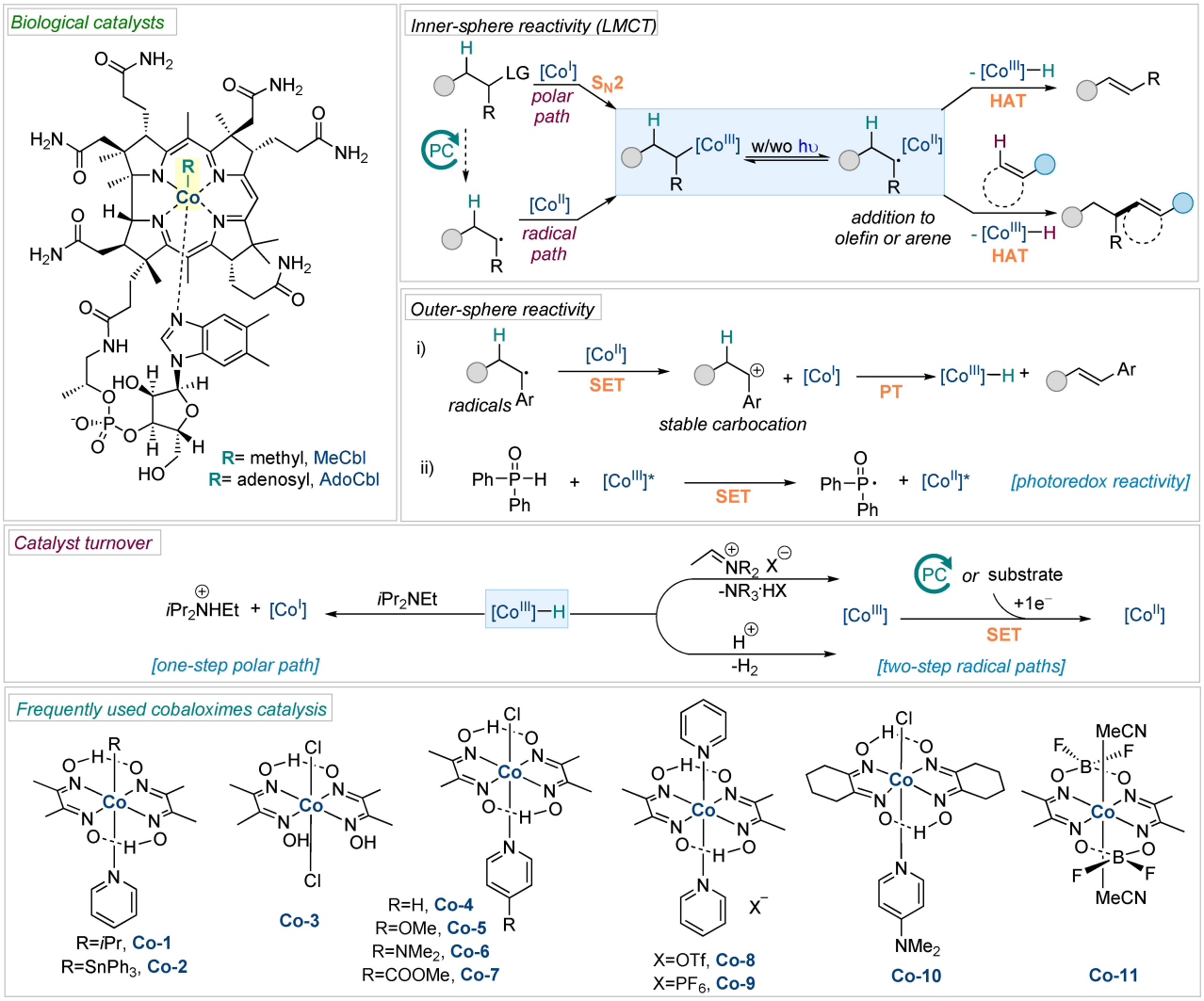

Scheme 1. Conceptualization of cobaloxime catalysis: from biological catalysis to small-molecule catalytic concepts.

transition state (TS) confirms the carbon–carbon coupling in the radical substrate via an intramolecular SET (Scheme 2, green). Intramolecular *endo*- or *exo*-radical addition furnishes a radical intermediate (**2.4**), which can recombine with [Co^{II}] to form another alkyl-[Co^{III}] intermediate (**2.5**). The cobalt species (**2.5**) under visible light irradiation results in the formation of the desired cyclic alkene (**2.6**) and a [Co^{III}]-hydride complex (Scheme 2, purple).

2.2. Radical Alkyl-Heck Reaction

The previously mentioned polar-based Heck reactions are mostly limited to intramolecular transformations of primary alkyl iodides. To overcome these limitations, efforts were directed towards the generation of alkyl radicals under visible light conditions using a co-catalyst followed by addition of the radicals to olefins, while a suitable cobaloxime enables the regeneration of the double bond and the formation of alkene products (Scheme 3). In this regards, Wu and co-workers have first reported decarboxylative alkyl Heck reaction using a dual photoredox/cobaloxime dual catalysis.[20] Carboxylic acids were used as precursors of a broad range of primary, secondary and tertiary alkyl radicals under oxidative photoredox conditions. Two years later, Leonori and co-workers disclosed alkyl Heck reaction of alkyl iodides and bromides.[21] The radical generation was enabled by halogen atom transfer (XAT) strategy. This XAT approach is proposed to be achieved via aminoalkyl radical reagent, which could be in situ generated using Et_3N and photocatalyst (4CzIPN). More recently, Melchiorre and co-workers outlined the merger of the alkyl radical generation using electron donating acceptor complex (EDA) photoactivation with cobalt catalyzed dehydrogenation.[22] The authors have used electron-rich radical precursors bearing redox auxiliaries such as 1,4-dihydropyridines, silicates and trifluoroborates together with tetrachlorophthalimides as EDA acceptor catalyst.

In all cases, the subsequent addition of the alkyl radical to olefin followed by the β-hydrogen eliminations using

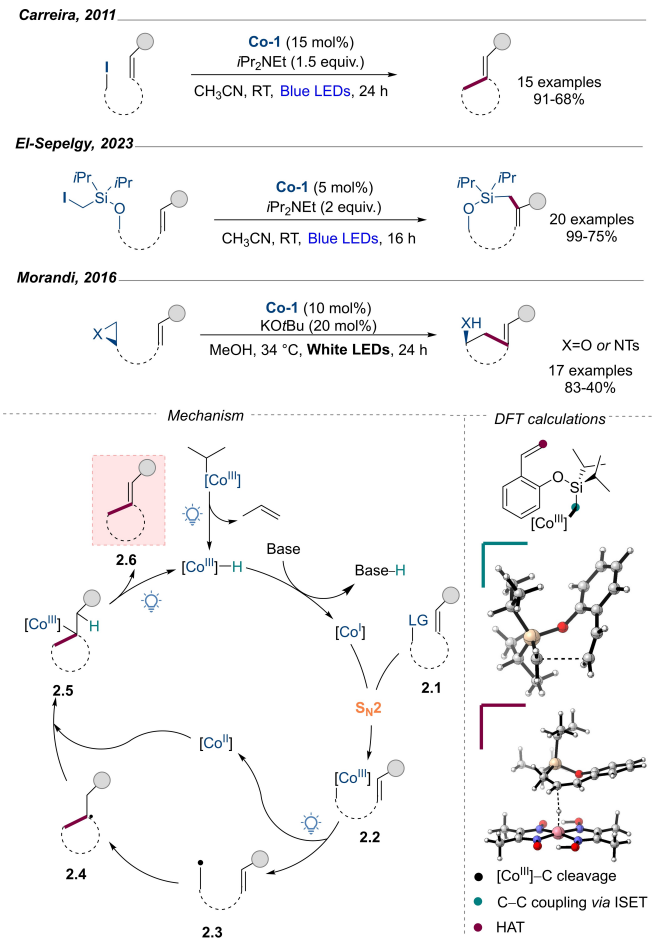

Scheme 2. Cobaloxime catalysed polar alkyl-Heck reaction.

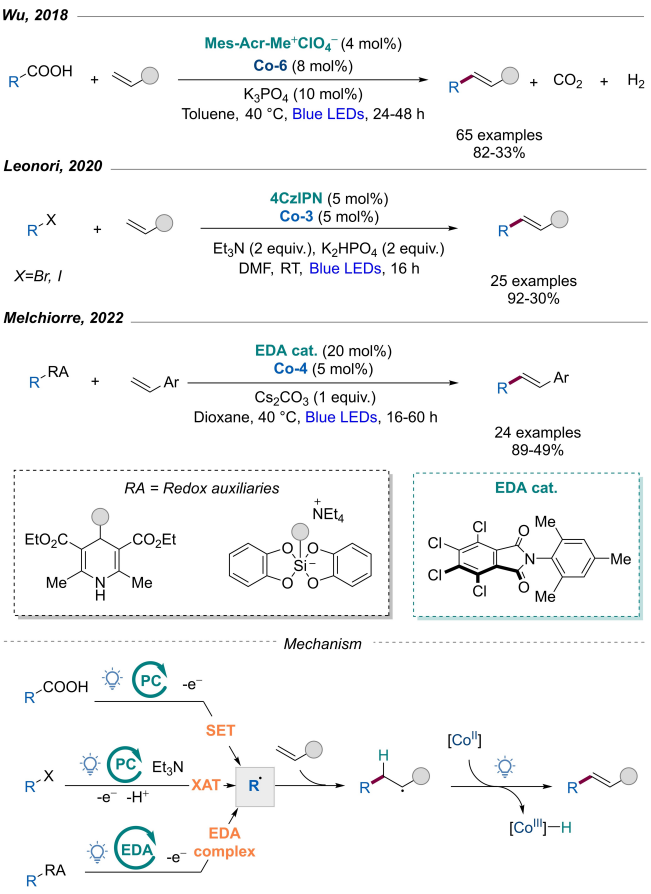

Scheme 3. Radical-type alkyl Heck reaction.

cobaloxime catalysis leads to the formation of the desired Heck product and [Co^{III}]–H intermediate. To enable the catalytic turnover, [Co^{III}]–H is initially converted to [Co^{III}] by reaction with another proton or iminium salt intermediate. Afterwards the electron poor [Co^{III}] undergoes SET reduction, leading to the regeneration of [Co^{II}] species and the photocatalyst or the EDA catalyst.

3. Desaturation of Aliphatic Compounds

The transformation of alkanes into alkenes stands as a fundamental pursuit in synthetic chemistry, offering pathways to valuable unsaturated compounds crucial in various industrial applications.[23] In this section, we summarize the recent achievements on the use of cobaloxime catalysis for the oxidant free desaturation of aliphatic compounds under visible light conditions at room temperature.

3.1. Nondirected Desaturation

In 2015, Sorensen and colleagues reported a pioneering example of radical and oxidant free desaturation of non-functionalized alkanes such as cyclooctane to the cyclooctene in low yield.[12b] This approach utilized tetrabutylammonium decatungstate catalyst (TBADT) as HAT catalyst for a hard hydrogen atom abstraction to generate a carbon-centered radical, followed by cobaloxime catalyzed desaturation under near UV light irradiation.[24] More recently, Huang and Xu further enhanced this nondirected desaturation of functionalized alkanes by using a dual 2-chloroanthraquinone photocatalyst and in situ generated cobaloxime catalysis (Scheme 4).[25]

The reaction selectivity is governed by the strength and electronic properties of sp^3 C–H bonds. For example, the catalytic system shows a very good reactivity and selectivity for the conversion of alkyl (hetero)arenes such as ethylbenzene to the corresponding styrenes. The detailed reaction mechanism is described in Scheme 4. The reaction was initiated though a HAT process with excited anthraquinone, resulting in ketyl radical (**4.2**) and alkyl radical (**4.1**). This intermediate (**4.1**) can be captured by [Co^{II}] to generate [Co^{III}]-alkyl species (**4.3**), which under irradiation leads to the formation of the desired olefin and [Co^{III}]–H species. The SET and PT from the ketyl radical (**4.2**) to [Co^{III}]–H result in the regeneration of the [Co^{II}] species and the HAT photocatalyst (Scheme 4).

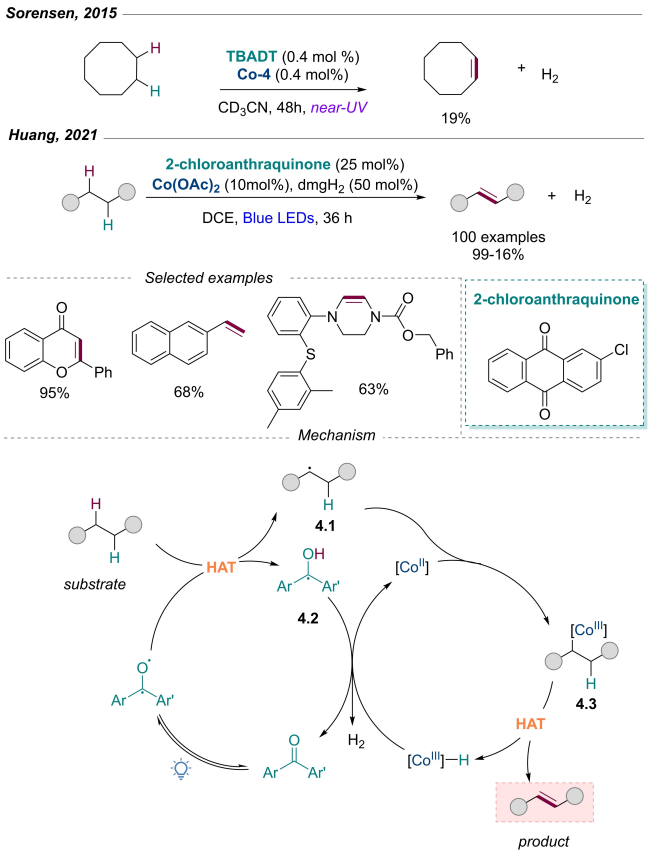

Scheme 4. Synthesis of olefins via nondirected desaturation of alkanes.

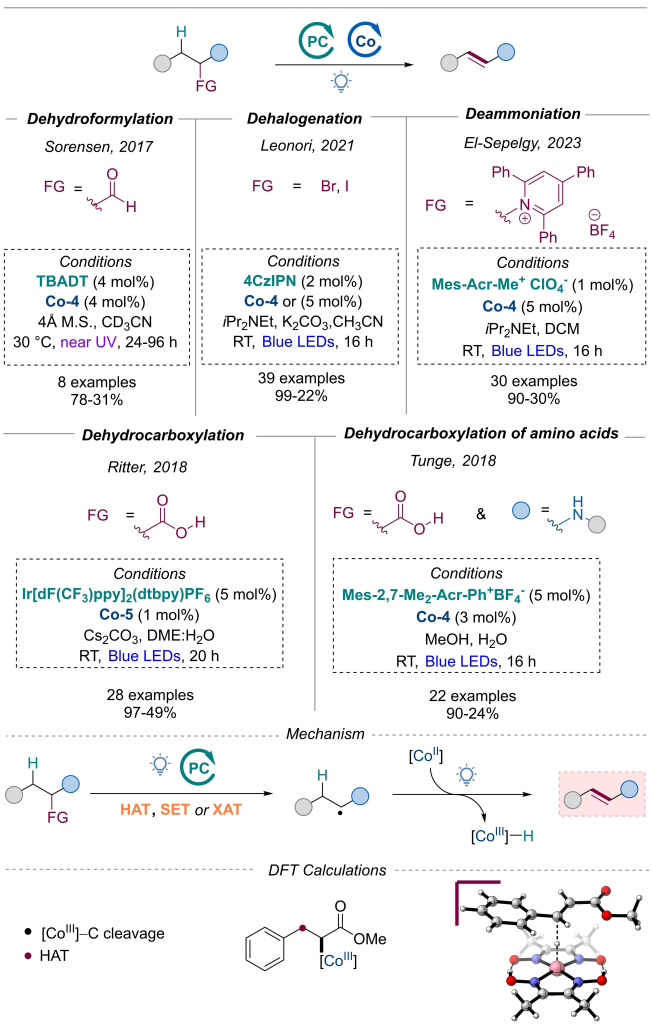

Scheme 5. Dehydrofunctionalization enabled by photoredox/cobaloxime dual catalysis.

3.2. Dehydrofunctionalisation

Defunctionalization chemistry facilitates the transition from fossil-based to bio-based chemicals, promoting sustainability. By selectively removing functional groups and substituting them with alkenes, it streamlines the synthesis of bio-derived compounds from renewable feedstocks. This reduces reliance on finite fossil resources and minimizes environmental impact. Through tailored catalysts and reaction conditions, defunctionalization enables the conversion of biomass into value-added chemicals while adhering to green chemistry principles.[26]

In comparison with the non-directed desaturation, the use of functional group as a radical precursor enables excellent regioselectivity of the produced alkene. In this regard, Sorensen and co-workers have reported a mild method for the dehydroformylation of α-quaternary aliphatic aldehydes using a dual HAT and cobaloxime catalysis (Scheme 5).[27] The dehydroformylation cycle begins with HAT of the aldehyde hydrogen excited-state tungsten photocatalyst resulting in the formation of acyl radicals, which undergo decarbonylation to extrude CO and generate alkyl radicals. The radical intermediate undergoes cobaloxime desaturation to produce the corresponding olefin and [Co^{III}]–H. Next, the groups of Ritter and Tunge have independently developed the dehydrodecarboxlation of a wide range of carboxylic acids[28] and amino acids[14b] using a combined photoredox and cobaloxime system. The photocatalyst enables the oxidation of the carboxylic acid to its corresponding alkyl radical while the cobaloxime catalyst act as H-abstractor and β-hydrogen elimination agent. Shortly thereafter, Larionov showcased the viability of a similar cobaloxime/photoredox system for upgrading biomass-derived carboxylic acids.[29] Building on these findings, Summerlin and Seidel have recently established elegant methods for the degradation of carboxylate-containing polymers under visible light irradiation.[30]

In 2021, Leonori et al. reported a photochemical dehalogenative olefination of alkyl halides by using photoredox/cobaloxime system.[31] The radical generation from the alkyl halides is enable by XAT using α-amino radical that could be in situ generated using photocatalyst and simple organic base such as *i*Pr$_2$NEt. Notably, the authors have shown that the regioselectivity of products can be controlled by modulating suitable steric and electric properties of the cobalt catalysts. Very recently, El-Sepelgy et al. have developed a biomimetic method for the dehydroammoniation of primary amines.[32] Pyridinium salts were used as

redox-active amines, together with acridinium photocatalyst and cobaloxime, providing the first mild alternative to the classical Hoffmann[33] and Cope elimination.[34] The methodology allows the dehydroamination of wide range of primary amines including amino acids, pharmaceuticals, and natural products. DFT calculations suggests that the homolysis of [Co^{III}]-alkyl bonds is taking place by the action of visible light in the excited (triplet) state. An example of transition state of β-hydrogen elimination is shown in the bottom of Scheme 5.

A related dehydrofunctionalization approach was also reported independently by Rueping and Wu.[35] Dual photoredox/cobaloxime catalytic system was used for the dehydrogenative conversion of electron-rich tertiary alcohols to form remotely dehydrogenated ketones (Scheme 6). The mechanism initiates with a SET from aryl substituents of alcohols to the excited state of the photoredox catalyst, generating cation radical species (**6.1**). These intermediates undergo intramolecular PCET in the presence of base to yield alkoxyl radical species (**6.2**), which can cleave into alkyl radicals and carbonyl moiety (**6.3**) via β-scission of the neighbouring C–C bond. The formed alkyl radical subsequently undergoes the desaturation process via cobaloxime catalysis, resulting in the formation of remotely dehydrogenated ketones.

3.3. Remote Desaturation of Aliphatic Compounds

Motivated by the groundbreaking advancements in dehydrofunctionalization chemistry catalysed by dual photoredox/cobaloxime systems, the group of El-Sepelgy decided to integrate this approach with intramolecular hydrogen atom transfer to achieve remote C–H desaturation.[16] It's noteworthy that a similar strategy was concurrently reported by Xu's group.[36] To validate the concept, the authors focused on exploring the desaturation of aliphatic amines and amides tethered with *o*-iodo-benzoyl tethers.[37] Initial trials employing combined photoredox/cobaloxime catalysis failed to yield any desaturated products, primarily due to challenges in activating the aryl iodide.

Nevertheless, employing cobaloxime-triphenyltin complex (**Co-2**) enabled the efficient conversion of a broad scope of amides and imides into the corresponding enamides and enimides at room temperature without the need for additional photocatalyst. Drawing from both experimental observations and theoretical investigations, the authors proposed a mechanistic pathway illustrated in Scheme 7. Upon visible light irradiation, homolytic cleavage of Co–$SnPh_3$ complex generates a metalloradical Co(II) species alongside a triphenyltin radical. The latter is believed to promote the formation of an α-amino radical from iPr_2NEt, serving as an XAT reagent to abstract iodo or bromo atoms

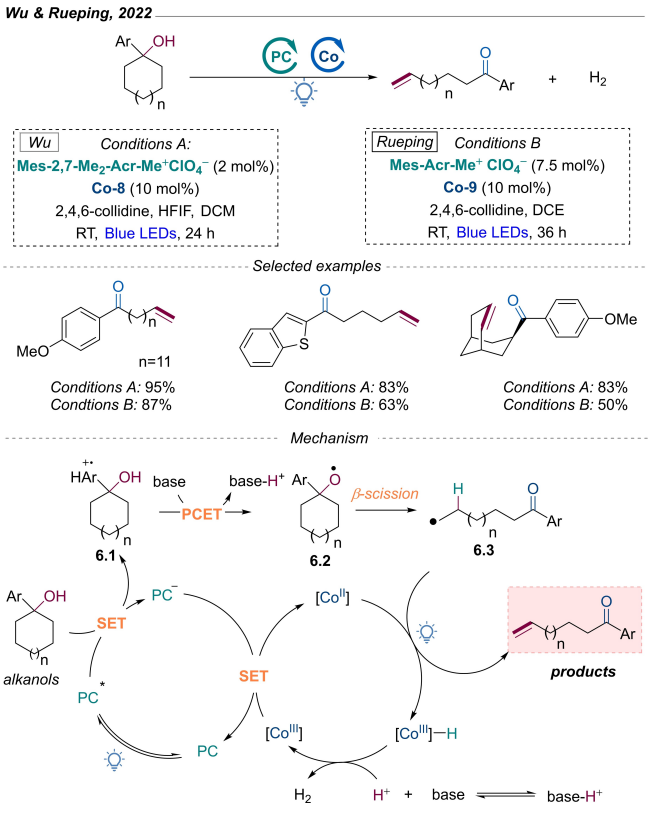

Scheme 6. Synthesis of distally unsaturated ketones via dehydrogenated alcohols.

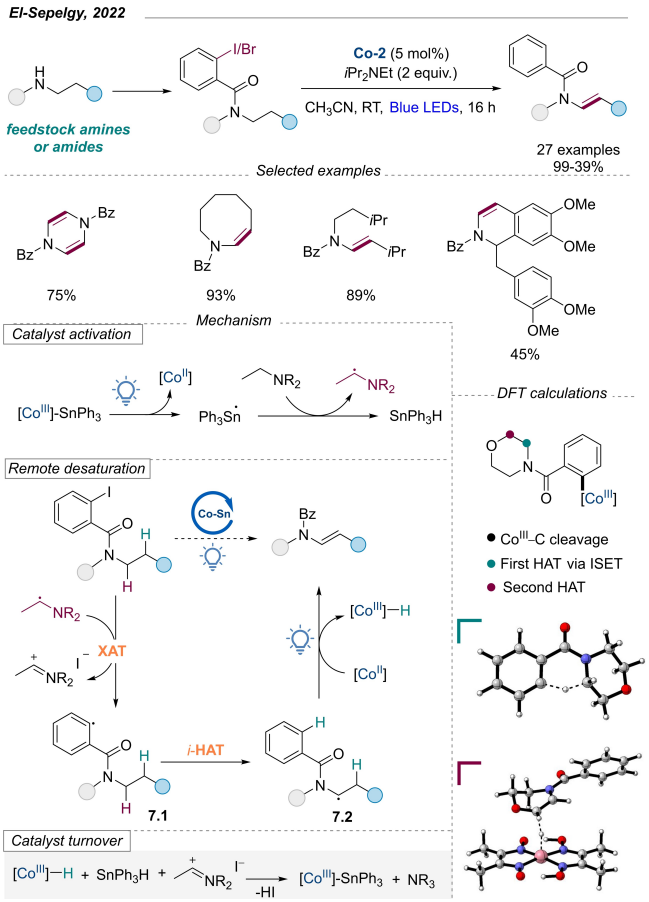

Scheme 7. Remote desaturation of aliphatic amines and amides.

from the substrate to generate aryl radical (**7.1**). Subsequently, this radical undergoes 1,5-HAT, leading to radical formation at an unactivated site of the alkyl chain (**7.2**). The alkyl radical (**7.2**) then undergoes desaturation utilizing the Co(II) species to furnish the unsaturated product along with [Co^{III}]–H. This hydride species facilitates the catalyst turnover by the reaction between $SnPh_3H$ and an iminium salt to regenerate the cobalt-tin catalyst. DFT investigations suggest that the excitation strategy of the cobaloxime-substrate complex plays a pivotal role in two key stages of the process. Initially, homolytic cleavage of the [Co^{III}]–C bond enables 1,5-HAT via intramolecular single electron transfer (SET) in the radical species (Scheme 7, green). Also, the desaturation of the alkyl intermediate (**7.2**) takes place in the excited state under visible light irradiation (Scheme 7, purple).

4. Desaturative Synthesis of Aromatics

Recently, Leonori group has developed several methodologies for converting aliphatic substrates into high-value aromatic products.[38] These transformations involve multiple acceptorless dehydrogenation steps utilizing dual catalytic systems including cobaloxime catalysis.

In 2020, Leonori group introduced a general and site-selective approach for synthesizing anilines from corresponding cyclohexanes and ammonia, primary, or secondary amines.[38a] The reaction commences with a straightforward condensation between the amine or ammonia and the cyclohexane derivative to form the corresponding enamine (**8.1**) (Scheme 8). The enamine intermediate undergoes single-electron oxidation with an iridium photocatalyst, generating an enaminium radical (**8.2**) which then deprotonates to yield the β-enamine radical (**8.3**). This radical subsequently reacts with a [Co^{II}] metalloradical via HAT, leading to the formation of the di-enamine (**8.4**) along with a [Co^{III}]–H species. This di-enamine is proposed to undergo a second oxidation-dehydrogenation process with the cobaloxime/photocatalyst system, resulting in the complete aromatization of the aniline derivatives. The reaction demonstrates excellent tolerance for various functional groups in the *ortho*-, *meta*-, and *para*- positions of the cyclohexanone. This method has been showcased to simplify the preparation of a wide range of pharmaceuticals. During the review of this manuscript, the same group has extended this methodology to the synthesis of aminated heteroaromatics from the corresponding amines and cyclic ketones.[39]

In 2021, Leonori and co-workers outlined a method for synthesizing a wide range of substituted aromatic aldehydes from the corresponding cyclohexanecarbaldehydes.[38b] This new approach involves a triple catalytic system comprising an amine catalyst, a photocatalyst, and cobaloxime, resulting in the production of aromatic aldehydes and hydrogen gas as the sole side-product. In this method, the morpholine catalyst reacts with the aldehyde, leading to the formation of the corresponding enamine. Similar to the dehydrogenative synthesis of anilines, the enamine intermediate undergoes two cycles of oxidation-deprotonation using an iridium photocatalyst, followed by desaturation with cobaloxime (Scheme 9). Finally, hydrolysis leads to the formation of the desired aldehydes.

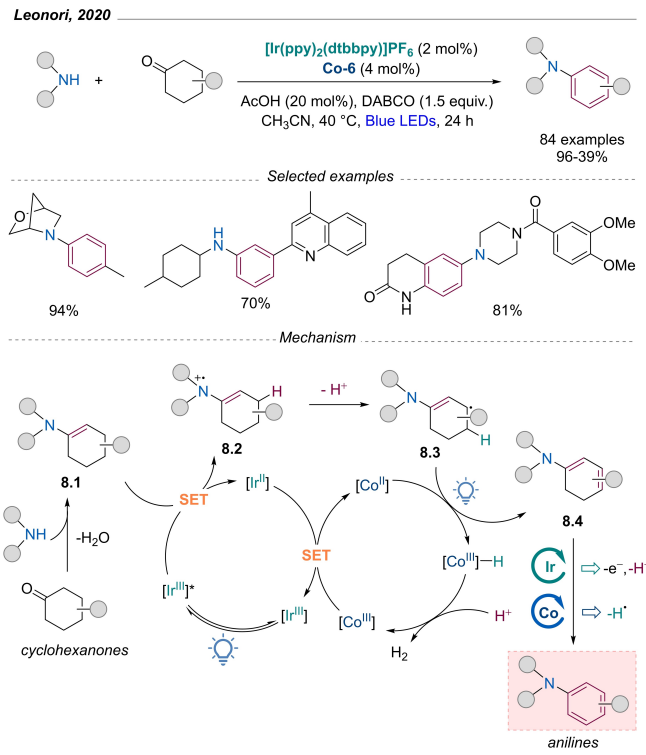

Scheme 8. Synthesis of anilines from amines and cyclohexanones.

More recently, Leonori et al. have introduced a new method for the complete aromatization of cyclohexanones to phenols (Scheme 10).[38c] This innovative strategy exploits the synergistic interplay of photocatalytic HAT and cobalt catalysis, alternating between each other, to sequentially remove four hydrogen atoms from the saturated precursors.

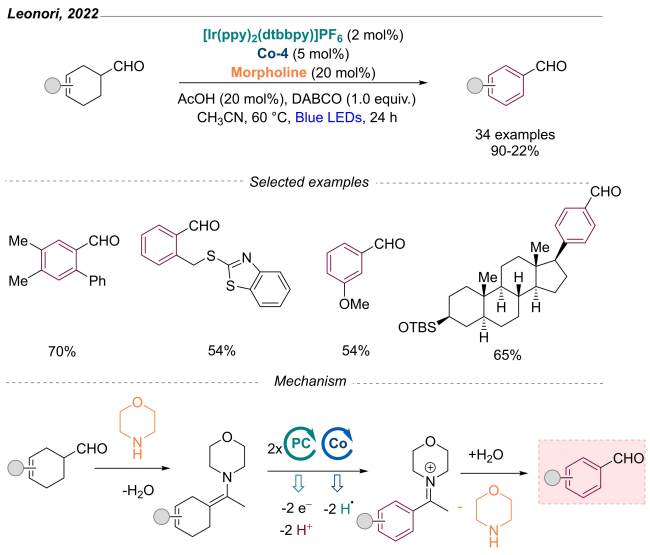

Scheme 9. Dehydrogenative synthesis of aldehydes.

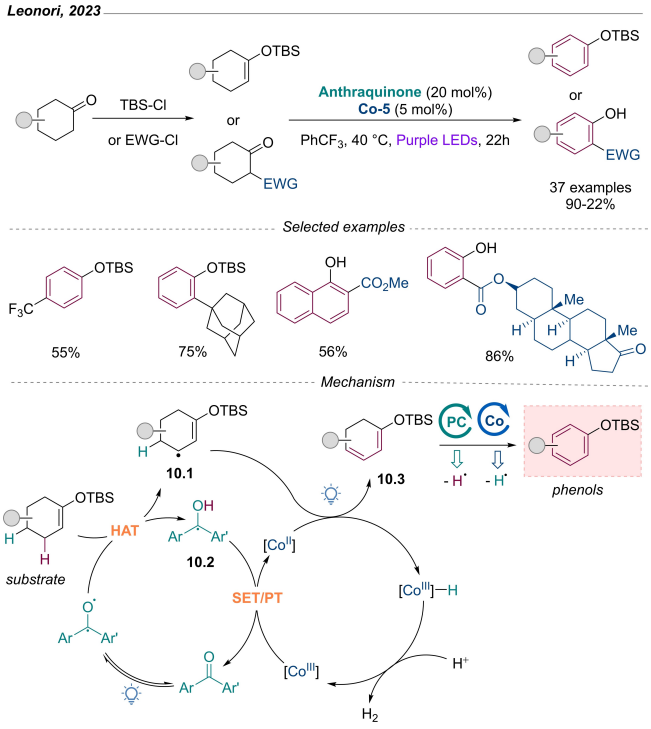

Scheme 10. Synthesis of phenols via desaturation of cyclohexanones.

To facilitate a facile HAT process, the authors initially convert the cyclohexenes to the corresponding enol ether or introduce an electron-withdrawing group (e.g., acetyl, ester) at the α-position to favour the enol tautomer over the ketone form. The catalysis starts with HAT process, hydrogen is transferred from the substrate to the triplet excited state of the HAT catalyst the allylic radical (**10.1**) and a ketyl radical (**10.2**). Subsequently, radical (**10.1**) undergoes desaturation with [Co^{II}] species, producing a diene (**10.3**). This diene then undergoes a second round of HAT and desaturation catalysis, resulting in the formation of phenol derivatives.

5. Cross Dehydrogenative Coupling (CDC)

Cross dehydrogenative coupling (CDC) is a powerful synthetic method in organic chemistry used to form new carbon–carbon or carbon–heteroatom bonds by coupling two different C–H bonds from two different molecules without requiring prefunctionalization. This process allows for the direct transformation of readily available and relatively inert C–H bonds into more complex structures, facilitating the synthesis of diverse organic compounds. In this section, we summarize the application of the cobaloxime catalysis in CDC reactions of olefins and arenes. However, the CDC reactions that involves iminium and oxonium cation intermediates[12a,40] and formal cycloaddition reactions[41] are already summarized elsewhere.[8a]

5.1 CDC of Olefins

The dehydrogenative functionalization of alkenes presents a promising avenue for sustainable synthesis by streamlining chemical transformations and minimizing waste generation. Leveraging the inherent reactivity of alkenes and strategically employing transition metal catalysts, this methodology facilitates the direct conversion of abundant, renewable feedstocks into valuable chemical products. Cobaloxime catalysis has emerged as a notable approach, either as a single catalyst or in conjunction with co-catalysts, for acceptorless dehydrogenation functionalization of olefins.

In general, these transformations can be initiated through two mechanistic scenarios: on one hand, SET oxidation of alkenes into their corresponding radical cations followed by reaction with neutral nucleophiles (Scheme 11); on the other hand, addition of an in situ radical to a neutral olefin (Scheme 12). In both pathways, the newly generated carbon-centered radical intermediates undergo desaturation catalyzed by cobaloxime to yield the desired olefin and [Co^{III}]–H. The interception between the radical generation cycle and the dehydrogenation cycles enables the catalysis turnover.

In line with the first scenario, Lei et al. have reported the anti-Markovnikov oxidation of β-alkyl styrenes using

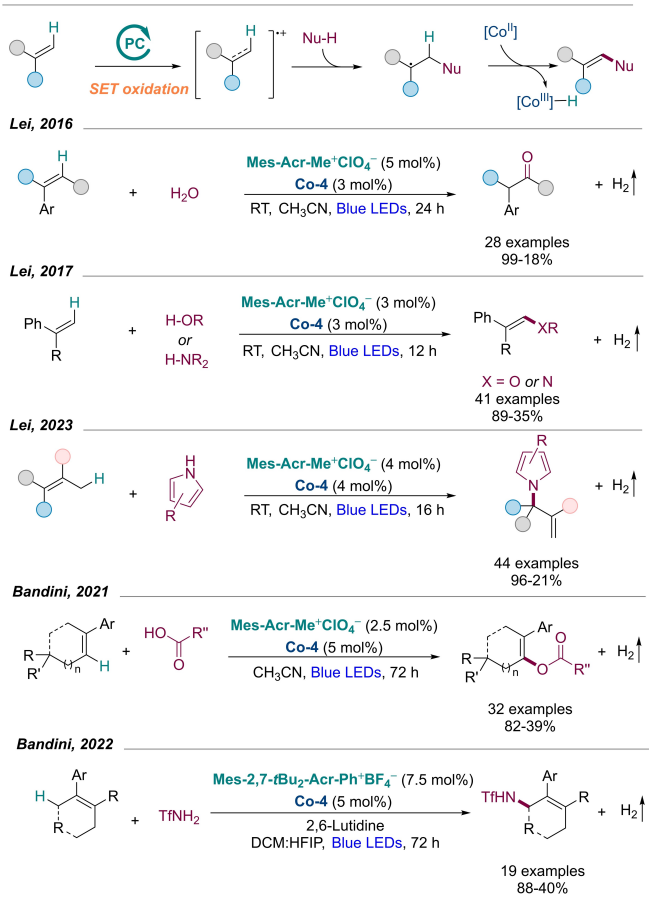

Scheme 11. Dehydrogenative functionalization of olefins via olefin SET oxidation.

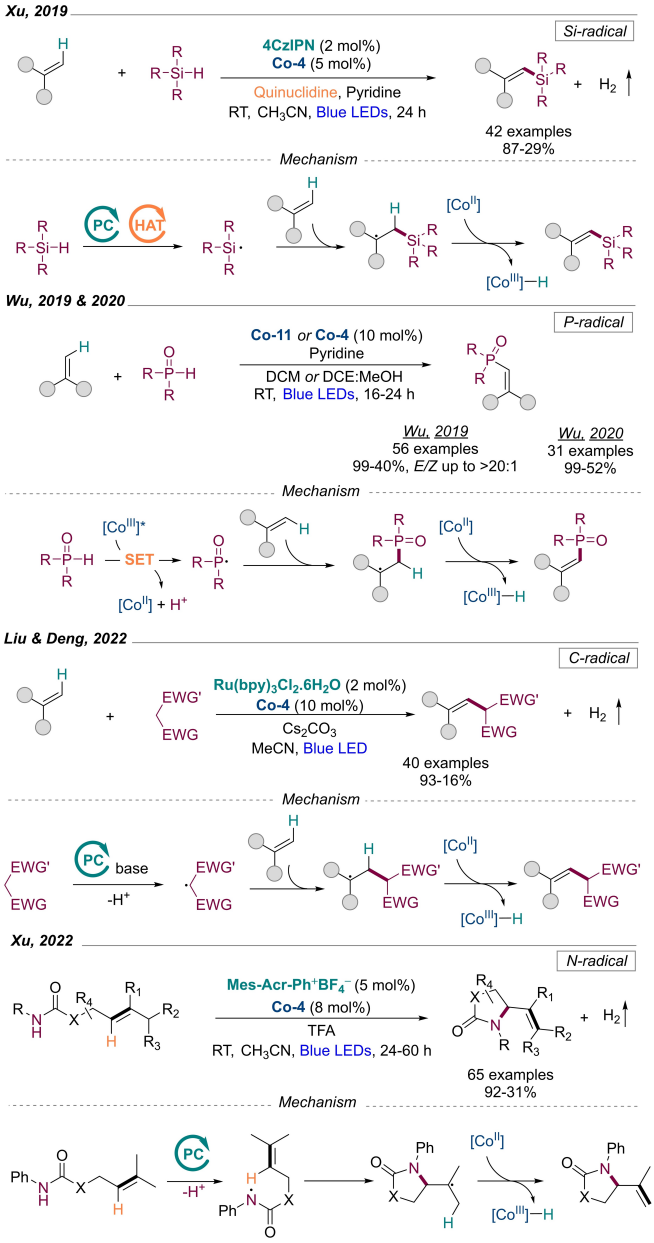

Scheme 12. Dehydrogenative functionalization via radical addition to olefins.

water as ideal oxidant.[42] Shortly after, the same group explored the dehydrogenative cross-coupling of alkenes with alcohols and azoles utilizing Acr–Mes–$Me^+ClO_4^-$ as a strongly oxidizing photocatalyst in conjunction with cobaloxime.[43] This reaction facilitates the formation of new $C(sp^2)$–O and $C(sp^2)$–N bonds. Furthermore, the same research group recently demonstrated the application of this catalytic system for coupling methyl-substituted alkenes with amines to produce allylazoles.[44] Additionally, Bandini et al. disclosed a similar acridinium/cobaloxime catalytic system for the dehydrogenative functionalization of styrenes with carboxylic acids and triflamides.[45]

In the second scenario, Xu et al. have demonstrated the in situ generation of silyl radicals from tris(trimethylsilyl)silane (TTMSS) through a combined photoredox and HAT catalysis.[46] Subsequent addition of the silyl radical to the olefin yields a carbon-centered radical intermediate, which undergoes desaturation catalysed by cobalt, resulting in the formation of allylsilane and [Co^{III}]–H. In 2019, Wu et al. reported the synthesis of alkenylphosphine oxides from corresponding alkenes and H-phosphines using cobaloxime catalysis, without the need for additional photocatalyst.[47] The authors highlighted the unique dual functionality of the cobaloxime catalyst, serving as both a photoredox catalyst and an inner-sphere desaturation catalyst. The [Co^{III}] complex acts as an outer-sphere photocatalyst for the activation of H-phosphine oxides, leading to the formation of phosphinoyl-centered radicals and [Co^{II}] species. The resulting phosphorus radical intermediate subsequently reacts with an olefin or enamine,[48] yielding an organic radical intermediate. This intermediate can then be trapped by [Co^{II}] species to produce the alkenylphosphine oxide product and [Co^{III}]–H. Very recently, the same group reported the addition of the P-radical to isocyanides and the subsequent synthesis of phosphorylated heteroaromatics.[49]

More recently, Liu and Deng developed dehydrogenative allylic $C(sp^3)$–H alkylation via triple Brønsted base/cobaloxime/photoredox catalysis.[50] The Brønsted base/photoredox catalysis facilitates the conversion of active methylene compounds to the corresponding radical followed by addition to methyl substituted olefins to produce carbon-centered radicals which can undergo cobaloxime dehydrogenation to deliver the desired allylic $C(sp^3)$–H allylation products.

Furthermore, Xu et al. also reported on the intramolecular dehydrogenative amination of alkenes through synergistic photoredox and cobaloxime catalysis, resulting in the formation of a diverse array of five-membered *N*-heterocycles.[51] Photoredox catalysis facilitates the formation of nitrogen radicals, which undergo 5-*exo*-trig cyclization to form a radical intermediate. This intermediate is subsequently captured by [Co^{II}] to generate [Co^{III}]–H and the dehydrogenative amination product.

5.2 CDC of Arenes

Similarly to the previously summarized dehydrogenative functionalization of olefins, few examples of intramolecular cross-dehydrogenative coupling of arenes catalyzed by cobaloxime catalysis have been reported in recent years (Scheme 13). An early example was presented by Wu and Lei in 2015, demonstrating aromatic C–H thiolation and the construction of $C(sp^2)$–S bonds.[12c] The photoredox catalyst is suggested to convert *N*-phenylthioamides to the corresponding S-radicals in the presence of a base, which then undergoes 5-*exo*-trig cyclization followed by rearomatization facilitated by cobaloxime catalysis. Similarly, utilizing dual photoredox/cobaloxime catalysis, *N*-arylenamines could be transformed into the corresponding indoles via the generation of C-radicals[52] and lactonization of 2-arylbenzoic acidthrough carboxylate radicals formation.[53] Recently, Wu's group reported a sustainable method for converting 2-

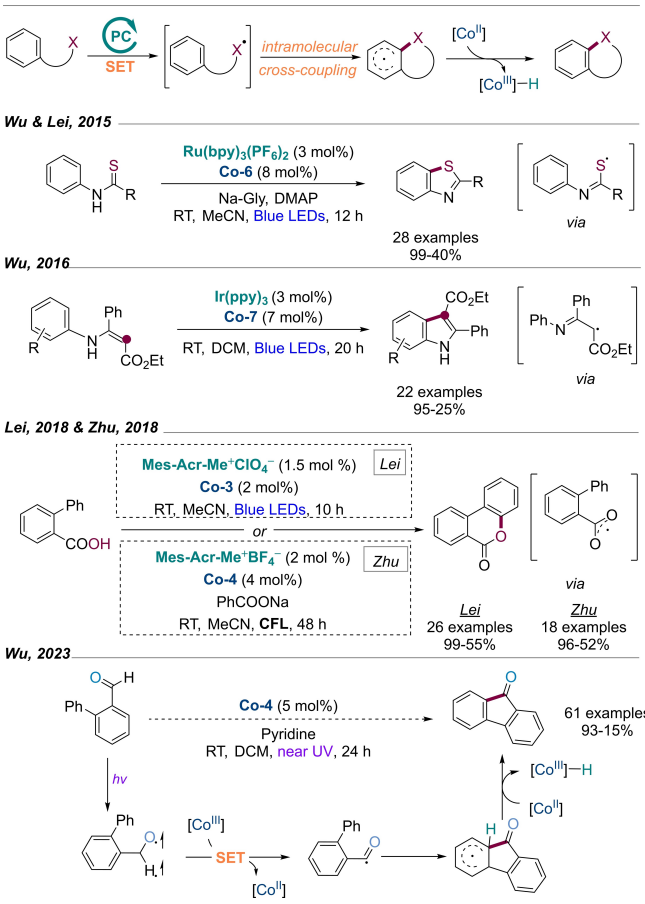

Scheme 13. Intramolecular dehydrogenative functionalization of arenes.

phenylbenzaldehydes into the corresponding fluorenones using cobaloxime catalysis without the need for a photoredox catalyst.[54] The authors proposed that under near UV light irradiation, the aromatic aldehydes enter a highly reactive triplet excited state, which is intercepted by cobaloxime in its ground state, leading to the formation of acyl radicals and [Co^{II}] species. Subsequent radical cyclization followed by rearomatization and fluorenone formation is enabled by the [Co^{II}] species.

It is worth noting that, a related intremolecular dehydrogenative Minisci alkylation between heteroarene and numerous carbon radical precursors has been reported. The C–C cross-coupling was realized by a photoredox/cobaloxime dual photocatalytic system, producing hydrogen gas as side product.[55]

The alternative approach for the arene dehydrogenative substitution involves the oxidation of the arene moiety with highly oxidizing photocatalyst (Scheme 14). In 2016 and 2017, Wu and Tung have reported the use of the highly oxidizing quinolinium ion QuCN$^+$ catalysts ($E^*_{red} = 2.72$ V) under UV light irradiation for the amination, hydroxylation and etherification of benzene in the presence of the cobaloxime catalysis for the rearomatization of the benzene.[56] The SET from the QuCN radical to the [Co^{III}] intermediate enables the catalysts regeneration. Simultaneously, Lei and co-workers demonstrated the possibility of

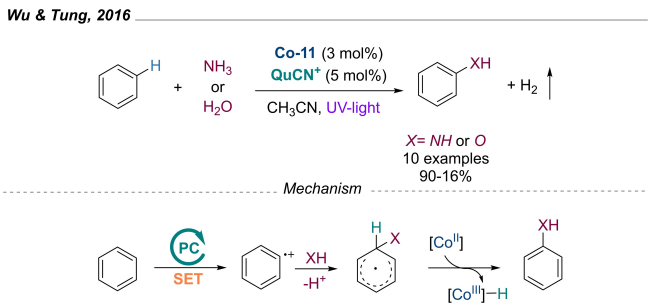

Scheme 14. Direct functionalization of arenes.

using acridinium visible light catalysis for the oxidation of arene and subsequent amination, however, the scope is limited to the electron rich arenes.[57]

6. Asymmetric Catalysis

The first application of cobaloxime in asymmetric synthesis was demonstrated by Luo and Wu in 2017.[58] A triple enamine/photoredox/cobaloxime catalysis was used for the asymmetric CDC of tetrahydroisoquinolines with carbonyl compounds. Recently Luo and co-workers have demonstrated the application of a related triple catalytic system for dehydrogenative allylic alkylation of 2-arylpropenes with β-ketocarbonyls (Scheme 15).[59] The reaction between the chiral primary amine organocatalyst and the β-ketocarbonyl compound yielded the enamines (**15.1**). These enamines undergo SET oxidation to generate α-iminoradicals, which readily react with the in situ generated [Co^{II}] species to form the organocobalt intermediate (**15.2**). Subsequent radical addition to the 2-arylpropenes, followed by dehydrogenation, leads to the formation of (**15.4**) via the cobalt intermediate (**15.3**). The hydrolysis of the imine (**15.4**) yields the desired product along with the regenerated organocatalyst (Scheme 15).

7. Conclusion and Outlook

In recent years, significant strides have been taken toward developing sustainable desaturative transformations, notably catalyzed by cost-effective cobaloxime catalysts. Cobaloxime catalysts have found diverse applications, including catalyzing challenging transformations such as alkyl-Heck reactions in both polar and radical fashion, desaturation of functionalized and unfunctionalized alkanes, remote desaturation of aliphatic compounds, and dehydrodefunctionalization of various functional groups including aldehydes, carboxylic acids, amines, alkyl halides, and tertiary alcohols. Recent contributions have showcased innovative dehydrogenative methods for synthesizing anilines, heteroarylamines, phenols, and aromatic aldehydes under cobaloxime catalysis. Additionally, significant progress has been achieved in cross-dehydrogenative coupling reactions facilitated by cobaloxime catalysis. These developments underscore the

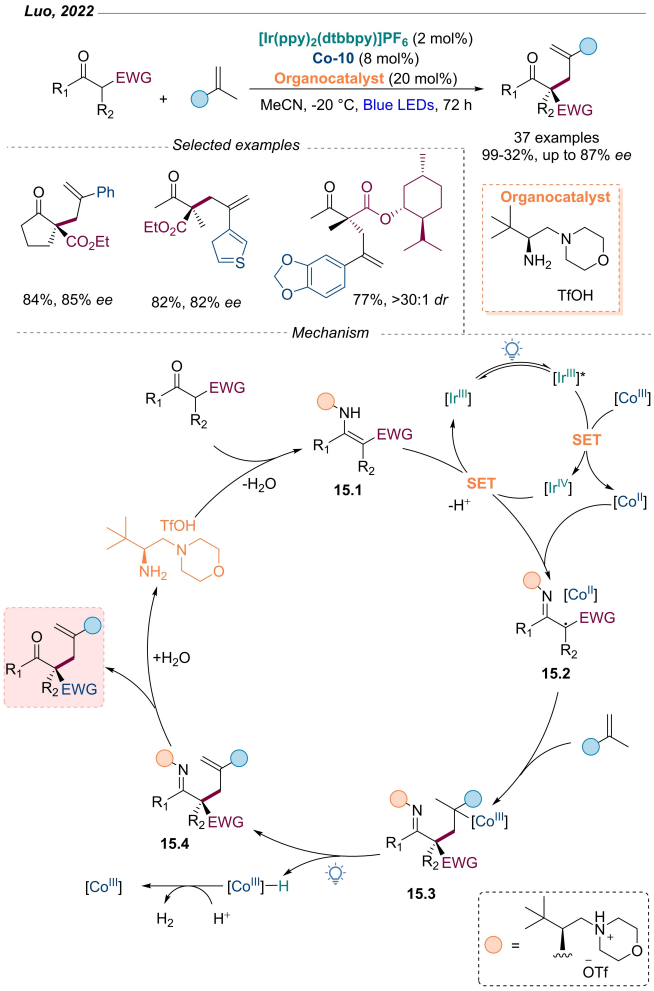

Scheme 15. Cobaloxime in asymmetric catalysis.

versatility and efficacy of cobaloxime catalysis in advancing sustainable synthetic methodologies, paving the way for further exploration and application in the field of organic synthesis. Despite the significant progress made, the application of cobaloxime catalysis is still in its infancy, and further academic and industrial research is anticipated, including progress in the practical applications of dehydrodefunctionalization of aliphatic compounds for upgrading biomass-derived compounds and upcycling of plastics, the expansion of remote and selective desaturation of aliphatic compounds,[60] exploration of Leonori's desaturative synthesis of aromatic compounds beyond enamine intermediates, the potential of merging cobaloxime with chiral catalysis for enhancing enantioselectivity, and the exploration of heterogenization of cobaloxime to facilitate catalyst recovery and reuse, thus improving the sustainability of cobaloxime catalysis. In addition to exploring new catalytic concepts and applications, cobaloxime catalysis lacks detailed theoretical and experimental studies, with several mechanistic steps currently under debate awaiting further investigations. For instance, there is discrepancy regarding the stepwise versus concerted hydrogen transfer, as well as the differentiation between homolytic cleavage of C–Co bonds in ground and excited states.

Acknowledgements

This work has been financially supported by the Deutsche Forschungsgemeinschaft (DFG, grant number EL 1041/3-1) and by the Leibniz Institute for Catalysis e.V. K.Z thanks Chinese Scholarship Council (CSC) for the predoctoral fellowship. L.M.A. is a Ramón y Cajal fellow (ref RYC2021-030994-I) and thanks MCIN/AEI and NextGenerationEU/PRTR for support. O.E.-S thanks Prof. Dr. Matthias Beller for his continued generous support. Open Access funding enabled and organized by Projekt DEAL.

Conflict of Interest

The authors declare no conflict of interest.

Data Availability Statement

Data sharing is not applicable to this article as no new data were created or analyzed in this study.

Keywords: Cobaloxime · photoredox catalysis · biomimetic chemistry · cobalt

[1] E. Poupon, B. Nay, *Biomimetic Organic Synthesis*, Wiley-VCH, Weinheim **2011**.
[2] a) B. Kräutler, *Vitamin B12 and B12-Proteins*, Wiley-VCH, Weinheim **1998**; b) G. Wohlfarth, G. Diekert, in *Chemistry and Biochemistry of B12*, Wiley-Interscience, New York **1999**.
[3] B. D. Martin, R. G. Finke, *J. Am. Chem. Soc.* **1992**, *114*, 585–592.
[4] a) B. E. Daikh, R. G. Finke, *J. Am. Chem. Soc.* **1992**, *114*, 2938–2943; b) Y. Wang, T. P. Begley, *J. Am. Chem. Soc.* **2020**, *142*, 9944–9954.
[5] G. N. Schrauzer, J. W. Sibert, R. J. Windgassen, *J. Am. Chem. Soc.* **1968**, *90*, 6681–6688.
[6] G. N. Schrauzer, *Acc. Chem. Res.* **1968**, *1*, 97–103.
[7] V. Artero, M. Chavarot-Kerlidou, M. Fontecave, *Angew. Chem. Int. Ed.* **2011**, *50*, 7238–7266.
[8] a) K. C. Cartwright, A. M. Davies, J. A. Tunge, *Eur. J. Org. Chem.* **2020**, *2020*, 1245–1258; b) A. Y. Chan, I. B. Perry, N. B. Bissonnette, B. F. Buksh, G. A. Edwards, L. I. Frye, O. L. Garry, M. N. Lavagnino, B. X. Li, Y. Liang, E. Mao, A. Millet, J. V. Oakley, N. L. Reed, H. A. Sakai, C. P. Seath, D. W. C. MacMillan, *Chem. Rev.* **2022**, *122*, 1485–1542; c) M. Kojima, S. Matsunaga, *Trends Chem.* **2020**, *2*, 410–426; d) K. Ram Bajya, S. Selvakumar, *Eur. J. Org. Chem.* **2022**, *2022*, e202200229.
[9] a) H. Bhandal, G. Pattenden, J. J. Russell, *Tetrahedron Lett.* **1986**, *27*, 2299–2302; b) B. P. Branchaud, M. S. Meier, Y. Choi, *Tetrahedron Lett.* **1988**, *29*, 167–170; c) A. Ghosez, T. Göbel, B. Giese, *Chem. Ber.* **1988**, *121*, 1807–1811; d) B. Giese, J. Hartung, J. He, O. Hüter, A. Koch, *Angew. Chem. Int. Ed.* **1989**, *28*, 325–327; e) M. Tada, K. Kaneko, *J. Org. Chem.* **1995**, *60*, 6635–6636.

[10] a) M. Okabe, M. Abe, M. Tada, *J. Org. Chem.* **1982**, *47*, 1775–1777; b) S. Torii, T. Inokuchi, T. Yukawa, *J. Org. Chem.* **1985**, *50*, 5875–5877; c) B. P. Branchaud, W. D. Detlefsen, *Tetrahedron Lett.* **1991**, *32*, 6273–6276; d) B. Giese, P. Erdmann, T. Göbel, R. Springer, *Tetrahedron Lett.* **1992**, *33*, 4545–4548; e) W. Affo, H. Ohmiya, T. Fujioka, Y. Ikeda, T. Nakamura, H. Yorimitsu, K. Oshima, Y. Imamura, T. Mizuta, K. Miyoshi, *J. Am. Chem. Soc.* **2006**, *128*, 8068–8077.

[11] M. E. Weiss, L. M. Kreis, A. Lauber, E. M. Carreira, *Angew. Chem. Int. Ed.* **2011**, *50*, 11125–11128.

[12] a) X.-W. Gao, Q.-Y. Meng, J.-X. Li, J.-J. Zhong, T. Lei, X.-B. Li, C.-H. Tung, L.-Z. Wu, *ACS Catal.* **2015**, *5*, 2391–2396; b) J. G. West, D. Huang, E. J. Sorensen, *Nat. Commun.* **2015**, *6*, 10093; c) G. Zhang, C. Liu, H. Yi, Q. Meng, C. Bian, H. Chen, J.-X. Jian, L.-Z. Wu, A. Lei, *J. Am. Chem. Soc.* **2015**, *137*, 9273–9280.

[13] F. Juliá, *ChemCatChem* **2022**, *14*, e202200916.

[14] a) D. D. M. Wayner, D. J. McPhee, D. Griller, *J. Am. Chem. Soc.* **1988**, *110*, 132–137; b) K. C. Cartwright, J. A. Tunge, *ACS Catal.* **2018**, *8*, 11801–11806.

[15] A. C. Frisch, M. Beller, *Angew. Chem. Int. Ed.* **2005**, *44*, 674–688.

[16] C. Wang, L. M. Azofra, P. Dam, M. Sebek, N. Steinfeldt, J. Rabeah, O. El-Sepelgy, *ACS Catal.* **2022**, *12*, 8868–8876.

[17] C. Wang, L. M. Azofra, P. Dam, E. J. Espinoza-Suarez, H. T. Do, J. Rabeah, A. Bruckner, O. El-Sepelgy, *Chem. Commun.* **2023**, *59*, 3862–3865.

[18] a) M. Parasram, V. O. Iaroshenko, V. Gevorgyan, *J. Am. Chem. Soc.* **2014**, *136*, 17926–17929; b) X. Dong, Y. Han, F. Yan, Q. Liu, P. Wang, K. Chen, Y. Li, Z. Zhao, Y. Dong, H. Liu, *Org. Lett.* **2016**, *18*, 3774–3777.

[19] G. Prina Cerai, B. Morandi, *Chem. Commun.* **2016**, *52*, 9769–9772.

[20] H. Cao, H. Jiang, H. Feng, J. M. C. Kwan, X. Liu, J. Wu, *J. Am. Chem. Soc.* **2018**, *140*, 16360–16367.

[21] T. Constantin, M. Zanini, A. Regni, N. S. Sheikh, F. Juliá, D. Leonori, *Science* **2020**, *367*, 1021–1026.

[22] W. Zhou, S. Wu, P. Melchiorre, *J. Am. Chem. Soc.* **2022**, *144*, 8914–8919.

[23] A. Kumar, T. M. Bhatti, A. S. Goldman, *Chem. Rev.* **2017**, *117*, 12357–12384.

[24] R. D. Kolb, N. Jain, B. König, *Adv. Synth. Catal.* **2023**, *365*, 605–611.

[25] M. J. Zhou, L. Zhang, G. Liu, C. Xu, Z. Huang, *J. Am. Chem. Soc.* **2021**, *143*, 16470–16485.

[26] R. Wohlgemuth, *ChemSusChem* **2022**, *15*, e202200402.

[27] D. J. Abrams, J. G. West, E. J. Sorensen, *Chem. Sci.* **2017**, *8*, 1954–1959.

[28] X. Sun, J. Chen, T. Ritter, *Nat. Chem.* **2018**, *10*, 1229–1233.

[29] V. T. Nguyen, V. D. Nguyen, G. C. Haug, H. T. Dang, S. Jin, Z. Li, C. Flores-Hansen, B. S. Benavides, H. D. Arman, O. V. Larionov, *ACS Catal.* **2019**, *9*, 9485–9498.

[30] a) A. Adili, A. B. Korpusik, D. Seidel, B. S. Sumerlin, *Angew. Chem. Int. Ed.* **2022**, *61*, e202209085; b) A. B. Korpusik, A. Adili, K. Bhatt, J. E. Anatot, D. Seidel, B. S. Sumerlin, *J. Am. Chem.* **2023**, *145*, 10480–10485.

[31] H. Zhao, A. J. McMillan, T. Constantin, R. C. Mykura, F. Julia, D. Leonori, *J. Am. Chem. Soc.* **2021**, *143*, 14806–14813.

[32] C. Wang, P. Dam, M. Elghobashy, A. Brückner, J. Rabeah, L. M. Azofra, O. El-Sepelgy, *ACS Catal.* **2023**, *13*, 14205–14212.

[33] A. W. von Hofmann, *Justus Liebigs Ann. Chem.* **1851**, *78*, 253–286.

[34] A. C. Cope, T. T. Foster, P. H. Towle, *J. Am. Chem. Soc.* **1949**, *71*, 3929–3934.

[35] a) L. Huang, T. Ji, C. Zhu, H. Yue, N. Zhumabay, M. Rueping, *Nat. Commun.* **2022**, *13*, 809; b) X. Wang, Y. Li, X. Wu, *ACS Catal.* **2022**, *12*, 3710–3718.

[36] W. L. Yu, Z. G. Ren, K. X. Ma, H. Q. Yang, J. J. Yang, H. Zheng, W. Wu, P. F. Xu, *Chem. Sci.* **2022**, *13*, 7947–7954.

[37] P. Chuentragool, M. Parasram, Y. Shi, V. Gevorgyan, *J. Am. Chem. Soc.* **2018**, *140*, 2465–2468.

[38] a) U. D. S. F. Julia, A. Luridiana, J. J. Douglas, D. Leonori, *Nature* **2020**, *584*, 75–81; b) H. Zhao, H. P. Caldora, O. Turner, J. J. Douglas, D. Leonori, *Angew. Chem. Int. Ed.* **2022**, *61*, e202201870; c) H. P. Caldora, Z. Zhang, M. J. Tilby, O. Turner, D. Leonori, *Angew. Chem. Int. Ed.* **2023**, *62*, e202301656.

[39] J. Corpas, H. P. Caldora, E. M. Di Tommaso, A. C. Hernandez-Perez, O. Turner, L. M. Azofra, A. Ruffoni, D. Leonori, *Nat. Catal.* **2024**, *7*, 593–603.

[40] a) E. Bergamaschi, C. Weike, V. J. Mayerhofer, I. Funes-Ardoiz, C. J. Teskey, *Org. Lett.* **2021**, *23*, 5378–5382; b) M. K. Sahoo, E. Balaraman, *Green Chem.* **2019**, *21*, 2119–2128; c) Z. Jia, Q. Yang, L. Zhang, S. Luo, *ACS Catal.* **2019**, *9*, 3589–3594; d) M. K. Sahoo, K. Saravanakumar, G. Jaiswal, E. Balaraman, *ACS Catal.* **2018**, *8*, 7727–7733; e) L. Niu, S. Wang, J. Liu, H. Yi, X.-A. Liang, T. Liu, A. Lei, *Chem. Commun.* **2018**, *54*, 1659–1662; f) K.-H. He, F.-F. Tan, C.-Z. Zhou, G.-J. Zhou, X.-L. Yang, Y. Li, *Angew. Chem. Int. Ed.* **2017**, *56*, 3080–3084; g) M. Xiang, Q.-Y. Meng, J.-X. Li, Y.-W. Zheng, C. Ye, Z.-J. Li, B. Chen, C.-H. Tung, L.-Z. Wu, *Chem. Eur. J.* **2015**, *21*, 18080–18084; h) J.-J. Zhong, Q.-Y. Meng, B. Liu, X.-B. Li, X.-W. Gao, T. Lei, C.-J. Wu, Z.-J. Li, C.-H. Tung, L.-Z. Wu, *Org. Lett.* **2014**, *16*, 1988–1991.

[41] a) G. Zhang, Y. Lin, X. Luo, X. Hu, C. Chen, A. Lei, *Nat. Commun.* **2018**, *9*, 1225; b) X. Hu, G. Zhang, F. Bu, A. Lei, *Angew. Chem. Int. Ed.* **2018**, *57*, 1286–1290.

[42] G. Zhang, X. Hu, C.-W. Chiang, H. Yi, P. Pei, A. K. Singh, A. Lei, *J. Am. Chem.* **2016**, *138*, 12037–12040.

[43] H. Yi, L. Niu, C. Song, Y. Li, B. Dou, A. K. Singh, A. Lei, *Angew. Chem. Int. Ed.* **2017**, *56*, 1120–1124.

[44] C. M. You, C. Huang, S. Tang, P. Xiao, S. Wang, Z. Wei, A. Lei, H. Cai, *Org. Lett.* **2023**, *25*, 1722–1726.

[45] a) Y. Liu, S. Battaglioli, L. Lombardi, A. Menichetti, G. Valenti, M. Montalti, M. Bandini, *Org. Lett.* **2021**, *23*, 4441–4446; b) S. Battaglioli, G. Bertuzzi, R. Pedrazzani, J. Benetti, G. Valenti, M. Montalti, M. Monari, M. Bandini, *Adv. Synth. Catal.* **2021**, *364*, 720–725.

[46] W. L. Yu, Y. C. Luo, L. Yan, D. Liu, Z. Y. Wang, P. F. Xu, *Angew. Chem. Int. Ed.* **2019**, *58*, 10941–10945.

[47] W.-Q. Liu, T. Lei, S. Zhou, X.-L. Yang, J. Li, B. Chen, J. Sivaguru, C.-H. Tung, L.-Z. Wu, *J. Am. Chem. Soc.* **2019**, *141*, 13941–13947.

[48] T. Lei, G. Liang, Y.-Y. Cheng, B. Chen, C.-H. Tung, L.-Z. Wu, *Org. Lett.* **2020**, *22*, 5385–5389.

[49] J.-X. Yu, Y.-Y. Cheng, B. Chen, C.-H. Tung, L.-Z. Wu, *Angew. Chem. Int. Ed.* **2022**, *61*, e202209293.

[50] M.-Y. Dong, C.-Y. Han, D.-S. Li, Y. Hong, F. Liu, H.-P. Deng, *ACS Catal.* **2022**, *12*, 9533–9539.

[51] W.-L. Yu, Z.-G. Ren, W. Ma, H. Zheng, W. Wu, P.-F. Xu, *Green Chem.* **2022**, *24*, 6131–6137.

[52] C.-J. Wu, Q.-Y. Meng, T. Lei, J.-J. Zhong, W.-Q. Liu, L.-M. Zhao, Z.-J. Li, B. Chen, C.-H. Tung, L.-Z. Wu, *ACS Catal.* **2016**, *6*, 4635–4639.

[53] a) M. Zhang, R. Ruzi, N. Li, J. Xie, C. Zhu, *Org. Chem. Front.* **2018**, *5*, 749–752; b) A. Shao, J. Zhan, N. Li, C.-W. Chiang, A. Lei, *J. Org. Chem.* **2018**, *83*, 3582–3589.

[54] J.-D. Guo, Y.-J. Chen, C.-H. Wang, Q. He, X.-L. Yang, T.-Y. Ding, K. Zhang, R.-N. Ci, B. Chen, C.-H. Tung, L.-Z. Wu, *Angew. Chem. Int. Ed.* **2023**, *62*, e202214944.

[55] a) J. Li, C.-Y. Huang, J.-T. Han, C.-J. Li, *ACS Catal.* **2021**, *11*, 14148–14158; b) S. Pillitteri, P. Ranjan, G. M. Ojeda-Carralero,

L. Y. Vázquez Amaya, J. E. Alfonso-Ramos, E. V. Van der Eycken, U. K. Sharma, *Org. Chem. Front.* **2022**, *9*, 6958–6967.
[56] a) Y.-W. Zheng, B. Chen, P. Ye, K. Feng, W. Wang, Q.-Y. Meng, L.-Z. Wu, C.-H. Tung, *J. Am. Chem. Soc.* **2016**, *138*, 10080–10083; b) Y.-W. Zheng, P. Ye, B. Chen, Q.-Y. Meng, K. Feng, W. Wang, L.-Z. Wu, C.-H. Tung, *Org. Lett.* **2017**, *19*, 2206–2209.
[57] L. Niu, H. Yi, S. Wang, T. Liu, J. Liu, A. Lei, *Nat. Commun.* **2017**, *8*, 14226.
[58] Q. Yang, L. Zhang, C. Ye, S. Luo, L.-Z. Wu, C.-H. Tung, *Angew. Chem. Int. Ed.* **2017**, *56*, 3694–3698.
[59] Z. Jia, L. Zhang, S. Luo, *J. Am. Chem. Soc.* **2022**, *144*, 10705–10710.
[60] Y. Wan, E. Ramírez, A. Ford, H. K. Zhang, J. R. Norton, G. Li, *J. Am. Chem.* **2024**, *146*, 4985–4992.

Manuscript received: March 26, 2024
Accepted manuscript online: May 22, 2024
Version of record online: July 15, 2024

Review 2:

Reductive depolymerization of plastics catalyzed with transition metal complexes

Wang, C.; El-Sepelgy, O.*

Curr. Opin. Green Sustain. Chem **2021**, *32*, 100547.

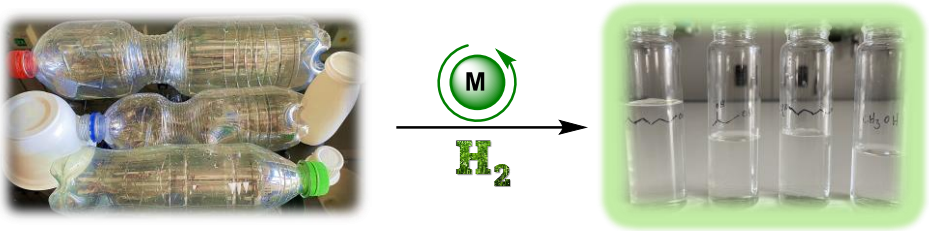

plastic waste

alcohols and amines
value-added products

Available online at www.sciencedirect.com

ScienceDirect

Current Opinion in
Green and Sustainable Chemistry

Reductive depolymerization of plastics catalyzed with transition metal complexes

Chenyang Wang and Osama El-Sepelgy

Herein we summarize the recent efforts of plastic waste management using homogenous transition metal catalysis. Pioneering studies involve the use of pincer type noble metal catalysis, in particular ruthenium and iridium complexes. Recent studies show more sustainable alternatives, including Earth-abundant transition metal catalysis, reusable catalysts, as well as supported single-atom catalysis. So far, organometallic chemists could depolymerize carbonyl-containing polymers such as polyesters, polylactic acids, polycarbonates, and polyamides with hydrogen gas which could be obtained from renewable resources. However, nonhydrolyzable polymers that resist enzymatic hydrolysis seem to be the real challenge of synthetic chemists.

Addresses
Leibniz-Institut für Katalyse e.V., Albert-Einstein-Str.29a, Rostock, 18059, Germany

Corresponding author: El-Sepelgy, Osama (Osama.Elsepelgy@catalysis.de)

Current Opinion in Green and Sustainable Chemistry 2021, **32:**100547

This review comes from a themed issue on **Metals 2021**

Edited by **Dmitry Valyaev**

Available online 18 August 2021

For complete overview of the section, please refer the article collection - Metals 2021

https://doi.org/10.1016/j.cogsc.2021.100547

Introduction

Synthetic plastics have become fundamental to almost every aspect of our lives, with nearly 368 million tonnes production per year, which is expected to increase to nearly 800 million tonnes by 2050. Subsequently, the growing consumption of plastics caused the generation of plastic waste around the world. Unfortunately, more than half of the plastic wastes are discarded into landfills and finally enter ecospheres, such as oceans and lakes, leading to serious environmental issues, including groundwater contamination. The second approach is the use of plastic waste as a source of energy [1]. However, burning plastics brings out the formation of more serious toxic airborne pollutants, including massive carbon emissions [2]. In contrast, the recycling of plastic could provide a sustainable solution for the global plastic issue. The most used method involves the application of mechanical forces to grind plastics into secondary raw materials, which leads to declined structural proprieties, thus with limited applications [3]. Consequently, the chemical treatment of plastic waste aims to convert the plastic feedstock to high-value chemicals, including the original monomer or intermediate oligomers has recently gained much attention. Different chemical recycling approaches have been investigated, including hydrogenolysis, photocatalysis, pyrolysis, solvolysis using both homogenous and heterogenous catalysis [4]. This mini-review sheds light on the recent development of homogenously metal catalyzed hydrogenative depolymerization of widely used plastic materials [5–8].

Depolymerization of polycarbonates

Polycarbonates are widely used in engineering as strong and tough materials, also in some grades as optically transparent, because they can be easily worked, molded, and thermoformed. However, most polycarbonates are recycled by re-melting and re-molding or burning, which often produce inferior polymer or hurt our living environment [9–11]. A more promising chemical-recycling route through controlled depolymerization is urgently demanded (Figure 1). In 2012, the Ding group accomplished the first hydrogenative depolymerization of waste poly(propylene carbonate) (PPC) to afford 1,2-propylenediol and methanol by using PNP-Ru pincer complex (**Ru-1**, 0.1 mol%) as catalyst. Hydrogen gas that can be produced using green energy was used as a reactant in the presence of catalytic amounts of a base under relatively mild conditions [12].

Subsequently, Robertson and coworkers have employed related Ru-PNN pincer complexes **Ru-2 or Ru-3** for the controlled depolymerization of polyethylene carbonate (PEC), as well as PPC under similar conditions [13]. Related catalytic systems were reported by Enthaler and coworkers for the depolymerization of poly-polycarbonates [14,15] In 2018, Klankermayer extended this strategy to the selective catalytic hydrogenolysis of the abundant poly(bisphenol A carbonate) P(BPA)C in gram scale by using a molecular ruthenium/Triphos **Ru-4** and $HNTf_2$ as catalyst system, resulting in bisphenol A and methanol in excellent yield and selectivity [16].

The replacement of noble-metal catalysts by earth-abundant base-metal alternatives is of high current interest due to the toxicity and high price of noble-metal complexes. Inspired by the recent progress in manganese catalyzed hydrogenation of carbonyl compounds [17], El-Sepelgy and Rueping have accomplished the first

Figure 1

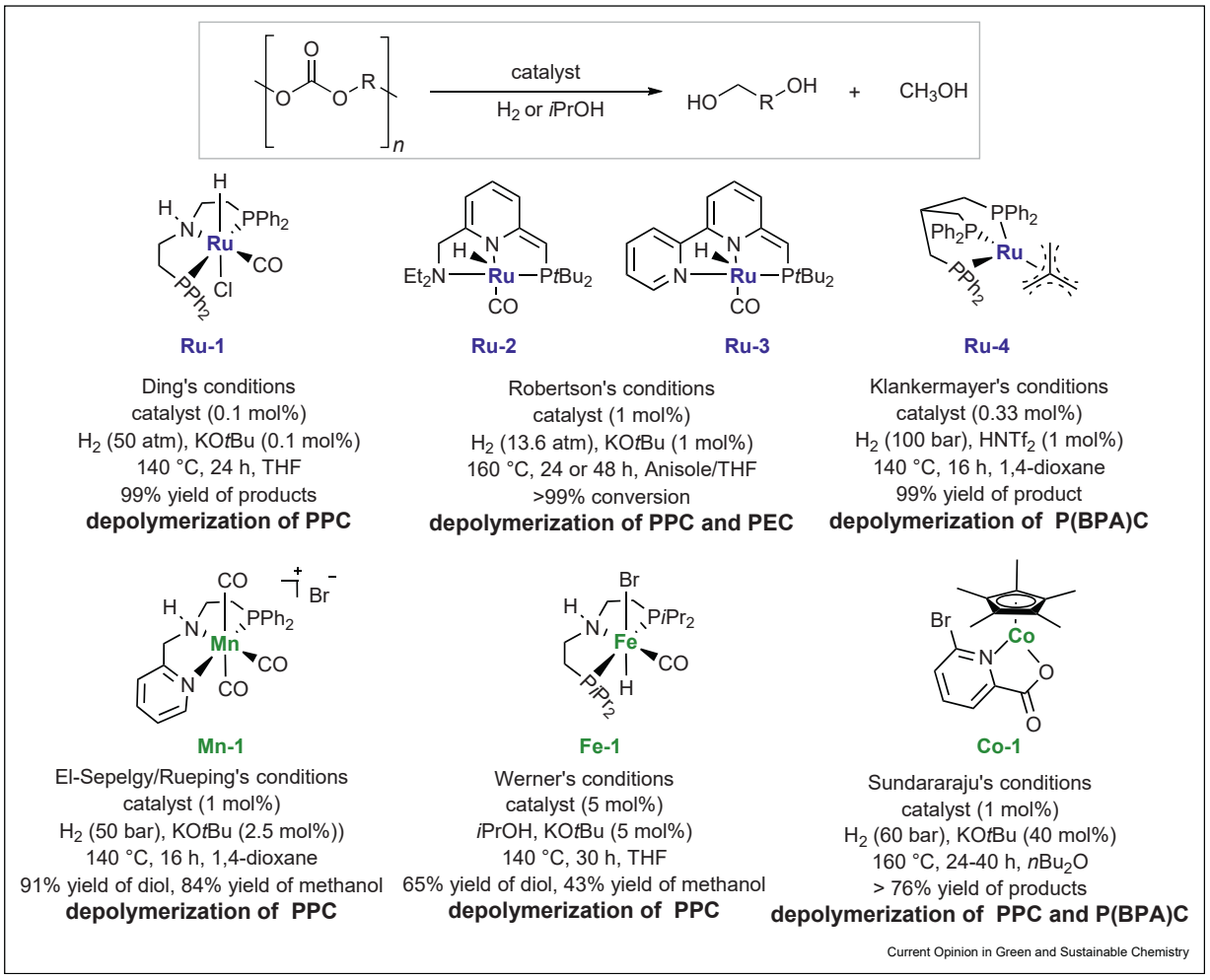

Depolymerization of polycarbonates.

example of base-metal catalyzed hydrogenative depolymerization. The application of the air-stable manganese catalysis **Mn1** for the depolymerization of PPC leads to the simultaneous formation of the corresponding diol (91% yield) and methanol (84% yield) [18]. Furthermore, the Werner group has reported the first base-metal catalyzed transfer hydrogenation of polycarbonates using isopropanol as practical and inexpensive hydrogen source. The authors have converted PPC to methanol and diol using PNP-Fe complex **Fe-1** [19]. In addition, Sundararaju and coworkers have outlined the application of a new phosphine-free base metal-catalyst **Co-1** for the hydrogenation of PPC and P(BPA)C [20,21].

Depolymerization of polyesters

Every year, nearly 70 million barrels of oil are used to prepare polyester, which is the most used fiber in textile industry. Thus, the development of sustainable technology for the polyester management is an elusive goal. The hydrogenative depolymerization of esters to valuable alcohols could be considered an attractive strategy to recycle the polyesters (Figure 2). Roberson and coworkers have reported the conversion of several polyesters, including polyethylene terephthalate (PET), poly(R-3-hydroxybutyric acid) (PHB), and poly(3-hydroxypropionic acid) (P3HP) to the corresponding alcohols using PNN-pincer ruthenium complexes (**Ru-2 or Ru-3**) [13]. Furthermore, Clarke and coworkers have reported another Ru catalyzed depolymerization of PET. Interestingly, air-sensitive aliphatic phosphines were replaced by a relatively stable tridentate amino-phosphine ligand [22].

In 2018, de Vries and coworkers reported the depolymerization of Dynacol 7360 using the iron pincer complex Fe-MACHO-BH **Fe-2**.The 1,6-hexanediol was produced in 87% isolated yield via the base-free transfer hydrogenation of Dynacol 7360 with EtOH as a hydrogen source [23].

Beyond the pincer type complexes, Fernandes and coworkers have recently reported the use of inexpensive

Figure 2

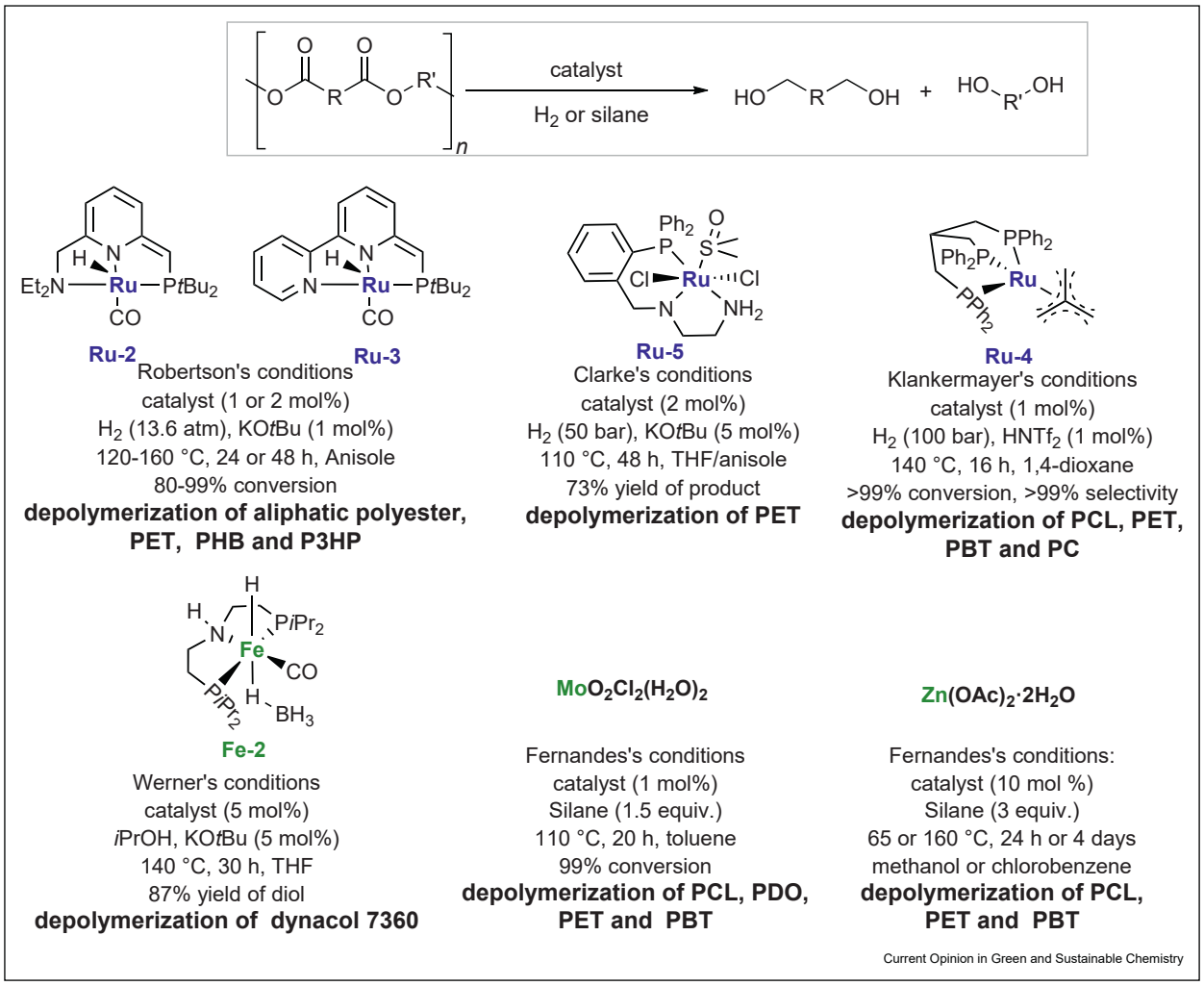

Depolymerization of polyesters.

and air-stable dioxomolybdenum complex $\mathbf{MoO_2Cl_2(H_2O)_2}$ as catalyst together with inexpensive silanes as reducing agents for the depolymerization of a variety of real plastic waste such as PET and polycaprolactone (PCL) to value-added chemicals [24]. Another promising approach was recently reported by the same group and involves the use of the simple, inexpensive, earth abundant zinc acetate (10 mol %) together with silane as reducing agent for depolymerization of several polyester [25]. Interestingly, the author has demonstrated the possibility of reusing the catalyst for at least seven cycles with good yields. These interesting findings may inspire the development of more industrially relevant catalytic systems that can offer a sustainable alternative to the current plastic management tactics.

Depolymerization of polylactic acid

In recent years, biodegradable polylactic acid is used in various packaging applications due to its physical properties that are similar to current synthetic plastics. There is a degradation pathway for recycling of PLA, biodegradable, but it needs very specific conditions so that biodegradability could occur [26–28]. To address this issue, Roberson disclosed the hydrogenative depolymerization of PLA using Ru-PNN complex **Ru-3** (Figure 3) [13]. Furthermore, Enthaler and coworkers reported the application of Ru-MACHO-BH complex **Ru-6** for the hydrogenative degradation of end-of-life Poly(lactide) to produce 1,2-propanediol [14]. Moreover, Klankermayer has also shown the possibility of the depolymerization of PLA using the homogenous ruthenium/Triphos catalytic system [16].

Similar to polyester, Fernandes has reported the use of inexpensive molybdenum and zinc salts for the hydrosilylation depolymerization of PLA in good yields [24,25].

In addition, Wood and Jones studied the degradation of PLA to produce methyl lactate (MeLa) by using Zn(II) complex as a catalyst in the presence of THF and

Figure 3

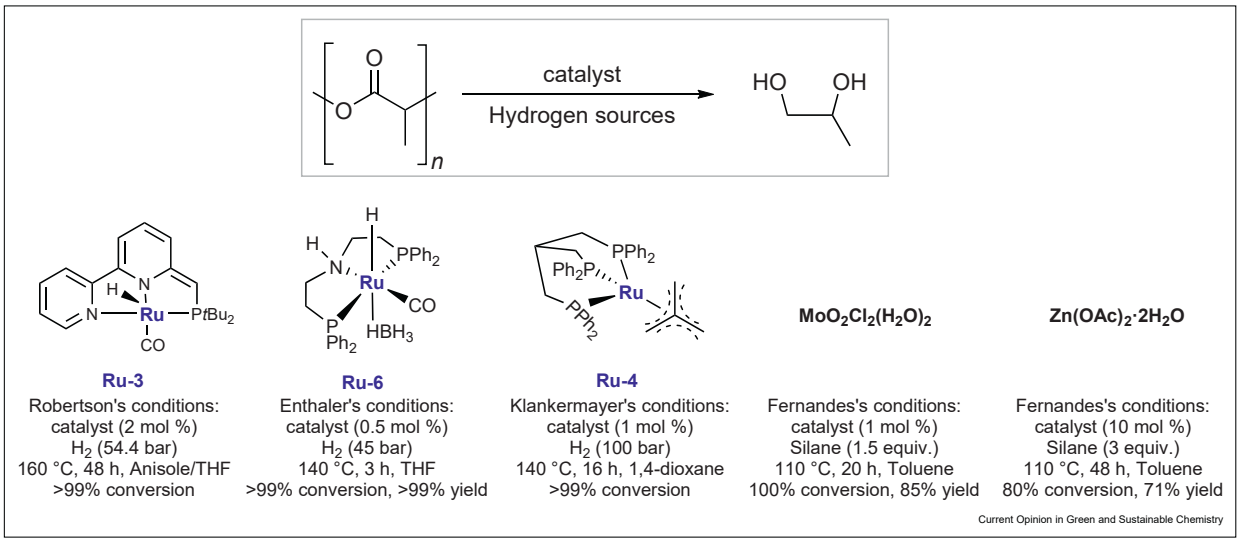

Depolymerization of polylactic acid.

methanol as the protic source [27]. Subsequently, the same group also studied the ethylenediamine Zn(II) complex catalyzed methanolysis of end-of-life poly (lactic acid) (PLA) to give methyl lactate, such as cup, toy, and three dimensional (3D) printing material [29]. In addition, the Cantat group achieved the depolymerization of PLA to selectively generate yield silyl ethers and corresponding alkanes in the presence of hydrosilanes and Brookhart's iridium(III) catalyst as [29,30].

Depolymerization of nylons and polyamides

Nylon polymers, with repeating units linked by amide bonds, have been found broad applications in our daily life, such as food packaging, apparel, cars, and electrical equipment because its properties of elasticity and strength. However, such commonly used plastics are not easily biodegradable, leading to land and water pollution. The current chemical recycling strategies for polyamides are focus on pyrolysis, hydrolysis, or aminolysis with pretty high temperatures (≥250−300 °C) [31−34].

The hydrogenative depolymerization of amide-based polymer is of particular interest because it will produce aminoalcohols, or a mixture of diols and diamines, which could be for the re-production of the same polymer and release of only hydrogen as a side product (Figure 4) [35].

Figure 4

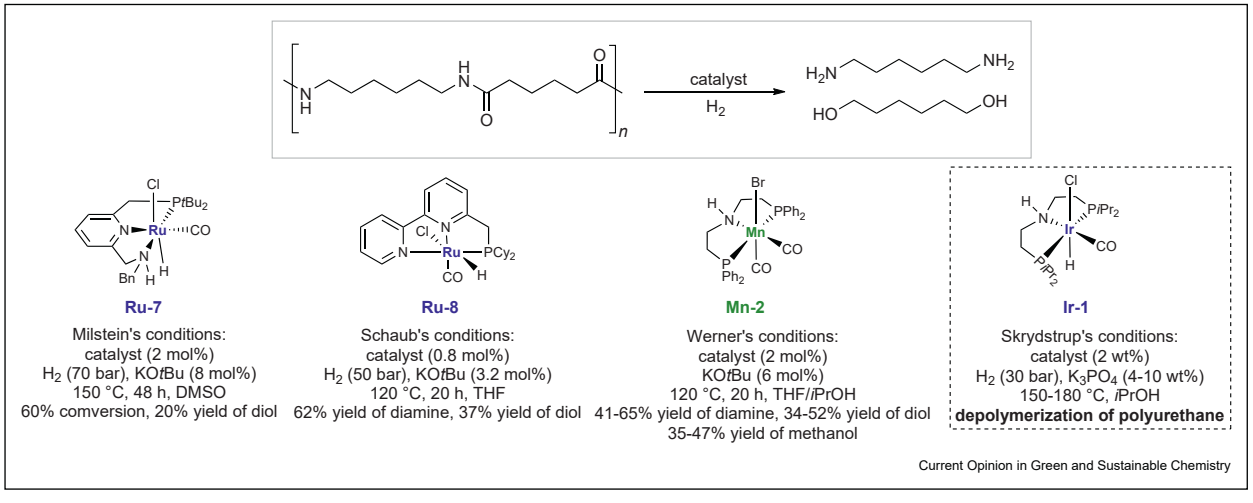

Depolymerization of polyamides (nylon).

In 2020, the Milstein group had reported the first transition-metal catalyzed reductive depolymerization of nylons and polyamides [36]. In the presence of a Ru–PNNH pincer complex **Ru-7** at 150 °C and 70 bar H_2 in DMSO, several polyamides were depolymerized under the optimized reaction conditions. First, nylon-6 (resins or powder) and nylon-12 were converted to 6-amino-1-hexanol in 24–30% yield, with the remaining being oligomers (dimer-tetramer). Furthermore, using the same catalytic system, nylon-66, poly(oligo)amides, and polyurethanes were also converted to the corresponding diols and diamines in high yield. Shortly after, Schaub and coworkers investigated an improved catalyst, **Ru-8,** for hydrogenative depolymerization of technical-grade nylon-66 and polyurethane in THF [37].

Very recently, the Werner group also reported a manganese pincer complex **Mn - 2** as a versatile catalyst in the transfer hydrogenation of polyurethanes to the corresponding alcohols, amines, and methanol as products [38]. Additionally, Kristensen and Skrydstrup described an effective deconstruction of polyurethane materials and products by applying the commercially available Ir-*i*PrMACHO complex **Ir-1** as under 30 bar H_2 and 150–180 °C in *i*PrOH as solvent [39]. The authors demonstrated the possibility of conversion of a variety of commercial polyurethane materials, including foams, inline skating wheels, shoe soles, and insulation materials, into value-added chemicals such as polyol and aniline.

Conclusion and perspective

Recently, plastic waste management has become one of the most serious challenges that face our society. Among the extensive efforts, homogenously catalyzed hydrogenative depolymerization of plastic waste via highly selective C–O and C–N bond cleavage represents one of the most promising approaches. This strategy leads to the direct conversion of plastic waste or even mixtures of plastic waste to value-added chemicals such as alcohols, diols, and amines. So far, most of the reported methods involve the use of expensive noble metal complexes in relatively high catalyst loading. However, recent preliminary efforts show the possibility of the use of base metal alternatives, as well as reusable homogenous and single-atom catalysis [40]. Another challenging task for organometallic chemists would be the development of new depolymerization transformation of the nonhydrolyzable polymers such as polyethylene (PE), polypropylene (PP), polystyrene (PS), and polyvinylchloride (PVC), which are resistant to the enzymatic degradation approaches [41].

Declaration of competing interest

Nothing declared.

Acknowledgements

O.E–S thanks Prof. Matthias Beller for his generous support. We thank Deutsche Forschungsgemeinschaft (DFG), as well as Leibniz institute for catalysis e.V. financial support.

References

Papers of particular interest, published within the period of review, have been highlighted as:

* of special interest
** of outstanding interest

1. Geyer R, Jambeck JR, Law KL: **Production, use, and fate of all plastics ever made**. *Sci Adv* 2017, **3**, e1700782.
2. Jambeck JR, Geyer R, Wilcox C, Siegler TR, Perryman M, Andrady A, Na R: **Plastic waste inputs from land into the ocean**. *Science* 2015, **347**:768–771.
3. Schyns ZOG, Shaver MP: **Mechanical recycling of packaging plastics: a review**. *Macromol Rapid Commun* 2021, **42**:2000415.
4. Chen X, Wang Y, Zhang L: **Recent progress in the chemical upcycling of plastic wastes**. *ChemSusChem* 2021. https://doi.org/10.1002/cssc.202100868.
5. Garbe M, Junge K, Beller M: **Homogeneous catalysis by manganese-based pincer complexes**. *Eur J Org Chem* 2017, **17**:4344–4362.
6. Gaillard S, Renaud J-L: **Iron-catalyzed hydrogenation, hydride transfer, and hydrosilylation: an alternative to precious-metal complexes?** *ChemSusChem* 2008, **1**:505–509.
7. Filonenko GA, van Putten R, Hensen EJM, Pidko EA: **Catalytic (de)hydrogenation promoted by non-precious metals-Co, Fe and Mn: recent advances in an emerging field**. *Chem Soc Rev* 2018, **47**:1459–1483.
8. Gunanathan C, Milstein D: **Bond activation and catalysis by ruthenium pincer complexes**. *Chem Rev* 2014, **114**:12024–12087.
9. Horn HW, Jones GO, Wei DS, Fukushima K, Lecuyer JM, Coady DJ, Hedrick JL, Rice JE: **Mechanisms of organocatalytic amidation and trans-esterification of aromatic esters as a model for the depolymerization of poly(ethylene) terephthalate**. *J Phys Chem A* 2012, **116**:12389–12398.
10. Leibfarth FA, Moreno N, Hawker AP, Shand JD: **Transforming polylactide into value-added materials**. *J Polym Sci, Part A: Polym Chem* 2012, **50**:4814–4822.
11. Fukushima K, Coulembier O, Lecuyer JM, Almegren HA, Alabdulrahman AM, Alsewailem FD, McNiel MA, Dubois P, Waymouth RM, Horn HW, Rice JE, Hedrick JL: **Organocatalytic depolymerization of poly(ethylene terephthalate)**. *J Polym Sci Part A: Polym Chem* 2011, **49**:1273–1281.
12. Han Z, Rong L, Wu J, Zhang L, Wang Z, Ding K: **Catalytic hydrogenation of cyclic carbonates: a practical approach from CO_2 and epoxides to methanol and diols**. *Angew Chem Int Ed* 2012, **51**:13041–13045.
13. Krall EM, Klein TW, Andersen RJ, Nett AJ, Glasgow RW, Reader DS, Dauphinais BC, Mc Ilrath SP, Fischer AA, Carney MJ, Hudson DJ, Robertson NJ: **Controlled hydrogenative depolymerization of polyesters and polycarbonates catalyzed by ruthenium(ii) PNN pincer complexes**. *Chem Commun* 2014, **50**:4884–4887.
14. Alberti C, Eckelt S, Enthaler S: **Ruthenium-catalyzed hydrogenative depolymerization of end-of-life poly(bisphenol A carbonate)**. *ChemistrySelect* 2019, **4**:12268–12271.
15. Kindler T-O, Alberti C, Sundermeier J, Enthaler S: **Hydrogenative depolymerization of end-of-life poly-(bisphenol A carbonate) catalyzed by a ruthenium-MACHO-complex**. *ChemistryOpen* 2019, **8**:1410–1412.

16. ** Westhues S, Idel J, Klankermayer J: **Molecular catalyst systems as key enablers for tailored polyesters and polycarbonate recycling concepts**. *Sci. Adv.* 2018, **14**:9669–9677.
The author shows the use of the commercially available Ru/Triphos catalytic system for the degradation of different plastic waste in gram scale. Additionally, mixed plastic waste could be degraded selectively upon the selection of the optimized reaction condition.

17. Elangovan S, Topf C, Fischer S, Jiao H, Spannenberg A, Baumann W, Ludwig R, Junge K, Beller M: **Selective catalytic hydrogenations of nitriles, ketones, and aldehydes by well-defined manganese pincer complexes**. *J Am Chem Soc* 2016, **138**:8809–8814.

18. * Zubar V, Lebedev Y, Azofra LM, Cavallo L, El-Sepelgy O, Rueping M: **Hydrogenation of CO_2-derived carbonates and polycarbonates to methanol and diols by metal-ligand cooperative manganese catalysis**. *Angew Chem Int Ed* 2018, **57**:13439–13443.
The first base-metal-catalyzed hydrogenation of poly(propylene carbonate) to alcohols is reported. Under mild conditions, the reaction proceeds smoothly in the presence of a manganese complex with loading as low as 0.25 mol%.

19. * Liu X, de Vries JG, Werner T: **Transfer hydrogenation of cyclic carbonates and polycarbonate to methanol and diols by iron pincer catalysts**. *Green Chem* 2019, **21**:5248–5255.
The authors described the first example of the use of an earth-abundant Fe complex as the catalyst for the direct hydrogenation polycarbonate to methanol and diols with isopropanol as the hydrogen source.

20. * Dahiya P, Gangwar MK, Sundararaju B: **Well-defined Cp*Co(III)-catalyzed hydrogenation of carbonates and polycarbonates**. *ChemCatChem* 2021, **13**:934–936.
By using well-defined cobalt complexes as a catalyst, the authors reported the catalytic hydrogenation of polycarbonates into their corresponding diols/alcohols with molecular hydrogen as a sole reductant or iPrOH as transfer hydrogenation source.

21. Ferretti F, Scharnagl FK, Dall'Anese A, Jackstell R, Dastgir S, Beller M: **Additive-free cobalt-catalysed hydrogenation of carbonates to methanol and alcohols**. *Catal Sci Technol* 2019, **9**:3548–3553.

22. Fuentes JA, Smith SM, Scharbert MT, Carpenter I, Cordes DB, Slawin AMZ, Clarke ML: **On the functional group tolerance of ester hydrogenation and polyester depolymerisation catalysed by ruthenium complexes of tridentate aminophosphine ligands**. *Chem Eur J* 2015, **21**:10851–10860.

23. Farrar-Tobar RA, Wozniak B, Savini A, Hinze S, Tin S, de Vries JG: **Base-free iron catalyzed transfer hydrogenation of esters using EtOH as hydrogen source**. *Angew Chem Int Ed* 2019, **58**:1129–1133.

24. ** Nunes BFS, Oliveira MC, Fernandes AC: **Dioxomolybdenum complex as an efficient and cheap catalyst for the reductive depolymerization of plastic waste into value-added compounds and fuels**. *Green Chem* 2020, **22**:2419–2425.
The reaction was catalyzed by an eco-friendly, cheap, and air-stable dioxomolybdenum complex $MoO_2Cl_2(H_2O)_2$ and using silanes as reducing agents at the same time, which was successfully applied in depolymerization of PLA, PCL, PDO, and PET.

25. * Fernandes AC: **Reductive depolymerization of plastic waste catalyzed by $Zn(OAc)_2 \cdot 2H_2O$**. *ChemSusChem* 2021. https://doi.org/10.1002/cssc.202100130.
First reusable homogenous catalyst for depolymerization of plastic waste

26. Bagheri AR, Laforsch C, Greiner A, Agarwal S: **Fate of so-called biodegradable polymers in seawater and freshwater**. *Global Challenges* 2017, **1**:1700048.

27. Haider TP, Völker C, Kramm J, Landfester K, Wurm FR: **Plastics of the future? The impact of biodegradable polymers on the environment and on society**. *Angew Chem Int Ed* 2019, **58**:50–62.

28. Román-Ramírez LA, Mckeown P, Jones MD, Wood J: **Poly(lactic acid) degradation into methyl lactate catalyzed by a well-defined Zn(II) complex**. *ACS Catal* 2019, **9**:409–416.

29. Román-Ramírez LA, McKeown P, Shah C, Abraham J, Jones MD, Wood J: *Ind Eng Chem Res* 2020, **59**:11149–11156.

30. Monsigny L, Berthet J-C, Cantat T: **Depolymerization of waste plastics to monomers and chemicals using a hydrosilylation strategy facilitated by Brookhart's iridium(III) catalyst**. *ACS Sustainable Chem Eng* 2018, **6**:10481–10488.

31. Mihut C, Captain DK, Gadala-Maria F, Amiridis MD: **Recycling of nylon from carpet waste**. *Polym Eng Sci* 2001, **41**:1457–1470.

32. Dimitis S, Andriotis LA, Koutsidis IA, Louka DA, Nianias NP, Siafaka P, Tsagkalias I, Tsintzou G: *Material recycling: trends and perspectives*. InTech; 2012.

33. Alberti C, Figueira R, Hofmann M, Koschke S, Enthaler S: **Chemical recycling of end-of-life polyamide 6 via ring closing depolymerization**. *ChemistrySelect* 2019, **4**:12638–12642.

34. Datta J, Błażek K, Włoch M, Bukowski R: **A new approach to chemical recycling of polyamide 6.6 and synthesis of polyurethanes with recovered intermediates**. *J Polym Environ* 2018, **26**:4415–4429.

35. Kumar A, Espinosa-Jalapa NA, Leitus G, Posner YD, Avram L, Milstein D: **Direct synthesis of amides by dehydrogenative coupling of amines with either alcohols or esters: manganese pincer complex as catalyst**. *Angew Chem Int Ed* 2017, **56**:14992–14996.

36. ** Kumar A, von Wolff N, Rauch M, Zou YQ, Shmul G, Ben-David Y, Leitus G, Avram L, Milstein D: **Hydrogenative depolymerization of nylons**. *J Am Chem Soc* 2020, **142**:14267–14275.
The widely used nylons and polyamides were first depolymerized to give amino alcohol or diol and diamine. This ruthenium pincer complex catalyzed hydrogenative depolymerization of nylons offers a new approach toward a cleaner route to recycling nylons.

37. Zhou W, Neumann P, Al Batal M, Rominger F, Hashmi ASK, Schaub T, ChemSusChem: *Depolymerization of technical-grade polyamide 66 and polyurethane materials through hydrogenation*. 2020. https://doi.org/10.1002/cssc.202002465.

38. X. Liu, T. Werner, Chem. Sci. Indirect reduction of CO_2 and recycling of polymers by manganese-catalyzed transfer hydrogenation of amides, carbamates, urea derivatives, and polyurethanes, DOI: 10.1039/D1SC02663A.

39. Gausas L, Kristensen SK, Sun H, Ahrens A, Donslund BS, Lindhardt AT, Skrydstrup T: **Catalytic hydrogenation of polyurethanes to base chemicals: from model systems to commercial and end-of-life polyurethane materials**. *JACS Au* 2021, **143**:517–524.

40. Kratish Y, Li J, Liu S, Gao Y, Marks TJ: **Polyethylene terephthalate deconstruction catalyzed by a carbon-supported single-site molybdenum-dioxo complex**. *Angew Chem Int Ed* 2020, **59**:19857–19861.

41. Ji Y, Lu Y, Puetz H, Schwaneberg U: **Chapter Thirteen - anchor peptides promote degradation of mixed plastics for recycling**. *Methods Enzymol* 2021, **648**:271–292.

Review 3:

Catalytic Methylation Using Methanol as C1 Source

Elghobashy, M.; El-Sepelgy, O.*

In *Dehydrogenation Reactions with 3d Metals*, Sundararaju, B. Ed.; Springer Nature Switzerland, **2024**; pp 173-197.

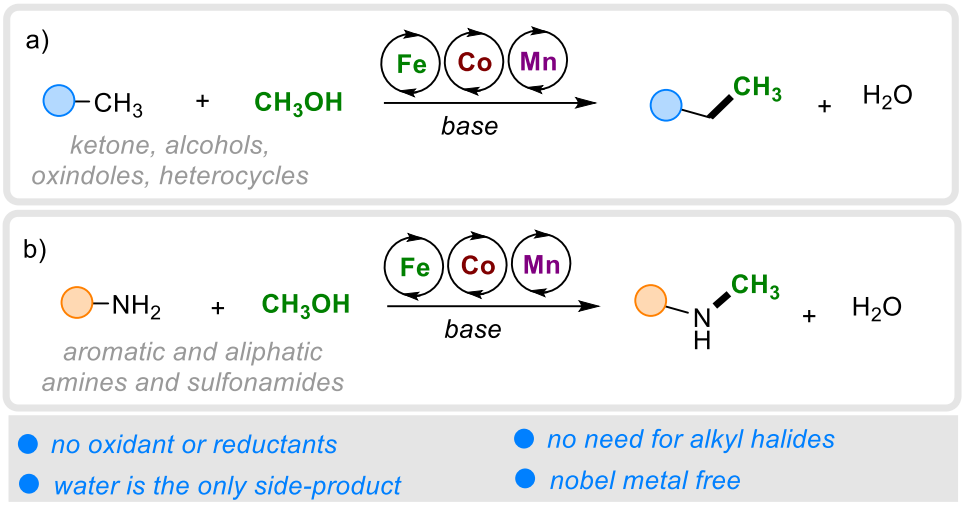

Top Organomet Chem (2024) 73: 173–198
https://doi.org/10.1007/3418_2023_109

Published online: 21 November 2023

Catalytic Methylation Using Methanol as C1 Source

Mohamed Elghobashy and Osama El-Sepelgy

Contents

Abstract The development of 3d metal-catalyzed molecular transformations has been a key focus of research in recent decades. One significant advancement is the discovery of the homogenous iron, cobalt, and manganese-catalyzed (de)-hydrogenation processes. Among these redox transformations, the "Borrowing Hydrogen" (BH) principle, also known as hydrogen auto-transfer, stands out as an

M. Elghobashy and O. El-Sepelgy (✉)
Leibniz Institute for Catalysis e.V., Rostock, Germany
e-mail: Osama.Elsepelgy@Catalysis.de

elegant and eco-friendly method that facilitates the self-transfer of hydrogen between reaction molecules and intermediates, eliminating the need for external hydrogen donors or acceptors. This concept allows for the eco-friendly use of alcohols, such as methanol, as environmentally benign C1 synthons for the alkylation of organic molecules, including pharmaceutically relevant candidates. In this context, the methyl group represents one of the most prevalent carbon fragments in small-molecule drugs. In this book chapter, we summarize the discovery and recent advancements in the use of 3d metal complexes for (multi)methylation of organic compounds using methanol via the hydrogen borrowing methodology. Additionally, we discuss current limitations, challenges, and the future prospects of this field.

Keywords methanol · hydrogen borrowing · catalysis · 3d-metals · C1 synthons

1 Introduction

The "magic methyl" group represents one of the most prevalent carbon fragments in small-molecule drugs. This basic alkyl segment is present in over 67% of top-selling drugs in 2011. It holds significant importance in shaping the pharmaceutical characteristics of diverse bioactive compounds by influencing binding affinities, binding selectivity, solubility, half-life, and various metabolic as well as pharmacokinetic/pharmacodynamic properties [1, 2].

Classical methods for introduction of methyl groups involve the use of toxic and hazardous and waste producing methylating agents such as methyl iodide, diazomethane, methyl triflate, trimethyl oxonium tetrafluoroborate, and dimethyl sulfate [3]. An industrially applied method for the methylation and dimethylation of amines involves the application of Eschweiler-Clarke reaction [4]. The reaction involves the reductive amination with the carcinogenic formaldehyde followed by hydrogenation. For sustainability reasons, the use of greener C1 alternatives such as methanol is of particular interest (*see* Fig. 1a, b). However, a major challenge lies in the energetically demanding dehydrogenation of methanol ($\Delta H = +84$ kJ mol–1) [5].

The key to the success of this chemistry is the use of appropriate transition metal catalysis that can enable the transformation using the concept of hydrogen borrowing or hydrogen autotransfer (*see* Fig. 1a, b) [6]. The initial step involves the transition-metal-catalyzed dehydrogenation of methanol, leading to the in-situ production of formaldehyde while storing the hydrogen on the transition metal catalyst. Then, base-catalyzed condensation between formaldehyde and the C- or N- nucleophiles, such as amines or active methylene or methyl compound, leads to the formation of imines or electron-deficient olefins. These intermediates can undergo hydrogenation with the borrowed hydrogen on the transition metal catalyst, leading to the formation of the C- or N-methylated products without the need for the use of and external oxidant or reductant (*see* Fig. 1c, d).

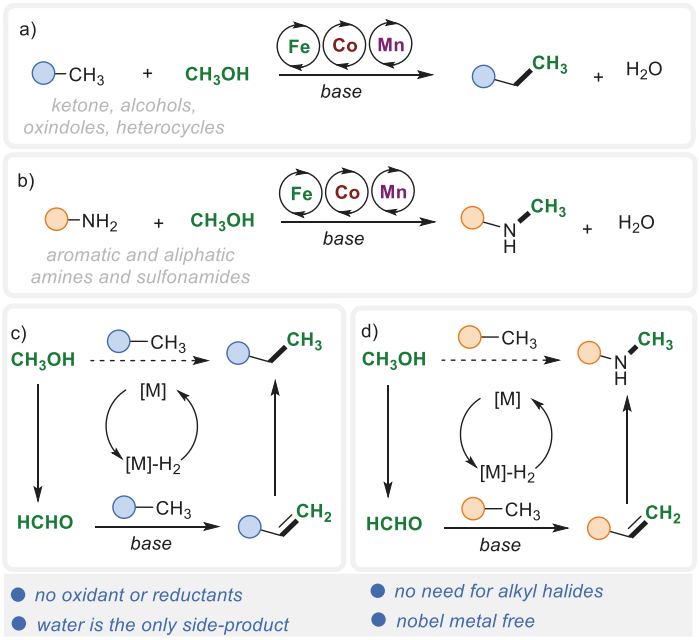

Fig. 1 Methylation using methanol via hydrogen borrowing concept

1.1 Catalyst Development

The use of alcohols, including methanol, as alkylating reagents was initially developed using noble-metal catalysis such as ruthenium and iridium catalysis. Yet, in recent times, a notable headway has been achieved in substituting these precious metals with base-metal alternatives, with a focus on iron, cobalt, and manganese [7]. In this context, we provide a succinct overview of the most important 3d transition metal catalytic systems that have been harnessed for C- and N-methylation reactions utilizing methanol through the concept of hydrogen borrowing (depicted in Fig. 2).

Iron catalysis: In 2007, Caesy [8] initially discovered the distinct catalytic capability of the iron hydride hydroxycyclopentadienyl complex **Fe-1a** [9] for heterolytic hydrogen activation. Subsequently, multiple research teams elucidated the in-situ formation of bifunctional iron (II) hydride complexes. This is achieved through the utilization of air- and moisture-stable iron (0) cyclopentadienone complexes, such as **Fe-1** and **Fe-2**. These pre-catalysts can be in situ activated through the removal of one carbonyl ligand using trimethylamine *N*-oxide [10], a suitable inorganic base [11], or light exposure [12] (*see* Fig. 3a). Notably, these phosphine-free complexes can be readily synthesized from economical materials, suggesting a promising potential for extensive industrial application [13].

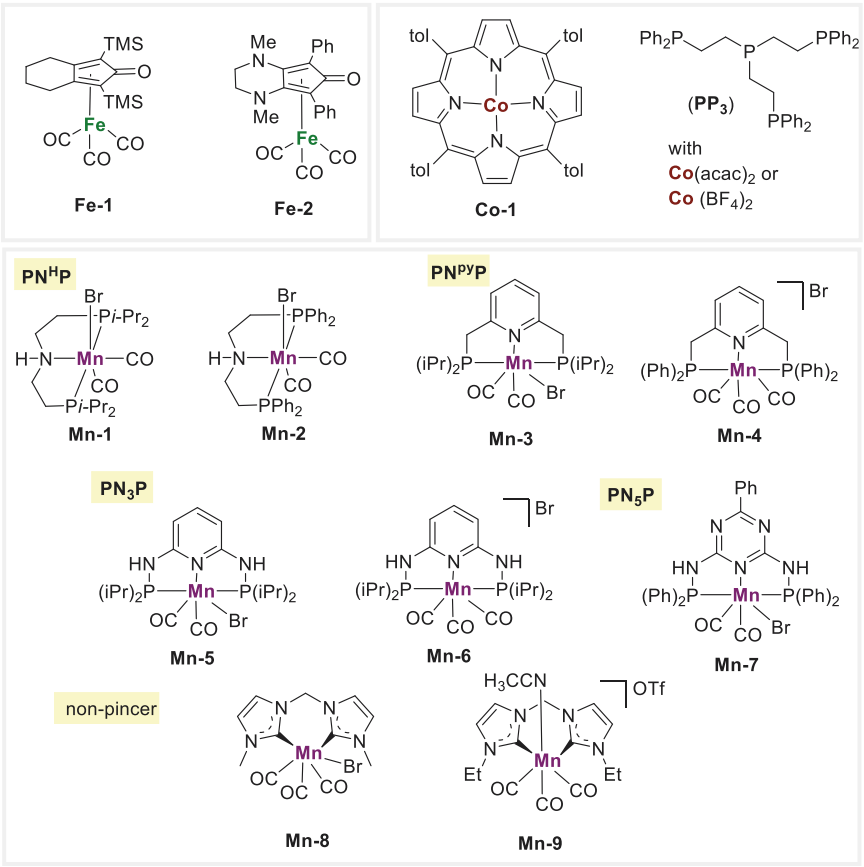

Fig. 2 3d transition metal catalysis used for methylation with methanol

Cobalt catalysis: Compared to iron and manganese, cooperative metal-ligand complexes based on cobalt have received relatively less attention. Nonetheless, a simple mixture of cobalt salts like $Co(acac)_2$ or $Co(BF_4)_2$ with tri- or tetra-dentate phosphines, such as 1,1,1-Tris(diphenylphosphinomethyl)ethane (Triphos) [14] or bis(diphenylphosphinoethyl)phenylphosphine (PP_3) [15], has demonstrated significant utility in (de)hydrogenation reactions, including the innovative concept of hydrogen borrowing methylation. Mechanistically, it involves the hydrogen activation through the classical monohydride pathway.

Manganese catalysis: In the spring of 2016, the breakthrough discovery of manganese hydrogenation catalysis was made by the research teams led by Beller [16] and Milstein [17]. Subsequent to this pioneering work, there has been a remarkable acceleration in advancements, propelling manganese to the forefront of 3d transition metals utilized in (de)hydrogenation transformations in under 3 years [18–20].

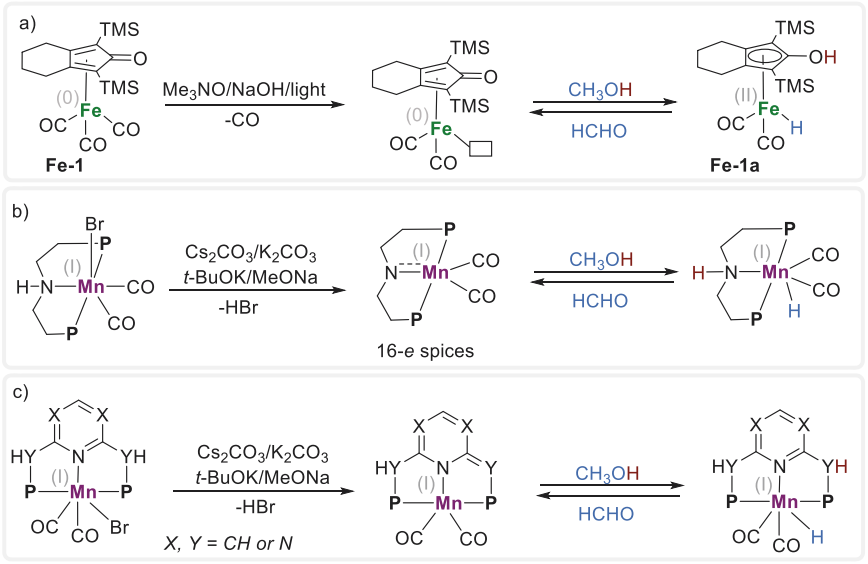

Fig. 3 Methanol dehydrogenation via metal ligand cooperation (MLC)

In terms of the mechanism, manganese catalysis employing the aliphatic PNHP "aminopincer" motif (such as **Mn-1 to Mn-2**), sharing structural similarities with Noyori's original catalysts, can undergo in situ activation through a suitable base. This leads to the formation of a catalytically active 16-electron species, as illustrated in Fig. 3b. Furthermore, the pyridine-based pincer ligands $PN^{Py}P$ and PN_3P, along with the trizine ligand PN_5P, have also seen extensive application in manganese (de)hydrogenation catalysis (**Mn-3** to **Mn-7**). Upon the introduction of a base, deprotonation of a CH_2 or NH group within the backbone results in the generation of an anionic, "dearomatized" pincer ligand with amide-like characteristics. Such dearomatized complexes can engage in stoichiometric, cooperative hydrogen activation through 1,3-addition across the metal-ligand framework, facilitated by the presence of a base (*see* Fig. 3c).

More recently, non-metal-ligand cooperative (MLC) pathways have also gained prominence in manganese (de)hydrogenation catalysis, exemplified by cases like **Mn-6** and **Mn-7**.

This book chapter provides a comprehensive overview of endeavors focused on the direct incorporation of methyl groups onto C–H and N–H bonds, utilizing methanol as a valuable C1 source. This advancement is made possible through the application of homogeneous catalysis anchored in 3d metals. Distinguishing itself from recent reviews [21–24], this chapter offers a critical synthesis of advancements in this domain, dissecting the progress achieved in each transformation. Notably, this chapter undertakes a systematic comparison of diverse catalytic systems, shedding light on their respective merits and limitations within this field of research.

2 N-Methylation

2.1 Methylation of Aromatic Amines

In 2016, Beller reported the first base-metal-catalyzed methylation using methanol. The authors have outlined the N-methylation of aniline derivatives with methanol using 3 mol% of a PNP manganese pincer complex (**Mn-1**) in the presence of *t*-BuOK (1 equiv.) at 100°C (Scheme 1, Condition A) [25]. Soratis et al. later reported a similar method using 5 mol% of PN_3P (**Mn-6**) at 120°C with only 20 mol% of *t*-BuOK (Condition B) [26]. Shortly after, Beller disclosed a modified method using 0.5 equiv. t-BuOK at 100°C (Condition C) [27]. More recently, an *N*-heterocyclic carbene-based Mn(I) catalyst (**Mn-8**) was showcased by Ke et al., utilizing 1.5 mol% of the non-pincer catalyst and 1 equivalent of *t*-BuOK at 120°C in toluene (Condition D) [28].

Meanwhile, Liu et al. demonstrated that a mixture of 5 mol% $Co(acac)_2$ and tetradentate phosphine ligand PP_3, with 1 equiv. K_3PO_4 at 140°C (Condition E) [29]. Also, Renaud et al. disclosed the use of the electron-rich Fe tricarbonyl complex (**Fe-2**) and only 10 mol% of CsOH at 110°C leading to similar results (Condition F) [30]. All the previously mentioned studies showed a great tolerance for a wide range of substitutions with electron-donating and electron withdrawing groups in ortho, meta and para positions. Interestingly, several hydrogen sensitive functional groups such as nitro, ketone, ester, amide, and olefins were tolerated under these conditions. These methodologies were also found to tolerate different heteroaromatic amines such as pyridines.

2.2 Reductive Methylation of Nitrobenzene Derivatives

In 2020, Morrill et al. demonstrated the direct conversion of nitrobenzene derivatives to *N*-methylarylamines using 5 mol% of Mn-PN_3P pincer complex (**Mn-6**) with KOH (2 equiv.) and 4 Å MS at 110°C [31]. The process involves tandem transfer hydrogenation followed by methylation, with methanol serving as both a hydrogen donor and a methylation reagent (Scheme 2).

The optimized method exhibited compatibility with meta- and para-electron-donating and electron-withdrawing substituents, but not with ortho-substitution due to hindered hydrogenation. The protocol also tolerated hydrogen-sensitive functional groups such as alcohols and alkenes, yielding moderate results.

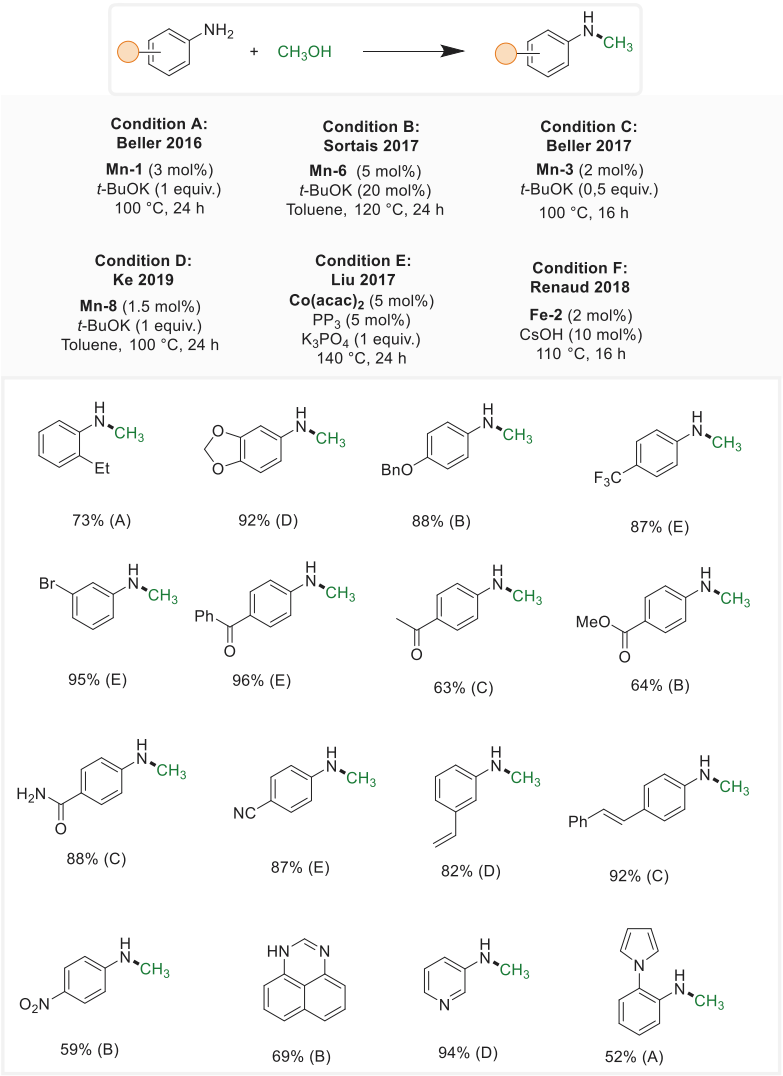

Scheme 1 N-methylation of arylamines

2.3 *Methylation of Sulfonamides*

Regarding sulfonamides methylation, Soratis et al. employed the PN_3P manganese catalyst **Mn-6** (Condition A). The procedure utilized 5 mol% of the Mn-pincer complex and 1.2 equivalents of *t*-BuOK as the base. The reaction occurred at 120° C in toluene as a cosolvent for 60 h [31]. Soon after, Morrill et al. introduced iron catalysts for the same process (Condition B). This involved 8 mol% of **Fe-2**, along

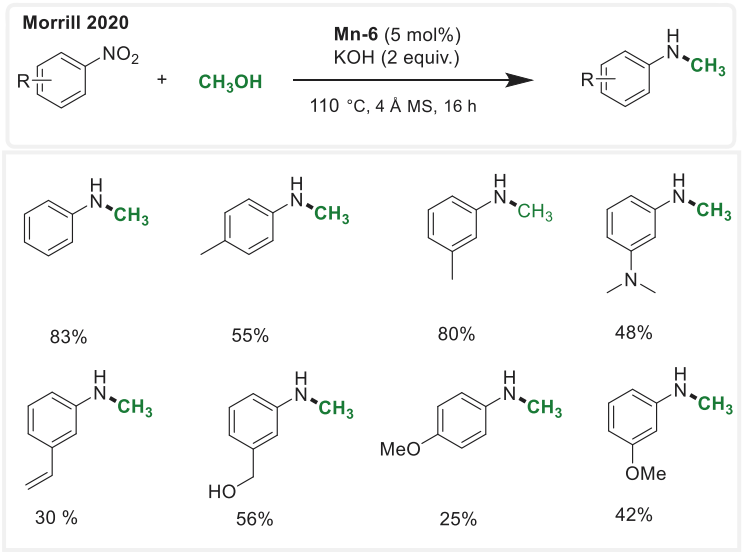

Scheme 2 Reductive methylation of nitrobenzene

with 4 mol% of trimethylamine *N*-oxide and 2 equivalents of K_2CO_3 at 100°C for only 24 h. These methods successfully produced a variety of monomethylated aromatic and aliphatic sulfonamides in excellent yields (Scheme 3) [32].

2.4 Methylation Aliphatic Amines

Using the hydrogen borrowing concept, aliphatic secondary and primary amines can also be mono-and dimethylated using methanol under base-metal catalysis conditions. In 2017, Liu et al. employed a mixture of 5 mol% of $Co(acac)_2$ with 5 mol% of the tetradentate phosphine ligand (PP_3). The reaction was carried out in the presence of 1 equivalent of K_3PO_4 as a base at 140°C (Scheme 4, Condition A) [29]. A year later, the groups of Renaud [30] and Morril [32] independently reported two methodologies based on the use of iron carbonyl complexes. Renaud et al. utilized 2 mol% **Fe-2** and 10 mol% CsOH at 110°C (Condition B). However, to ensure good yields, the reaction was conducted under 10 atm of H_2. On the other hand, the use of **Fe-1** (4 mol%) and Me_3NO (8 mol%) and 2 equivalents of K_2CO_3 led to similar results without the need of additional hydrogen gas (Condition C).

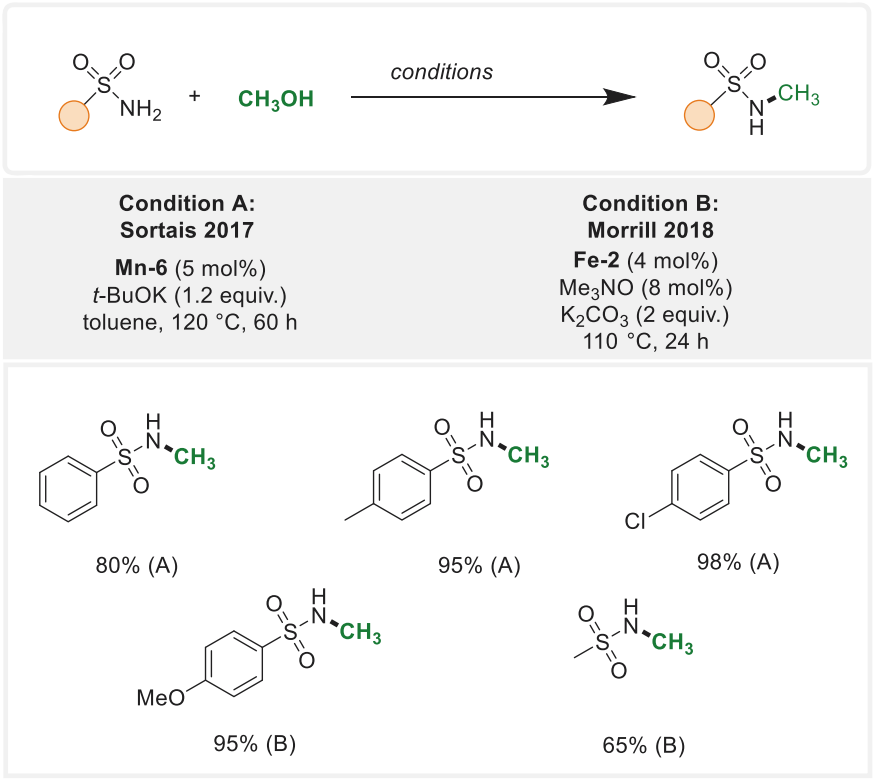

Scheme 3 Methylation of sulfonamides

3 C-Methylation

3.1 α-Methylation of Ketones

In 2019, El-Sepelgy/Rueping demonstrated a mild manganese-catalyzed approach for α-methylation and dimethylation of aromatic and aliphatic ketones. 2.5 mol% of the PNP manganese complex **Mn-4** was used, along with 2 equivalents of Cs_2CO_3 at 85°C (Scheme 5, Condition A) [33]. Meanwhile, Soratis et al. presented a related manganese-catalyzed α-methylation of ketones using 3 mol% of PN_3P complex (**Mn-6**) and 50 mol% of *t*-BuONa as a base at 120°C (Condition B) [34].

The iron version of this transformation was first reported by Morill et al. However, the scope of the iron-catalyzed transformation was limited to the relatively more active aromatic ketones. The iron-catalyzed methylation of ketones involves the use of 2 mol% of **Fe-1**, 4 mol% of Me_3NO and 2 equivalents of K_2CO_3 at 80 (Condition C) [32]. Very recently, Sundararaju et al. reported that 4 mol% of **Fe-1** in the presence of 2 equivalents of *t*-BuOK for 24 h at 42°C under visible light

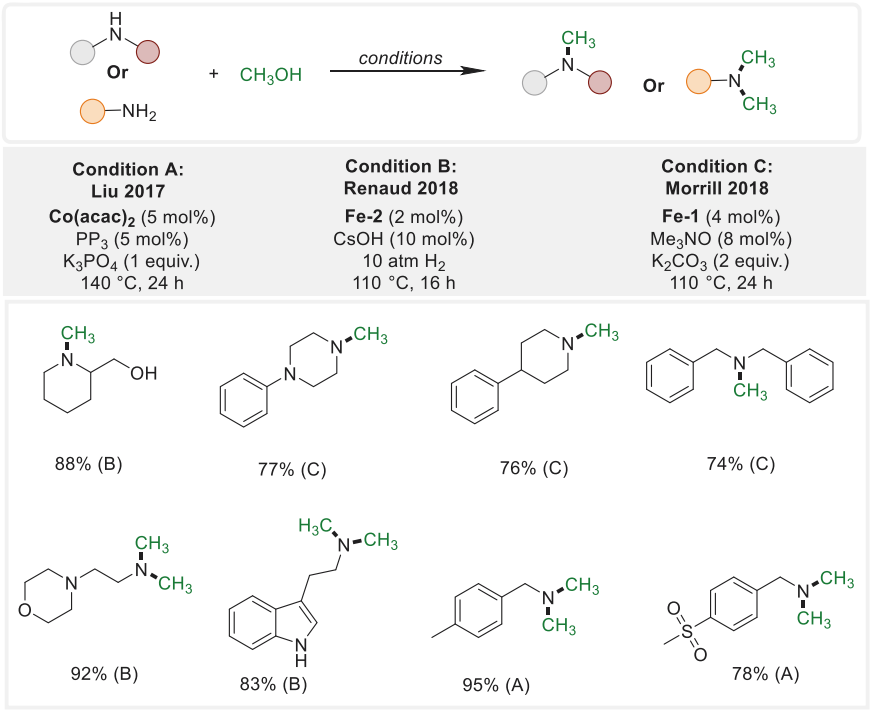

Scheme 4 Methylation of primary and secondary amines

irradiation (Condition D) [35]. Control experiments revealed that no reaction was observed in the absence of light at 40°C.

Furthermore, Liu et al. also disclosed cobalt catalytic system for the α-methylation of ketones with methanol. The authors demonstrated the need of 1 mol% $Co(BF_4)_2{\cdot}6H_2O$ and 1 mol% of a tetradentate phosphine ligand, $P(CH_2CH_2PPh_2)_3$ in the presence of 1 equivalent of K_3PO_4 at 100°C (Condition E) [36]. Similar to the iron catalytic system the reaction scope was limited to aromatic ketones.

Importantly, El-Sepelgy and Rueping have demonstrated the usefulness of the metal-ligand cooperation concept for the methylation of ketones with highly selective isotope labelling. An example is shown in Scheme 6, the methylation of propiophenone with four different labeled methanol, led to the formation of 4 different isotope-labeled isobutyrophenone derivatives.

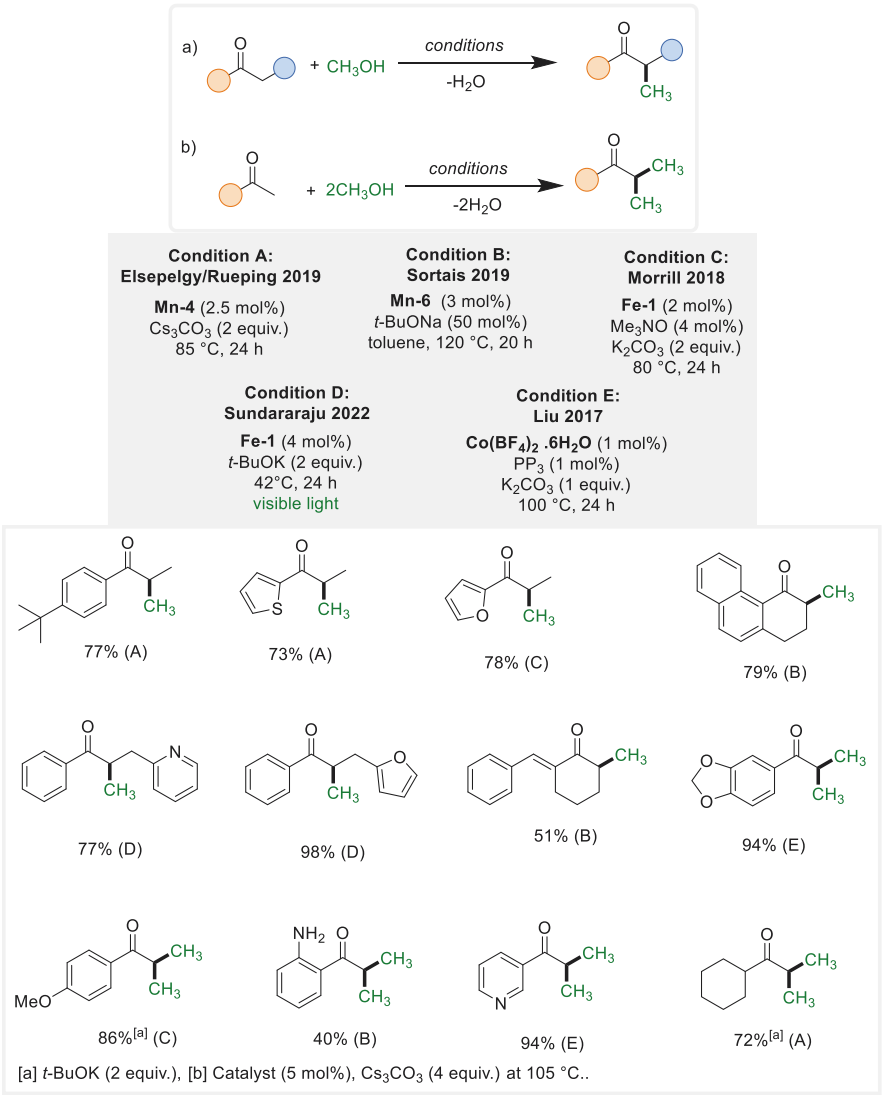

Scheme 5 α-methylation and double methylation of ketones

3.2 α-Methylation of Oxindoles

The α-methylation of ketones was further extended to activated amides (oxindole). In this regard, Morrill demonstrated that 2 mol% of **Fe-1** activated by 4 mol% of Me_3NO could be used for the methylation of oxindoles in the presence of 2 equivalents of K_2CO_3 at 80 to 110°C (Scheme 7). Interestingly, unprotected oxindoles bearing free NH was also amendable to the iron catalytic system [32].

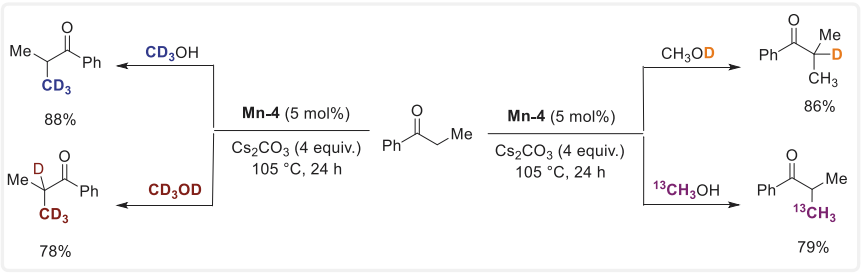

Scheme 6 Selective methylation of propiophenone using label methanol

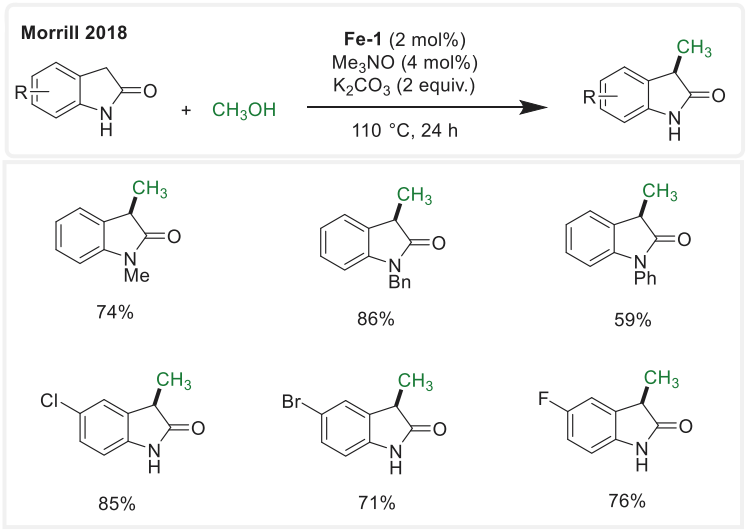

Scheme 7 α-methylation of oxindoles

3.3 Tandem Isomerization α-Methylation of Allylic Alcohols

In 2009, Morrill et al. demonstrated that α-methylated ketones can be synthetized upon the use of allylic alcohols instead of ketones (Scheme 8). The authors utilized 2 mol% of **Fe-2** catalyst in the presence of 2 equivalents of K_2CO_3 and 4 mol% of Me_3NO at 130°C for 24 h. This process involves tandem iron-catalyzed isomerization of the allylic alcohol to the corresponding ketone followed by iron-catalyzed methylation with methanol. The developed protocol was found to tolerate a wide range of allylic alcohols including aliphatic alcohols and heterocylic-containing substrates [37].

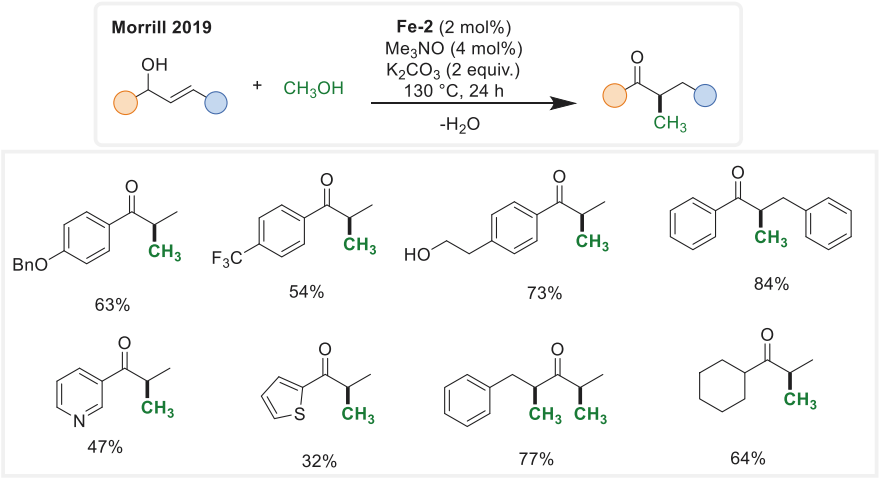

Scheme 8 Isomerization α-methylation of allylic alcohols

3.4 *Tandem Hydrogenation α-Methylation of α,β-Unsaturated Ketones*

Similarly, to the previous protocol, Kundu et al. decided to synthetize α-methylated ketones starting from α,β-unsaturated ketones. The authors have used a phosphine free bis-NHC manganese complex **Mn-9** combined with 0.5 equivalents of the strong base NaOH. The reaction was conducted at 120°C for 5 h [38]. The tandem transformation starts with manganese-catalyzed transfer hydrogenation to form ketones using methanol as a hydrogen donor followed by the typical manganese-catalyzed methylation. The reaction also showed a good tolerance to different functional groups including hydrogenation sensitive moieties (Scheme 9).

3.5 *β-Methylation of 2-Arylethanol*

Next to ketones, several groups have also investigated β-Methylation of alcohols with methanol. The reaction involves double hydrogen auto-transfer, where both methanol and the alcohol substrate undergo dehydrogenation followed by condensation. The formed α,β-unsaturated ketone then underwent double hydrogenation to produce the desired β-methylated alcohol.

The first base-metal-catalyzed alcohol methylation protocol was reported by Renaud in 2019. The catalytic system involves the use of the iron carbonyl complex **Fe-2** together with NaOH (10 mol%) and *t*-BuONa at 110°C for 40 h (Scheme 10, Condition A) [39]. However, the iron-catalyzed transformation is limited to the relatively high activation of 2-arylethanol. One year later, Leitner et al. developed

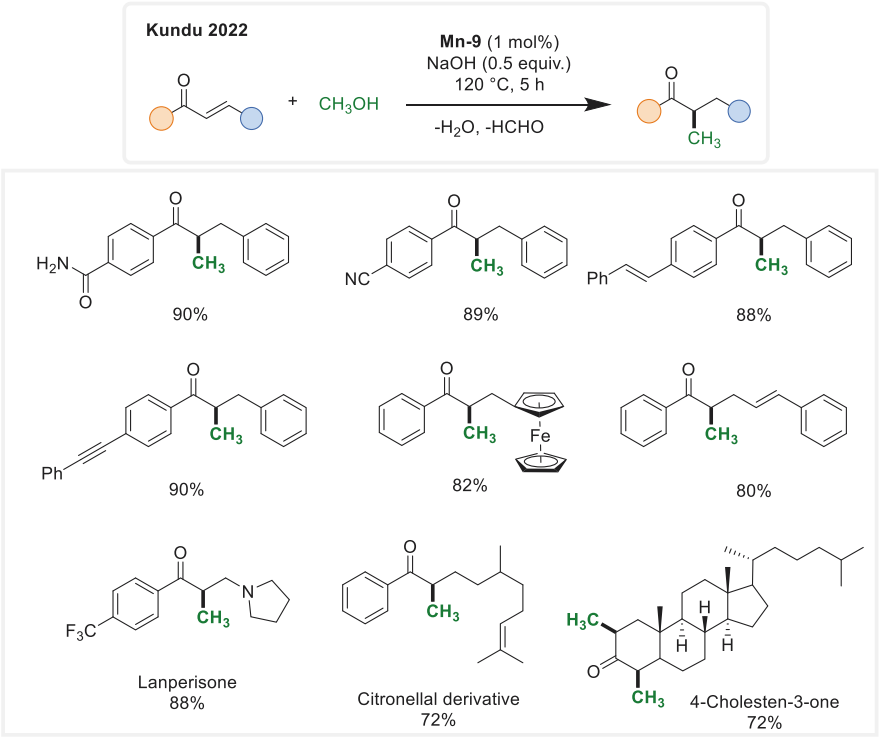

Scheme 9 Tandem hydrogenation α-methylation of α,β-unsaturated ketones

highly selective approach for the methylation of the same substates using 0.5 mol% of **Mn-1** and 2 equivalents NaOMe at 150°C (Scheme 10, Condition B) [40].

3.6 β-Methylation of Alcohols

Interestingly, the Leitner's protocol for the β-Methylation of 2-arylethanol was also found to be effective for the methylation of more challenging alcohols including purely aliphatic examples (Scheme 11, Condition A) [40]. Almost at the same time, Kempe et al. introduced another manganese-catalyzed methylation and multi-methylation of challenging alcohols using only 0.1 mol% of the **Mn-7** (Condition B) [41]. Selected examples from both protocols are shown in Scheme 11. These methodologies tolerate a diverse range of sensitive functional groups to produce the desired methylated and multi-methylated alcohols in high yields. Impressively, the methodologies exhibited good reactivity in the methylation of various aliphatic alcohols, encompassing those derived from biomass, diols, natural products, and drug molecules.

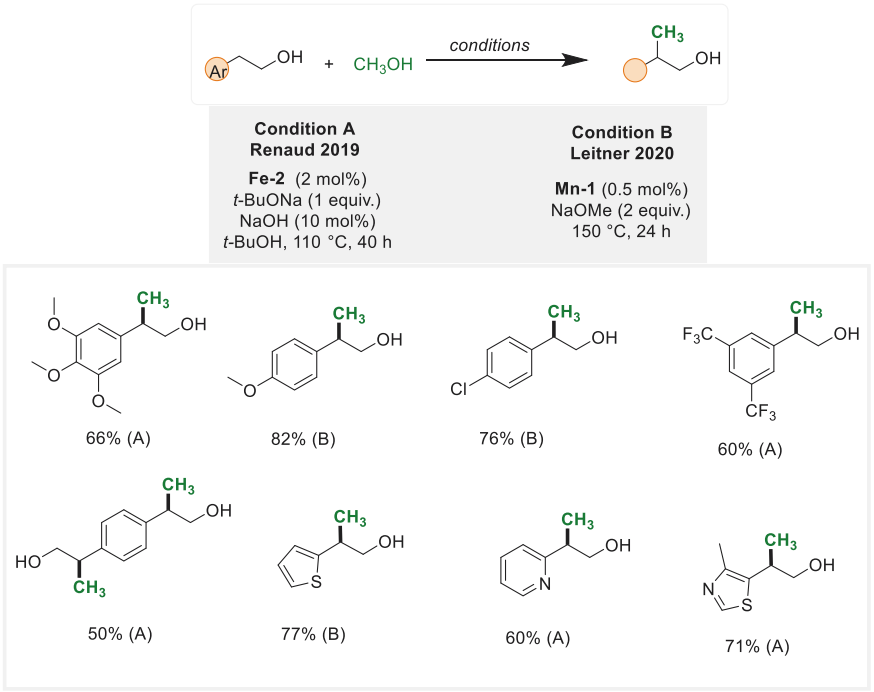

Scheme 10 β-Methylation of 2-arylethanol

3.7 α-Methylation of Nitriles

As presented in the previous section, most of the *C*-methylation protocols involve direct α-methylation of ketones or in situ formation of ketones from alcohols, allylic alcohols, and unsaturated ketones. In addition, most of these transformations require the use of equivalent amounts of base.

In 2019, Rueping/El-Sepelgy et al. demonstrated a manganese-catalyzed approach for α-methylation of nitriles under relatively mild conditions. This method utilized 5 mol% of the PNP manganese complex **(Mn-2)**, combined with 10 mol% of the mild base Cs_2CO_3. The reaction was conducted at 135°C in the presence of 1,4-dioxane as a cosolvent [42]. The key to success of this transformation even using only 10% of carbonate salt is the critical role of the bifunctional manganese catalyst for the activation of both methanol and the nitrile substrate. The proposed mechanism is shown in Scheme 12 below.

The cobalt version of this transformation was also reported by Liu et al. Employing conditions similar to those employed in the α-methylation of ketones, this method involved the use of a mixture of 1–2.5 mol% $Co(BF_4)_2{\cdot}6H_2O$ and tetradentate phosphine ligand (PP_3). The reaction was carried out in the presence of 1 equivalent of K_3PO_4, serving as the base, at 100°C for 24 to 48 h [36].

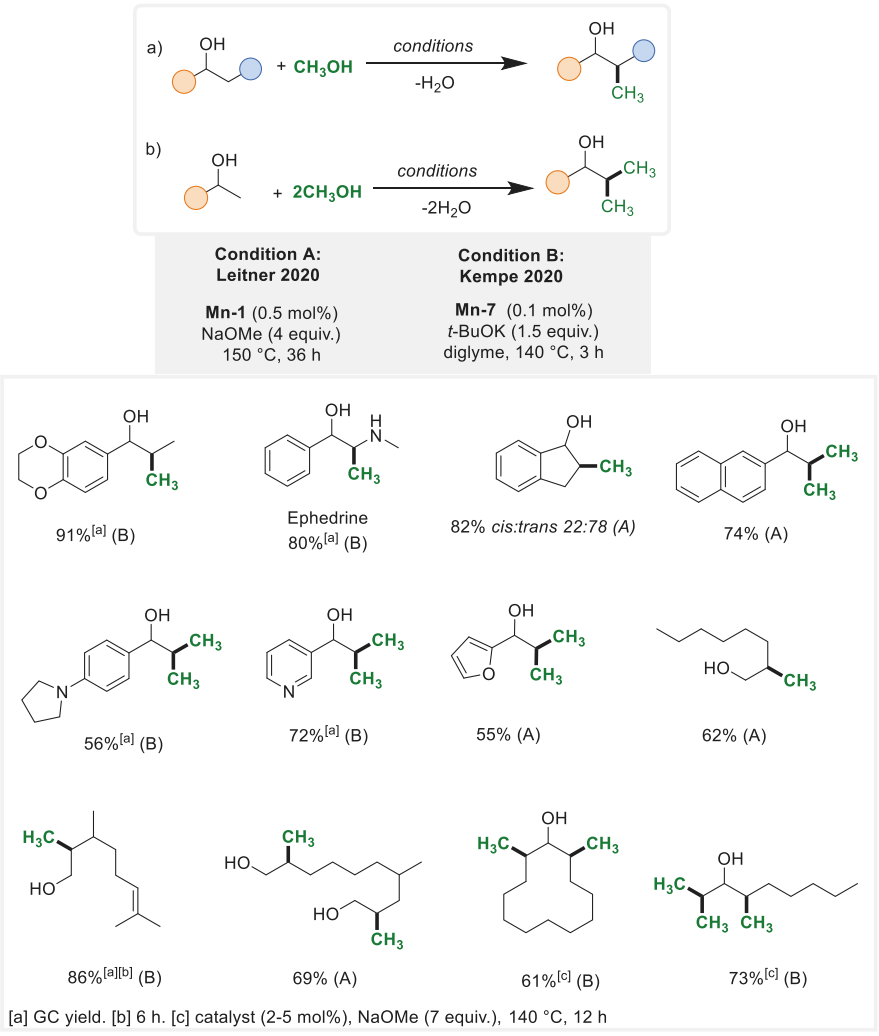

Scheme 11 β-Methylation of alcohols

3.8 Methylation of N-Heterocycles

Liu et al. also extended their cobalt-catalyzed methylation system ($Co(BF_4)_2{\cdot}6H_2O$/PP_3) to C(3)-methylation indoles. The reaction was carried out in the presence of 1 equivalent of K_3PO_4, serving as the base at 100°C (Scheme 13, Condition A) [36]. Also, Morill et al. have shown that iron could be used for the same transformation (Scheme 13, Condition B) [32].

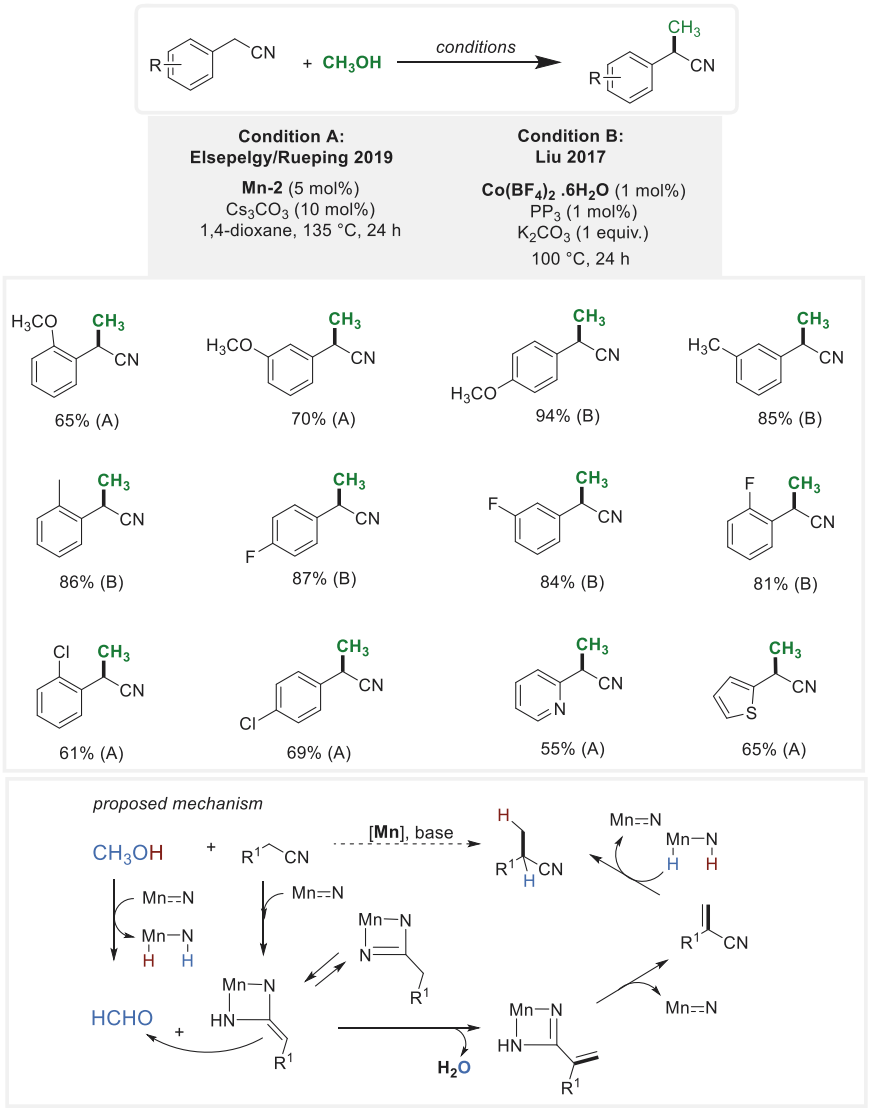

Scheme 12 α-Methylation of Nitriles

4 C- and Heteroatom Methylation

The chemistry of C- and N-methylation using hydrogen borrowing can be further applied to more complex transformations. In this regard, the hydrogen borrowing process is interrupted by the addition of nucleophile such as amines or alcohols.

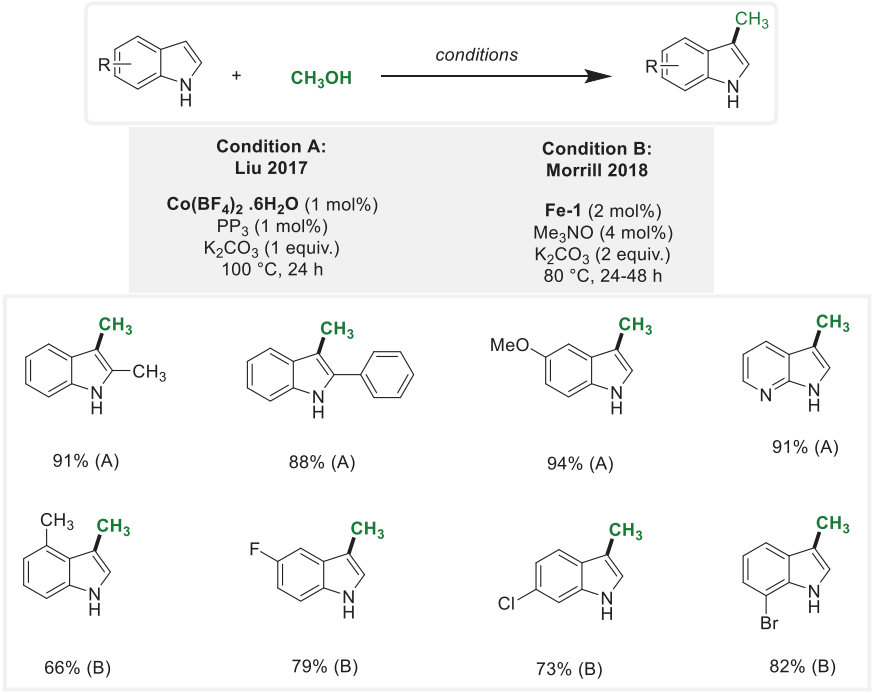

Scheme 13 Methylation of N-Heterocycles

4.1 Aminomethylation of Activated Aromatic Compounds

In 2017, Kichner et al. reported the first instance of manganese-catalyzed three-component aminomethylation of activated aromatic compounds. Their research employed the preprepared hydride form of (**Mn-5**) at 4 mol% loading, along with 1.3 equivalents of t-BuOK. The reaction took place at 130°C in toluene [43]. This method exhibited a broad substrate scope, encompassing diverse aromatic and heteroaromatic compounds, along with various amines and methanol. These conditions yielded the corresponding amino-methylated products in good-to-high yields (Scheme 14).

4.2 α-Aminomethylation of Ketones

In 2018, Xiao et al. introduced a successful cobalt-catalyzed approach for α-aminomethylation of ketones using methanol as the C1 source. This method involved a one-pot, two-step process for the three-component α-aminomethylation of ketones. The used catalyst was $CoCl_2 \cdot 6H_2O$ (3 mol%), along with 2 equivalents

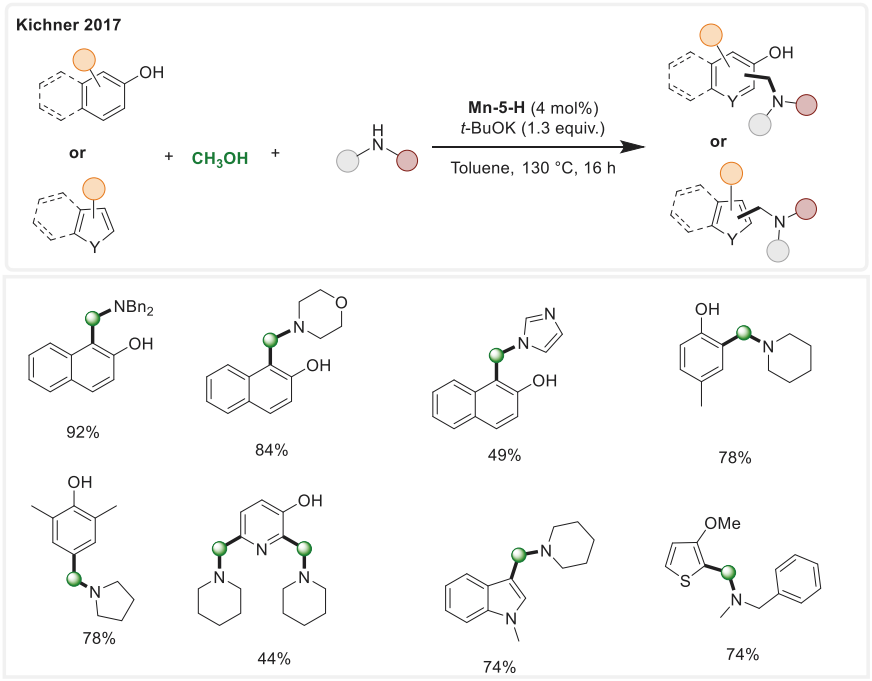

Scheme 14 Aminomethylation of activated aromatic compounds

of Cs_2CO_3 as the base and 1.5 equivalents of *t*-butyl hydroperoxide (TBHP) as the oxidizing agent. The reaction pathway, outlined in Scheme 15, emphasizes the amination of the in situ formed unsaturated ketone as the key step. TBHP's presence is proposed to prevent the completion of the hydrogen borrowing process. This established technique exhibited wide applicability that facilitate the synthesis of various α-aminomethylated ketones, including heterocyclic-based substrates [44].

4.3 α-Methoxymethylation of Ketones

The same group extended the established procedure for the aminomethylation of ketones to α-methoxymethylation of ketones. Interestingly, methanol plays a dual role as methylation and methoxylation source [44] (Scheme 16).

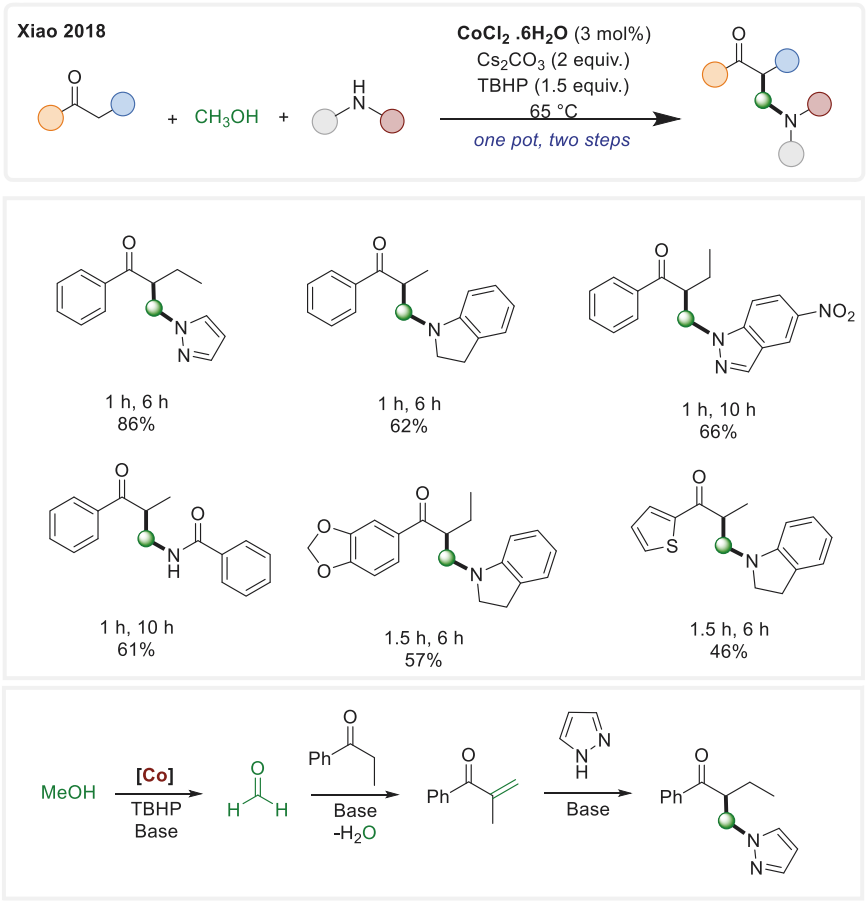

Scheme 15 α-aminomethylation of ketones

5 Two Carbon Methylation

In 2021, Chandrasekhar et al. presented a rare instance of utilizing methanol as a C1 source for synthesizing symmetrical 1,5-diketones. This innovative process employed a Co(II) porphyrin complex (**Co-1**) with *t*-butoxide salt at 135°C [45]. The sequence involves methanol dehydrogenation to formaldehyde, followed by base-catalyzed condensation, resulting in an α-methylenated intermediate. Within the described reaction conditions, this methylenated intermediate reacts with another ketone substrate molecule in the presence of the butoxide base, leading to Michael-type reactions. These steps culminate in the production of diverse 1,5-ketones with yields ranging from moderate to excellent (Scheme 17).

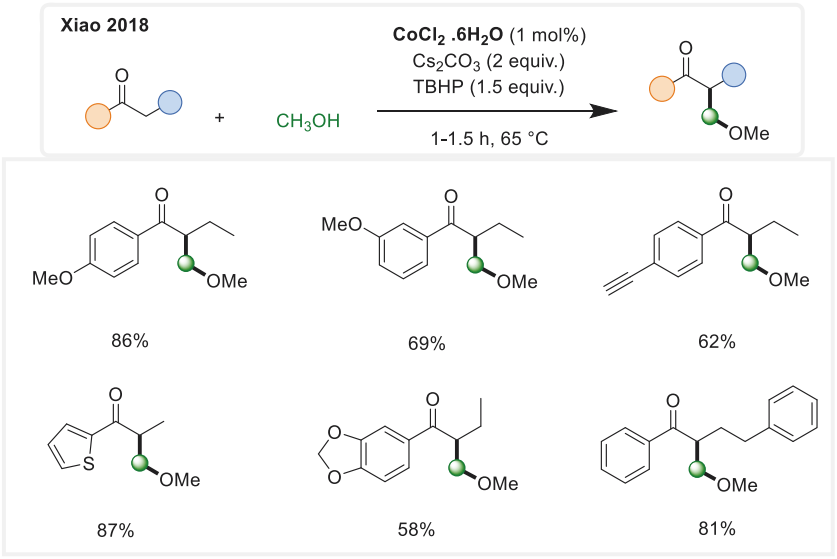

Scheme 16 α-methoxymethylation of ketones

6 Conclusion and Outlook

In summary, we have provided an overview of the chemistry involving methanol as a methylating reagent through the process of base-metal-catalyzed hydrogen borrowing. The inception of this chemistry dates back to 2016. It revolves around two primary processes: the hydrogen borrowing steps catalyzed by iron, cobalt, and manganese complexes, and the subsequent base-catalyzed condensation between the substrate and the in situ generated formaldehyde. Among these metals, manganese has exhibited the highest activity in most cases. Nonetheless, the cost-effective iron carbonyl complexes hold notable economic significance. Cobalt catalytic systems have demonstrated the advantage of not requiring pre-synthesized complexes.

Future endeavors might focus on the utilization of more affordable and stable homogeneous catalysis, specifically exploring combinations of readily available base metal salts such as Co(II), Fe(II), and Mn(II) with NHC or nitrogen-based ligands. Additionally, developing recyclable heterogeneous catalysis would mark a crucial advancement [46–49] for large-scale applications. Substituting high thermal energy with environmentally friendly visible light offers another avenue [50].

However, the central challenge lies in broadening the scope of this chemistry to encompass a wider range of substrates such as unactivated amides, esters, and other aromatic-aliphatic C-H containing compounds. This will entail devising alternatives to the base-catalyzed conditions that can be seamlessly integrated with hydrogen borrowing catalysis.

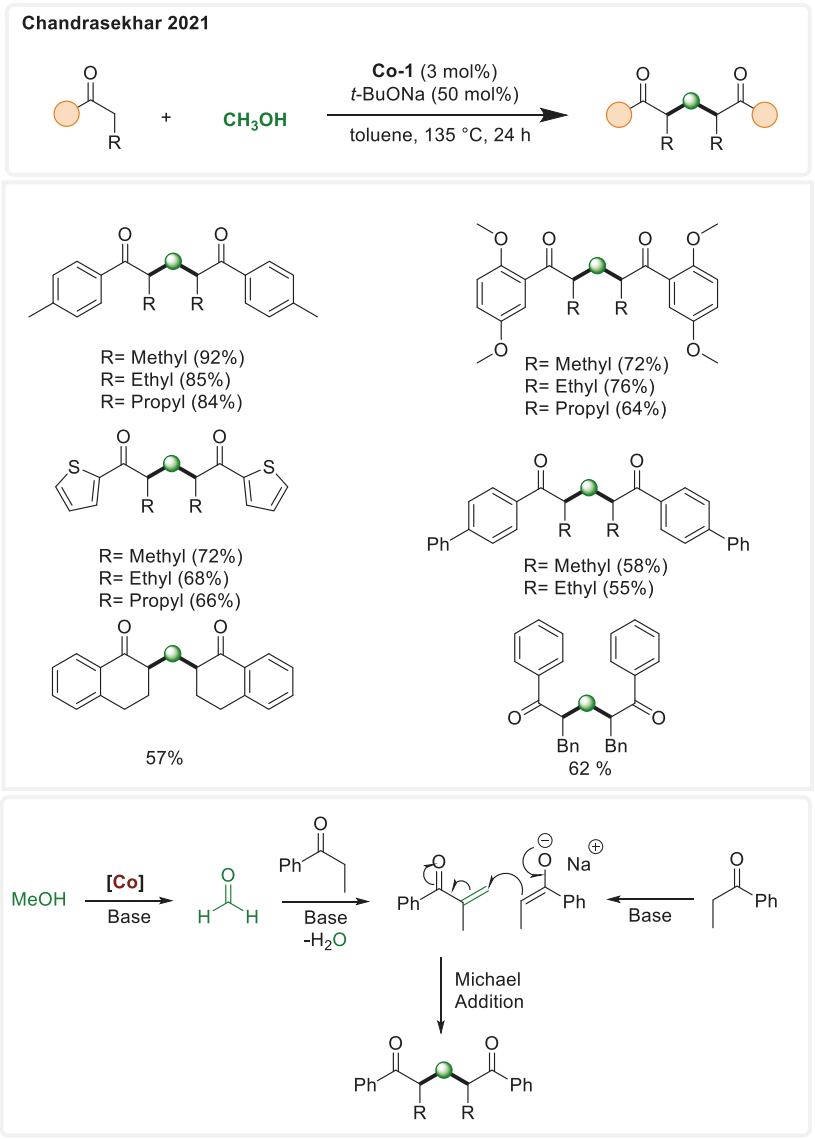

Scheme 17 Synthesis of symmetrical 1,5-diketons using methanol as C1 source

References

1. Aynetdinova D, Callens MC, Hicks HB, Poh CYX, Shennan BDA, Boyd AM, Lim ZH, Leitch JA, Dixon DJ (2021) Installing the "magic methyl" – C-H methylation in synthesis. Chem Soc Rev 50(9):5517-5563. https://doi.org/10.1039/D0CS00973C

2. Schönherr H, Cernak T (2013) Profound methyl effects in drug discovery and a call for new C–H methylation reactions. Angew Chem Int Ed 52(47):12256–12267. https://doi.org/10.1002/anie.201303207
3. Chen Y (2019) Recent advances in methylation: a guide for selecting methylation reagents. Chem A Eur J 25(14):3405–3439. https://doi.org/10.1002/chem.201803642
4. Pine SH, Sanchez BL (1971) Formic acid-formaldehyde methylation of amines. J Org Chem 36(6):829–832. https://doi.org/10.1021/jo00805a022
5. Selva M, Perosa A (2008) Green chemistry metrics: a comparative evaluation of dimethyl carbonate, methyl iodide, dimethyl sulfate and methanol as methylating agents. Green Chem 10(4):457–464. https://doi.org/10.1039/B713985C
6. Corma A, Navas J, Sabater MJ (2018) Advances in one-pot synthesis through borrowing hydrogen catalysis. Chem Rev 118(4):1410–1459. https://doi.org/10.1021/acs.chemrev.7b00340
7. Irrgang T, Kempe R (2019) 3d-metal catalyzed N- and C-alkylation reactions via borrowing hydrogen or hydrogen autotransfer. Chem Rev 119(4):2524–2549. https://doi.org/10.1021/acs.chemrev.8b00306
8. Casey CP, Guan H (2007) An efficient and chemoselective iron catalyst for the hydrogenation of ketones. J Am Chem Soc 129(18):5816–5817. https://doi.org/10.1021/ja071159f
9. Knölker H-J, Baum E, Goesmann H, Klauss R (1999) Demetalation of tricarbonyl (cyclopentadienone)iron complexes initiated by a ligand exchange reaction with NaOH – X-ray analysis of a complex with nearly square-planar coordinated sodium. Angew Chem Int Ed 38(13–14):2064–2066. https://doi.org/10.1002/(SICI)1521-3773(19990712)38:13/14<2064::AID-ANIE2064>3.0.CO;2-W
10. Pagnoux-Ozherelyeva A, Pannetier N, Mbaye MD, Gaillard S, Renaud J-L (2012) Knoelker′s iron complex: an efficient in situ generated catalyst for reductive amination of alkyl aldehydes an amines. Angew Chem Int Ed 51(20):4976-4980. https://doi.org/10.1002/anie.201201360
11. Fleischer S, Zhou S, Junge K, Beller M (2013) General and highly efficient iron-catalyzed hydrogenation of aldehydes, ketones, and α,β-unsaturated aldehydes. Angew Chem Int Ed 52(19):5120–5124. https://doi.org/10.1002/anie.201301239
12. Berkessel A, Reichau S, von der Höh A, Leconte N, Neudörfl J-M (2011) Light-induced enantioselective hydrogenation using chiral derivatives of Casey's iron–cyclopentadienone catalyst. Organometallics 30(14):3880–3887. https://doi.org/10.1021/om200459s
13. Quintard A, Rodriguez J (2014) Iron cyclopentadienone complexes: discovery, properties, and catalytic reactivity. Angew Chem Int Ed 53(16):4044–4055. https://doi.org/10.1002/anie.201310788
14. Korstanje TJ, Ivar van der Vlugt J, Elsevier CJ, de Bruin B (2015) Hydrogenation of carboxylic acids with a homogeneous cobalt catalyst. Science 350(6258):298–302. https://doi.org/10.1126/science.aaa8938
15. Liu W, Sahoo B, Junge K, Beller M (2018) Cobalt complexes as an emerging class of catalysts for homogeneous hydrogenations. Acc Chem Res 51(8):1858–1869. https://doi.org/10.1021/acs.accounts.8b00262
16. Elangovan S, Topf C, Fischer S, Jiao H, Spannenberg A, Baumann W, Ludwig R, Junge K, Beller M (2016) Selective catalytic hydrogenations of nitriles, ketones, and aldehydes by well-defined manganese pincer complexes. J Am Chem Soc 138(28):8809–8814. https://doi.org/10.1021/jacs.6b03709
17. Mukherjee A, Nerush A, Leitus G, Shimon LJW, Ben David Y, Espinosa Jalapa NA, Milstein D (2016) Manganese-catalyzed environmentally benign dehydrogenative coupling of alcohols and amines to form aldimines and H2: a catalytic and mechanistic study. J Am Chem Soc 138(13):4298–4301. https://doi.org/10.1021/jacs.5b13519
18. Alig L, Fritz M, Schneider S (2019) First-row transition metal (de)hydrogenation catalysis based on functional pincer ligands. Chem Rev 119(4):2681–2751. https://doi.org/10.1021/acs.chemrev.8b00555

19. Filonenko GA, van Putten R, Hensen EJM, Pidko EA (2018) Catalytic (de)hydrogenation promoted by non-precious metals – Co, Fe and Mn: recent advances in an emerging field. Chem Soc Rev 47(4):1459–1483. https://doi.org/10.1039/C7CS00334J
20. Kallmeier F, Kempe R (2018) Manganese complexes for (de)hydrogenation catalysis: a comparison to cobalt and iron catalysts. Angew Chem Int Ed 57(1):46–60. https://doi.org/10.1002/anie.201709010
21. Goyal V, Sarki N, Narani A, Naik G, Natte K, Jagadeesh RV (2023) Recent advances in the catalytic N-methylation and N-trideuteromethylation reactions using methanol and deuterated methanol. Coord Chem Rev 474:214827. https://doi.org/10.1016/j.ccr.2022.214827
22. Natte K, Neumann H, Beller M, Jagadeesh RV (2017) Transition-metal-catalyzed utilization of methanol as a C_1 source in organic synthesis. Angew Chem Int Ed 56(23):6384–6394. https://doi.org/10.1002/anie.201612520
23. Sarki N, Goyal V, Natte K, Jagadeesh RV (2021) Base metal-catalyzed C-methylation reactions using methanol. Adv Synth Catal 363(22):5028–5046. https://doi.org/10.1002/adsc.202100762
24. Sheetal, Mehara P, Das P (2023) Methanol as a greener C1 synthon under non-noble transition metal-catalyzed conditions. Coord Chem Rev 475:214851. https://doi.org/10.1016/j.ccr.2022.214851
25. Elangovan S, Neumann J, Sortais J-B, Junge K, Darcel C, Beller M (2016) Efficient and selective N-alkylation of amines with alcohols catalysed by manganese pincer complexes. Nat Commun 7(1):12641. https://doi.org/10.1038/ncomms12641
26. Bruneau-Voisine A, Wang D, Dorcet V, Roisnel T, Darcel C, Sortais J-B (2017) Mono-N-methylation of anilines with methanol catalyzed by a manganese pincer-complex. J Catal 347:57–62. https://doi.org/10.1016/j.jcat.2017.01.004
27. Neumann J, Elangovan S, Spannenberg A, Junge K, Beller M (2017) Improved and general manganese-catalyzed N-methylation of aromatic amines using methanol. Chem A Eur J 23(23):5410–5413. https://doi.org/10.1002/chem.201605218
28. Huang M, Li Y, Li Y, Liu J, Shu S, Liu Y, Ke Z (2019) Room temperature N-heterocyclic carbene manganese catalyzed selective N-alkylation of anilines with alcohols. Chem Commun 55(44):6213–6216. https://doi.org/10.1039/C9CC02989C
29. Liu Z, Yang Z, Yu X, Zhang H, Yu B, Zhao Y, Liu Z (2017) Efficient cobalt-catalyzed methylation of amines using methanol. Adv Synth Catal 359(24):4278–4283. https://doi.org/10.1002/adsc.201701044
30. Lator A, Gaillard S, Poater A, Renaud J-L (2018) Well-defined phosphine-free iron-catalyzed N-ethylation and N-methylation of amines with ethanol and methanol. Org Lett 20(19):5985–5990. https://doi.org/10.1021/acs.orglett.8b02080
31. Reed-Berendt BG, Mast N, Morrill LC (2020) Manganese-catalyzed one-pot conversion of nitroarenes into N-methylarylamines using methanol. Eur J Org Chem 2020(9):1136–1140. https://doi.org/10.1002/ejoc.201901854
32. Polidano K, Allen BDW, Williams JMJ, Morrill LC (2018) Iron-catalyzed methylation using the borrowing hydrogen approach. ACS Catal 8(7):6440–6445. https://doi.org/10.1021/acscatal.8b02158
33. Sklyaruk J, Borghs JC, El-Sepelgy O, Rueping M (2019) Catalytic C1 alkylation with methanol and isotope-labeled methanol. Angew Chem Int Ed 58(3):775–779. https://doi.org/10.1002/anie.201810885
34. Bruneau-Voisine A, Pallova L, Bastin S, César V, Sortais J-B (2019) Manganese catalyzed α-methylation of ketones with methanol as a C1 source. Chem Commun 55(3):314–317. https://doi.org/10.1039/C8CC08064J
35. Emayavaramban B, Chakraborty P, Dahiya P, Sundararaju B (2022) Iron-catalyzed α-methylation of ketones using methanol as the C1 source under photoirradiation. Org Lett 24(33):6219–6223. https://doi.org/10.1021/acs.orglett.2c02545
36. Liu Z, Yang Z, Yu X, Zhang H, Yu B, Zhao Y, Liu Z (2017) Methylation of C(sp3)–H/C(sp2)–H bonds with methanol catalyzed by cobalt system. Org Lett 19(19):5228–5231. https://doi.org/10.1021/acs.orglett.7b02462

37. Latham DE, Polidano K, Williams JMJ, Morrill LC (2019) One-pot conversion of allylic alcohols to α-methyl ketones via iron-catalyzed isomerization–methylation. Org Lett 21(19): 7914–7918. https://doi.org/10.1021/acs.orglett.9b02900
38. Ganguli K, Mandal A, Kundu S (2022) Well-defined bis(NHC)Mn(I) complex catalyzed tandem transformation of α,β-unsaturated ketones to α-methylated ketones using methanol. ACS Catal 12(19):12444–12457. https://doi.org/10.1021/acscatal.2c04131
39. Bettoni L, Gaillard S, Renaud J-L (2019) Iron-catalyzed β-alkylation of alcohols. Org Lett 21(20):8404–8408. https://doi.org/10.1021/acs.orglett.9b03171
40. Kaithal A, van Bonn P, Hölscher M, Leitner W (2020) Manganese(I)-catalyzed β-methylation of alcohols using methanol as C1 source. Angew Chem Int Ed 59(1):215–220. https://doi.org/10.1002/anie.201909035
41. Schlagbauer M, Kallmeier F, Irrgang T, Kempe R (2020) Manganese-catalyzed β-methylation of alcohols by methanol. Angew Chem Int Ed 59(4):1485–1490. https://doi.org/10.1002/anie.201912055
42. Borghs JC, Tran MA, Sklyaruk J, Rueping M, El-Sepelgy O (2019) Sustainable alkylation of nitriles with alcohols by manganese catalysis. J Org Chem 84(12):7927–7935. https://doi.org/10.1021/acs.joc.9b00792
43. Mastalir M, Pittenauer E, Allmaier G, Kirchner K (2017) Manganese-catalyzed aminomethylation of aromatic compounds with methanol as a sustainable C1 building block. J Am Chem Soc 139(26):8812–8815. https://doi.org/10.1021/jacs.7b05253
44. Yang J, Chen S, Zhou H, Wu C, Ma B, Xiao J (2018) Cobalt-catalyzed α-methoxymethylation and aminomethylation of ketones with methanol as a C1 source. Org Lett 20(21):6774–6779. https://doi.org/10.1021/acs.orglett.8b02892
45. Biswal P, Samser S, Nayak P, Chandrasekhar V, Venkatasubbaiah K (2021) Cobalt(II)-porphyrin-mediated selective synthesis of 1,5-diketones via an interrupted-borrowing hydrogen strategy using methanol as a C1 source. J Org Chem 86(9):6744–6754. https://doi.org/10.1021/acs.joc.1c00476
46. Das J, Singh K, Vellakkaran M, Banerjee D (2018) Nickel-catalyzed hydrogen-borrowing strategy for α-alkylation of ketones with alcohols: a new route to branched gem-Bis(alkyl) ketones. Org Lett 20(18):5587–5591. https://doi.org/10.1021/acs.orglett.8b02256
47. Charvieux A, Duguet N, Métay E (2019) α-Methylation of ketones with methanol catalyzed by Ni/SiO2-Al2O3. Eur J Org Chem 2019(22):3694–3698. https://doi.org/10.1002/ejoc.201900602
48. Zhang H, Wang J, Liu M, Liu D (2020) Cu/Al2O3 catalyst prepared by a double hydrolysis method for a green, continuous and controlled N-methylation reaction of nitroarenes with methanol. Appl Surf Sci 526:146708. https://doi.org/10.1016/j.apsusc.2020.146708
49. Ma Z, Zhou B, Li X, Kadam RG, Gawande MB, Petr M, Zbořil R, Beller M, Jagadeesh RV (2022) Reusable Co-nanoparticles for general and selective N-alkylation of amines and ammonia with alcohols. Chem Sci 13(1):111–117. https://doi.org/10.1039/D1SC05913K
50. Li H, Li C, Liu W, Yao Y, Li Y, Zhang B, Qiu C Photo-induced C1 substitution using methanol as a C1 source. ChemSusChem:e202300377. https://doi.org/10.1002/cssc.202300377

2 Cobalt catalyzed desaturation

Paper 1: Wang, C.; Azofra, L. M.; Dam, P.; Sebek, M.; Steinfeldt, N.; Rabeah, J.; El-Sepelgy, O.* Catalytic Desaturation of Aliphatic Amides and Imides Enabled by Excited-State Base-Metal Catalysis. *ACS Catal.* **2022**, *12*, 8868-8876.

Paper 2: Zuo K, Zhu J, Akhtar F, Dam P, Azofra, LM, El-Sepelgy O.* Biomimetic Catalytic Remote Desaturation of Aliphatic Alcohols. *Org. Lett.* **2025**, *27*, 30-35.

Paper 3: Wang, C.; Dam, P.; Elghobashy, M.; Brückner, A.; Rabeah, J.; Azofra, L. M.; El-Sepelgy, O.* Biomimetic Dehydroamination of Primary Amines. *ACS Catal.* **2023**, *13*, 14205-14212.

Paper 4: Wang, C.; Azofra, L. M.; Dam, P.; Espinoza-Suarez, E. J.; Do, H. T.; Rabeah, J.; Brückner, A.; El-Sepelgy, O.* Photoexcited cobalt catalysed endo-selective alkyl Heck reaction. *Chem. Commun.* **2023**, *59*, 3862-3865.

Authors Contributions

O.E.-S. conceived and designed the studies, secured funding, led the research, wrote the manuscripts, and revised the supporting information. C.W., P.D., F.A., J.Z., M.E., H.T.D., and E.-S.E. performed all synthesis experiments and prepared the supporting information files. J.R., P.D., and A.B. conducted the EPR and UV-Vis experiments and prepared the corresponding figures. L.M.A. performed the DFT calculations and generated the figures. N.S. and M.S. contributed to the design of the micro-flow reactor.

Paper 1:

Catalytic Desaturation of Aliphatic Amides and Imides Enabled by Excited-State Base-Metal Catalysis.

Wang, C.; Azofra, L. M.; Dam, P.; Sebek, M.; Steinfeldt, N.; Rabeah, J.; El-Sepelgy, O.*

ACS Catal. **2022**, *12*, 8868-8876.

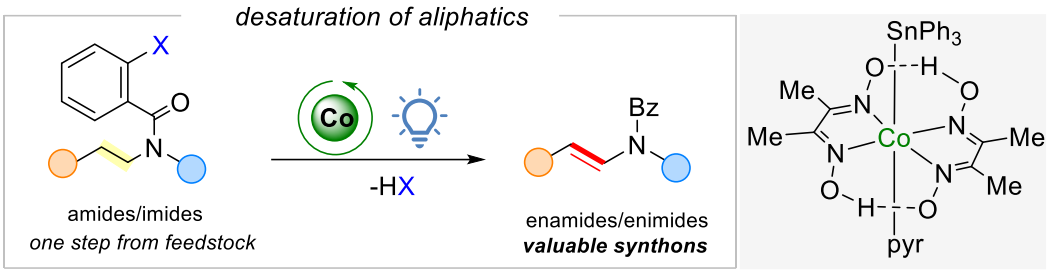

ACS Catalysis

pubs.acs.org/acscatalysis

Research Article

Catalytic Desaturation of Aliphatic Amides and Imides Enabled by Excited-State Base-Metal Catalysis

Chenyang Wang, Luis Miguel Azofra, Phong Dam, Michael Sebek, Norbert Steinfeldt, Jabor Rabeah, and Osama El-Sepelgy*

Cite This: *ACS Catal.* 2022, 12, 8868–8876

Read Online

ACCESS | Metrics & More | Article Recommendations | Supporting Information

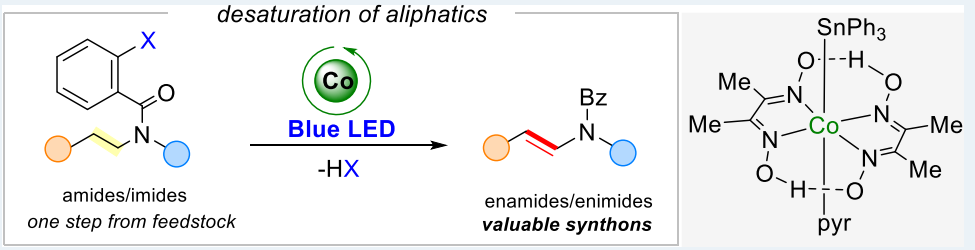

ABSTRACT: Herein, we report a photoexcited base-metal-catalyzed selective desaturation of aliphatic amides and imides. The reaction is catalyzed by a base-metal cobalt complex under visible-light irradiation. This transformation can be efficiently processed at room temperature and enables the synthesis of valuable cyclic and acyclic enamides and enimides from abundant chemicals. Density functional theory (DFT) analysis, electron paramagnetic resonance (EPR), and UV−vis studies rationalized the discovered reactivity of the cobalt catalyst for the photochemical C(sp^3)−H activation reaction. Finally, we demonstrated the potential of our process by scaling-up experiments using a continuous flow photoreactor.

KEYWORDS: *visible light, excited state, base metals, desaturation, cobalt, flow chemistry*

Over the last few decades, ground-state transition-metal catalysis has further developed, and it plays a crucial role in the production of fine and bulk chemicals.[1] However, excited-state catalysis has recently attracted significant attention, leading to the discovery of novel transformations that are inaccessible under conventional thermal conditions.[2] In contrast to the well-established transition-metal/photoredox dual catalysis, photoexcited transition-metal catalysis employs a single catalyst as both photosensitizers and bond-forming and -cleaving catalysts. To date, most of the reported catalytic systems rely on the use of noble metal catalysts such as palladium,[3] ruthenium,[4] gold,[5] rhodium,[6] and iridium.[7] However, the merger of earth-abundant base-metal catalysis and photochemistry has not been broadly developed.[8]

Enamines, enamides, and enimides are among the most common functional groups found in pharmaceutical and agrochemical industries.[9] Conventional methods involve the use of prefunctionalized substrates as well as equivalent amounts of waste-producing reagents.[10] An ideal approach would be the direct and selective desaturation of aliphatic amides and imides to enamides and enimides at room temperature. In general, the design and development of innovative strategies for the selective sustainable conversion of alkanes to alkenes comprise a central challenge for synthetic chemists.[11,12] Toward this elusive goal, several groups have independently developed a few elegant approaches (Figure 1).[13−20] However, these methods suffer from several drawbacks, including the use of highly sensitive substrates, high loading of noble metal and expensive ligands, regioselectivity issues, as well as the need for very high or very low temperatures. In contrast, nature utilizes 3d-transition-metal-based enzymes called desaturases for highly selective desaturation of aliphatic chains under mild conditions.[21] Importantly, 3d-transition-metal complexes have inherent preferences to undergo single electron transfer (SET) processes as opposed to two-electron redox events common to noble metal catalysis.[22]

Accordingly, we envisage the feasibility of mimicking the nature reactivity via the development of a nonenzymatic base-metal-catalyzed process. Inspired by the literature,[23] we report herein a mild practical catalytic system for selective desaturation of aliphatic chains using photoexcited cobaloxime catalysis, which is a model system of Vitamin B12.[24] This method represents the first room-temperature, oxidant-free, base-metal-catalyzed desaturation of amides and imides. Our

Received: April 8, 2022
Revised: June 26, 2022
Published: July 11, 2022

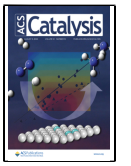

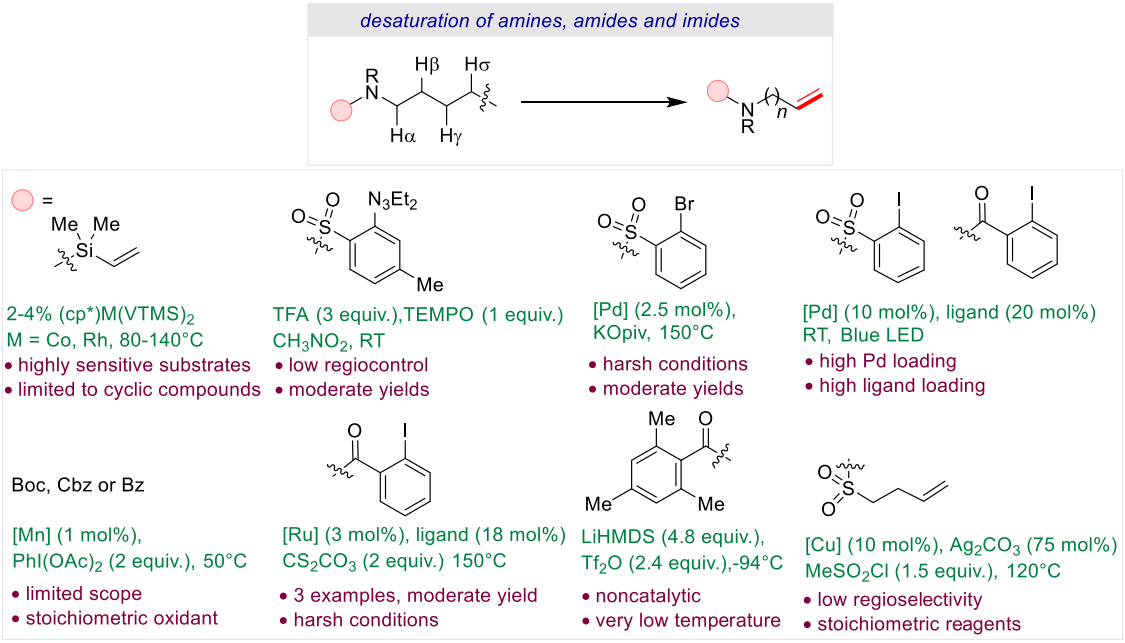

Figure 1. State-of-the-art of desaturation of amines, amides, and imides.[13−20]

strategy involves the installation of a commercially available benzoyl tether at the nitrogen atom of the aliphatic amine or the amide. Then, the photoexcited cobaloxime catalyst is postulated to form an aryl−[Co(III)] species at the tether, which, via photoinduced 1,5-hydrogen atom transfer (HAT),[25] produces the alkyl−[Co(III)] species at a selective unactivated C(sp^3)−H bond. Finally, the corresponding enamide or enimide could form upon a photoinduced β-hydride elimination event and the formation of cobalt-hydride species. The catalyst turnover could be enabled upon the use of a suitable base.

Our proposal for the desaturation of amides was put into practice by employing **Co-1** (5 mol %) as a catalyst and *i*-Pr_2NEt as a base in CH_3CN. Morpholine protected with commercially available *o*-iodobenzoyl chloride tether **1a** was used as a model substrate for the reaction development (Table 1). Under these mild conditions, **1a** was converted to **2a** in 99% yield (Table 1, entry 1). It is worth noting that the related Pd-catalyzed process required the use of 10 mol % Pd salt as well as 20 mol % ferrocene-based ligand (dtbdppf).[16] These preliminary results of the Co-catalyzed transformation highlight the potential of merging of 3d-metal catalysis and photochemistry. Control experiments revealed no background reactivity in the absence of the cobalt catalyst or in the dark (Table 1, entries 2, 3). Importantly, only trace amounts of **2a** were obtained under thermal conditions, indicating the potential of visible-light irradiation. The application of the pyridine-substituted catalyst **Co-2** bearing an electron-donating group led to similar results to the **Co-1** complex (Table 1, entry 4).

Next, we tested the catalytic activity of the **Co-3**/photoredox system, which has recently been reported by Leonori for the E2 eliminations of aliphatic alkyl halides.[26,27] Surprisingly, no desired product was detected (Table 1, entry 5). Also, the combination of the photoredox catalyst 4CzIPN with the Co(II) catalyst **Co-5** does not lead to any catalytic activity (Table 1, entry 6). Interestingly, **Co-4** bearing the *i*-Pr ligand showed no catalytic activity (Table 1, entry 7). Afterward,

Table 1. Reaction Development[a]

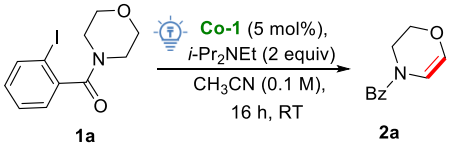

1a 2a

entry	deviation from the standard conditions	yield (%)
1	none	99
2	no **Co-1** or no light	n.d.
3	70°C instead of light	trace
4	**Co-2** as catalyst	99
5	**Co-3** and 4CzIPN (2 mol%)	n.d.
6	**Co-5** and 4CzIPN (2 mol%)	n.d.
7	**Co-4** as catalyst	n.d.
8	1 equiv. K_2CO_3 as base	59
9	1 equiv. K_2CO_3, 0.2 equiv. *i*-Pr_2NEt as base	99
10	DMAP as base	13
11	DABCO as base	29
12	DBU as base	trace
13	no base, **Co-1** (50 mol%)	37
14	TEMPO was added	n.d.

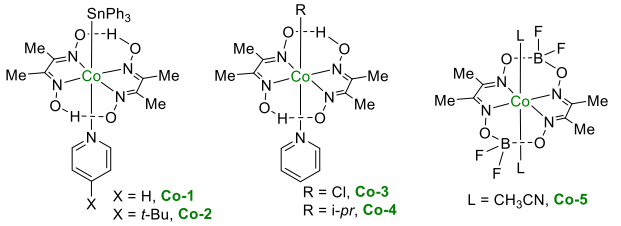

[a]Standard condition: substrate **1a** (0.1 mmol), **Co-1** (0.005 mmol, 3.6 mg), *i*-Pr_2NEt (0.2 mmol, 35 μL), CH_3CN (1 mL), RT, blue LED (10 W, Ledxon), 6−16 h, isolated yields. 4CzIPN is an organic photoredox catalyst. Bz is the benzoyl group.

different bases were investigated (Table 1, entries 8−12). The use of 1 equiv of K_2CO_3 as a base furnished a lower yield of 59%, but full reactivity was restored upon the addition of

https://doi.org/10.1021/acscatal.2c01723
ACS Catal. 2022, 12, 8868−8876

Scheme 1. Further Control Experiments

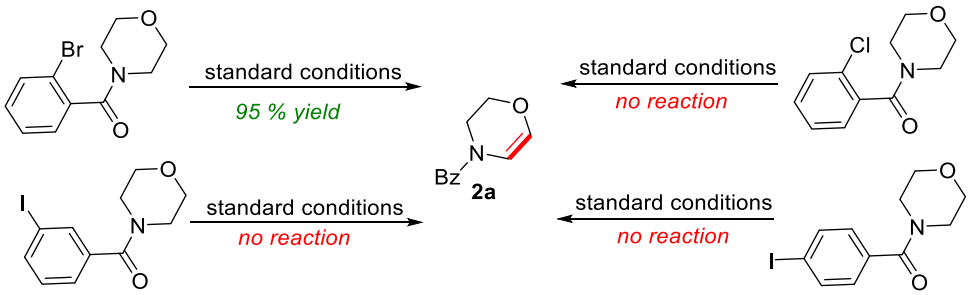

Scheme 2. Desaturation of Amides[b]

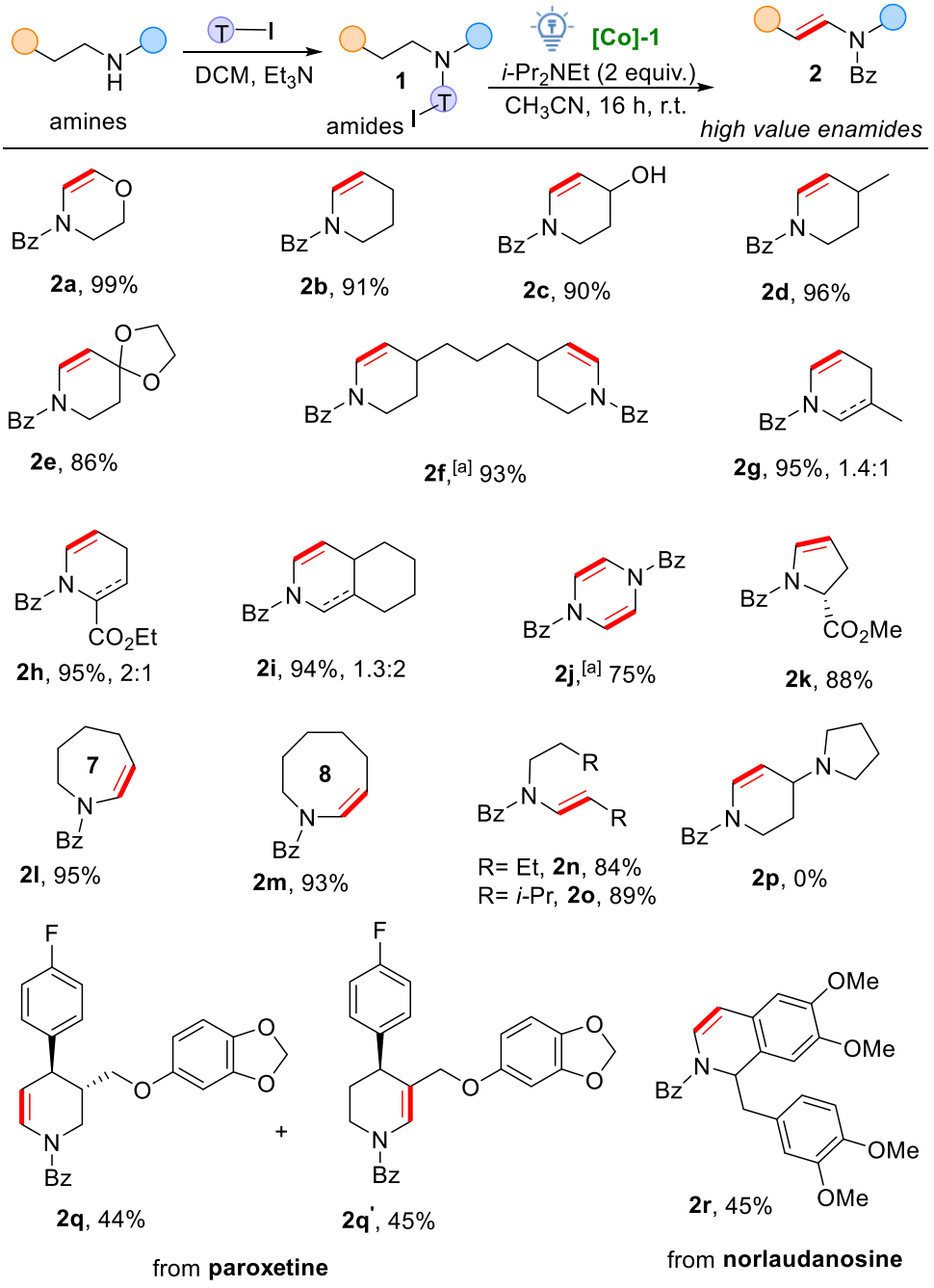

[a]**Co-1** (0.02 mmol, 14.4 mg), *i*-Pr_2NEt (0.8 mmol, 140 μL). [b]Reaction conditions: substrate **1** (0.2 mmol), **Co-1** (0.01 mmol, 7.2 mg), *i*-Pr_2NEt (0.4 mmol, 70 μL), CH_3CN (2 mL), RT, blue LED (10 W, Ledxon), 16 h, isolated yields.

https://doi.org/10.1021/acscatal.2c01723
ACS Catal. 2022, 12, 8868−8876

Scheme 3. Desaturation of Imides[b]

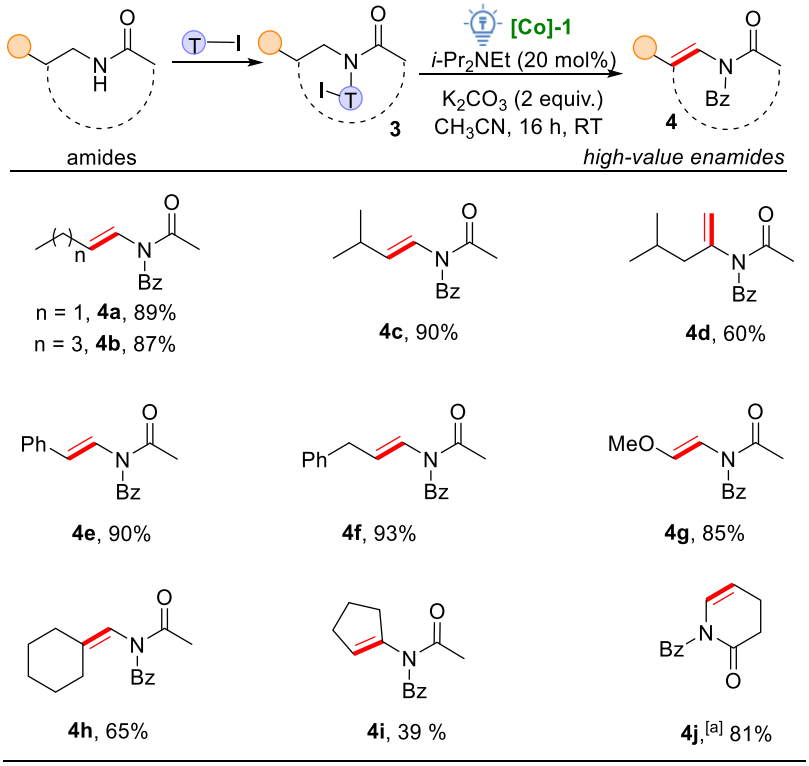

[a]**Co-1** (0.01 mmol, 7.2 mg), *i*-Pr_2NEt (0.4 mmol, 70 μL). [b]Reaction conditions: substrate **1** (0.2 mmol), **Co-2** (0.02 mmol, 14.4 mg), *i*-Pr_2NEt (0.04 mmol, 7 μL), K_2CO_3 (55 mg, 0.4 mmol), CH_3CN (2 mL), RT, 16 h, blue LED (Ledxon), isolated yields.

catalytic amounts of *i*-Pr_2NEt. Additionally, we found that bases, such as DMAP, DABCO, and DBU, led to a drastic decrease in yield. The use of 50 mol % **Co-1** in the absence of the base gave 37% yield of **2a** (Table 1, entry 13). Furthermore, the addition of the radical scavenger TEMPO to the reaction mixture led to no product formation (Table 1, entry 14). Afterward, we examined different halogen-substituted benzoyl tethers (Scheme 1). To our delight, the use of a bromide-substituted tether gave similar results to the heavier iodide analogue; however, the chloride derivative was inactive under the reaction conditions. Furthermore, we found that 3- or 4-iodobenzoyl tethers are unsuitable tethers, which can be attributed to the selective 1,5-HAT process.

With the optimized reaction conditions in hand, the generality of the desaturation of aliphatic amides was investigated. Generally, five-, six-, seven-, and eight-membered cyclic amide derivatives reacted efficiently, leading to the corresponding enamides in very good to excellent yields (**2a**−**2m**). In more details, the unsubstituted piperidine **1b**, piperidines bearing the unprotected hydroxyl group **1c**, the 4-methyl substituent **1d**, and the labile spiro acetal moiety **1e** have been tolerated efficiently, leading to the corresponding cyclic enamides in excellent yields of up to 96%. Similarly, the substrate **1f** possessing double piperidine moieties gave the corresponding double dehydrogenated product in 93% yield. Furthermore, different unsymmetrical piperidine derivatives reacted very well, albeit with the formation of regioisomers (**2g**−**2i**). Interestingly, the desaturation of piperazine **1j**, containing two amide moieties, was tolerated, producing the double desaturation product **2j** in 75% isolated yield. Notably, the desaturation of the proline ester **1k** led to the formation of **2k** with high regioselectivity >20:1. It is worth noting that amide **1k** produced a mixture of isomers with the ratio of 4:1 using palladium catalysis.[16] In contrast with previously reported methods,[17,19] the substrate reactivity was not decreased when increasing the ring size. Protected azepane and azocane underwent selective desaturation to the cyclic enamides **2l** and **2m**. These results represent a practical synthesis of endocyclic enamides that are difficult to synthetize by traditional methods (Scheme 2).

To our delight, this photoexcited Co catalysis proved to be applicable for linear amides **1n** and **1o**, leading to exclusively *E*-selectivity in very good yields. It is important to note that substrates that can form α-aminoalkyl radicals such as **1p** proved to be incompatible with this method. Then, we turned our attention to the application of our methodology on the late-stage functionalization of commercially available drugs and natural products. The antidepressant drug paroxetine was desaturated to produce two isolable enamides **2q** and **2q′** in 44 and 45% yields. Also, the benzoyl derivative of norlaudanosine **1r**, a dopamine metabolite, was desaturated to the corresponding enamide **2r** in moderate yield.

Following the successful development of this process, we decided to examine the more challenging imides using a modified catalytic system with catalytic amounts of the organic base and K_2CO_3. Notably, different aliphatic acetimides **3a**−**3i** were found to be amendable to this method and led to the formation of the corresponding enimides **4** in good to excellent yields (Scheme 3). Gratifyingly, we found that this photo-excited base-metal catalytic system is also applicable to cyclic imides such as δ-valerolactam **3j**, leading to selective desaturation at an unusual reaction site.

To showcase the synthetic utility of the products, we performed a postfunctionalization reaction. The enamide **2k**,

https://doi.org/10.1021/acscatal.2c01723
ACS Catal. 2022, 12, 8868−8876

Scheme 4. Application of the Functionalized L-Proline Amino Acid

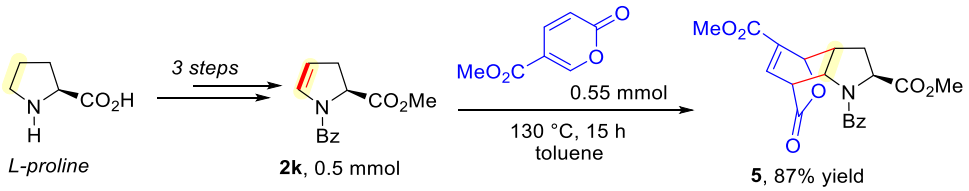

which is prepared from the naturally occurring *L*-proline, undergoes the inverse electron-demand Diels–Alder (IEDDA) reaction with methyl coumalate, leading to the formation of the endo-selective cycloaddition product **5** in 87% yield (Scheme 4).[28]

To prove the practical applicability of this photochemical transformation protocol, we carried out scale-up attempts in batch; unfortunately, a drop in yield was observed due to the limited light penetration through the reaction mixture. However, the problem was solved with the use of continuous flow microreaction technology, which could be considered an enabling technology to operationally scale up photochemical transformations. The channel of the microreactor (XXL series, Little Things Factory, Germany) has a total length of about 3000 mm with a cross section of 2.2 × 2.2 mm^2, giving a total volume of 8 mL, and it was arranged on an area of 150 × 150 mm^2. To improve the mixing of the reaction solution, the channel contained a continuous mixing structure. For liquid cooling, a separate channel system was implemented above and below the reaction channel.

The LED array (105 × 125 mm^2) was dimensioned to irradiate the entire area of the reaction channel with 240 blue-light LEDs with total 19.2 W. The LED wavelength maximum was 467 nm, and the distance between the LED array and the microreactor was adjusted to 8 mm. Additionally, the LED array was cooled using an air cooler (Figure 2). In an initial

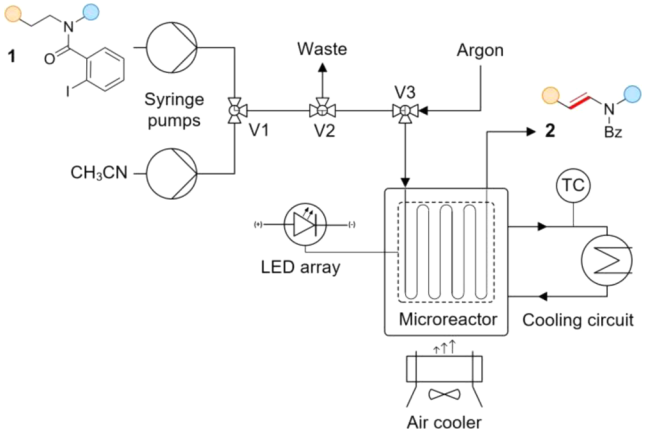

Figure 2. Schematic diagram of the experimental photoreactor setup.

experiment, the desaturation of the benzoyl derivative of the paroxetine drug **2p** in the flow reactor with residence time t_R = 80 min (flow rate = 0.1 mL min^{-1}) led to 95% conversion, and the desired enamides were isolated in 86% yield (2 mmol, 741 mg). These results illustrate the significant acceleration of the process enabled by the combination of microreaction technology and photochemistry.

To shed more light into the mechanism, we performed preliminary experimental mechanistic studies. First, the reaction profile was studied (Figure 3a). Furthermore, to exclude the possibility of a radical chain process, light on–off experiments were carried out. During the light-off cycles no reaction was observed (Figure 3b). In addition, we obtained the quantum yield of Φ = 0.008 for the photoexcited cobalt reaction (see the Supporting Information for details). Next, we performed *in situ* UV–vis studies (Figure 3c,d). Before the irradiation of the reaction mixture, we observed a strong peak with an absorption maximum at 358 nm. Subsequent irradiation of the reaction mixture with blue light led to the generation of a new peak at 430 nm along with a decrease at 358 nm, which is indicative of the formation of the catalytically active $Co^{(II)}$ species. After the complete conversion of the substrate, we observed a decrease in the absorption at 430 nm.

To gain more insights into the light-driven desaturation reaction, *in situ* EPR experiments were performed (Figure 4). The EPR spectrum of the cobalt precatalyst **Co-1** in CH_3CN at −173 °C in the dark showed no EPR signal, which is attributed to the presence of the EPR inactive $Co^{(III)}$ complex. However, the irradiation of **Co-1** for 5 min with blue light at room temperature generated the EPR-active $Co^{(II)}$ species, which exhibited a characteristic $Co^{(II)}$ (S = 1/2) axial signal at $g_\perp$ = 2.282 and $g_\parallel$ = 2.013 with a resolvable ^{59}Co hyperfine structure (I = 7/2) of the parallel component: A = 113 G. The hyperfine structure, especially the middle lines, exhibited a quintet super-hyperfine splitting with ∼1:4:6:4:1 relative intensity due to the nearly equal interaction with two ^{14}N nuclei (I = 1), indicating the coordination of the amino ligands with the $Co^{(II)}$ center. Additionally, there is a very weak signal superimposed with the hyperfine structure of Co^{II} at g = 2.042, most probably due to the formation of the Ph_3Sn radical. It seems that the light-induced homolytic cleavage of the cobaloxime precatalyst **Co-1** leads to the formation of the EPR-active $Co^{(II)}$ species and the Ph_3Sn radical. The EPR signal intensity of $Co^{(II)}$ increased with time upon the addition of the substrate **1a**, *i*-Pr_2NEt, and irradiation for 5 and 60 min. After 16 h of the reaction mixture irradiation and full conversion, we observed a dramatic decrease in the intensity of the EPR signals.

Next, the reaction mechanism was studied using DFT techniques (Figure 5). First, the triphenyl tin cobaloxime complex, **A**, was excited and split into [$Co^{(II)}$] and the Ph_3Sn radical through light irradiation. The Ph_3Sn radical traps the iodide from the substrate **1a**, and the substrate radical combines with the [$Co^{(II)}$] species to form complex **C**, −4.8 kcal mol^{-1}. Then, we analyzed the key step of the internal HAT process, which enables the selective C(sp^3)–H activation of the α-position of the amide substrate. The complex **C** is excited from the singlet (S_0) to the triplet (T_1) state. This vertical (Franck–Condon, FC) excitation brings the complex to a high-energy state, 36.6 kcal mol^{-1}. The formation of this high-energetic excited-state species is crucial for enabling this transformation, which cannot take place under thermal conditions. After relaxation, pyridine (pyr) is released to

https://doi.org/10.1021/acscatal.2c01723
ACS Catal. 2022, 12, 8868–8876

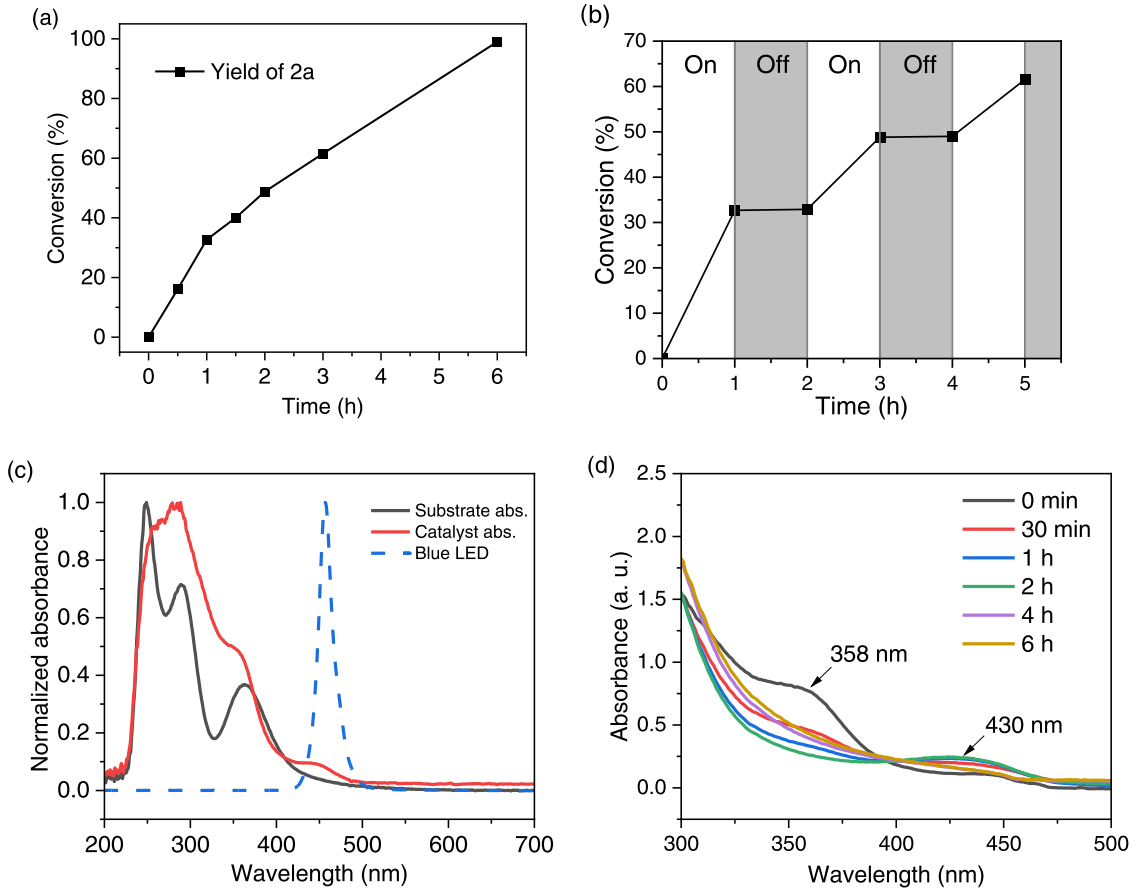

Figure 3. (a) Reaction profile at standard conditions. (b) Light on−off experiment. (c) Absorption spectra of substrates **1a** (25 mM) and **Co-1** (2.5 mM) and emission spectra of blue LED. (d) UV−vis study (concentration diluted twice compared to standard conditions) upon irradiation.

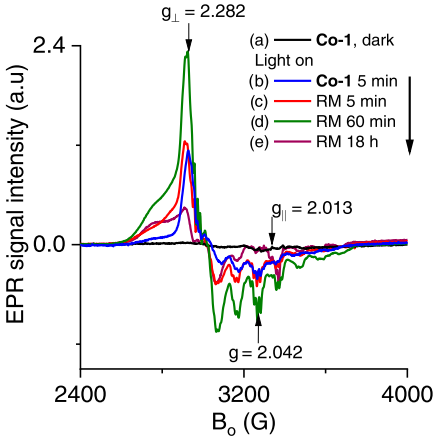

Figure 4. EPR spectra of **Co-1** (5 mM) in CH_3CN at −173 °C: (a) **Co-1** before irradiation; (b) **Co-1** after 5 min light on; (c) reaction mixture of **1a** (RM) after 5 min light on; (d) RM after 60 min light on; and (e) RM after 18 h light on (RM is the reaction mixture).

form the complex $\mathbf{D}(T_1)$, followed by the breakage of the $Co^{(III)}$−C bond into the $[Co^{(II)}]$ and the radical species **E**, both in the doublet state (D), and therefore, we observed the EPR-active species. Interestingly, the transition state for the hydrogen atom transfer (TS_{HAT}) promoted by an internal single electron transfer (ISET) event lies just 0.6 kcal mol^{-1} above in the relative free energy with respect to **E**. As a result of this, complex $\mathbf{G}(S_0)$ is formed by recombination of $[Co^{(II)}]$, the alkyl radical species **F**, and pyridine, being highly stabilized at −10.6 kcal mol^{-1}.

Afterward, we analyzed the step of the product formation *via* *β* hydrogen elimination. Under visible-light irradiation, complex $\mathbf{G}(S_0)$ undergoes a second vertical (FC) excitation, lying at 33.9 kcal mol^{-1}. Pyridine is newly released from the complex leading to $\mathbf{H}(T_1)$, −1.9 kcal mol^{-1}. The *β* hydrogen elimination event takes place in the triplet state to form the $[Co^{(III)}]$−H and the enamine product **2a**. It is important to note that the $TS_{\beta HE}(T_1)$ is only 11.1 kcal mol^{-1} above in free energy relative to **H**.

To enable the catalytic turnover and the halogen atom transfer (XAT),[29] the produced organocobalt (III) species needs to react with a new substrate to produce the complex **D** {$[Co^{(III)}]$−sub} and the hydrogen iodide side-product. There are three possibilities to this process: the first hypothesis involves the deprotonation of $[Co^{(III)}]$−H to generate the anionic Co (I) species using a base (see the NMR study in the Supporting Information). The XAT is then enabled upon nucleophilic substitution (SN_2) with the substrate to generate the complex D (Scheme 5a). This pathway could be excluded because the tin-free **Co-4** that produces $[Co^{(III)}]$−H upon irradiation is catalytically inactive. That is attributed to the use of aryl halides, which cannot undergo SN_2 transformations.

The second proposed pathway suggests that the XAT should take place directly using the $SnPh_3^{\bullet}$ to form the substrate radical. Then, the generated Ph_3SnI may react with $[Co^{(III)}]$-H in the presence of an organic or inorganic base to regenerate the SnPh3$^{\bullet}$ and $[Co^{(II)}]$ species, which combines with the

https://doi.org/10.1021/acscatal.2c01723
ACS Catal. 2022, 12, 8868−8876

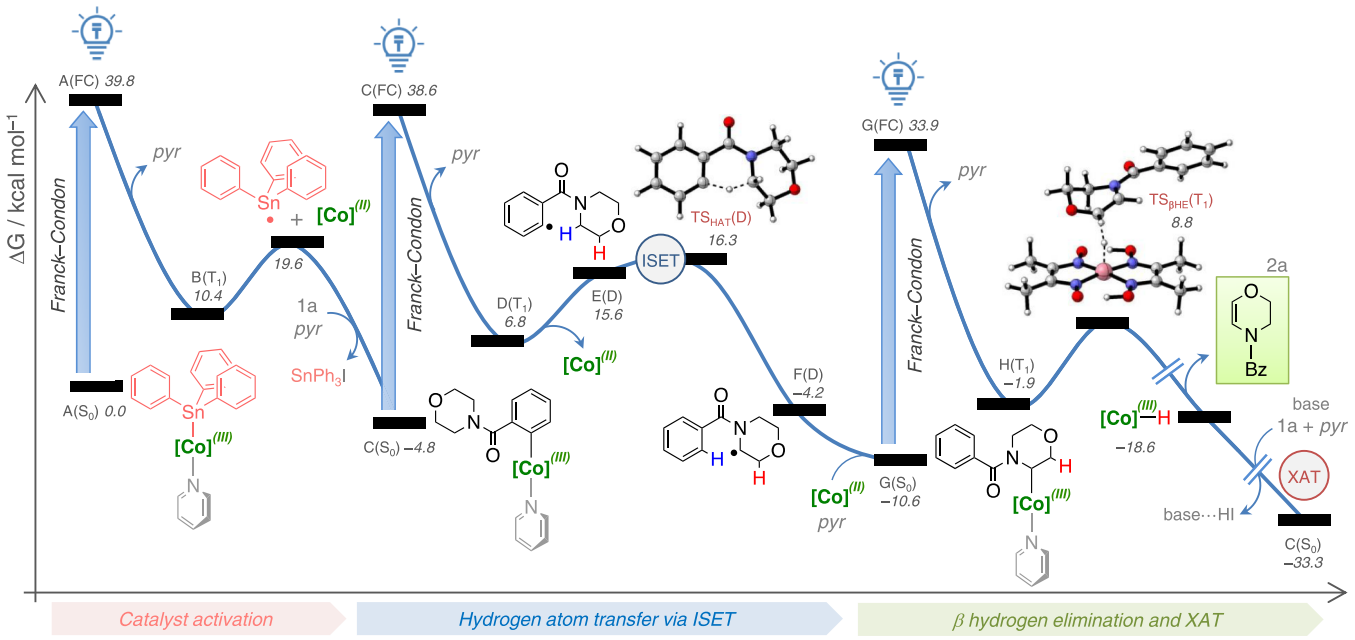

Figure 5. Detailed description of the potential energy surface (PES) for the precatalyst activation (PCA) and metal-assisted desaturation cycle (MADC) involving the hydrogen atom transfer (HAT) and the β hydrogen elimination (βHE) steps. Free energy results are shown in kcal mol^{-1} at the PBE96/TZVP//BP86/6−31G-SVP(Sn,I) level of theory in acetonitrile as the solvent.

Scheme 5. Catalyst Turnover and Halogen Atom Transfer (XAT)

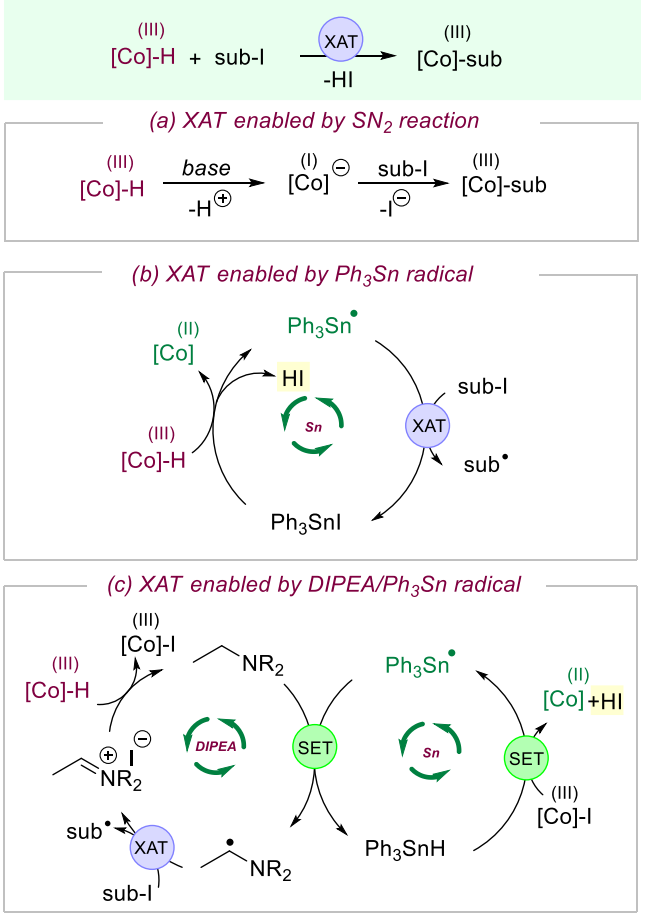

substrate radical to produce the complex **D** (Scheme 5b). This proposal explains the moderate catalytic activity in the presence of K_2CO_3 (Table 1, entry 8). The third suggested mechanism is proposed to take place in the presence of an organic base such as *i*-Pr_2NEt (Scheme 5c). The $SnPh_3^{\bullet}$ reacts with the amine to form the α-amino radical and Ph_3SnH via SET. The XAT is then enabled by the organocatalytic α-amino radical.[29a] This latter proposal is most likely to occur in the presence of organic bases that could form the α-amino radical. This could explain the incompatibility of the substrate **1p** bearing a moiety that can form the α-amino radical.

In summary, we have described a new photochemical C(sp^3)−H functionalization of aliphatic amides and imides.[30] This protocol relies on the use of an air-stable earth-abundant cobalt catalyst with visible-light irradiation as an inexpensive renewable energy source. The method enabled the conversion of saturated aliphatics to highly valuable enamides and enimides under mild conditions in batch and flow. It is expected that this operationally simple and scalable catalytic method would serve as a basis for further practical applications in desaturation of different aliphatic compounds. Most importantly, the unlocking of the novel catalytic activity of the reported cobalt catalysis offers novel possibilities for the discovery of greener alternatives of the hybrid-Pd radical catalysis.[3,31]

■ ASSOCIATED CONTENT

Supporting Information

The Supporting Information is available free of charge at https://pubs.acs.org/doi/10.1021/acscatal.2c01723.

Experimental procedures, analytical data for all new compounds, and NMR spectra (PDF)

■ AUTHOR INFORMATION

Corresponding Author

Osama El-Sepelgy − *Leibniz Institute for Catalysis e.V., 18059 Rostock, Germany;* orcid.org/0000-0003-3131-4988; Email: Osama.Elsepelgy@Catalysis.de

https://doi.org/10.1021/acscatal.2c01723
ACS Catal. 2022, 12, 8868−8876

Authors

Chenyang Wang − *Leibniz Institute for Catalysis e.V., 18059 Rostock, Germany*

Luis Miguel Azofra − *Instituto de Estudios Ambientales y Recursos Naturales (i-UNAT), Universidad de Las Palmas de Gran Canaria (ULPGC), 35017 Las Palmas de Gran Canaria, Spain;* orcid.org/0000-0003-4974-1670

Phong Dam − *Leibniz Institute for Catalysis e.V., 18059 Rostock, Germany*

Michael Sebek − *Leibniz Institute for Catalysis e.V., 18059 Rostock, Germany*

Norbert Steinfeldt − *Leibniz Institute for Catalysis e.V., 18059 Rostock, Germany;* orcid.org/0000-0003-0491-6481

Jabor Rabeah − *Leibniz Institute for Catalysis e.V., 18059 Rostock, Germany;* orcid.org/0000-0003-2162-0981

Complete contact information is available at: https://pubs.acs.org/10.1021/acscatal.2c01723

Funding

This work was financially supported by Deutsche Forschungsgemeinschaft (DFG, Grant Number 456582392) and by the Leibniz Institute for Catalysis e.V.

Notes

The authors declare no competing financial interest.

■ ACKNOWLEDGMENTS

Prof. Dr. Matthias Beller is gratefully acknowledged for his continued generous support, and the paper is dedicated to him on the occasion of his 60th birthday. Gratitude is also due to KAUST for the use of supercomputer Shaheen II for providing the computational resources.

■ REFERENCES

(1) Cornils, B.; Hermann, W. A. *Applied Homogenous Catalysis and Organometallic Compounds*, 2nd ed.; Wiley-VCH: Weinheim, 2002.

(2) (a) Cheung, K. P. S.; Sarkar, S.; Gevorgyan, V. Visible Light-Induced Transition Metal Catalysis. *Chem. Rev.* **2022**, *122*, 1543−1625. (b) Baslé, O. Visible-light-induced 3d transition metal-catalysis: A focus on C−H bond functionalization. *Curr. Opin. Green Sustainable Chem.* **2021**, *32*, 100539. (c) Cheng, W.-M.; Shang, R. Transition Metal-Catalyzed Organic Reactions under Visible Light: Recent Developments and Future Perspectives. *ACS Catal.* **2020**, *10*, 9170−9196. (d) Kancherla, R.; Muralirajan, K.; Sagadevan, A.; Rueping, M. Visible Light-Induced Excited-State Transition-Metal Catalysis. *Trends Chem.* **2019**, *1*, 510−523.

(3) (a) Chuentragool, P.; Kurandina, D.; Gevorgyan, V. Catalysis with Palladium Complexes Photoexcited by Visible Light. *Angew. Chem., Int. Ed.* **2019**, *58*, 11586−11598. (b) Huang, H.-M.; Koy, M.; Serrano, E.; Pflüger, P. M.; Schwarz, J. L.; Glorius, F. Catalytic radical generation of π-allylpalladium complexes. *Nat. Catal.* **2020**, *3*, 393−400.

(4) (a) Korvorapun, K.; Struwe, J.; Kuniyil, R.; Zangarelli, A.; Casnati, A.; Waeterschoot, M.; Ackermann, L. Photo-Induced Ruthenium-Catalyzed C−H Arylations at Ambient Temperature. *Angew. Chem., Int. Ed.* **2020**, *59*, 18103−18109. (b) Jana, S.; Pei, C.; Bahukhandi, S. B.; Koenigs, R. M. Photoinduced ruthenium-catalyzed alkyl-alkyl cross-coupling reactions. *Chem. Catal.* **2021**, *1*, 467−479.

(5) Witzel, S.; Hashmi, A. S. K.; Xie, J. Light in Gold Catalysis. *Chem. Rev.* **2021**, *121*, 8868−8925.

(6) Thongpaen, J.; Manguin, R.; Dorcet, V.; Vives, T.; Duhayon, C.; Mauduit, M.; Baslé, O. Visible Light Induced Rhodium(I)-Catalyzed C−H Borylation. *Angew. Chem., Int. Ed.* **2019**, *58*, 15244−15248.

(7) Zhang, L.; Meggers, E. Steering Asymmetric Lewis Acid Catalysis Exclusively with Octahedral Metal-Centered Chirality. *Acc. Chem. Res.* **2017**, *50*, 320−330.

(8) (a) Jamatia, R.; Mondal, A.; Srimani, D. Visible-Light-Induced Manganese-Catalyzed Reactions: Present Approach and Future Prospects. *Adv. Synth. Catal.* **2021**, *363*, 2969−2995. (b) Mendelsohn, L. N.; MacNeil, C. S.; Tian, L.; Park, Y.; Scholes, G. D.; Chirik, P. J. Visible-Light-Enhanced Cobalt-Catalyzed Hydrogenation: Switchable Catalysis Enabled by Divergence between Thermal and Photochemical Pathways. *ACS Catal.* **2021**, *11*, 1351−1360. (c) Bergamaschi, E.; Beltran, F.; Teskey, C. J. Visible-Light Controlled Divergent Catalysis Using a Bench-Stable Cobalt(I) Hydride Complex. *Chem. − Eur. J.* **2020**, *26*, 5180−5184. (d) Beltran, F.; Bergamaschi, E.; Funes-Ardoiz, I.; Teskey, C. J. Photocontrolled Cobalt Catalysis for Selective Hydroboration of α,β-Unsaturated Ketones. *Angew. Chem., Int. Ed.* **2020**, *59*, 21176−21182. (e) Liu, W.-Q.; Lei, T.; Zhou, S.; Yang, X.-L.; Li, J.; Chen, B.; Sivaguru, J.; Tung, C.-H.; Wu, L.-Z. Cobaloxime Catalysis: Selective Synthesis of Alkenylphosphine Oxides under Visible Light. *J. Am. Chem. Soc.* **2019**, *141*, 13941−13947. (f) Ye, J.-H.; Miao, M.; Huang, H.; Yan, S.-S.; Yin, Z.-B.; Zhou, W.-J.; Yu, D.-G. Visible-Light-Driven Iron-Promoted Thiocarboxylation of Styrenes and Acrylates with CO_2. *Angew. Chem., Int. Ed.* **2017**, *56*, 15416−15420. (g) Kainz, Q. M.; Matier, C. D.; Bartoszewicz, A.; Zultanski, S. L.; Peters, J. C.; Fu, G. C. Asymmetric copper-catalyzed C-N cross-couplings induced by visible light. *Science* **2016**, *351*, 681−684.

(9) *The Chemistry of Enamines, Parts 1 & 2* Rappoport, Z., Ed.; Wiley: New York, 1994.

(10) For reviews, see: (a) Dehli, J. R.; Legros, J.; Bolm, C. Synthesis of enamines, enol ethers and related compounds by cross-coupling reactions. *Chem. Commun.* **2005**, 973−986. (b) Gopalaiah, K.; Kagan, H. B. Use of Nonfunctionalized Enamides and Enecarbamates in Asymmetric Synthesis. *Chem. Rev.* **2011**, *111*, 4599−4657.

(11) Weissermel, K.; Arpe, H.-J. *Olefins, Industrial Organic Chemistry*; Wiley-VCH: Weinheim, 2008; p 59.

(12) (a) Resasco, D. E. Dehydrogenation by Heterogeneous Catalysts. In *Encyclopedia of Catalysis* Horvath, I. T., Ed.; Wiley-VCH: Weinheim, 2002. (b) Dobereiner, G. E.; Crabtree, R. H. Dehydrogenation as a Substrate-Activating Strategy in Homogeneous Transition-Metal Catalysis. *Chem. Rev.* **2010**, *110*, 681−703. (c) Kumar, A.; Bhatti, T. M.; Goldman, A. S. Dehydrogenation of Alkanes and Aliphatic Groups by Pincer-Ligated Metal Complexes. *Chem. Rev.* **2017**, *117*, 12357−12384. (d) Budweg, S.; Junge, K.; Beller, M. Catalytic oxidations by dehydrogenation of alkanes, alcohols and amines with defined (non)-noble metal pincer complexes. *Catal. Sci. Technol.* **2020**, *10*, 3825−3842.

(13) Bolig, A. D.; Brookhart, M. Activation of sp3 C−H Bonds with Cobalt(I): Catalytic Synthesis of Enamines. *J. Am. Chem. Soc.* **2007**, *129*, 14544−14545.

(14) Voica, A.-F.; Mendoza, A.; Gutekunst, W. R.; Fraga, J. O.; Baran, P. S. Guided desaturation of unactivated aliphatics. *Nat. Chem.* **2012**, *4*, 629−635.

(15) Bheeter, C. B.; Jin, R.; Bera, J. K.; Dixneuf, P. H.; Doucet, H. Palladium-Catalysed Dehydrogenative sp^3 C-H Bonds Functionalisation into Alkenes: A Direct Access to N-Alkenylbenzenesulfonamides. *Adv. Synth. Catal.* **2014**, *356*, 119−124.

(16) Chuentragool, P.; Parasram, M.; Shi, Y.; Gevorgyan, V. General, Mild, and Selective Method for Desaturation of Aliphatic Amines. *J. Am. Chem. Soc.* **2018**, *140*, 2465−2468.

(17) Li, G.; Kates, P. A.; Dilger, A. K.; Cheng, P. T.; Ewing, W. R.; Groves, J. T. Manganese-Catalyzed Desaturation of N-Acyl Amines and Ethers. *ACS Catal.* **2019**, *9*, 9513−9517.

(18) Huang, L.; Bismuto, A.; Rath, S. A.; Trapp, N.; Morandi, B. Ruthenium-Catalyzed Dehydrogenation Through an Intermolecular Hydrogen Atom Transfer Mechanism. *Angew. Chem., Int. Ed.* **2021**, *60*, 7290−7296.

(19) Spieß, P.; Berger, M.; Kaiser, D.; Maulide, N. Direct Synthesis of Enamides via Electrophilic Activation of Amides. *J. Am. Chem. Soc.* **2021**, *143*, 10524−10529.

(20) Xia, Y.; Jana, K.; Studer, A. Remote Radical Desaturation of Unactivated C−H Bonds in Amides. *Chem. − Eur. J.* **2021**, *27*, 16621−16625.
(21) (a) Kim, C.; Dong, Y.; Que, L. Modeling Nonheme Diiron Enzymes: Hydrocarbon Hydroxylation and Desaturation by a High-Valent Fe_2O_2 Diamond Core. *J. Am. Chem. Soc.* **1997**, *119*, 3635−3636. (b) Buist, P. H. Fatty acid desaturases: selecting the dehydrogenation channel. *Nat. Prod. Rep.* **2004**, *21*, 249−262.
(22) Fürstner, A. Iron Catalysis in Organic Synthesis: A Critical Assessment of What It Takes To Make This Base Metal a Multitasking Champion. *ACS Cent. Sci.* **2016**, *2*, 778−789.
(23) (a) Schrauzer, G. N.; Holland, R. J. Hydridocobaloximes. *J. Am. Chem. Soc.* **1971**, *93*, 1505−1506. (b) Weiss, M. E.; Kreis, L. M.; Lauber, A.; Carreira, E. M. Cobalt-Catalyzed Coupling of Alkyl Iodides with Alkenes: Deprotonation of Hydridocobalt Enables Turnover. *Angew. Chem., Int. Ed.* **2011**, *50*, 11125−11128. (c) Kreis, L. M.; Krautwald, S.; Pfeiffer, N.; Martin, R. E.; Carreira, E. M. Photocatalytic Synthesis of Allylic Trifluoromethyl Substituted Styrene Derivatives in Batch and Flow. *Org. Lett.* **2013**, *15*, 1634−1637.
(24) (a) Brown, K. L. Chemistry and Enzymology of Vitamin B12. *Chem. Rev.* **2005**, *105*, 2075−2150. (b) Bam, R.; Pollatos, A. S.; Moser, A. J.; West, J. G. Mild olefin formation via bio-inspired vitamin B12 photocatalysis. *Chem. Sci.* **2021**, *12*, 1736−1744.
(25) (a) Han, G.; LaPorte, M. G.; McIntosh, M. C.; Weinreb, S. M.; Parvez, M. Exploratory Synthetic Studies of the α-Methoxylation of Amides via Cuprous Ion-Promoted Decomposition of o-Diazobenzamides. *J. Org. Chem.* **1996**, *61*, 9483−9493. (b) Shaaban, S.; Roller, A.; Maulide, N. Visible-Light, Metal-Free α-Amino $C(sp^3)$−H Activation through 1,5-Hydrogen Migration: A Concise Method for the Preparation of Bis(indolyl)alkanes. *Eur. J. Org. Chem.* **2015**, *2015*, 7643−7647. (c) Shaaban, S.; Oh, J.; Maulide, N. Redox-Neutral α-Amino C−H Functionalization: When the Catalyst Is Also the Nucleophile. *Org. Lett.* **2016**, *18*, 345−347. (d) Du, S.; Kimball, E. A.; Ragains, J. R. Visible-Light-Promoted Remote C−H Functionalization of o-Diazoniaphenyl Alkyl Sulfones. *Org. Lett.* **2017**, *19*, 5553−5556. For a recent review, (e) Sarkar, S.; Cheung, K. P. S.; Gevorgyan, V. C−H functionalization reactions enabled by hydrogen atom transfer to carbon-centered radicals. *Chem. Sci.* **2020**, 12974−12993.
(26) Zhao, H.; McMillan, A. J.; Constantin, T.; Mykura, R. C.; Juliá, F.; Leonori, D. Merging Halogen-Atom Transfer (XAT) and Cobalt Catalysis to Override E2-Selectivity in the Elimination of Alkyl Halides: A Mild Route toward contra-Thermodynamic Olefins. *J. Am. Chem. Soc.* **2021**, *143*, 14806−14813.
(27) For selected examples on Co/photoredox catalytic systems (a) Zhou, M.-J.; Zhang, L.; Liu, G.; Xu, C.; Huang, Z. Site-Selective Acceptorless Dehydrogenation of Aliphatics Enabled by Organophotoredox/Cobalt Dual Catalysis. *J. Am. Chem. Soc.* **2021**, *143*, 16470−16485. (b) Sun, X.; Chen, J.; Ritter, T. Catalytic dehydrogenative decarboxyolefination of carboxylic acids. *Nat. Chem.* **2018**, *10*, 1229−1233. (c) Kojima, M.; Matsunaga, S. The Merger of Photoredox and Cobalt Catalysis. *Trends Chem.* **2020**, *2*, 410−426. (d) West, J. G.; Huang, D.; Sorensen, E. J. Acceptorless dehydrogenation of small molecules through cooperative base metal catalysis. *Nat. Commun.* **2015**, *6*, No. 10093.
(28) For selcted methods of deprotection of benzoyl protecting groups (a) Spaggiari, A.; Blaszczak, L. C.; Prati, F. Low-Temperature Deacylation of N-Monosubstituted Amides. *Org. Lett.* **2004**, *6*, 3885−3888. (b) Tanaka, H.; Ogasawara, K. Utilization of lithium triethylborohydride as a selective N-acyl deprotecting agent. *Tetrahedron Lett.* **2002**, *43*, 4417−4420. (c) Boger, D. L.; McKie, J. A.; Nishi, T.; Ogiku, T. Total Synthesis of (+)-Duocarmycin A, epi-(+)-Duocarmycin A and Their Unnatural Enantiomers: Assessment of Chemical and Biological Properties. *J. Am. Chem. Soc.* **1997**, *119*, 311−325. (d) Boger, D. L.; Machiya, K. Total synthesis of (+)-duocarmycin SA. *J. Am. Chem. Soc.* **1992**, *114*, 10056−10058. (e) Hughes, P.; Clardy, J. Total synthesis of cyclobutane amino acids from Atelia herbert smithii. *J. Org. Chem.* **1988**, *53*, 4793−4796. (f) Ben-Ishai, D.; Altman, J.; Peled, N. The synthesis of p-substituted d,l-phenylglycines by the amidoalkylation of benzylchloride and N-benzylbenzamide. *Tetrahedron* **1977**, *33*, 2715−2717. (g) Matsuura, S.; Niu, C.-H.; Cohen, J. S. Pyridinium polyhydrogen fluoride, a deprotecting reagent in peptide chemistry. *J. Chem. Soc., Chem. Commun.* **1976**, 451−452. (h) Gutzwiller, J.; Uskokovic, M. Total synthesis of quinine and quinidine. II. *J. Am. Chem. Soc.* **1970**, *92*, 204−205.
(29) (a) Constantin, T.; Zanini, M.; Regni, A.; Sheikh, N. S.; Juliá, F.; Leonori, D. Aminoalkyl radicals as halogen-atom transfer agents for activation of alkyl and aryl halides. *Science* **2020**, *367*, 1021−1026. (b) Juliá, F.; Constantin, T.; Leonori, D. Applications of Halogen-Atom Transfer (XAT) for the Generation of Carbon Radicals in Synthetic Photochemistry and Photocatalysis. *Chem. Rev.* **2022**, *122*, 2292−2352.
(30) (a) Gandeepan, P.; Müller, T.; Zell, D.; Cera, G.; Warratz, S.; Ackermann, L. 3d Transition Metals for C−H Activation. *Chem. Rev.* **2019**, *119*, 2192−2452. (b) Laudadio, G.; Deng, Y.; Wal, K.; Ravelli, D.; Nuño, M.; Fagnoni, M.; Guthrie, D.; Sun, Y.; Noël, T. $C(sp^3)$−H functionalizations of light hydrocarbons using decatungstate photocatalysis in flow. *Science* **2020**, *369*, 92−96.
(31) Amadeo, P.; Bhaskararao, B.; Yang, Y.-F.; Kozlowski, M. C. Inherent Selectivity of Pd C−H Activation from Different Metal Oxidation States. *Organometallics* **2021**, *40*, 2290−2294.

https://doi.org/10.1021/acscatal.2c01723
ACS Catal. 2022, 12, 8868−8876

Paper 2:

Biomimetic Catalytic Remote Desaturation of Aliphatic Alcohols.

Zuo, K.; Zhu, J.; Akhtar, F.; Dam, P.; Azofra, L. M.; El-Sepelgy, O.*

Org. Lett. **2025**, *27*, 30-35.

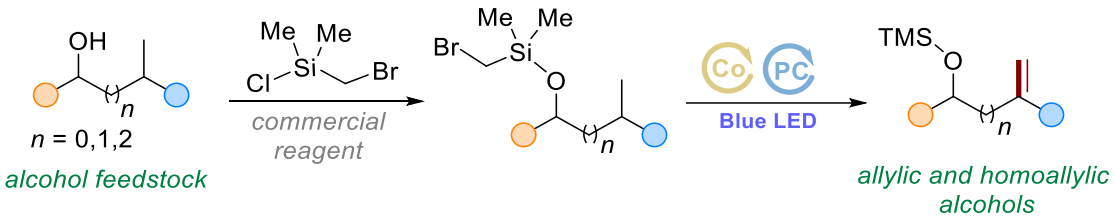

OL Organic Letters

pubs.acs.org/OrgLett

Letter

Biomimetic Catalytic Remote Desaturation of Aliphatic Alcohols

Kaiming Zuo, Jing Zhu, Faral Akhtar, Phong Dam, Luis Miguel Azofra, and Osama El-Sepelgy*

Cite This: *Org. Lett.* 2025, 27, 30−35

Read Online

ACCESS | Metrics & More | Article Recommendations | Supporting Information

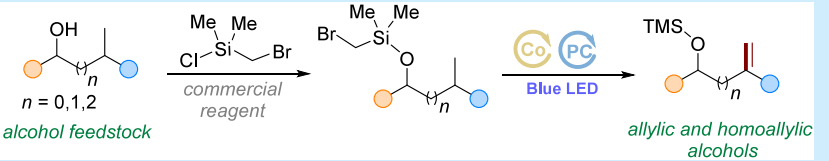

ABSTRACT: Herein we present photoinduced cobaloxime-catalyzed selective remote desaturation of aliphatic alcohols. This transformation, which proceeds efficiently at room temperature, facilitates the synthesis of valuable cyclic and acyclic allylic and homoallylic alcohols from readily available saturated aliphatic alcohols. Remarkably, this method obviates the need for external oxidants, noble metal catalysts, and phosphine ligands.

Remote desaturation of aliphatic compounds is a valuable transformation in organic chemistry that enables the introduction of unsaturation at positions distant from functional groups or reactive sites within a molecule.[1−3] This process is particularly challenging due to the inherent stability and inertness of the C−H bonds in aliphatic chains.[4] We have recently reported cobaloxime-catalyzed remote desaturation of aliphatic amines and amides.[5] Our next goal involves the further exploration of the catalytic method for the more challenging remote desaturation of aliphatic alcohols.[6,7]

In 2012, Baran introduced an innovative method for remote C−H desaturation of aliphatics using an aryl triazine tether (Scheme 1a).[8] This approach utilized a tether containing an aryl radical hydrogen abstracting group that, due to its geometric configuration, preferentially facilitates γ-C−H HAT at the tertiary sites.[9] The reaction involves the formation of a translocated radical[10−12] followed by radical oxidation using stochiometric oxidant. In 2019, an elegant silicon auxiliary[13,14] enabled photoexcited Pd-catalyzed remote desaturation of alcohols (Scheme 1b).[15] The hybrid Pd−radical nature of this protocol enabled the efficient functionalization of different unactivated C−H sites. However, the reaction suffers from the need to use a 10 mol % loading of palladium salt together with expensive phosphine ligand. Importantly, the method also suffers from the necessity to use the highly sensitive and difficult to handle dimethyl(iodomethyl)silane tether for secondary and tertiary alcohols. Inspired by the pioneering work of Gevorgyan,[13,15−17] Zhang,[18,19] and Ackermann[20] and our previous work,[5,21] we sought on the development of a mild base-metal-catalyzed alcohol desaturation (Scheme 1c).

Cobaloxime catalysis,[22] which mimics the action of vitamin B_{12},[23,24] offers an intriguing method for the desaturation of aliphatic compounds.[25−27] This approach leverages its unique ability to convert carbon-centered radicals into the corresponding olefins with high efficiency under mild conditions. These vitamin B_{12} mimics have already demonstrated significant potential in facilitating these challenging desaturation reactions.[21,28−34]

We began our study by using naturally occurring (−)-menthol as a model substrate for desaturation. Initially, we introduced a diisopropyl(iodomethyl)silane tether, commonly employed in Pd-catalyzed transformations. To our

Scheme 1. Radical Remote Desaturation of Alcohols

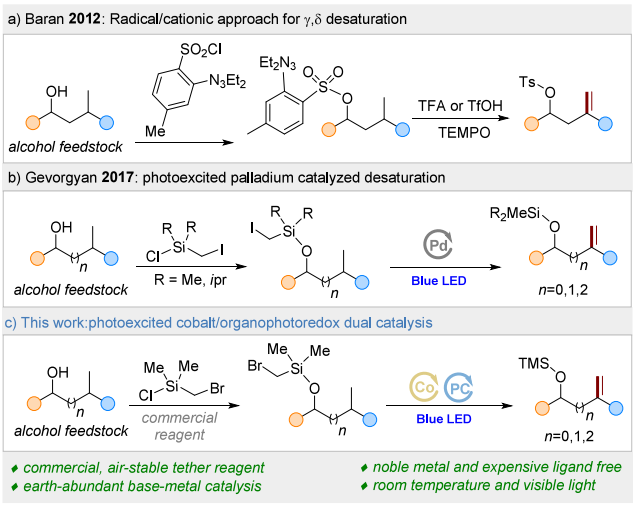

Received: September 27, 2024
Revised: December 10, 2024
Accepted: December 17, 2024
Published: December 23, 2024

delight, using 5 mol % **Co-1** as a single catalyst along with an organic base (condition A) produced the desired product **2a** as a single regioisomer in 70% yield. (Scheme 2) This result

Scheme 2. Remote Desaturation of (−)-Menthol

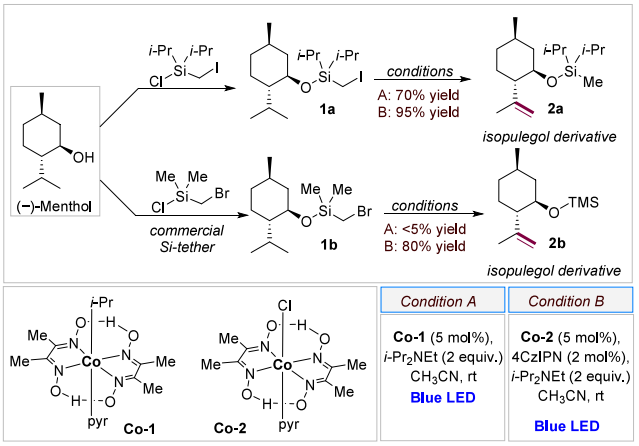

suggests a more efficient and sustainable alternative to the Pd/ferrocene-based phosphine catalytic system.[15] The reaction initiates with the conversion of **Co-1** to the corresponding $[Co]^{III}$−H species under visible-light irradiation, followed by the formation of the supernucleophilic $[Co]^{I}$ species.[21] The reaction proceeds via an S_N2 mechanism on the alkyl iodide moiety.

To avoid the multistep synthesis associated with diisopropyl(iodomethyl)silane and handling difficulties of the highly sensitive dimethyl(iodomethyl)silane, we explored using the commercially available and air-stable dimethyl(bromomethyl)silane. However, under condition A, the reaction of **1b** to give **2b** did not proceed due to the lower reactivity of the alkyl bromide **1b** compared to the alkyl iodide substrate **1a** in the S_N2 pathway. Therefore, we tested the possibility of using an additional organic photocatalyst[35−37] to generate the silyl methyl radical, which could be trapped by the *in situ*-generated $[Co]^{II}$ species. To our delight, using just a 2 mol % loading of the organic dye 4CzIPN along with **Co-2** (condition B) led to the TMS-protected isoeugenol **2b** as a single regioisomer in 80% yield. Additionally, subjecting the iodo substrate **1a** to reaction condition B afforded the desaturated product **2a** in 95% yield (Scheme 2).

After establishing optimal conditions using naturally occurring menthol, we investigated the generality of the developed catalytic system (Scheme 3). In general, we focused on the use of the commercially available dimethylsilyl tether. However, in some cases we observed slightly higher yields or selectivity when the diisopropylsilyl derivative was used. We began by examining a range of alcohol substrates (**1c**−**1i**) that possess a single tertiary Hγ site and lack of tertiary Hβ or Hδ positions. Various primary and secondary alcohols underwent exclusive γ-/δ-desaturation, yielding their respective homoallylic derivatives in moderate to very good yields (**2c**−**2i**). Notably, the reaction tolerated alcohol derivative **1f**, which contains an additional unsaturation site. Subsequently, to study the competitive selective C−H abstraction and the subsequent cobaloxime-catalyzed desaturation, we tested several challenging substrates with various competitive C−H sites. Desaturation of substrate **1j**, which has both secondary and tertiary Hγ sites, led exclusively to the formation of a tertiary radical and the subsequent γ-/δ-desaturation product **2j** in a good yield. In the case of substrate **1k**, which has different tertiary Hγ sites, a mixture of regioisomers was formed, favoring HAT at the cyclic position. Importantly, competition between 1,5-HAT and 1,6-HAT in alcohol derivatives **1l** and **1m** produced γ-/δ-desaturation products with a very high regioselectivity. Substrates **1n** and **1o**, which have competitive tertiary Hδ sites along with tertiary Hγ sites, reacted exclusively at the γ-C−H sites, yielding **2n** and **2o** in good yields (56−70%). Additionally, tertiary alcohol **1p** was found to be compatible with our desaturation method.

After developing a highly regioselective protocol for converting alcohols with Hγ sites to the corresponding homoallylic alcohols, we aimed to extend this method to alcohols lacking Hγ sites. We investigated the desaturation of different secondary and tertiary alcohols bearing isopropyl units to produce the corresponding valuable allylic alcohols **2q**−**2u**. The β-/γ-desaturation process, involving the abstraction of β-sites, occurs via 1,5-HAT. It is worth noting that the hydrogen abstraction from tertiary Hβ site is more favorable than from the secondary Hγ and the tertiary Hδ, as shown in the model examples **2r**−**2u**. Next, we explored the possibility of more challenging distal δ-/ε-desaturation. The secondary and primary alcohols **1v** and **1w** underwent selective δ-/ε-desaturation, yielding desaturated alcohols **2v** and **2w** in moderate yields. Based on the experimental results, our radical desaturation protocol strongly favors the abstraction of tertiary hydrogen atoms at β, γ, and δ over the secondary hydrogen atoms. In addition, the direct competition between the alcohol substrates **1m**, **1n**, and **1s** possessing 3° C−H sites and bearing the same silyl tether enables us to conclude the following preference: 1,6 HAT of Hγ ≫ 1,5 HAT of Hβ > 1,7 HAT.

Finally, an additive robustness study[38] was conducted on the reaction of **1b** to give **2b** to assess the tolerance of various reactive functional groups. Representative examples demonstrate that the desaturation process uniquely accommodates the presence of aromatic amines, aryl bromides, aldehydes, and ketones with minimal impact on the yield or selectivity (Scheme 3).

To gain deeper insight into the preference for 1,6-HAT regioselectivity, we proceeded with the modeling of saddle points for a series of model substrates that present a varied catalog of HAT events (Figure 1). In this sense, calculations were performed at the PBE0+D3/TZVP//BP91/SVP level of theory in acetonitrile solvent (see the Supporting Information (SI) for details). Cases **a** and **b** show the preference of 1,6-HAT events (red) over 1,5- and 1,7-HAT events (blue), respectively, in tertiary radicals. Since kinetic control determines the preference for the obtained regioisomer in the desaturation process, the transition state (TS) for 1,6- versus 1,5-HAT is favored by 1.0 kcal/mol in case **a**, and the TS for 1,6- versus 1,7-HAT is favored by 2.6 kcal/mol in case **b**, entailing calculated regioisomeric ratios of 84:16 and 99:1, respectively. Case **c** analyzes the competition for HAT between tertiary and secondary radicals, with 1,6-HAT in both cases, showing a preference for 3° Hγ over 2° Hγ by 2.3 kcal/mol, which leads to a theoretically estimated regioisomeric ratio of 98:2. In all cases, calculated Boltzmann populations are in good agreement with the experimental results obtained for these substrates.

To understand the nature of this stabilization at the thermodynamic level, we observe that in all cases 1,6-HAT presents a lower enthalpy variation than 1,5- and 1,7-HAT (see

https://doi.org/10.1021/acs.orglett.4c03623
Org. Lett. 2025, 27, 30−35

Scheme 3. Remote Desaturation of Alcohols

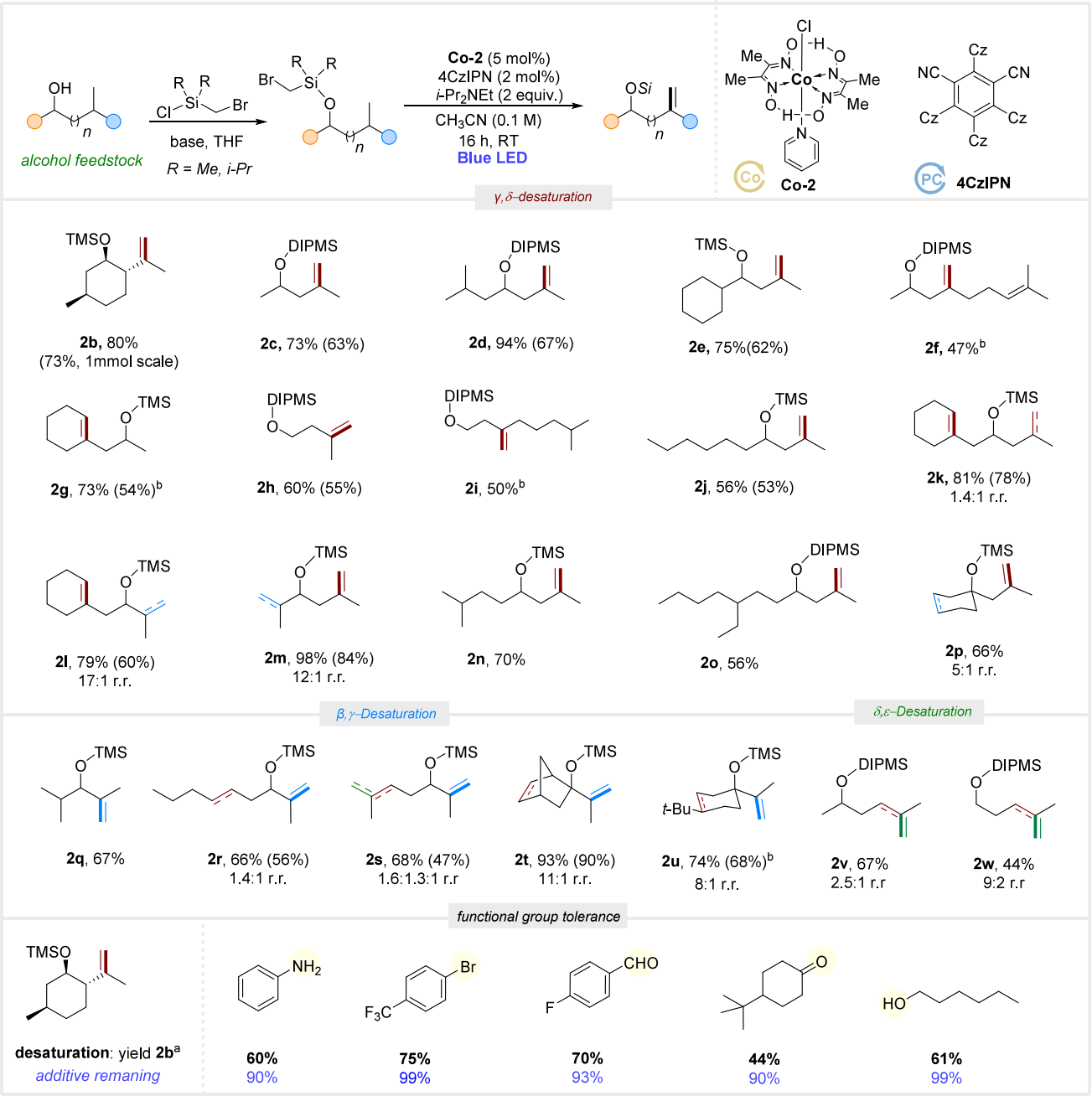

[a]**1** (0.2 mmol), **Co-2** (0.01 mmol, 4.0 mg), 4CzIPN (0.004 mmol, 3.2 mg), *i*-Pr_2NEt (0.2 mmol, 70 μL), CH_3CN (2 mL), RT, 16 h. NMR yields (1,3,5-trimethoxybenzene as internal standard) are given outside parentheses, and isolated yields are given in parentheses. [b]Contains a minor amount of hydrodehalogenation byproduct. r.r. is the regioisomeric ratio, and DIPMS is diisopropylmethylsilane

the SI for details). On the other hand, in cases **b** and **c** we find a more favorable entropy variation for 1,6- versus 1,7-HAT and 3° Hγ versus 2° Hγ, respectively. Although in case **a** a greater disorder is computed for 1,5- versus 1,6-HAT, the TS characterizing 1,5-HAT presents higher angular stress than that for 1,6-HAT. In this sense, the angular stress between 1,6- and 1,7-HAT TSs, whatever the nature of the carbon is (3° or 2°), does not play an important role, as it does in 1,5-HAT.

To gain further insight into the reaction mechanism, a series of UV−vis measurements were performed. Initially, we measured the UV−vis spectrum of the photocatalyst 4CzIPN, which displayed a strong $\pi-\pi^*$ intraligand transition at 240 nm and a broad band between approximately 320 and 460 nm, representing both localized and delocalized charge transfer regions (Figure 2, black curve).[39]

After the addition of Co catalyst and *i*-Pr_2NEt, the spectrum's intensity increased due to the appearance of a strong $\pi-\pi^*$ absorption transition at 250 nm from cobaloxime.[40] Upon irradiation under blue light, there is a new appearance of a shoulder at 430 nm, which corresponds to the ligand-to-metal charge transfer (LMCT) of $[Co]^{II}$ species (Figure 2, blue curve). The formation of this $[Co]^{II}$ species result from the quenching process of the excited state of 4CzIPN by cobaloxime. The subsequent introduction of a

https://doi.org/10.1021/acs.orglett.4c03623
Org. Lett. 2025, 27, 30−35

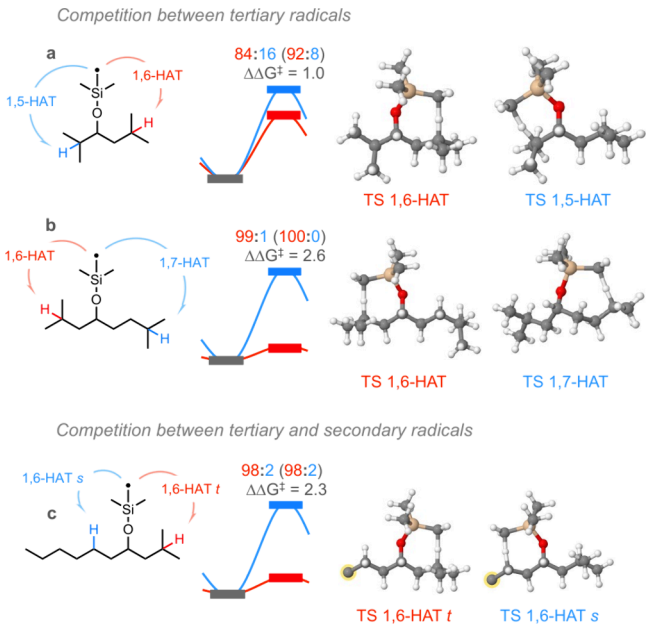

Figure 1. DFT analysis for kinetic control imposing regioselectivity in the desaturation of alcohols. Relative activation free energies, $\Delta\Delta G^{\ddagger}$, are shown in kcal/mol, and Boltzmann populations, expressed as regioisomeric ratios, were calculated at 25 °C (experimental values are also shown in parentheses for comparison). Optimized structures for TSs are displayed, where carbon atoms highlighted in yellow refer to a $CH_2CH_2CH_2CH_3$ moiety, which has been omitted for clarity.

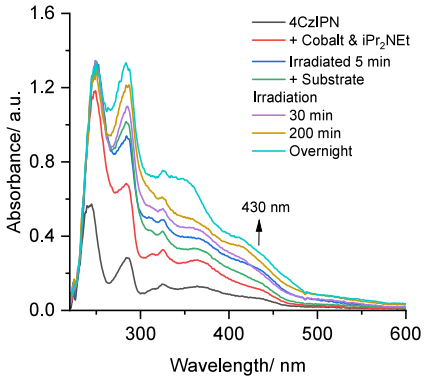

Figure 2. UV−vis spectra of the reaction mixture upon different component additions and irradiation times.

substrate to the mixture led to the disappearance of $[Co]^{II}$ species, indicating the formation of a $[Co]^{III}$−substrate intermediate (Figure 2, green curve). Further irradiation of the complete reaction mixture resulted in stable UV−vis spectra, indicating that the catalyst quickly achieved a steady state, establishing an effective $[Co]^{III}/[Co]^{II}$ cycle (Figure 2, purple and yellow curves).

The plausible mechanism is illustrated in Figure 3. The reaction mechanism involves two photocatalytic cycles, two single electron transfer (SET) events, two hydrogen atom transfer (HAT) steps, and a halogen atom transfer (XAT). The reaction starts with the quenching of the excited photocatalyst 4CzIPN* with the cobaloxime catalyst, leading to the formation of the 4CzIPN radical cation and $[Co]^{II}$ species. The XAT of the substrate is enabled by α-amino radical **A**, which is generated in situ from Hünig's base and the 4CzIPN radical cation.[34] The carbon-centered radical **C** undergoes

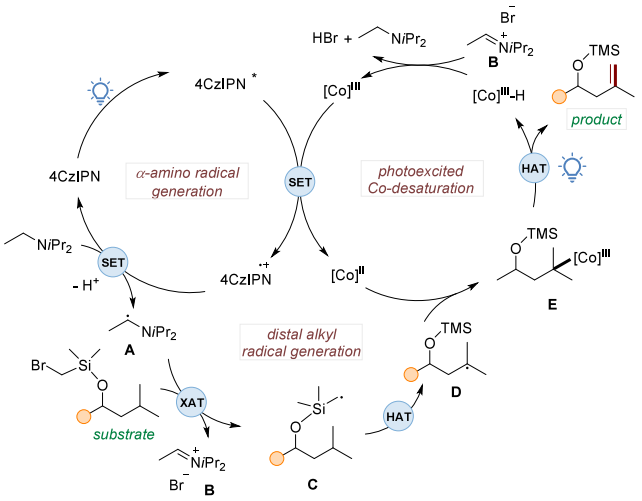

Figure 3. Plausible mechanism.

internal HAT, leading to the formation of the alkyl radical **D**, and subsequent trapping by the $[Co]^{II}$ results in the formation of the alkylcobalt intermediate **E**. Under visible-light irradiation, the cobalt species **E** undergoes radical-type β-hydrogen elimination, resulting in the formation of the desired unsaturated product and $[Co]^{III}$−H. The reaction between the imine salt **B** and the $[Co]^{III}$−H leads to the regeneration of the $[Co]^{III}$ species and Hünig's base.

In summary, we have developed a mild and selective catalytic remote desaturation method for aliphatic alcohols. This approach utilizes two commercially available photocatalysts, 4CzIPN and cobaloxime, eliminating the need for noble metals and complex ligands. DFT calculations indicated a preference for 1,6-HAT over 1,5- and 1,7-HAT in tertiary radicals with energy differences that correlate well with experimental regioisomeric ratios. We believe that this method overcomes limitations of previous approaches, providing a promising new catalytic system for synthesizing valuable allylic and homoallylic alcohols.

■ ASSOCIATED CONTENT

Data Availability Statement

The data underlying this study are available in the published article and its Supporting Information.

Supporting Information

The Supporting Information is available free of charge at https://pubs.acs.org/doi/10.1021/acs.orglett.4c03623.

Experimental procedures, analytical data for all new compounds, NMR spectra, and computational information (PDF)

■ AUTHOR INFORMATION

Corresponding Author

Osama El-Sepelgy − *Leibniz Institute for Catalysis e.V., 18059 Rostock, Germany;* orcid.org/0000-0003-3131-4988; Email: Osama.Elsepelgy@Catalysis.de

Authors

Kaiming Zuo − *Leibniz Institute for Catalysis e.V., 18059 Rostock, Germany*

Jing Zhu − *Leibniz Institute for Catalysis e.V., 18059 Rostock, Germany*

https://doi.org/10.1021/acs.orglett.4c03623
Org. Lett. 2025, 27, 30−35

Faral Akhtar − *Leibniz Institute for Catalysis e.V., 18059 Rostock, Germany*
Phong Dam − *Leibniz Institute for Catalysis e.V., 18059 Rostock, Germany*
Luis Miguel Azofra − *Instituto de Estudios Ambientales y Recursos Naturales (i-UNAT), Universidad de Las Palmas de Gran Canaria (ULPGC), 35017 Las Palmas de Gran Canaria, Spain;* orcid.org/0000-0003-4974-1670

Complete contact information is available at: https://pubs.acs.org/10.1021/acs.orglett.4c03623

Notes

The authors declare no competing financial interest.

■ ACKNOWLEDGMENTS

This research was supported by the Deutsche Forschungsgemeinschaft (DFG) (Grant EL 1041/3-1) and the Leibniz Institute for Catalysis e.V. Gratitude is also due to the KAUST Supercomputer Laboratory (KSL), KSA, for providing the computational resources (Shaheen III). K.Z. acknowledges the Chinese Scholarship Council (CSC) for a predoctoral fellowship. L.M.A., a Ramón y Cajal Fellow (ref RYC2021-030994-I), is grateful for the support of MCIN/AEI and NextGenerationEU/PRTR. F.A. thanks the Erasmus Mundus Program (ASC) for a Master's scholarship. O.E.-S. expresses gratitude to Prof. Dr. Matthias Beller (LIKAT Rostock) for his continuous support. We also thank Dr. Marcus Klahn (LIKAT Rostock) for assistance with mass spectrometry measurements.

■ REFERENCES

(1) Choi, J.; MacArthur, A. H. R.; Brookhart, M.; Goldman, A. S. Dehydrogenation and Related Reactions Catalyzed by Iridium Pincer Complexes. *Chem. Rev.* **2011**, *111*, 1761−1779.
(2) Giri, R.; Maugel, N.; Foxman, B. M.; Yu, J.-Q. Dehydrogenation of Inert Alkyl Groups via Remote C−H Activation: Converting a Propyl Group into a π-Allylic Complex. *Organometallics* **2008**, *27*, 1667−1670.
(3) Baudoin, O.; Herrbach, A.; Guéritte, F. The Palladium-Catalyzed C−H Activation of Benzylic *gem*-Dialkyl Groups. *Angew. Chem., Int. Ed.* **2003**, *42*, 5736−5740.
(4) Zhang, X.-M. Homolytic Bond Dissociation Enthalpies of the C−H Bonds Adjacent to Radical Centers. *J. Org. Chem.* **1998**, *63*, 1872−1877.
(5) Wang, C.; Azofra, L. M.; Dam, P.; Sebek, M.; Steinfeldt, N.; Rabeah, J.; El-Sepelgy, O. Catalytic Desaturation of Aliphatic Amides and Imides Enabled by Excited-State Base-Metal Catalysis. *ACS Catal.* **2022**, *12*, 8868−8876.
(6) Čeković, Ž.; Dimttruević, L.; Djokić, G.; Srnić, T. Remote functionalisation by ferrous ion-cupric ion induced decomposition of alkyl hydroperoxides. *Tetrahedron* **1979**, *35*, 2021−2026.
(7) Breslow, R.; Baldwin, S.; Flechtner, T.; Kalicky, P.; Liu, S.; Washburn, W. Remote oxidation of steroids by photolysis of attached benzophenone groups. *J. Am. Chem. Soc.* **1973**, *95*, 3251−3262.
(8) Voica, A.-F.; Mendoza, A.; Gutekunst, W. R.; Fraga, J. O.; Baran, P. S. Guided desaturation of unactivated aliphatics. *Nat. Chem.* **2012**, *4*, 629−635.
(9) Hollister, K. A.; Conner, E. S.; Spell, M. L.; Deveaux, K.; Maneval, L.; Beal, M. W.; Ragains, J. R. Remote Hydroxylation through Radical Translocation and Polar Crossover. *Angew. Chem., Int. Ed.* **2015**, *54*, 7837−7841.
(10) Nechab, M.; Mondal, S.; Bertrand, M. P. 1,*n*-Hydrogen-Atom Transfer (HAT) Reactions in Which $n \neq 5$: An Updated Inventory. *Chem.—Eur. J.* **2014**, *20*, 16034−16059.
(11) Sarkar, S.; Cheung, K. P. S.; Gevorgyan, V. C-H functionalization reactions enabled by hydrogen atom transfer to carbon-centered radicals. *Chem. Sci.* **2020**, *11*, 12974−12993.
(12) Friese, F. W.; Mück-Lichtenfeld, C.; Studer, A. Remote C−H functionalization using radical translocating arylating groups. *Nat. Commun.* **2018**, *9*, 2808.
(13) Parasram, M.; Gevorgyan, V. Silicon-Tethered Strategies for C−H Functionalization Reactions. *Acc. Chem. Res.* **2017**, *50*, 2038−2053.
(14) Wilt, J. W.; Lusztyk, J.; Peeran, M.; Ingold, K. U. Absolute rate constants for some intermolecular and intramolecular reactions of α-, β-, and γ-silicon-substituted radicals. *J. Am. Chem. Soc.* **1988**, *110*, 281−287.
(15) Parasram, M.; Chuentragool, P.; Wang, Y.; Shi, Y.; Gevorgyan, V. General, Auxiliary-Enabled Photoinduced Pd-Catalyzed Remote Desaturation of Aliphatic Alcohols. *J. Am. Chem. Soc.* **2017**, *139*, 14857−14860.
(16) Chuentragool, P.; Yadagiri, D.; Morita, T.; Sarkar, S.; Parasram, M.; Wang, Y.; Gevorgyan, V. Aliphatic Radical Relay Heck Reaction at Unactivated C(sp^3)-H Sites of Alcohols. *Angew. Chem., Int. Ed.* **2019**, *58*, 1794−1798.
(17) Kurandina, D.; Yadagiri, D.; Rivas, M.; Kavun, A.; Chuentragool, P.; Hayama, K.; Gevorgyan, V. Transition-Metal- and Light-Free Directed Amination of Remote Unactivated C(sp^3)−H Bonds of Alcohols. *J. Am. Chem. Soc.* **2019**, *141*, 8104−8109.
(18) Cao, Z.; Li, J.; Sun, Y.; Zhang, H.; Mo, X.; Cao, X.; Zhang, G. Photo-induced copper-catalyzed alkynylation and amination of remote unactivated C(sp^3)−H bonds. *Chem. Sci.* **2021**, *12*, 4836−4840.
(19) Cao, Z.; Li, J.; Zhang, G. Photo-induced copper-catalyzed sequential 1,*n*-HAT enabling the formation of cyclobutanols. *Nat. Commun.* **2021**, *12*, 6404.
(20) Wang, Y.; Chen, S.; Chen, X.; Zangarelli, A.; Ackermann, L. Photo-Induced Ruthenium-Catalyzed Double Remote C(sp^2)−H/C(sp^3)−H Functionalizations by Radical Relay. *Angew. Chem., Int. Ed.* **2022**, *61*, e202205562.
(21) Wang, C.; Azofra, L. M.; Dam, P.; Espinoza-Suarez, E. J.; Do, H. T.; Rabeah, J.; Brückner, A.; El-Sepelgy, O. Photoexcited cobalt catalysed endo-selective alkyl Heck reaction. *Chem. Commun.* **2023**, *59*, 3862−3865.
(22) Dam, P.; Zuo, K.; Azofra, L. M.; El-Sepelgy, O. Biomimetic Photoexcited Cobaloxime Catalysis in Organic Synthesis. *Angew. Chem., Int. Ed.* **2024**, *63*, e202405775.
(23) Tahara, K.; Pan, L.; Ono, T.; Hisaeda, Y. Learning from B12 enzymes: biomimetic and bioinspired catalysts for eco-friendly organic synthesis. *Beilstein J. Org. Chem.* **2018**, *14*, 2553−2567.
(24) Giedyk, M.; Goliszewska, K.; Gryko, D. Vitamin B_{12} catalysed reactions. *Chem. Soc. Rev.* **2015**, *44*, 3391−3404.
(25) Yu, W.-L.; Ren, Z.-G.; Ma, K.-X.; Yang, H.-Q.; Yang, J.-J.; Zheng, H.; Wu, W.; Xu, P.-F. Cobalt-catalyzed chemoselective dehydrogenation through radical translocation under visible light. *Chem. Sci.* **2022**, *13*, 7947−7954.
(26) Zhou, M.-J.; Zhang, L.; Liu, G.; Xu, C.; Huang, Z. Site-Selective Acceptorless Dehydrogenation of Aliphatics Enabled by Organo-photoredox/Cobalt Dual Catalysis. *J. Am. Chem. Soc.* **2021**, *143*, 16470−16485.
(27) West, J. G.; Huang, D.; Sorensen, E. J. Acceptorless dehydrogenation of small molecules through cooperative base metal catalysis. *Nat. Commun.* **2015**, *6*, 10093.
(28) Abrams, D. J.; West, J. G.; Sorensen, E. J. Toward a mild dehydroformylation using base-metal catalysis. *Chem. Sci.* **2017**, *8*, 1954−1959.
(29) Cartwright, K. C.; Tunge, J. A. Decarboxylative Elimination of *N*-Acyl Amino Acids via Photoredox/Cobalt Dual Catalysis. *ACS Catal.* **2018**, *8*, 11801−11806.
(30) Huang, L.; Ji, T.; Zhu, C.; Yue, H.; Zhumabay, N.; Rueping, M. Bioinspired desaturation of alcohols enabled by photoredox proton-coupled electron transfer and cobalt dual catalysis. *Nat. Commun.* **2022**, *13*, 809.

(31) Sun, X.; Chen, J.; Ritter, T. Catalytic dehydrogenative decarboxyolefination of carboxylic acids. *Nat. Chem.* **2018**, *10*, 1229−1233.
(32) Wang, C.; Dam, P.; Elghobashy, M.; Brückner, A.; Rabeah, J.; Azofra, L. M.; El-Sepelgy, O. Biomimetic Dehydroamination of Primary Amines. *ACS Catal.* **2023**, *13*, 14205−14212.
(33) Wang, X.; Li, Y.; Wu, X. Photoredox/Cobalt Dual Catalysis Enabled Regiospecific Synthesis of Distally Unsaturated Ketones with Hydrogen Evolution. *ACS Catal.* **2022**, *12*, 3710−3718.
(34) Zhao, H.; McMillan, A. J.; Constantin, T.; Mykura, R. C.; Juliá, F.; Leonori, D. Merging Halogen-Atom Transfer (XAT) and Cobalt Catalysis to Override E2-Selectivity in the Elimination of Alkyl Halides: A Mild Route toward contra-Thermodynamic Olefins. *J. Am. Chem. Soc.* **2021**, *143*, 14806−14813.
(35) Chan, A. Y.; Perry, I. B.; Bissonnette, N. B.; Buksh, B. F.; Edwards, G. A.; Frye, L. I.; Garry, O. L.; Lavagnino, M. N.; Li, B. X.; Liang, Y.; Mao, E.; Millet, A.; Oakley, J. V.; Reed, N. L.; Sakai, H. A.; Seath, C. P.; MacMillan, D.W. C. Metallaphotoredox: The Merger of Photoredox and Transition Metal Catalysis. *Chem. Rev.* **2022**, *122*, 1485−1542.
(36) Ram Bajya, K.; Selvakumar, S. Dual Photoredox and Cobalt Catalysis Enabled Transformations. *Eur. J. Org. Chem.* **2022**, *2022*, e202200229.
(37) Kojima, M.; Matsunaga, S. The Merger of Photoredox and Cobalt Catalysis. *Trends Chem.* **2020**, *2*, 410−426.
(38) Collins, K. D.; Glorius, F. A robustness screen for the rapid assessment of chemical reactions. *Nat. Chem.* **2013**, *5* (7), 597−601.
(39) Brannan, A. C.; Beaumont, E. F. P.; Phuoc, N. L.; Whitehead, G. F. S.; Linnolahti, M.; Romanov, A. S. Organic thermally activated delayed fluorescence material with strained benzoguanidine donor. *Beilstein J. Org. Chem.* **2023**, *19*, 1289−1298.
(40) Kilic, A.; Durgun, M.; Yorulmaz, N.; Yavuz, R. The synthesis and investigation of different cobaloximines by spectroscopic methods. *J. Mol. Struct.* **2018**, *1174*, 25−31.

https://doi.org/10.1021/acs.orglett.4c03623
Org. Lett. 2025, 27, 30−35

Paper 3:

Biomimetic Dehydroamination of Primary Amines.

Wang, C.; Dam, P.; Elghobashy, M.; Brückner, A.; Rabeah, J.; Azofra, L. M.; El-Sepelgy, O.*

ACS Catal. **2023**, *13*, 14205-14212.

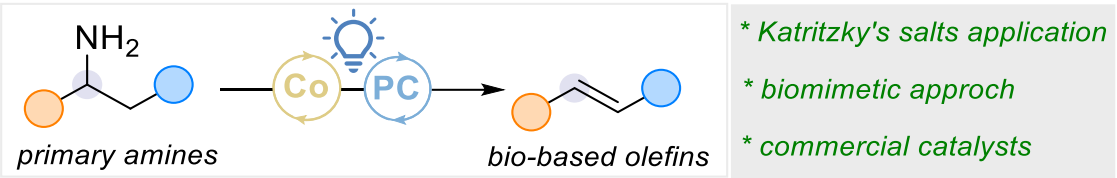

ACS Catalysis

pubs.acs.org/acscatalysis

Research Article

Biomimetic Dehydroamination of Primary Amines

Chenyang Wang, Phong Dam, Mohamed Elghobashy, Angelika Brückner, Jabor Rabeah, Luis Miguel Azofra, and Osama El-Sepelgy*

Cite This: *ACS Catal.* 2023, 13, 14205−14212

Read Online

ACCESS | Metrics & More | Article Recommendations | Supporting Information

ABSTRACT: Herein, we present a biomimetic method for the catalytic deammoniation of diverse primary amines, including amino acids, natural products, and pharmaceuticals. This innovative approach, characterized by its operational simplicity and high selectivity, provides a rapid and easily accessible pathway to a wide range of olefin products derived from nonfossil-based chemicals. The transformation relies on the utilization of two readily available photoactive catalysts: acridinium salt and cobaloxime. Through a combination of experimental and theoretical studies, we have gained valuable insights into the fundamental steps underlying this unconventional dehydroamination process.

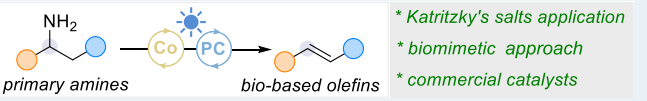

KEYWORDS: *visible light, excited-state, base metals, biomimetic, desaturation*

Biomimetic organic synthesis, inspired by nature's efficient and selective pathways, has emerged as a powerful strategy for the development of novel chemical transformations that mimic enzymatic processes.[1] Deammoniation plays a crucial role in a range of biological processes, including the biosynthesis of natural products and the metabolism of amino acids. For instance, phenylalanine ammonia lyase converts L-phenylalanine to cinnamic acid,[2] a critical precursor for the biosynthesis of lignols, flavonoids, coumarins, aurones, and stilbenes (Scheme 1a).[3]

Despite recent advancements in biomimetic synthesis and the growing interest in replacing fossil-based chemicals with biobased alternatives in the chemical industry, it is surprising that there is a lack of readily available and mild in vitro methods for converting primary amines into alkenes.[4,5] To the best of our knowledge, two classical methods are known for this transformation: Hofmann elimination,[5] which involves exhaustive methylation of primary amines to quaternary ammonium salts, followed by counterion exchange with stoichiometric silver oxide. While Cope elimination[6] involves the oxidation of *t*-amines with peroxides. The production of the alkenes mostly requires harsh thermal and vacuum conditions (Scheme 1b).[7] In addition, unlike alcohols, Burgess reagent proved to be an unsuccessful defunctionalization reagent.[8]

We envisage the feasibility of mimicking the natural reactivity via the development of a nonenzymatic process (Scheme 1c). Our design makes use of the recent progress on the mild generation of C-centered radicals from activated primary amines such as pyridinium salt.[9−11] A major challenge is the subsequent fast reduction of the formed radicals and the generation of the corresponding alkanes.[12] To solve the problem, we decided to employ cobaloxime catalysis, a model of vitamin B12, for the mild conversion of the alkyl radicals to the corresponding olefin.[13] Indeed, this concept draws inspiration from the natural ability of methylcobalamin to act as a reversible free radical carrier that effectively stabilizes highly reactive methyl radicals via the formation of weak carbon−cobalt bonds.[14] Thus, we reported herein the first example of mild dehydroamination of primary amines enabled by a synergistic combination of two photoactive catalysis: organic dye and cobaloxime.[15−17] It is noteworthy that in 1982, Katritzky converted primary amines into tetrahydrobenzoacridium salts, followed by thermolysis at 150−180 °C, yielding the respective olefins.[18]

Our mechanistic proposal is initiated by the generation of *α*-amino radical **A** from *N*,*N*-diisopropylethylamine (*i*-Pr_2NEt) upon the use of highly oxidizing excited-state organic dye such as [Mes-Acr-Me^+]* ($E_{1/2}^{red}$ = +2.06 V vs SCE).[19] The formed *α*-amino radical **A** enables the single electron transfer (SET) reduction of the pyridinium salt, producing the corresponding C-centered radical **B**. Subsequently, the open-shell species **B** are intercepted by a persistent 17-electron $[Co]^{II}$ radical,[20] forming an alkyl-$[Co]^{III}$ intermediate **C** that undergoes C−cobalt bond homolysis upon light irradiation. At this stage, $[Co]^{II}$ performs *α*,*β*-hydrogen abstraction, resulting in the formation of the desired olefin and a $[Co]^{III}$−H species. The cobalt and photoredox catalytic cycles culminate through a simultaneous SET event between the $[Co]^{III}$ intermediate ($E_{1/2}^{red}$ = −0.68 V vs SCE)[21] and the reduced form of the photocatalyst (PC) Mes-Acr-Me•. By employing this envisioned approach, we aim to provide a milder and more

Received: September 11, 2023
Revised: October 4, 2023
Published: October 20, 2023

Scheme 1. State-of-the-Art of the Dehydroamination

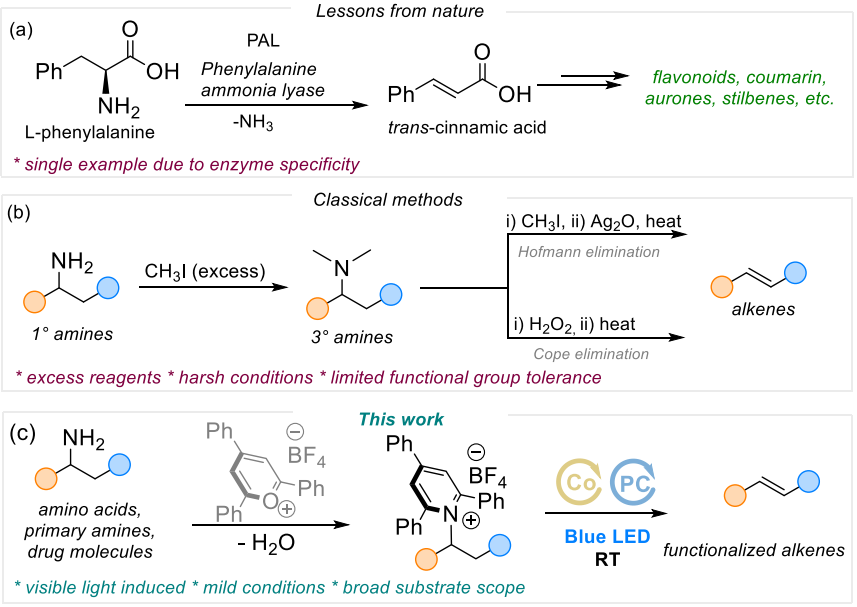

Scheme 2. Our Envisioned Mechanistic Proposal

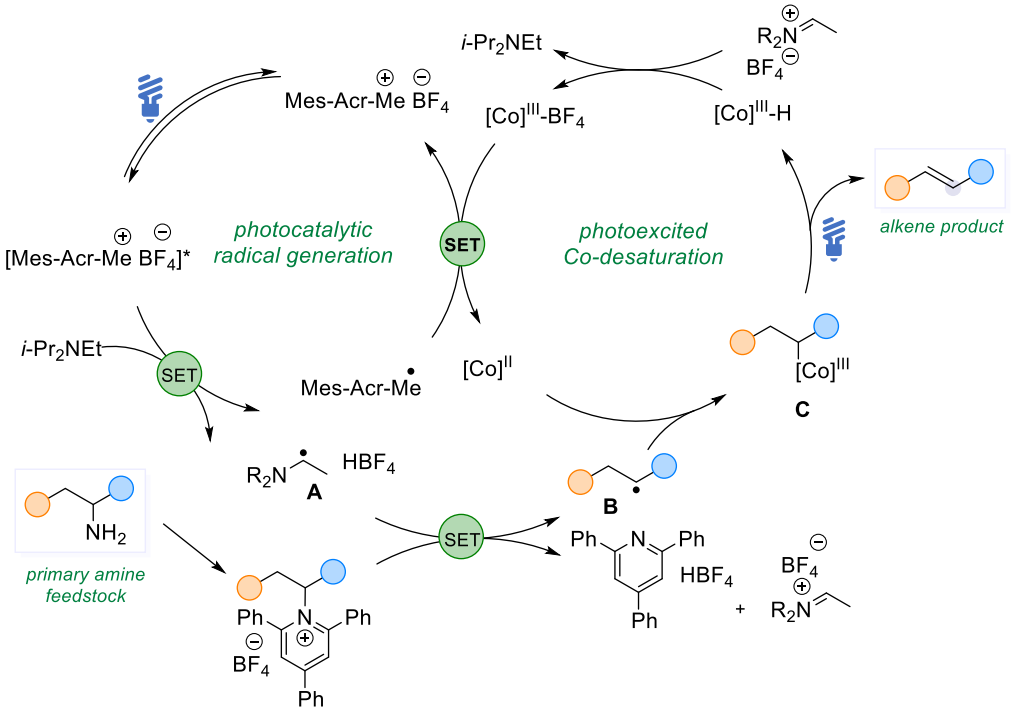

accessible alternative for dehydroamination, contributing to the development of sustainable and efficient synthetic organic chemistry (Scheme 2).

The optimization of the reaction conditions for the synergistic combination of photoredox and cobalt catalysis is summarized in Table 1. Initially, the evaluation focused on essential amino acid derivative **1**, mimicking the transformation by phenylalanine ammonia lyase (Scheme 1a). Optimized conditions applied the use of two commercially available catalysts: Mes-Acr-$MeClO_4$ (1 mol %) and $Co(dmgH)_2PyCl$ ([**Co**]-**1**, 5 mol %). The reaction was carried out in a 0.1 M dichloromethane (DCM) solution with 2 equiv of diisopropylethylamine (*i*-Pr_2NEt) as a base at room temperature, using blue light-emitting diodes for irradiation. This condition yielded the desired methyl cinnamate product **31** in 84% nuclear magnetic resonance (NMR) yield and excellent *E*-selectivity (>20:1) (Table 1, entry 1). The use of Mes-Acr-$MeBF_4$ as a PC led to comparable results (Table 1, entry 2). However, less oxidizing photosensitizers, such as Eosin Y* ($E_{1/2}^{red}$ = +0.83 V vs SCE),[22] 4CzIPN* ($E_{1/2}^{red}$ = +1.35 V vs SCE),[23] and Riboflavin* ($E_{1/2}^{red}$ = +1.50 V vs SCE),[24] resulted in lower product yields (Table 1, entries 3−5). This suggests that the reaction pathway likely involves SET from an electron donor to the excited-state PC. Similar results were obtained when the reaction was conducted in acetonitrile instead of DCM (Table 1, entry 6). Screening of different organic and

https://doi.org/10.1021/acscatal.3c04305
ACS Catal. 2023, 13, 14205−14212

Table 1. Reaction Development[a]

entry	deviation from the standard conditions	yield (%)	E/Z ratio
1	none	84	>20:1
2	Mes-Acr-MeBF$_4$ as PC	82	>20:1
3	Eosin Y as PC	22	>20:1
4	Riboflavin as PC	38	10:1
5	4CzIPN as PC	40	>20:1
6	CH_3CN as solvent	80	>20:1
7	DBU as base	37	>20:1
8	K_2CO_3 as base	Trace	
9	Et_3N as base	30	10:1
10	[**Co**]-**2** instead of [**Co**]-**1**	82	>20:1
11	[**Co**]-**3** (single catalyst)	23	15:1
12	no light/PC/[Co]/base	n.r	

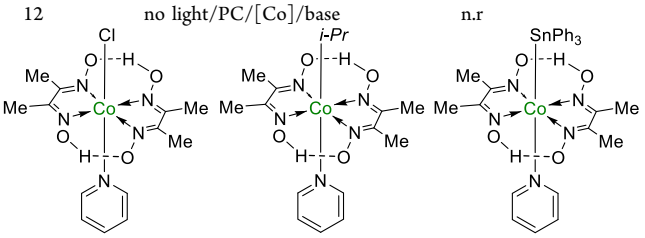

[a]Standard conditions: substrate **1** (0.2 mmol), [**Co**]-**1** (0.005 mmol, 4 mg), Mes-Acr-MeClO$_4$ (0.002 mmol, 0.8 mg), i-Pr$_2$NEt (0.4 mmol, 70 μL), DCM (2 mL), RT, 16 h, NMR yields.

inorganic bases revealed that i-Pr$_2$NEt is the optimal choice (Table 1, entries 7−9). Furthermore, the use of Co(dmgH)$_2$(i-Pr)(py) [**Co**]-**2**[25] resulted in an NMR yield of 82% (Table 1, entry 10). Importantly, the application of the bifunctional [Co]-SnPh$_3$ catalyst [**Co**]-**3** as a single catalyst[26] led to a significant decrease in yield and selectivity (Table 1, entry 11). Finally, we conducted control experiments by individually omitting the PC, [**Co**] catalyst, base, or light. In each instance, no product was detected (Table 1, entry 12).

After establishing optimal conditions, we investigated the dehydroamination of various Katritzky salts[9] (Scheme 3). Our visible-light protocol demonstrated tolerance toward a wide range of primary amines, amino acids, natural products, and drug molecules (**1**−**30**). We initiated the substrate scope exploration with different amino acids, including a variety of common amino acids. Methyl and benzyl phenylalanine derivatives could be transformed to the corresponding cinnamates **31** and **32** with isolated yields of 82% and 85%, respectively. Phenylalanine derivatives bearing electron-withdrawing groups provided the desired α,β-unsaturated esters (**33**−**35**) along with varying amounts of saturated products. Conversely, the electron-rich tyrosine selectively furnished the corresponding *trans*-cinnamate **36**.

Furthermore, homophenylalanine successfully underwent our protocol, yielding ester **37** with an 80% yield and moderate E/Z selectivity. Aliphatic amino acids such as leucine and norleucine readily afforded the corresponding α,β-unsaturated esters **38** and **39** with excellent yields and selectivity. Also, isoleucine yielded the trisubstituted olefin **40** with a high yield and an E/Z ratio of 1.2:1. Notably, the sulfur-containing amino acid methionine could be selectively converted to E-alkene **41** in 71% yield. Aspartic acid and glutamic acid, which are dicarboxylic amino acids, furnished the desired selective E-olefins **42** and **43** with yields of 60 and 71%, respectively. Additionally, the carboxamide-containing amino acid asparagine produced the olefin **44** with an 86% yield and excellent stereocontrol, while glutamine resulted in the unsaturated ester **45** with moderate selectivity. Lysine was successfully converted to alkene **46** in 59% yield with complete selectivity. Furthermore, tryptophan, a heterocyclic-based amino acid, tolerated our system and provided excellent yields and selectivity for products **47** and **48**.

Next, we explored primary amines beyond amino acids. Gratifyingly, 2-aminoindane, a designer drug, yielded indene (**49**) in 70% yield. Amphetamine resulted in a 58% yield mixture of terminal and internal olefins (ratio 2:1) due to the competitive nature of the Co catalyst in abstracting both the reactive benzylic and less hindered terminal hydrogen atoms. In contrast, 4-phenyl-2-butanamine exclusively formed terminal alkene **51**. Cyclic amines were amendable to the reaction, delivering the desired products **52**−**55**. It is worth noting the excellent regioselectivity of the formation of olefin **54**. This highlighting the tendency of the cobaloxime to abstract the less hindered β-hydrogen atom. Gratifyingly, phenylalaninol also delivered cinnamyl alcohol (**56**) in 65% yield. In addition, a testosterone derivative underwent dehydroamination to produce olefin **58**, albeit in a mixture of regioisomers. The cardic drug mexiletine was also converted to its corresponding terminal olefin **59** with moderate regioselectivity. Interestingly, the application of a β-aminoglucose derivative led to the formation of the unsaturated deoxysugar **60** with the elimination of the β-OAc group instead of the β-hydrogen.

To confirm the proposed reaction mechanism of the synergetic photoredox-cobalt catalytic system depicted in Scheme 2, a combination of experimental and theoretical methods was applied. Fluorescence measurements were conducted under inert conditions at room temperature to differentiate between oxidative and reductive quenching of the acridine PC. No quenching of the excited state PC was observed with the substrate and cobaloxime catalyst, while i-Pr$_2$NEt effectively quenched the excited state of the PC, supporting the proposed reductive quenching pathway. Figure 1a shows the Stern−Volmer plot for the fluorescence quenching of Mes-Acr-MeClO$_4$ with i-Pr$_2$NEt. Further electron paramagnetic resonance (EPR) measurements at room temperature of the irradiated [Mes-Acr-Me$^+$ClO$_4$]* did not show any EPR signal. However, a gradual development of a new EPR signal at g = 2.004 was observed with time in the presence of i-Pr$_2$NEt due to the formation of Mes-Acr-Me• (Figure 1b).[27] The formed spectra are in accordance with the theoretical simulation of Mes-Acr-Me• (See Supporting Information for details).

Density functional theory (DFT) calculations shown in Figure 2 supported the fluorescence and EPR results, showing that PC undergoes light-induced vertical (Franck−Condon) excitation to triplet state [**PC**(FC)] at 45.3 kcal/mol. After relaxation, PC transitions to the relaxed triplet state [**PC**(T$_1$)] at 38.4 kcal/mol. The highly oxidizing excited-state species undergoes SET from i-Pr$_2$NEt, leading to the reduction of the acridine PC to the radical Mes-Acr-Me• in the double state. The reductive quenching process is spontaneous, releasing 17.2 kcal/mol. As depicted in Figure 2, the complex of i-

https://doi.org/10.1021/acscatal.3c04305
ACS Catal. 2023, 13, 14205−14212

Scheme 3. Scope of Visible Light Induced Dehydroamination of Primary Amines.[a-c] (See Supporting Information[a])

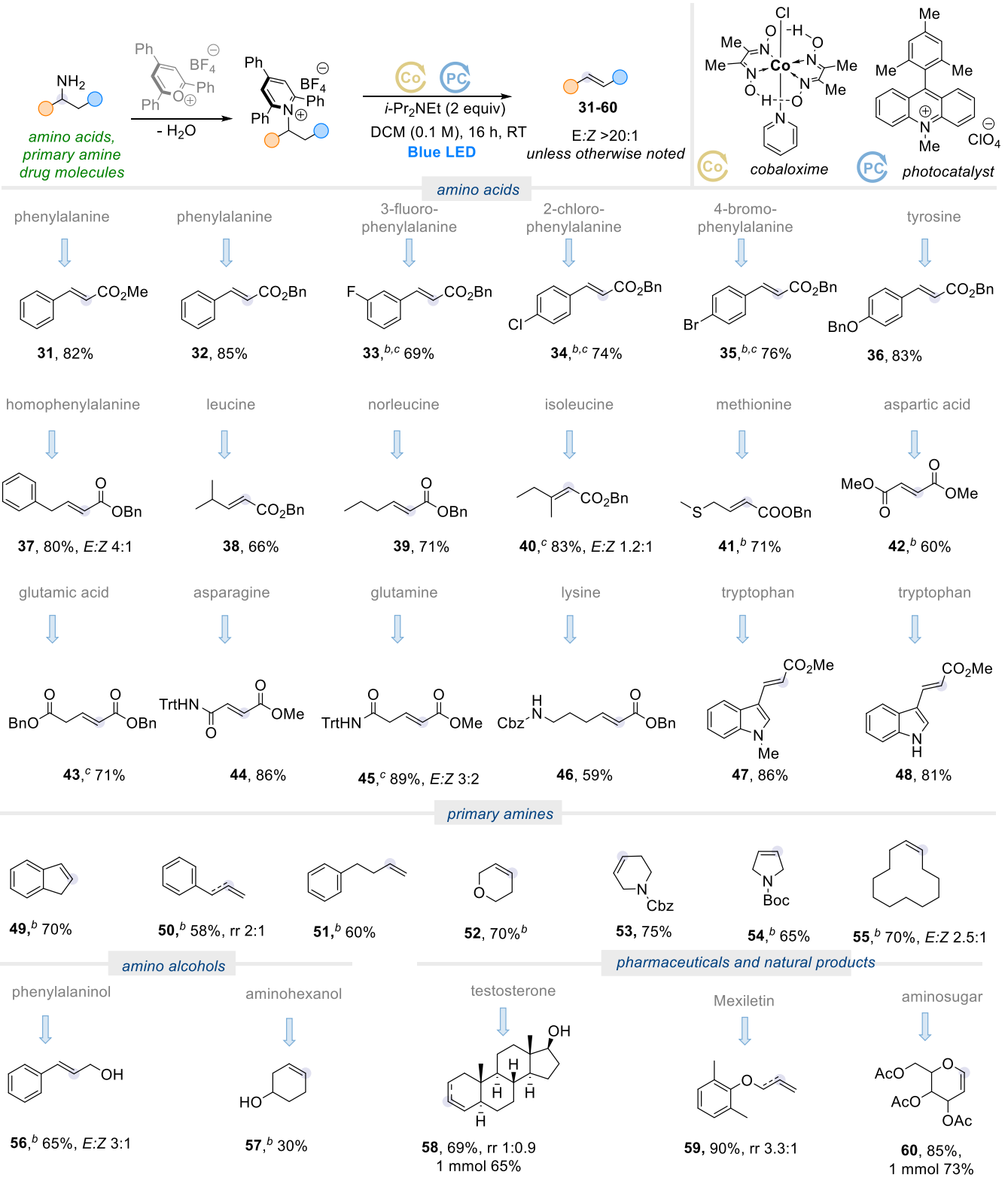

[a]Standard conditions: pyridinium salt (0.2 mmol), [Co]-1 (0.01 mmol, 0.8 mg), Acr-MeClO4 (0.002 mmol, 0.8 mg), i-Pr_2NEt (0.4 mmol, 70 μL), DCM (2 mL), RT, 16 h, the reported yields refer to the conversion of the pyridinium salts to the olefins (see supporting information for details). [b]NMR yield. [c]Contains minor amount of hydrodeamination by-product.

$Pr_2NEt^{\bullet+}$ and HBF_4 facilitates the exergonic formation of a carbon-centered radical, releasing 36.5 kcal/mol. Subsequent addition of pyridinium salt **1** to the reaction mixture results in the formation of organic radical intermediate **sub** (D). This was confirmed by a spin trapping experiment using 5,5-dimethyl-1-pyrroline-*N*-oxide (DMPO), resulting in a six-line EPR signal due to the formation of a DMPO-$^{\bullet}$R adduct (Figure 1c). According to the proposed reaction mechanism,

https://doi.org/10.1021/acscatal.3c04305
ACS Catal. 2023, 13, 14205−14212

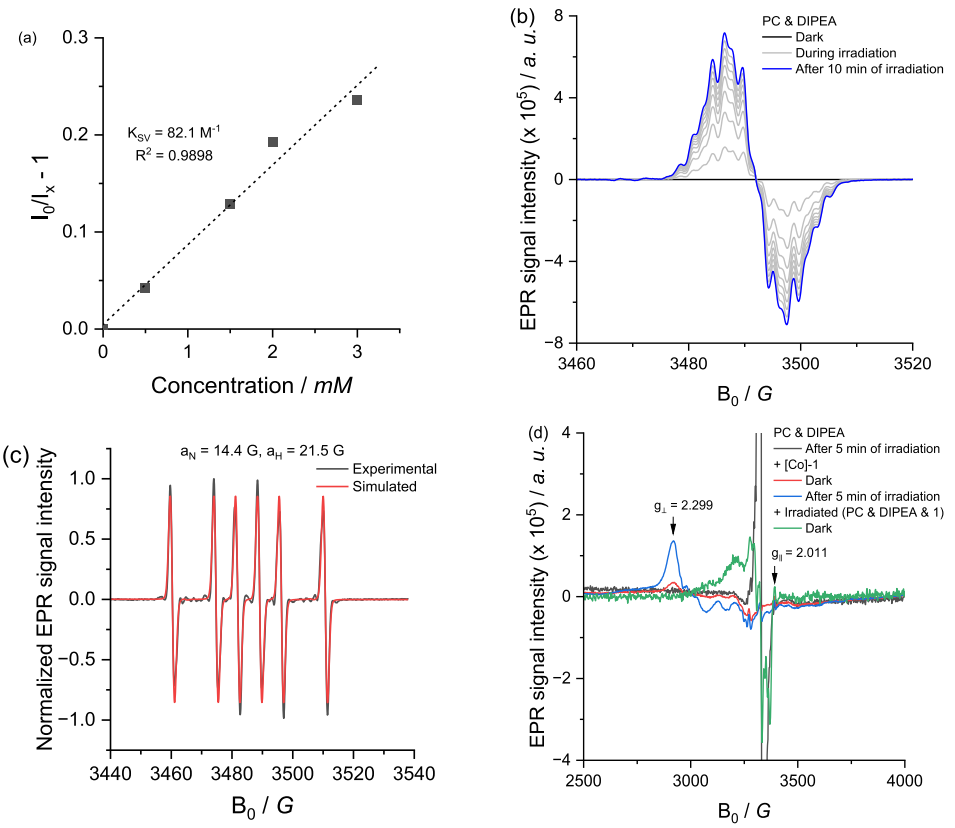

Figure 1. (a) Stern−Volmer plot for fluorescence quenching of Mes-Acr-MeClO$_4$ with *i*-Pr$_2$NEt; (b) EPR spectra recorded at room temperature of the mixture of PC and *i*-Pr$_2$NEt before and after the irradiation; (c) Experimental and simulated EPR spectrum of the irradiated mixture between PC and *i*-Pr$_2$NEt after the addition of substrate and DMPO; (d) EPR spectra recorded at −173 °C of the irradiated mixture of PC and *i*-Pr$_2$NEt with the addition of [**Co**]-**1**, then subsequential addition of the irradiated solution of PC, *i*-Pr$_2$NEt, and substrate.

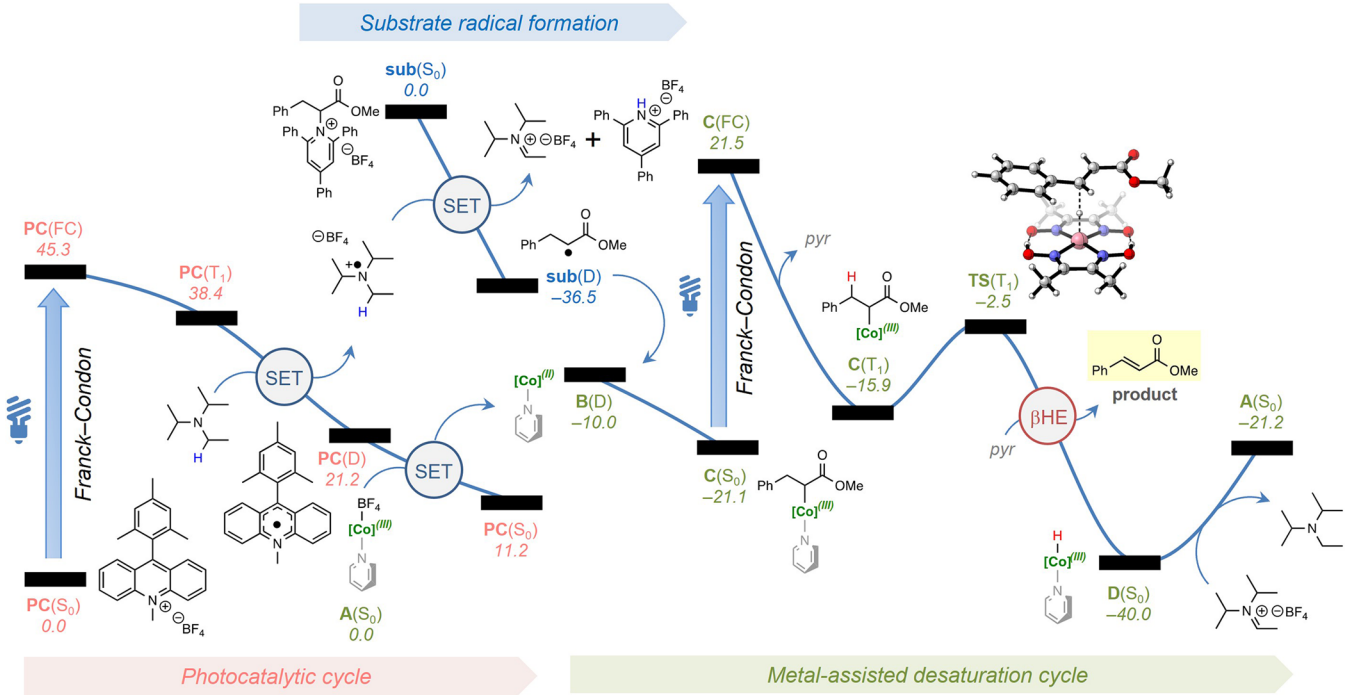

Figure 2. Potential energy surface (PES) for the light-assisted deamination process constituted by the photocatalytic cycle, substrate radical formation, and the metal-assisted desaturation cycle. Free energies (room temperature) are shown in kcal mol^{-1} at the BP91/TZVP//BP91/SVP computational level, using acetonitrile (ε = 35.688) as solvent.

https://doi.org/10.1021/acscatal.3c04305
ACS Catal. 2023, 13, 14205−14212

the organic radical intermediate is trapped by the $[Co]^{II}$ species to form $[Co]^{III}$-substrate. Low-temperature EPR measurements at −173 °C were performed to monitor the [Co] species since it is EPR-inactive at reaction temperature. As we mentioned before, the photocatalytic radical generation cycle results in the formation of a PC radical anion. This radical was also detected at −173 °C, however, with a much higher signal intensity (Figure 1d, black line). Upon the addition of [**Co**]-**1** to PC and *i*-Pr_2NEt mixture, the EPR signal of the reduced PC vanished with time, accompanied by appearing of a new signal at $g_\perp = 2.299$ and $g_\parallel = 2.011$ (Figure 1d, red and blue lines) due to the formation of EPR-active $[Co]^{II}$ species. DFT calculations revealed that this SET process is spontaneous, with an energy release of −10.0 kcal/mol. The presence of pyridinium salt **1** caused the disappearance of the $[Co]^{II}$ signal and the *in-situ*-generated substrate radical due to the formation of EPR-silent $[Co]^{III}$-substrate (Figure 1d, green line). DFT calculations supported the formation of the highly stable complex **C**(S0) at −21.1 kcal/mol (Figure 2). This can be attributed to the photolysis of relatively weak $C(sp^3)-[Co]^{III}$ bonds (BDE < 30 kcal/mol). In more detail, the excitation of $\mathbf{C}(S_0)$ by light leads to the formation of the Franck−Condon triplet state, **C**(FC), and its subsequent relaxation to the triplet state, $\mathbf{C}(T_1)$, accompanied by the release of pyridine. In this spin state, the subsequent elimination of the hydrogen at the β-position occurs, resulting in the desaturation of the substrate and the formation of $[Co]^{III}$-H, $\mathbf{D}(S_0)$, via homolytic cleavage of the $C(sp^3)-[Co]^{III}$ bond. This transition state, $\mathbf{TS}(T_1)$, was located and found to be only 12.8 kcal/mol higher in free energy relative to $\mathbf{C}(T_1)$. Finally, the $[Co]^{III}$-hydride complex regenerates *i*-Pr_2NEt and complex $\mathbf{A}(S_0)$, completing the cycle.

In conclusion, we have reported a straightforward conversion of various primary amines, including amino acids, natural products, and drug molecules, into their respective alkenes with selectivity for the trans-configured isomers. This biomimetic transformation was achieved using a dual organic dye/photoexcited base metal[28] catalysis system under visible light irradiation at room temperature. The protocol offers the flexibility to employ a diverse range of common amino acids and allows for late-stage functionalization of drug molecules. Given its simplicity, effectiveness, mild reaction conditions, and broad applicability, we anticipate that this photocatalytic dehydroamination method will find widespread use in both academic and industrial settings.

■ ASSOCIATED CONTENT

Supporting Information

The Supporting Information is available free of charge at https://pubs.acs.org/doi/10.1021/acscatal.3c04305.

Experimental procedures, analytical data for all new compounds, and NMR spectra (PDF)

■ AUTHOR INFORMATION

Corresponding Author

Osama El-Sepelgy − *Leibniz Institute for Catalysis e.V., Rostock 18059, Germany;* orcid.org/0000-0003-3131-4988; Email: Osama.Elsepelgy@Catalysis.de

Authors

Chenyang Wang − *Leibniz Institute for Catalysis e.V., Rostock 18059, Germany;* orcid.org/0000-0001-6210-4129

Phong Dam − *Leibniz Institute for Catalysis e.V., Rostock 18059, Germany*

Mohamed Elghobashy − *Leibniz Institute for Catalysis e.V., Rostock 18059, Germany*

Angelika Brückner − *Leibniz Institute for Catalysis e.V., Rostock 18059, Germany;* orcid.org/0000-0003-4647-1273

Jabor Rabeah − *Leibniz Institute for Catalysis e.V., Rostock 18059, Germany;* orcid.org/0000-0003-2162-0981

Luis Miguel Azofra − *Instituto de Estudios Ambientales y Recursos Naturales (i-UNAT), Universidad de Las Palmas de Gran Canaria (ULPGC), Las Palmas de Gran Canaria 35017, Spain;* orcid.org/0000-0003-4974-1670

Complete contact information is available at: https://pubs.acs.org/10.1021/acscatal.3c04305

Author Contributions

The manuscript was written through contributions of all authors. All authors have given approval to the final version of the manuscript.

Funding

This work has been financially supported by the Deutsche Forschungsgemeinschaft (DFG, grant number EL 1041/3-1) and by the Leibniz Institute for Catalysis e.V.

Notes

The authors declare no competing financial interest.

■ ACKNOWLEDGMENTS

M.E. thanks the Erasmus Munds program of the EU (SusCat) for the master scholarship. L.M.A. is a Ramón y Cajal fellow (ref RYC2021-030994-I) and thanks MCIN/AEI and NextGenerationEU/PRTR for support. We thank the KAUST Supercomputer Laboratory (KSL), KSA for providing the computational resources (Shaheen II). O.E.-S thanks Prof. Dr. Matthias Beller for his continued generous support.

■ REFERENCES

(1) Erwan, P.; Bastien, N. *Biomimetic Organic Synthesis*; Wiley VCH Verlag GmbH & Co. KGaA, 2021.

(2) Camm, E. L.; Towers, G. H. N. Phenylalanine ammonia lyase. *Phytochemistry* **1973**, *12*, 961−973.

(3) Vogt, T. Phenylpropanoid Biosynthesis. *Mol. Plant* **2010**, *3*, 2−20.

(4) (a) Wohlgemuth, R. Selective Biocatalytic Defunctionalization of Raw Materials. *ChemSusChem* **2022**, *15*, No. e202200402. (b) Berger, K. J.; Levin, M. D. Reframing primary alkyl amines as aliphatic building blocks. *Org. Biomol. Chem.* **2021**, *19*, 11−36. (c) Modak, A.; Maiti, D. Metal catalyzed defunctionalization reactions. *Org. Biomol. Chem.* **2016**, *14*, 21−35.

(5) (a) Schwartz, Z.; Valiton, C.; Lovasz, M.; Roberts, A. G. Recent Applications of Ammonium Ylide Based [2,3]-Sigmatropic and [1,2]-Stevens Rearrangements To Transform Amines into Natural Products. *Synthesis* **2023**. (b) McFadden, T. P.; Nwachukwu, C. I.; Roberts, A. G. An amine template strategy to construct successive C-C bonds: synthesis of benzo[h]quinolines by a deaminative ring contraction cascade. *Org. Biomol. Chem.* **2022**, *20*, 1379−1385.

(6) (a) von Hofmann, A. W. Beitrage zur Kenntniss der fluchtigen organischen Basen. *Ann. Chem. Pharm.* **1851**, *78*, 253−286. (b) Bach, R. D. trans-CYCLOOCTENE. *Org. Synth.* **1969**, *49*, 39. (c) Trauner, D. Richard Willstatter and the 1915 Nobel Prize in Chemistry. *Angew. Chem., Int. Ed.* **2015**, *54*, 11910−11916.

(7) (a) Cope, A. C.; Ciganek, E.; Horning, E. C. Methylenecyclohexane And *N,N*-Dimethylhydroxylamine Hydrochloride. *Org. Synth.* **1959**, *39*, 40. (b) Cope, A. C.; Foster, T. T.; Towle, P. H. Thermal

Decomposition of Amine Oxides to Olefins and Dialkylhydroxylamines. *J. Am. Chem. Soc.* **1949**, *71*, 3929−3934. (c) Serna, A. V.; Kürti, L.; Siitonen, J. H. Synthesis of (±)-Setigerumine I: Biosynthetic Origins of the Elusive Racemic Papaveraceae Isoxazolidine Alkaloids. *Angew. Chem., Int. Ed.* **2021**, *60*, 27236−27240.

(8) (a) Nicolaou, K. C.; Snyder, S. A.; Longbottom, D. A.; Nalbandian, A. Z.; Huang, X. New Uses for the Burgess Reagent in Chemical Synthesis: Methods for the Facile and Stereoselective Formation of Sulfamidates, Glycosylamines, and Sulfamides. *Chem.—Eur. J.* **2004**, *10*, 5581−5606. (b) De Christopher, P. J.; Adamek, J. P.; Lyon, G. D.; Galante, J. J.; Haffner, H. E.; Boggio, R. J.; Baumgarten, R. J. Approach to deamination. III. High-yield conversion of primary aliphatic amines into alkyl halides and alkenes via the use of sulfonimide leaving groups. *J. Am. Chem. Soc.* **1969**, *91*, 2384−2385. (c) Curtis, V. A.; Knutson, F. J.; Baumgarten, R. J. New deaminations IX - pyrolysis of N-alkyl-N,N-disulfonimides. *Tetrahedron Lett.* **1981**, *22*, 199−202.

(9) for reviews; (a) Katritzky, A. R.; Marson, C. M. Pyrylium Mediated Transformations of Primary Amino Groups into Other Functional Groups. New Synthetic Methods. *Angew. Chem., Int. Ed.* **1984**, *23*, 420−429. (b) He, F.-S.; Ye, S.; Wu, J. Recent Advances in Pyridinium Salts as Radical Reservoirs in Organic Synthesis. *ACS Catal.* **2019**, *9*, 8943−8960. (c) Correia, J. T.; Fernandes, V.; Matsuo, B. T.; Delgado, J. A.; de Souza, W. C.; Paixão, M. W. Photoinduced deaminative strategies: Katritzky salts as alkyl radical precursors. *Chem. Commun.* **2020**, *56*, 503−514. (d) Pang, Y.; Moser, D.; Cornella, J. Pyrylium Salts: Selective Reagents for the Activation of Primary Amino Groups in Organic Synthesis. *Synthesis* **2020**, *52*, 489−503. (e) Li, Y.-N.; Xiao, F.; Guo, Y.; Zeng, Y.-F. Recent Developments in Deaminative Functionalization of Alkyl Amines. *Eur. J. Org Chem.* **2021**, *2021*, 1215−1228.

(10) (a) Basch, C. H.; Liao, J.; Xu, J.; Piane, J. J.; Watson, M. P. Harnessing Alkyl Amines as Electrophiles for Nickel-Catalyzed Cross Couplings via C-N Bond Activation. *J. Am. Chem. Soc.* **2017**, *139*, 5313−5316. (b) Klauck, F. J. R.; James, M. J.; Glorius, F. Deaminative Strategy for the Visible-Light-Mediated Generation of Alkyl Radicals. *Angew. Chem. Int. Ed.* **2017**, *56*, 12336−12339.

(11) Selected examples: (a) Hu, J.; Wang, G.; Li, S.; Shi, Z. Selective C-N Borylation of Alkyl Amines Promoted by Lewis Base. *Angew. Chem., Int. Ed.* **2018**, *57*, 15227−15231. (b) Ociepa, M.; Turkowska, J.; Gryko, D. Redox-Activated Amines in $C(sp^3)$-$C(sp)$ and $C(sp^3)$-$C(sp^2)$ Bond Formation Enabled by Metal-Free Photoredox Catalysis. *ACS Catal.* **2018**, *8*, 11362−11367. (c) Sandfort, F.; Strieth-Kalthoff, F.; Klauck, F. J. R.; James, M. J.; Glorius, F. Deaminative Borylation of Aliphatic Amines Enabled by Visible Light Excitation of an Electron Donor-Acceptor Complex. *Chem.—Eur. J.* **2018**, *24*, 17210−17214. (d) Wu, J.; He, L.; Noble, A.; Aggarwal, V. K. Photoinduced Deaminative Borylation of Alkylamines. *J. Am. Chem. Soc.* **2018**, *140*, 10700−10704. (e) James, M. J.; Strieth-Kalthoff, F.; Sandfort, F.; Klauck, F. J. R.; Wagener, F.; Glorius, F. Visible-Light-Mediated Charge Transfer Enables C-C Bond Formation with Traceless Acceptor Groups. *Chem.—Eur. J.* **2019**, *25*, 8240−8244. (f) Jiang, X.; Zhang, M.-M.; Xiong, W.; Lu, L.-Q.; Xiao, W.-J. Deaminative (Carbonylative) Alkyl-Heck-type Reactions Enabled by Photocatalytic C-N Bond Activation. *Angew. Chem., Int. Ed.* **2019**, *58*, 2402−2406. (g) Klauck, F. J. R.; Yoon, H.; James, M. J.; Lautens, M.; Glorius, F. Visible-Light-Mediated Deaminative Three-Component Dicarbofunctionalization of Styrenes with Benzylic Radicals. *ACS Catal.* **2019**, *9*, 236−241. (h) Plunkett, S.; Basch, C. H.; Santana, S. O.; Watson, M. P. Harnessing Alkylpyridinium Salts as Electrophiles in Deaminative Alkyl-Alkyl Cross-Couplings. *J. Am. Chem. Soc.* **2019**, *141*, 2257−2262. (i) Sun, S.-Z.; Romano, C.; Martin, R. Site-Selective Catalytic Deaminative Alkylation of Unactivated Olefins. *J. Am. Chem. Soc.* **2019**, *141*, 16197−16201. (j) Wu, J.; Grant, P. S.; Li, X.; Noble, A.; Aggarwal, V. K. Catalyst-Free Deaminative Functionalizations of Primary Amines by Photoinduced Single-Electron Transfer. *Angew. Chem., Int. Ed.* **2019**, *58*, 5697−5701. (k) Yang, Z.-K.; Xu, N.-X.; Wang, C.; Uchiyama, M. Photoinduced $C(sp^3)$-N Bond Cleavage Leading to the Stereoselective Syntheses of Alkenes. *Chem.—Eur. J.* **2019**, *25*, 5433−5439. (l) Yue, H.; Zhu, C.; Shen, L.; Geng, Q.; Hock, K. J.; Yuan, T.; Cavallo, L.; Rueping, M. Nickel-catalyzed C-N bond activation: activated primary amines as alkylating reagents in reductive cross-coupling. *Chem. Sci.* **2019**, *10*, 4430−4435. (m) Kim, I.; Im, H.; Lee, H.; Hong, S. N-Heterocyclic carbene-catalyzed deaminative cross-coupling of aldehydes with Katritzky pyridinium salts. *Chem. Sci.* **2020**, *11*, 3192−3197. (n) Lübbesmeyer, M.; Mackay, E. G.; Raycroft, M. A. R.; Elfert, J.; Pratt, D. A.; Studer, A. Base-Promoted C-C Bond Activation Enables Radical Allylation with Homoallylic Alcohols. *J. Am. Chem. Soc.* **2020**, *142*, 2609−2616. (o) Wang, C.; Qi, R.; Xue, H.; Shen, Y.; Chang, M.; Chen, Y.; Wang, R.; Xu, Z. Visible-Light-Promoted $C(sp^3)$-H Alkylation by Intermolecular Charge Transfer: Preparation of Unnatural α-Amino Acids and Late-Stage Modification of Peptides. *Angew. Chem., Int. Ed.* **2020**, *59*, 7461−7466. (p) Wang, J.; Hoerrner, M. E.; Watson, M. P.; Weix, D. J. Nickel-Catalyzed Synthesis of Dialkyl Ketones from the Coupling of N-Alkyl Pyridinium Salts with Activated Carboxylic Acids. *Angew. Chem., Int. Ed.* **2020**, *59*, 13484−13489. (q) Zeng, X.; Yan, W.; Zacate, S. B.; Cai, A.; Wang, Y.; Yang, D.; Yang, K.; Liu, W. Copper-Catalyzed Deaminative Difluoromethylation. *Angew. Chem., Int. Ed.* **2020**, *59*, 16398−16403. (r) Cai, Z.; Gu, R.; Si, W.; Xiang, Y.; Sun, J.; Jiao, Y.; Zhang, X. Photoinduced allylic defluorinative alkylation of trifluoromethyl alkenes with Katritzky salts under catalyst- and metal-free conditions. *Green Chem.* **2022**, *24*, 6830−6835.

(12) Berger, K. J.; Driscoll, J. L.; Yuan, M.; Dherange, B. D.; Gutierrez, O.; Levin, M. D. Direct Deamination of Primary Amines via Isodiazene Intermediates. *J. Am. Chem. Soc.* **2021**, *143*, 17366−17373.

(13) Brown, K. L. Chemistry and Enzymology of Vitamin B12. *Chem. Rev.* **2005**, *105*, 2075−2150.

(14) (a) Daikh, B. E.; Finke, R. G. The persistent radical effect: a prototype example of extreme, 105 to 1, product selectivity in a free-radical reaction involving persistent.cntdot.CoII[macrocycle] and alkyl free radicals. *J. Am. Chem. Soc.* **1992**, *114*, 2938−2943. (b) Wang, Y.; Begley, T. P. Mechanistic Studies on CysS - A Vitamin B12-Dependent Radical SAM Methyltransferase Involved in the Biosynthesis of the tert-Butyl Group of Cystobactamid. *J. Am. Chem. Soc.* **2020**, *142*, 9944−9954.

(15) For reviews; (a) Ram Bajya, K.; Selvakumar, S. Dual Photoredox and Cobalt Catalysis Enabled Transformations. *Eur. J. Org Chem.* **2022**, *2022*, No. e202200229. (b) Kojima, M.; Matsunaga, S. The Merger of Photoredox and Cobalt Catalysis. *Trends Chem.* **2020**, *2*, 410−426.

(16) Selected examples: (a) Abrams, D. J.; West, J. G.; Sorensen, E. J. Toward a mild dehydroformylation using base-metal catalysis. *Chem. Sci.* **2017**, *8*, 1954−1959. (b) Cartwright, K. C.; Tunge, J. A. Decarboxylative Elimination of N-Acyl Amino Acids via Photoredox/Cobalt Dual Catalysis. *ACS Catal.* **2018**, *8*, 11801−11806. (c) Sun, X.; Chen, J.; Ritter, T. Catalytic dehydrogenative decarboxyolefination of carboxylic acids. *Nat. Chem.* **2018**, *10*, 1229−1233. (d) Zhao, H.; McMillan, A. J.; Constantin, T.; Mykura, R. C.; Juliá, F.; Leonori, D. Merging Halogen-Atom Transfer (XAT) and Cobalt Catalysis to Override E2-Selectivity in the Elimination of Alkyl Halides: A Mild Route toward contra-Thermodynamic Olefins. *J. Am. Chem. Soc.* **2021**, *143*, 14806−14813. (e) Huang, L.; Ji, T.; Zhu, C.; Yue, H.; Zhumabay, N.; Rueping, M. Bioinspired desaturation of alcohols enabled by photoredox proton-coupled electron transfer and cobalt dual catalysis. *Nat. Commun.* **2022**, *13*, 809. (f) Wang, X.; Li, Y.; Wu, X. Photoredox/Cobalt Dual Catalysis Enabled Regiospecific Synthesis of Distally Unsaturated Ketones with Hydrogen Evolution. *ACS Catal.* **2022**, *12*, 3710−3718. (g) Caldora, H. P.; Zhang, Z.; Tilby, M. J.; Turner, O.; Leonori, D. Dual Photochemical H-Atom Transfer and Cobalt Catalysis for the Desaturative Synthesis of Phenols from Cyclohexanones. *Angew. Chem., Int. Ed.* **2023**, *62*, No. e202301656.

(17) (a) West, J. G.; Huang, D.; Sorensen, E. J. Acceptorless dehydrogenation of small molecules through cooperative base metal catalysis. *Nat. Commun.* **2015**, *6*, 10093. (b) Sahoo, M. K.; Balaraman, E. Room temperature catalytic dehydrogenation of cyclic amines with the liberation of H_2 using water as a solvent. *Green Chem.* **2019**, *21*,

https://doi.org/10.1021/acscatal.3c04305
ACS Catal. 2023, 13, 14205−14212

2119−2128. (c) Zhou, M.-J.; Zhang, L.; Liu, G.; Xu, C.; Huang, Z. Site-Selective Acceptorless Dehydrogenation of Aliphatics Enabled by Organophotoredox/Cobalt Dual Catalysis. *J. Am. Chem. Soc.* **2021**, *143*, 16470−16485. (d) Ritu Kolb, D.; Kolb, D.; Jain, N.; König, B. Synthesis of Linear Enamides and Enecarbamates via Photoredox Acceptorless Dehydrogenation. *Adv. Synth. Catal.* **2023**, *365*, 605−611.

(18) Katritzky, A. R.; El-Mowafy, A. M. Pyrylium-mediated conversion of primary alkyl primary amines into olefins via tetrahydrobenzoacridiniums: a mild alternative to the Hofmann elimination. *J. Org. Chem.* **1982**, *47*, 3506−3511.

(19) (a) Fukuzumi, S.; Kotani, H.; Ohkubo, K.; Ogo, S.; Tkachenko, N. V.; Lemmetyinen, H. Electron-Transfer State of 9-Mesityl-10-methylacridinium Ion with a Much Longer Lifetime and Higher Energy Than That of the Natural Photosynthetic Reaction Center. *J. Am. Chem. Soc.* **2004**, *126*, 1600−1601. (b) Uygur, M.; Danelzik, T.; Mancheño, O. G. Metal-free desilylative C-C bond formation by visible-light photoredox catalysis. *Chem. Commun.* **2019**, *55*, 2980−2983.

(20) Leifert, D.; Studer, A. The Persistent Radical Effect in Organic Synthesis. *Angew. Chem., Int. Ed.* **2020**, *59*, 74−108.

(21) Ng, F. T. T.; Rempel, G. L. Ligand effects on transition metal-alkyl bond dissociation energies. *J. Am. Chem. Soc.* **1982**, *104*, 621−623.

(22) Hari, D. P.; König, B. Synthetic applications of eosin Y in photoredox catalysis. *Chem. Commun.* **2014**, *50*, 6688−6699.

(23) Shang, T.-Y.; Lu, L.-H.; Cao, Z.; Liu, Y.; He, W.-M.; Yu, B. Recent advances of 1,2,3,5-tetrakis(carbazol-9-yl)-4,6-dicyanobenzene (4CzIPN) in photocatalytic transformations. *Chem. Commun.* **2019**, *55*, 5408−5419.

(24) Ramirez, N. P.; König, B.; Gonzalez-Gomez, J. C. Decarboxylative Cyanation of Aliphatic Carboxylic Acids via Visible-Light Flavin Photocatalysis. *Org. Lett.* **2019**, *21*, 1368−1373.

(25) Wang, C.; Azofra, L. M.; Dam, P.; Espinoza-Suarez, E. J.; Do, H. T.; Rabeah, J.; Brückner, A.; El-Sepelgy, O. Photoexcited cobalt catalysed endo-selective alkyl Heck reaction. *Chem. Commun.* **2023**, *59*, 3862−3865.

(26) Wang, C.; Azofra, L. M.; Dam, P.; Sebek, M.; Steinfeldt, N.; Rabeah, J.; El-Sepelgy, O. Catalytic Desaturation of Aliphatic Amides and Imides Enabled by Excited-State Base-Metal Catalysis. *ACS Catal.* **2022**, *12*, 8868−8876.

(27) Fukuzumi, S.; Ohkubo, K.; Suenobu, T.; Kato, K.; Fujitsuka, M.; Ito, O. Photoalkylation of 10-Alkylacridinium Ion via a Charge-Shift Type of Photoinduced Electron Transfer Controlled by Solvent Polarity. *J. Am. Chem. Soc.* **2001**, *123*, 8459−8467.

(28) (a) Ye, J.-H.; Miao, M.; Huang, H.; Yan, S.-S.; Yin, Z.-B.; Zhou, W.-J.; Yu, D.-G. Visible-Light-Driven Iron-Promoted Thiocarboxylation of Styrenes and Acrylates with CO2. *Angew. Chem., Int. Ed.* **2017**, *56*, 15416−15420. (b) Gandeepan, P.; Müller, T.; Zell, D.; Cera, G.; Warratz, S.; Ackermann, L. 3d Transition Metals for C-H Activation. *Chem. Rev.* **2019**, *119*, 2192−2452. (c) Jamatia, R.; Mondal, A.; Srimani, D. Visible-Light-Induced Manganese-Catalyzed Reactions: Present Approach and Future Prospects. *Adv. Synth. Catal.* **2021**, *363*, 2969−2995.

https://doi.org/10.1021/acscatal.3c04305
ACS Catal. 2023, 13, 14205−14212

Paper 4:

Photoexcited cobalt catalysed endo-selective alkyl Heck reaction.

Wang, C.; Azofra, L. M.; Dam, P.; Espinoza-Suarez, E. J.; Do, H. T.; Rabeah, J.; Brückner, A.; El-Sepelgy, O.*

Chem. Commun. **2023**, *59*, 3862-3865.

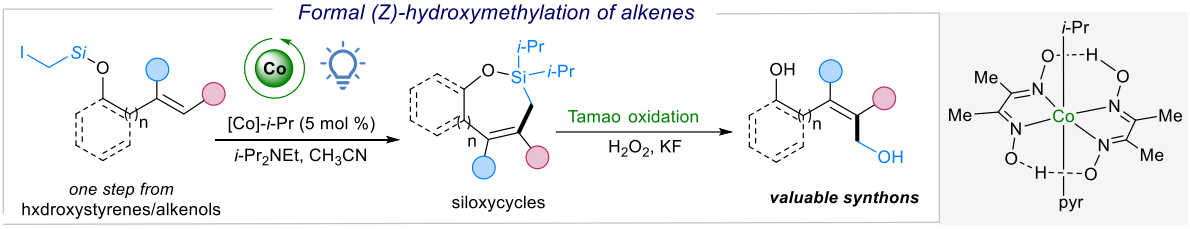

ChemComm

COMMUNICATION

View Article Online
View Journal | View Issue

Cite this: *Chem. Commun.*, 2023, **59**, 3862

Received 22nd December 2022,
Accepted 23rd February 2023

DOI: 10.1039/d2cc06967a

rsc.li/chemcomm

Photoexcited cobalt catalysed *endo*-selective alkyl Heck reaction†

Chenyang Wang,[a] Luis Miguel Azofra,[b] Phong Dam,[a] Edelman J. Espinoza-Suarez,[a] Hieu Trung Do,[a] Jabor Rabeah,[a] Angelika Brückner[a] and Osama El-Sepelgy*[a]

Herein, we report an intramolecular *endo*-selective Heck reaction of iodomethylsilyl ethers of phenols and alkenols. The reaction leads to the formation of seven- and eight-membered siloxycycles in excellent yields, which could be further converted into the corresponding allylic alcohols upon oxidation. Thus, this method could be used for the selective (*Z*)-hydroxymethylation of *o*-hydroxystyrenes and alkenols. Rapid scan EPR experiments and DFT calculations suggest a concerted *β*-hydrogen elimination event to take place in the triplet state.

The Mizoroki–Heck reaction[1] is a fundamental synthetic method for C–C bond formation and was awarded the Nobel prize in Chemistry in 2010.[2] Most of the transformations involve the use of aryl halides while the application of C(sp^3) halides has been less investigated due to the slow rate of oxidative addition.[3] Despite these difficulties, Fu has reported the first example of an intramolecular alkyl-Heck reaction using an NHC ligand together with palladium salts.[4] Furthermore, Alexanian has disclosed an elegant example of an alkyl-Heck reaction *via* a hybrid organometallic radical mechanism using palladium catalysis under thermal conditions.[5] Both methodologies involve conventional intramolecular 5-*exo*-trig and 6-*exo*-trig selective cyclization.[4,5] However, the *endo*-trig alkyl-Heck reaction is very rare and we are only aware of two examples. In 2014, Gevorgean disclosed the *endo* selective alkyl-Heck cyclization of iodomethylsilyl to the corresponding siloxycycles,[6] a reaction that has been previously reported by Koreeda under reductive conditions (Scheme 1).[7] The second example was reported by Liu for the synthesis of 5-phenyltetrahydropyridine derivatives from the alkyl iodide bearing a 1-aryl-substituted alkene moiety.[8] These two examples involve the use of 10 mol% of palladium salt and operate *via* a hybrid palladium radical mechanism under thermal conditions. The requirement of the use of 20 mol% of expensive ferrocene-based phosphine (dtbdppf) and equivalent amounts of silver salts limits the large-scale application.[6,8] To the best of our knowledge, there are no reports on base-metal catalysed *endo*-selective alkyl Heck reactions.

Motivated by our previous work on photoexcited cobalt-catalyzed desaturation of amides,[9] we decided to investigate whether the thermal palladium/dtbdppf/Ag(OTf) catalytic system can be replaced by a visible light photocatalytic phosphine-free alternative with base metals.[10] To validate our proposal, we decided to test the cyclization reaction of iodomethylsilyl ethers of phenols and aliphatic alkenols. Herein, we report a new photoexcited cobalt catalysed *endo*-selective alkyl-Heck reaction.[11,12]

Our hypothesis involves the use of a nucleophilic $[Co]^{I}$ complex, which could be photo-generated *in situ* from a simple [Co]-*i*-Pr catalyst and a suitable base under visible light irradiation. This cobalt species could react with alkyl halide to give the corresponding alkyl–$[Co]^{III}$ intermediate, which under visible light irradiation could form a $[Co]^{II}$ species and an alkyl radical intermediate.[12,13] Then the alkyl radical undergoes intramolecular radical addition followed by recombination with $[Co]^{II}$. Under visible light irradiation, the formed $[Co]^{III}$ species generates the Heck product together with $[Co]^{III}$–H, which could then be deprotonated by a suitable base to restore the nucleophilic $[Co]^{I}$ species (Scheme 2).

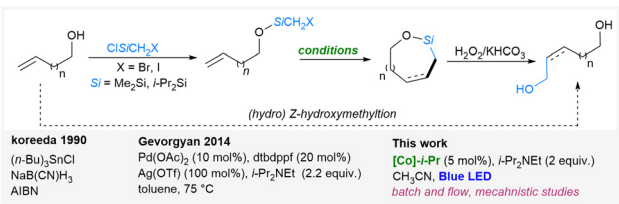

Scheme 1 Formal (hydro) (*Z*)-hydroxymethylation of alkenes.

[a] *Leibniz Institute for Catalysis e.V., Albert-Einstein-Str. 29a, Rostock 18059, Germany. E-mail: Osama.Elsepelgy@Catalysis.de*

[b] *Instituto de Estudios Ambientales y Recursos Naturales (i-UNAT), Universidad de Las Palmas de Gran Canaria (ULPGC), Campus de Tafira, Las Palmas de Gran Canaria 35017, Spain*

† Electronic supplementary information (ESI) available: experimental details and characterization of all compounds, and copies of ^{1}H and ^{13}C NMR spectra for selected compounds. See DOI: https://doi.org/10.1039/d2cc06967a

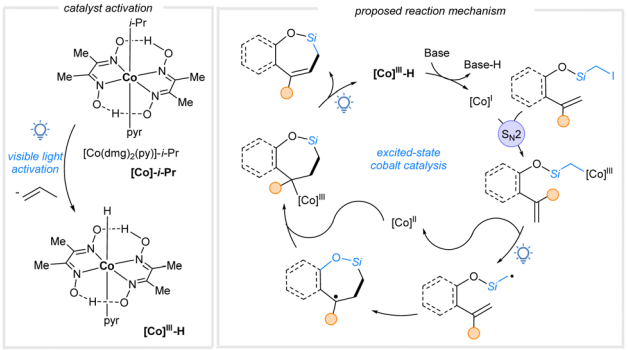

Scheme 2 Plausible mechanism of the *endo*-selective cyclization.

Our study was initiated by the investigation of silyl-tethered *o*-hydroxystyrene **1a** as a model substrate for the intramolecular Heck-reaction. We found that the combination of 5 mol% of [Co(dmg)$_2$(py)*i*-Pr] and Hünig's base (DIPEA) in acetonitrile under blue LED irradiation at room temperature was optimal for affording the 7-membered siloxycycle **2a** in quantitative yield (Table 1, entry 1). It is worth noting that this catalytic system does not require the use of an additional photoredox catalyst,[14] strong reductive conditions,[15] or Grignard reagents.[16] Control experiments revealed no background reactivity in the absence of the cobalt catalyst or blue light (Table 1, entries 2 and 3). Investigation of different organic and inorganic bases revealed that Hünig's base is the best choice (Table 1, entries 4–7). Switching of the reaction solvent from CH_3CN to DCM or THF led to lower yields (Table 1, entries 8 and 9). Finally, the addition of TEMPO leads to no product formation (Table 1, entry 10).

Next, the generality of our catalytic system was investigated under the optimized reaction conditions (Table 2). Arene-tethered substrates bearing different substituents (Cl, Br, F, Me and OMe) in the 4 different positions of the phenyl ring afforded the corresponding *endo*-selective Heck products **2b–2j** in excellent yields (95–99%). Importantly, the use of the alkyl bromide analogue of **1d** led to the formation of the desired

Table 1 Control reactions of the optimized conditions[a]

Entry	Deviation from the standard conditions	Yield (%)
1	None	99
2	No **[Co]-*i*-Pr** or no light	n.d.
3	70 °C instead of light	Trace
4	1 equiv. K_2CO_3 as base	72
5	1 equiv. K_2CO_3, 20 mol% i-Pr$_2$NEt as base	81
6	DMAP as base	Trace
7	DBU as base	Trace
8	DCM as solvent	85
9	THF as solvent	71
10	TEMPO was added	n.d.

[a] Standard conditions: substrate **1a** (0.1 mmol), **[Co]-*i*-Pr** (0.005 mmol, 3.6 mg), *i*-Pr$_2$NEt (0.2 mmol, 35 μL), CH_3CN (1 mL), rt, Blue LED (19 W, Ledxon), 16 h, isolated yields.

Table 2 Scope of *o*-hydroxystyrenes and alkenols[a]

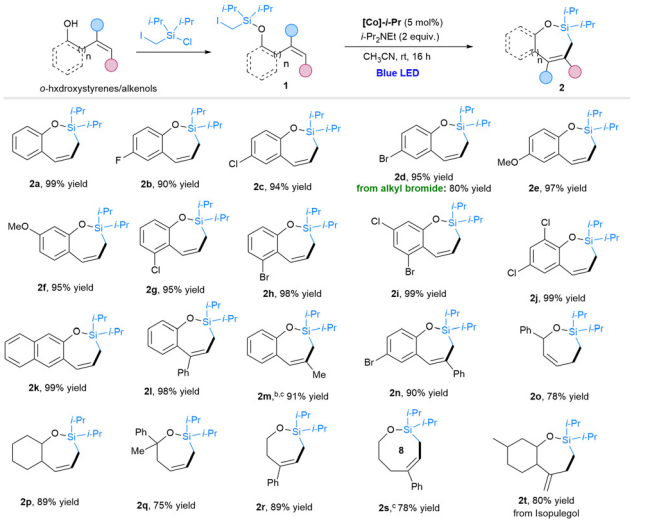

[a] Reaction conditions: **1** (0.2 mmol), **[Co]-i-Pr** (0.01 mmol, 7.2 mg), *i*-Pr$_2$NEt (0.4 mmol, 70 μL), CH_3CN (2 mL), rt, Blue LED (19 W, Ledxon), 16 h, isolated yields. [b] Mixture of isomers (6.4 : 1:1.6 : 1.6), see ESI for details. [c] NMR yield.

product in 80% yield. Furthermore, the naphthyl derivative **1k** furnished the cyclic product in quantitative yield. Then, substrates bearing substituents in the olefin were studied. The substrate with the substituent on the α-position produced the *endo*-product **2l**. In addition, **1m** bearing substituents in the β-position led to the formation of the oxasilepine **2m**, albeit with moderate selectivity (60% of major isomer). As for the (*E*)-2-styrylphenol **1n**, the selectivity of the formation of **2n** was extremely improved.

Encouraged by these promising results, we tested more challenging systems such as aliphatic alkenols. The cyclization of the secondary homoallylic alcohol **1o** led to the formation of the allylic siloxycycle **2o** in 78% yield. Interestingly, the substrate bearing two vicinal substitutions at the α- and β-positions of the tethered alcohol efficiently furnish the siloxysilane **2p** in very good yield. Remarkably, tethered tertiary alcohol **1r** was also found to tolerate the catalytic system and produce the desired product in 75% yield. Importantly, the tethered primary alcohols **1r** and **1s** underwent 7-*endo*-trig and 8-*endo*-trig cyclization in 89% and 78% yield, respectively. In addition, the application of the methodology on the naturally occurring isopulegol led to the formation of **2t** in very good yield and excellent *endo*-selectivity.

To showcase the practical applicability of this photoexcited catalytic transformation, we carried out a 3 mmol scale alkyl-Heck reaction for substrate **1d** in batch mode. Fortunately, the desired product **2d** was obtained in 90% yield in 24 hours. To further improve the efficiency of the developed methodology, we reperformed the reaction using a microflow reactor. Impressively, 76% of the isolated cyclic product **2d** was obtained after only 2.5 hours. Afterwards, we turned our attention to further derivatization of the cyclic products. To our delight, the oxasilepine **2d** was smoothly oxidized to the (*Z*)-allylic alcohol **3d** *via* Tamao oxidation (Scheme 3).

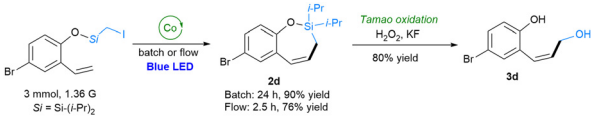

Scheme 3 Gram scale formal (*Z*)-hydroxymethylation of styrene derivatives.

To gain more insights into the reaction mechanism, we performed preliminary experimental mechanistic studies. First, the reaction profile was studied (see the ESI† for details), which showed that more than 75% conversion was obtained after 4 h. Furthermore, to exclude the possibility of a radical chain process, light on–off experiments were carried out. In the absence of light, no reaction was observed (Fig. 1a). Under light irradiation, we obtained the quantum yield of $\Phi = 0.045$ for the photoexcited cobalt-catalyzed Heck reaction (see the ESI† for details).

Additional controlled UV-vis, EPR and NMR experiments were performed. The UV-vis spectrum of the initial $[Co]^{III}$-*i*-Pr complex showed three poorly resolved Ligand-to-Metal Charge Transfer (LMCT) absorption bands at 330, 390 and 450 nm (Fig. 1b-black line).[17] These bands decreased quickly during the first minute of irradiation and a new LMCT band appeared at $\lambda_{max} = 430$ nm due to the formation of $[Co]^{II}$ species. This was also evident from the EPR spectrum of the irradiated $[Co]^{III}$-*i*-Pr complex, which showed an axial signal at $g_{\perp} = 2.282$ and $g_{\parallel} = 2.029$ with resolved ^{59}Co hyperfine structure ($I = 7/2$) of the parallel component (Fig. 1c). On the other hand, the ^{1}H NMR spectrum of irradiated $[Co]^{III}$-*i*-Pr in DCM-d_2 points to the formation of $[Co]^{III}$-H and propene (see supporting information for details). The formation of $[Co]^{II}$ observed in the EPR spectrum might be due to a homolytic cleavage of the $[Co]^{III}$-H bond upon irradiation.[18] In order to distinguish between the stepwise and the concerted pathways of the formation of the alkene, we performed a spin trap experiment using 5,5-dimethyl-1-pyrrolin-*N*-oxide (DMPO) by rapid scan EPR spectroscopy. Interestingly, an unstable DMPO-H species ($a_N = 14.8$ G, $a_{H2} = 19.3$ G) was formed instead of the stable DMPO-*i*-Pr spin adduct, suggesting a concerted mechanism (Fig. 1d). During the catalytic reaction in the presence of *i*-Pr_2NEt and the substrate **1d**, the amount of EPR-active $[Co]^{II}$ species was by about 70% lower than in the $[Co]^{III}$ pre-catalyst after irradiating for 1 min and stayed nearly constant during prolonged irradiation. This indicates that the catalyst quickly reached a steady state in which an effective $[Co]^{I}/[Co]^{III}/[Co]^{II}$ cycle is established that keeps the $[Co]^{II}$ constant in time average. UV-Vis results also confirmed this hypothesis by showing a decrease of the LMCT band at 430 nm of the $[Co]^{II}$ complex along with a new band at 367 nm that might arise from the coordination of the substrate to [Co] sites during the catalytic reaction.

Next, the reaction mechanism for the light-driven Heck reaction has been studied by means of DFT techniques (Fig. 2) using **1a** as a model substrate. The mechanism involves the carbon-carbon coupling *via* internal single electron transfer (ISET) and the β hydrogen elimination and S_N2 steps. Thus, complex **A** is excited from the singlet (S_0) to the triplet (T_1) state through a vertical (Franck–Condon, FC) excitation that brings the complex to a high-energy state, 40.5 kcal mol^{-1}. After relaxation, pyridine (pyr) is released to form complex **B**(T_1), followed by the breakage of the $[Co]^{III}$–C bond into the $[Co]^{II}$ and the radical species **C**, both in the doublet state (D) and therefore being EPR active species. The species **C** contains an unpaired electron in the terminal carbon directly bound to the tether, making it quite reactive. Through an internal single electron transfer (ISET) process, the radical carbon reacts with the C(sp^2) of the vinyl group. This entails a carbon–carbon coupling whose transition state (TS_{CCC}) lies just 3.6 kcal mol^{-1} above in relative free energy with respect to **B** to finally produce the seven-membered ring at **D** in a very spontaneous process (−9.1 kcal mol^{-1} relative to **A**). It should be noted that the formation of the highly energetic (excited) **C** species, promoted

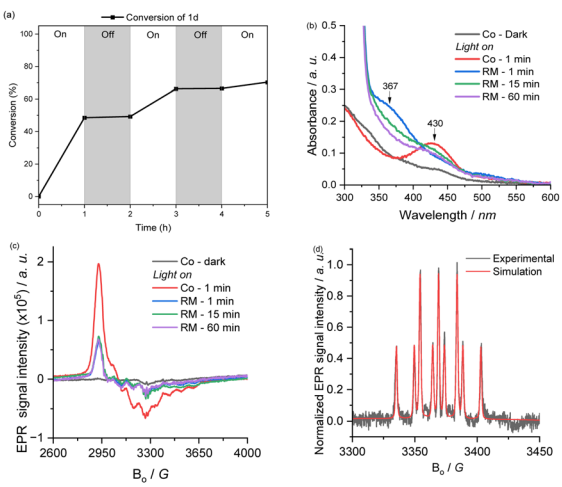

Fig. 1 (a) Light on-off experiment; (b) UV-vis spectra of (0.005 mmol [Co]-*i*-Pr in 6 ml MeCN, black line) and reaction mixture ([Co]-*i*-Pr, 0.1 mmol **1d**, 0.2 mmol *i*-Pr_2NEt) before and after irradiation with time; (c) EPR spectra measured at −173 °C of (0.005 mmol [Co]-*i*-Pr, 1 ml MeCN) and reaction mixture (0.005 mmol [Co]-*i*-Pr, 0.1 mmol **1d**, 0.2 mmol *i*-Pr_2NEt, 1 ml MeCN) before and after irradiation with time. (d) Experimental and simulated EPR spectra for [Co]-*i*-Pr with DMPO using rapid scan EPR spectroscopy.

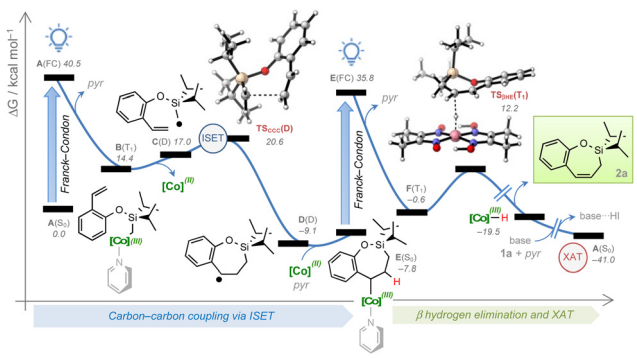

Fig. 2 Detailed description of the potential energy surface (PES). Free energy results are shown in kcal mol^{-1} at the PBE96/TZVP//BP86/6-31G-SVP(l) level of theory in acetonitrile as solvent.

by light irradiation, is decisive to boost the carbon–carbon coupling step that could not otherwise occur through classical thermal catalysis. The radical species **D** is recombined with $[Co]^{II}$ and pyridine forming complex $\mathbf{E}(S_0)$. This can also be excited by visible light, undergoing a second vertical (FC) transition, lying at 35.8 kcal mol^{-1}. In a similar mechanistic fashion, pyridine is again released from the complex leading to $\mathbf{F}(T_1)$, −0.6 kcal mol^{-1}. In accordance with the rapid scan EPR experiment, the desaturation process takes place *via* a concerted β-hydrogen elimination event in the triplet state, with a transition state ($TS_{\beta HE}$) just lying 12.8 kcal mol^{-1} above in free energy with respect to **F**. As a result of this, the hydride $[Co]^{III}$–H complex and product **2a** are formed, and complex $\mathbf{A}(S_0)$ is regenerated by action of the organic base and substrate **1a** *via* the S_N2 pathway to be newly integrated in the photoexcited cobalt cycle.

As an exception, the intermediate $\mathbf{E}(S_0)$ of the substrate **2l** bearing a highly stable double benzylic radical is suggested to follow an outer sphere mechanism.

In summary, we have developed a highly selective cobalt catalyzed cyclization of iodomethylsilyl ethers of phenol and of aliphatics. Upon further oxidation of the formed siloxycycles, the corresponding allylic alcohols are produced. This method could be used for the formal hydroxymethylation of allylic alcohols and *o*-hydroxystyrenes.[19] The reaction mechanism has been studied using different experimental and theoretical tools. It is anticipated that this operationally simple and scalable photoexcited base metal methodology would serve as a basis for the development of a greener alternative to the Pd-catalyzed alkyl-Heck reaction.[20]

This work has been finically supported by Deutsche Forschungsgemeinschaft (DFG, grant number 456582392) and by Leibniz institute for catalysis e.V (LIKAT Rostock). E. J. E.-S acknowledges the Erasmus Munds program of the EU (SusCat) for the master scholarship. H.T.D. thanks RoHan SDG Graduate School funded by the German Academic Exchange Service (DAAD, 57315854) for the postdoctoral fellowship. L.M.A. is a Ramón y Cajal fellow (ref. RYC2021-030994-I) and thanks MCIN/AEI and NextGenerationEU/PRTR for support and the KAUST Supercomputer Laboratory (KSL) for providing the computational resources (Shaheen II). O.E.-S. gratefully thanks Prof. Dr Matthias Beller for his continued generous support.

Conflicts of interest

There are no conflicts of interest to declare.

Notes and references

1 M. Oestreich, *The Mizoroki-Heck Reaction*, John Wiley & Sons, Ltd, 2009.
2 (*a*) M. Tsutomu, M. Kunio and O. Atsumu, *Bull. Chem. Soc. Jpn.*, 1971, **44**, 581; (*b*) H. A. Dieck and R. F. Heck, *J. Am. Chem. Soc.*, 1974, **96**, 1133–1136; (*c*) R. F. Heck, *J. Am. Chem. Soc.*, 1969, **91**, 6707–6714.
3 (*a*) S. Bräse and A. d Meijere, *Metal-Catalyzed Cross-Coupling Reactions and More*, ed. A. de Meijere, S. Bräse and M. Oestreich, 2014, pp. 533–663; (*b*) D. Kurandina, P. Chuentragool and V. Gevorgyan, *Synthesis*, 2019, 985–1005.
4 (*a*) L. Firmansjah and G. C. Fu, *J. Am. Chem. Soc.*, 2007, **129**, 11340–11341; (*b*) Y. Wu, B. Xu, G. Zhao, Z. Pan, Z.-M. Zhang and J. Zhang, *Chin. J. Chem.*, 2021, **39**, 3255–3260.
5 K. S. Bloome, R. L. McMahen and E. J. Alexanian, *J. Am. Chem. Soc.*, 2011, **133**, 20146–20148.
6 M. Parasram, V. O. Iaroshenko and V. Gevorgyan, *J. Am. Chem. Soc.*, 2014, **136**, 17926–17929.
7 M. Koreeda and L. G. Hamann, *J. Am. Chem. Soc.*, 1990, **112**, 8175–8177.
8 X. Dong, Y. Han, F. Yan, Q. Liu, P. Wang, K. Chen, Y. Li, Z. Zhao, Y. Dong and H. Liu, *Org. Lett.*, 2016, **18**, 3774–3777.
9 C. Wang, L. M. Azofra, P. Dam, M. Sebek, N. Steinfeldt, J. Rabeah and O. El-Sepelgy, *ACS Catal.*, 2022, **12**, 8868–8876.
10 For selected reviews and examples, (*a*) K. P. S. Cheung, S. Sarkar and V. Gevorgyan, *Chem. Rev.*, 2022, **122**, 1543–1625; (*b*) L.-L. Liao, L. Song, S.-S. Yan, J.-H. Ye and D.-G. Yu, *Trends Chem.*, 2022, **4**, 512–527; (*c*) L. Huang, T. Ji, C. Zhu, H. Yue, N. Zhumabay and M. Rueping, *Nat. Commun.*, 2022, **13**, 809; (*d*) D. Kalsi, N. Barsu, S. Chakrabarti, P. Dahiya, M. Rueping and B. Sundararaju, *Chem. Commun.*, 2019, **55**, 11626–11629.
11 (*a*) W.-K. Tang, Z.-W. Xu, J. Xu, F. Tang, X.-X. Li, J.-J. Dai, H.-J. Xu and Y.-S. Feng, *Org. Lett.*, 2019, **21**, 196–200; (*b*) L. M. Kreis, S. Krautwald, N. Pfeiffer, R. E. Martin and E. M. Carreira, *Org. Lett.*, 2013, **15**, 1634–1637.
12 M. E. Weiss, L. M. Kreis, A. Lauber and E. M. Carreira, *Angew. Chem., Int. Ed.*, 2011, **50**, 11125–11128.
13 G. Prina Cerai and B. Morandi, *Chem. Commun.*, 2016, **52**, 9769–9772.
14 H. Cao, H. Jiang, H. Feng, J. M. C. Kwan, X. Liu and J. Wu, *J. Am. Chem. Soc.*, 2018, **140**, 16360–16367.
15 (*a*) M. Okabe, M. Abe and M. Tada, *J. Org. Chem.*, 1982, **47**, 1775–1777; (*b*) M. Ladlow and G. Pattenden, *Tetrahedron Lett.*, 1984, **25**, 4317–4320; (*c*) S. Torii, T. Inokuchi and T. Yukawa, *J. Org. Chem.*, 1985, **50**, 5875–5877; (*d*) B. P. Branchaud and Y. L. Choi, *Tetrahedron Lett.*, 1988, **29**, 6037–6038; (*e*) B. P. Branchaud and M. S. Meier, *Tetrahedron Lett.*, 1988, **29**, 3191–3194; (*f*) B. P. Branchaud, M. S. Meier and Y. Choi, *Tetrahedron Lett.*, 1988, **29**, 167–170; (*g*) B. P. Branchaud and M. S. Meier, *J. Org. Chem.*, 1989, **54**, 1320–1326; (*h*) S. Busato, O. Tinembart, Z.-D. Zhang and R. Scheffold, *Tetrahedron*, 1990, **46**, 3155–3166; (*i*) B. P. Branchaud and W. D. Detlefsen, *Tetrahedron Lett.*, 1991, **32**, 6273–6276; (*j*) B. Giese, P. Erdmann, T. Göbel and R. Springer, *Tetrahedron Lett.*, 1992, **33**, 4545–4548.
16 (*a*) Y. Ikeda, T. Nakamura, H. Yorimitsu and K. Oshima, *J. Am. Chem. Soc.*, 2002, **124**, 6514–6515; (*b*) Y. Ikeda, H. Yorimitsu, H. Shinokubo and K. Oshima, *Adv. Synth. Catal.*, 2004, **346**, 1631–1634; (*c*) W. Affo, H. Ohmiya, T. Fujioka, Y. Ikeda, T. Nakamura, H. Yorimitsu, K. Oshima, Y. Imamura, T. Mizuta and K. Miyoshi, *J. Am. Chem. Soc.*, 2006, **128**, 8068–8077.
17 S. Varma, C. E. Castillo, T. Stoll, J. Fortage, A. G. Blackman, F. Molton, A. Deronzier and M.-N. Collomb, *Phys. Chem. Chem. Phys.*, 2013, **15**, 17544–17552.
18 G. N. Schrauzer, J. W. Sibert and R. J. Windgassen, *J. Am. Chem. Soc.*, 1968, **90**, 6681–6688.
19 T. Fujiwara, K. Yanai, K. Shimane, M. Takamori and T. Takeda, *Eur. J. Org. Chem.*, 2001, 155–161.
20 (*a*) K. Muralirajan, R. Kancherla, A. Gimnkhan and M. Rueping, *Org. Lett.*, 2021, **23**, 6905–6910; (*b*) G. S. Lee, D. Kim and S. H. Hong, *Nat. Commun.*, 2021, **12**, 991; (*c*) N. Kvasovs, V. Iziumchenko, V. Palchykov and V. Gevorgyan, *ACS Catal.*, 2021, **11**, 3749–3754; (*d*) X. Jia, Z. Zhang and V. Gevorgyan, *ACS Catal.*, 2021, **11**, 13217–13222; (*e*) B. Zhao, R. Shang, G.-Z. Wang, S. Wang, H. Chen and Y. Fu, *ACS Catal.*, 2020, **10**, 1334–1343; (*f*) R. Kancherla, K. Muralirajan, B. Maity, C. Zhu, P. E. Krach, L. Cavallo and M. Rueping, *Angew. Chem., Int. Ed.*, 2019, **58**, 3412–3416; (*g*) D. Kurandina, M. Rivas, M. Radzhabov and V. Gevorgyan, *Org. Lett.*, 2018, **20**, 357–360; (*h*) W.-J. Zhou, G.-M. Cao, G. Shen, X.-Y. Zhu, Y.-Y. Gui, J.-H. Ye, L. Sun, L.-L. Liao, J. Li and D.-G. Yu, *Angew. Chem., Int. Ed.*, 2017, **56**, 15683–15687.

3 Manganese catalyzed (de)hydrogenation

Paper 5: Zubar, V.; Lebedev, Y.; Azofra, L. M.; Cavallo, L.; El-Sepelgy, O.*; Rueping, M.* Hydrogenation of CO2-Derived Carbonates and Polycarbonates to Methanol and Diols by Metal-Ligand Cooperative Manganese Catalysis. *Angew. Chem. Int. Ed.* **2018**, *57*, 13439-13443.

Paper 6: Brzozowska, A.; Azofra, L. M.; Zubar, V.; Atodiresei, I.; Cavallo, L.; Rueping, M.; El-Sepelgy, O.* Highly Chemo- and Stereoselective Transfer Semihydrogenation of Alkynes Catalyzed by a Stable, Well-Defined Manganese(II) Complex. *ACS Catal.* **2018**, *8*, 4103-4109.

Paper 7: Sklyaruk, J.; Borghs, J. C.; El-Sepelgy, O.*; Rueping, M.* Catalytic C1 Alkylation with Methanol and Isotope-Labeled Methanol. *Angew. Chem. Int. Ed.* **2019**, *58*, 775-779.

Paper 8: El-Sepelgy, O.*; Matador, E.; Brzozowska, A.; Rueping, M.* C-Alkylation of Secondary Alcohols by Primary Alcohols through Manganese-Catalyzed Double Hydrogen Autotransfer. *ChemSusChem* **2019**, *12*, 3099.

Paper 9: Jang, Y. K.; Krückel, T.; Rueping, M.*; El-Sepelgy, O.* Sustainable Alkylation of Unactivated Esters and Amides with Alcohols Enabled by Manganese Catalysis. *Org. Lett.* **2018**, 7779-7783.

Paper 10: Borghs, J. C.; Tran, M. A.; Sklyaruk, J.; Rueping, M.*; El-Sepelgy, O.* Sustainable Alkylation of Nitriles with Alcohols by Manganese Catalysis. *J. Org. Chem.* **2019**, *84*, 7927-7935.

Paper 11: Azofra, L. M.; Tran, M. A.; Zubar, V.; Cavallo, L.; Rueping, M.; El-Sepelgy, O.* Conversion of racemic alcohols to optically pure amine precursors enabled by catalyst dynamic kinetic resolution: experiment and computation. *Chem. Commun.* **2020**, *56*, 9094-9097.

Paper 12: Borghs, J. C.; Lebedev, Y.; Rueping, M.*; El-Sepelgy, O.* Sustainable Manganese-Catalyzed Solvent-Free Synthesis of Pyrroles from 1,4-Diols and Primary Amines. *Org. Lett.* **2019**, *21*, 70-74.

Paper 13: Borghs, J. C.; Azofra, L. M.; Biberger, T.; Linnenberg, O.; Cavallo, L.; Rueping, M.*; El-Sepelgy, O.* Manganese-Catalyzed Multicomponent Synthesis of Pyrroles through Acceptorless Dehydrogenation Hydrogen Autotransfer Catalysis: Experiment and Computation. ChemSusChem 2019, 12, 3083.

Authors Contributions

O.E.-S. conceived and designed the studies, led the research, wrote the manuscripts, and revised the supporting information. M.R. secured funding and proofread the final manuscripts. A.B., J.B., J.S., V.S., Y.K.J., E.M., M.A.T., O.L., and T.B. performed all synthesis experiments and prepared the supporting information. L.M.A. and L.C. carried out the DFT calculations and generated the figures. I.A. and Y.L. conducted the X-ray analysis.

Paper 5:

Hydrogenation of CO2-Derived Carbonates and Polycarbonates to Methanol and Diols by Metal-Ligand Cooperative Manganese Catalysis.

Zubar, V.; Lebedev, Y.; Azofra, L. M.; Cavallo, L.*; El-Sepelgy, O.*; Rueping, M.*

Angew. Chem. Int. Ed. **2018**, *57*, 13439-13443.

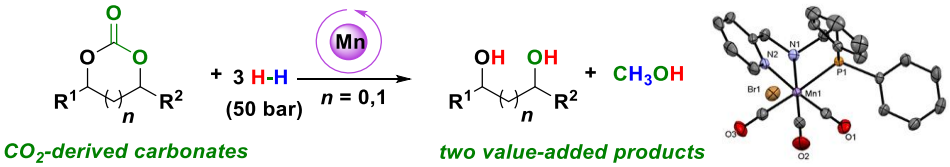

CO_2-derived carbonates and polycarbonate

Carbon Dioxide Conversion

International Edition: DOI: 10.1002/anie.201805630
German Edition: DOI: 10.1002/ange.201805630

Hydrogenation of CO_2-Derived Carbonates and Polycarbonates to Methanol and Diols by Metal–Ligand Cooperative Manganese Catalysis

Viktoriia Zubar, Yury Lebedev, Luis Miguel Azofra, Luigi Cavallo, Osama El-Sepelgy,* and Magnus Rueping**

Abstract: *The first base-metal-catalysed hydrogenation of CO_2-derived carbonates to alcohols is presented. The reaction proceeds under mild conditions in the presence of a well-defined manganese complex with a loading as low as 0.25 mol %. The non-precious-metal homogenous catalytic system provides an indirect route for the conversion of CO_2 into methanol with the co-production of value-added (vicinal) diols in yields of up to 99 %. Experimental and computational studies indicate a metal–ligand cooperative catalysis mechanism.*

The transition-metal-catalysed hydrogenation of polar bonds is a key technology in modern industrial chemistry. Thus far, most of these catalytic systems rely on the use of precious-metal catalysts.[1] However, the replacement of noble-metal catalysts by earth-abundant alternatives is a topic of current interest.[2] Accordingly, significant advances have been made in the hydrogenation of aldehydes,[3] ketones,[3] esters,[4] carboxylic acids,[4d] and amides[5] using base-metal catalysts. On the other hand, the hydrogenation of carbonic acid derivatives is significantly more difficult owing to the resonance stabilisation effect of the adjacent alkoxy groups, which lowers the electrophilicity of the carbonyl group. To the best of our knowledge, a catalytic hydrogenation of carbonic acid derivatives has never been reported using a homogenous non-precious-metal catalyst.[6]

Among the carbonic acid derivatives, the hydrogenation of cyclic organic carbonates (COCs) to alcohols is of particular interest because COCs are industrially synthesised by the direct coupling between carbon dioxide and oxiranes or oxetanes. Hence, developing mild conditions for the hydrogenation of COCs would lead to a practical two-step route for the conversion of CO_2 into methanol, which also leads to the production of value-added diols (Scheme 1).

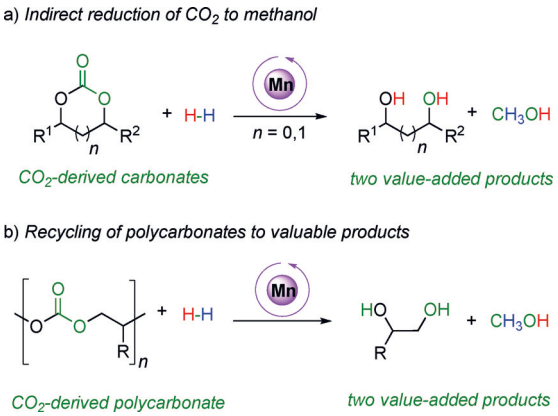

Scheme 1. Unprecedented base-metal-catalysed hydrogenation of organic carbonates.

More specifically, the industrial production of ethylene glycol (EG) involves the use of the so-called "omega process", in which CO_2 is inserted into ethylene oxide to produce ethylene carbonate, followed by catalytic hydrolysis of the former carbonate to EG and CO_2.[7] The replacement of the catalytic hydrolysis by catalytic hydrogenation would lead to the formation of methanol instead of CO_2, thus giving a great advantage in terms of sustainability. The catalytic production of methanol from CO_2 is an elegant alternative for the recycling of carbon and could enable a "methanol economy", which is a suggested scenario in which methanol might play a central role as a hydrogen storage material and C_1 building block.[8] This reaction has been studied with heterogeneous catalysts. Nevertheless, these catalytic systems have to operate at elevated temperature (> 200 °C) and suffer from the formation of several side products.[9] In contrast, well-defined homogenous catalysts are potentially more active and can be tuned based on insight gained in mechanistic studies. In that regard, only recently, seminal reports outlined preliminary results on the direct[10] and indirect[6,11] hydrogenation of CO_2 to methanol.

However, an efficient catalytic system based on an earth-abundant metal remains an elusive goal. Thus the development of a base-metal catalyst that could be used at low catalyst loadings for the reduction of CO_2-derived organic carbonates to value-added alcohols would be an important

[*] M. Sc. V. Zubar, Dr. O. El-Sepelgy, Prof. Dr. M. Rueping
Institute of Organic Chemistry, RWTH Aachen University
Landoltweg 1, 52074 Aachen (Germany)
E-mail: Osama.Elsepelgy@RWTH-Aachen.de
Magnus.Rueping@rwth-aachen.de
Dr. Y. Lebedev, Dr. L. M. Azofra, Prof. Dr. L. Cavallo, Prof. Dr. M. Rueping
KAUST Catalysis Center (KCC)
King Abdullah University of Science and Technology (KAUST)
Thuwal 23955-6900 (Saudi Arabia)
E-mail: luigi.cavallo@kaust.edu.sa
Supporting information and the ORCID identification number(s) for the author(s) of this article can be found under: https://doi.org/10.1002/anie.201805630.

advancement in achieving the requirements of an ecologically and economically benign process (Scheme 1 a). Furthermore, the successful development of such a process may also be extended to the recycling of polycarbonates with the simultaneous formation of valuable diols and methanol (Scheme 1 b).

Inspired by recent progress in manganese catalysis[12] and our interest in developing sustainable transformations using inexpensive base metals stabilised by stable non-innocent ligands,[13,14] we herein present a new manganese complex that reduces COCs and recycles polycarbonates into methanol and vicinal diols under mild reaction conditions. For the first time, a combined experimental and computational study provides insight into the reaction mechanism and explains the role of the non-innocent ligand in the cascade hydrogenation of the CO_2-derived COCs.

To develop a practical reduction method for the rather challenging cyclic carbonates, we started our studies with the synthesis of a new bench-stable ^{Ph}PNN-Mn complex **Mn-1**, which is supported by the air- and moisture-stable ^{Ph}PNN ligand **L1**.[15] Following the typical route for the synthesis of pincer manganese carbonyl complexes,[12] **Mn-1** was readily prepared by treatment of **L1** with 1 equiv of $Mn(CO)_5Br$ as the metal precursor in THF at 80 °C for 16 h. The pale yellow complex was isolated in 84 % yield and characterised by multinuclear NMR spectroscopy, IR spectroscopy, and mass spectrometry as well as single-crystal X-ray diffraction. To study the role of the N–H group, we also synthetized the corresponding N-methylated ligand and complex **Mn-2** in 88 % yield (Scheme 2).

With the aim to find the right reaction conditions, ethylene carbonate was selected as a benchmark substrate for the catalytic hydrogenation of COCs. To our delight, our complex **Mn-1** showed excellent reactivity and provided EG in > 99 % yield and methanol in 92 % yield when the reaction was performed under 50 bar H_2 pressure in 1,4-dioxane (Table 1, entry 1). Importantly, the application of **Mn-2** resulted in the formation of only 14 % of EG and no methanol was detected (Table 1, entry 2). This result highlights the crucial role of the free N–H group in the pincer ligand. Further screening of different manganese complexes led to unsatisfactory results (see the Supporting Information, Table S4 for details). Subsequently, the influence of different solvents and bases was investigated. Employing K_2CO_3 as the base did not improve the results while Cs_2CO_3 was similarly effective as KO*t*Bu (Table 1, entries 3 and 4). Furthermore, testing various solvents such as THF, 2-methyltetrahydrofuran, and toluene did not provide better results (Table 1, entries 5–7). Hence, 1,4-dioxane was chosen as the appropriate solvent. The reduction of the catalyst loading to 0.5 mol % resulted in > 99 % of EG and 89 % of methanol (Table 1, entry 8). Pleasingly, the reaction proceeded equally well when the catalyst loading was reduced to 0.25 mol % and the substrate concentration was increased to 1.46 M (Table 1, entries 9–11).

Table 1: Optimisation of the reaction conditions.[a]

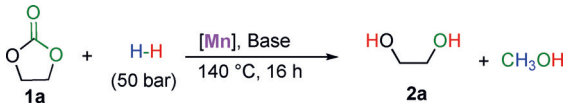

Entry	[Mn] (mol %)	Base (mol %)	Solvent	Yield of EG [%][b]	Yield of MeOH [%][b]
1	**Mn-1** (1)	KO*t*Bu (2.5)	1,4-dioxane	> 99	92
2	**Mn-2** (1)	KO*t*Bu (2.5)	1,4-dioxane	14	0
3	**Mn-1** (1)	K_2CO_3 (2.5)	1,4-dioxane	> 99	86
4	**Mn-1** (1)	Cs_2CO_3 (2.5)	1,4-dioxane	> 99	92
5	**Mn-1** (1)	KO*t*Bu (2.5)	THF	> 99	77
6	**Mn-1** (1)	KO*t*Bu (2.5)	2-Me-THF	90	80
7	**Mn-1** (1)	KO*t*Bu (2.5)	toluene	61	52
8	**Mn-1** (0.5)	KO*t*Bu (1.25)	1,4-dioxane	> 99	89
9	**Mn-1** (0.25)	KO*t*Bu (0.63)	1,4-dioxane	54	36
10[c]	**Mn-1** (0.25)	KO*t*Bu (0.63)	1,4-dioxane	99	92
11[c]	**Mn-1** (0.1)	KO*t*Bu (0.25)	1,4-dioxane	40	20

[a] Reaction conditions: **1a** (1 mmol), **Mn-1**, base, solvent (0.25 M) at 140 °C under 50 bar of H_2 for 16 h. [b] Determined by GC analysis using *m*-xylene as the internal standard. [c] With **1a** (5.7 mmol, 500 mg) in 1,4-dioxane (1.46 M).

To demonstrate the potential and applicability of the newly developed method, a range of COCs **1b–1m** were tested under the optimised reaction conditions (Table 2). An array of monosubstituted five-membered 1,3-dioxolan-2-ones bearing different alkyl and aryl substituents such as Me, Et, *n*-Bu, pentyl, *t*-Bu, and Ph were efficiently and selectively hydrogenated to the corresponding vicinal 1,2-diols and methanol in very good yields (Table 2, entries 1–6). The reaction tolerates the benzyloxymethyl and methoxymethyl derivatives **1h** and **1i**, and the desired alcohols were produced in excellent yields (Table 2, entries 7 and 8). It should be noted that the disubstituted cyclic carbonate **1j** was successfully converted into methanol and 2,3-butylene glycol (**2j**) in very good yields (Table 2, entry 9). Under the same reaction conditions, different unsubstituted and substituted six-membered COCs **1k–1m** reacted in excellent yields to give methanol and the corresponding 1,3-diols (Table 2, entries 10–12).

Additionally, our catalytic system was found to catalyse the hydrogenative depolymerisation of polycarbonates to the corresponding diol and methanol. An example is shown in Table 2, entry 13: Poly(propylene carbonate), which can be prepared by copolymerisation of propylene oxide and CO_2,[16] was hydrogenated using 1 mol % of **Mn-1** to produce methanol (84 % yield) and 1,2-propyleneglycol (**2b**, 91 % yield).

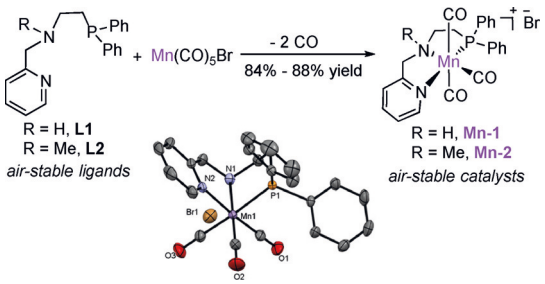

Scheme 2. Synthesis of two manganese complexes and the single-crystal X-ray structure of **Mn-1**, with ellipsoids set at 50 % probability.

Table 2: Manganese-catalysed hydrogenation of COCs.[a]

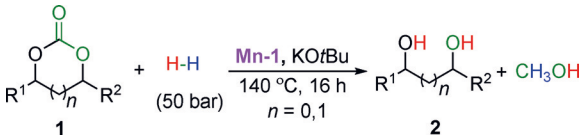

1 2

Entry	Substrate		Yield of diol [%][b]	Yield of methanol [%][c]
1	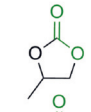	**1b**	99[c]	85
2	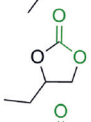	**1c**	94[c]	92
3	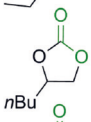	**1d**	96	88
4	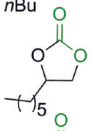	**1e**	99	95
5	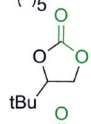	**1f**	99	94
6	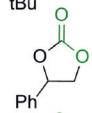	**1g**	99	95
7	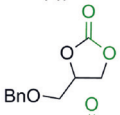	**1h**	99	90
8	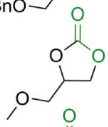	**1i**	99	94
9	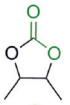	**1j**	99	85
10		**1k**	99[c]	95
11		**1l**	99	80
12[d]	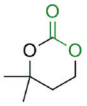	**1m**	99	99
13	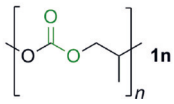	**1n**	91	84

[a] Reaction conditions: **1** (1 mmol), **Mn-1** (0.01 mmol), and KO*t*Bu (0.025 mmol) in 1,4-dioxane (4 mL) at 140 °C under 50 bar of H_2 for 16 h. [b] Yields of isolated products. [c] Determined by GC analysis using *m*-xylene as the internal standard. [d] With **Mn-1** (0.012 mmol) and KO*t*Bu (0.03 mmol).

This result might open new avenues for developing efficient base-metal catalysts for the recycling of widely used polycarbonate plastic materials.

To gain more insight into the reaction mechanism, we performed deuterium labelling studies by using D_2 instead of H_2 (see the Supporting Information for details). The manganese-catalysed deuteration of ethylene carbonate resulted in the production of methanol with >95% deuterium incorporation in the methyl group while the ethylene glycol was produced with no deuterium incorporation. Thus the deuteration of ethylene carbonate is much faster than the dehydrogenation–deuteration of EG. This result provides a practical alternative method for the production of widely used deuterated methanol. On the other hand, the treatment of EG with D_2 at 140 °C caused significant deuterium substitution at the carbon atoms, which indicates the potential of the manganese catalyst in dehydrogenative deuteration reactions.

The mechanism of the Mn^I-PNN-catalysed hydrogenation of COC substrates was also investigated by DFT calculations.[17] The overall hydrogenation of ethylene carbonate to EG and methanol can be separated into three independent C=O hydrogenation events, each with a corresponding catalytic cycle (Figure 1). The first one is the hydrogenation of ethylene carbonate (**1a**) into 2-hydroxyethyl formate (**3**), the second one is the hydrogenation of **3** into EG (**2a**) and formaldehyde (**4**), and the third one is the hydrogenation of **4** into CH_3OH. In the following, we discuss the first hydrogenation cycle only, **1a** to **3** (Figure 1). The other two catalytic cycles, composed of similar steps, are shown in the Supporting Information (Figure S3). Calculations were performed using the most active **Mn-1** catalyst.

During the initiation process concerning the H_2 addition to the Mn active site (steps **A** to **C**, where **A** is a 16-electron species), H_2 coordination to Mn is a non-spontaneous process demanding 14.6 kcal mol^{-1} at the M06/TZVP//ωB97XD/SVP(H,C,N,O,P)-TZVP(Mn) level of theory in 1,4-dioxane as the solvent and relative to **A**. The heterolytic cleavage of H_2, via transition state **B-C** (at 21.3 kcal mol^{-1} relative to **A**), leads to the hydrogenation of the catalytic species by hydride addition to the Mn centre and protonation of the non-pyridinic N atom.

The resulting [Mn]-H_2 species **C** (zero energy reference) promotes the reduction of the C=O bond of the substrates (**1a**, **3**, and **4**) in the three catalytic cycles. The C=O hydrogenation step is characterised by two main mechanistic events. On the one hand, the nucleophilic character of the hydride on Mn promotes hydride transfer from Mn to the C(sp^2) atom of the substrate (steps **D** to **E**). On the other hand, in agreement with the literature, proton transfer is achieved through cleavage of the H–H bond of a H_2 molecule η^2-coordinated to the metal (steps **F** to **H**).[18] This prevents formation of the 16-electron species **A** by deprotonation of the N–H functionality.

In more detail, the first step is the hydride transfer from the catalyst to the substrate via transition state **D-E** at 16.4 kcal mol^{-1}, leading to the Mn alkoxide intermediate **E**, at −3.9 kcal mol^{-1}. It can be seen that as a consequence of this hydride transfer, 1,3-dioxolan-2-olate is transformed into 2-(formyloxy)ethan-1-olate by charge reorganisation in the substrate. The second step is proton transfer from a coordinated H_2 molecule, releasing the product. In the presence of

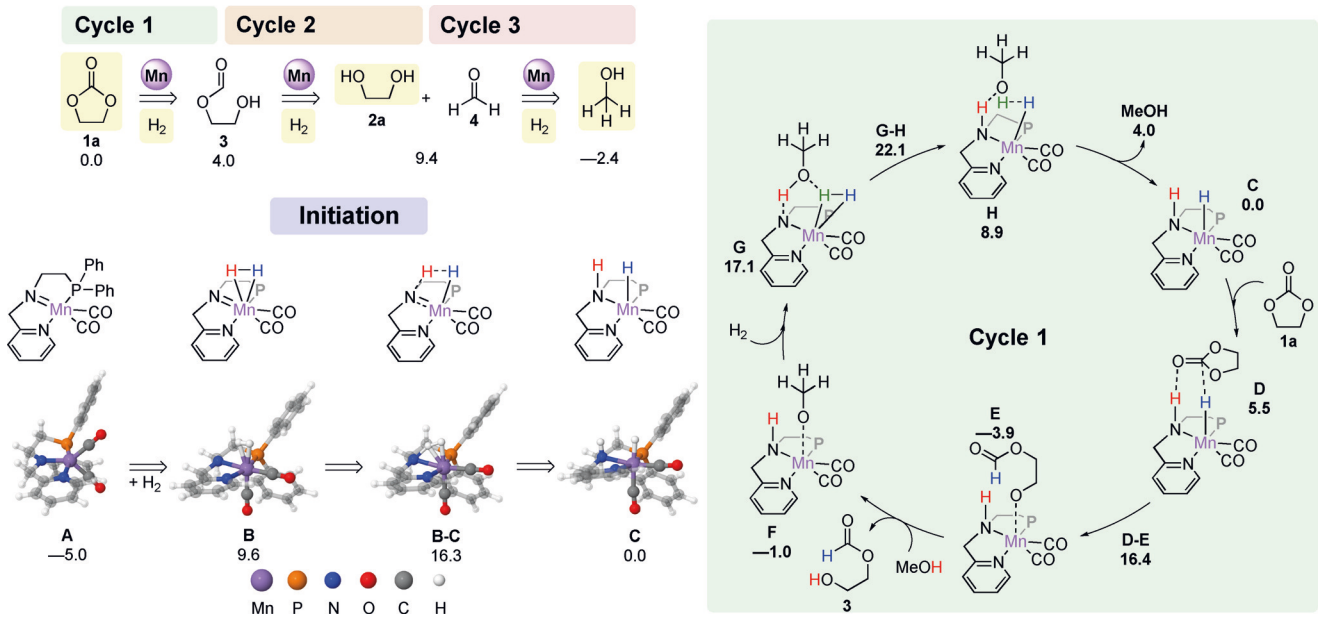

Figure 1. Proposed reaction mechanism for the three-cascade hydrogenation of ethylene carbonate into methanol and EG catalysed by **Mn-1** (**P** = PPh_2). Steps **A** to **C** refer to the initiation by catalyst hydrogenation while steps **D** to **H** concern the substrate hydrogenation and catalyst regeneration by MeOH and η^2-H_2 assistance. Calculated Gibbs free reaction and activation energies, at 140 °C and 50 bar reaction conditions, are given in kcal mol^{-1} and were obtained at the M06/TZVP//ωB97XD/SVP(H,C,N,O,P)-TZVP(Mn) level of theory in 1,4-dioxane as the solvent. Note: The H-N-Mn-H species (**C**, cycle 1) corresponds to an energy of zero.

an excess of methanol, which is expected as the reaction evolves, metathesis of **E** with CH_3OH can lead to the methoxide species **F**. Coordination of H_2 leads to **G** and triggers rehydration of the Mn active site and proton transfer to methanolate via transition state **G-H** (at 22.1 kcal mol^{-1}). This entails the regeneration of CH_3OH as well as the catalytic species. Based on calculations, the rate-determining transition state along the cycle is this proton transfer, with an overall activation barrier of 25.0 kcal mol^{-1} from **E** to **G-H**. Of course, this proton transfer can also occur without involving initial metathesis of CH_3OH with **E**, with very similar reaction steps involving the Mn alkoxide bond of **E**.

The impact of the phosphine substituents was analysed by comparing **Mn-1** with catalysts presenting aliphatic and bulky *t*Bu substituents on the P atom and the less sterically impeded *i*Pr. Hydrogenation during the initiation process of both alkyl-substituted catalysts, via transition state **B-C**, exhibits larger barriers of 25.3 and 23.7 kcal mol^{-1} compared to **Mn-1** (21.3 kcal mol^{-1}) and relative to **A**. In this sense, our DFT predictions are in agreement with experiments suggesting that the ^{Ph}PNN ligand confers to the manganese catalyst superior behaviour over those functionalised with aliphatic phosphines.

In conclusion, we have reported the hydrogenation of CO_2-derived COCs to alcohols using a homogenous base-metal complex.[19] The reaction is catalysed by a bench-stable Mn-PNN complex and proceeds with high selectivity under mild conditions, without generation of any waste or side products. A variety of five- and six-membered COCs were employed to furnish methanol and vicinal diols in very good to quantitative yields, providing a milder and indirect route for the production of methanol from CO_2. Furthermore, polycarbonates were successfully recycled with the simultaneous formation of valuable diols and methanol. These preliminary results might lead to further developments of more cost-effective catalytic hydrogenation systems, which could offer a sustainable alternative for ethylene carbonate hydrolysis as well as the existing waste recycling methods. The reaction mechanism was studied by deuterium labelling experiments and density functional theory. The process is characterised by three catalytic cycles involving the heterolytic cleavage of three dihydrogen molecules by metal–ligand cooperation.

Acknowledgements

L.M.A. and L.C. thank King Abdullah University of Science and Technology (KAUST) for support. Gratitude is also due to the KAUST Supercomputing Laboratory for providing computational resources and granting access to the supercomputer Shaheen II.

Conflict of interest

The authors declare no conflict of interest.

Keywords: carbon dioxide · carbonates · manganese · methanol · reduction

How to cite: *Angew. Chem. Int. Ed.* **2018**, *57*, 13439–13443
Angew. Chem. **2018**, *130*, 13627–13631

[1] a) J. G. de Vries, C. J. Elsevier, *Handbook of Homogeneous Hydrogenation* (3 Vols.), Wiley-VCH, Weinheim, **2007**; for

selected reviews, see: b) A. M. Smith, R. Whyman, *Chem. Rev.* **2014**, *114*, 5477 – 5510; c) S. Werkmeister, K. Junge, M. Beller, *Org. Process Res. Dev.* **2014**, *18*, 289 – 302; d) P. A. Dub, T. Ikariya, *ACS Catal.* **2012**, *2*, 1718 – 1741; e) M. L. Clarke, *Catal. Sci. Technol.* **2012**, *2*, 2418 – 2423; for selected examples: f) X. Cui, Y. Li, C. Topf, K. Junge, M. Beller, *Angew. Chem. Int. Ed.* **2015**, *54*, 10596 – 10599; *Angew. Chem.* **2015**, *127*, 10742 – 10745; g) M. Naruto, S. Saito, *Nat. Commun.* **2015**, *6*, 8140; h) T. Miura, M. Naruto, K. Toda, T. Shimomura, S. Saito, *Sci. Rep.* **2017**, *7*, 1586; i) M. Naruto, S. Agrawal, K. Toda, S. Saito, *Sci. Rep.* **2017**, *7*, 3425.

[2] a) J. Sa, A. Srebowata, *Hydrogenation with Low-Cost Transition Metals*, CRC, Boca Raton, **2017**; b) R. M. Bullock, *Catalysis without Precious Metals*, Wiley-VCH, Weinheim, **2010**.

[3] a) C. P. Casey, H. Guan, *J. Am. Chem. Soc.* **2007**, *129*, 5816 – 5817; b) R. Langer, G. Leitus, Y. Ben-David, D. Milstein, *Angew. Chem. Int. Ed.* **2011**, *50*, 2120 – 2124; *Angew. Chem.* **2011**, *123*, 2168 – 2172; c) G. Zhang, B. L. Scott, S. K. Hanson, *Angew. Chem. Int. Ed.* **2012**, *51*, 12102 – 12106; *Angew. Chem.* **2012**, *124*, 12268 – 12272; d) S. Elangovan, C. Topf, S. Fischer, H. Jiao, S. Spannenberg, W. Baumann, R. Ludwig, K. Junge, M. Beller, *J. Am. Chem. Soc.* **2016**, *138*, 8809 – 8814.

[4] a) S. Chakraborty, H. Dai, P. Bhattacharya, N. T. Fairweather, M. S. Gibson, J. A. Krause, H. Guan, *J. Am. Chem. Soc.* **2014**, *136*, 7869 – 7872; b) S. Werkmeister, K. Junge, B. Wendt, E. Alberico, H. Jiao, W. Baumann, H. Junge, F. Gallou, M. Beller, *Angew. Chem. Int. Ed.* **2014**, *53*, 8722 – 8726; *Angew. Chem.* **2014**, *126*, 8867 – 8871; c) D. Srimani, A. Mukherjee, A. F. G. Goldberg, G. Leitus, Y. Diskin, L. Posner, J. W. Shimon, Y. B. David, D. Milstein, *Angew. Chem. Int. Ed.* **2015**, *54*, 12357 – 12360; *Angew. Chem.* **2015**, *127*, 12534 – 12537; d) T. J. Korstanje, J. I. van der Vlugt, C. J. Elsevier, B. de Bruin, *Science* **2015**, *350*, 298 – 302; e) S. Elangovan, M. Garbe, H. Jiao, A. Spannenberg, K. Junge, M. Beller, *Angew. Chem. Int. Ed.* **2016**, *55*, 15364 – 15368; *Angew. Chem.* **2016**, *128*, 15590 – 15594; f) N. A. Espinosa-Jalapa, A. Nerush, L. J. W. Shimon, G. Leitus, L. Avram, Y. Ben-David, D. Milstein, *Chem. Eur. J.* **2017**, *23*, 5934 – 5938; g) M. B. Widegren, G. J. Harkness, A. M. Z. Slawin, D. B. Cordes, M. L. Clarke, *Angew. Chem. Int. Ed.* **2017**, *56*, 5825 – 5828; *Angew. Chem.* **2017**, *129*, 5919 – 5922.

[5] a) N. M. Rezayee, D. C. Samblanet, M. S. Sanford, *ACS Catal.* **2016**, *6*, 6377 – 6383; b) V. Papa, J. R. Cabrero-Antonio, E. Alberico, A. Spanneberg, K. Junge, H. Junge, M. Beller, *Chem. Sci.* **2017**, *8*, 3576 – 3585.

[6] For homogenous noble-metal catalysis, see: a) E. Balaraman, C. Gunanathan, J. Zhang, L. J. W. Shimon, D. Milstein, *Nat. Chem.* **2011**, *3*, 609 – 614; b) Z. Han, L. Rong, J. Wu, L. Zhang, Z. Wang, K. Ding, *Angew. Chem. Int. Ed.* **2012**, *51*, 13041 – 13045; *Angew. Chem.* **2012**, *124*, 13218 – 13222; c) S. H. Kim, S. H. Hong, *ACS Catal.* **2014**, *4*, 3630 – 3636; d) T. vom Stein, M. Meuresch, D. Limper, M. Schmitz, M. Hölscher, J. Coetzee, D. J. Cole-Hamilton, J. Klankermayer, W. Leitner, *J. Am. Chem. Soc.* **2014**, *136*, 13217 – 13225.

[7] The "Omega process" is a process by *Shell Global Solutions* that is used to produce ethylene glycol (automotive antifreeze compound).

[8] a) G. A. Olah, A. Goeppert, G. K. S. Prakash, *Beyond Oil and Gas: The Methanol Economy*, Wiley-VCH, Weinheim, **2009**; b) M. Aresta, *Carbon Dioxide as Chemical Feedstock*, Wiley-VCH, Weinheim, **2010**.

[9] W. Wang, S. Wang, X. Ma, J. Gong, *Chem. Soc. Rev.* **2011**, *40*, 3703 – 3727.

[10] a) K.-I. Tominaga, Y. Sasaki, M. Kawai, T. Watanabe, M. Saito, *J. Chem. Soc. Chem. Commun.* **1993**, 629 – 631; b) C. A. Huff, M. S. Sanford, *J. Am. Chem. Soc.* **2011**, *133*, 18122 – 18125; c) S. Wesselbaum, T. Vom Stein, J. Klankermayer, W. Leitner, *Angew. Chem. Int. Ed.* **2012**, *51*, 7499 – 7502; *Angew. Chem.* **2012**, *124*, 7617 – 7620; d) J. Schneidewind, R. Adam, W. Baumann, R. Jackstel, M. Beller, *Angew. Chem. Int. Ed.* **2017**, *56*, 1890 – 1893; *Angew. Chem.* **2017**, *129*, 1916 – 1919.

[11] a) N. M. Rezayee, C. A. Huff, M. S. Sanford, *J. Am. Chem. Soc.* **2015**, *137*, 1028 – 1031; b) J. R. Khusnutdinova, J. A. Garg, D. Milstein, *ACS Catal.* **2015**, *5*, 2416 – 2422; c) J. Kothandaraman, A. Goeppert, M. Czaun, G. A. Olah, G. K. Prakash, *J. Am. Chem. Soc.* **2016**, *138*, 778 – 781; d) S. Kar, A. Goeppert, J. Kothandaraman, J. K. S. Prakash, *ACS Catal.* **2017**, *7*, 6347 – 6351; e) S. Kar, R. Sen, A. Goeppert, G. K. S. Prakash, *J. Am. Chem. Soc.* **2018**, *140*, 1580 – 1583.

[12] For recent reviews, see: a) G. A. Filonenko, R. van Putten, E. J. M. Hensen, E. A. Pidko, *Chem. Soc. Rev.* **2018**, *47*, 1459; b) F. Kallmeier, R. Kempe, *Angew. Chem. Int. Ed.* **2018**, *57*, 46 – 60; *Angew. Chem.* **2018**, *130*, 48 – 63; c) T. Zell, R. Langer, *ChemCatChem* **2018**, *10*, 1930 – 1940; d) B. Maji, M. K. Barman, *Synthesis* **2017**, *49*, 3377 – 3393; e) M. Garbe, K. Junge, M. Beller, *Eur. J. Org. Chem.* **2017**, 4344 – 4362; on C–H functionalization: f) C. Wang, *Synlett* **2013**, *24*, 1606 – 1613; g) W. Liu, L. Ackermann, *ACS Catal.* **2016**, *6*, 3743 – 3752; h) D. A. Valyaev, G. Lavigne, N. Lugan, *Coord. Chem. Rev.* **2016**, *308*, 191 – 235.

[13] a) O. El-Sepelgy, N. Alandini, M. Rueping, *Angew. Chem. Int. Ed.* **2016**, *55*, 13602 – 13605; *Angew. Chem.* **2016**, *128*, 13800 – 13803; b) O. El-Sepelgy, A. Brzozowska, M. Rueping, *ChemSusChem* **2017**, *10*, 1664 – 1668; c) O. El-Sepelgy, A. Brzozowska, L. M. Azofra, Y. K. Jang, L. Cavallo, M. Rueping, *Angew. Chem. Int. Ed.* **2017**, *56*, 14863 – 14867; *Angew. Chem.* **2017**, *129*, 15059 – 15063; d) O. El-Sepelgy, A. Brzozowska, J. Sklyaruk, Y. K. Jang, V. Zubar, M. Rueping, *Org. Lett.* **2018**, *20*, 696 – 699.

[14] For reviews on metal–ligand catalysis, see: a) R. Khusnutdinova, D. Milstein, *Angew. Chem. Int. Ed.* **2015**, *54*, 12236 – 12273; *Angew. Chem.* **2015**, *127*, 12406 – 12445; b) V. Lyaskovskyy, B. de Bruin, *ACS Catal.* **2012**, *2*, 270 – 279.

[15] D. Spasyuk, D. G. Gusev, *Organometallics* **2012**, *31*, 5239 – 5242.

[16] X.-B. Lu, Y. Wang, *Angew. Chem. Int. Ed.* **2004**, *43*, 3574 – 3577; *Angew. Chem.* **2004**, *116*, 3658 – 3661.

[17] Optimised geometries were located using the ωB97XD functional together with the SVP basis set for main-group atoms and the TZVP basis set for Mn. To obtain more accurate energy values, single-point refinement calculations were done using the M06 functional and TZVP basis set on all atoms. Solvent effects (1,4-dioxane) were included with the PCM model at both steps. All calculations were performed through the facilities provided by the Gaussian09 package. See the Supporting Information for full computational details.

[18] For selected key examples, see: a) F. Hasanayn, R. H. Morris, *Inorg. Chem.* **2012**, *51*, 10808 – 10818; b) F. Hasanayn, A. Baroudi, A. A. Bengali, A. S. Goldman, *Organometallics* **2013**, *32*, 6969 – 6985; c) P. A. Dub, N. J. Henson, R. L. Martin, J. C. Gordon, *J. Am. Chem. Soc.* **2014**, *136*, 3505 – 3521; d) D. G. Gusev, *ACS Catal.* **2016**, *6*, 6967 – 6981; e) M. Glatz, B. Stöger, D. Himmelbauer, L. F. Veiros, K. Kirchner, *ACS Catal.* **2018**, *8*, 4009 – 4016.

[19] For independent parallel studies, see: a) A. Kumar, T. Janes, N. A. Espinosa-Jalapa, D. Milstein, *Angew. Chem. Int. Ed.* **2018**, https://doi.org/10.1002/anie.201806289; *Angew. Chem.* **2018**, https://doi.org/10.1002/ange.201806289; b) A. Kaithal, M. Hölscher, W. Leitner, *Angew. Chem. Int. Ed.* **2018**, https://doi.org/10.1002/anie.201808676; *Angew. Chem.* **2018**, https://doi.org/10.1002/ange.201808676.Angew. Chem. 2018, 10.1002/ange.201808676

Manuscript received: May 15, 2018
Revised manuscript received: July 26, 2018
Accepted manuscript online: August 13, 2018
Version of record online: September 3, 2018

Paper 6:

Highly Chemo- and Stereoselective Transfer Semihydrogenation of Alkynes Catalyzed by a Stable, Well-Defined Manganese(II) Complex.

Brzozowska, A.; Azofra, L. M.*; Zubar, V.; Atodiresei, I.; Cavallo, L.; Rueping, M.; El-Sepelgy, O.*

ACS Catal. **2018**, *8*, 4103-4109.

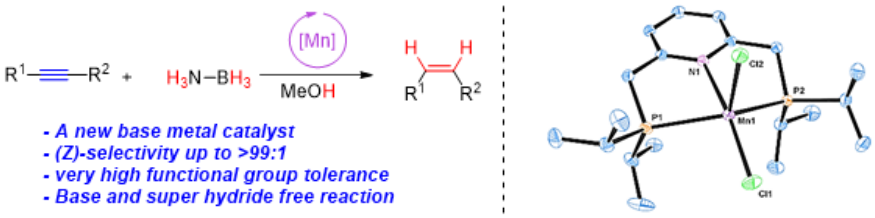

ACS Catalysis

Research Article

Cite This: ACS Catal. 2018, 8, 4103−4109

pubs.acs.org/acscatalysis

Highly Chemo- and Stereoselective Transfer Semihydrogenation of Alkynes Catalyzed by a Stable, Well-Defined Manganese(II) Complex

Aleksandra Brzozowska,[‡] Luis Miguel Azofra,*[,†] Viktoriia Zubar,[‡] Iuliana Atodiresei,[‡] Luigi Cavallo,[†] Magnus Rueping,[†,‡] and Osama El-Sepelgy*[,‡]

[‡]Institute of Organic Chemistry, RWTH Aachen University, Landoltweg 1, 52074 Aachen, Germany

[†]KAUST Catalysis Center, King Abdullah University of Science and Technology, Thuwal 23955-6900, Saudi Arabia

Supporting Information

ABSTRACT: Herein we report unprecedented manganese-catalyzed semihydrogenation of internal alkynes to (*Z*)-alkenes using ammonia borane as a hydrogen donor. The reaction is catalyzed by a pincer complex of the earth-abundant manganese(II) salt in the absence of any additives, base, or superhydride. The ammonia borane smoothly reduces the manganese precatalyst [Mn(II)−PNP][Cl]$_2$ to the catalytically active species [Mn(I)−PNP]−hydride in the triplet spin state. This manganese hydride is highly stabilized by complexation with the alkyne substrate. Computational density functional theory (DFT) analysis studies of the reaction mechanism rationalize the origin of stereoselectivity toward formation of (*Z*)-alkenes.

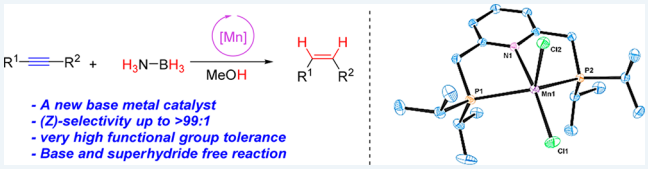

KEYWORDS: *base metals, manganese, pincer complexes, ammonia borane, alkynes, semihydrogenation*

INTRODUCTION

Stereodefined alkenes are among the most important organic compounds, ubiquitous in chemical, material, and pharmaceutical industries.[1] Semihydrogenation of alkynes to alkenes is a very important reaction in organic synthesis.[2] Until today, triple-bond semireduction relies mainly on the use of precious metal catalysis. Among the known heterogeneous catalysts, the palladium-based Lindlar catalyst is the most prominent one.[3] However, the necessity to use toxic lead salts as additive and the product isomerization under the reaction conditions are the major drawbacks of this method. Besides, various modern heterogeneous catalysts,[4] homogeneous counterparts, such as the Rh-based Wilkinson's and Schrock−Osborn catalyst,[5] palladium,[6] ruthenium,[7] and iridium[8] catalysts have been intensively investigated for this reaction.

Economic and environmental aspects persuade chemists to replace toxic noble metal catalysts by first row base metal alternatives. In this regard, few homogeneous catalytic systems have been reported so far. In 2013, Srimani et al. have reported the use of acridine-based PNP iron catalyst for the (*Z*)-selective semihydrogenation of alkynes followed by rapid isomerization to (*E*)-alkenes under pressurized dihydrogen.[9] More recently, processes relaying on the use of nickel,[10] cobalt,[11] and copper[12] based catalysts have been disclosed. Nonetheless, these protocols may suffer from the use of high catalyst loading, limited substrate scope, and low levels of chemoselectivity or over-reduction. Despite these advances, new efficient catalytic systems based on earth-abundant metal catalysts would be highly desirable.

During the past months, manganese-catalyzed hydrogenation reactions have emerged. However, so far these are limited to the hydrogenation of C═O and C≡N bonds.[13] To the best of our knowledge, a well-defined manganese complex catalyzing the (transfer) hydrogenation of unsaturated hydrocarbons has never been reported. Therefore, it was not surprising that our initial attempts to employ these complexes in semihydrogenation of alkynes were also unsuccessful.

The mechanism of the metal hydride catalyzed (*Z*)-selective semireduction of alkynes typically takes place via hydrometalation followed by reductive elimination steps, which requires a vacant coordination site on the metal center. However, the recently reported manganese hydrogenation catalysts are hexacoordinated pincer−Mn(I) complexes. Thus, in order to design a proper catalyst for this transformation, our attention was directed to the use of the five-coordinate manganese(II) dichloride, which after activation might be converted to tetracoordinate manganese(I) hydride. In contrast to the well-established iron(II) and cobalt(II) hydrogenation catalysts, manganese(II) dichloride has been reported to be inactive for the hydrogenation of carbonyl compounds. This might be attributed to the low stability of the formed Mn(I) hydride in the absence of carbonyl ligands.[13a,b]

Ammonia borane (AB) is a low molecular weight (30.87 g mol^{-1}), bench-stable, inexpensive solid bearing both protic N−H and hydric B−H bonds. The good hydrogen capacity (16.9% wt) and possibility of recycling its dehydrogenated products has inspired intensive studies toward the use of ammonia borane as H_2 storage molecule. However, reports pertaining to the use of

Received: March 14, 2018
Revised: March 28, 2018
Published: March 30, 2018

DOI: 10.1021/acscatal.8b00983
ACS Catal. 2018, 8, 4103−4109

ammonia borane as a chemical reagent and, in particular, as hydrogen donor are scarce.[14] We report herein the first example of manganese-catalyzed transfer hydrogenation of unsaturated carbon−carbon bonds using ammonia borane as an environmentally benign hydrogen donor (Scheme 1).

Scheme 1. Manganese-Catalyzed Transfer Semihydrogenation of Alkynes

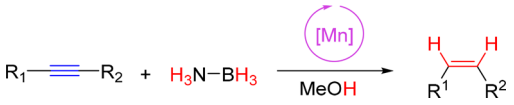

RESULTS AND DISCUSSION

We started our study with the synthesis of several PNP and NNN manganese pincer complexes (**Mn-1**−**Mn-4**, Figure 1).

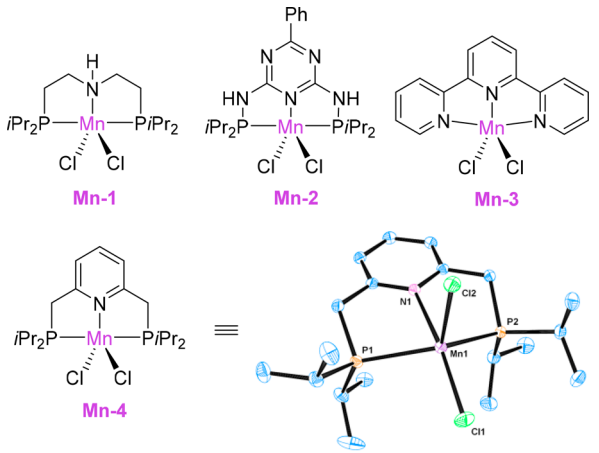

Figure 1. Manganese complexes tested in this study and X-ray crystal structure analysis of **Mn-4** (hydrogen atoms omitted for clarity).

These five-coordinated Mn-complexes could be easily prepared by the reaction of the anhydrous manganese dichloride with 1.2 equiv of the corresponding ligand in THF at room temperature. The synthesis and the characterization of the complexes **Mn-1** and **Mn-2** were recently reported by Elangovan et al.[13a] and Kallmeier et al.,[13b] respectively. However, these complexes were inactive hydrogenation catalysts. **Mn-3** was prepared from literature report.[15] Furthermore, we have synthesized a new pyridine-based manganese complex **Mn-4** in 80% yield. The crystal structure analysis of **Mn-4** showed that the coordination geometry of the manganese center is distorted square pyramidal (Figure 1).

Next, we investigated the catalytic activity of the manganese complexes **Mn-1**−**Mn-4** in the hydrogenation of diphenylacetylene (**1a**) as a model substrate. Methanol was used as a solvent and ammonia borane as both the potential catalyst activator and hydrogen donor. The NH-based PNP manganese complex **Mn-1** provided only low conversion (27%) with 84:16 *Z*/*E* ratio (Table 1, entry 1). Higher yield (69%) and a slightly higher *Z*/*E* ratio (88:12) were observed by the application of triazine-based PNP−manganese complex **Mn-2** (Table 1, entry 2). Subsequently, we tested the catalytic performance of the readily available terpyridine−Mn(II) complex **Mn-3**; however, only moderate results were obtained (Table 1, entry 3). To our delight, the newly synthesized pyridyl-based PNP complex **Mn-4** showed full conversion and very good selectivity (97:3, Table 1, entry 4). The use of $MnCl_2$ as a catalyst afforded low conversion and selectivity (Table 1, entry 5), highlighting the crucial role of the ligand.

Table 1. Optimization of the Reaction Conditions[a]

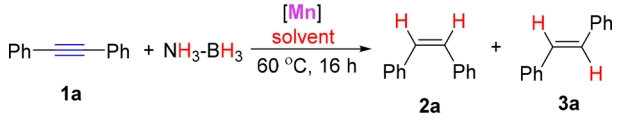

entry	[Mn] (mol %)	solvent	conversion (%)	2a:3a
1	**Mn-1** (2)	MeOH	27	84:16
2	**Mn-2** (2)	MeOH	69	88:12
3	**Mn-3** (2)	MeOH	62	79:21
4	**Mn-4** (2)	MeOH	>99	97:03
5	$MnCl_2$ (2)	MeOH	29	78:22
6	**Mn-4** (2)	EtOH	99	85:15
7	**Mn-4** (2)	*i*-PrOH	41	95:05
8	**Mn-4** (2)	HFIP	06	ND
9	**Mn-4** (2)	TFE	08	ND
10	**Mn-4** (2)	THF	87	72:28
11	**Mn-4** (2)	dioxane	63	79:21
12	**Mn-4** (2)	DMF	14	80:20
13	**Mn-4** (2)	NMP	21	83:17
14	**Mn-4** (2)	toluene	14	83:17
15	**Mn-4** (2)	hexane	<5	ND
16[b]	**Mn-4** (2)	MeOH	<5	ND
17[c]	**Mn-4** (2)	MeOH	<5	ND
18	**Mn-4** (1)	MeOH	>99	99:01
19	**Mn-4** (0.5)	MeOH	76	95:05

[a]Reaction conditions: **1** (0.25 mmol), AB (0.25 mmol), **Mn** catalyst in 1 mL of solvent at 60 °C for 16 h. Conversion was determined by ^{1}H NMR using mesitylene as the internal standard. *Z*/*E* ratio was determined by GC analysis. [b]AB (0.025 mmol), H_2 (10 bar). [c]AB (0.025 mmol), HCOOH (0.5 mmol).

Next, different solvents were tested. Replacing MeOH by EtOH resulted in the same conversion but lower *Z*/*E* ratio (Table 1, entry 6). The promising results in methanol and ethanol have encouraged us to investigate more alcohols such as *i*-PrOH and more acidic fluorinated solvents: trifluoroethanol (TFE) and hexafluoroisopropyl alcohol (HFIP). However, these alcohols proved to be unsuitable for this reaction (Table 1, entries 7−9). Interestingly, running the reaction in THF or dioxane afforded moderate results (Table 1, entries 10−11). Furthermore, reactions performed in DMF or NMP led to very low conversions, probably due to the strong coordination of these solvents with the catalyst (Table 1, entries 12−13). The solvent screening shows that the nonpolar solvents hexane and toluene failed to give the desired product (Table 1, entries 14−15).

Moreover, in order to exclude molecular hydrogen as a reactant in the described process, the reaction was examined under hydrogen atmosphere (10 bar) in the presence of catalytic amounts of AB. Importantly, only traces of the desired product were detected (Table 1, entry 16). This result suggests that the reaction takes place via direct transfer hydrogenation and not via AB solvolysis followed by hydrogenation. Also, formic acid has been demonstrated to be an unsuitable hydrogen donor in this process (Table 1, entry 17).

Following these results, we turned our attention to screening of the reaction conditions with the respect to the catalyst loading (**Mn-4**). Pleasingly, the reaction still proceeded well with a catalyst loading as low as 1 mol % (Table 1, entry 18).

DOI: 10.1021/acscatal.8b00983
ACS Catal. 2018, 8, 4103−4109

Subsequent reduction of the catalyst to 0.5 mol % resulted in lower conversion of 76% after 16 h (Table 1, entry 19).

In order to demonstrate the applicability of our manganese catalyst system, we tested the transfer hydrogenation of various internal alkyne substrates bearing different electronic and steric properties (Table 2). Generally, all investigated aromatic substrates with electron-withdrawing groups and electron-donating groups were converted into the corresponding (*Z*)-alkenes with very good yields and excellent (*Z*):(*E*) selectivity **1a**−**1n**. Interestingly, sensitive functional groups such as nitrile, ester, and heterocycles were well-tolerated under the mild reaction conditions. The semitransfer hydrogenation could also be applied to the mono- and dialkylacetylene **1o** and **1p** after using more catalyst loading and ammonia borane. The protected allyl alcohol **2q** could be obtained in 81% yield and good selectivity. Finally, the pentynol-derived alkyne **1r** could be selectively semihydrogenated in good yield (66%).

Apart from the synthetic value of the conversion of alkynes to alkenes, we decided to investigate the application of the newly developed catalytic system in the purification of alkenes from alkyne impurities, which is a highly important industrial process to valorize the steam cracking bulk feedstocks.[4g] To demonstrate the process feasibility, we hydrogenated diphenylacetylene in the presence of a large excess of (*Z*)-stilbene. To our delight, 0.03 mmol of diphenylacetylene could be hydrogenated in the presence 100 equiv of (*Z*)-stilbene using only 0.0003 mmol of the **Mn-4**. Importantly, (*Z*)-alkenes were obtained with 99% purity with only traces of the isomerized (*E*)-alkene **3a** and no overhydrogenation product was detected (Scheme 2).

Table 2. Manganese-Catalyzed (*Z*)-Selective Transfer Hydrogenation of Alkynes[a]

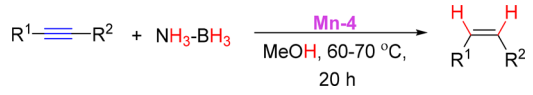

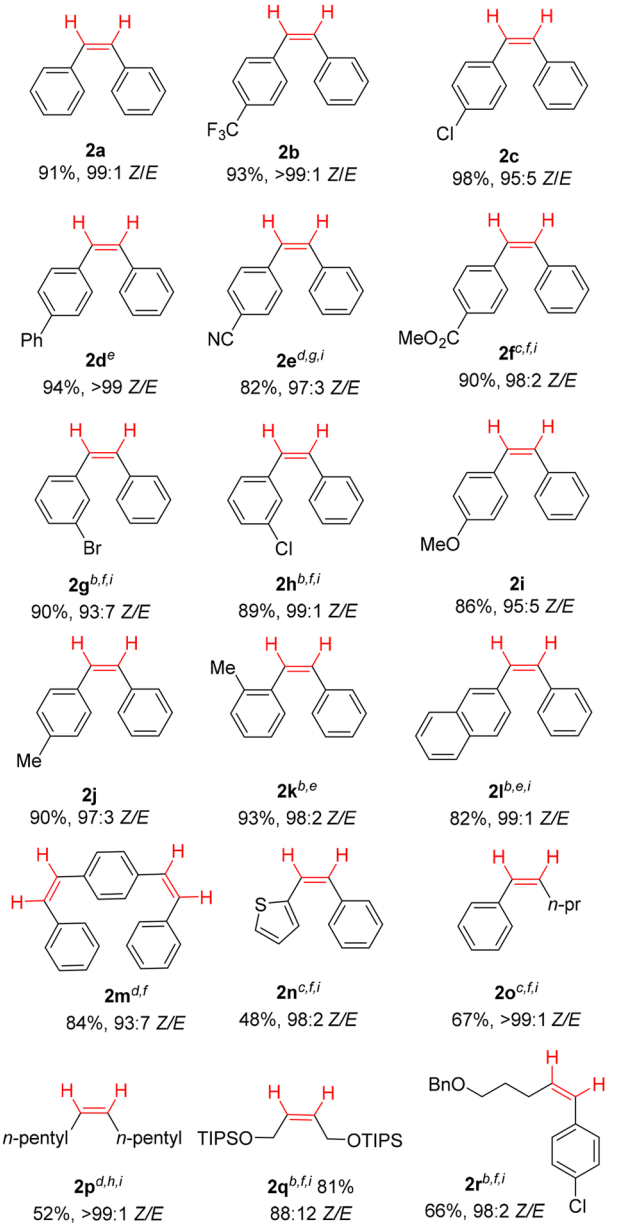

[a]Reaction conditions: **1** (0.5 mmol), AB (0.5 mmol), **Mn-4** (1 mol %) in 2 mL of methanol at 60 °C for 20 h, yields after column chromatography, *Z*/*E* ratio is determined by GC analysis of the crude reaction mixture. [b]**Mn-4** (2 mol %). [c]**Mn-4** (3 mol %). [d]**Mn-4** (4 mol %). [e]AB (0.75 mmol). [f]AB (1 mmol). [g]AB (1.5 mmol). [h]AB (2 mmol). [i]70 °C.

Scheme 2. Showcase of Manganese-Catalyzed Purification of *Cis* Alkenes without Isomerization

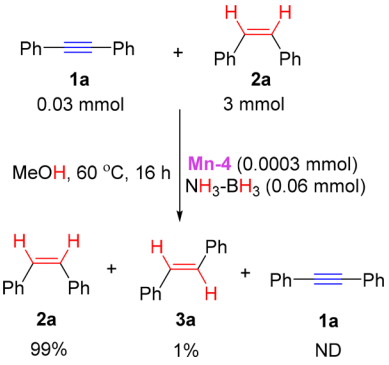

With this background knowledge we studied the reaction mechanism for diphenylacetylene reduction into stilbene through density functional theory (DFT) modeling (Figure 2).[17] Gibbs free reaction and activation energies were calculated at 50 °C in methanol as a solvent. The precatalyst we considered is **Mn-4**, which we suggest can be reduced into the active catalytic [Mn(I)−PNP]−hydride species (**A**, at Figure 2) by NH_3BH_3. This hypothesis is based on the consideration that thermogravimetric analysis and differential scanning calorimetric studies proved that $CoCl_2$ to be reduced into cobalt(I) by induction of NH_3BH_3 decomposition. These findings served as the basis for demonstrating the reducing power of NH_3BH_3 toward other compounds such as $FeCl_3$ and $AlCl_3$ species.[16] Starting from the proposed active species **A**, two catalytic cycles working simultaneously can be proposed to explain the product distribution. One is the alkyne reduction cycle, converting diphenylacetylene into (*Z*)-stilbene; the second is the alkene isomerization cycle, converting (*Z*)-stilbene into (*E*)-stilbene.

Calculations indicate that the reaction occurs through a triplet state spin route (Table S1). For example, in the case of the catalytic species **A** the triplet spin state is more stable than the singlet spin state by 27.5 and 32.4 kcal mol^{-1} at the PBE/

DOI: 10.1021/acscatal.8b00983
ACS Catal. 2018, 8, 4103−4109

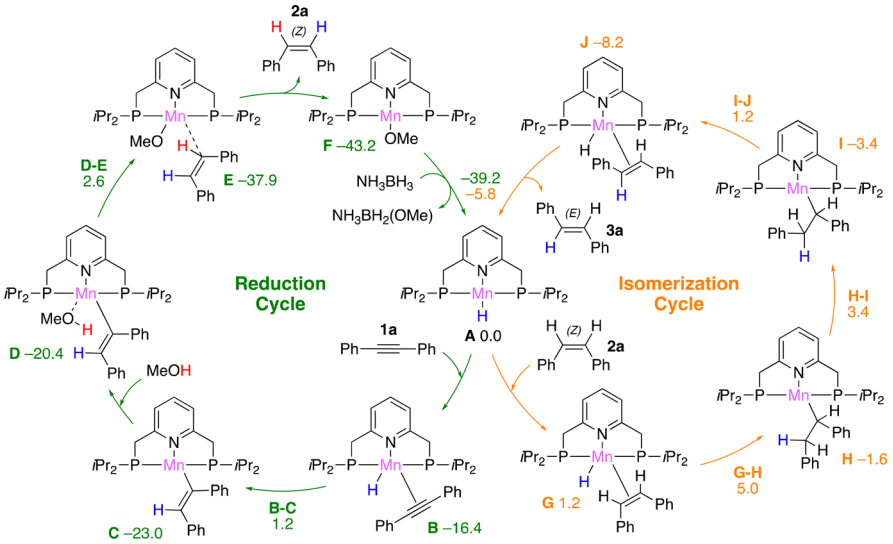

Figure 2. Proposed reaction mechanism for manganese-catalyzed semitransfer hydrogenation of diphenylacetylene (**1a**) into (*Z*)-stilbene (**2a**) (reduction cycle) and internal conversion of (*Z*)-stilbene (**2a**) into (*E*)-stilbene (**3a**) (isomerization cycle). Calculated Gibbs free reaction and activation energies, at 50 °C, are shown in kcal mol^{-1} at the PBE0+D3(BJ)/TZVP//PVE/SVP computational level in methanol as solvent.

SVP and PBE0+D3(BJ)/TZVP//PVE/SVP levels of theory in methanol. These values are consistent with the value of 33.5 kcal mol^{-1} calculated at the OPBE/SVP level in the gas phase.[18]

The alkyne reduction cycle, converting diphenylacetylene into (*Z*)-stilbene, starts with coordination of diphenylacetylene to the [Mn(I)−PNP]−hydride catalyst **A**, spontaneously forming the stable complex **B**, with a binding Gibbs free energy at 50 °C of −16.4 kcal mol^{-1} in methanol. The overall structure of **B** (see Figure S2) has a strong metallacycloolefin character, as the C−C−Ph angles are severely bent from 180° in the isolated substrate, to assume an average value of 143°. The C−C bond, 1.34 Å, is close to the value of 1.36 Å as in the isolated (*Z*)-stilbene, compared to 1.23 Å in the isolated diphenylacetylene.

This first hydrogenation of the substrate, leading to intermediate **C**, exhibits a Gibbs free activation energy of 17.6 kcal mol^{-1} via transition state **B**−**C**. Intermediate **C** presents a *cis* disposition of the Ph substituents on the formed C═C double bond. The overall skeleton of the reacting carbonaceous moiety is perpendicular to the PNP plane, see Figure 3. The formed Mn−C bond is nearly collinear with the Mn−N bond, with a Mn−N−C angle of 161°, and the large distance between Mn and the transferred H atom, 3.17 Å, indicates no agostic interaction.

The next step corresponds to MeOH interaction with the Mn center, leading to intermediate **D**, with a free energy increasing in 2.6 kcal mol^{-1}. The long distance between the Mn and the O atom of MeOH, 3.60 Å, suggests this interaction being dominated by dispersion forces. Indeed, the enthalpy of association (between MeOH and **C** to reach **D**) at the PBE0/TZVP//PVE/SVP level amounts to −6.6 kcal mol^{-1}, while at the PBE0+D3(BJ)/TZVP//PVE/SVP level, which is after addition of an empirical dispersion term, it amounts to −11.1 kcal mol^{-1}. Proton transfer from MeOH to the substrate occurs via transition state **D**−**E**, indicated to be the rate-limiting step with a relative activation Gibbs free energy of 25.6 kcal mol^{-1} (energy span from **C** to **D**−**E**). Once (*Z*)-stilbene is released in a spontaneous process, the formed [Mn]−OMe intermediate **F** reacts with NH_3BH_3 to regenerate the starting [Mn(I)−PNP]−hydride catalytic species **A**.

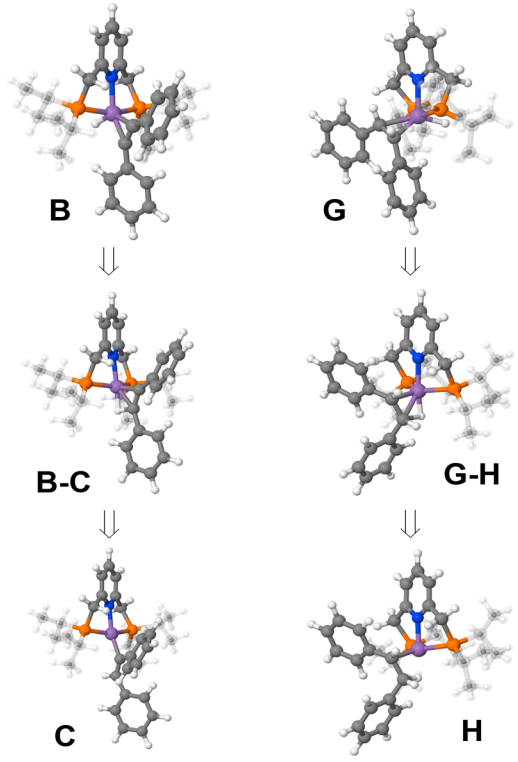

Figure 3. Minima and transition states for the hydride transfer steps in the reduction (B−C) and isomerization (G−H) cycles. (For clarity, *i*-Pr_2 groups are in soft color.)

A key feature of the above reaction pathway is that the initial hydrogen transfer to diphenylacetylene, step **B** to **C**, occurs with formation of a Mn−vinyl bond presenting a *cis* disposition of the Ph substituents. Since no free rotation around the C═C double bond of the substrate is possible, stereoselectivity toward the (*Z*)-alkene is imposed. Our attempts to locate an alternative transition state in which proton transfer from an external MeOH to diphenylacetylene occurs first followed by the hydride transfer from the Mn−H moiety failed.

DOI: 10.1021/acscatal.8b00983
ACS Catal. 2018, 8, 4103−4109

Furthermore, the potential role of NH_3BH_3 as proton donor instead of MeOH during the **D′** to **E′** step has been also investigated. The large activation Gibbs free energy of 37.1 kcal mol^{-1} (relative to **C**) clearly rules out this route in the presence of MeOH (Figure S3). Finally, we also analyzed both the reduction and isomerization cycles in THF, where NH_3BH_3 is the sole source of proton (see Figure S4). Proton transfer from NH_3BH_3 to the substrate via transition state **D′−E′**, with a Gibbs free energy of activation of 35.5 kcal mol^{-1}, is again of high energy, which depresses reactivity. These results are in agreement with experimental solvent screening experiments in Table 1.

The formation of (*E*)-stilbene may also be explained via the alkene isomerization cycle shown in Figure 2. Within this cycle the catalytic species **A** interacts with (*Z*)-stilbene leading to complex **G**. This is a slightly endergonic step, with a binding Gibbs free energy of 1.2 kcal mol^{-1}, which contrasts with the large binding energy of diphenylacetylene to **A** (−16.4 kcal mol^{-1}). Hydride transfer from Mn(I) of **G** to the closest C atom of stilbene leads to intermediate **H**. This hydrogenation transfer exhibits a low relative activation barrier of 5.0 kcal mol^{-1} and leads to an sp^3 hybridization of the C atom of stilbene, which indeed allows easy rotation around the C−C bond, step **H** to **I** (the relative rotational activation barrier is calculated to be 5.0 kcal mol^{-1}). *β*-H transfer to the Mn atom from **I** via transition state **I−J** with Gibbs free energy barrier of 4.6 kcal mol^{-1} leads to (*E*)-stilbene, intermediate **J**. Finally, dissociation of (*E*)-stilbene from the metal regenerates the catalytic species **A**.

Comparison between the reduction and the isomerization cycles shows that coordination of diphenylacetylene to the catalytic species **A** is favored by 17.6 kcal mol^{-1} over (*Z*)-stilbene coordination (−16.4 vs 1.2 kcal mol^{-1}). Steric effects play a minor role in determining this large difference in the binding energies, as a similarly large difference, 14.0 kcal mol^{-1}, is calculated for coordination of diphenylacetylene and (*Z*)-stilbene to a model system where the *i*-Pr substituents on the P atoms of PNP ligands are replaced by smaller methyl groups, −17.3 and −3.3 kcal mol^{-1}, respectively. Further, coordination of the simplest alkyne (acetylene) and alkene (ethylene) to this model system with methyl substituents on the P atoms displays again a large difference in the binding Gibbs free energies, −18.3 and −7.8 kcal mol^{-1}, confirming that preferential alkyne coordination over alkene coordination is dominated by electronic effects.

Considering that the substrate-coordinated intermediates **B** and **G** are connected by intermediate **A**, the Curtin−Hammett principle can be used to relate the faster kinetics of the alkyne reduction cycle to the energy difference between the highest-laying transition states along the two cycles, which is transition states **D−E** and **G−H**. Consistent with the experimental evidence, the former, along the alkyne reduction cycle, is favored by 2.4 kcal mol^{-1} over the latter, taking place along the alkene isomerization cycle.

CONCLUSIONS

A new manganese-catalyzed hydrogenation of unsaturated hydrocarbons is reported herein.[19] Notably, the newly developed catalytic system is based on an earth-abundant metal which is shown to be highly active for semitransfer hydrogenation of internal alkynes under base- and super-hydride-free conditions. Ammonia borane was used as both potential hydrogen donor and catalyst activator. Under mild conditions a broad scope of internal alkynes bearing different functional groups are converted to (*Z*)-alkenes in up to 98% yield and >99:1 (*Z*):(*E*) selectivity. Importantly, this base metal catalyst allows for the purification of alkenes from alkyne impurities without alkene isomerization. The ammonia borane smoothly reduces the manganese precatalyst [Mn(II)−PNP]-$[Cl]_2$ to the active catalytic species [Mn(I)−PNP]−hydride in the triplet spin state which is highly stabilized by the complexation with the alkyne substrate. DFT calculations indicate that two catalytic cycles, one for hydrogenation of diphenylacetylene to (*Z*)-stilbene (the reduction cycle), the other for isomerization of (*Z*) to (*E*)-stilbene (the isomerization cycle), are in competition. The strong thermodynamics control imposed during the early catalyst···substrate coordination steps explains the selectivity showed by the [Mn(I)−PNP]−hydride species for the preferred reduction of diphenylacetylene into (*Z*)-stilbene over the (*E*) isomer.

ASSOCIATED CONTENT

Supporting Information

The Supporting Information is available free of charge on the ACS Publications website at DOI: 10.1021/acscatal.8b00983.

Experimental and DFT details, and cartesian coordinates (PDF)

Crystallographic data (CIF)

AUTHOR INFORMATION

Corresponding Authors

*E-mail: luis.azoframesa@kaust.edu.sa.

*E-mail: Osama.Elsepelgy@rwth-aachen.de.

ORCID

Luis Miguel Azofra: 0000-0003-4974-1670

Luigi Cavallo: 0000-0002-1398-338X

Magnus Rueping: 0000-0003-4580-5227

Osama El-Sepelgy: 0000-0003-3131-4988

Notes

The authors declare no competing financial interest.

ACKNOWLEDGMENTS

L.M.A. and L.C. acknowledge King Abdullah University of Science and Technology (KAUST) for support. Gratitude is also due to the KAUST Supercomputing Laboratory using the supercomputer Shaheen II for providing the computational resources.

REFERENCES

(1) Williams, J. M. J. *Preparation of Alkenes: A Practical Approach*; Oxford University Press: Oxford, U.K., 1996.

(2) (a) Oger, C.; Balas, L.; Durand, T.; Galano, J.-M. Are Alkyne Reductions Chemo-, Regio-, and Stereoselective Enough To Provide Pure (*Z*)-Olefins in Polyfunctionalized Bioactive Molecules? *Chem. Rev.* **2013**, *113*, 1313−1350. (b) Rylander, P. N. *Catalytic Hydrogenation in Organic Syntheses*; Academic Press: New York, 1979. (c) De Vries, J. G.; Elsevier, C. J. *Handbook of Homogeneous Hydrogenation*; Wiley-VCH: Weinheim, Germany, 2007. (d) Andersson, P. G.; Munslow, I. J. *Modern Reduction Methods*; Wiley: New York, 2008.

(3) (a) Lindlar, H. Ein neuer Katalysator für selektive Hydrierungen. *Helv. Chim. Acta* **1952**, *35*, 446−450. (b) Lindlar, H.; Dubuis, R. Palladium catalyst for partial reduction of acetylenes. *Org. Synth.* **1966**, *46*, 89.

(4) For selected examples of semihydrogenation of alkynes using heterogeneous catalysts see: (a) Mitsudome, T.; Takahashi, Y.; Ichikawa, S.; Mizugaki, T.; Jitsukawa, K.; Kaneda, K. Metal−Ligand

DOI: 10.1021/acscatal.8b00983
ACS Catal. 2018, 8, 4103−4109

Core−Shell Nanocomposite Catalysts for the Selective Semihydrogenation of Alkynes. *Angew. Chem., Int. Ed.* **2013**, *52*, 1481−1485. (b) Gieshoff, T. N.; Welther, A.; Kessler, M. T.; Prechtl, M. H. G.; Jacobi von Wangelin, A. Stereoselective Iron-Catalyzed Alkyne Hydrogenation in Ionic Liquids. *Chem. Commun.* **2014**, *50*, 2261−2264. (c) Karunananda, M. K.; Mankad, N. P. *E*-Selective Semi-Hydrogenation of Alkynes by Heterobimetallic Catalysis. *J. Am. Chem. Soc.* **2015**, *137*, 14598−14601. (d) Mitsudome, T.; Yamamoto, M.; Maeno, Z.; Mizugaki, T.; Jitsukawa, K.; Kaneda, K. One-step Synthesis of Core-Gold/Shell-Ceria Nanomaterial and Its Catalysis for Highly Selective Semihydrogenation of Alkynes. *J. Am. Chem. Soc.* **2015**, *137*, 13452−13455. (e) Vasilikogiannaki, E.; Titilas, I.; Vassilikogiannakis, G.; Stratakis, M. *Cis*-Semihydrogenation of Alkynes with Amine Borane Complexes Catalyzed by Gold Nanoparticles under Mild Conditions. *Chem. Commun.* **2015**, *51*, 2384−2387. (f) Konnerth, H.; Prechtl, M. H. G. Selective Partial Hydrogenation of Alkynes To (*Z*)-Alkenes with Ionic Liquid-Doped Nickel Nanocatalysts at Near Ambient Conditions. *Chem. Commun.* **2016**, *52*, 9129−9132. (g) Chen, F.; Kreyenschulte, C.; Radnik, J.; Lund, H.; Surkus, A.-E.; Junge, K.; Beller, M. Selective Semihydrogenation of Alkynes with N-Graphitic-Modified Cobalt Nanoparticles Supported on Silica. *ACS Catal.* **2017**, *7*, 1526−1532. (h) Lu, Y.; Feng, X.; Takale, B. S.; Yamamoto, Y.; Zhang, W.; Bao, M. Highly Selective Semihydrogenation of Alkynes to Alkenes by Using an Unsupported Nanoporous Palladium Catalyst: No Leaching of Palladium into the Reaction Mixture. *ACS Catal.* **2017**, *7*, 8296−8303.

(5) (a) Osborn, J. A.; Jardine, F. H.; Young, J. F.; Wilkinson, G. The Preparation and Properties of Tris(Triphenylphosphine)-Halogenorhodium(I) and Some Reactions Thereof Including Catalytic Homogeneous Hydrogenation of Olefins and Acetylenes and Their Derivatives. *J. Chem. Soc. A* **1966**, 1711−1732. (b) Schrock, R. R.; Osborn, J. A. Catalytic Hydrogenation Using Cationic Rhodium Complexes. I. Evolution of the Catalytic System and the Hydrogenation of Olefins. *J. Am. Chem. Soc.* **1976**, *98*, 2134−2143.

(6) (a) van Laren, M. W.; Elsevier, C. J. Selective Homogeneous Palladium(0)-Catalyzed Hydrogenation of Alkynes to (*Z*)-Alkenes. *Angew. Chem., Int. Ed.* **1999**, *38*, 3715−3717. (b) Shen, R.; Chen, T.; Zhao, Y.; Qiu, R.; Zhou, Y.; Yin, S.; Wang, X.; Goto, M.; Han, L.-B. Facile Regio- and Stereoselective Hydrometalation of Alkynes with a Combination of Carboxylic Acids and Group 10 Transition Metal Complexes: Selective Hydrogenation of Alkynes with Formic Acid. *J. Am. Chem. Soc.* **2011**, *133*, 17037−17044. (c) Drost, R. M.; Bouwens, T.; van Leest, N. P.; de Bruin, B.; Elsevier, C. J. Convenient Transfer Semihydrogenation Methodology for Alkynes Using a Pd(II)-NHC Precatalyst. *ACS Catal.* **2014**, *4*, 1349−1357.

(7) (a) Radkowski, K.; Sundararaju, B.; Fürstner, A. A Functional-Group-Tolerant Catalytic *trans* Hydrogenation of Alkynes. *Angew. Chem., Int. Ed.* **2013**, *52*, 355−360. (b) Leutzsch, M.; Wolf, L. M.; Gupta, P.; Fuchs, M.; Thiel, W.; Farès, C.; Fürstner, A. Formation of Ruthenium Carbenes by *gem*-Hydrogen Transfer to Internal Alkynes: Implications for Alkyne *trans*-Hydrogenation. *Angew. Chem., Int. Ed.* **2015**, *54*, 12431−12436. (c) Neumann, K. T.; Klimczyk, S.; Burhardt, M. N.; Bang-Andersen, B.; Skrydstrup, T.; Lindhardt, A. T. Direct trans-Selective Ruthenium-Catalyzed Reduction of Alkynes in Two-Chamber Reactors and Continuous Flow. *ACS Catal.* **2016**, *6*, 4710−4714. (d) Kusy, R.; Grela, K. *E*- and *Z*-Selective Transfer Semihydrogenation of Alkynes Catalyzed by Standard Ruthenium Olefin Metathesis Catalysts. *Org. Lett.* **2016**, *18*, 6196−6199.

(8) Tani, K.; Iseki, A.; Yamagata, T. Efficient transfer hydrogenation of alkynes and alkenes with methanol catalysed by hydrido(methoxo)-iridium(III) complexes. *Chem. Commun.* **1999**, 1821−1822.

(9) Srimani, D.; Diskin-Posner, Y.; Ben-David, Y.; Milstein, D. Iron pincer complex catalyzed, environmentally benign, E-selective semi-hydrogenation of alkynes. *Angew. Chem., Int. Ed.* **2013**, *52*, 14131−14134.

(10) (a) Barrios-Francisco, R.; García, J. Semihydrogenation of alkynes in the presence of Ni(0) catalyst using ammonia-borane and sodium borohydride as hydrogen sources. *Appl. Catal., A* **2010**, *385*, 108−113. (b) Richmond, E.; Moran, J. Ligand Control of *E*/*Z* Selectivity in Nickel-Catalyzed Transfer Hydrogenative Alkyne Semireduction. *J. Org. Chem.* **2015**, *80*, 6922−6929.

(11) (a) Fu, S.; Chen, N.-Y.; Liu, X.; Shao, Z.; Luo, S.-P.; Liu, Q. Ligand-Controlled Cobalt-Catalyzed Transfer Hydrogenation of Alkynes: Stereodivergent Synthesis of *Z*- and *E*-Alkenes. *J. Am. Chem. Soc.* **2016**, *138*, 8588−8594. (b) Tokmic, K.; Fout, A. R. Alkyne Semihydrogenation with a Well-Defined Nonclassical Co−H_2 Catalyst: A H_2 Spin on Isomerization and *E*-Selectivity. *J. Am. Chem. Soc.* **2016**, *138*, 13700−13705. (c) Chen, C.; Huang, Y.; Zhang, Z.; Dong, X.-Q.; Zhang, X. Cobalt-Catalyzed (*Z*)-Selective semihydrogenation of alkynes with molecular hydrogen. *Chem. Commun.* **2017**, *53*, 4612−4615.

(12) (a) Pape, F.; Thiel, N. O.; Teichert, J. F. *Z*-Selective Copper(I)-Catalyzed Alkyne Semihydrogenation with Tethered Cu−Alkoxide Complexes. *Chem. - Eur. J.* **2015**, *21*, 15934−15938. (b) Korytiaková, E.; Thiel, N. O.; Pape, F.; Teichert, J. F. Copper(I)-Catalyzed Transfer Hydrogenations with Ammonia Borane. *Chem. Commun.* **2017**, *53*, 732−735.

(13) For seminal examples on manganese-catalyzed hydrogenation see: (a) Elangovan, S.; Topf, C.; Fischer, S.; Jiao, H.; Spannenberg, A.; Baumann, W.; Ludwig, R.; Junge, K.; Beller, M. Selective Catalytic Hydrogenations of Nitriles, Ketones, and Aldehydes by Well-Defined Manganese Pincer Complexes. *J. Am. Chem. Soc.* **2016**, *138*, 8809−8814. (b) Kallmeier, F.; Irrgang, T.; Dietel, T.; Kempe, R. Highly Active and Selective Manganese C═O Bond Hydrogenation Catalysts: The Importance of the Multidentate Ligand, the Ancillary Ligands, and the Oxidation State. *Angew. Chem., Int. Ed.* **2016**, *55*, 11806−11809. (c) Elangovan, S.; Garbe, M.; Jiao, H.; Spannenberg, A.; Junge, K.; Beller, M. Hydrogenation of Esters to Alcohols Catalyzed by Defined Manganese Pincer Complexes. *Angew. Chem., Int. Ed.* **2016**, *55*, 15364−15368. (d) Papa, V.; Cabrero-Antonino, J. R.; Alberico, E.; Spanneberg, A.; Junge, K.; Junge, H.; Beller, M. Efficient and Selective Hydrogenation of Amides to Alcohols and Amines using a Well-Defined Manganese−PNN Pincer Complex. *Chem. Sci.* **2017**, *8*, 3576−3585. (e) Espinosa-Jalapa, N. A.; Nerush, A.; Shimon, L. J. W.; Leitus, G.; Avram, L.; Ben-David, Y.; Milstein, D. Manganese-Catalyzed Hydrogenation of Esters to Alcohols. *Chem. - Eur. J.* **2017**, *23*, 5934−5938. (f) van Putten, R.; Uslamin, E. A.; Garbe, M.; Liu, C.; Gonzalez-de-Castro, A.; Lutz, M.; Junge, K.; Hensen, E. J. M.; Beller, M.; Lefort, L.; Pidko, E. A. Non-Pincer-Type Manganese Complexes as Efficient Catalysts for the Hydrogenation of Esters. *Angew. Chem., Int. Ed.* **2017**, *56*, 7531−7534.

(14) Commercially available from several providers with reasonable price, e.g., $75/50 g from Shanghai Forxine Pharmaceutical Company.

(15) Kabir, M. K.; Kawahara, M.; Kumagai, H.; Adachi, K.; Kawata, S.; Ishii, T.; Kitagawa, S. The Rational Syntheses of Manganese−Chloranilate Compounds: Crystal Structures and Magnetic Properties. *Polyhedron* **2001**, *20*, 1417−1422.

(16) (a) Chiriac, R.; Toche, F.; Demirci, U. B.; Krol, O.; Miele, P. Ammonia Borane Decomposition in the Presence of Cobalt Halides. *Int. J. Hydrogen Energy* **2011**, *36*, 12955−12964. (b) Benzouaa, R.; Demirci, U. B.; Chiriac, F.; Toche, P.; Miele, P. Metal Chloride-Doped Ammonia Borane Thermolysis: Positive Effect on Induction Period as well as Hydrogen and Borazine Release. *Thermochim. Acta* **2010**, *509*, 81−86. (c) Semproni, S. P.; Milsmann, C.; Chirik, P. J. Four-Coordinate Cobalt Pincer Complexes: Electronic Structure Studies and Ligand Modification by Homolytic and Heterolytic Pathways. *J. Am. Chem. Soc.* **2014**, *136*, 9211−9224. (d) Srimani, D.; Mukherjee, A.; Goldberg, A. F. G.; Leitus, G.; Diskin-Posner, Y.; Shimon, L. J. W.; Ben David, Y.; Milstein, D. Cobalt-Catalyzed Hydrogenation of Esters to Alcohols: Unexpected Reactivity Trend Indicates Ester Enolate Intermediacy. *Angew. Chem., Int. Ed.* **2015**, *54*, 12357−12360.

(17) Geometries were located with the G09 package using the PBE functional together with the SVP basis set for main group atoms and the TZVP basis set for Mn. The reported free energies were obtained via single-point energy calculations using the PBE0-D3 functional and the TZVP basis set on all atoms. Solvent effects (methanol) were evaluated with the PCM model, including nonelectrostatic terms. (Full computational details can be found in the Supporting Information.)

DOI: 10.1021/acscatal.8b00983
ACS Catal. 2018, 8, 4103−4109

(18) Conradie, J.; Ghosh, A. Electronic Structure of Trigonal-Planar Transition-Metal−Imido Complexes: Spin-State Energetics, Spin-Density Profiles, and the Remarkable Performance of the OLYP Functional. *J. Chem. Theory Comput.* **2007**, *3*, 689−702.
(19) During the publication process, a related manganese-catalyzed semihydrogenation of alkynes to (*E*)-olefins has been reported, see: Zhou, Y.-P.; Mo, Z.; Luecke, M.-P.; Driess, M. Stereoselective Transfer Semi-Hydrogenation of Alkynes to *E*-Olefins with N-Heterocyclic Silylene−Manganese Catalysts. *Chem. - Eur. J.* [Online early access]. DOI: 10.1002/chem.201705745. Published Online: Dec 20, **2017**. https://onlinelibrary.wiley.com/doi/abs/10.1002/chem.201705745.

DOI: 10.1021/acscatal.8b00983
ACS Catal. 2018, 8, 4103−4109

Paper 7:

Catalytic C1 Alkylation with Methanol and Isotope-Labeled Methanol.

Sklyaruk, J.; Borghs, J. C.; El-Sepelgy, O.*; Rueping, M.*

Angew. Chem. Int. Ed. **2019**, *58*, 775-779.

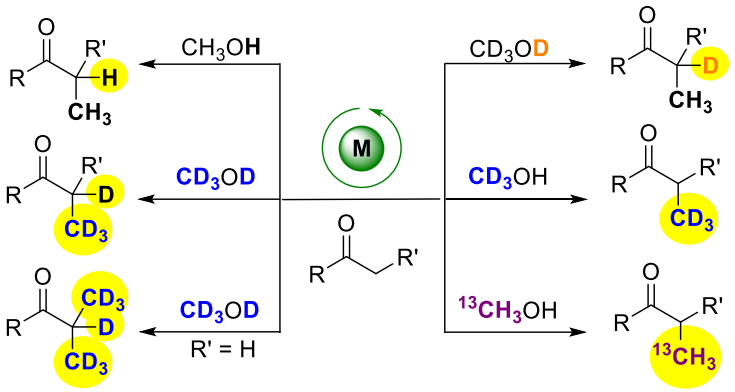

Methylation

International Edition: DOI: 10.1002/anie.201810885
German Edition: DOI: 10.1002/ange.201810885

Catalytic C_1 Alkylation with Methanol and Isotope-Labeled Methanol

Jan Sklyaruk, Jannik C. Borghs, Osama El-Sepelgy, and Magnus Rueping**

Abstract: *A metal-catalyzed methylation process has been developed. By employing an air- and moisture-stable manganese catalyst together with isotopically labeled methanol, a series of D-, CD_3-, and ^{13}C-labeled products were obtained in good yields under mild reaction conditions with water as the only byproduct.*

Isotope labeling is a very important topic in various fields of the life sciences.[1] Deuterium-labeled compounds are widely used as internal standards for spectroscopy and for biochemical applications.[2] Replacing carbon–hydrogen bonds by more stable carbon–deuterium bonds may have a positive effect on metabolic stability while retaining the potency and selectivity of the compound.[1c] As a consequence, deuterated drugs have been intensively studied.[3] The incorporation of deuterium can be achieved by different strategies, either by heterogeneously and homogeneously catalyzed H/D exchange or by organic synthesis with deuterium-labeled building blocks.[4]

In general, the methyl group has an extraordinary significance, being one of the most common fragments in biologically active molecules.[5] Furthermore, many pharmaceuticals feature improved properties if methyl groups are incorporated.[5] However, the exchange of methyl groups by the corresponding labeled analogue is not always straightforward and is traditionally accomplished by the use of either electrophilic or nucleophilic CD_3 sources, which may have drawbacks. Aside from their toxicity, carcinogenic properties, and high cost, a further disadvantage is the waste production (Scheme 1 A). In this regard, recent efforts focused on trideuteromethylation with deuterated dimethyl sulfoxide[6] or the generation of aryl methyl ethers, Ar–OCD_3, with the aid of deuterated methanol.[7]

Given the importance of the methyl group in medicinal and pharmaceutical chemistry and the improved metabolic properties of deuterated analogues, together with the current synthetic limitations, we decided to examine a new base-metal-catalyzed methylation of carbonyl groups using inexpensive and readily available isotope-labeled methanol as the

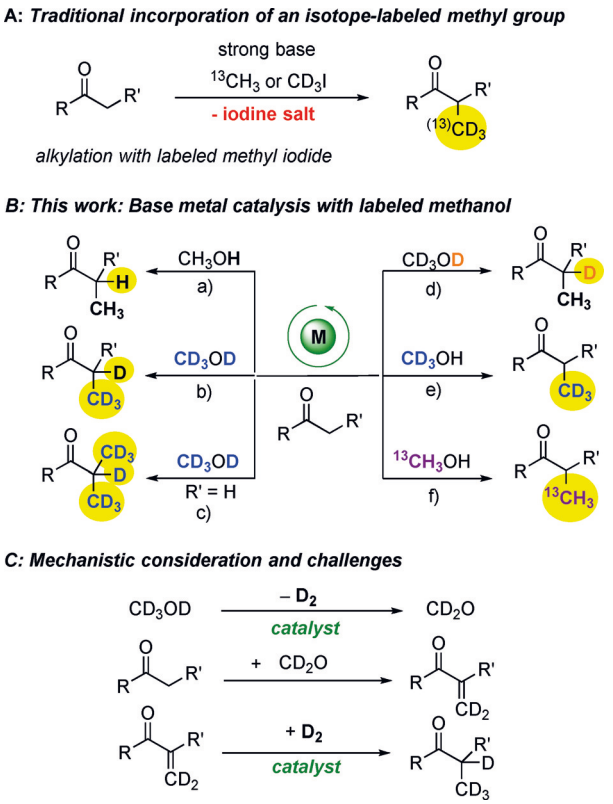

Scheme 1. Comparison of different methods for the isotope labeling of ketones.

C_1 building block.[8] The successful development of such a reaction would provide access to diverse labeled products, with water being generated as the only byproduct (Scheme 1 B). In particular, we decided to investigate a new C_1 alkylation reaction[9,10] with methanol following a dehydrogenation, aldol condensation, and hydrogenation pathway (Scheme 1 C).

To develop this sustainable reaction, we needed to address several challenges: 1) A general restriction for the use of methanol is its high stability towards dehydrogenation and the low stability of the intermediates, which often leads to the formation of CO_2 and hydrogen;[11] 2) aldol condensation with formaldehyde can generate side products; 3) the following hydrogenation needs to be chemoselective towards the olefinic bond to avoid carbonyl reduction; and 4) the base-metal catalyst needs to be reactive, readily available, stable, and moisture-tolerant as water is formed as a byproduct.

To the best of our knowledge, a general and practical base-metal-catalyzed C_1 alkylation of carbonyl compounds with isotope-labeled methanol had not been reported previously. Manganese is the third most-abundant transition metal in the Earth's crust and currently considered for the

[*] M. Sc. J. Sklyaruk, M. Sc. J. C. Borghs, Dr. O. El-Sepelgy, Prof. Dr. M. Rueping
Institute of Organic Chemistry, RWTH Aachen University
Landoltweg 1, 52074 Aachen (Germany)
E-mail: osama.elsepelgy@rwth-aachen.de
magnus.rueping@rwth-aachen.de
Prof. Dr. M. Rueping
KAUST Catalysis Center (KCC)
King Abdullah University of Science and Technology (KAUST)
Thuwal, 23955-6900 (Saudi Arabia)
Supporting information and the ORCID identification number(s) for the author(s) of this article can be found under: https://doi.org/10.1002/anie.201810885.

development of sustainable catalytic transformations,[12] including alkylations.[9a] Thus we initiated our studies with the synthesis of different manganese complexes (**Mn-1** to **Mn-4**), starting from the corresponding ligands and the precursor $Mn(CO)_5Br$ (Table 1).[13]

Table 1: Optimization of the reaction conditions.[a]

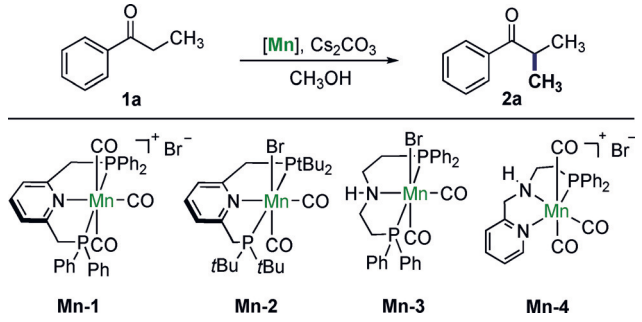

Entry	Catalyst (mol%)	Cs_2CO_3 [equiv]	*T* [°C]	Yield [%]
1	**Mn-1** (5)	4	85	97
2	**Mn-2** (5)	4	85	0
3	**Mn-3** (5)	4	85	22
4	**Mn-4** (5)	4	85	0
5	$Mn(CO)_5Br$ (5)	4	85	0
6	–	4	85	0
7	**Mn-1** (5)	–	85	0
8	**Mn-1** (2.5)	4	85	94
9	**Mn-1** (1)	4	85	57
10	**Mn-1** (2.5)	4	70	36
11[b]	**Mn-1** (2.5)	2	85	99
12[b]	**Mn-1** (2.5)	0.2	105	80

[a] Reaction conditions: **1a** (0.2 mmol), [**Mn**], Cs_2CO_3, MeOH (2 mL), 24 h. Yields were determined by GC analysis using ethylbenzene as an internal standard. [b] MeOH (1 mL).

However, before directly applying isotope-labeled methanol, we decided to first develop the variant with non-labeled methanol. Hence, we tested different manganese complexes in the α-methylation of propiophenone **1a** with methanol (Table 1).[14] To our delight, the air-stable aromatic and cationic diphenylphosphine-based complex [**Mn-1**] gave the desired product in quantitative yield (Table 1, entry 1). In contrast, the *tert*-butylphosphine-based complex **Mn-2** proved to be inactive (Table 1, entry 2). The aliphatic diphenylphosphine-based complex **Mn-3** provided the desired product in a lower yield of 22% (Table 1, entry 3). Furthermore, the pyridine- and diphenylphosphine-containing complex **Mn-4**, which we recently applied in the hydrogenation of carbonates, was inactive under these reaction conditions (Table 1, entry 4). The catalyst screen showed that the presence of an aromatic pyridyl-based backbone together with an aromatic phosphine is required for good activity and chemoselectivity.

Control experiments using either the manganese precursor $Mn(CO)_5Br$, **Mn-1** without base, or only Cs_2CO_3 did not provide the product (Table 1, entries 5–7). As the subsequent base screening (see the Supporting Information) did not result in improved reaction conditions, Cs_2CO_3 was used as the base. Decreasing the catalyst loading to 2.5 mol% gave also almost quantitative conversion (Table 1, entry 8). However, when the catalyst loading was lowered to 1 mol%, the yield dropped to 57% (Table 1, entry 9). Lowering the temperature to 70°C as well as decreasing the amount of base also resulted in diminished yield (Table 1, entries 10). However, when the concentration of **1a** was increased, a quantitative yield was achieved (Table 1, entry 11). Fur-

Table 2: Manganese-catalyzed methylation of ketones.[a]

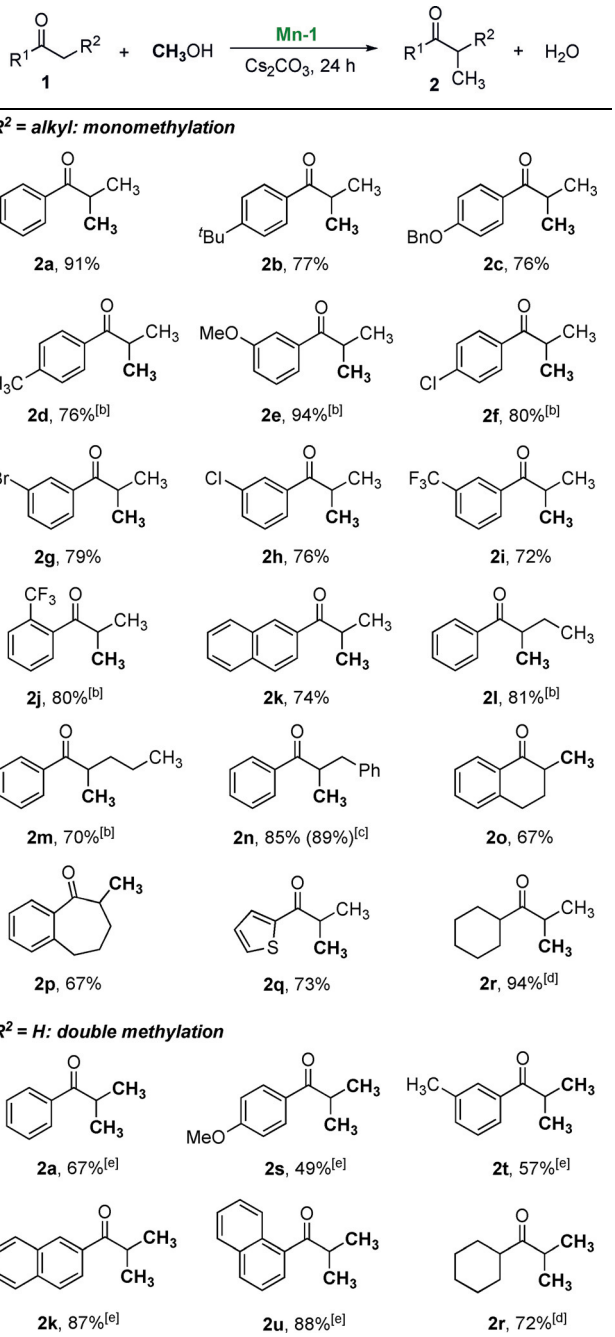

[a] Reaction conditions: **1** (1 mmol), Cs_2CO_3 (2 mmol), **Mn-1** (2.5 mol%) in CH_3OH (5 mL) at 85°C for 24 h. [b] **Mn-1** (5 mol%). [c] **1n** (10 mmol), Cs_2CO_3 (2 mmol), CH_3OH (10 mL), 105°C, 24 h. [d] **1** (1 mmol), Cs_2CO_3 (4 mmol), **Mn-1** (5 mol%), CH_3OH (2 mL) at 105°C. [e] **1** (1 mmol), Cs_2CO_3 (4 mmol), **Mn-1** (5 mol%), CH_3OH (5 mL) at 85°C.

Table 3: Manganese-catalyzed trideuteromethylation of ketones.[a]

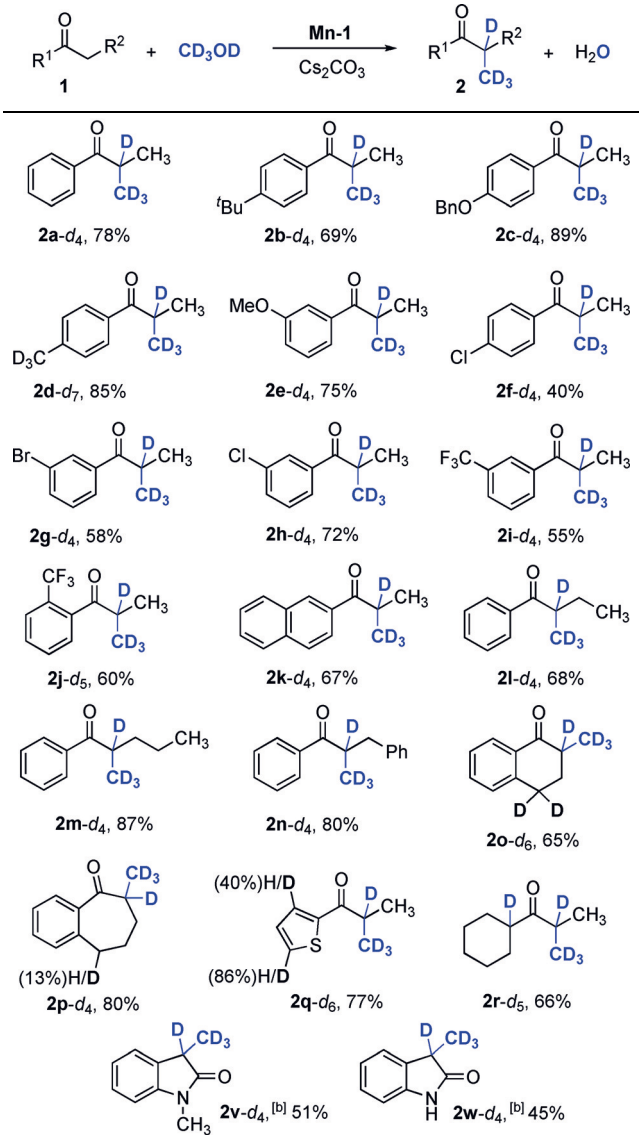

[a] Reaction conditions: **1** (0.5 mmol), Cs_2CO_3 (2 mmol), **Mn-1** (5 mol%), CD_3OD (1 mL) at 105 °C for 24 h. [b] CD_3OD (0.5 mL), 1,4-dioxane (0.5 mL), 135 °C.

thermore, at higher temperature, the base can be used in catalytic amounts (Table 1, entries 12).

With optimized reaction conditions in hand, we examined the scope of the manganese-catalyzed C_1 alkylation of carbonyl compounds (Table 2). In general, the reaction proceeded well, and differently substituted propiophenone derivatives as well as cyclic, heteroaromatic, and aliphatic ketones were converted into the corresponding α-methylated products **2a**–**2r** in good yields. Furthermore, using acetophenone derivatives, double alkylation was also achieved, and the corresponding products were obtained in good yields (Table 2, bottom). The practical applicability of the **Mn-1** catalytic system was demonstrated by performing the α-methylation of **1n** on a 10 mmol scale using 2.5 mol% of **Mn-1** and 20 mol% of Cs_2CO_3.

Following the successful development of this process using methanol as the alkylating reagent, we turned our attention to D- and ^{13}C-labeled methanol. Owing to the kinetic isotope effect ($k_{CH_3OH}/k_{CD_3OD} = 2.4$), we had to adjust the reaction conditions. Again, the manganese-catalyzed C_1 alkylation proceeded well when fully deuterated CD_3OD was used, and the corresponding trideuteromethylated products **2**-d_4 were obtained in good yields (Table 3). According to the proposed mechanism, deuterium incorporation in the α-carbonyl position is observed. Overall the yields are comparable to those of the non-deuterated version (Table 2). Interestingly, we also observed H/D exchange for substrates with benzylic positions (**2d**, **2o**, **2p**), indicating that the manganese catalyst can be used beyond the C_1 deuteromethylation. Subsequently, we also used acetophenone and derivatives thereof in the alkylation reaction and obtained the doubly deuteromethylated products **2**-d_7 in good yields (Table 4).

Table 4: Manganese-catalyzed double trideuteromethylation of ketones.[a]

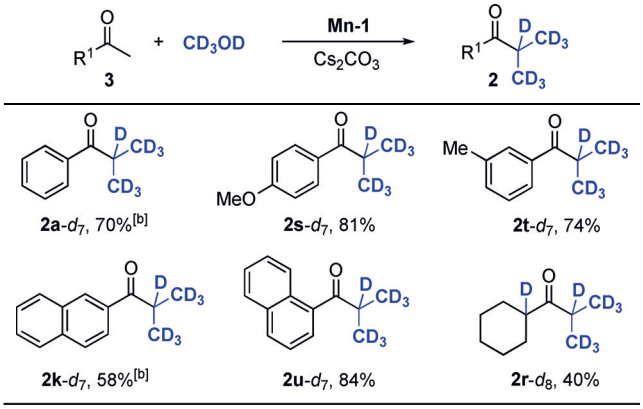

[a] Reaction conditions: **1** (0.5 mmol), Cs_2CO_3 (2 mmol), **Mn-1** (5 mol%), CD_3OD (1 mL) at 105 °C for 24 h. [b] 48 h.

To show the regioselectivity of the deuterium incorporation and illustrate the different possibilities for highly selective isotope labeling, we applied three other isotope-labeled methanol variants, CH_3OD, CD_3OH, and $^{13}CH_3OH$, in the manganese-catalyzed alkylation (Scheme 2). Ketone **2a**-d_1 was isolated in 86% yield, giving almost exclusively the α-deuterated isotopomer. In the case of CD_3OH, **2a**-d_3 was isolated in 88%, giving the desired β-trideuterated product. To confirm the generality of our process, we also applied ^{13}C-labeled methanol, and pure **2a**-^{13}C was obtained in 79% yield.

In summary, we have developed a manganese-catalyzed C_1 alkylation with methanol as an environmentally benign alkylating reagent that provides methylated products in good yields under mild reaction conditions, with water being generated as the only byproduct. Differently isotope-labeled methanol variants were subjected to this base-metal-catalyzed process to selectively generate CD_3-, $(CD_3)_2$-, and ^{13}C-labeled products. Given the simplicity of the procedure and the use of readily available substrates and catalysts as well as inexpensive labeled reagents, both the newly developed

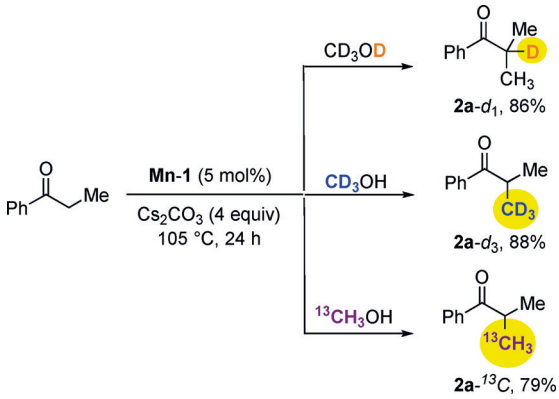

Scheme 2. Selective isotope labeling of propiophenone **1a** using different methanol variants.

methylation as well as the labeling reaction should be of interest for the straightforward synthesis of methyl-containing bioactive compounds.

Acknowledgements

J.S. is grateful for a doctoral fellowship provided by the Fonds der Chemischen Industrie. J.C.B. acknowledges the DBU for a doctoral fellowship.

Conflict of interest

The authors declare no conflict of interest.

Keywords: alkylation · manganese · methylation · transition-metal catalysis · trideuteromethylation

How to cite: *Angew. Chem. Int. Ed.* **2019**, *58*, 775–779
Angew. Chem. **2019**, *131*, 785–789

[1] a) T. G. Gant, *J. Med. Chem.* **2014**, *57*, 3595–3611; b) J. Atzrodt, V. Derdau, W. J. Kerr, M. Reid, *Angew. Chem. Int. Ed.* **2018**, *57*, 1758–1784; *Angew. Chem.* **2018**, *130*, 1774–1802; c) V. Zachleder, M. Vítová, M. Hlavová, Š. Moudříková, P. Mojzeš, H. Heumann, J. R. Becher, K. Bišová, *Biotechnol. Adv.* **2018**, *36*, 784–797.

[2] a) J. Atzrodt, V. Derdau, *J. Labelled Compd. Radiopharm.* **2010**, *53*, 674–685; b) D. J. Kushner, A. Baker, T. G. Dunstall, *Can. J. Physiol. Pharmacol.* **1999**, *77*, 79–88.

[3] a) A. Mullard, *Nat. Rev. Drug Discovery* **2016**, *15*, 219–221; b) C. Schmidt, *Nat. Biotechnol.* **2017**, *35*, 493–494.

[4] a) J. Atzrodt, V. Derdau, T. Fey, J. Zimmermann, *Angew. Chem. Int. Ed.* **2007**, *46*, 7744–7765; *Angew. Chem.* **2007**, *119*, 7890–7911; b) J. Atzrodt, V. Derdau, W. J. Kerr, M. Reid, *Angew. Chem. Int. Ed.* **2018**, *57*, 3022–3047; *Angew. Chem.* **2018**, *130*, 3074–3101.

[5] a) H. Schönherr, T. Cernak, *Angew. Chem. Int. Ed.* **2013**, *52*, 12256–12267; *Angew. Chem.* **2013**, *125*, 12480–12492; b) E. J. Barreiro, A. E. Kümmerle, C. A. M. Fraga, *Chem. Rev.* **2011**, *111*, 5215–5246.

[6] a) R. Caporaso, S. Manna, S. Zinken, A. R. Kochnev, E. R. Lukyanenko, V. Kurkin, A. P. Antonchick, *Chem. Commun.* **2016**, *52*, 12486–12489; b) R. Zhang, H. Yu, Z. Li, Q. Yan, P. Li, J. Wu, *Adv. Synth. Catal.* **2018**, *360*, 1384–1388.

[7] a) S. Vanderheiden, B. Bulat, T. Zevaco, N. Jung, S. Bräse, *Chem. Commun.* **2011**, *47*, 9063–9065; b) S. Gowrisankar, H. Neumann, M. Beller, *Chem. Eur. J.* **2012**, *18*, 2498–2502; c) C. W. Cheung, S. L. Buchwald, *Org. Lett.* **2013**, *15*, 3998–4001.

[8] For key examples of the use of methanol as a C_1 building block, see: a) B. Sam, B. Breit, M. J. Krische, *Angew. Chem. Int. Ed.* **2015**, *54*, 3267–3274; *Angew. Chem.* **2015**, *127*, 3317–3325; b) K. Natte, H. Neumann, M. Beller, R. V. Jagadeesh, *Angew. Chem. Int. Ed.* **2017**, *56*, 6384–6394; *Angew. Chem.* **2017**, *129*, 6482–6492; for further examples, see: c) J. Moran, A. Preetz, R. A. Mesch, M. J. Krische, *Nat. Chem.* **2011**, *3*, 287–291; d) K. D. Nguyen, D. Herkommer, M. J. Krische, *J. Am. Chem. Soc.* **2016**, *138*, 14210–14213; e) M. Holmes, K. D. Nguyen, L. A. Schwartz, T. Luong, M. J. Krische, *J. Am. Chem. Soc.* **2017**, *139*, 8114–8117.

[9] For leading examples of base-metal-catalyzed C alkylation reactions with alcohols, see: manganese: a) M. Peña-López, P. Piehl, S. Elangovan, H. Neumann, M. Beller, *Angew. Chem. Int. Ed.* **2016**, *55*, 14967–14971; *Angew. Chem.* **2016**, *128*, 15191–15195; b) S. Fu, Z. Shao, Y. Wang, Q. Liu, *J. Am. Chem. Soc.* **2017**, *139*, 11941–11948; c) N. V. Kulkarni, W. W. Brennessel, W. D. Jones, *ACS Catal.* **2018**, *8*, 997–1002; d) T. Liu, L. Wang, K. Wu, Z. Yu, *ACS Catal.* **2018**, *8*, 7201–7207; e) A. Jana, C. B. Reddy, B. Maji, *ACS Catal.* **2018**, *8*, 9226–9231; f) O. El-Sepelgy, E. Matador, A. Brzozowska, M. Rueping, *ChemSusChem* **2018**, https://doi.org/10.1002/cssc.201801660; cobalt: g) N. Deibl, R. Kempe, *J. Am. Chem. Soc.* **2016**, *138*, 10786–10789; h) G. Zhang, J. Wu, H. Zeng, S. Zhang, Z. Yin, S. Zheng, *Org. Lett.* **2017**, *19*, 1080–1083; i) F. Freitag, T. Irrgang, R. Kempe, *Chem. Eur. J.* **2017**, *23*, 12110–12113; iron: j) G. Tang, C.-H. Cheng, *Adv. Synth. Catal.* **2011**, *353*, 1918–1922; k) S. Elangovan, J.-B. Sortais, M. Beller, C. Darcel, *Angew. Chem. Int. Ed.* **2015**, *54*, 14483–14486; *Angew. Chem.* **2015**, *127*, 14691–14694; l) W. Ma, S. Cui, H. Sun, W. Tang, D. Xue, C. Li, J. Fan, J. Xiao, C. Wang, *Chem. Eur. J.* **2018**, *24*, 13118–13123.

[10] For manganese-catalyzed C–N bond formation and N alkylation using methanol, see: a) S. Elangovan, J. Neumann, J.-B. Sortais, K. Junge, C. Darcel, M. Beller, *Nat. Commun.* **2016**, *7*, 12641; b) M. Mastalir, E. Pittenauer, G. Allmaier, K. Kirchner, *J. Am. Chem. Soc.* **2017**, *139*, 8812–8815; c) S. Chakraborty, U. Gellrich, Y. Diskin-Posner, G. Leitus, L. Avram, D. Milstein, *Angew. Chem. Int. Ed.* **2017**, *56*, 4229–4233; *Angew. Chem.* **2017**, *129*, 4293–4297; d) A. J. Neumann, S. Elangovan, A. Spannenberg, K. Junge, M. Beller, *Chem. Eur. J.* **2017**, *23*, 5410–5413; e) A. Bruneau-Voisine, D. Wang, V. Dorcet, T. Roisnel, C. Darcel, J.-B. Sortais, *J. Catal.* **2017**, *347*, 57–62; f) R. Fertig, T. Irrgang, F. Freitag, J. Zander, R. Kempe, *ACS Catal.* **2018**, *8*, 8525–8530.

[11] M. Andérez-Fernández, L. K. Vogt, S. Fischer, W. Zhou, H. Jiao, M. Garbe, S. Elangovan, K. Junge, H. Junge, R. Ludwig, M. Beller, *Angew. Chem. Int. Ed.* **2017**, *56*, 559–562; *Angew. Chem.* **2017**, *129*, 574–577.

[12] For recent reviews on manganese catalysis, see: a) N. Gorgas, K. Kirchner, *Acc. Chem. Res.* **2018**, *51*, 1558–1569; b) G. A. Filonenko, R. van Putten, E. J. M. Hensen, E. A. Pidko, *Chem. Soc. Rev.* **2018**, *47*, 1459–1483; c) F. Kallmeier, R. Kempe, *Angew. Chem. Int. Ed.* **2018**, *57*, 46–60; *Angew. Chem.* **2018**, *130*, 48–63; d) T. Zell, R. Langer, *ChemCatChem* **2018**, *10*, 1930–1940; e) B. Maji, M. K. Barman, *Synthesis* **2017**, *49*, 3377–3393; f) M. Garbe, K. Junge, M. Beller, *Eur. J. Org. Chem.* **2017**, 4344–4362; g) W. Liu, L. Ackermann, *ACS Catal.* **2016**, *6*, 3743–3752; for further examples from our group, see: h) A. Brzozowska, L. M. Azofra, V. Zubar, I. Atodiresei, L. Cavallo, M. Rueping, O. El-Sepelgy, *ACS Catal.* **2018**, *8*, 4103–4109; i) V. Zubar, Y. Lebedev, L. M. Azofra, L. Cavallo, O. El-Sepelgy, *Angew. Chem.*

Int. Ed. **2018**, *57*, 13439 – 13443; *Angew. Chem.* **2018**, *130*, 13627 – 13631.
[13] For further details, see the Supporting Information.
[14] For leading examples, see: a) L. K. M. Chan, D. L. Poole, D. Shen, M. P. Healy, T. J. Donohoe, *Angew. Chem. Int. Ed.* **2014**, *53*, 761 – 765; *Angew. Chem.* **2014**, *126*, 780 – 784; b) S. Ogawa, Y. Obora, *Chem. Commun.* **2014**, *50*, 2491 – 2493; c) F. Li, J. Ma, N. Wang, *J. Org. Chem.* **2014**, *79*, 10447 – 10455; d) X. Quan, S. Kerdphon, P. G. Andersson, *Chem. Eur. J.* **2015**, *21*, 3576 – 3579; e) D. Shen, D. L. Poole, C. C. Shotton, A. F. Kornahrens, M. P. Healy, T. J. Donohoe, *Angew. Chem. Int. Ed.* **2015**, *54*, 1642 – 1645; *Angew. Chem.* **2015**, *127*, 1662 – 1665; f) T. Thanh, M. A. Seayad, *Adv. Synth. Catal.* **2016**, *358*, 3373 – 3380; g) K. Chakrabarti, M. Maji, D. Panja, B. Paul, S. Shee, G. K. Das, S. Kundu, *Org. Lett.* **2017**, *19*, 4750 – 4753; h) Z. Liu, Z. Yang, X. Yu, H. Zhang, B. Yu, Y. Zhao, Z. Liu, *Org. Lett.* **2017**, *19*, 5228 – 5231; i) S. M. A. H. Siddiki, A. S. Touchy, M. A. R. Jamil, T. Toyao, K.-I. Shimizu, *ACS Catal.* **2018**, *8*, 3091 – 3103; j) K. Polidano, B. D. W. Allen, J. M. J. Williams, L. C. Morrill, *ACS Catal.* **2018**, *8*, 6440 – 6445.

Manuscript received: September 21, 2018
Revised manuscript received: November 8, 2018
Accepted manuscript online: November 20, 2018
Version of record online: December 17, 2018

Paper 8:

C-Alkylation of Secondary Alcohols by Primary Alcohols through Manganese-Catalyzed Double Hydrogen Autotransfer.

El-Sepelgy, O.*; Matador, E.; Brzozowska, A.; Rueping, M.*

ChemSusChem **2019**, *12*, 3099.

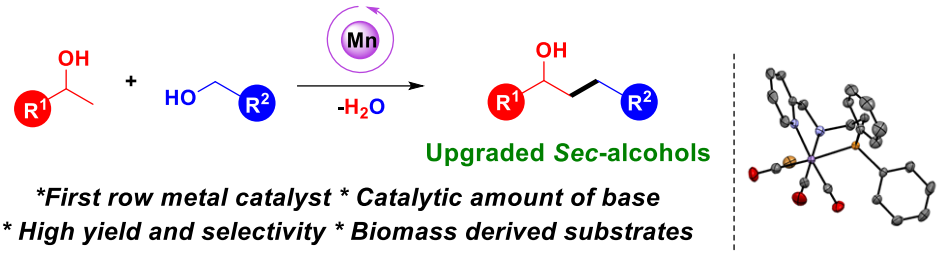

ChemPubSoc Europe

DOI: 10.1002/cssc.201801660

CHEMSUSCHEM Communications

C-Alkylation of Secondary Alcohols by Primary Alcohols through Manganese-Catalyzed Double Hydrogen Autotransfer

Osama El-Sepelgy,*[a] Esteban Matador+,[a] Aleksandra Brzozowska+,[a] and Magnus Rueping*[a, b]

A new Mn-catalyzed alkylation of secondary alcohols with non-activated alcohols is presented. The use of a stable and well-defined manganese pincer complex, stabilized by a PNN ligand, together with a catalytic amount of base enabled the conversion of renewable alcohol feedstocks to a broad range of higher-value alcohols in good yields with water as the sole byproduct. The strategy eliminates the need for exogenous and detrimental alkyl halides as well as the use of noble metal catalysts, making the C-alkylation through double hydrogen autotransfer a highly sustainable and environmentally benign process. Mechanistic investigations support a hydrogen autotransfer mechanism in which a non-innocent ligand plays a crucial role.

β-Alkylation of alcohols is one of the most fundamental carbon-carbon bond-forming reactions. The conventional route requires three chemical steps (i.e., stoichiometric oxidation, alkylation with alkyl halides, and stoichiometric reduction), making the overall process environmentally unfriendly.[1] With aim to avoid the use of mutagenic and waste-forming reagents,[2] modern processes have emerged, which are based on the hydrogen autotransfer strategy[3] utilizing biomass-derived alcohols as alkylating agents.[4] Hence, a strategy that comprises the dehydrogenation of both of the primary and secondary alcohols followed by base-catalyzed aldol condensation to produce α,β-unsaturated ketones and subsequent double hydrogenation can provide β-alkylated alcohols. Thus, stoichiometric oxidation and reduction reagents as well as alkyl halides can be substituted by abundantly available alcohols.

So far, the vast majority of these approaches rely on the use of more expensive noble-metal catalysts, such as Ir,[5] Ru,[6] Rh[7] and Pd.[8] Replacement of the precious-metal catalysts by earth-abundant low-toxicity base-metal catalysts is a topic of current interest.[9] Processes relying on the use of Fe[10] Ni[11] and Cu[12] catalysts have been disclosed. More recently, Co catalysis has been successfully used. However, higher catalyst loading (5 mol%) along with superstoichiometric amounts of a more sensitive and expensive base [potassium bis(trimethylsilyl)amide (KHMDS)] may be a drawback.[13]

Despite all these efforts, the alkylation of secondary alcohols with primary alcohols often leads to mixtures of the desired β-alkylated alcohols along with the corresponding undesired ketones, presenting a crucial selectivity issue. Therefore, the development of a base-metal catalyst for the selective alkylation of secondary alcohols would be highly desirable.

Based on our recent experience in Mn catalysis and its application in the reduction of alkynes and organic carbonates,[14] we questioned if highly reactive Mn catalysts may be suitable for the efficient hydrogenation of the intermediate α,β-unsaturated ketone, resulting exclusively in the desired alkylated alcohols. However, at the outset of this work, the alkylation of secondary alcohols using/from primary alcohols by Mn catalysis was not known to the best of our knowledge. During the preparation of this Communication a related parallel study was reported by Yu and co-workers.[15] Here, we demonstrate that the Mn–PNN pincer complex **Mn-1** is a remarkably active and selective catalyst for the alkylation reaction of alcohols (Scheme 1).[16,17]

The cross-coupling between 1-phenylethanol (**1a**) and benzyl alcohol (**2a**) was selected as a model reaction (Table 1). Initially, we screened the catalytic properties of different Mn complexes (**Mn-1** to **Mn-4**) in combination with 10 mol% of

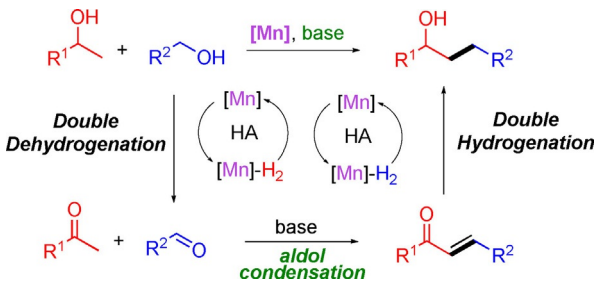

Scheme 1. Mn-catalyzed double hydrogen autotransfer.

[a] Dr. O. El-Sepelgy, E. Matador,+ A. Brzozowska,+ Prof. Dr. M. Rueping
Institute of Organic Chemistry
RWTH Aachen University
Landoltweg 1, 52074 Aachen (Germany)
E-mail: osama.elsepelgy@rwth-aachen.de
magnus.rueping@rwth-aachen.de

[b] Prof. Dr. M. Rueping
KAUST Catalysis Center (KCC)
King Abdullah University of Science and Technology (KAUST)
Thuwal 23955-6900 (Saudi Arabia)

[+] These authors contributed equally to this work.

Supporting Information and the ORCID identification number(s) for the author(s) of this article can be found under: https://doi.org/10.1002/cssc.201801660.

This publication is part of a Special Issue on "Sustainable Organic Synthesis".
Please visit the issue at http://doi.org/10.1002/cssc.v12.13

Table 1. Optimization of the reaction conditions.[a]

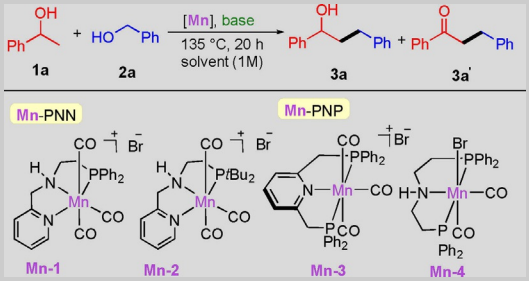

Entry	Catalyst ([mol%])	Base ([mol%])	Solvent	Conv. [%]	Yield of **3a**/**3a**′ [%]
1	**Mn-1** (3)	Cs_2CO_3 (10)	TAA	57	49/8
2	**Mn-2** (3)	Cs_2CO_3 (10)	TAA	60	42/14
3	**Mn-3** (3)	Cs_2CO_3 (10)	TAA	>99	69/30
4	**Mn-4** (3)	Cs_2CO_3 (10)	TAA	90	55/34
5	**Mn-1** (3)	Cs_2CO_3 (10)	1,4-dioxane	62	20/3
6	**Mn-1** (3)	Cs_2CO_3 (10)	2-Me-THF	60	30/4
7	**Mn-1** (3)	Cs_2CO_3 (10)	toluene	73	50/22
8	**Mn-1** (3)	KHMDS (10)	toluene	77	50/8
9	**Mn-1** (3)	KH (10)	toluene	90	65/8
10	**Mn-1** (3)	KOH (10)	toluene	93	76/5
11	**Mn-1** (3)	KO*t*Bu (10)	toluene	88	81/5
12	**Mn-1** (3)	KO*t*Bu (5)	toluene	85	57/17
13	**Mn-1** (3)	KO*t*Bu (25)	toluene	>99	92/8
14	**Mn-1 (1)**	**KO*t*Bu (25)**	toluene	>**99**	**92/8**
15[b]	**Mn-1 (1)**	KO*t*Bu (25)	toluene	>99	83/13

[a] Reaction conditions: **1a** (0.5 mmol), **2a** (0.55 mmol), [**Mn**] and base in 0.5 mL of solvent at 135 °C in a glass tube under argon for 20 h. Conversions and yields were determined by the H^1 NMR analysis of the crude reaction mixture using mesitylene as an internal standard. TAA = *tert*-amyl alcohol. [b] A drop of mercury was added.

Cs_2CO_3 in *tert*-amyl alcohol (TAA) as solvent. The use of 3 mol% of our PNN complex **Mn-1** led to promising results, providing the desired product **3a** in 49% yield along with 8% of the corresponding ketone **3a**′ (Table 1, entry 1). The application of the di-*tert*-butyl complex **Mn-2** resulted in similar dehydrogenation activity and slightly lower hydrogenation activity (Table 1, entry 2).[16f] In the presence of PNP complexes, such as **Mn-3** and **Mn-4**, excellent conversion was observed. However, the inefficient hydrogenation of the unsaturated intermediate provided considerable amount of the undesired ketone **3a**′ (Table 1, entries 3 and 4). Thus, we decided to further optimize the model reaction using **Mn-1** in combination with different bases and solvents. 1,4-Dioxane and 2-Me-THF proved to be unsuitable for this reaction. However, performing the reaction in toluene resulted in better results (Table 1, entries 5–7). Additionally, we tested various bases such as KHMDS, KH, KOH, and KO*t*Bu (Table 1, entries 8–13). From these experiments the reaction proceeded best when 25 mol% of KO*t*Bu were applied and the desired product was obtained in 92% yield (Table 1, entry 13). Interestingly, we could reduce the catalyst loading to 1 mol% while still obtaining excellent yield (Table 1, entry 14). Finally, full conversion was still observed upon adding Hg to the reaction mixture, proving the homogenous nature of the Mn catalyst (Table 1, entry 15).

Next, the substrate scope of the β-alkylation of different secondary alcohols **1** with benzyl alcohol **2a** was conducted (Scheme 2a). The 1-phenylethanol derivatives **1b**–**1d** bearing electron-donating substituents in *ortho*, *meta*, and *para* positions gave the desired products **3b**–**3d** in good yields. Similarly, the electron-deficient substrates **1e** and **1f** furnished the upgraded alcohols **3e** and **3f** in good yields. Furthermore, the alkylation of the naphthyl substrate **1g** afforded the expected product in 71% yield. Importantly, the substrate scope could be extended to the use of the less active aliphatic secondary alcohols **1h**–**1l**; the corresponding alcohols **3h**–**3l** were obtained in good-to-moderate yields. Noteworthy, even the sterically demanding alcohol **1k** was tolerated in this Mn-catalyzed reaction.

After successfully varying the secondary alcohols, we became interested in studying the scope of the β-alkylation of 1-phenylethanol (**1a**) with different primary alcohols **2** (Scheme 2b). The alkylation of **1a** with the electron-rich benzyl alcohols **2b**–**2f** as well as the electron-poor substrates **2g**–**2i** resulted in the secondary alcohols **4b**–**4i** in good yields. Also, the alcohol **4j** containing a naphthyl group was obtained in 77% yield. Additionally, various aliphatic primary alcohols could also be used as a coupling partner to afford the alcohols **4k**–**4m**.

Encouraged by these promising results, we decided to investigate the more challenging coupling reaction between saturated aliphatic primary and secondary alcohols (Scheme 2c). Indeed, our catalytic system also proved to be suitable to couple the branched cyclohexanemethanol and unbranched 1-octanol with 1-cyclohexylethanol and the products **5a** and **5b** were isolated in good yields. Furthermore, 1-cyclopenylethanol and 1-cyclopropylethanol were alkylated with different linear and non-linear alcohols to produce the alcohols **5c**–**5e** in good yields.

To gain insight into the reaction mechanism, we performed deuterium-labeling experiments (Scheme 3). When 1-phenylethanol-α-d_1 [D_1]**1a** was reacted with benzyl alcohol-α,α-d_2 [D_2]**2a**, a very strong kinetic isotope effect was observed and **3a**′′ was obtained in 31% yield with 86% deuteration in the α-position and 60% deuterium incorporation at C3. No deuteration occurred at the OH moiety and only 10% deuterium incorporation occurred at the C2 position (Scheme 3a). Similarly, the reaction between [D_1]**1a** and **2a** gave the alkylated product with deuterium incorporations of 32% at C1, 15% at C3, and >3% at C2 (Scheme 3b). The presence of only 40% deuterium incorporation at C3 in the reaction between **1a** and [D_2]**2a** indicates the reversibility of the primary alcohol dehydrogenation process and supports the hydrogen autotransfer pathway (Scheme 3c).

Interestingly, the high deuterium content at C1 and C3 and the low deuterium incorporation at C2 are not in alignment with both the classical dihydride mechanism and proposed amidate-assisted pathway.[16e] The presented deuterium experiments support a monohydride mechanism and highlight the involvement of both the metal and the non-innocent ligand in the transfer-hydrogenation pathways.[18–20]

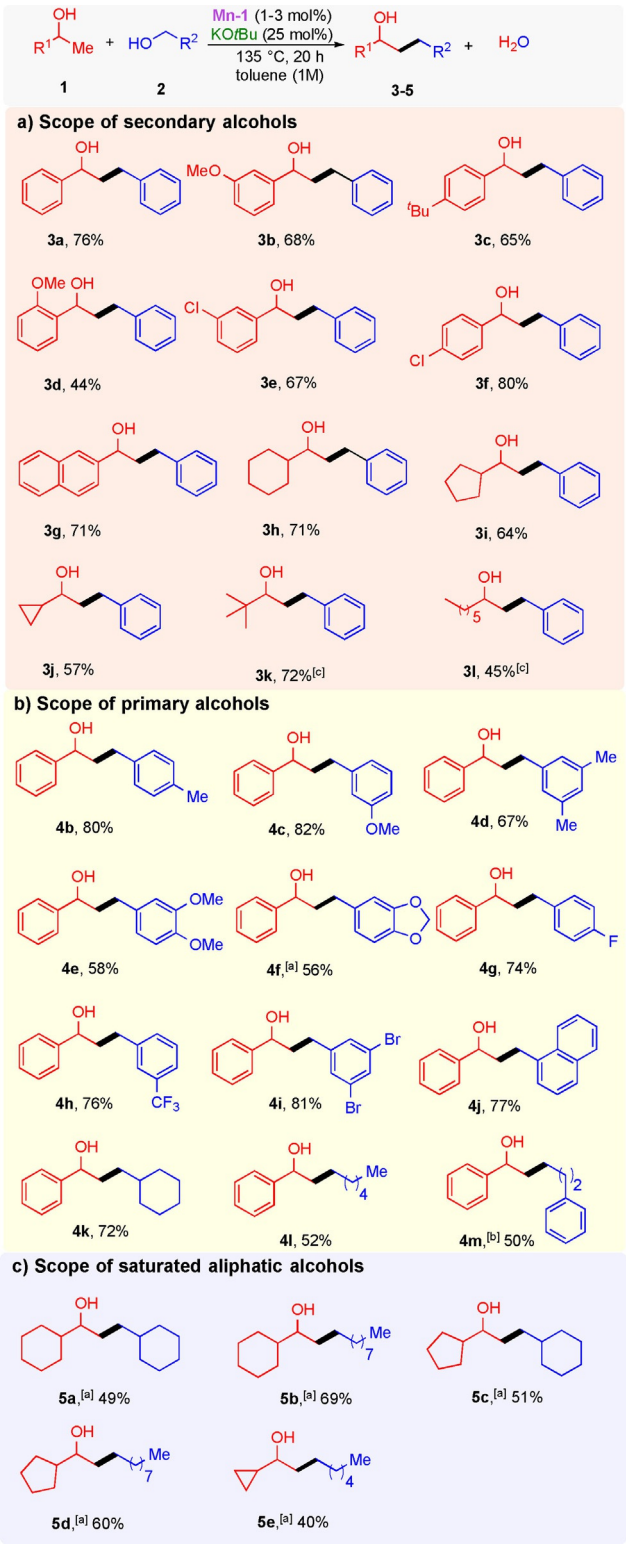

Scheme 2. Scope of Mn-catalyzed C-alkylation of secondary alcohols by primary alcohols. Reaction conditions: **1** (0.5 mmol), **2** (0.55 mmol), **Mn-1** (0.005 mmol) and KO*t*Bu (0.125 mmol) in toluene (0.5 mL) were stirred at 135 °C for 20 h in a glass tube under an inert atmosphere. Yields after column chromatography. [a] **Mn-1** (0.015 mmol). [b] **Mn-1** (0.01 mmol). [c] NMR yield.

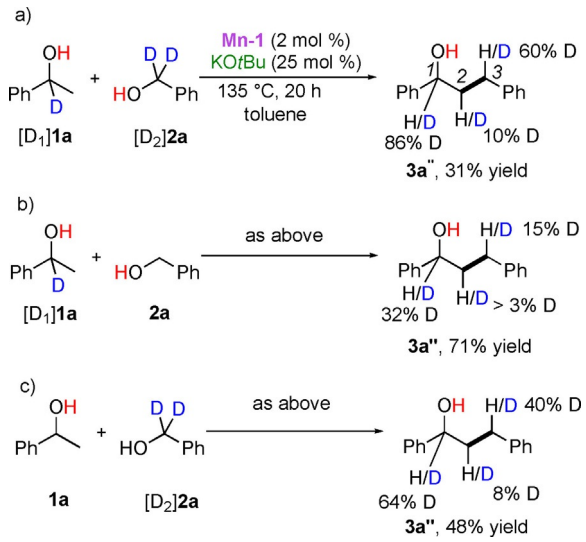

Scheme 3. Deuterium labeling experiments.

The metal monohydride can be formed by the β-hydride elimination of the Mn alkoxide (inner sphere pathway). Alternatively, the alcohol can be (de)hydrogenated through the outer sphere of the metal without coordination of the alcohol to the metal center.[20] Subsequently, we investigated the progress of the model reaction between **1a** and **2a** as a function of time (see the Supporting Information for details). The investigation indicates that the dehydrogenation of the alcohol substrates is most likely the rate-limiting step. The proposed reaction mechanism is shown in Scheme 4. Initially, the precatalyst **Mn-1** reacts with the base to form the 16e species **A**. This active species can reversibly react with an alcohol to form the corresponding ketone and the hydrogenated catalyst **B** (Scheme 4a). The alkylation reaction starts with the dehydrogenation of both alcohols to form carbonyl compounds and the hydrogenated catalyst **B**. Then, the base-catalyzed aldol condensation leads to the irreversible formation of the α,β-unsaturated ketone intermediate. Based on the experimental re-

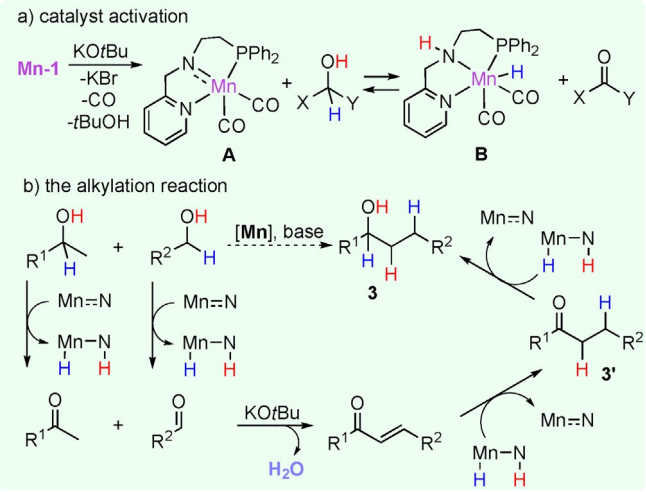

Scheme 4. Proposed reaction mechanism.

sults and the reaction profile, it is suggested that the hydrogenation of the C=C double bond of the α,β-unsaturated ketone takes place prior to the reduction of the ketone **3′** to the desired alcohol product **3** (Scheme 4b).

In conclusion, we report here the synthesis of C-alkylated secondary alcohols through a hydrogen autotransfer strategy using a stable and well-defined Mn catalyst. The newly developed catalytic system distinguishes itself through the absence of noble metals and stoichiometric amounts of base as well as external hydrogen acceptors or hydrogen donors not being required. The environmentally benign, atom-economical process operates under relatively mild conditions and water is the only byproduct. The Mn-catalyzed reaction features a wide substrate scope and, importantly, the cross-coupling between two different aliphatic saturated alcohols is feasible, resulting in the desired secondary aliphatic alcohols with excellent chemoselectivity.

Acknowledgements

E.M. acknowledges Ministerio of Economía y Competitividad and Universidad de Sevilla for predoctoral fellowships.

Conflict of interest

The authors declare no conflict of interest.

Keywords: alcohols · alkylation · base metals · hydrogen autotransfer · manganese catalysis

[1] a) D. Caine in *Comprehensive Organic Synthesis, Vol. 3* (Eds.: B. M. Trost, I. Fleming, G. Patternden), Pergamon Press, Oxford, **1991**, pp. 1–63; b) *Modern Carbonyl Chemistry* (Ed.: J. Otera), Wiley-VCH, Weinheim, **2000**.

[2] K. Sawatari, Y. Nakanishi, T. Matsushima, *Ind. Health* **2001**, *39*, 341–345.

[3] Selected reviews: a) A. Corma, J. Navas, M. J. Sabater, *Chem. Rev.* **2018**, *118*, 1410–1459; b) G. Chelucci, *Coord. Chem. Rev.* **2017**, *331*, 1–36; c) F. Huang, Z. Liu, Z. Yu, *Angew. Chem. Int. Ed.* **2016**, *55*, 862–875; *Angew. Chem.* **2016**, *128*, 872–885; d) A. Nandakumar, S. P. Midya, V. G. Landge, E. Balaraman, *Angew. Chem. Int. Ed.* **2015**, *54*, 11022–11034; *Angew. Chem.* **2015**, *127*, 11174–11186; e) Q. Yang, Q. Wang, Z. Yu, *Chem. Soc. Rev.* **2015**, *44*, 2305–2329; f) J. Leonard, A. J. Blacker, S. P. Marsden, M. F. Jones, K. R. Mulholland, R. A. Newton, *Org. Process Res. Dev.* **2015**, *19*, 1400–1410; g) Y. Obora, *ACS Catal.* **2014**, *4*, 3972–3981; h) G. Guillena, D. J. Ramón, M. Yus, *Chem. Rev.* **2010**, *110*, 1611–1641.

[4] T. P. Vispute, H. Zhang, A. Sanna, R. Xiao, G. W. Huber, *Science* **2010**, *330*, 1222–1227.

[5] Selected examples: a) K.-i. Fujita, C. Asai, T. Yamaguchi, F. Hanasaka, R. Yamaguchi, *Org. Lett.* **2005**, *7*, 4017–4019; b) S. Ruiz-Botella, E. Peris, *Chem. Eur. J.* **2015**, *21*, 15263–15271; c) M. V. Jiménez, J. Fernandez-Tornos, F. J. Modrego, J. J. Perez-Torrente, L. A. Oro, *Chem. Eur. J.* **2015**, *21*, 17877–17889.

[6] Selected examples: a) D. Gnanamgari, C. H. Leung, N. D. Schley, S. T. Hilton, R. H. Crabtree, *Org. Biomol. Chem.* **2008**, *6*, 4442–4445; b) H. W. Cheung, T. Y. Lee, H. Y. Lui, C. H. Yeung, C. P. Lau, *Adv. Synth. Catal.* **2008**, *350*, 2975–2983; c) Q. Wang, K. Wu, Z. Yu, *Organometallics* **2016**, *35*, 1251–1256; d) B. C. Roy, K. Chakrabarti, S. Shee, S. Paul, S. Kundu, *Chem. Eur. J.* **2016**, *22*, 18147–18155.

[7] P. Satyanarayana, H. Maheswaran, G. M. Reddy, M. L. Kantam, *Adv. Synth. Catal.* **2013**, *355*, 1859–1867.

[8] O. Kose, S. Saito, *Org. Biomol. Chem.* **2010**, *8*, 896–900.

[9] *Catalysis without Precious Metals* (Ed.: R. M Bullock), Wiley-VCH, Weinheim, **2010**.

[10] J. Yang, X. Liu, D.-L. Meng, H.-Y. Chen, Z.-H. Zong, T.-T. Feng, K. Sun, *Adv. Synth. Catal.* **2012**, *354*, 328–334.

[11] G. Tang, C.-H. Cheng, *Adv. Synth. Catal.* **2011**, *353*, 1918–1922.

[12] a) S. Liao, K. Yu, Q. Li, H. Tian, Z. Zhang, X. Yu, Q. Xu, *Org. Biomol. Chem.* **2012**, *10*, 2973–2978; for metal-free examples: b) Q. Xu, J. Chen, Q. Liu, *Adv. Synth. Catal.* **2013**, *355*, 697–704; c) L. J. Allen, R. H. Crabtree, *Green Chem.* **2010**, *12*, 1362–1364.

[13] F. Freitag, T. Irrgang, R. Kempe, *Chem. Eur. J.* **2017**, *23*, 12110–12113.

[14] a) A. Brzozowska, L. M. Azofra, V. Zubar, I. Atodiresei, L. Cavallo, M. Rueping, O. El-Sepelgy, *ACS Catal.* **2018**, *8*, 4103–4109; b) V. Zubar, Y. Lebedev, L. M. Azofra, L. Cavallo, O. El-Sepelgy, M. Rueping, *Angew. Chem. Int. Ed.* **2018**, https://doi.org/10.1002/anie.201805630; *Angew. Chem.* **2018**, https://doi.org/10.1002/ange.201805630.

[15] T. Liu, L. Wang, K. Wu, Z. Yu, *ACS Catal.* **2018**, *8*, 7201–7207.

[16] Selected examples on Mn catalysis: a) A. Mukherjee, A. Nerush, G. Leitus, L. J. W. Shimon, Y. Ben-David, N. A. Espinosa-Jalapa, D. Milstein, *J. Am. Chem. Soc.* **2016**, *138*, 4298–4301; b) S. Elangovan, C. Topf, S. Fischer, H. Jiao, A. Spannenberg, W. Baumann, R. Ludwig, K. Junge, M. Beller, *J. Am. Chem. Soc.* **2016**, *138*, 8809–8814; c) S. Elangovan, J. Neumann, J.-B. Sortais, K. Junge, C. Darcel, M. Beller, *Nat. Commun.* **2016**, *7*, 12641; d) F. Kallmeier, T. Irrgang, T. Dietel, R. Kempe, *Angew. Chem. Int. Ed.* **2016**, *55*, 11806–11809; *Angew. Chem.* **2016**, *128*, 11984–11988; e) M. Peña-López, P. Piehl, S. Elangovan, H. Neumann, M. Beller, *Angew. Chem. Int. Ed.* **2016**, *55*, 14967–14971; *Angew. Chem.* **2016**, *128*, 15191–15195; f) S. Fu, Z. Shao, Y. Wang, Q. Liu, *J. Am. Chem. Soc.* **2017**, *139*, 11941–11948; g) N. V. Kulkarni, W. W. Brennessel, W. D. Jones, *ACS Catal.* **2018**, *8*, 997–1002.

[17] For recent reviews on Mn catalysis: a) G. A. Filonenko, R. van Putten, E. J. M. Hensen, E. A. Pidko, *Chem. Soc. Rev.* **2018**, *47*, 1459–1483; b) T. Zell, R. Langer, *ChemCatChem* **2018**, *10*, 1930–1940; c) F. Kallmeier, R. Kempe, *Angew. Chem. Int. Ed.* **2018**, *57*, 46–60; *Angew. Chem.* **2018**, *130*, 48–63; d) B. Maji, M. K. Barman, *Synthesis* **2017**, 3377–3393; on the C–H functionalizations: e) C. Wang, *Synlett* **2013**, *24*, 1606–1613; f) W. Liu, L. Ackermann, *ACS Catal.* **2016**, *6*, 3743–3752; g) D. A. Valyaev, G. Lavigne, N. Lugan, *Coord. Chem. Rev.* **2016**, *308*, 191–235.

[18] Selected reviews on cooperative metal–ligand catalysis: a) R. Khusnutdinova, D. Milstein, *Angew. Chem. Int. Ed.* **2015**, *54*, 12236–12273; *Angew. Chem.* **2015**, *127*, 12406–12445; b) O. R. Luca, R. H. Crabtree, *Chem. Soc. Rev.* **2013**, *42*, 1440–1459; c) V. Lyaskovskyy, B. de Bruin, *ACS Catal.* **2012**, *2*, 270–279.

[19] Examples from our group: a) O. El-Sepelgy, N. Alandini, M. Rueping, *Angew. Chem. Int. Ed.* **2016**, *55*, 13602–13605; *Angew. Chem.* **2016**, *128*, 13800–13803; b) O. El-Sepelgy, A. Brzozowska, M. Rueping, *ChemSusChem* **2017**, *10*, 1664–1668; c) O. El-Sepelgy, A. Brzozowska, L. M. Azofra, Y. K. Jang, L. Cavallo, M. Rueping, *Angew. Chem. Int. Ed.* **2017**, *56*, 14863–14867; *Angew. Chem.* **2017**, *129*, 15059–15063; d) O. El-Sepelgy, A. Brzozowska, J. Sklyaruk, Y. K. Jang, V. Zubar, M. Rueping, *Org. Lett.* **2018**, *20*, 696–699.

[20] a) S. E. Clapham, A. Hadzovic, R. H. Morris, *Coord. Chem. Rev.* **2004**, *248*, 2201–2237; b) P. A. Dub, N. J. Henson, R. L. Martin, J. C. Gordon, *J. Am. Chem. Soc.* **2014**, *136*, 3505–3521; c) J. S. M. Samec, J.-E. Bäckvall, P. G. Andersson, P. Brandt, *Chem. Soc. Rev.* **2006**, *35*, 237–248.

Manuscript received: July 22, 2018
Revised manuscript received: August 14, 2018
Version of record online: September 21, 2018

Paper 9:

Sustainable Alkylation of Unactivated Esters and Amides with Alcohols Enabled by Manganese Catalysis.

Jang, Y. K.; Krückel, T.; Rueping, M.*; El-Sepelgy, O.*

Org. Lett. **2018**, 7779-7783.

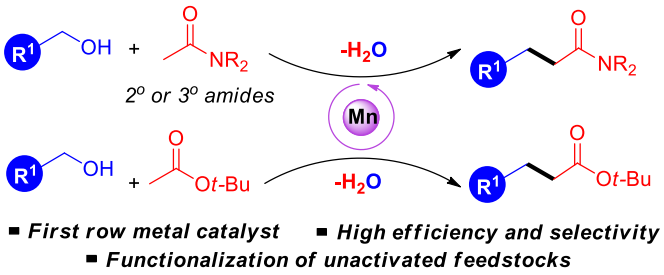

Organic LETTERS

Letter

Cite This: Org. Lett. 2018, 20, 7779–7783

pubs.acs.org/OrgLett

Sustainable Alkylation of Unactivated Esters and Amides with Alcohols Enabled by Manganese Catalysis

Yoon Kyung Jang,[†] Tobias Krückel,[†] Magnus Rueping,*[,†,‡] and Osama El-Sepelgy*[,†]

[†]Institute of Organic Chemistry, RWTH Aachen University, Landoltweg 1, 52074 Aachen, Germany

[‡]KAUST Catalysis Center (KCC), King Abdullah University of Science and Technology (KAUST), Thuwal 23955-6900, Saudi Arabia

Supporting Information

ABSTRACT: The first example of manganese-catalyzed *C*-alkylation of the carboxylic acid derivatives is reported. The bench-stable homogeneous manganese complex enables the transformation of the renewable alcohol and carboxylic acid derivative feedstock to higher value esters and amides. The reaction operates via hydrogen autotransfer and ideally produces water as the only side product. Importantly, aliphatic-, benzylic-, and heterocyclic-containing alcohols can be used as alkylating reagents, eliminating the need for mutagenic alkyl halides.

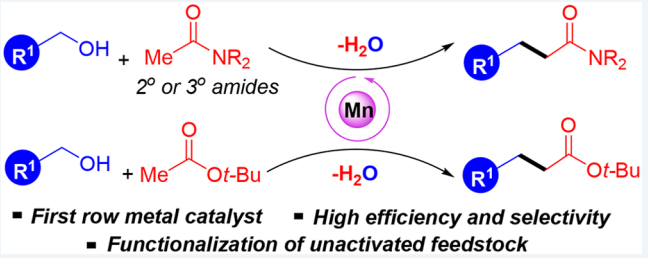

The catalytic functionalization of the C−H bonds is a central challenge in modern chemistry.[1] Carboxylic acids and their derivatives are pervasive in nature. Accordingly, an elegant approach to utilize the readily available esters and amides is to convert them to more valuable intermediates upon α-alkylation reaction. Conventional noncatalytic methods for the α-alkylation of the carbonyl compounds involve the generation of the corresponding enolate nucleophile using superbase (such as organolithium or alkali metal amides) at very low temperature. In addition to the need for toxic alkyl halide electrophiles, such methods suffer from low atom economy and the generation of copious amounts of waste.[2]

Recently, alkylation of the carbonyl compounds with primary alcohols using a hydrogen autotransfer strategy has emerged as an environmentally friendly alternative for conventional alkylation methods.[3] The key features of this hydrogen-neutral process are the use of the alcohols as a green electrophile, and the only stoichiometric byproduct is water. Alcohols are renewably available from the lignocellulosic biomass and a variety of industrial processes.[4] In fact, progress has been made in the α-alkylation of ketones and β-alkylation of alcohols.[5,6] In contrast, the α-C−H bonds of the esters and amides exhibit comparably low Brønsted acidity owing to the resonance stabilization effect of the adjacent NR_2 group. Furthermore, esters typically undergo side reactions such as self-condensation and transesterification. Among the carboxylic acid derivatives, the functionalization of dimethylacetamide (DMA) and *tert*-butyl acetate is of particular interest because these compounds can be obtained in one step from acetic acid and are frequently used as solvents in synthetic chemistry. Only a few reports are known for the α-alkylation of esters and amides using iridium[7] and ruthenium[8] catalysis. Very recently, Kempe and co-workers have reported an elegant cobalt-catalyzed alkylation of esters and amides. However, the extensive need for a glovebox may complicate large-scale application.[9]

For sustainability reasons, the current key challenge is the development of efficient catalytic systems that rely on the use of widely abundant, inexpensive metals.[10] Manganese, the third most abundant transition metal, was recently recognized by several groups including ours as a potential alternative for the toxic noble metal in the hydrogenation of polar[11] and nonpolar bonds,[12] acceptorless dehydrogenation transformations,[13] and *C*- and *N*-alkylation with primary alcohols.[5e−j,6c,14] Despite recent advances,[15] alkylation of the esters and amides via a hydrogen autotransfer strategy remains an unsolved challenge. Herein, we report the first example of manganese-catalyzed α-alkylation of unactivated esters and amides with alcohols (Scheme 1). Our catalytic system features a bench-stable catalyst stabilized by an air-stable PNN ligand.

The *C*-alkylation of DMA with benzyl alcohol (**1a**) was selected as a model reaction for the optimization of the reaction conditions (Table 1). Initially, we tested the catalytic

Scheme 1. Unprecedented Manganese-Catalyzed C−H Functionalization of Esters and Amides

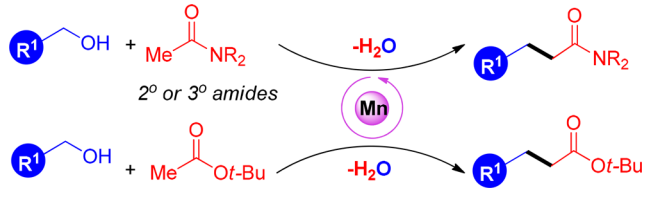

Received: October 5, 2018
Published: December 3, 2018

DOI: 10.1021/acs.orglett.8b03184
Org. Lett. 2018, 20, 7779–7783

Table 1. Optimization of the Reaction Conditions[a]

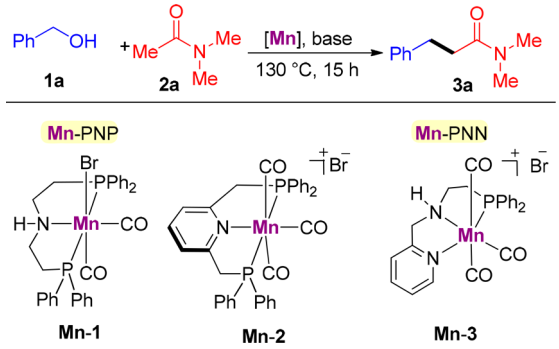

entry	[Mn]	base	solvent	yield (%)
1	**Mn-1**	*t*-BuOK	1,4-dioxane	22
2	**Mn-2**	*t*-BuOK	1,4-dioxane	15
3	**Mn-3**	*t*-BuOK	1,4-dioxane	91
4	**Mn-3**	*t*-BuOLi	1,4-dioxane	9
5	**Mn-3**	*t*-BuONa	1,4-dioxane	28
6	**Mn-3**	Cs_2CO_3	1,4-dioxane	0
7	**Mn-3**	Na_2CO_3	1,4-dioxane	0
8	**Mn-3**	NaOH	1,4-dioxane	0
9	**Mn-3**	KOH	1,4-dioxane	0
10	**Mn-3**	*t*-BuOK	2-Me-THF	57
11	**Mn-3**	*t*-BuOK	diglyme	9
12	**Mn-3**	*t*-BuOK	toluene	62

[a]Reaction conditions: **1a** (0.5 mmol), **2a** (1.5 mmol), [**Mn**] (0.015 mmol), base (0.6 mmol), solvent (1 mL), 130 °C, 15 h. Yields determined by GC analysis using *m*-xylene as an internal standard.

activity of different manganese complexes (**Mn-1**–**Mn-3**)[16] in 1,4-dioxane using *t*-BuOK as a base. While the PNP–Mn complexes **Mn-1** and **Mn-2** gave unsatisfactory results, **Mn-3** bearing a PNN ligand afforded the desired alkylated amide **3a** in 91% yield (Table 1, entries 1–3). Thus, **Mn-3** was selected for the further optimization of the common reaction parameters such as base and solvent. It was found that efficiency of the reaction was reduced upon use of *t*-BuOLi and *t*-BuONa (Table 1, entries 4 and 5). Additionally, relatively weak bases such as Cs_2CO_3 and Na_2CO_3 were inert in this transformation (Table 1, entries 6 and 7). Similarly, NaOH and KOH proved unsuitable for this reaction (Table 1, entries 8 and 9). Next, we examined different solvents. The use of other polar aprotic solvents such as 2-Me-THF and diglyme resulted in the formation of the desired product in 57% and 9% yields, respectively (Table 1, entries 10 and 11). The application of the nonpolar toluene led to lower yield compared to that of 1,4-dioxane (Table 1, entry 12). In summary, the reaction works best using 3 mol % of **Mn-3** and 1.2 equiv of *t*-BuOK in 1,4-dioxane at 130 °C.

With the optimized conditions in hand, we explored the scope of the α-alkylation of amides with alcohols (Table 2). First, the scope of the alkylation of *N*,*N*-dimethylacetamide with alcohols was investigated. Benzylic alcohols bearing electron-donating or electron substituents in the *ortho*, *meta*, and *para* positions delivered the corresponding alkylated amide **3a**–**d** in good to excellent yield (Table 2, entries 1–4). Similarly, 1-naphthalenemethanol performed well in this transformation and gave **3e** in 72% yield (Table 2, entry 5). Importantly, alcohols bearing different heterocyclic moieties; furan, thiophene, and pyridine, were tolerated, and the high-value-added amides **3f**–**h** were obtained in good yield (Table 2, entries 6–8). Furthermore, long-chain and α-branched aliphatic alcohols could be used in this new method to produce the *C*-alkylated amide derivatives **3i**–**k** in good yields (Table 2, entries 9–11). Afterward, we investigated different types of amides. Pleasantly, when *N*,*N*-diethylacetamide and 4-acetylmorpholine **2b** and **2c** were subjected to the reaction, the alkylation products were obtained in moderate yields (Table 2, entries 12 and 13). Importantly, this catalytic system was not limited to the alkylation of the tertiary amide. Thus, the selective alkylation of *N*-methylacetamide resulted in the formation of the desired *C*-alkylated products **3n** and **3o** in

Table 2. Manganese Catalyzed Alkylation of Amides[a]

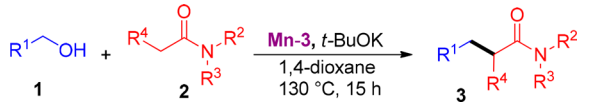

entry	**3**, yield	entry	**3**, yield
1	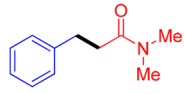 **3a** (90%)	9	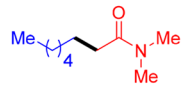 **3i** (72%)
2	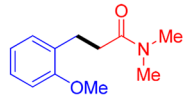 **3b** (78%)	10	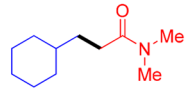 **3j** (71%)[b]
3	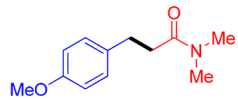 **3c** (92%)	11	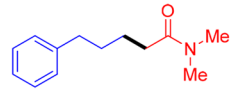 **3k** (52%)
4	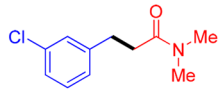 **3d** (62%)	12	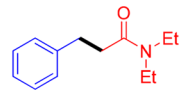 **3l** (56%)
5	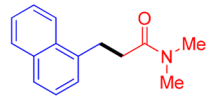 **3e** (72%)	13	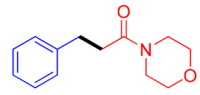 **3m** (59%)
6	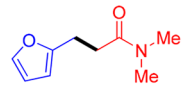 **3f** (61%)	14	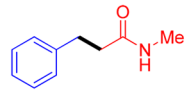 **3n** (53%)
7	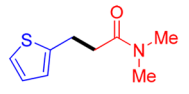 **3g** (80%)[c]	15	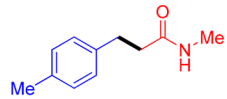 **3o** (86%)
8	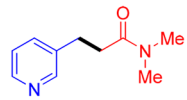 **3h** (76%)	16	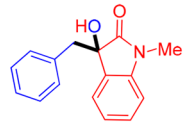 **3p** (87%)[b]

[a]Reaction conditions: **1** (0.5 mmol), **2** (1.5 mmol), **Mn-3** (0.015 mmol), *t*-BuOK (0.6 mmol), 1,4-dioxane (1.0 mL), 15 h, 130 °C. Isolated yields are shown. [b]**Mn-3** (0.02 mmol) and *t*-BuOK (1.0 mmol). [c]1 mmol scale.

DOI: 10.1021/acs.orglett.8b03184
Org. Lett. 2018, 20, 7779–7783

53% and 86% yields (Table 2, entries 14 and 15). It is worth noting that the conventional alkylation of secondary amides using alkyl halides often leads to the *N*-alkylation products.[2c] Afterward, we examined our catalytic system for the alkylation of the 2-oxindole derivative **2p**. Indeed, the alkylation reaction proceeds well followed by C−H hydroxylation to afford the C3-hydroxy-functionalized 2-oxoindole **3p** in 87% yield (Table 1, entry 16).

Encouraged by these results, we decided to further expand the scope to the alkylation of esters. Thus, the reaction conditions for the *tert*-butyl acetate alkylation with benzyl alcohol were investigated. In summary, the best conditions involve the use **Mn-3** and 2 equiv of *t*-BuOK in toluene at 100 °C for 4 h. We then focused on the substrate scope (Table 3).

Table 3. Manganese Catalyzed Alkylation of Esters[a]

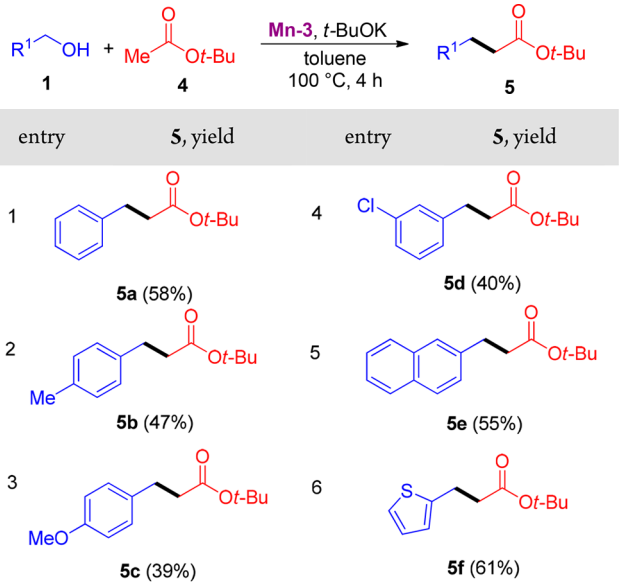

[a]Reaction conditions: **1** (0.5 mmol), **4** (2 mmol), **Mn-3** (0.025 mmol) and *t*-BuOK (1 mmol), toluene (1 mL), 100 °C, 4 h. Isolated yields are shown.

The application of the benzyl alcohol as a coupling partner gave the desired product **5a** in 58% yield (Table 3, entry 1). Benzylic alcohols containing *p*-methyl, *p*-methoxy, and *m*-chloro were compatible with the reaction conditions, and the *C*-alkylated esters **5b−d** were obtained in moderate yields (Table 3, entries 2−4). The application of 1-naphthaleneme-thanol led also to the desired product **5e** in moderate yield (Table 3, entry 5). Noteworthy, thiophene-containing substrate and products such as **5f** are tolerated in this alkylation reaction (Table 3, entry 6).

In order to gain more insight in the reaction mechanism, we carried out a deuterium-labeled experiment (Scheme 2). In more detail, [D_2]**1a** was used an alkylating reagent for the

Scheme 2. Deuterium-Labeled Experiment

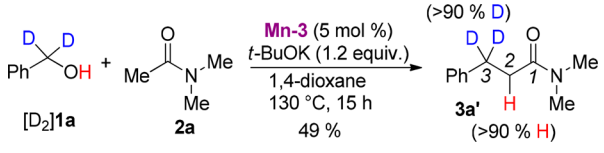

DMA. However, when the catalyst loading was increased to 5 mol %, only 49% yield was observed, which indicates a very strong kinetic isotope effect. Furthermore, the alkylated amide **3a′** was obtained with >90% deuterium incorporation at C3 and very low deuteration at C2. The deuterium experiment indicates that the hydrogen autotransfer reaction takes place via a monohydride mechanism with involvement of both the metal and the non innocent ligand in the dehydrogenation and hydrogenation steps.[17−19]

On the basis of our experimental observations, the proposed reaction mechanism is presented in Scheme 3. Initially, proton

Scheme 3. Proposed Reaction Mechanism

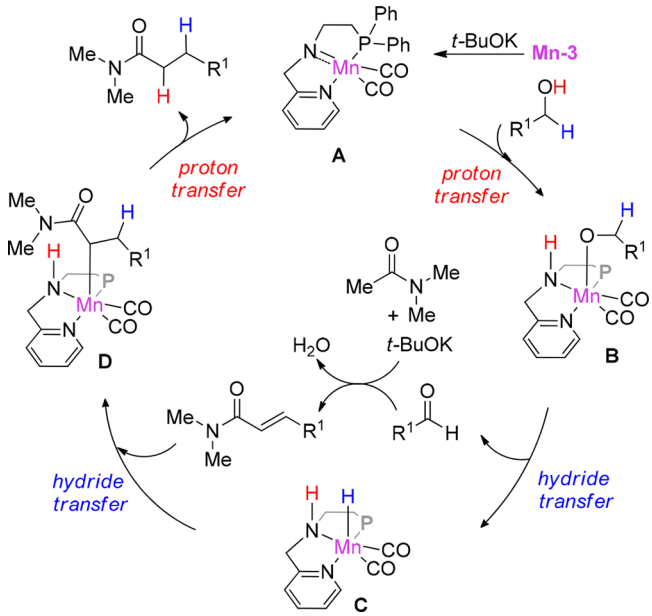

transfer from the alcohol to the 16e species **A** takes place to generate the manganese alkoxide intermediate **B**. Subsequently, *β*-hydride elimination leads to the formation of an aldehyde and the hydrogenated catalyst **C**, storing the abstracted hydrogen on the metal ligand catalyst. The base-catalyzed condensation between the in situ generated aldehyde and carboxylic acid derivative result in the formation of an unsaturated amide. The shuttled hydrogen on the hydrogenated catalyst **C** is then transferred to the C═C bond in two discrete steps. First, the the C═C bond is inserted into the Mn−H bond to produce the intermediate **D**. Second, the desired product is released upon proton transfer and the manganese species **A** is regenerated. The proton transfer may also occur by transferring a proton directly from an alcohol, producing the desired product and the intermediate **B** without the regeneration of the 16e species **A**.[20]

In conclusion, we have reported the first example of manganese-catalyzed environmentally benign *C*-alkylation of unactivated esters and amides with unactivated alcohols.[21] The reaction tolerates a wide range of functional groups and heterocyclic moieties, providing highly useful upgraded amides and esters in excellent efficiency. The presented sustainable alkylation reaction liberates water as the only side product.

DOI: 10.1021/acs.orglett.8b03184
Org. Lett. 2018, 20, 7779−7783

■ ASSOCIATED CONTENT

Supporting Information

The Supporting Information is available free of charge on the ACS Publications website at DOI: 10.1021/acs.orglett.8b03184.

Experimental details and characterization data (PDF)

■ AUTHOR INFORMATION

Corresponding Authors

*E-mail: magnus.rueping@rwth-aachen.de.
*E-mail: osama.elsepelgy@rwth-aachen.de.

ORCID

Magnus Rueping: 0000-0003-4580-5227
Osama El-Sepelgy: 0000-0003-3131-4988

Notes

The authors declare no competing financial interest.

■ REFERENCES

(1) (a) Liu, W.; Ackermann, L. *ACS Catal.* **2016**, *6*, 3743−3752. (b) Wang, C. *Synlett* **2013**, *24*, 1606−1613. For a recent example, see Liu, W.; Cera, G.; Oliveira, J. C. A.; Shen, Z.; Ackermann, L. *Chem. - Eur. J.* **2017**, *23*, 11524−11528.

(2) (a) Carey, F. A.; Sundberg, R. K. *Advanced Organic Chemistry*, 5th ed.; Springer: Heidelberg, 2007; Part B, pp 1−31. (b) Hoyle, J. In *The Chemistry of Acid Derivatives*; Patai, S., Ed.; Wiley: Chichester, UK, 1992; Vol. 2, pp 615−702. (c) Challis, B. C.; Challis, J. *The Chemistry of Amides*; Zabicky, J., Ed.; John Wiley & Sons: London, 1970; pp 731−857.

(3) Selected recent reviews: (a) Corma, A.; Navas, J.; Sabater, M. J. *Chem. Rev.* **2018**, *118*, 1410−1459. (b) Crabtree, R. H. *Chem. Rev.* **2017**, *117*, 9228−9246. (c) Chelucci, G. *Coord. Chem. Rev.* **2017**, *331*, 1−36. (d) Huang, F.; Liu, Z.; Yu, Z. *Angew. Chem., Int. Ed.* **2016**, *55*, 862−875. (e) Nandakumar, A.; Midya, S. P.; Landge, V. G.; Balaraman, E. *Angew. Chem., Int. Ed.* **2015**, *54*, 11022−11034. (f) Yang, Q.; Wang, Q.; Yu, Z. *Chem. Soc. Rev.* **2015**, *44*, 2305−2329. (g) Obora, Y. *ACS Catal.* **2014**, *4*, 3972−3981. (h) Gunanathan, C.; Milstein, D. *Science* **2013**, *341*, 1229712. (i) Guillena, G.; Ramón, D. J.; Yus, M. *Chem. Rev.* **2010**, *110*, 1611−1641.

(4) Vispute, T. P.; Zhang, H.; Sanna, A.; Xiao, R.; Huber, G. W. *Science* **2010**, *330*, 1222−1227.

(5) Iron catalysis: (a) Yang, J.; Liu, X.; Meng, D.-L.; Chen, H.-Y.; Zong, Z.-H.; Feng, T.-T.; Sun, K. *Adv. Synth. Catal.* **2012**, *354*, 328−334. (b) Elangovan, S.; Sortais, J.-B.; Beller, M.; Darcel, C. *Angew. Chem., Int. Ed.* **2015**, *54*, 14483−14486. Cobalt catalysis: (c) Freitag, F.; Irrgang, T.; Kempe, R. *Chem. - Eur. J.* **2017**, *23*, 12110−12113. (d) Zhang, G.; Wu, J.; Zeng, H.; Zhang, S.; Yin, Z.; Zheng, S. *Org. Lett.* **2017**, *19*, 1080−1083. Manganese catalysis: (e) Pena-Lopez, M.; Piehl, P.; Elangovan, S.; Neumann, H.; Beller, M. *Angew. Chem., Int. Ed.* **2016**, *55*, 14967−14971. (f) Fu, S.; Shao, Z.; Wang, Y.; Liu, Q. *J. Am. Chem. Soc.* **2017**, *139*, 11941−11948. (g) El-Sepelgy, O.; Matador, E.; Brzozowska, A.; Rueping, M. *ChemSusChem* **2018**, DOI: 10.1002/cssc.201801660. (h) Liu, T.; Wang, L.; Wu, K.; Yu, Z. *ACS Catal.* **2018**, *8*, 7201−7207. (i) Kulkarni, N. V.; Brennessel, W. W.; Jones, W. D. *ACS Catal.* **2018**, *8*, 997−1002. (j) Barman, M. K.; Jana, A.; Maji, B. *Adv. Synth. Catal.* **2018**, *360*, 3233−3238.

(6) Methylation of ketones by base metal catalysis: (a) Liu, Z.; Yang, Z.; Yu, X.; Zhang, H.; Yu, B.; Zhao, Y.; Liu, Z. *Org. Lett.* **2017**, *19*, 5228−5231. (b) Polidano, K.; Allen, B. D. W.; Williams, J. M. J.; Morrill, L. C. *ACS Catal.* **2018**, *8*, 6440−6445. (c) Sklyaruk, J.; Borghs, J. C.; El-Sepelgy, O.; Rueping, M. *Angew. Chem., Int. Ed.* **2018**, DOI: 10.1002/anie.201810885.

(7) (a) Guo, L.; Ma, X.; Fang, H.; Jia, X.; Huang, Z. *Angew. Chem., Int. Ed.* **2015**, *54*, 4023−4027. (b) Guo, L.; Liu, Y.; Yao, W.; Leng, X.; Huang, Z. *Org. Lett.* **2013**, *15*, 1144−1147. (c) Iuchi, Y.; Obora, Y.; Ishii, Y. *J. Am. Chem. Soc.* **2010**, *132*, 2536−2537.

(8) (a) Kuwahara, T.; Fukuyama, T.; Ryu, I. *RSC Adv.* **2013**, *3*, 13702−13704. (b) Chaudhari, M. B.; Bisht, G. S.; Kumari, P.; Gnanaprakasam, B. *Org. Biomol. Chem.* **2016**, *14*, 9215−9220.

(9) Deibl, N.; Kempe, R. *J. Am. Chem. Soc.* **2016**, *138*, 10786−10789.

(10) (a) Chirik, P.; Morris, R. *Acc. Chem. Res.* **2015**, *48*, 2495−2495. (b) Bauer, I.; Knölker, H.-J. *Chem. Rev.* **2015**, *115*, 3170−3387. (c) Morris, R. H. *Acc. Chem. Res.* **2015**, *48*, 1494−1502. (d) Bullock, R. M. *Catalysis without Precious Metals*; Wiley-VCH: Weinheim, 2010. (e) Plietker, B. *Iron Catalysis in Organic Chemistry: Reactions and applications*, 2nd ed.; Wiley-VCH: Weinheim, 2008.

(11) Selected examples: (a) Elangovan, S.; Topf, C.; Fischer, S.; Jiao, H.; Spannenberg, A.; Baumann, W.; Ludwig, R.; Junge, K.; Beller, M. *J. Am. Chem. Soc.* **2016**, *138*, 8809−8814. (b) Kallmeier, F.; Irrgang, T.; Dietel, T.; Kempe, R. *Angew. Chem., Int. Ed.* **2016**, *55*, 11806−11809. (c) Widegren, M. B.; Harkness, G. J.; Slawin, A. M. Z.; Cordes, D. B.; Clarke, M. L. *Angew. Chem., Int. Ed.* **2017**, *56*, 5825−5828. (d) Bruneau-Voisine, A.; Wang, D.; Dorcet, V.; Roisnel, T.; Darcel, C.; Sortais, J. B. *Org. Lett.* **2017**, *19*, 3656−3659. (e) Perez, M.; Elangovan, S.; Spannenberg, A.; Junge, K.; Beller, M. *ChemSusChem* **2017**, *10*, 83−86. (f) Zirakzadeh, A.; de Aguiar, S. R. M. M.; Stöger, B.; Widhalm, M.; Kirchner, K. *ChemCatChem* **2017**, *9*, 1744−1748. (g) Garbe, M.; Junge, K.; Walker, S.; Wei, Z.; Jiao, H.; Spannenberg, A.; Bachmann, S.; Scalone, M.; Beller, M. *Angew. Chem., Int. Ed.* **2017**, *56*, 11237−11241. (h) Wang, D.; Bruneau-Voisine, A.; Sortais, J.-B. *Catal. Commun.* **2018**, *105*, 31−36. (i) Bruneau-Voisine, A.; Wang, D.; Roisnel, T.; Darcel, C.; Sortais, J.-B. *Catal. Commun.* **2017**, *92*, 1−4. (j) Glatz, M.; Stöger, B.; Himmelbauer, D.; Veiros, L. F.; Kirchner, K. *ACS Catal.* **2018**, *8*, 4009−4016. (k) Zubar, V.; Lebedev, Y.; Azofra, L. M.; Cavallo, L.; El-Sepelgy, O.; Rueping, M. *Angew. Chem., Int. Ed.* **2018**, *57*, 13439−13443. (l) Wei, D.; Bruneau-Voisine, A.; Chauvin, T.; Dorcet, V.; Roisnel, T.; Valyaev, D. A.; Lugan, N.; Sortais, J.-B. *Adv. Synth. Catal.* **2018**, *360*, 676−681.

(12) (a) Brzozowska, A.; Azofra, L. M.; Zubar, V.; Atodiresei, I.; Cavallo, L.; Rueping, M.; El-Sepelgy, O. *ACS Catal.* **2018**, *8*, 4103−4109. (b) Zhou, Y. P.; Mo, Z.; Luecke, M. P.; Driess, M. *Chem. - Eur. J.* **2018**, *24*, 4780−4784.

(13) For Mn-catalyzed olefination with primary alcohols, see: (a) Chakraborty, S.; Das, U. K.; Ben-David, Y.; Milstein, D. *J. Am. Chem. Soc.* **2017**, *139*, 11710−11713. (b) Zhang, G.; Irrgang, T.; Dietel, T.; Kallmeier, F.; Kempe, R. *Angew. Chem., Int. Ed.* **2018**, *57*, 9131−9135. (c) Barman, M. K.; Waiba, S.; Maji, B. *Angew. Chem., Int. Ed.* **2018**, *57*, 9126−9130. For Mn-catalyzed C-alkylation of nitriles with primary alcohols, see: (d) Jana, A.; Reddy, C. B.; Maji, B. *ACS Catal.* **2018**, *8*, 9226−9231.

(14) For Mn-catalyzed N-alkylation with primary alcohols, see: (a) Elangovan, S.; Neumann, J.; Sortais, J.-B.; Junge, K.; Darcel, C.; Beller, M. *Nat. Commun.* **2016**, *7*, 12641. (b) Neumann, J.; Elangovan, S.; Spannenberg, A.; Junge, K.; Beller, M. *Chem. - Eur. J.* **2017**, *23*, 5410−5413. (c) Bruneau-Voisine, A.; Wang, D.; Dorcet, V.; Roisnel, T.; Darcel, C.; Sortais, J.-B. *J. Catal.* **2017**, *347*, 57−62. (d) Mastalir, M.; Pittenauer, E.; Allmaier, G.; Kirchner, K. *J. Am. Chem. Soc.* **2017**, *139*, 8812−8815. (e) Fertig, R.; Irrgang, T.; Freitag, F.; Zander, J.; Kempe, R. *ACS Catal.* **2018**, *8*, 8525−8530.

(15) For recent reviews on Mn catalysis, see: (a) Gorgas, N.; Kirchner, K. *Acc. Chem. Res.* **2018**, *51*, 1558−1569. (b) Filonenko, G. A.; van Putten, R.; Hensen, E. J. M.; Pidko, E. A. *Chem. Soc. Rev.* **2018**, *47*, 1459−1483. (c) Zell, T.; Langer, R. *ChemCatChem* **2018**, *10*, 1930−1940. (d) Kallmeier, F.; Kempe, R. *Angew. Chem., Int. Ed.* **2018**, *57*, 46−60. (e) Maji, B.; Barman, M. K. *Synthesis* **2017**, *49*, 3377−3393. (f) Garbe, M.; Junge, K.; Beller, M. *Eur. J. Org. Chem.* **2017**, *2017*, 4344−4362. (g) Valyaev, D. A.; Lavigne, G.; Lugan, N. *Coord. Chem. Rev.* **2016**, *308*, 191−235. (h) Carney, J. R.; Dillon, B. R.; Thomas, S. P. *Eur. J. Org. Chem.* **2016**, 3912−3929.

(16) For details, see the Supporting Information.

(17) For reviews on metal−ligand catalysis, see: (a) Khusnutdinova, R.; Milstein, D. *Angew. Chem., Int. Ed.* **2015**, *54*, 12236−12273.

DOI: 10.1021/acs.orglett.8b03184
Org. Lett. 2018, 20, 7779−7783

(b) Luca, O. R.; Crabtree, R. H. *Chem. Soc. Rev.* **2013**, *42*, 1440−1459. (c) Lyaskovskyy, V.; de Bruin, B. *ACS Catal.* **2012**, *2*, 270−279.
(18) (a) Clapham, S. E.; Hadzovic, A.; Morris, R. H. *Coord. Chem. Rev.* **2004**, *248*, 2201−2237. (b) Samec, J. S. M.; Bäckvall, J.-E.; Andersson, P. G.; Brandt, P. *Chem. Soc. Rev.* **2006**, *35*, 237−248.
(19) (a) El-Sepelgy, O.; Alandini, N.; Rueping, M. *Angew. Chem., Int. Ed.* **2016**, *55*, 13602−13605. (b) El-Sepelgy, O.; Brzozowska, A.; Rueping, M. *ChemSusChem* **2017**, *10*, 1664−1668. (c) El-Sepelgy, O.; Brzozowska, A.; Azofra, L. M.; Jang, Y. K.; Cavallo, L.; Rueping, M. *Angew. Chem., Int. Ed.* **2017**, *56*, 14863−14867. (d) El-Sepelgy, O.; Brzozowska, A.; Sklyaruk, J.; Jang, Y. K.; Zubar, V.; Rueping, M. *Org. Lett.* **2018**, *20*, 696−679.
(20) (a) Hasanayn, F.; Morris, R. H. *Inorg. Chem.* **2012**, *51*, 10808−10818. (b) Hasanayn, F.; Baroudi, A.; Bengali, A. A.; Goldman, A. S. *Organometallics* **2013**, *32*, 6969−6985. (c) Dub, P. A.; Henson, N. J.; Martin, R. L.; Gordon, J. C. *J. Am. Chem. Soc.* **2014**, *136*, 3505−3521. (d) Pan, H.-J.; Zhang, Y.; Shan, C.; Yu, Z.; Lan, Y.; Zhao, Y. *Angew. Chem., Int. Ed.* **2016**, *55*, 9615−9619.
(21) During the review of this manuscript, a related paper was published with only NMR or GC yields: Chakraborty, S.; Daw, P.; Ben David, Y.; Milstein, D. *ACS Catal.* **2018**, *8*, 10300−10305.

DOI: 10.1021/acs.orglett.8b03184
Org. Lett. 2018, 20, 7779−7783

Paper 10:

Sustainable Alkylation of Nitriles with Alcohols by Manganese Catalysis.

Borghs, J. C.; Tran, M. A.; Sklyaruk, J.; Rueping, M.*; El-Sepelgy, O.*

J. Org. Chem. **2019**, *84*, 7927-7935.

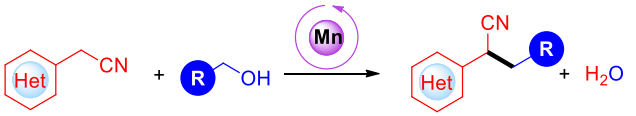

readily abandant feedstocks *value-added alkyl nitriles*

First row metal catalyst * Catalytic amount of base
**** Methanol as C1 source * High yield and excellent selectivity***

JOC The Journal of Organic Chemistry
Cite This: J. Org. Chem. 2019, 84, 7927−7935
Article
pubs.acs.org/joc

Sustainable Alkylation of Nitriles with Alcohols by Manganese Catalysis

Jannik C. Borghs,[†] Mai Anh Tran,[†] Jan Sklyaruk,[†] Magnus Rueping,*[,†,‡] and Osama El-Sepelgy*[,†]

[†]Institute of Organic Chemistry, RWTH Aachen University, Landoltweg 1, 52074 Aachen, Germany
[‡]KAUST Catalysis Center (KCC), King Abdullah University of Science and Technology (KAUST), Thuwal 23955-6900, Saudi Arabia

Supporting Information

ABSTRACT: A general and chemoselective catalytic alkylation of nitriles using a homogeneous nonprecious manganese catalyst is presented. This alkylation reaction uses naturally abundant alcohols and readily available nitriles as coupling partners. The reaction tolerates a wide range of functional groups and heterocyclic moieties, efficiently providing useful cyanoalkylated products with water as the only side product. Importantly, methanol can be used as a C1 source and the chemoselective C-methylation of nitriles is achieved. The mechanistic investigations support the multiple role of the metal−ligand manganese catalyst, the dehydrogenative activation of the alcohol, α-C−H activation of the nitrile, and hydrogenation of the in-situ-formed unsaturated intermediate.

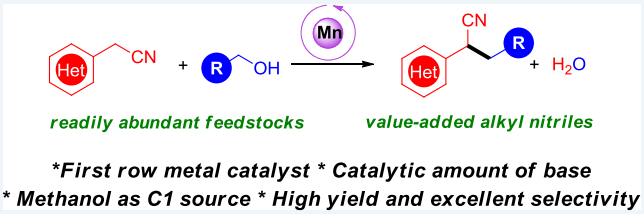

INTRODUCTION

The construction of C−C bonds via the hydrogen autotransfer strategy is of particular academic and industrial interest. The key motivation for this strategy is the application of alcohol feedstock as a benign alkylating reagent[1] while liberating water as the sole byproduct. Thus, the procedure eliminates the need for mutagenic alkyl halides and avoids the production of copious waste. To date, the majority of appropriate catalytic systems are based on noble metals including Ru, Rh, Ir, Pd and Pt.[2] The low availability of these precious metals has triggered the development of alternative catalytic systems based on earth abundant metals.[3] In this context, progress has been made in the alkylation of ketones,[4] alcohols,[5] esters,[6] and amides[6] using base metal catalysts. In contrast, the alkylation of nitriles is more challenging due to the sensitivity of the cyano group toward the activated hydrogen and the water side product. In more details, the metal catalyst can transfer hydrogen from the alcohol to the nitriles to form primary amines and aldehydes[7] and these can subsequently be converted to secondary amines[8] or amides.[9] However, water might result in the hydrolysis of the nitrile functionality to the corresponding amide.[10] In addition, the alkylation of nitriles with alcohols often leads to a mixture of the alkylnitrile product along with the corresponding olefin intermediate,[11] giving rise to critical selectivity issues. Thus, until recently, the direct alkylation of nitriles with alcohols was only known with precious metal catalysis such as Ru,[12] Ir,[13] Rh,[14] Os,[15] and Pd.[16]

Our interest in the development of an improved synthesis of alkylnitriles is due to their great importance as valuable intermediates in the fine chemical industry. Importantly, the cyanoalkyl moiety is also ubiquitous in different natural products and pharmaceuticals.[17] Very recently, Wang and co-workers have reported an interesting iron-catalyzed alkylation of nitriles with primary alcohols by applying stoichiometric amount of strong base (NaOH).[18] Pursuant to our interest in developing sustainable transformations based on nonprecious metal catalysis,[19] and inspired by the recent advances in manganese catalysis,[20−22] we herein report highly reactive and selective manganese-catalyzed alkylation of nonactivated nitriles with a broad range of alcohols (Scheme 1). A related study has also been reported by Maji et al.[23] In our study, we focused on a catalytic system that utilizes a bench stable catalyst that can easily be prepared in one step from the commercially available and air stable MACHO ligand and $Mn(CO)_5Br$. Interestingly, the presented catalytic system is not limited to the long-chain alcohols as the more challenging C-alkylation can also be achieved with methanol as the C1 source. Furthermore, the manganese catalyst does not require any sensitive reagent for activation and is simply activated with catalytic amounts of suitable base.

Scheme 1. Manganese-Catalyzed Alkylation of Nitriles with Alcohols

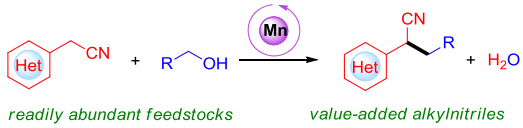

Received: March 20, 2019
Published: May 22, 2019

DOI: 10.1021/acs.joc.9b00792
J. Org. Chem. 2019, 84, 7927−7935

RESULTS AND DISCUSSION

To develop the base metal-catalyzed alkylation reaction, we started to investigate the reaction between phenylacetonitrile (**1a**) and the *n*-butanol (**2a**) applying different manganese catalysts (Table 1). Initially, we screened the catalytic activity

Table 1. Optimization of the Reaction Conditions[a]

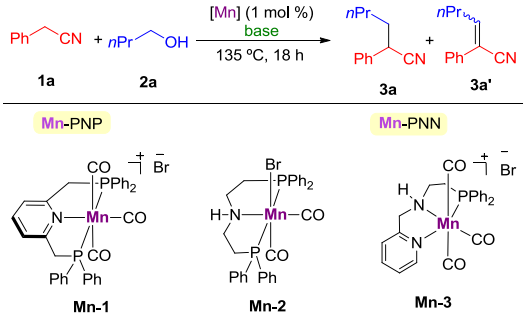

entry	cat.	base (mol %)	conv. (%)	yield **3a**/**3a′** (%)
1	**Mn-1**	*t*-BuOK (3)	38	>5/>5
2	**Mn-2**	*t*-BuOK (3)	97	86/11
3	**Mn-3**	*t*-BuOK (3)	96	70/09
4	**Mn-2**	*t*-BuOK (1)	66	35/12
5[b]	**Mn-2**	*t*-BuOK (3)	95	77/12
6[c]	**Mn-2**	*t*-BuOK (3)	48	25/06
7[d]	**Mn-2**	*t*-BuOK (3)	78	60/10
8	**Mn-2**	KOH (3)	>99	96/04
9	**Mn-2**	K_2CO_3 (3)	84	67/12
10	**Mn-2**	Cs_2CO_3 (3)	>99	79/08
11	**Mn-2**	Cs_2CO_3 (10)	>99	99/00

[a]Reaction conditions: **1a** (0.5 mmol), **2a** (1 mmol), [**Mn**] (0.005 mmol), and base in toluene (0.5 mL) at 135 °C in a glass tube under an inert atmosphere for 18 h. Conversions and yields were determined by gas chromatography analysis of the crude reaction mixture using mesitylene as an internal standard. [b]Reaction in *t*-amyl alcohol. [c]Reaction in 2-MeTHF. [d]Reaction in 1,4-dioxane.

of the different manganese complexes **Mn-1**−**3** in toluene using *t*-BuOK as the catalyst activator. The pyridyl-based PNP complex **Mn-1**[22j] led to unsatisfactory results, providing only a trace amount of the product (Table 1, entry 1). However, in the presence of the complex **Mn-2**,[22k] bearing an aliphatic NH group, excellent conversion was observed and 86% of the desired product **3a** along with 11% of the unsaturated olefin **3a′** (Table 1, entry 2) was obtained. Use of the Mn-PNN pincer complex **Mn-3**[20b] (Table 1, entry 3) provided similar results. Due to the facile access of **Mn-2** and the availability of the ligand, we decided to further optimize the model reaction using **Mn-2** in combination with different bases and solvents. Running the reaction using equimolar amounts of manganese and the base resulted in 66% conversion and 47% combined yield of **3a** and **3a′** (Table 1, entry 4). Using polar solvents such as *t*-amyl alcohol, 1,4-dioxane, or 2-methyltetrahydrofuran (2-Me-THF) did not lead to improved results (Table 1, entries 5−7). In addition, we tested various bases including KOH, K_2CO_3, and Cs_2CO_3 (Table 1, entries 8−10). From these experiments, the best results were obtained using Cs_2CO_3 and the desired product was obtained in 79% yield along with 8% of the alkenyl nitrile **3a′**. Pleasingly, slightly increasing the base loading to 10 mol % led to quantitative yield with complete chemoselectivity (Table 1, entry 11).

Scheme 2. Manganese-Catalyzed Alkylation of Nitriles with Different Alcohols

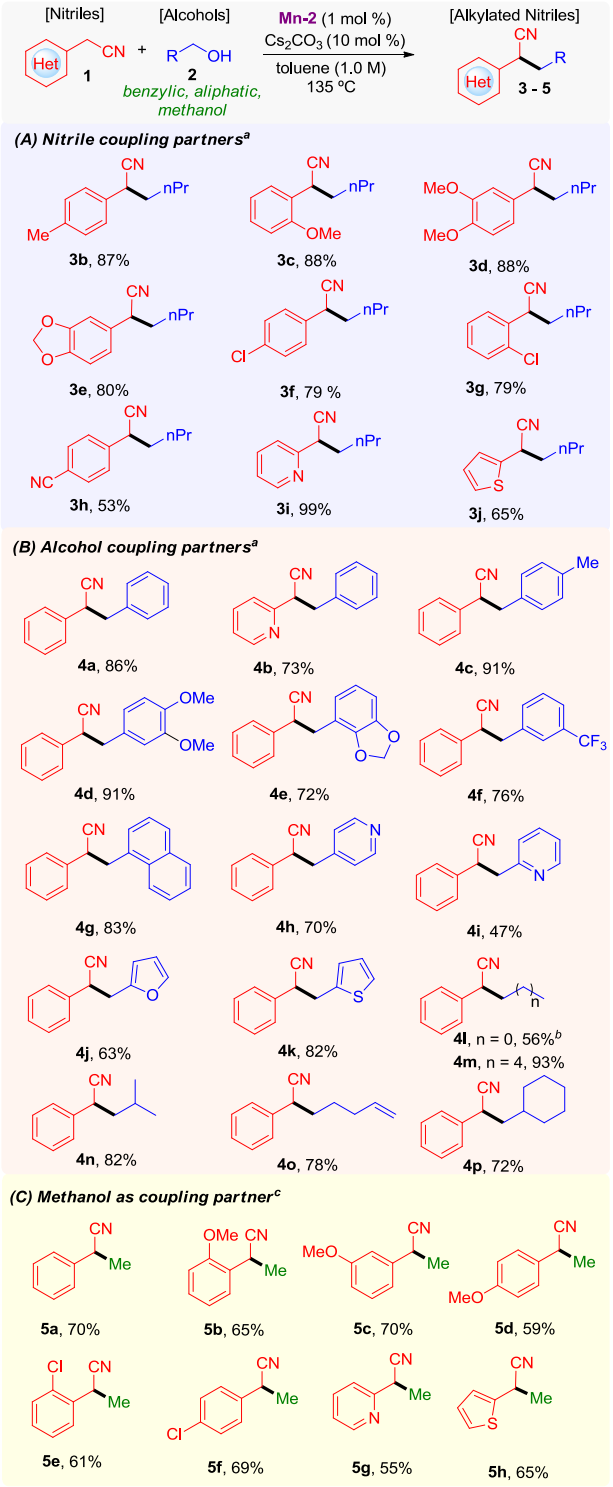

[a]Reaction conditions: **1** (0.5 mmol), **2** (1 mmol), **Mn-2** (0.005 mmol), Cs_2CO_3 (0.05 mmol), toluene (0.5 mL), 135 °C (aluminum block), 18 h. [b]**Mn-2** (0.025 mmol). [c]Reaction conditions: **1** (0.5 mmol), methanol (1 mL), **Mn-2** (0.025 mmol), Cs_2CO_3 (0.05 mmol), 1,4-dioxane (1 mL), 24 h.

Having established the optimized reaction conditions, we next investigated the generality of this protocol by exploring the scope of the nitrile alkylation partner (Scheme 2A). To our

DOI: 10.1021/acs.joc.9b00792
J. Org. Chem. 2019, 84, 7927−7935

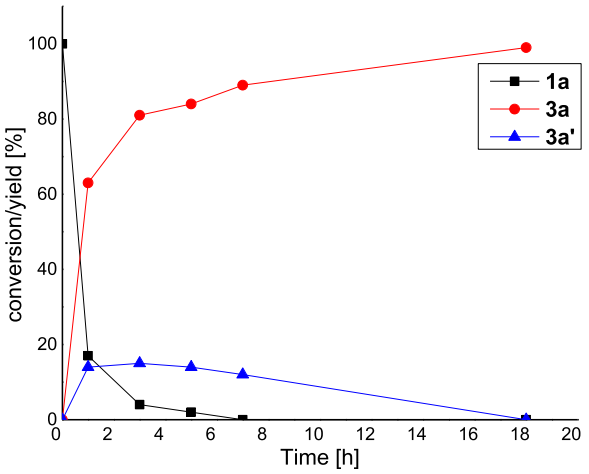

Figure 1. Monitoring of the reaction progress (reaction conditions as in Table 1, entry 11).

delight, in all cases, the reaction was accomplished within 18 h using 1 mol % of the bench stable catalyst **Mn-2**. Notably, a diverse range of substituted benzyl cyanides can be used to yield the C-alkylated nitrile derivatives **3b−g** in very good yields and with excellent chemoselectivity. It is important to highlight that the benzonitrile moiety was tolerated to give the desired product **3h**. Importantly, heterocycle containing benzylic nitriles, such as **3i** and **3j**, can also be efficiently alkylated.

We next decided to explore the scope of primary alcohols as alkylating agents (Scheme 2B). Importantly, a large array of benzyl alcohols bearing electron-withdrawing and electron-donating groups in different positions could be applied to give the desired products **4a−f** in very good isolated yields. Furthermore, a naphthyl-substituted product **4g** was obtained in 83% yield. Similar to the scope of the nitrile, alcohols bearing heterocycles (pyridine, thiophene, and furane) could also be used to access the corresponding products **4h−k**. Moreover, this protocol is not limited to benzylic alcohols, as exemplified by the rapid incorporation of different aliphatic alcohols under the same reaction conditions (**4l−p**), whereby unsaturated C═C bonds remain intact (**4o**).

However, a higher activation energy barrier needs to be overcome for the dehydrogenation of the methanol; compared with other alcohols, our catalytic system proved to be suitable for the challenging α-methylation of nitriles. Slightly modified reaction conditions have to be used to successfully accomplish the C1-alkylation. Indeed, a broad series of differently substituted nitriles, including heterocycles, can be methylated to deliver the products **5a−h** in moderate-to-good yields (Scheme 2C). Interestingly, our base metal-catalyzed procedure shows superior catalytic activity to the recently disclosed Ru-catalyzed protocol.[12a]

To gain more insight into the reaction mechanism, we monitored the reaction progress between phenylacetonitrile (**1a**) and 1-butanol (**2a**) catalyzed by **Mn-2** (Figure 1). After 1 h, we observed 83% of conversion of the nitrile **1a** and the formation of 66% yield of **3a** along with 15% of the unsaturated intermediate **3a′**. After 3 h, almost full conversion of **1a** was obtained with 80% yield of the **3a**, whereas the amount of the remaining intermediate **3a′** was still constant (ca. 15%). Complete conversion was observed after 18 h. Subsequently, we decided to carry out several control NMR experiments (Figure 2). The treatment of **Mn-2** with 1 equiv of *t*-BuOK at room temperature (RT) for 1 h in C_6D_6 led to the formation of the soluble imido complex **Mn-2a**, as confirmed by the ^{31}P NMR spectrum (91.02 ppm). When 1 equiv of 4-flurophenylacetonitrile was added, we immediately observed the formation of two new broad peaks at 73.65 and 78.82 ppm at ^{31}P NMR, indicating the coordination between the manganese catalyst and the nitrile substrate.

Based on the experimental background and the density functional theory studies, a proposed reaction mechanism is shown in Scheme 3. Initially, the manganese precatalyst reacts with the base to generate an imido complex as the active catalytic species (Scheme 3a). This imido complex activates the alcohol via dehydrogenation with the simultaneous formation of the manganese species H−Mn−N−H. Most likely, this reaction takes place via the formation of a Mn-alkoxide intermediate. In addition to the role of the manganese catalyst in the alcohol activation, the NMR experiment indicates the role of the metal catalyst in the C−H activation of the nitrile substrate.[24] The two new broad peaks in Figure 2c most likely correlate to the species **A** and **B** in Scheme 3b.

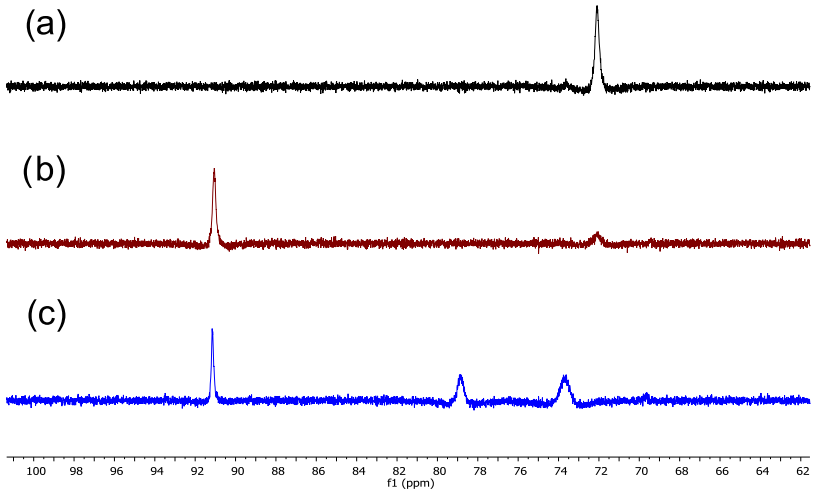

Figure 2. ^{31}P NMR spectra at RT. (a) **Mn-2** in CD_2Cl_2. (b) **Mn-2** + 1 equiv *t*-BuOK in C_6D_6. (c) **Mn-2** + 1 equiv of *t*-BuOK + 1 equiv of 4-flurophenylacetonitrile in C_6D_6.

DOI: 10.1021/acs.joc.9b00792
J. Org. Chem. 2019, 84, 7927−7935

Scheme 3. Proposed Reaction Mechanism

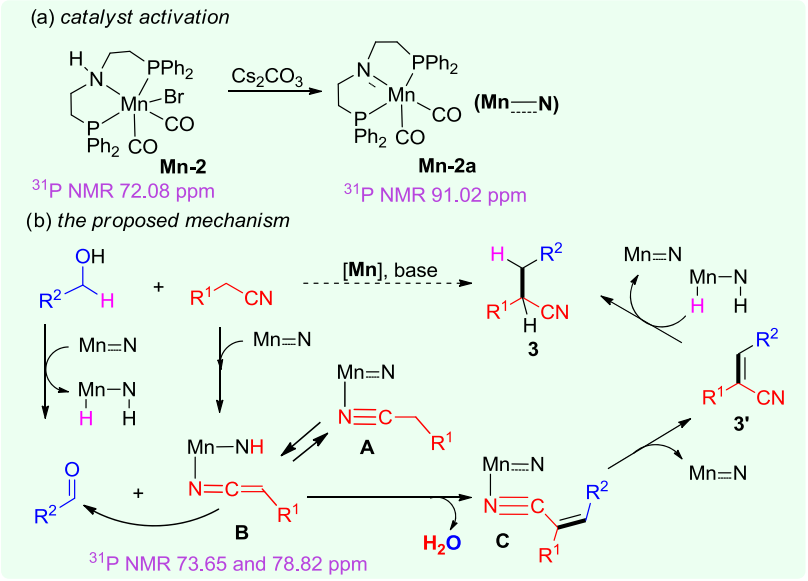

The initial coordination of the nitrile substrate with the 16e species lead to the formation of molecule **A**. Then, the ligand plays a crucial role in hydrogen abstraction and the generation of the highly nucleophilic species **B**.[25] Thus, the same metal catalyst simultaneously activates both of the substrates to produce the electrophile (aldehyde) and nucleophile **B**. The addition of the intermediate **B** to the in-situ-generated aldehyde delivers the intermediate **C** and one molecule of water. This intermediate leads to the formation of the olefin intermediate **3′** and regenerates the **Mn-2a**. Finally, the shuttled hydrogen on the H−Mn−N−H is transferred to **3′** to produce the α-alkylated nitrile **3** via a metal−ligand cooperative mechanism.

CONCLUSIONS

In summary, manganese PNP pincer-catalyzed alkylation of nitriles with alcohols is reported. This environmentally benign hydrogen autotransfer reaction is characterized by the absence of noble metals and stoichiometric reagents, generating water as the only side product. A broad range of alcohols could be used as green alkylating reagents and, importantly, the challenging methylation reaction is feasible, resulting in the desired C-methylated nitriles with excellent chemoselectivity. The experimental studies support the reaction mechanism in which the manganese catalyst plays a multiple role in activating both the reaction partners and the subsequent hydrogenation of the alkenyl nitrile to selectively produce the highly value-added α-alkylated nitriles.

EXPERIMENTAL SECTION

General Method. All reactions were carried out under an argon atmosphere using oven-dried glassware. Purified compounds were further dried under high vacuum (0.01−0.05 Torr). Yields refer to purified compounds. Analytical thin-layer chromatography was performed using silica gel 60 precoated aluminum plates (Macherey-Nagel, 0.20 mm thickness) with a fluorescent indicator UV254. Visualization was performed with standard phosphomolybdic acid stain (10 g in 100 mL of EtOH) or UV light. Column chromatography was performed using Macherey-Nagel aluminum oxide 90 neutral (50−200 μm). ^{1}H NMR, ^{13}C NMR, and ^{31}P NMR spectra were recorded on a VNMRS-400, VNMRS-600, or Mercury 300 spectrometer in $CDCl_3$. Chemical shifts (δ) are reported in ppm and multiplicities are indicated: singlet (s), doublet (d), doublet of doublet (dd), triplet (t), doublet of triplet (dt), triplet of doublet (td), quartet (q), quintet (quint), multiplet (m); coupling constants (J) are in hertz (Hz). The abbreviation "vt" corresponds to a "virtual triplet" due to scalar coupling with two magnetically nonequivalent phosphorus nuclei. Mass spectra were acquired on a Finnigan SSQ7000 (electron impact (EI)/chemical ionization (CI)) spectrometer, and high-resolution mass spectra (HRMS) were acquired on a Finnigan MAT 95 (EI/CI) or on a ThermoFisher Scientific LTQ Orbitrap XL (electrospray ionization (ESI)) using ion trap as analyzer type. IR spectra were recorded on a PerkinElmer Spectrum 100 spectrometer and were reported in terms of frequency of absorption (cm^{-1}).

*Synthesis of Tricarbonyl(2,6-bis((diphenylphosphaneyl)methyl)-pyridine)manganese(I) Bromide (**Mn-1**).*[22j] A flame-dried Schlenk tube was charged with $Mn(CO)_5Br$ (420 mg, 1.53 mmol, 1.0 equiv) and the pincer PNP ligand (800 mg, 1.68 mmol, 1.1 equiv). The tube was evacuated and backfilled with argon three times. Tetrahydrofuran (THF) (25 mL) was added, and the resulting orange suspension was heated to 60 °C (oil bath) and stirred for 20 h. The solution was allowed to cool to room temperature, and THF was removed in vacuo. The workup was done under an ambient atmosphere. The yellow solid was washed three times with *n*-hexane (3 × 5 mL). The crude yellow powder was taken into dichloromethane and transferred into a 50 mL round bottom flask to remove insoluble inorganic side products. The solution was concentrated under reduced pressure, and the complex **Mn-1** was isolated as a yellow powder (1.02 g, 95%); ^{1}H NMR (300 MHz, CD_2Cl_2) δ 8.09 (s, 2H), 7.81−7.26 (m, 21H), 4.65 (s, 4H); ^{31}P{^{1}H} NMR (243 MHz, CD_2Cl_2) δ 69.4. (s, 2P); IR (attenuated total reflection (ATR)) 1918, 1840, 1571, 1435, 1284, 1172, 1097, 964, 833, 696 cm^{-1}; HRMS (ESI+): m/z $[M - Br]^+$ calcd for $C_{34}H_{27}MnNO_3P_2$, 614.0841; found, 614.0853.

*Synthesis of Bromodicarbonyl(bis(2-(diphenylphosphaneyl)-ethyl)-amine)manganese(I) (**Mn-2**).*[22k] A flame-dried Schlenk tube was charged with the HCl salt of the PNP pincer ligand (478 mg, 1.0 mmol, 1.0 equiv), toluene (8 mL), water (2 mL), and NaOH (120 mg, 3.0 mmol, 3.0 equiv). The reaction mixture was stirred at 45 °C (oil bath) for 30 min. The two phases were separated, and the organic layer was washed with water (5 × 5 mL). The pH value was checked until the solution turned neutral. The organic layer was concentrated under reduced pressure. Subsequently, toluene (12 mL) and the $Mn(CO)_5Br$ precursor were added to the Schlenk tube. The reaction mixture was heated up to 110 °C (oil bath), and the atmosphere was exchanged three times by evacuating and backfilled with argon. After

DOI: 10.1021/acs.joc.9b00792
J. Org. Chem. 2019, 84, 7927−7935

the mixture was stirred for 20 h at reflux temperature, it was cooled to room temperature and concentrated in vacuo. The crude precipitate was washed with pentane and extracted with dichloromethane/diethyl ether to remove insoluble inorganic side products. The solution was concentrated under reduced pressure and dried to afford the complex **Mn-2** as a yellow powder (410 mg, 65%). ^{1}H NMR (600 MHz, CD_2Cl_2) δ 7.92−7.89 (m, 4H, CH_{Ar}), 7.60−7.57 (m, 4H, CH_{Ar}), 7.43−7.29 (m, 12H, CH_{Ar}), 3.74−3.59 (m, 2H, NCH_2CH_2), 3.52 (br, 1H, NH), 3.32−3.23 (m, 2H, NCH_2CH_2), 2.78−2.73 (m, 2H, NCH_2CH_2), 2.44−2.40 (m, 2H, NCH_2CH_2); ^{31}P{^{1}H} NMR (243 MHz, CD_2Cl_2) δ = 69.7 (s); ^{13}C{^{1}H} NMR (151 MHz, CD_2Cl_2) δ = 231.6 (br, CO), 226.0 (br, CO), 137.9 (vt, J = 19.1 Hz, $PC_{Ar,ipso}$), 135.5 (vt, J = 19.1 Hz, $PC_{Ar,\ ipso}$), 133.8 (vt, J = 5.0 Hz, CH_{Ar}), 130.6 (vt, J = 5.0 Hz, CH_{Ar}), 130.3 (s, CH_{Ar}), 129.6 (s, CH_{Ar}), 129.0 (vt, J = 4.3 Hz, CH_{Ar}), 128.7 (vt, J = 4.6 Hz, CH_{Ar}), 53.0 (vt, J = 4.7 Hz, NCH_2CH_2), 28.4 (vt, J = 8.9 Hz, NCH_2CH_2); IR (ATR): ν^{-1} 3189, 1910, 1826 cm^{-1}; HRMS (ESI+): m/z [M − Br]$^+$: calcd for $C_{30}H_{29}MnNO_2P_2$, 552.1049; found, 552.1050.

*Synthesis of Dicarbonyl(bis(2-(diphenylphosphaneyl)ethyl)-amide)manganese(I) (**Mn-2a**).* In an argon-filled glovebox, complex **Mn-2** (127 mg, 0.2 mmol) was introduced into a 25 mL Schlenk tube and was dissolved in toluene (5 mL). After 2 min of stirring, *t*-BuOK (34 mg, 0.3 mmol) was added, which turned the yellow solution into deep red. The reaction mixture was stirred for 1 h at 50 °C (oil bath). Then, the mixture was filtered and the solution was concentrated under reduced pressure to give a deep red powder (75 mg, 68%) that was stored in a glovebox. ^{1}H NMR (600 MHz, C_6D_6) δ 7.73−7.71 (m, 8H, CH_{Ar}), 7.10−7.08 (m, 8H, CH_{Ar}), 7.04−7.02 (m, 4H), 3.25−3.24 (m, 4H, NCH_2CH_2), 2.35−2.32 (m, 4H, NCH_2CH_2); ^{31}P{^{1}H} NMR (243 MHz, C_6D_6) δ 91.06 (s); ^{13}C{^{1}H} NMR (151 MHz, C_6D_6) δ = 233.5 (br, CO), 136.6 (vt, J = 18.0 Hz, $PC_{Ar,ipso}$), 132.7 (s, CH_{Ar}), 129.8 (s, CH_{Ar}), 128.8 (vt, J = 4.3 Hz, CH_{Ar}), 62.1 (NCH_2CH_2), 33.7 (NCH_2CH_2); IR (ATR): 1903, 1828 cm^{-1} (no ν_{NH} band observed).

*Synthesis of Tricarbonyl(2-(diphenylphosphaneyl)-N-(pyridin-2-ylmethyl)ethan-1-amine)manganese(I) Bromide (**Mn-3**).*[20b] A flame-dried Schlenk tube was charged with the PNN pincer ligand (300 mg, 1.07 mmol, 1 equiv) and $Mn(CO)_5Br$ (293 mg, 1.07 mmol, 1.0 equiv). The Schlenk tube was evacuated and backfilled with argon several times. Afterward, 15 mL of degassed THF was added and the reaction mixture was stirred at 80 °C (oil bath) for 20 h. The suspension was allowed to cool to room temperature, and the yellow precipitate was filtered off and washed with diethyl ether and *n*-hexane. The remaining solid was dried under vacuum to afford the complex **Mn-3** as a yellow powder (0.49 g, 84%); ^{1}H NMR (600 MHz, dimethyl sulfoxide (DMSO)-d_6): δ 7.93−7.92 (m, 1H), 7.87−7.84 (m, 2H), 7.81−7.78 (m, 1H), 7.58−7.49 (m, 4H), 7.39−7.37 (m, 1H), 7.31−7.29 (m, 2H), 7.20−7.09 (m, 2H), 6.94−6.92 (m, 1H), 4.58−4.54 (m, 1H), 4.38 (m, 1H), 3.28−3.20 (m, 1H), 3.04−3.00 (m, 1H), 2.95−2.89 (m, 1H), 2.40−2.27 (m, 1H); ^{13}C{^{1}H} NMR (151 MHz, DMSO-d_6) δ 221.2, 219.9, 215.3, 162.1, 153.0, 139.2, 132.4, 132.0, 131.1, 131.0, 130.9, 130.8, 129.9, 129.8, 129.6, 125.0, 122.4, 59.8, 53.8 (d, J = 8.8 Hz), 22.7 (d, J = 22.7 Hz); ^{31}P{^{1}H} NMR (242 MHz, DMSO-d_6) δ 65.86; IR (ATR): 3045, 2891, 2024, 1914, 1843, 1477, 1434, 1099, 892, 752, 693 cm$^{-1;}$ HRMS (ESI): m/z [M − Br]$^+$ calcd for $C_{23}H_{21}MnN_2O_3P$, 459.0665; found, 459.0675.

General Procedure of C-Alkylation of Nitriles Using Aliphatic and Benzylic Alcohols. A glass pressure tube (10 mL) equipped with a magnetic stirrer was charged with **Mn-2** (3.2 mg, 0.005 mmol) and Cs_2CO_3 (16.3 mg, 0.05 mmol). A rubber septum was attached to the tube, and the reaction vessel was evacuated and backfilled with argon three times. Under an inert atmosphere, primary alcohol (1.0 mmol), nitrile (0.5 mmol), and toluene (0.5 mL) were added and the tube was closed with a screw cap. The resulting mixture was stirred at 135 °C (aluminum block) for 18 h under an argon atmosphere. Upon cooling down to room temperature, the residue was directly purified by flash column chromatography on silica gel eluting with pentane/diethyl ether (20:1 (v/v)) to give the pure alkylated nitrile.

*2-Phenylhexanenitrile (**3a**).*[12a] Colorless oil; 78 mg (88%) ^{1}H NMR (400 MHz, $CDCl_3$) δ 7.46−7.27 (m, 5H), 3.77 (dd, J = 8.5, 6.3 Hz, 1H), 2.04−1.74 (m, 2H), 1.60−1.25 (m, 4H), 0.92 (t, J = 7.2 Hz, 3H); ^{13}C{^{1}H} NMR (101 MHz, $CDCl_3$) δ 136.2, 129.1, 128.0, 127.3, 121.0, 37.5, 35.7, 29.2, 22.2, 13.8.

*2-(p-Tolyl)hexanenitrile (**3b**).*[13d] Colorless oil; 81 mg (87%); ^{1}H NMR (600 MHz, $CDCl_3$) δ 7.25−7.16 (m, 4H), 3.74 (dd, J = 8.6, 6.3 Hz, 1H), 2.36 (s, 3H), 1.99−1.77 (m, 2H), 1.55−1.29 (m, 4H), 0.92 (t, J = 7.3 Hz, 3H); ^{13}C{^{1}H} NMR (151 MHz, $CDCl_3$) δ 137.8, 133.1, 129.7, 127.2, 121.2, 37.0, 35.7, 29.2, 22.2, 21.1, 13.9.

*2-(2-Methoxyphenyl)hexanenitrile (**3c**).*[12a] Colorless oil; 96 mg (94%); eluent mixture: pentane/diethyl ether (10:1 (v/v)), ^{1}H NMR (400 MHz, $CDCl_3$) δ 7.42−7.40 (m, 1H), 7.30−7.27 (m, 1H), 7.00−6.96 (m, 1H), 6.91−6.82 (m, 1H), 4.19 (dd, J = 8.2, 6.3 Hz, 1H), 3.85 (s, 3H), 1.86 (m, 2H), 1.62−1.23 (m, 4H), 0.92 (t, J = 7.2 Hz, 3H); ^{13}C{^{1}H} NMR (101 MHz, $CDCl_3$) δ 156.1, 129.3, 128.3, 124.5, 121.4, 120.9, 110.8, 55.5, 33.5, 31.4, 29.4, 22.1, 13.8.

*2-(3,4-Dimethoxyphenyl)hexanenitrile (**3d**).* Colorless oil; 103 mg (88%); eluent mixture: pentane/diethyl ether (5:1 (v/v)); ^{1}H NMR (600 MHz, $CDCl_3$) δ 6.85−6.76 (m, 3H), 3.86 (s, 3H), 3.84 (s, 3H), 3.68 (dd, J = 8.7, 6.3 Hz, 1H), 1.94−1.75 (m, 2H), 1.50−1.26 (m, 4H), 0.87 (t, J = 7.3 Hz, 3H); ^{13}C{^{1}H} NMR (151 MHz, $CDCl_3$) δ 149.3, 148.7, 128.4, 121.2, 119.5, 111.3, 110.2, 110.1, 56.0, 55.9, 36.9, 35.6, 29.1, 22.1, 13.8; IR: 2936, 2865, 2087, 1906, 1595, 1457, 1343, 1253, 1146, 1026, 913, 809, 759 cm^{-1}. HRMS (ESI+): m/z [M]$^+$ calcd for $C_{14}H_{19}O_2N$, 233.1410; found 233.1413.

*2-(Benzo[d][1,3]dioxol-5-yl)hexanenitrile (**3e**).*[12a] Colorless oil; 87 mg (80%); eluent mixture: pentane/diethyl ether (5:1 (v/v)); ^{1}H NMR (600 MHz, $CDCl_3$) δ 6.81−6.73 (m, 3H), 5.96 (s, 2H), 3.67 (dd, J = 8.5, 6.4 Hz, 1H), 1.93−1.74 (m, 2H), 1.50−1.27 (m, 4H), 0.94−0.85 (m, 3H); ^{13}C{^{1}H} NMR (151 MHz, $CDCl_3$) δ 148.2, 147.4, 129.8, 121.1, 120.7, 108.6, 107.7, 107.7, 101.4, 37.1, 35.7, 29.1, 22.1, 13.8.

*2-(4-Chlorophenyl)hexanenitrile (**3f**).*[26a] Colorless oil; 82 mg (79%); ^{1}H NMR (600 MHz, $CDCl_3$) δ 7.35−7.25 (m, 4H), 3.75 (dd, J = 8.6, 6.2 Hz, 1H), 1.97−1.77 (m, 2H), 1.51−1.28 (m, 4H), 0.90 (t, J = 7.3 Hz, 3H); ^{13}C{^{1}H} NMR (151 MHz, $CDCl_3$) δ 134.6, 134.0, 129.3, 128.7, 120.6, 36.9, 35.6, 29.1, 22.1, 13.8.

*2-(2-Chlorophenyl)hexanenitrile (**3g**).* Colorless oil; 82 mg (79%); ^{1}H NMR (600 MHz, $CDCl_3$) δ 7.56−7.55 (m, 1H), 7.42−7.36 (m, 1H), 7.32−7,31 (m, 1H), 7.28−7.25 (m, 1H), 4.28 (dd, J = 9.0, 5.6 Hz, 1H), 1.96−1.79 (m, 2H), 1.61−1.30 (m, 4H), 0.92 (t, J = 7.4 Hz, 3H). ^{13}C{^{1}H} NMR (151 MHz, $CDCl_3$) δ 134.0, 132.6, 130.0, 129.5, 128.9, 127.7, 120.5, 34.7, 34.0, 29.3, 22.1, 13.9; IR: 3424, 2935, 2866, 2666, 2323, 2103, 1921, 1728, 1466, 1278, 1040, 754 cm^{-1}; HRMS (ESI+): m/z [M + Na]$^+$ calcd for $C_{12}H_{14}N_1Cl_1Na_1$ 230.0707; found, 230.0707.

*4-(1-Cyanopentyl)benzonitrile (**3h**).* Yellowish oil; 52 mg (53%); ^{1}H NMR (600 MHz, CDCl3) δ 7.70−7.68 (m, 2H), 7.47−7.46 (m, 2H), 3.85 (dd, J = 8.6, 6.1 Hz, 1H), 1.98−1.82 (m, 2H), 1.54−1.29 (m, 4H), 0.91 (t, J = 7.3 Hz, 3H); ^{13}C{^{1}H} NMR (151 MHz, $CDCl_3$) δ 141.3, 133.0, 128.2, 119.8, 118.3, 112.4, 37.6, 35.5, 29.1, 22.2, 13.9; IR: 3470, 3064, 2958, 2867, 2231, 1610, 1506, 1462, 1414, 1381, 1115, 1021, 841 cm^{-1}; HRMS (ESI+): m/z [M + H]$^+$ calcd for $C_{13}H_{15}N_2$ 199.1230; found 199.1230.

*2-(Pyridin-2-yl)hexanenitrile (**3i**).* Colorless oil; 86 mg (99%); eluent mixture: pentane/diethyl ether (10:1 (v/v)); ^{1}H NMR (600 MHz, $CDCl_3$) δ 8.58−8.51 (m, 1H), 7.70−7.67 (m, 1H), 7.42−7.37 (m, 1H), 7.22−7.20 (m, 1H), 3.94 (dd, J = 8.3, 6.4 Hz, 1H), 1.99−1.95 (m, 2H), 1.53−1.25 (m, 4H), 0.86 (t, J = 7.4 Hz, 3H); ^{13}C{^{1}H} NMR (151 MHz, $CDCl_3$) δ 155.4, 149.9, 137.3, 122.9, 121.7, 120.2, 39.9, 33.9, 29.1, 22.1, 13.8; IR: 3180, 2933, 2867, 2322, 1920, 1738, 1586, 1467, 1437, 1301, 1206, 994, 755, 665 cm^{-1}; HRMS (ESI+): m/z [M]$^+$ calcd for $C_{11}H_{14}N_2$, 174.1152; found 174.1145.

*2-(Thiophen-2-yl)hexanenitrile (**3j**).* Yellowish oil; 58 mg (65%), ^{1}H NMR (600 MHz, $CDCl_3$) δ 7.27−7.26 (m, 1H), 7.06−7.05 (d, J = 3.5 Hz, 1H), 6.98−6.97 (m, 1H), 4.06 (dd, J = 8.4, 6.3 Hz, 1H), 2.06−1.91 (m, 2H), 1.58−1.43 (m, 2H), 1.43−1.33 (m, 2H), 0.93 (t, J = 7.3 Hz, 3H); ^{13}C{^{1}H} NMR (151 MHz, $CDCl_3$) δ 138.2, 127.1, 126.1, 125.5, 120.1, 35.7, 32.6, 29.1, 22.1, 13.9; IR: 3468, 3109, 2957,

DOI: 10.1021/acs.joc.9b00792
J. Org. Chem. 2019, 84, 7927−7935

2865, 2242, 1728, 1461, 1379, 1238, 1038, 836, 703 cm^{-1}; HRMS (ESI+): m/z $[M + Na]^+$ calcd for $C_{10}H_{13}N_1NaS$, 202.0661; found 202.0659.

*2,3-Diphenylpropanenitrile (**4a**).*[10] Colorless oil; 89 mg (86%); ^1H NMR (600 MHz, $CDCl_3$) δ 7.41−7.26 (m, 8H), 7.18−7.14 (m, 2H), 4.02 (dd, J = 8.5, 6.4 Hz, 1H), 3.21 (dd, J = 13.6, 8.4 Hz, 1H), 3.15 (dd, J = 13.7, 6.4 Hz, 1H); $^{13}C\{^1H\}$ NMR (151 MHz, $CDCl_3$) δ 136.4, 135.3, 129.3, 129.1, 128.7, 128.3, 127.6, 127.5, 120.5, 42.3, 39.9.

*3-Phenyl-2-(pyridin-2-yl)propanenitrile (**4b**).*[13c] Yellowish oil; 76 mg (73%); eluent mixture: pentane/diethyl ether (10:1 (v/v)); ^1H NMR (600 MHz, $CDCl_3$) δ 8.65−8.64 (m, 1H), 7.68−7.65 (m, 1H), 7.30−7.24 (m, 5H), 7.18−7.16 (m, 2H), 4.21 (dd, J = 8.7, 5.9 Hz, 1H), 3.37 (dd, J = 13.6, 5.9 Hz, 1H), 3.26 (dd, J = 13.6, 8.7 Hz, 1H); $^{13}C\{^1H\}$ NMR (151 MHz, $CDCl_3$) δ 154.6, 150.1, 137.3, 136.4, 129.3, 128.8, 127.5, 123.2, 122.3, 119.8, 42.2, 40.2.

*2-Phenyl-3-(p-tolyl)propanenitrile (**4c**).*[14] White solid; 101 mg (91%); ^1H NMR (600 MHz, $CDCl_3$) δ 7.39−7.33 (m, 3H), 7.29−7.28 (m, 2H), 7.13−7.11 (m, 2H), 7.06−7.04 (m, 2H), 3.99 (dd, J = 8.5, 6.3 Hz, 1H), 3.16 (dd, J = 13.7, 8.5 Hz, 1H), 3.11 (dd, J = 13.7, 6.4 Hz, 1H), 2.34 (s, 3H); $^{13}C\{^1H\}$ NMR (151 MHz, $CDCl_3$) δ 137.1, 135.4, 133.3, 129.4, 129.2, 129.1, 128.2, 127.6, 120.6, 41.9, 40.0, 21.2.

*3-(3,4-Dimethoxyphenyl)-2-phenylpropanenitrile (**4d**).*[13c] Off-white solid; 121 mg (91%); eluent mixture: pentane/diethyl ether (10:1 (v/v)); ^1H NMR (600 MHz, $CDCl_3$) δ 7.38−7.30 (m, 3H), 7.26−7.22 (m, 2H), 6.78−6.79 (m, 1H), 6.71−6.69 (m, 1H), 6.52−6.51 (m, 1H), 3.98 (dd, J = 7.8, 6.4 Hz, 1H), 3.86 (s, 3H), 3.76 (s, 3H), 3.14 (dd, J = 13.7, 7.9 Hz, 1H), 3.09 (dd, J = 13.7, 6.4 Hz, 1H); $^{13}C\{^1H\}$ NMR (151 MHz, $CDCl_3$) δ 148.8, 148.4, 135.3, 129.1, 128.7, 128.3, 127.7, 121.5, 120.6, 112.5, 111.2, 56.0, 55.9, 41.9, 40.0.

*3-(Benzo[d][1,3]dioxol-4-yl)-2-phenylpropanenitrile (**4e**).* Colorless oil; 91 mg (72%); eluent mixture: pentane/diethyl ether (5:1 (v/v)); ^1H NMR (600 MHz, $CDCl_3$) δ 7.39−7.30 (m, 3H), 7.28−7.25 (m, 2H), 6.73−6.72 (m, 1H), 6.63−6.58 (m, 2H), 5.94 (s, 2H), 3.96 (dd, J = 8.4, 6.4 Hz, 1H), 3.10 (dd, J = 13.7, 8.3 Hz, 1H), 3.05 (dd, J = 13.8, 6.5 Hz, 1H); $^{13}C\{^1H\}$ NMR (151 MHz, $CDCl_3$) δ 147.8, 147.0, 135.2, 130.0, 129.1, 128.3, 127.6, 122.6, 120.5, 109.6, 108.5, 101.2, 42.0, 40.1; IR: 3064, 3031, 2899, 2241, 1685, 1605, 1495, 1446, 1249, 1194, 1100, 1039, 810, 751, 699 cm^{-1}; HRMS (ESI+): m/z $[M + H]^+$ calcd for $C_{16}H_{14}O_2N$, 252.1019; found 252.1017.

*2-Phenyl-3-(3-(trifluoromethyl)phenyl)propanenitrile (**4f**).* Colorless oil; 105 mg (76%); ^1H NMR (600 MHz, $CDCl_3$) δ 7.55−7.53 (m, 1H), 7.44−7.42 (m, 1H), 7.39−7.33 (m, 4H), 7.30−7.29 (m, 1H), 7.26−7.23 (m, 2H), 4.04 (dd, J = 8.1, 6.5 Hz, 1H), 3.25 (dd, J = 13.7, 8.1 Hz, 1H), 3.21 (dd, J = 13.7, 6.5 Hz, 1H); $^{13}C\{^1H\}$ NMR (151 MHz, $CDCl_3$) δ 137.1, 134.6, 130.9 (q, J = 32.4 Hz), 129,3, 129,2, 128.6, 127.6, 126.2 (q, J = 3.8 Hz), 124.4 (q, J = 3.8 Hz), 123.9 (q, J = 272.2 Hz), 41.9, 39.5; ^{19}F NMR (282 MHz, $CDCl_3$) δ −62.73; IR: 3066, 3035, 2933, 2243, 1599, 1495, 1451, 1330, 1166, 1126, 1075, 911, 792, 754, 701 cm^{-1}; HRMS (ESI+): m/z $[M + Na]^+$ calcd for $C_{16}H_{12}NF_3Na$, 298.0814; found 298.0814.

*3-(Naphthalen-1-yl)-2-phenylpropanenitrile (**4g**).*[26b] Colorless oil; 107 mg (83%); ^1H NMR (400 MHz, $CDCl_3$) δ 7.97−7.89 (m, 2H), 7.82−7.80 (m, 1H), 7.59−7.50 (m, 2H), 7.43−7.29 (m, 7H), 4.18 (dd, J = 8.7, 6.7 Hz, 1H), 3.70−3.57 (m, 2H); $^{13}C\{^1H\}$ NMR (101 MHz, $CDCl_3$) δ 135.8, 134.1, 132.4, 131.4, 129.4, 129.3, 128.5, 128.4, 128.3, 127.5, 126.7, 125.9, 125.6, 122.7, 120.6, 39.7, 39.0 ppm.

*2-Phenyl-3-(pyridin-4-yl)propanenitrile (**4h**).*[14] Yellowish oil; 73 mg (70%); ^1H NMR (600 MHz, $CDCl_3$) δ 8.62−8.60 (m, 1H), 7.65−7.62 (m, 1H), 7.37−7.36 (m, 4H), 7.34−7.30 (m, 1H), 7.23−7.20 (m, 1H), 7.15−7.14 (m, 1H), 4.50 (dd, J = 9.3, 6.6 Hz, 1H), 3.36 (dd, J = 13.9, 9.3 Hz, 1H), 3.30 (dd, J = 13.9, 6.6 Hz, 1H); $^{13}C\{^1H\}$ NMR (151 MHz, $CDCl_3$) δ 156.1, 149.5, 136.9, 135.4, 129.1, 128.2, 127.4, 124.0, 120.5, 44.1, 37.3.

*2-Phenyl-3-(pyridin-2-yl)propanenitrile (**4i**).*[10] Yellowish oil; 49 mg (47%); ^1H NMR (600 MHz, $CDCl_3$) δ 8.61−8.59 (m, 1H), 7.62−7.60 (m, 1H), 7.36−7.35 (m, 4H), 7.34−7.29 (m, 1H), 7.21−7.18 (m, 1H), 7.13−7.12 (m, 1H), 4.48 (dd, J = 9.3, 6.5 Hz, 1H), 3.35 (dd, J = 13.9, 9.3 Hz, 1H), 3.28 (dd, J = 13.9, 6.5 Hz, 1H); $^{13}C\{^1H\}$ NMR (151 MHz, $CDCl_3$) δ 156.3, 149.8, 136.9, 135.5, 129.2, 128.3, 127.5, 124.0, 122.5, 120.7, 44.3, 37.4.

*3-(Furan-2-yl)-2-phenylpropanenitrile (**4j**).*[26c] Colorless oil; 62 mg (63%); ^1H NMR (600 MHz, $CDCl_3$) δ 7.39−7.25 (m, 6H), 6.30−6.29 (m, 1H), 6.12−6.11 (m, 1H), 4.15 (dd, J = 8.6, 6.5 Hz, 1H), 3.27 (dd, J = 15.0, 8.6 Hz, 1H), 3.19−3.13 (m, 1H); $^{13}C\{^1H\}$ NMR (151 MHz, $CDCl_3$) δ 150.1, 142.3, 135.0, 129.2, 128.7, 128.5, 110.6, 108.4, 37.2, 34.8.

*2-Phenyl-3-(thiophen-2-yl)propanenitrile (**4k**).*[18] Colorless oil; 87 mg (82%); ^1H NMR (600 MHz, $CDCl_3$) δ 7.40−7.26 (m, 5H), 7.17 (m, 1H), 6.92 (m, 1H), 6.85 (m, 1H), 4.04 (dd, J = 8.1, 6.4 Hz, 1H), 3.43 (dd, J = 14.8, 8.2 Hz, 1H), 3.34 (dd, J = 14.8, 6.3 Hz, 1H); $^{13}C\{^1H\}$ NMR (151 MHz, $CDCl_3$) δ 138.0, 134.8, 129.2, 128.5, 127.5, 127.2, 127.1, 125.0, 40.1, 36.2.

*2-Phenylbutanenitrile (**4l**).*[12a] Colorless oil; 38 mg (52%); ^1H NMR (600 MHz, $CDCl_3$) δ 7.41−7.29 (m, 5H), 3.74 (t, J = 7.2 Hz, 1H), 1.97−1.92 (m, 2H), 1.08 (t, J = 7.4 Hz, 3H); $^{13}C\{^1H\}$ NMR (151 MHz, $CDCl_3$) δ 135.9, 129.1, 128.1, 127.4, 120.9, 39.0, 29.4, 11.6.

*2-Phenyloctanenitrile (**4m**).*[10] Colorless oil; 94 mg (93%); ^1H NMR (600 MHz, $CDCl_3$) δ 7.39−7.37 (m, 2H), 7.34−7.31 (m, 3H), 3.77 (dd, J = 8.7, 6.2 Hz, 1H), 1.97−1.82 (m, 2H), 1.55−1.42 (m, 2H), 1.36−1.25 (m, 6H), 0.88 (t, J = 6.9 Hz, 3H); $^{13}C\{^1H\}$ NMR (151 MHz, $CDCl_3$) δ 136.2, 129.1, 128.0, 127.3, 121.0, 37.5, 36.0, 31.6, 28.7, 27.0, 22.6, 14.1.

*4-Methyl-2-phenylpentanenitrile (**4n**).*[13c] Colorless oil; 71 mg (82%); ^1H NMR (600 MHz, $CDCl_3$) δ 7.40−7.30 (m, 5H), 3.81 (dd, J = 9.8, 6.4 Hz, 1H), 1.91 (ddd, J = 13.4, 9.8, 5.5 Hz, 1H), 1.88−1.80 (m, 1H), 1.64 (ddd, J = 13.3, 8.4, 6.3 Hz, 1H), 0.99 (dd, J = 8.0, 6.5 Hz, 6H); $^{13}C\{^1H\}$ NMR (151 MHz, $CDCl_3$) δ 136.4, 129.2, 128.1, 127.3, 121.1, 45.1, 35.61, 26.2, 22.7, 21.7.

*2-Phenylhept-6-enenitrile (**4o**).*[26d] Colorless oil; 78 mg (78%); ^1H NMR (600 MHz, $CDCl_3$) δ δ 7.41−7.30 (m, 5H), 5.76 (ddt, J = 17.0, 10.2, 6.7 Hz, 1H), 5.05−4.97 (m, 2H), 3.79 (dd, J = 8.6, 6.2 Hz, 1H), 2.13−2.08 (m, 2H), 1.98−1.84 (m, 2H), 1.67−1.52 (m, 2H); $^{13}C\{^1H\}$ NMR (151 MHz, $CDCl_3$) δ 137.6, 136.0, 129.1, 128.1, 127.3, 120.9, 115.5, 37.3, 35.3, 33.0, 26.2.

*3-Cyclohexyl-2-phenylpropanenitrile (**4p**).*[14] Colorless oil; 77 mg (72%); ^1H NMR (600 MHz, $CDCl_3$) δ 7.40−7.30 (m, 5H), 3.85 (dd, J = 10.1, 6.2 Hz, 1H), 1.92−1.81 (m, 2H), 1.78−1.62 (m, 5H), 1.57−1.49 (m, 1H), 1.31−1.13 (m, 3H), 1.01−0.92 (m, 2H); $^{13}C\{^1H\}$ NMR (151 MHz, $CDCl_3$) δ 136.6, 129.2, 128.0, 127.3, 121.2, 43.8, 35.4, 34.9, 33.4, 32.4, 26.4, 26.0, 25.9.

General Procedure of C-Methylation of Nitriles. A glass Ace pressure tube (22 mL) equipped with a magnetic stir bar was charged with **Mn-2** (8 mg, 0.025 mmol) and Cs_2CO_3 (16.3 mg, 0.05 mmol). A rubber septum was attached to the tube, and the reaction vessel was evacuated and backfilled with argon three times. Under an inert atmosphere, nitrile (0.5 mmol), methanol (1 mL), and 1,4-dioxane (1 mL) were added and the tube was closed with a screw cap. The resulting mixture was stirred at 135 °C (aluminum block) for 24 h under an argon atmosphere. Upon cooling down to room temperature, the residue was directly purified by flash column chromatography on silica gel eluting with pentane/diethyl ether mixtures to give the pure desired product.

*2-Phenylpropanenitrile (**5a**).*[26e] Yellowish oil; 46 mg (70%); ^1H NMR (600 MHz, $CDCl_3$) δ 7.41−7.31 (m, 5H), 3.90 (q, J = 7.3 Hz, 1H), 1.65 (d, J = 7.3 Hz, 3H); $^{13}C\{^1H\}$ NMR (151 MHz, $CDCl_3$) δ 137.2, 129.3, 128.2, 126.8, 121.7, 31.4, 21.6.

*2-(2-Methoxyphenyl)propanenitrile (**5b**).*[26f] Yellowish oil 52 mg (65%); eluent mixture: pentane/diethyl ether (10:1 (v/v)); ^1H NMR (600 MHz, $CDCl_3$) δ 7.43−7.41 (m, 1H), 7.32−7.29 (m, 1H), 7.01−6.98 (m, 1H), 6.91−6.89 (m, 1H), 4.25 (q, J = 7.2 Hz, 1H), 3.87 (s, 3H), 1.58 (d, J = 7.2 Hz, 3H); $^{13}C\{^1H\}$ NMR (151 MHz, $CDCl_3$) δ 156.2, 129.4, 127.7, 125.5, 122.1, 121.1, 110.9, 55.6, 25.7, 19.6.

*2-(3-Methoxyphenyl)propanenitrile (**5c**).*[26g] Yellowish oil 56 mg (70%); ^1H NMR (600 MHz, $CDCl_3$) δ 7.30 (m, 1H), 6.94−6.93 (m, 1H), 6.89 (m, 1H), 6.87−6.85 (m, 1H), 3.87 (q, J = 7.3 Hz, 1H), 3.83 (s, 3H), 1.64 (d, J = 7.4 Hz, 3H); $^{13}C\{^1H\}$ NMR (151 MHz, $CDCl_3$) δ 160.2, 138.6, 130.3, 121.7, 119.1, 113.5, 112.7, 55.5, 31.4, 21.5.

DOI: 10.1021/acs.joc.9b00792
J. Org. Chem. 2019, 84, 7927−7935

*2-(4-Methoxyphenyl)propanenitrile (**5d**).*[26e] Yellowish oil 48 mg (59%); ^{1}H NMR (600 MHz, $CDCl_3$) δ 7.30−7.28 (m, 2H), 6.94−6.91 (m, 2H), 3.87 (q, J = 7.4 Hz, 1H), 3.83 (s, 3H), 1.64 (d, J = 7.3 Hz, 3H); ^{13}C{^{1}H} NMR (151 MHz, $CDCl_3$) δ 159.4, 129.2, 128.0, 122.0, 114.6, 55.5, 30.6, 21.7.

*2-(2-Chlorophenyl)propanenitrile (**5e**).*[26e] Yellowish oil; 51 mg (61%); ^{1}H NMR (600 MHz, $CDCl_3$) δ 7.58 (m, 1H), 7.41−7.39 (m, 1H), 7.36−7.32 (m, 1H), 7.30−7.27 (m, 1H), 4.36 (q, J = 7.1 Hz, 1H), 1.63 (d, J = 7.1 Hz, 3H); ^{13}C{^{1}H} NMR (151 MHz, $CDCl_3$) δ 134.9, 132.6, 130.2, 129.6 128.4, 127.9, 121.2, 29.0, 20.1.

*2-(4-Chlorophenyl)propanenitrile (**5f**).*[26e] Yellowish oil; 57 mg (69%); ^{1}H NMR (600 MHz, $CDCl_3$) δ 7.38−7.35 (m, 2H), 7.31−7.28 (m, 2H), 3.88 (q, J = 7.4 Hz, 1H), 1.63 (d, J = 7.3 Hz, 3H); ^{13}C{^{1}H} NMR (151 MHz, $CDCl_3$) δ 135.6, 134.2, 129.5, 128.2, 121.3, 30.9, 21.5.

*2-(Pyridin-2-yl)propanenitrile (**5g**).*[26h] 36 mg (55%), yellowish oil; ^{1}H NMR (600 MHz, $CDCl_3$) δ 8.62−8.61 (m, 1H), 7.77−7.74 (m, 1H), 7.48−7.47 (m, 1H), 7.29−7.27 (m, 1H), 4.08 (q, J = 7.4 Hz, 1H), 1.73 (d, J = 7.4 Hz, 3H); ^{13}C{^{1}H} NMR (151 MHz, $CDCl_3$) δ 156.2, 150.0, 137.6, 123.1, 121.2, 121.1, 33.9, 19.8.

*2-(Thiophen-2-yl)propanenitrile (**5h**).*[26i] Yellowish oil; 42 mg (61%); ^{1}H NMR (600 MHz, $CDCl_3$) δ 7.28−7.27 (m, 1H), 7.08−7.07 (m, 1H), 6.99−6.98 (m, 1H), 4.18 (q, J = 7.4 Hz, 1H), 1.74 (d, J = 7.2 Hz, 3H); ^{13}C{^{1}H} NMR (151 MHz, $CDCl_3$) δ 139.3, 127.2, 125.7, 125.5, 120.8, 26.7, 21.6.

*Representative Procedure for Gram-Scale Synthesis of 2-Phenyl-3-(p-tolyl)propanenitrile (**4c**).* A glass pressure tube (25 mL) equipped with a magnetic stirrer was charged with **Mn-2** (35.2 mg, 0.055 mmol) and Cs_2CO_3 (179.3 mg, 0.55 mmol). A rubber septum was attached to the tube, and the reaction vessel was evacuated and backfilled with argon three times. Under an inert atmosphere, *p*-tolylmethanol (1.34 g, 11.0 mmol), 2-phenylacetonitrile (632 μL, 644 mg, 5.5 mmol), and toluene (5.5 mL) were added and the tube was closed with a screw cap. The resulting mixture was stirred at 135 °C (aluminum block) for 24 h under an argon atmosphere. Upon cooling down to room temperature, the residue was concentrated under reduced pressure and purified by flash column chromatography on silica gel eluting with pentane/diethyl ether (20:1 (v/v)) to give the pure **4c** (1022 mg, 84% yield).

■ ASSOCIATED CONTENT

Supporting Information

The Supporting Information is available free of charge on the ACS Publications website at DOI: 10.1021/acs.joc.9b00792.

Copies of NMR spectra of the manganese complexes, copies of the NMR spectra of the control NMR experiments, copies of the NMR spectra of the products, and robustness screening (PDF)

■ AUTHOR INFORMATION

Corresponding Authors

*E-mail: Magnus.Rueping@rwth-aachen.de (M.R.).
*E-mail: Osama.Elsepelgy@rwth-aachen.de (O.E.-S.).

ORCID

Magnus Rueping: 0000-0003-4580-5227
Osama El-Sepelgy: 0000-0003-3131-4988

Notes

The authors declare no competing financial interest.

■ ACKNOWLEDGMENTS

J.C.B. acknowledges the German Federal Environmental Foundation (DBU) for a doctoral fellowship. J.S. is grateful for a doctoral fellowship provided by the Fonds der Chemischen Industrie.

■ REFERENCES

(1) Vispute, T. P.; Zhang, H.; Sanna, A.; Xiao, R.; Huber, G. W. Renewable Chemical Commodity Feedstocks from Integrated Catalytic Processing of Pyrolysis Oils. *Science* **2010**, *330*, 1222−1227.

(2) Selected Recent Reviews: (a) Corma, A.; Navas, J.; Sabater, M. J. Advances in One-Pot Synthesis through Borrowing Hydrogen Catalysis. *Chem. Rev.* **2018**, *118*, 1410. (b) Crabtree, R. H. Homogeneous Transition Metal Catalysis of Acceptorless Dehydrogenative Alcohol Oxidation: Applications in Hydrogen Storage and to Heterocycle Synthesis. *Chem. Rev.* **2017**, *117*, 9228−9246. (c) Chelucci, G. Ruthenium and osmium complexes in C-C bond-forming reactions by borrowing hydrogen catalysis. *Coord. Chem. Rev.* **2017**, *331*, 1−36. (d) Huang, F.; Liu, Z.; Yu, Z. C-Alkylation of Ketones and Related Compounds by Alcohols: Transition-Metal-Catalyzed Dehydrogenation. *Angew. Chem., Int. Ed.* **2016**, *55*, 862−875. (e) Nandakumar, A.; Midya, S. P.; Landge, V. G.; Balaraman, E. Transition-Metal-Catalyzed Hydrogen-Transfer Annulations: Access to Heterocyclic Scaffolds. *Angew. Chem., Int. Ed.* **2015**, *54*, 11022−11034. (f) Yang, Q.; Wang, Q.; Yu, Z. Substitution of alcohols by N-nucleophiles via transition metal-catalyzed dehydrogenation. *Chem. Soc. Rev.* **2015**, *44*, 2305−2329. (g) Obora, Y. Recent Advances in α-Alkylation Reactions using Alcohols with Hydrogen Borrowing Methodologies. *ACS Catal.* **2014**, *4*, 3972−3981. (h) Gunanathan, C.; Milstein, D. Applications of Acceptorless Dehydrogenation and Related Transformations in Chemical Synthesis. *Science* **2013**, *341*, No. 1229712. (i) Guillena, G.; Ramln, D. J.; Yus, M. Hydrogen Autotransfer in the *N*-Alkylation of Amines and Related Compounds using Alcohols and Amines as Electrophiles. *Chem. Rev.* **2010**, *110*, 1611.

(3) Bullock, R. M. *Catalysis without Precious Metals*; Wiley-VCH: Weinheim, 2010.

(4) (a) Bruneau-Voisine, A.; Pallova, L.; Bastin, S.; César, V.; Sortais, J.-B. Manganese catalyzed α-methylation of ketones with methanol as a C1 source. *Chem. Commun.* **2019**, *55*, 314−317. (b) Sklyaruk, J.; Borghs, J.; El-Sepelgy, O.; Rueping, M. Catalytic C_1 Alkylation with Methanol and Isotope Labelled Methanol. *Angew. Chem., Int. Ed.* **2018**, *131*, 785−789. (c) Barman, M. K.; Jana, A.; Maji, B. Phosphine-Free NNN-Manganese Complex Catalyzed α-Alkylation of Ketones with Primary Alcohols and Friedlaender Quinoline Synthesis. *Adv. Synth. Catal.* **2018**, *360*, 3233−3238. (d) Zhang, G.; Wu, J.; Zeng, H.; Zhang, S.; Yin, Z.; Zheng, S. Cobalt-Catalyzed α-Alkylation of Ketones with Primary Alcohols. *Org. Lett.* **2017**, *19*, 1080−1083. (e) Peña-López, M.; Piehl, P.; Elangovan, S.; Neumann, H.; Beller, M. Manganese Catalyzed Hydrogen-Autotransfer C-C Bond Formation: α-Alkylation of Ketones with Primary Alcohols. *Angew. Chem., Int. Ed.* **2016**, *55*, 14967−14971. (f) Elangovan, S.; Sortais, J.-B.; Beller, M.; Darcel, C. Iron-Catalyzed α-Alkylation of Ketones with Alcohols. *Angew. Chem., Int. Ed.* **2015**, *54*, 14483−14486.

(5) (a) El-Sepelgy, O.; Matador, E.; Brzozowska, A.; Rueping, M. C-Alkylation of Secondary Alcohols by Primary Alcohols through Manganese-Catalyzed Double Hydrogen Autotransfer. *ChemSusChem* **2019**, DOI: 10.1002/cssc.201801660. (b) Liu, T.; Wang, L.; Wu, K.; Yu, Z. Manganese-Catalyzed β-Alkylation of Secondary Alcohols with Primary Alcohols under Phosphine-Free Conditions. *ACS Catal.* **2018**, *8*, 7201−7207. (c) Kulkarni, N. V.; Brennessel, W. W.; Jones, W. D. Catalytic Upgrading of Ethanol to n-Butanol via Manganese-Mediated Guerbet Reaction. *ACS Catal.* **2018**, *8*, 997−1002. (d) Fu, S.; Shao, Z.; Wang, Y.; Liu, Q. Manganese-Catalyzed Upgrading of Ethanol into 1-Butanol. *J. Am. Chem. Soc.* **2017**, *139*, 11941−11948. (e) Freitag, F.; Irrgang, T.; Kempe, R. Cobalt-Catalyzed Alkylation of Secondary Alcohols with Primary Alcohols via Borrowing Hydrogen/Hydrogen Autotransfer. *Chem. − Eur. J.* **2017**, *23*, 12110−12113.

(6) (a) Jang, Y. K.; Krückel, T.; Rueping, M.; El-Sepelgy, O. Sustainable Alkylation of Unactivated Esters and Amides with Alcohols Enabled by Manganese Catalysis. *Org Lett.* **2018**, *20*, 7779−7783. (b) Chakraborty, S.; Daw, P.; Ben David, Y.; Milstein, D. Manganese-Catalyzed α-Alkylation of Ketones, Esters, and Amides Using Alcohols. *ACS Catal.* **2018**, *8*, 10300−10305. (c) Deibl, N.; Kempe, R. General and Mild Cobalt-Catalyzed C-Alkylation of

DOI: 10.1021/acs.joc.9b00792
J. Org. Chem. 2019, 84, 7927−7935

Unactivated Amides and Esters with Alcohols. *J. Am. Chem. Soc.* **2016**, *138*, 10786−10789.
(7) Werkmeister, S.; Bornschein, C.; Junge, K.; Beller, M. Selective Ruthenium-Catalyzed Transfer Hydrogenations of Nitriles to Amines with 2-Butanol. *Chem. − Eur. J.* **2013**, *19*, 4437−4440.
(8) (a) Paul, B.; Shee, S.; Panja, D.; Chakrabarti, K.; Kundu, S. Direct Synthesis of N,N-Dimethylated and β-Methyl N,N-Dimethylated Amines from Nitriles Using Methanol: Experimental and Computational Studies. *ACS Catal.* **2018**, *8*, 2890−2896. (b) Werkmeister, S.; Bornschein, C.; Junge, K.; Beller, M. Ruthenium-Catalyzed Transfer Hydrogenation of Nitriles: Reduction and Subsequent N-Monoalkylation to Secondary Amines. *Eur. J. Org. Chem.* **2013**, 3671−3674.
(9) (a) Kang, B.; Hong, S. H. Hydrogen Acceptor- and Base-Free N-Formylation of Nitriles and Amines using Methanol as C1 Source. *Adv. Synth. Catal.* **2015**, *357*, 834−840. (b) Kang, B.; Fu, Z.; Hong, S. H. Ruthenium-Catalyzed Redox-Neutral and Single-Step Amide Synthesis from Alcohol and Nitrile with Complete Atom Economy. *J. Am. Chem. Soc.* **2013**, *135*, 11704−11707.
(10) Li, F.; Zou, X.; Wang, N. Direct Coupling of Arylacetonitriles and Primary Alcohols to α-Alkylated Arylacetamides with Complete Atom Economy Catalyzed by a Rhodium Complex−Triphenylphosphine−Potassium Hydroxide System. *Adv. Synth. Catal.* **2015**, *357*, 1405−1415.
(11) Chakraborty, S.; Das, U. K.; Ben-David, Y.; Milstein, D. Manganese Catalyzed α-Olefination of Nitriles by Primary Alcohols. *J. Am. Chem. Soc.* **2017**, *139*, 11710−11713.
(12) (a) Thiyagarajan, S.; Gunanathan, C. Facile Ruthenium(II)-Catalyzed α-Alkylation of Arylmethyl Nitriles Using Alcohols Enabled by Metal−Ligand Cooperation. *ACS Catal.* **2017**, *7*, 5483−5490. (b) Alós, J.; Bolaño, T.; Esteruelas, M. A.; Oliván, M.; Oñate, E.; Valencia, M. POP−Pincer Ruthenium Complexes: d6 Counterparts of Osmium d4 Species. *Inorg. Chem.* **2014**, *53*, 1195−1209. (c) Kuwahara, T.; Fukuyama, T.; Ryu, I. Synthesis of Alkylated Nitriles by $[RuHCl(CO)(PPh_3)_3]$-Catalyzed Alkylation of Acetonitrile Using Primary Alcohols. *Chem. Lett.* **2013**, *42*, 1163−1165. (d) Cheung, H. W.; Li, J.; Zheng, W.; Zhou, Z.; Chiu, Y. H.; Lin, Z.; Lau, C. P. Dialkylamino Cyclopentadienyl Ruthenium(ii) Complex-Catalyzed α-Alkylation of Arylacetonitriles with Primary Alcohols. *Dalton Trans.* **2010**, *39*, 265−274. (e) Motokura, K.; Fujita, N.; Mori, K.; Mizugaki, T.; Ebitani, K.; Jitsukawa, K.; Kaneda, K. Environmentally Friendly One-Pot Synthesis of α-Alkylated Nitriles Using Hydrotalcite-Supported Metal Species as Multifunctional Solid Catalysts. *Chem. − Eur. J.* **2006**, *12*, 8228−8239. (f) Motokura, K.; Nishimura, D.; Mori, K.; Mizugaki, T.; Ebitani, K.; Kaneda, K. A. Ruthenium-Grafted Hydrotalcite as a Multifunctional Catalyst for Direct α-Alkylation of Nitriles with Primary Alcohols. *J. Am. Chem. Soc.* **2004**, *126*, 5662−5663. (g) Zhu, Z.-H.; Li, Y.; Wang, Y.-B.; Lan; Xinju, Z.-G.; Zhu, X.; Hao, X.-Q.; Song, M.-P. α-Alkylation of Nitriles with Alcohols Catalyzed by NNN′Pincer Ru(II) Complexes Bearing Bipyridyl Imidazoline Ligands. *Organometallics* **2019**, *38*, 2156.
(13) (a) Sawaguchi, T.; Obora, Y. Iridium Catalyzed α-Alkylation of Acetonitrile with Primary and Secondary Alcohols. *Chem. Lett.* **2011**, *40*, 1055−1057. (b) Anxionnat, B.; Gomez Pardo, D.; Ricci, G.; Cossy, J. Monoalkylation of Acetonitrile by Primary Alcohols Catalyzed by Iridium Complexes. *Org. Lett.* **2011**, *13*, 4084−4087. (c) Morita, M.; Obora, Y.; Ishii, Y. Alkylation of active methylene compounds with alcohols catalyzed by an iridium complex. *Chem. Commun.* **2007**, 2850−2852. (d) Löfberg, C.; Grigg, R.; Whittaker, M. A.; Keep, A.; Derrick, A. Efficient Solvent-Free Selective Monoalkylation of Arylacetonitriles with Mono-, Bis-, and Tris-primary Alcohols Catalyzed by a Cp*Ir Complex. *J. Org. Chem.* **2006**, *71*, 8023−8027. (e) Ishii, Y.; Iwahama; Takahiro, N. Tatsuya Preparation of Nitriles by α-Alkylation by Alcohols. JP2005-64657, 2005.
(14) (a) Li, J.; Liu, Y.; Tang, W.; Xue, D.; Li, C.; Xiao, J.; Wang, C. Atmosphere-Controlled Chemoselectivity: Rhodium-Catalyzed Alkylation and Olefination of Alkylnitriles with Alcohols. *Chem. − Eur. J.* **2017**, *23*, 14445−14449.
(15) Buil, M. L.; Esteruelas, M. A.; Herrero, J.; Izquierdo, S.; Pastor, I. M.; Yus, M. Osmium Catalyst for the Borrowing Hydrogen Methodology: α-Alkylation of Arylacetonitriles and Methyl Ketones. *ACS Catal.* **2013**, *3*, 2072−2075.
(16) Corma, A.; Rjdenas, T.; Sabater, M. J. Monoalkylations with alcohols by a cascade reaction on bifunctional solid catalysts: Reaction kinetics and mechanism. *J. Catal.* **2011**, *279*, 319−327.
(17) (a) López, R.; Palomo, C. Cyanoalkylation: Alkylnitriles in Catalytic C-C Bond Forming Reactions. *Angew. Chem., Int. Ed.* **2015**, *54*, 13170−13184. and the references cited in (b) Rappoport, Z.; Patai, S. *Chemistry of the Cyano Group*; Wiley: London, 1970.
(18) Ma, W.; Cui, S.; Sun, H.; Tang, W.; Xue, D.; Li, C.; Fan, J.; Xiao, J.; Wang, C. Iron Catalyzed Alkylation of Nitriles with Alcohols. *Chem. − Eur. J.* **2018**, *24*, 13118−13123.
(19) (a) El-Sepelgy, O.; Alandini, N.; Rueping, M. Merging Iron Catalysis and Biocatalysis—Iron Carbonyl Complexes as Efficient Hydrogen Autotransfer Catalysts in Dynamic Kinetic Resolutions. *Angew. Chem., Int. Ed.* **2016**, *55*, 13602−13605. (b) El-Sepelgy, O.; Brzozowska, A.; Azofra, L. M.; Jang, Y. K.; Cavallo, L.; Rueping, M. Experimental and Computational Study of an Unexpected Iron-Catalyzed Carboetherification by Cooperative Metal and Ligand Substrate Interaction and Proton Shuttling. *Angew. Chem., Int. Ed.* **2017**, *56*, 14863−14867. (c) El-Sepelgy, O.; Brzozowska, A.; Rueping, M. Asymmetric Chemoenzymatic Reductive Acylation of Ketones by a Combined Iron-Catalyzed Hydrogenation-Racemization and Enzymatic Resolution Cascade. *ChemSusChem* **2017**, *10*, 1664−1668. (d) El-Sepelgy, O.; Brzozowska, A.; Sklyaruk, J.; Jang, Y. K.; Zubar, V.; Rueping, M. Cooperative Metal−Ligand Catalyzed Intramolecular Hydroamination and Hydroalkoxylation of Allenes Using a Stable Iron Catalyst. *Org. Lett.* **2018**, *20*, 696−699.
(20) Mn-catalyzed hydrogenation of polar bonds, seminal example: (a) Elangovan, S.; Topf, C.; Fischer, S.; Jiao, H.; Spannenberg, A.; Baumann, W.; Ludwig, R.; Junge, K.; Beller, M. Selective Catalytic Hydrogenations of Nitriles, Ketones, and Aldehydes by Well-Defined Manganese Pincer Complexes. *J. Am. Chem. Soc.* **2016**, *138*, 8809−8814. Example from our group: (b) Zubar, V.; Lebedev, Y.; Azofra, L. M.; Cavallo, L.; El-Sepelgy, O.; Rueping, M. Hydrogenation of CO_2-Derived Carbonates and Polycarbonates to Methanol and Diols by Metal−Ligand Cooperative Manganese Catalysis. *Angew. Chem., Int. Ed.* **2018**, *57*, 13439−13443.
(21) Mn-catalyzed hydrogenation of non-polar bonds: (a) Brzozowska, A.; Azofra, L. M.; Zubar, V.; Atodiresei, I.; Cavallo, L.; Rueping, M.; El-Sepelgy, O. Highly Chemo- and Stereoselective Transfer Semihydrogenation of Alkynes Catalyzed by a Stable, Well-Defined Manganese(II) Complex. *ACS Catal.* **2018**, *8*, 4103−4109. (b) Zhou, Y. P.; Mo, Z.; Luecke, M. P.; Driess, M. Stereoselective Transfer Semi-Hydrogenation of Alkynes to E-Olefins with N-Heterocyclic Silylene−Manganese Catalysts. *Chem. − Eur. J.* **2018**, *24*, 4780−4784.
(22) For recent reviews on Mn-catalysis: Recent Reviews: (a) Zell, T.; Langer, R. From Ruthenium to Iron and Manganese—A Mechanistic View on Challenges and Design Principles of Base-Metal Hydrogenation Catalysts. *ChemCatChem* **2018**, *10*, 1930−1940. (b) Mukherjee, A.; Milstein, D. Homogeneous Catalysis by Cobalt and Manganese Pincer Complexes. *ACS Catal* **2018**, *8*, 11435−11469. (c) Kallmeier, F.; Kempe, R. Manganese Complexes for (De)Hydrogenation Catalysis: A Comparison to Cobalt and Iron Catalysts. *Angew. Chem., Int. Ed.* **2018**, *57*, 46−60. (d) Gorgas, N.; Kirchner, K. Isoelectronic Manganese and Iron Hydrogenation/Dehydrogenation Catalysts: Similarities and Divergences. *Acc. Chem. Res.* **2018**, *51*, 1558−1569. (e) Filonenko, G. A.; van Putten, R.; Hensen, E. J. M.; Pidko, E. A. Catalytic (de)hydrogenation promoted by non-precious metals − Co, Fe and Mn: recent advances in an emerging field. *Chem. Soc. Rev.* **2018**, *47*, 1459−1483. (f) Maji, B.; Barman, M. K. Recent Developments of Manganese Complexes for Catalytic Hydrogenation and Dehydrogenation Reactions. *Synthesis* **2017**, *49*, 3377−3393. (g) Garbe, M.; Junge, K.; Beller, M. Homogeneous Catalysis by Manganese-Based Pincer Complexes. *Eur. J. Org. Chem.* **2017**, 4344−4362. (h) Valyaev, D. A.; Lavigne, G.; Lugan, N. Manganese organometallic compounds in homogeneous

DOI: 10.1021/acs.joc.9b00792
J. Org. Chem. 2019, 84, 7927−7935

catalysis: Past, present, and prospects. *Coord. Chem. Rev.* **2016**, *308*, 191−235. (i) Carney, J. R.; Dillon, B. R.; Thomas, S. P. Recent Advances of Manganese Catalysis for Organic Synthesis. *Eur. J. Org. Chem.* **2016**, 3912−3929. For recent examples from our group: (j) Borghs, J. C.; Azofra, L. M.; Biberger, T.; Linnenberg, O.; Cavallo, L.; Rueping, M.; El-Sepelgy, O. Manganese-Catalyzed Multicomponent Synthesis of Pyrroles through Acceptorless Dehydrogenation Hydrogen Autotransfer Catalysis: Experiment and Computation. *ChemSusChem* **2019**, DOI: 10.1002/cssc.201802416. (k) Borghs, J. C.; Lebedev, Y.; Rueping, M.; El-Sepelgy, O. Sustainable Manganese-Catalyzed Solvent-Free Synthesis of Pyrroles from 1,4-Diols and Primary Amines. *Org. Lett.* **2019**, *21*, 70−74.

(23) Jana, A.; Reddy, C. B.; Maji, B. Manganese Catalyzed α-Alkylation of Nitriles with Primary Alcohols. *ACS Catal.* **2018**, *8*, 9226−9231.

(24) Liu, W.; Ackermann, L. Manganese-Catalyzed C−H Activation. *ACS Catal.* **2016**, *6*, 3743−3752.

(25) For a recent detailed DFT study: (a) Luque-Urrutia, J. A.; Solà, M.; Milstein, D.; Poater, A. Mechanism of the Manganese-Pincer-Catalyzed Acceptorless Dehydrogenative Coupling of Nitriles and Alcohols. *J. Am. Chem. Soc.* **2019**, *141*, 2398−2403. (b) Lu, Y.; Zhao, R.; Guo, J.; Liu, Z.; Dagnaw, W. M.; Wang, Z. A Unified Mechanism to Account for Manganese or Ruthenium Catalyzed Nitrile α-Olefinations by Primary or Secondary Alcohols: A DFT Mechanistic Study. *Chem. − Eur. J.* **2019**, *25*, 3939−3949. For related observations: (c) Vogt, M.; Nerush, A.; Iron, M. A.; Leitus, G.; Diskin-Posner, Y.; Shimon, L. J. W.; Ben-David, Y.; Milstein, D. Activation of Nitriles by Metal Ligand Cooperation. Reversible Formation of Ketimido- and Enamido-Rhenium PNP Pincer Complexes and Relevance to Catalytic Design. *J. Am. Chem. Soc.* **2013**, *135*, 17004−17018. (d) Perdriau, S.; Zijlstra, D. S.; Heeres, H. J.; de Vries, J. G.; Otten, E. A Metal−Ligand Cooperative Pathway for Intermolecular Oxa-Michael Additions to Unsaturated Nitriles. *Angew. Chem., Int. Ed.* **2015**, *54*, 4236−4240. (e) Nerush, A.; Vogt, M.; Gellrich, U.; Leitus, G.; Ben-David, Y.; Milstein, D. Template Catalysis by Metal−Ligand Cooperation. C−C Bond Formation via Conjugate Addition of Non-activated Nitriles under Mild, Base-free Conditions Catalyzed by a Manganese Pincer Complex. *J. Am. Chem. Soc.* **2016**, *138*, 6985−6997.

(26) (a) Shang, R.; Ji, D.-S.; Chu, L.; Fu, Y.; Liu, L. Synthesis of α-Aryl Nitriles through PalladiumCatalyzed Decarboxylative Coupling of Cyanoacetate Salts with Aryl Halides and Triflates. *Angew. Chem., Int. Ed.* **2011**, *50*, 4470−4474. (b) Xiao, J.; Yang, J.; Chen, T.; Hana, L.-B. Nickel Catalyzed α-Benzylation of Arylacetonitriles via C-O Activation. *Adv. Synth. Catal.* **2016**, *358*, 816−819. (c) Kulp, S. S.; Caldwell, C. B. Reduction of alpha, beta-diarylacrylonitriles by sodium borohydride. *J. Org. Chem.* **1980**, *45*, 171−173. (d) Choi, J.; Fu, G. C. Catalytic Asymmetric Synthesis of Secondary Nitriles via Stereoconvergent Negishi Arylations and Alkenylations of Racemic α-Bromonitriles. *J. Am. Chem. Soc.* **2012**, *134*, 9102−9105. (e) Huang, Y.; Yu, Y.; Zhu, Z.; Zhu, C.; Cen, J.; Li, X.; Wu, W.; Jiang, H. Copper-Catalyzed Cyanation of N-Tosylhydrazones with Thiocyanate Salt as the "CN" Source. *J. Org. Chem.* **2017**, *82*, 7621−7627. (f) Chen, G.; Wang, Z.; Wu, J.; Ding, K. Facile Preparation of α-Aryl Nitriles by Direct Cyanation of Alcohols with TMSCN Under the Catalysis of InX_3. *Org. Lett.* **2008**, *10*, 4573−4576. (g) Cheng, A.; Uyeno, E.; Polgar, W.; Toll, L.; Lawson, J. A.; DeGraw, J. I.; Loew, G.; Camerman, A.; Camerman, N. N-Substituent modulation of opiate agonist/antagonist activity in resolved 3-methyl-3-(m-hydroxyphenyl)piperidines. *J. Med. Chem.* **1986**, *29*, 531−537. (h) Möhrle, H.; Pycior, M. 2-(Pyridyl)-propionitriles and their Aminomethylation. *Arch. Pharm.* **1995**, *328*, 293−296. (i) Guin, J.; Varseev, G.; List, B. Catalytic Asymmetric Protonation of Silyl Ketene Imines. *J. Am. Chem. Soc.* **2013**, *135*, 2100−2103.

DOI: 10.1021/acs.joc.9b00792
J. Org. Chem. 2019, 84, 7927−7935

Paper 11:

Conversion of racemic alcohols to optically pure amine precursors enabled by catalyst dynamic kinetic resolution: experiment and computation.

Azofra, L. M.*; Tran, M. A.; Zubar, V.; Cavallo, L.; Rueping, M.; El-Sepelgy, O.*

Chem. Commun. **2020**, *56*, 9094-9097.

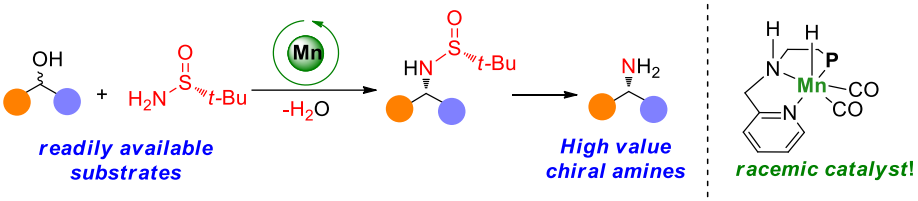

Volume 56
Number 64
18 August 2020
Pages 9043–9224

ChemComm

Chemical Communications

rsc.li/chemcomm

ISSN 1359-7345

ROYAL SOCIETY OF CHEMISTRY

COMMUNICATION

Luis Miguel Azofra, Osama El-Sepelgy *et al.*
Conversion of racemic alcohols to optically pure amine precursors enabled by catalyst dynamic kinetic resolution: experiment and computation

ChemComm

COMMUNICATION

View Article Online
View Journal | View Issue

Cite this: *Chem. Commun.*, 2020, **56**, 9094

Received 21st April 2020,
Accepted 29th June 2020

DOI: 10.1039/d0cc02881a

rsc.li/chemcomm

Conversion of racemic alcohols to optically pure amine precursors enabled by catalyst dynamic kinetic resolution: experiment and computation†

Luis Miguel Azofra,[a] Mai Anh Tran,[b] Viktoriia Zubar,[b] Luigi Cavallo,[c] Magnus Rueping[bc] and Osama El-Sepelgy[b]

An unprecedented base metal catalysed asymmetric synthesis of α-chiral amine precursors from racemic alcohols is reported. This redox-neutral reaction utilises a bench-stable manganese complex and Ellman's sulfinamide as a versatile ammonia surrogate. DFT calculations explain the unusual finding of the highly stereoselective transformation enabled by a catalyst that undergoes an unusual dynamic kinetic resolution.

Chiral primary amines are of great importance in the pharmaceutical and agrochemical industries. In fact, at least 40% of the optically active drugs are chiral amines. Biocatalytic kinetic resolution of racemic amines with 50% maximum yield is probably the most widely practiced method for the production of enantiopure primary amines. Additionally, hydrogenation using man-made catalysis (transition-metal catalysis and organocatalysis), which requires hydrogen gas under high pressure or stoichiometric amounts of a reductant, often involves the use of hard to remove protecting groups. Besides, methods involving chemoenzymatic dynamic kinetic resolution, cascade deracemization of racemic amines, have been reported.[1]

The hydrogen autotransfer (HA) strategy has captured much attention during the last few years, mainly due to its synthetic importance as a powerful environmentally benign approach for the construction of C–C and C–N bonds. In this regard, progress has been made in transition-metal catalysed *C*-alkylations and *N*-alkylations with non-activated alcohols. The reactions mainly rely on the production of achiral or racemic products.[2]

The direct asymmetric amination of alcohols to produce chiral aniline,[3] amino alcohols,[4] oxazolidinones,[5] and hydrazones[6] has been demonstrated using ruthenium and iridium catalysis. In contrast, the direct production of chiral primary amines from racemic alcohols is significantly more challenging. In this regard, a ruthenium catalysed protocol was disclosed. However, this noble metal method is limited to the methyl substituted chiral amines.[7] Apart from metal catalysis, the use of a dual enzymatic system for the direct amination of secondary alcohols has been reported.[8] Therefore, the development of a new catalytic system, ideally based on a non-precious metal catalyst,[9] which can transform a broad range of racemic alcohols to enantiopure primary amines, is an elusive goal.[10]

Ellman's sulfinamide represents as an industrially relevant reagent, frequently used as an ammonia surrogate in the synthesis of enantiopure primary amines.[11] This transformation typically requires three chemical steps, *i.e.*, stoichiometric

Luis Miguel Azofra

Luis Miguel Azofra loves Quantum Chemistry as much as the sea. The latter was a gift he received for being born in the Canary Islands, the first is a passion he learned during his PhD in Prof. Alkorta's lab (CSIC, Spain). In 2015, Dr Sun and Prof. MacFarlane introduced him to the field of catalysis (Monash University, Australia), and in 2016 he joined Prof. Cavallo's group as an in silico designer (KAUST, Saudi Arabia). Currently, Dr Azofra is an early-career research leader at Universidad de Las Palmas de Gran Canaria, where he combines his efforts as a researcher and lecturer.

[a] *Instituto de Estudios Ambientales y Recursos Naturales (i-UNAT), Universidad de Las Palmas de Gran Canaria (ULPGC), Campus de Tafira, 35017, Las Palmas de Gran Canaria, Spain. E-mail: luismiguel.azofra@ulpgc.es*
[b] *Institute of Organic Chemistry, RWTH Aachen University, Landoltweg 1, 52074 Aachen, Germany. E-mail: Osama.Elsepelgy@rwth-aachen.de*
[c] *KAUST Catalysis Center (KCC), King Abdullah University of Science and Technology (KAUST), Thuwal 23955-6900, Saudi Arabia*

† Electronic supplementary information (ESI) available: Full experimental and computational details and optimised Cartesian coordinates. See DOI: 10.1039/d0cc02881a

oxidation, condensation using stoichiometric titanium reagent and stoichiometric reduction, producing large quantities of waste.

Encouraged by recent studies on metal catalysed hydrogen autotransfer,[2,12,13] we envisioned that an effective base-metal catalyst might potentially catalyse the oxidative dehydrogenation of the *sec*-alcohols (*rac*-**1**), to form the corresponding ketone and shuttle the abstracted hydrogen required for the stereoselective hydrogenation. The *in situ* formed ketone undergoes condensation with an ammonia equivalent to produce an imine and only water as a by-product. Finally, the imine will be reduced in a stereoselective fashion to produce the desired product. The chemoselectivity of the reaction depends on the potential of the metal catalyst to return the stored hydrogen to the final product.

Herein, we present a new manganese catalysed synthesis of optically active amines from racemic alcohols. Interestingly, our DFT mechanistic study on this stereoselective reaction explains how a racemic catalyst could lead to optically pure product. Notably, we found that the high stereocontrol is enabled by unusual catalyst dynamic kinetic resolution (Scheme 1a). The chiral imine intermediate kinetically discriminates the catalyst racemic mixture (Scheme 1b). While only one enantiomer of the catalyst can be involved in the stereoselective hydrogenation reaction, the ketone intermediate plays the crucial role in the racemisation of the second catalyst enantiomer (Scheme 1a). We are not aware of a literature report with such an unusual observation.

We started our study with the selection of the appropriate base metal catalyst and the optimisation of the suitable reaction parameters. After careful investigations, we found that the use of the air stable PNN-Mn complex (5 mol%) in combination

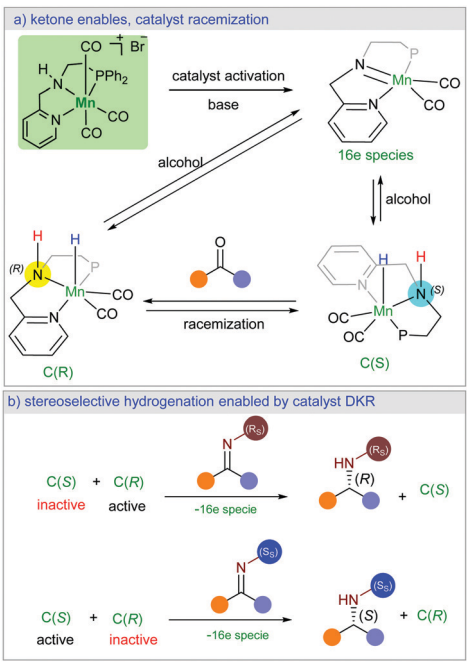

Scheme 1 Manganese-catalysed diasteroselective hydrogen autotransfer.

Table 1 Manganese catalysed asymmetric amination of *sec*-alcohols[a]

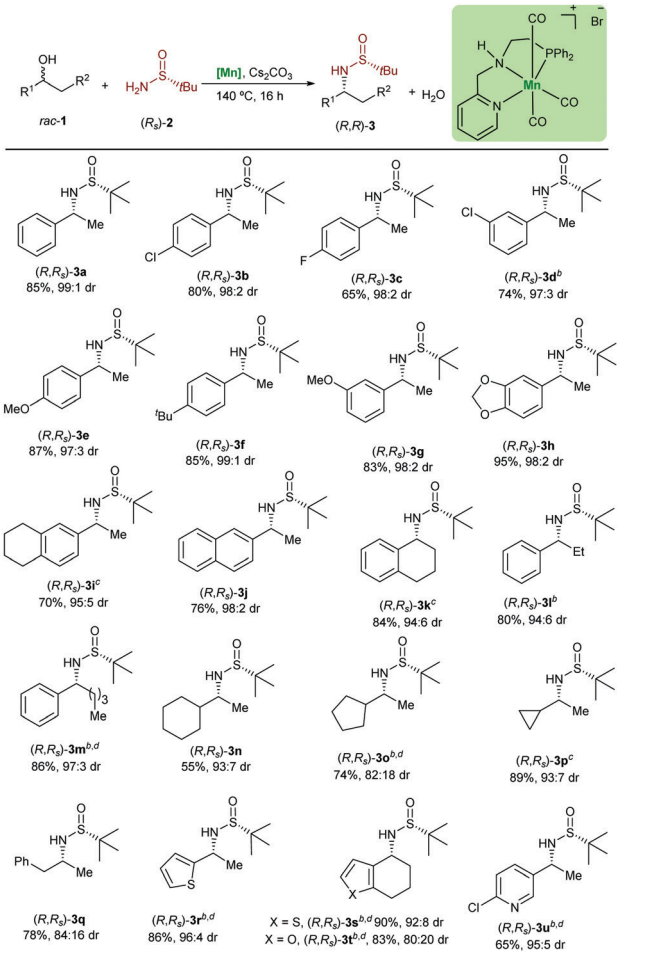

[a] Reaction conditions: **1** (0.75 mmol), (*R*)-**2a** (0.5 mmol), [Mn] (0.025 mmol) and Cs_2CO_3 (0.05 mmol) in *t*-amyl alcohol (1 mL) were stirred at 140 °C (aluminum block), for 16 h in a glass tube under argon. Yields after column chromatography are given. [b] [Mn] (0.05 mmol), Cs_2CO_3 (0.1 mmol). [c] 48 h. [d] **1** (1 mmol).

with Cs_2CO_3 (10 mol%) and *t*-amyl alcohol (0.5 M) is the optimal combination for this reaction (see the ESI† for details).

Next, the variability and the applicability of the asymmetric hydrogen autotransfer reaction were investigated (Table 1). We initially explored different racemic benzylic alcohols. The alcohols **1a–1i** bearing different electron donating and electron withdrawing groups were applicable without significant effect on the reactivity or the stereochemical outcome and all desired products **3a–3i** were isolated in very good yields and optical purity. Similarly, the naphthyl substituted sulfinamide (R,R_S)-**3j** was isolated in very good yield and selectivity. Importantly, some of these amines are key intermediates in the synthesis of pharmaceuticals and bioactive molecules. For example, carpropamid,[14] an agriculture fungicide, can be prepared from (R,R_S)-**3b**, whereas the Alzheimer's and Parkinson's drug rivastigmine can be produced using the sulfinylamine (S,S_S)-**3g**.[15] It is noteworthy that the classical synthesis of these α-chiral amines involves the addition of MeLi to *N*-*tert*-butylsulfinyl

aldimes. However, this reaction often suffers from unfavourable diastereocontrol, even at lower temperature. To our delight, our catalytic system was found not to be limited to the *sec*-phenethyl alcohol derivatives. Thus, 1-tetralol (**1k**) was converted to the desired product in 84% yield. This amine is of relevance as it is used in the synthesis of diverse bio-related compounds.[16] The ethyl substituted alcohol **1l** and the more challenging alcohol **1m** were found to be reactive using the presented catalytic system. With this success, we turned our attention to the more demanding non-benzylic alcohols **1n–1q**. The chiral amines bearing a cyclohexyl substituent (R,R_s)-**3n** and cyclopropyl substituent (R,R_s)-**3p** were produced in a very good diastereomeric ratio as well. Interestingly, the amphetamine, which is used in the treatment of attention deficit hyperactivity disorder, can be obtained from the *rac*-**1q** in 78% yield. Heterocycle-containing alcohols were also tolerated and underwent the reaction to afford the chiral amine precursors (R,R_s)-**3r** to (R,R_s)-**3u** in very good yields and with high diastereoselectivity. Interestingly, despite the importance of the optically pure **3s** and **3r** in the synthesis of HIV protease inhibitors,[17] the asymmetric synthesis of the corresponding primary amines is not yet reported. It is noteworthy that even pyridine containing substrates and products, such as **3u** are tolerated in this manganese catalysed reaction.

In order to understand the origin of the stereoselective hydrogenation, we have carried out DFT modelling for the asymmetric amination of 1-phenylethanol (Scheme 2). The 16e species **A**, which can be generated by treating the manganese pre-catalyst [Mn] with appropriate bases, dehydrogenates the alcohol substrate *rac*-**1a** to produce acetophenone and manganese hydride complex **C**. Based on our DFT results, the alcohol dehydrogenation step takes place in a stepwise fashion *via* the formation of four different diastereoisomers of manganese alkoxide intermediates **B**, bearing chiral nitrogen and carbon atoms. However, the proton transfer **A–B** is a barrier-less process. The calculated free activation energy for the hydride transfer **B–C** steps are between 19.9 and 20.1 kcal mol^{-1} at the M06/TZVP level of theory. The β-hydride elimination will lead to the formation of a racemic mixture of the hydrogenated catalyst **C**(***S***) and **C**(***R***).

The condensation reaction between the *in situ* generated ketone and (R_s)-**2** results in the generation of a C=N bond which can be potentially hydrogenated by the action of racemic manganese catalyst **C**(***S***) and **C**(***R***). Similarly, to the alcohol substrate dehydrogenation, we found that the hydrogenation of the imine intermediate takes place *via* a stepwise mechanism. Since the hydrogenated catalyst exists as a racemic mixture, it establishes the possibility of the hydride transfer (**C–D**) to form four different intermediates **D**. Importantly, we found that the hydride transfer step (**C–D**) is the rate determining step as well as the stereodetermining step. When the manganese catalyst **C**(***R***) was used for the hydrogenation of an imine bearing (R)-sulfinamide group, the computed barrier for the hydride transfer is 29.1 kcal mol^{-1} for the creation of a new (R) stereogenic centre, while the barrier for the generation of the (S) stereogenic centre is 33.1 kcal mol^{-1}. On the other hand, the barriers for the hydride transfer using the catalyst enantiomer **C**(***S***) are 39.5 and 36.3 kcal mol^{-1}. Interestingly, when an imine bearing (S)-sulfinamide group is used as a substrate, only the (S) enatiomer of the catalyst is involved in the imine hydrogenation step and creates a new stereogenic centre with the (S) configuration. With this process being controlled by kinetics, it

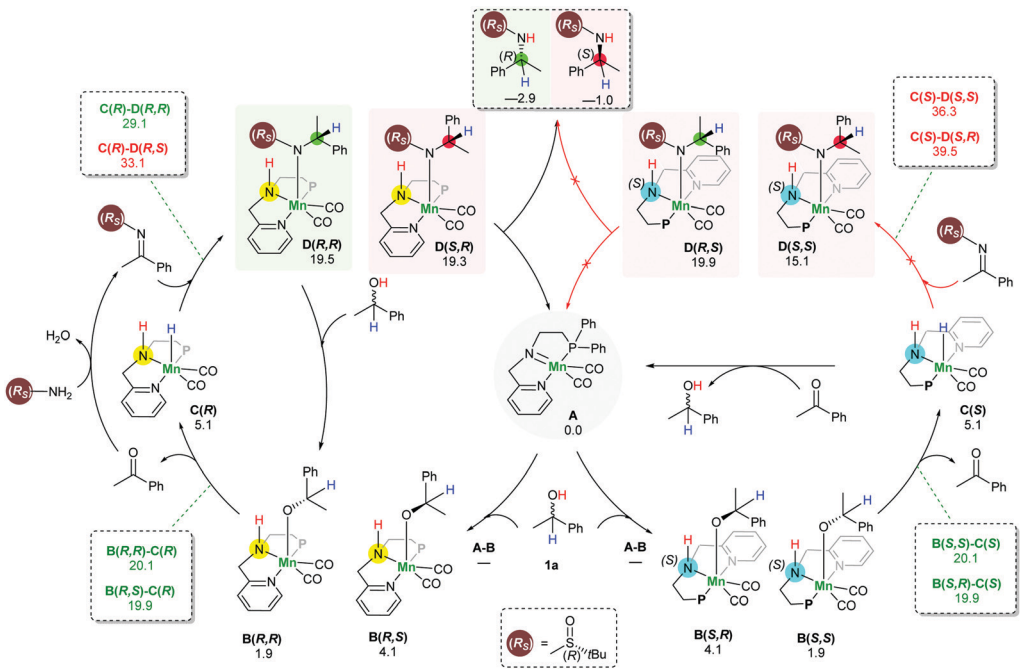

Scheme 2 Proposed reaction mechanism for the stereoselective manganese catalysed hydrogen autotransfer amination of *rac*-alcohols. Free reaction and activation energies (at 140 °C) are shown in kcal mol^{-1} at the M06/TZVP level using toluene as a solvent.

supposes a diasteoisomeric ratio equal to 99 : 1. This is fully in agreement with our experimental results.

The last step involves the proton transfer to the product nitrogen atom. The proton could be internally transferred from the catalyst NH group to generate the product and the 16e species **A**. Alternatively, in the presence of excess *rac*-**1a**, direct proton transfer from the alcohol substrate could take place to produce the desired product and the intermediates **B** without the regeneration of the 16e species **A**.[18] Notably, calculations show that the undesired catalyst enantiomer **C(*S*)** can be easily racemised with the assistance of the acetophenone intermediate. In other words, the steps **C(*S*)–B(*S*,*R*)**, **C(*S*)–B(*S*,*S*)**, **B(*S*,*S*)–A** and **B(*S*,*R*)–A** are reversible. We are not aware of a previously reported mechanism with a similar observation of the catalyst racemisation assisted by the *in situ* generated intermediate.

In conclusion, we have developed an unprecedented base-metal catalysed stereoselective amination of racemic alcohols using the hydrogen autotransfer strategy. The produced enatiomerically pure sulfinamides could be easily converted to the corresponding α-chiral amine upon stirring in methanolic HCl at room temperature.[19] Notably, the protocol uses an inexpensive earth-abundant manganese complex and readily available substrates. Our DFT calculations demonstrate the origin of high diastereoselectivity which is enabled by an unusual catalyst dynamic kinetic resolution process. We found that the alcohol dehydrogenation and imine hydrogenation reactions occur in a stepwise fashion, while the hydride transfer to the imine intermediate represents the rate and stereodetermining step of the whole reaction. Given the operational simplicity, the presented catalytic system will serve as a basis for further application in the synthesis of relevant optically pure α-chiral amines and heterocycles.

L. M. A. thanks Universidad de Las Palmas de Gran Canaria (ULPGC) for support. Gratitude is also due to the KAUST for use of the supercomputer Shaheen II for providing the computational resources.

Conflicts of interest

There are no conflicts to declare.

Notes and references

1 (*a*) C. Aranda, G. Oksdath-Mansilla, F. R. Bisogno and G. de Gonzalo, *Adv. Synth. Catal.*, 2020, **362**, 1233–1257; (*b*) D. Ghislieri and N. J. Turner, *Top. Catal.*, 2014, **57**, 284–300; (*c*) C. E. Humphrey, M. Ahmed, A. Ghanem and N. J. Turner, in *Separation of Enantiomers: Synthetic Methods*, ed. M. Todd, Wiley-VCH, Weinheim, 2014, pp. 123–160; (*d*) M. D. Truppo, N. J. Turner and J. D. Rozzell, *Chem. Commun.*, 2009, 2127–2129; (*e*) T. C. Nugent, *Chiral Amine Synthesis*, Wiley-VCH, Weinheim, 2010; (*f*) M. Rueping, E. Sugiono, C. Azap, T. Theissmann and M. Bolte, *Org. Lett.*, 2005, **7**, 3781–3783.

2 (*a*) A. Corma, J. Navas and M. J. Sabater, *Chem. Rev.*, 2018, **118**, 1410–1459; for the production of chiral products using biocatalysis: (*b*) E. Tassano and M. Hall, *Chem. Soc. Rev.*, 2019, **48**, 5596–5615.

3 (*a*) Y. Zhang, C.-S. Lim, D. S. B. Sim, H.-J. Pan and Y. Zhao, *Angew. Chem., Int. Ed.*, 2014, **53**, 1399–1403; (*b*) Z.-Q. Rong, Y. Zhang, R. H. B. Chua, H.-J. Pan and Y. Zhao, *J. Am. Chem. Soc.*, 2015, **137**, 4944–4947; (*c*) C. S. Lim, T. T. Quach and Y. Zhao, *Angew. Chem., Int. Ed.*, 2017, **56**, 7176–7180.

4 (*a*) A. E. Putra, Y. Oe and T. Ohta, *Eur. J. Org. Chem.*, 2013, 6146–6151; (*b*) L.-C. Yang, Y.-N. Wang, Y. Zhang and Y. Zhao, *ACS Catal.*, 2017, **7**, 93–97.

5 M. Peña-López, H. Neumann and M. Beller, *Angew. Chem., Int. Ed.*, 2016, **55**, 7826–7830.

6 P. Yang, C. Zhang, Y. Ma, C. Zhang, A. Li, B. Tang and J. S. Zhou, *Angew. Chem., Int. Ed.*, 2017, **56**, 14702–14706.

7 N. J. Oldenhuis, V. M. Dong and Z. Guan, *J. Am. Chem. Soc.*, 2014, **136**, 12548–12551.

8 (*a*) F. G. Mutti, T. Knaus, N. S. Scrutton, M. Breuer and N. J. Turner, *Science*, 2015, **349**, 1525–1529; (*b*) S. L. Montgomery, J. Mangas-Sanchez, M. P. Thompson, G. A. Aleku, B. Dominguez and N. J. Turner, *Angew. Chem., Int. Ed.*, 2017, **56**, 10491–10494; (*c*) M. P. Thompson and N. J. Turner, *ChemCatChem*, 2017, **9**, 3833–3836; (*d*) W. Böhmer, T. Knaus and F. G. Mutti, *ChemCatChem*, 2018, **10**, 731–735; (*e*) M. L. Corrado, T. Knaus and F. G. Mutti, *Green Chem.*, 2019, **21**, 6246–6251.

9 (*a*) R. M. Bullock, *Catalysis without Precious Metals*, Wiley-VCH Verlag GmbH & Co. KGaA, Weinheim, 2010; (*b*) B. Plietker, *Iron Catalysis in Organic Chemistry: Reactions and applications*, Wiley-VCH, Weinheim, 2008.

10 M. Xiao, X. Yue, R. Xu, W. Tang, D. Xue, C. Li, M. Lei, J. Xiao and C. Wang, *Angew. Chem., Int. Ed.*, 2019, **58**, 10528–10536.

11 (*a*) G. C. Liu, D. A. Cogan and J. A. Ellman, *J. Am. Chem. Soc.*, 1997, **119**, 9913–9914; (*b*) M. T. Robak, M. A. Herbage and J. A. Ellman, *Chem. Rev.*, 2010, **110**, 3600–3740; (*c*) M. Wakayama and J. A. Ellman, *J. Org. Chem.*, 2009, **74**, 2646–2650.

12 Recent reviews: (*a*) T. Irrgang and R. Kempe, *Chem. Rev.*, 2019, **119**, 2524–2549; (*b*) A. Mukherjee and D. Milstein, *ACS Catal.*, 2018, **8**, 11435–11469; (*c*) F. Kallmeier and R. Kempe, *Angew. Chem., Int. Ed.*, 2018, **57**, 46–60; (*d*) N. Gorgas and K. Kirchner, *Acc. Chem. Res.*, 2018, **51**, 1558–1569; (*e*) G. A. Filonenko, R. van Putten, E. J. M. Hensen and E. Pidko, *Chem. Soc. Rev.*, 2018, **47**, 1459–1483; (*f*) M. Garbe, K. Junge and M. Beller, *Eur. J. Org. Chem.*, 2017, 4344–4362.

13 Mn-Catalysed achiral *N*-alkylation with primary alcohols to produce achiral products: (*a*) S. Elangovan, J. Neumann, J.-B. Sortais, K. Junge, C. Darcel and M. Beller, *Nat. Commun.*, 2016, **7**, 12641; (*b*) J. Neumann, S. Elangovan, A. Spannenberg, K. Junge and M. Beller, *Chem. – Eur. J.*, 2017, **23**, 5410–5413; (*c*) A. Bruneau-Voisine, D. Wang, V. Dorcet, T. Roisnel, C. Darcel and J.-B. Sortais, *J. Catal.*, 2017, **347**, 57–62; (*d*) M. Mastalir, E. Pittenauer, G. Allmaier and K. Kirchner, *J. Am. Chem. Soc.*, 2017, **139**, 8812–8815; (*e*) R. Fertig, T. Irrgang, F. Freitag, J. Zander and R. Kempe, *ACS Catal.*, 2018, **8**, 8525–8530; (*f*) K. Das, A. Mondal, D. Pal, H. K. Srivastava and D. Srimani, *Organometallics*, 2019, **38**, 1815–1825; (*g*) B. G. Reed-Berendt and L. C. Morrill, *J. Org. Chem.*, 2019, **84**, 3715–3724.

14 G. Tsuji, T. Takeda, I. Furusawa, O. Horino and Y. Kubo, *Pestic. Biochem. Physiol.*, 1997, **57**, 211–219.

15 C. M. Spencer and S. Noble, *Drugs Aging*, 1998, **13**, 391–411.

16 R. Webster, A. Boyer, M. J. Fleming and M. Lautens, *Org. Lett.*, 2010, **12**, 5418–5421.

17 D. J. Kucera and R. W. Scott, *US Pat. Appl. Publ.*, 20040204591, 2004.

18 (*a*) P. A. Dub, N. J. Henson, R. L. Martin and J. C. Gordon, *J. Am. Chem. Soc.*, 2014, **136**, 3505–3521; (*b*) H.-J. Pan, Y. Zhang, C. Shan, Z. Yu, Y. Lan and Y. Zhao, *Angew. Chem., Int. Ed.*, 2016, **55**, 9615–9619.

19 A. Adamkiewicz and J. Mlynarski, *Eur. J. Org. Chem.*, 2016, 1060–1065.

Paper 12:

Sustainable Manganese-Catalyzed Solvent-Free Synthesis of Pyrroles from 1,4-Diols and Primary Amines.

Borghs, J. C.; Lebedev, Y.; Rueping, M.*; El-Sepelgy, O.*

Org. Lett. **2019**, *21*, 70-74.

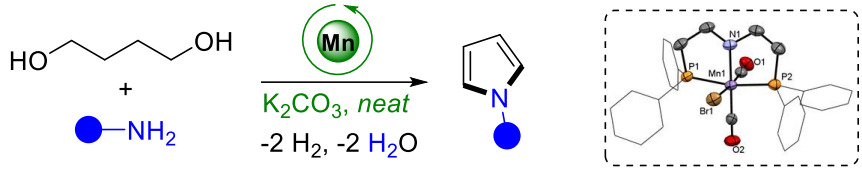

- ***Unprecedented selectivity***
- ***First row metal catalyst***
- ***Feedstock to high-value pyrrole***
- ***Catalytic amount of K_2CO_3***

OL | Organic Letters

Letter

Cite This: Org. Lett. 2019, 21, 70−74

pubs.acs.org/OrgLett

Sustainable Manganese-Catalyzed Solvent-Free Synthesis of Pyrroles from 1,4-Diols and Primary Amines

Jannik C. Borghs,[†] Yury Lebedev,[‡] Magnus Rueping,*[,†,‡] and Osama El-Sepelgy*[,†]

[†]Institute of Organic Chemistry, RWTH Aachen University, Landoltweg 1, 52074 Aachen, Germany

[‡]KAUST Catalysis Center (KCC), King Abdullah University of Science and Technology (KAUST), Thuwal 23955-6900, Saudi Arabia

Supporting Information

ABSTRACT: A general and selective metal-catalyzed conversion of biomass-derived primary diols and amines to the highly valuable 2,5-unsubstituted pyrroles has been developed. The reaction is catalyzed by a stable nonprecious manganese complex (1 mol %) in the absence of organic solvents whereby water and molecular hydrogen are the only side products. The manganese catalyst shows unprecedented selectivity, avoiding the formation of pyrrolidines, cyclic imides, and lactones.

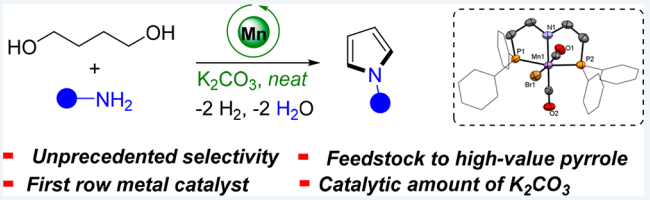

The discovery of new sustainable catalytic systems for upgrading renewable feedstocks to value-added fine and bulk chemicals represents a central challenge for chemists.[1] In this context, lignocellulosic biomass-derived alcohols offer a green alternative to mutagenic alkyl halides. Thus, substantial work was dedicated to the metal-catalyzed activation of alcohols by hydrogen shuttling with transfer of hydrogen from the alcohol to the final product. Besides, the catalytic dehydrogenation of alcohols leads to *in situ* formation of carbonyl intermediates which can undergo coupling reactions via condensation cascades to give more complex target molecules.[2]

Pyrroles represent an important class of synthetic intermediates which have found numerous applications in medicinal and advanced materials chemistry.[3] While 2,5-substituted pyrroles are conventionally prepared through the Paal−Knorr synthesis,[4] approaches for the synthesis of N-substituted pyrroles, and in particular 2,5-unsubstituted pyrroles, include the Clauson−Kaas reaction[5] as well as N-alkylation of pyrrole. However, these methods may suffer from the formation of stoichiometric amounts of waste and limited substrate scope. More modern methods rely on the ruthenium- or iron-catalyzed condensation of the more expensive 2-butyne-1,4-diol with primary amines to give N-substituted pyrroles.[6] Recently, a chemoenzymatic synthesis of N-substituted pyrrole was achieved via an olefin metathesis−aromatization cascade.[7]

A selective catalytic synthesis of N-substituted pyrroles from the readily available 1,4-butanediol (**1**) would be an ideal alternative, producing water and hydrogen gas as the only side products. However, the reaction of diol **1** with primary amines often leads to a mixture of pyrrolidine, cyclic imide, pyrrole, and lactone (Scheme 1).[8] Saturated pyrrolidine can be accessed from the primary diol **1** and amines using iridium,

Scheme 1. Metal-Catalyzed Coupling of Primary Diols and Primary Amines

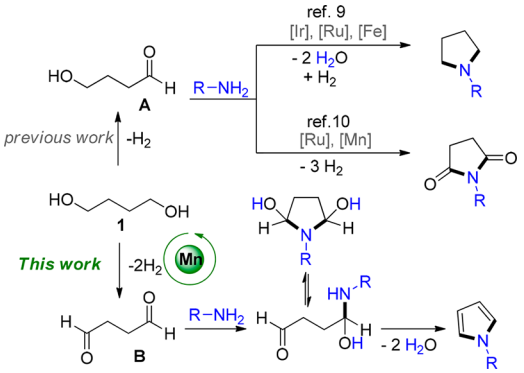

ruthenium and iron catalysts.[6a,9] Furthermore, Hong et al. reported the selective synthesis of cyclic imides using PNNH-Ru catalyst, whereas a base-metal-catalyzed version was recently reported by Milstein using the PNNH−Mn complex.[10] Moreover, the cyclization of 1,4-dialdehyde to γ-butyrolactone was outlined using ruthenium bisphosphine diamine catalyst.[11] In contrast, a general catalytic system to access pyrroles from diol **1** and primary amines has not been reported so far, although it could provide a desirable green and sustainable synthesis.[12]

Manganese is the third most abundant transition metal in the Earth's crust and has recently been recognized by several groups including ours as a sustainable alternative for Ru and Ir (de)hydrogenation catalysis.[13−17] Indeed, several catalytic systems have been developed for the hydrogenation of polar

Received: November 2, 2018
Published: December 24, 2018

DOI: 10.1021/acs.orglett.8b03506
Org. Lett. 2019, 21, 70−74

and nonpolar bonds,[15] dehydrogenation reactions,[16] and hydrogen autotransfer.[17] Encouraged by these advances and our experience in metal−ligand cooperative catalysis,[18,19] we envisioned the possibility of developing a new catalytic system for the efficient *in situ* generation of the dialdehyde **B** from the diol **1**. This reactive intermediate **B** would likely undergo condensation with a primary amine to afford the corresponding pyrrole upon dehydration of the cyclic hemiaminal intermediate, whereas the pyrrolidine and imide synthesis typically involves the reaction between the primary amine and the hydroxyaldehyde intermediate **A**.[9,10]

Here, we report our results on the sustainable transformation of the readily available diols and primary amines to pyrroles in a highly chemoselective fashion using an earth-abundant metal complex based on the inexpensive base metal manganese.

We started our study by the preparation of different manganese complexes bearing air- and moisture-stable ligands (**Mn-1**−**Mn-3**). For example, the manganese complex **Mn-3** could be readily prepared from the commercially available "MACHO" PNP pincer ligand and the inexpensive manganese precursor, $Mn(CO)_5Br$. Suitable crystals of **Mn-3** were obtained and characterized by X-ray diffraction (Figure 1).

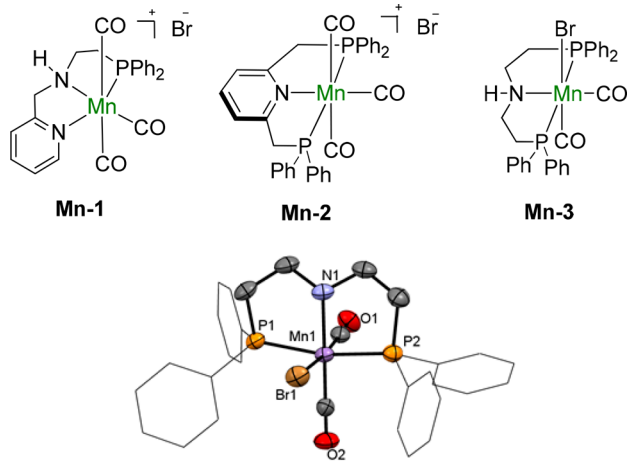

Figure 1. Manganese complexes used in this study and the single-crystal X-ray structure of **Mn-3** with ellipsoid set at 50% probability level.

Subsequently, the reaction between 1,4-butanediol (**1**) and *n*-hexylamine (**2a**) was thoroughly investigated in order to find the appropriate reaction conditions for the synthesis of the desired pyrrole **3a** while suppressing the formation of the undesired side products **3a′** and **3a″** (Table 1). To evaluate the most efficient catalyst, the manganese complexes **Mn-1**−**Mn-3** were tested in combination with Cs_2CO_3 in 1,4-dioxane as a solvent. Indeed, the application of **Mn-1** bearing a PNN ligand led to full conversion with 24% of the desired pyrrole **3a** along with 29% of the imide **3a′** (Table 1, entry 1). The high yield of the imide may be explained by the presence of the hemilabile pyridine ligand. In contrast, the pyridyl-based PNP pincer complex **Mn-2** showed low reactivity and excellent chemoselectivity toward the formation of the desired pyrrole **3a**. To our delight, **Mn-3** bearing a backbone N−H group resulted in 47% yield of pyrrole **3a** and 10% of cyclic imide **3a″** (Table 1, entry 3). We then turned our attention toward fine-tuning of the catalytic system by investigating different solvents

Table 1. Optimization of the Reaction Conditions[a]

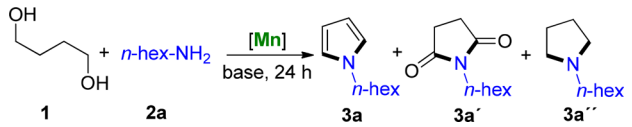

1 2a 3a 3a′ 3a″

entry	[Mn] (mol %)	base (mol %)	conv. [%]	yield of 3a:3a′:3a″ [%]
1	**Mn-1** (2)	Cs_2CO_3 (3)	99	24:29:00
2	**Mn-2** (2)	Cs_2CO_3 (3)	99	11:00:00
3	**Mn-3** (2)	Cs_2CO_3 (3)	99	47:10:01
4[b]	**Mn-3** (2)	Cs_2CO_3 (3)	99	41:13:01
5[c]	**Mn-3** (2)	Cs_2CO_3 (3)	99	40:10:02
6[d]	**Mn-3** (2)	Cs_2CO_3 (3)	99	57:02:06
7[d]	**Mn-3** (2)	*t*-BuOK (3)	99	54:03:03
8[d]	**Mn-3** (2)	KOH (3)	99	60:02:10
9[d]	**Mn-3** (2)	K_2CO_3 (3)	99	62:02:05
10[d,e]	**Mn-3** (2)	K_2CO_3 (3)	99	41:00:06
11[d]	**Mn-3 (1)**	**K_2CO_3 (1)**	**99**	**77:00:09**
12[d]	$Mn(CO)_5Br$ (3)	Cs_2CO_3 (5)	95	<5
13[d]	-	Cs_2CO_3 (5)	95	<5

[a]Reaction conditions: **1** (0.5 mmol) and **2a** (1.0 mmol) in 1,4-dioxane (1.0 M) at 150 °C for 24 h under argon atmosphere. Conversions and yields were determined by GC using mesitylene (0.2 mmol) as an internal standard. [b]Reaction in toluene. [c]Reaction in CPME. [d]Neat conditions. [e]4 Å mol sieves added. It is worth noting that the difference between yields and conversion is attributed to the formation of oligomeric side products that cannot be detected by GC analysis.

and bases. When 1,4-dioxane was replaced by toluene or CPME, both yield and selectivity slightly decreased (Table 1, entries 4−5). Surprisingly, running the reaction under neat conditions led to improved reactivity and selectivity (Table 1, entry 6). The influence of different bases, such as *t*-BuOK, KOH, and K_2CO_3, was also examined (Table 1, entries 7−9). We found that the inexpensive K_2CO_3 could be used as a catalyst activator providing 62% of pyrrole **3a** and only trace amounts of **3a′** and **3a″**. Unfortunately, the addition of 4 Å molecular sieves did not improve the yield (Table 1, entry 10). Gratifyingly, decreasing the manganese catalyst and base loading to 1 mol % afforded the desired product **3a** in 77% yield (Table 1, entry 11). Use of manganese pentacarbonyl bromide or only the base did not afford any product, indicating the crucial role of the metal−ligand catalyst (Table 1, entries 12 and 13).

In order to demonstrate the general applicability of the reaction, a variety of primary amines were reacted with 1,4-butanediol (**1**) as a coupling partner (Scheme 2). Long-chain primary amines reacted smoothly with **1**, leading to the pyrroles **3a** and **3b** in good yields. When cyclohexyl amine was used as a substrate, the desired product **3c** was obtained in 68% yield. Slightly better yield was obtained when phenylethylamine was used, and the corresponding pyrrole **3d** was obtained in very good yield. Likewise, the reaction could also be applied successfully to medicinally relevant tryptamine, affording the pyrrole **3e** in 78% yield. Furthermore, benzylamines bearing electron-withdrawing and electron-donating groups were successfully reacted and provided the corresponding pyrroles **3f**−**3i** in moderate to good yields. Interestingly, amines bearing heterocycles such as pyridine and furane could also be used as coupling partners providing the desired pyrroles **3j** and **3k** in moderate to good yields. In addition, α-

DOI: 10.1021/acs.orglett.8b03506
Org. Lett. 2019, 21, 70−74

Scheme 2. Manganese-Catalyzed Coupling of Primary Amines with 1,4-Butanediol[a]

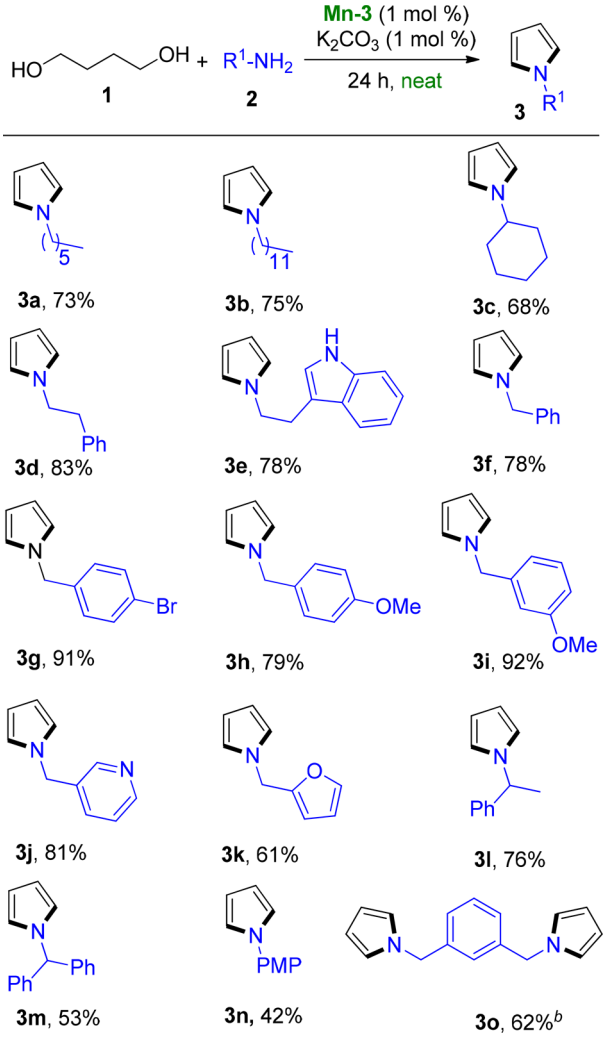

[a]Reaction conditions: **1** (0.5 mmol), **2** (1.0 mmol), **Mn-3** (0.005 mmol), and K_2CO_3 (0.005 mmol) at 150 °C for 24 h. [b]Diamine (0.5 mmol) and **1** (1.5 mmol).

substituted amines such as α-methylbenzylamine and benzhydrylamine were successfully applied and afforded the pyrroles **3l** and **3m** in moderate to good yields. Utilizing aromatic amines such as *para*-methoxy aniline appeared to be more challenging due to the lower nucleophilicity, and only 42% of the desired product **3n** could be isolated. Next, we successfully extended the scope by accessing symmetrical bispyrrole **3o** from the corresponding diamine.

Encouraged by these results, we decided to further expand the scope and to use secondary diols, such as 2,5-hexanediol (**4a**) as a coupling partner (Scheme 3).[8] In analogy to Scheme 2, different α-branched and unbranched primary amines and aniline derivatives are tolerated, and the desired substituted pyrroles **5a**–**5i** were obtained in good to excellent yields. However, the PMP-derived pyrrole **5j** was obtained in only 33% yield. In order to further prove the generality of the presented catalytic system, mono- and diphenylbutanediol were investigated and readily converted to the corresponding pyrroles **5k** and **5l** in moderate yields. Finally, further extension led to the synthesis of the symmetrical bispyrroles **5m** and **5n** in good yields.

Scheme 3. Scope of Different Symmetrical and Unsymmetrical Diols[a]

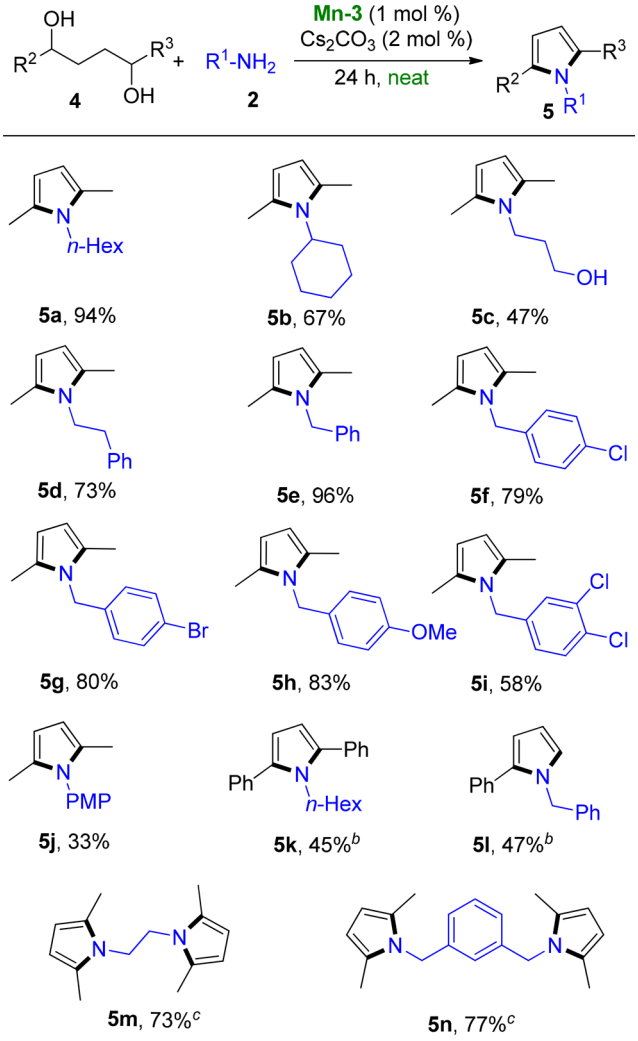

[a]Reaction conditions: **4** (0.5 mmol), **2** (1.0 mmol), **Mn-3** (0.005 mmol), and Cs_2CO_3 (0.01 mmol) at 150 °C for 24 h. [b]**Mn-3** (0.01 mmol) and Cs_2CO_3 (0.025 mmol). [c]Diamine (0.5 mmol) and diol (1.5 mmol).

To demonstrate the practicability of this newly developed methodology, we conducted a gram-scale synthesis of the tryptamine-substituted pyrrole **7**, and the desired product was isolated in excellent yield without the need of purification by chromatography (Scheme 4).

In summary, we report a general and selective synthesis of N-substituted pyrroles from low-cost renewable diols and primary amines. The reaction is catalyzed by a well-defined, bench-stable, homogeneous base metal catalyst which circumvents the use of stoichiometric amounts of mutagenic reagents

Scheme 4. Gram-Scale Synthesis of Tryptamine-Substituted Pyrrole 7

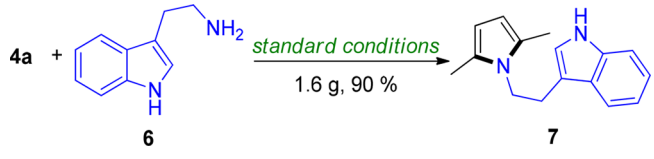

DOI: 10.1021/acs.orglett.8b03506
Org. Lett. 2019, 21, 70–74

and produces water and hydrogen gas as the sole byproducts. The high potential of this catalytic system was demonstrated by the synthesis of a wide variety of pyrroles in good to excellent yields.

■ ASSOCIATED CONTENT

Supporting Information

The Supporting Information is available free of charge on the ACS Publications website at DOI: 10.1021/acs.orglett.8b03506.

Experimental data (PDF)

Accession Codes

CCDC 1863450 contains the supplementary crystallographic data for this paper. These data can be obtained free of charge via www.ccdc.cam.ac.uk/data_request/cif, or by emailing data_request@ccdc.cam.ac.uk, or by contacting The Cambridge Crystallographic Data Centre, 12 Union Road, Cambridge CB2 1EZ, UK; fax: + 44 1223 336033.

■ AUTHOR INFORMATION

Corresponding Authors

*E-mail: magnus.rueping@rwth-aachen.de.
*E-mail: osama.elsepelgy@rwth-aachen.de.

ORCID

Yury Lebedev: 0000-0003-2985-6876
Magnus Rueping: 0000-0003-4580-5227
Osama El-Sepelgy: 0000-0003-3131-4988

Notes

The authors declare no competing financial interest.

■ ACKNOWLEDGMENTS

J.C.B. is thankful for financial support of the German Federal Environmental Foundation (DBU).

■ REFERENCES

(1) (a) *Biomass and Biofuels*; Jose, S., Bhaskar, T., Eds.; CRC Press, 2015. (b) Vispute, T. P.; Zhang, H.; Sanna, A.; Xiao, R.; Huber, G. W. *Science* **2010**, *330*, 1222−1227.

(2) Selected reviews: (a) Corma, A.; Navas, J.; Sabater, M. J. *Chem. Rev.* **2018**, *118*, 1410−1459. (b) Chelucci, G. *Coord. Chem. Rev.* **2017**, *331*, 1−36. (c) Huang, F.; Liu, Z.; Yu, Z. *Angew. Chem., Int. Ed.* **2016**, *55*, 862−875. (d) Nandakumar, A.; Midya, S. P.; Landge, V. G.; Balaraman, E. *Angew. Chem., Int. Ed.* **2015**, *54*, 11022−11034. (e) Yang, Q.; Wang, Q.; Yu, Z. *Chem. Soc. Rev.* **2015**, *44*, 2305−2329. (f) Leonard, J.; Blacker, A. J.; Marsden, S. P.; Jones, M. F.; Mulholland, K. R.; Newton, R. A. *Org. Process Res. Dev.* **2015**, *19*, 1400−1410. (g) Gunanathan, C.; Milstein, D. *Science* **2013**, *341*, 1229712. (h) Obora, Y. *ACS Catal.* **2014**, *4*, 3972−3981. (i) Guillena, G.; Ramón, D. J.; Yus, M. *Chem. Rev.* **2010**, *110*, 1611−1641. (j) Dobereiner, G. E.; Crabtree, R. H. *Chem. Rev.* **2010**, *110*, 681−703. (k) Hamid, M. H. S. A.; Slatford, P. A.; Williams, J. M. J. *Adv. Synth. Catal.* **2007**, *349*, 1555−1575.

(3) (a) *Heterocyclic Chemistry*, 5th ed.; Joule, J. A., Mills, K., Eds.; Wiley: UK, 2010. (b) *Chemistry of Heterocyclic Compounds: Pyrroles, Part 1 and 2*; Jones, R. A., Ed.; 2008; Vol. *48*. (c) Setsune, J.-I. *Chem. Rev.* **2017**, *117*, 3044−3101. (d) MacDiarmid, A. G. *Angew. Chem., Int. Ed.* **2001**, *40*, 2581−2590. (e) Vernitskaya, T. V.; Efimov, O. N. *Russ. Chem. Rev.* **1997**, *66*, 443−457.

(4) (a) Paal, C. *Ber. Dtsch. Chem. Ges.* **1885**, *18*, 367−371. (b) Knorr, L. *Ber. Dtsch. Chem. Ges.* **1884**, *17*, 1635−1642. (c) Hantzsch, A. *Ber. Dtsch. Chem. Ges.* **1890**, *23*, 1474−1476.

(5) (a) Clauson-Kaas, N. *Acta Chem. Scand.* **1952**, *6*, 667−670. (b) Guida, W. C.; Mathre, D. J. J. *J. Org. Chem.* **1980**, *45*, 3172−3176.

(6) (a) Tsuji, Y.; Yokoyama, Y.; Huh, K. T.; Watanabe, Y. *Bull. Chem. Soc. Jpn.* **1987**, *60*, 3456−3458. (b) Yan, T.; Barta, K. *ChemSusChem* **2016**, *9*, 2321−2325. (c) Emayavaramban, B.; Sen, M.; Sundararaju, B. *Org. Lett.* **2017**, *19*, 6−9.

(7) Scalacci, N.; Black, G. W.; Mattedi, G.; Brown, N. L.; Turner, N. J.; Castagnolo, D. *ACS Catal.* **2017**, *7*, 1295−1300.

(8) (a) Schley, N. D.; Dobereiner, G. E.; Crabtree, R. H. *Organometallics* **2011**, *30*, 4174−4179. (b) Daw, P.; Chakraborty, S.; Garg, J. A.; Ben-David, Y.; Milstein, D. *Angew. Chem., Int. Ed.* **2016**, *55*, 14373−14377.

(9) (a) Fujita, K.-i.; Fujii, T.; Yamaguchi, R. *Org. Lett.* **2004**, *6*, 3525−3528. (b) Hamid, M.; Haniti, S. A.; Allen, C. L.; Lamb, G. W.; Maxwell, A. C.; Maytum, H. C.; Watson, A. J. A.; Williams, J. M. J. *J. Am. Chem. Soc.* **2009**, *131*, 1766−1774. (c) Yan, T.; Feringa, B. L.; Barta, K. *Nat. Commun.* **2014**, *5*, 5602.

(10) (a) Zhang, J.; Senthilkumar, M.; Ghosh, S. C.; Hong, S. H. *Angew. Chem., Int. Ed.* **2010**, *49*, 6391−6395. (b) Espinosa-Jalapa, N. A.; Kumar, A.; Milstein, D. *J. Am. Chem. Soc.* **2017**, *139*, 11722−11725.

(11) (a) Zhao, J.; Hartwig, J. F. *Organometallics* **2005**, *24*, 2441−2446. (b) Nguyen, D. H.; Trivelli, X.; Capet, F.; Paul, J.-F.; Dumeignil, F.; Gauvin, R. M. *ACS Catal.* **2017**, *7*, 2022−2032.

(12) For pyrrole synthesis from amino alcohols and secondary alcohols: (a) Michlik, S.; Kempe, R. A. *Nat. Chem.* **2013**, *5*, 140−144. (b) Srimani, D.; Ben-David, Y.; Milstein, D. *Angew. Chem., Int. Ed.* **2013**, *52*, 4012−4015. (c) Iida, k.; Miura, T.; Ando, J.; Saito, S. *Org. Lett.* **2013**, *15*, 1436−1439. (d) Kallmeier, F.; Dudziec, B.; Irrgang, T.; Kempe, R. *Angew. Chem., Int. Ed.* **2017**, *56*, 7261−7265. For three-component synthesis of pyrrole: (e) Zhang, M.; Neumann, H.; Beller, M. *Angew. Chem., Int. Ed.* **2013**, *52*, 597−601. (f) Zhang, M.; Fang, X. J.; Neumann, H.; Beller, M. *J. Am. Chem. Soc.* **2013**, *135*, 11384−11388. (g) Dang, T. T.; Seayad, A. M. *Chem. - Asian J.* **2017**, *12*, 2383−2387. (h) Borghs, J. C.; Azofra, L. M.; Biberger, T.; Linnenberg, O.; Cavallo, L.; Rueping, M.; El-Sepelgy, O. *ChemSusChem* **2018**, in press.

(13) Selected reviews: (a) Filonenko, G. A.; van Putten, R.; Hensen, E. J. M.; Pidko, E. A. *Chem. Soc. Rev.* **2018**, *47*, 1459−1483. (b) Zell, T.; Langer, R. *ChemCatChem* **2018**, *10*, 1930−1940. (c) Kallmeier, F.; Kempe, R. *Angew. Chem., Int. Ed.* **2018**, *57*, 46−60. (d) Maji, B.; Barman, M. K. *Synthesis* **2017**, *49*, 3377−3393. (e) Liu, W.; Ackermann, L. *ACS Catal.* **2016**, *6*, 3743−3752. (f) Valyaev, D. A.; Lavigne, G.; Lugan, N. *Coord. Chem. Rev.* **2016**, *308*, 191−235.

(14) For general reviews on base metal catalysis: (a) Chirik, P.; Morris, R. *Acc. Chem. Res.* **2015**, *48*, 2495−2495. (b) Bauer, I.; Knölker, H.-J. *Chem. Rev.* **2015**, *115*, 3170−3387. (c) Morris, R. H. *Acc. Chem. Res.* **2015**, *48*, 1494−1502. (d) Bullock, R. M. *Catalysis without Precious Metals*; Wiley-VCH: Weinheim, 2010. (e) Plietker, B. *Iron Catalysis in Organic Chemistry: Reactions and applications*, 2nd ed.; Wiley-VCH: Weinheim, 2008.

(15) Selected examples: (a) Elangovan, S.; Topf, C.; Fischer, S.; Jiao, H.; Spannenberg, A.; Baumann, W.; Ludwig, R.; Junge, K.; Beller, M. *J. Am. Chem. Soc.* **2016**, *138*, 8809−8814. (b) Kallmeier, F.; Irrgang, T.; Dietel, T.; Kempe, R. *Angew. Chem., Int. Ed.* **2016**, *55*, 11806−11809. (c) Widegren, M. B.; Harkness, G. J.; Slawin, A. M. Z.; Cordes, D. B.; Clarke, M. L. *Angew. Chem., Int. Ed.* **2017**, *56*, 5825−5828. (d) Bruneau-Voisine, A.; Wang, D.; Dorcet, V.; Roisnel, T.; Darcel, C.; Sortais, J. B. *Org. Lett.* **2017**, *19*, 3656−3659. (e) Perez, M.; Elangovan, S.; Spannenberg, A.; Junge, K.; Beller, M. *ChemSusChem* **2017**, *10*, 83−86. (f) Zirakzadeh, A.; de Aguiar, S. R. M. M.; Stöger, B.; Widhalm, M.; Kirchner, K. *ChemCatChem* **2017**, *9*, 1744−1748. (g) Glatz, M.; Stöger, B.; Himmelbauer, D.; Veiros, L. F.; Kirchner, K. *ACS Catal.* **2018**, *8*, 4009−4016. (h) Brzozowska, A.; Azofra, L. M.; Zubar, V.; Atodiresei, I.; Cavallo, L.; Rueping, M.; El-Sepelgy, O. *ACS Catal.* **2018**, *8*, 4103−4109. (i) Zubar, V.; Lebedev, Y.; Azofra, L. M.; Cavallo, L.; El-Sepelgy, O.; Rueping, M. *Angew. Chem., Int. Ed.* **2018**, *57*, 13439−13443. (j) Zhou, Y. P.; Mo, Z.; Luecke, M. P.; Driess, M. *Chem. - Eur. J.* **2018**, *24*, 4780−4784.

DOI: 10.1021/acs.orglett.8b03506
Org. Lett. 2019, 21, 70−74

(16) (a) Mukherjee, A.; Nerush, A.; Leitus, G.; Shimon, L. J. W.; Ben-David, Y.; Espinosa Jalapa, N. A.; Milstein, D. *J. Am. Chem. Soc.* **2016**, *138*, 4298−4301. (b) Mastalir, M.; Glatz, M.; Pittenauer, E.; Allmaier, G.; Kirchner, K. *J. Am. Chem. Soc.* **2016**, *138*, 15543−15546. (c) Deibl, N.; Kempe, R. *Angew. Chem., Int. Ed.* **2017**, *56*, 1663−1666. (d) Daw, P.; Kumar, A.; Espinosa-Jalapa, N. A.; Diskin-Posner, Y.; Ben-David, Y.; Milstein, D. *ACS Catal.* **2018**, *8*, 7734−7741. (e) Das, K.; Mondal, A.; Srimani, D. J. *J. Org. Chem.* **2018**, *83*, 9553−9560. (f) Das, K.; Mondal, A.; Srimani, D. *Chem. Commun.* **2018**, *54*, 10582−10585.

(17) Selected examples: (a) Elangovan, S.; Neumann, J.; Sortais, J.-B.; Junge, K.; Darcel, C.; Beller, M. *Nat. Commun.* **2016**, *7*, 12641. (b) Pena-Lopez, M.; Piehl, P.; Elangovan, S.; Neumann, H.; Beller, M. *Angew. Chem., Int. Ed.* **2016**, *55*, 14967−14971. (c) Fu, S.; Shao, Z.; Wang, Y.; Liu, Q. *J. Am. Chem. Soc.* **2017**, *139*, 11941−11948. (d) Bruneau-Voisine, A.; Wang, D.; Dorcet, V.; Roisnel, T.; Darcel, C.; Sortais, J.-B. *J. Catal.* **2017**, *347*, 57−62. (e) Mastalir, M.; Pittenauer, E.; Allmaier, G.; Kirchner, K. *J. Am. Chem. Soc.* **2017**, *139*, 8812−8815. (f) Fertig, R.; Irrgang, T.; Freitag, F.; Zander, J.; Kempe, R. *ACS Catal.* **2018**, *8*, 8525−8530. (g) El-Sepelgy, O.; Matador, E.; Brzozowska, A.; Rueping, M. *ChemSusChem* **2018**, DOI: 10.1002/cssc.201801660. (h) Liu, T.; Wang, L.; Wu, K.; Yu, Z. *ACS Catal.* **2018**, *8*, 7201−7207. (i) Kulkarni, N. V.; Brennessel, W. W.; Jones, W. *ACS Catal.* **2018**, *8*, 997−1002. (j) Jana, A.; Reddy, C. B.; Maji, B. *ACS Catal.* **2018**, *8*, 9226−9231. (k) Sklyaruk, J.; Borghs, J. C.; El-Sepelgy, O.; Rueping, M. *Angew. Chem., Int. Ed.* **2018**, DOI: 10.1002/anie.201810885. (l) Jang, Y. K.; Krückel, T.; Rueping, M.; El-Sepelgy, O. *Org. Lett.* **2018**, DOI: 10.1021/acs.orglett.8b03184.

(18) (a) El-Sepelgy, O.; Alandini, N.; Rueping, M. *Angew. Chem., Int. Ed.* **2016**, *55*, 13602−13605. (b) El-Sepelgy, O.; Brzozowska, A.; Rueping, M. *ChemSusChem* **2017**, *10*, 1664−1668. (c) El-Sepelgy, O.; Brzozowska, A.; Azofra, L. M.; Jang, Y. K.; Cavallo, L.; Rueping, M. *Angew. Chem., Int. Ed.* **2017**, *56*, 14863−14867. (d) El-Sepelgy, O.; Brzozowska, A.; Sklyaruk, J.; Jang, Y. K.; Zubar, V.; Rueping, M. *Org. Lett.* **2018**, *20*, 696−679.

(19) For reviews on metal-ligand catalysis: (a) Khusnutdinova, R.; Milstein, D. *Angew. Chem., Int. Ed.* **2015**, *54*, 12236−12273. (b) Lyaskovskyy, V.; de Bruin, B. *ACS Catal.* **2012**, *2*, 270−279.

DOI: 10.1021/acs.orglett.8b03506
Org. Lett. 2019, 21, 70−74

Paper 13:

Manganese-Catalyzed Multicomponent Synthesis of Pyrroles through Acceptorless Dehydrogenation Hydrogen Autotransfer Catalysis: Experiment and Computation.

Borghs, J. C.; Azofra, L. M.; Biberger, T.; Linnenberg, O.; Cavallo, L.*; Rueping, M.*; El-Sepelgy, O.*

ChemSusChem **2019**, *12*, 3083.

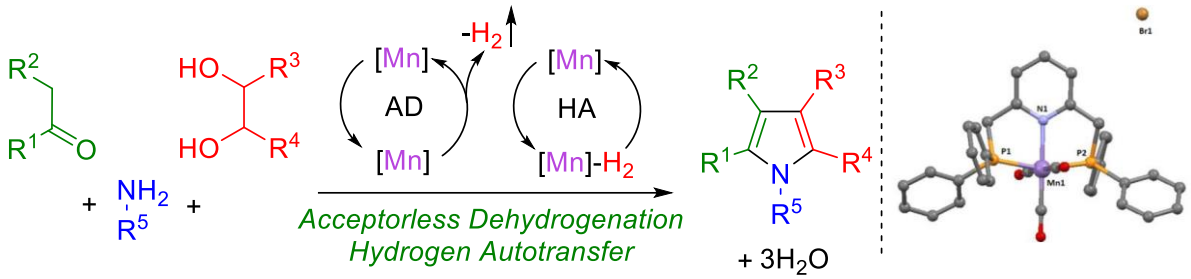

ChemPubSoc Europe

DOI: 10.1002/cssc.201802416

CHEMSUSCHEM Communications

Manganese-Catalyzed Multicomponent Synthesis of Pyrroles through Acceptorless Dehydrogenation Hydrogen Autotransfer Catalysis: Experiment and Computation

Jannik C. Borghs,[a] Luis Miguel Azofra,[b] Tobias Biberger,[a] Oliver Linnenberg,[c] Luigi Cavallo,*[b] Magnus Rueping,*[a, b] and Osama El-Sepelgy*[a]

A new base metal catalyzed sustainable multicomponent synthesis of pyrroles from readily available substrates is reported. The developed protocol utilizes an air- and moisture-stable catalyst system and enables the replacement of themutagenic α-haloketones with readily abundant 1,2-diols. Moreover, the presented method is catalytic in base and the sole byproducts of this transformation are water and hydrogen gas. Experimental and computational mechanistic studies indicate that the reaction takes place through a combined acceptorless dehydrogenation hydrogen autotransfer methodology.

Multicomponent reactions are valuable sustainable processes for the construction of complex molecules in one pot from three or more substrates. This strategy merges several elementary reaction steps, which leads to minimization of the amount of waste, and simplifies the workup and purification steps.[1]

Pyrroles represent prominent and important chemical motifs in medicinal, agro, and advanced materials chemistry. Classical synthetic routes suffer from drawbacks mainly resulting from the generation of substantial amounts of waste produced during the multi-step pre-functionalization of substrates or by-product formation.[2] Accordingly, there is a continuous need to develop new catalytic systems that allow the direct and atom-economic conversion of renewable and readily available substrates to pyrroles.

Alcohols can be obtained from renewable biomass resources and present promising sustainable feedstock chemicals. The utilization of alcohols as substrates in the synthesis of fine chemicals will hence contribute not only to the reduction of toxic chemical waste but also to decrease CO_2 emissions by avoiding the use of carbon fossil sources.[3] One of the key concepts for alcohol functionalization is hydrogen autotransfer (HA), which has become a powerful tool for utilizing abundant alcohols as building blocks for environmentally benign C–C and C–N bond formations, releasing water as the only byproduct (Scheme 1 A).[4] A related concept is acceptorless dehydrogenation (AD), which permits the conversion of alcohols to car-

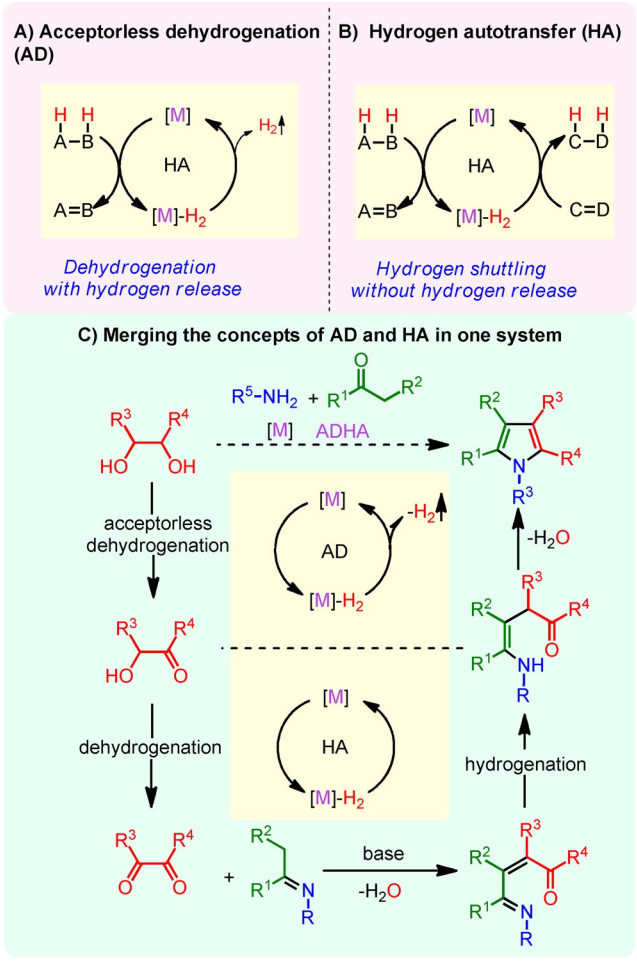

Scheme 1. Acceptorless dehydrogenation and hydrogen autotransfer catalysis.

[a] J. C. Borghs, T. Biberger, Prof. Dr. M. Rueping, Dr. O. El-Sepelgy
Institute of Organic Chemistry
RWTH Aachen University
Landoltweg 1, 52074 Aachen (Germany)
E-mail: magnus.rueping@rwth-aachen.de
osama.elsepelgy@rwth-aachen.de

[b] Dr. L. M. Azofra, Prof. Dr. L. Cavallo, Prof. Dr. M. Rueping
KAUST Catalysis Center (KCC)
King Abdullah University of Science and Technology (KAUST)
Thuwal 23955-6900 (Saudi Arabia)
E-mail: luigi.cavallo@kaust.edu.sa

[c] O. Linnenberg
Institute of Inorganic Chemistry
RWTH Aachen University
Landoltweg 1, 52074 Aachen (Germany)

Supporting Information and the ORCID identification number(s) for the author(s) of this article can be found under: https://doi.org/10.1002/cssc.201802416.

This publication is part of a Special Issue on "Sustainable Organic Synthesis". Please visit the issue at http://doi.org/10.1002/cssc.v12.13

bonyl compounds by liberating hydrogen gas without the need for a stoichiometric oxidant (Scheme 1 B).[5]

Following the concept of HA, pyrroles can be synthetized from unsaturated 1,4-diols and primary amines.[6] Furthermore, catalytic systems have been developed for the synthesis of pyrroles by using the AD concept from 1,4-diols and primary amines or secondary alcohols and amino alcohols.[7] Moreover, Beller and co-workers have reported a three-component synthesis of pyrroles by using a $[Ru_3(CO)_{12}]$/Xantphos catalytic system. The authors proposed that the reaction might proceed through the AD concept.[8]

The replacement of noble metal catalysts by first-row transition metal catalysts is highly desirable owing to ecological and economic benefits and may also lead to the discovery of new chemical reactivity.[9] Manganese is the third most abundant transition metal in the earth's crust and is recognized as a sustainable alternative for toxic noble metal catalysts.[10–12] In our continuous efforts to develop new sustainable transformations enabled by metal–ligand catalysts,[13,14] we now report an unprecedented manganese-catalyzed construction of pyrroles starting from readily available substrates: 1,2-diols, ketones, and primary amines (Scheme 1 C). Notably, our experimental and computational mechanistic studies on this multicomponent transformation suggest that the reaction proceeds through a unified acceptorless dehydrogenation hydrogen autotransfer strategy. To the best of our knowledge, this is the first study that proves the involvement of both processes of AD and HA in heterocyclic synthesis.[15] In fact, we found that this strategy is crucial for the successful activation of the vicinal 1,2-diols, providing a greener alternative to the mutagenic α-haloketones.[16]

We commenced our experimental study by synthesizing various manganese pincer complexes and identified **Mn-1** to be most effective for the desired transformation. The new PNP^{Ph}-based complex is bench stable and thus enables an operationally simple, glovebox-free reaction set up. Suitable crystals of **Mn-1** could be grown and were characterized by X-ray diffraction (Table 1, top).

For our model reaction system, we investigated the formation of the substituted pyrrole **4a** by using propiophenone (**1a**), 2-phenylethylamine (**2a**), and ethylene glycol (**3a**). Thus, a solution containing substrates in dried solvent, Mn complex, and 20 mol% of a base was heated to 135 °C for 24 h. To our delight, by applying **Mn-1**, promising catalytic activity was observed and the desired pyrrole was obtained in 65% yield (Table 1, entry 1). Control experiments demonstrated the crucial role of both the metal and the pincer ligand (Table 1, entries 2, 3). Next, we further optimized other reaction parameters. Our investigation revealed that the reaction is most effective in the polar protic solvent *t*-amyl alcohol, as other solvents proved less effective (Table 1, entries 4–7). Screening of various bases confirmed that inexpensive KO*t*Bu is the best for this transformation (Table 1, entries 8–10). Further experiments revealed that increasing the concentration to 1.0 M offers an increased yield of 86% (Table 1entries 11 and 12).

Having established optimal conditions for the heterocyclization, we moved on to demonstrate the applicability of our catalytic system. An array of aryl and alkyl ketones in combination with 2-phenylethylamine (**2a**) and ethylene glycol (**3a**) as model substrates (Scheme 2 A) could be transformed into the corresponding pyrroles. Initially, we were interested in using various less active and challenging non-benzylic ketones. Pleasingly, all the shown examples bearing different substituents were isolated in high yields (**4a**–**4h**). Notably, abundant alkyl ketones were also successfully converted to the corresponding bicyclic products **4g** and **4h** in very good yields. When we turned our attention to the use of benzylic ketones, we obtained the respective pyrroles **4i**–**4m**. To prove the scalability, we conducted a gram-scale synthesis of the pyrrole **4k"** and the desired product was isolated in 78% yield. Regarding their importance in medicinal chemistry,[17] we also targeted heteroatom-substituted pyrroles by applying the respective α-functionalized ketones. In fact, an α-alkoxy ketone showed high reactivity and could be transformed into the product **4n** in good yield. Importantly, the benzamide-containing pyrrole **4o** was obtained in excellent yield (94%). Next, various amines were tested in combination with different ketones while keeping ethylene glycol as a coupling partner (Scheme 2 B). All corresponding pyrroles were obtained in moderate to excellent yields. Specifically, different ketones in combination with *n*-hexylamine afforded products in good yields (**5a**–**5f**). It was further demonstrated that different amines such as benzylamine or cyclohexylamine were also suitable for this cascade transformation (**5g**–**5i**). Despite its weak nucleophilicity, toluidine showed significant reactivity and could be transformed into *N*-aryl-substituted pyrrole **5j** in moderate yield. Gratifyingly, even

Table 1. Optimization of the reaction conditions.[a]

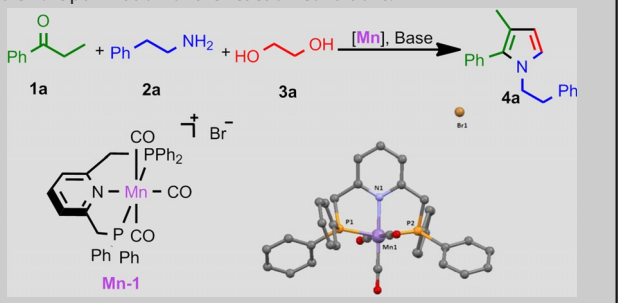

Entry	Catalyst	Solvent	Base	Yield [%]
1	**Mn-1**	*t*-amyl alcohol	KO*t*Bu	65
2	$Mn(CO)_5Br$	*t*-amyl alcohol	KO*t*Bu	< 5
3	–	*t*-amyl alcohol	KO*t*Bu	< 5
4	**Mn-1**	toluene	KO*t*Bu	20
5	**Mn-1**	1,4-dioxane	KO*t*Bu	28
6	**Mn-1**	Me-THF	KO*t*Bu	16
7	**Mn-1**	CPME	KO*t*Bu	16
8	**Mn-1**	*t*-amyl alcohol	KOH	43
9	**Mn-1**	*t*-amyl alcohol	K_2CO_3	23
10	**Mn-1**	*t*-amyl alcohol	Cs_2CO_3	41
11[b]	**Mn-1**	*t*-amyl alcohol	KO*t*Bu	86
12	**Mn-1**	neat	KO*t*Bu	70

[a] Reaction conditions: **1a** (0.5 mmol), **2a** (0.75 mmol), **3a** (1.5 mmol), [**Mn**] catalyst (2 mol%) in *t*-amyl alcohol (0.5 M), 135 °C, 24 h under argon atmosphere. Yield determined by GC by using mesitylene as an internal standard. [b] 1.0 M reaction mixture. CPME = cyclopentyl methyl ether.

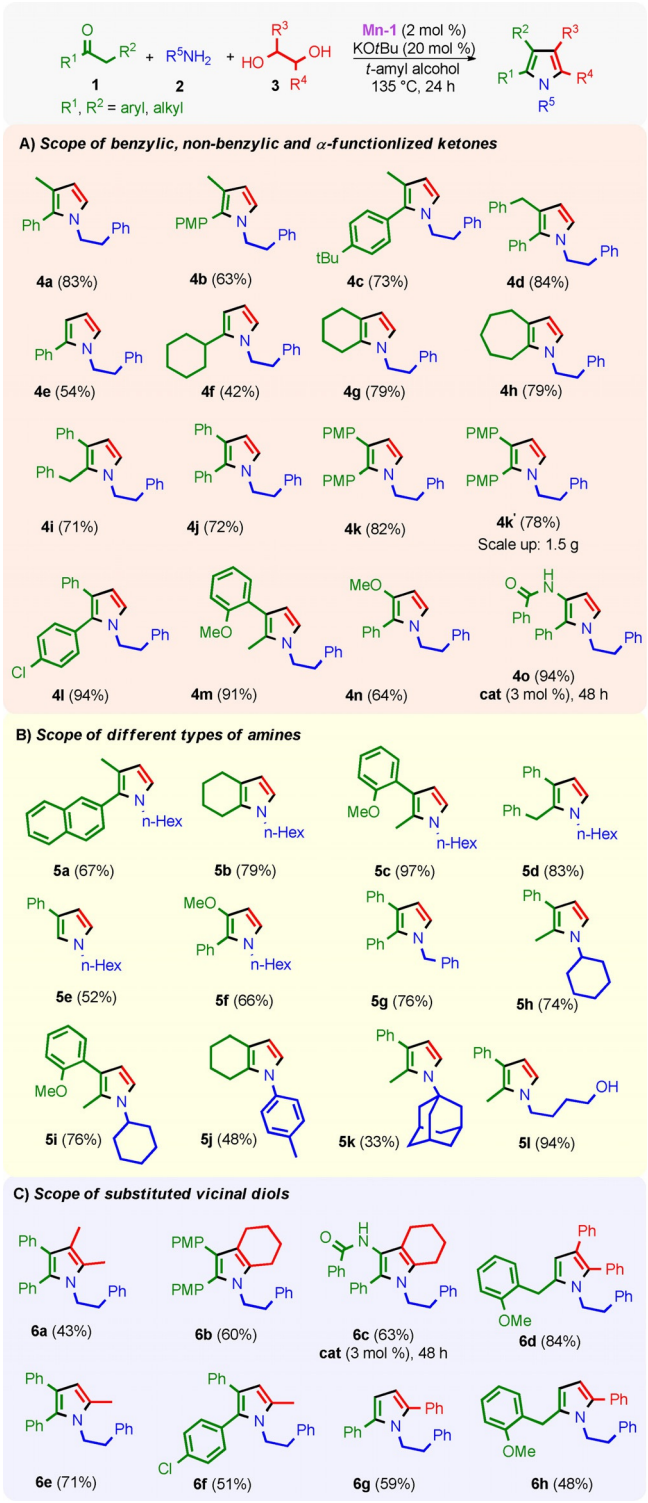

Scheme 2. Manganese-catalyzed acceptorless dehydrogenation hydrogen autotransfer: Synthesis of multisubstituted pyrroles.

the sterically demanding 1-adamantylamine could be converted into the respective pyrrole **5k**. To our delight, an amino alcohol was selectively converted to the pyrrole **5l**.

To provide highly substituted pyrroles, we employed an array of different vicinal diols, which gave the corresponding pyrroles in high yields (Scheme 2C). Interestingly, symmetrical disubstituted aromatic, aliphatic as well as cyclic diols could be used for this transformation, giving good yields of the corresponding fully substituted pyrroles **6a**–**6c** and tetra-substituted pyrrole **6d**. If mono-substituted unsymmetrical diols were employed, two regioisomers can be formed. However, in all cases, either a single regioisomer or a very high regioselectivity (95:5) was obtained with substitution occurring at R^4 in pyrroles **6e**–**6h**. It is important to note that when the 1-(2-methoxyphenyl)propan-2-one was used as a ketone in combination with ethylene glycol, the C–H alkylation usually takes place at the benzylic carbon (Scheme 2A, example **4m**). To our surprise, when using the same ketone in combination with phenyl- or diphenyl-substituted diols, the alkylation reaction occurs on the free methyl group, affording a different regioisomer (Scheme 2C, examples **6d** and **6h**). This observation led to the synthesis of new highly substituted pyrroles, which are difficult to prepare by other methods.

Afterwards, we decided to conduct experiments to prove the role of the metal–ligand catalyst. When we performed the reaction shown in Scheme 3 without catalyst and replacing the

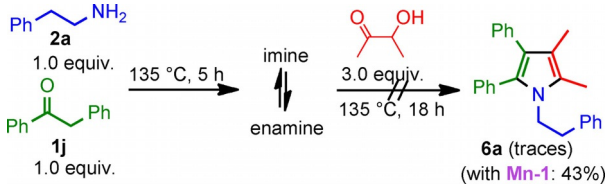

Scheme 3. Experimental mechanistic investigations.

1,2-diol by an α-hydroxy ketone, only trace amounts of the pyrrole **6a** were observed. However, when 2,3-butandiol and **Mn-1** were used, **6a** was obtained in 43% yield (Scheme 3). Furthermore, we have analyzed the reaction atmosphere of the model reaction by using gas chromatography (Table 1, entry 11) and detected the presence of hydrogen gas. These experimental results indicate that the metal–ligand complex not only catalyzes the AD process but also the HA process.

We subsequently carried out a detailed DFT study and selected the multicomponent reaction between glyceraldehyde, propiophenone, and *n*-hexylamine catalyzed by **Mn-1** as the model reaction.[18,19] Initially, the uncatalyzed reaction between the primary amine and the ketone leads to the formation of an imine, which is in equilibrium with the corresponding enamine. The latter may undergo a C–H or N–H addition reaction with the in situ generated glycolaldehyde or glyoxal. This establishes the existence of four plausible reaction pathways (see Figure S3 in the Supporting Information). The DFT calculations, the experimental investigations, and the observed selectivity (Scheme 2, examples **6e**–**6h**) suggest that the reaction most likely occurs through the C–H alkylation of enamine with in situ generated glyoxal (see the Supporting Information for details).

Figure 1 illustrates that the Mn complex acts as a catalyst for acceptorless dehydrogenation hydrogen autotransfer processes. The first catalytic cycle involves AD of ethylene glycol to glycolaldehyde and hydrogen gas (Figure 1A). The second cat-

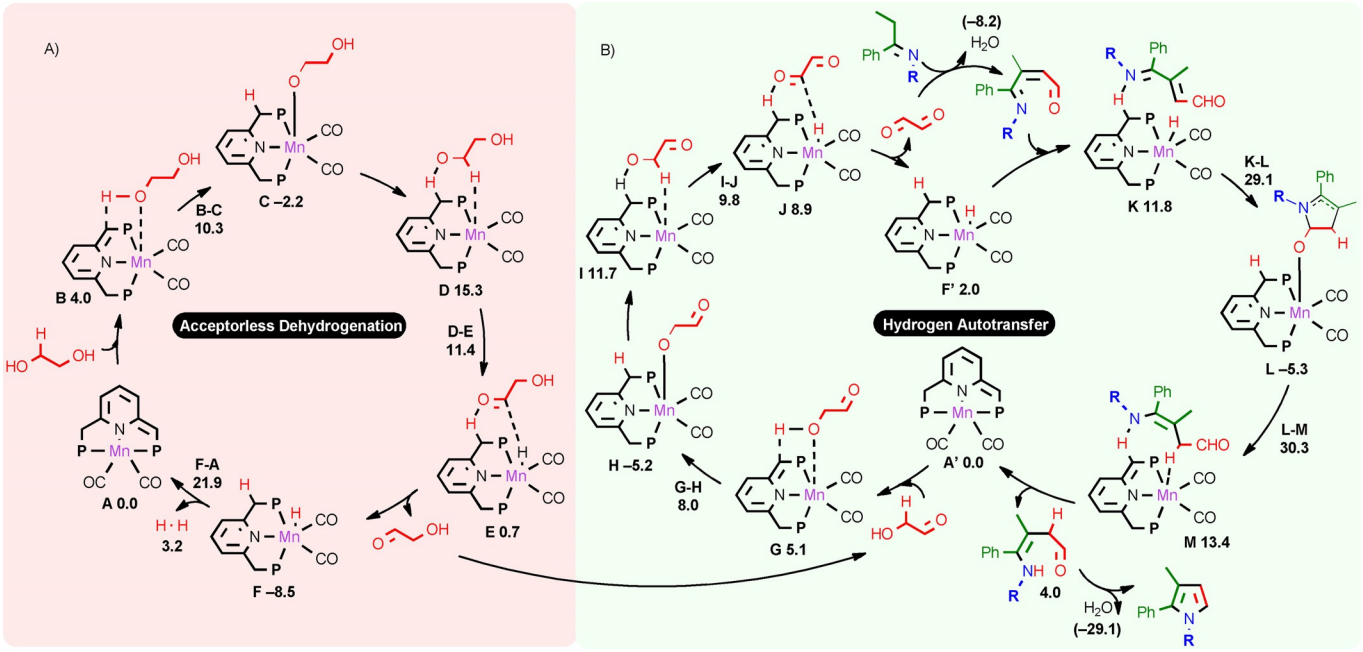

Figure 1. Proposed reaction mechanism of the heterocyclization through a unified acceptorless dehydrogenation hydrogen autotransfer concept catalyzed by **Mn-1**. Calculated Gibbs free reaction and activation energies at 135 °C are shown in kcal mol^{-1} at the M06/TZVP//PBE/SVP(H,C,N,O,P)-TZVP(Mn) computational level by using 1-butanol as the solvent. Note: **P** and **R** groups refer to PPh_2 and *n*-hexyl, respectively.

alytic cycle involves a crucial HA process consisting of metal-catalyzed activation of glycolaldehyde by shuttling a hydrogen molecule, which is required for the hydrogenation of the azadiene intermediate (Figure 1 B). Specifically, the ethylene glycol dehydrogenation (AD cycle) starts with one of the -OH groups of ethylene glycol interacting with the [Mn] species **A** to give complex **B**, with a slightly endergonic binding Gibbs free energy of 4.0 kcal mol^{-1} at 135 °C and by using 1-butanol as the solvent. This complex is characterized by the presence of two interactions, in which Mn acts as electrophilic center through a Mn···O interaction, whereas the sp^2 carbon in one of the arms of the non-innocent PNP ligand acts as nucleophilic center through a C···H interaction with the H atom of the ethylene glycol OH group. Proton transfer from the alcohol occurs via transition state **B**–**C** with a free energy barrier of 10.3 kcal mol^{-1} from **A**, and leads to intermediate **C** laying −2.2 kcal mol^{-1} below **A**. This aromatization/dearomatization process has been thoroughly studied in metal–PNP and PNN complexes as an important process providing the lowest energy pathways.[20]

The following hydride transfer occurs via the formation of complex **D**, which represents the highest energy intermediate of the dehydrogenation cycle, 15.3 kcal mol^{-1} relative to **A**. The hydride transfer occurs through transition state **D**–**E**. This is assumed to be an almost barrier-free process, as transition state **D**–**E** is only 1.1 kcal mol^{-1} above intermediate **D** when electronic energies in solution at the PBE/SVP(H,C,N,O,P)-TZVP(Mn) level of theory are considered (i.e., the computational protocol used to locate geometries). The resulting [Mn]–H_2···glycolaldehyde complex **E** is located 0.7 kcal mol^{-1} above **A**. The following release of glycolaldehyde is exergonic by 8.5 kcal mol^{-1} and leads to **F**. The acceptorless dehydrogenation cycle closes with the regeneration of the catalyst by H_2 release, in a process presenting a kinetic penalty of 30.5 kcal mol^{-1} relative to **F**.

We have also carried out calculations for the case in which proton and hydride transfers from glyceraldehyde to the Mn^{I}–PNP catalytic species occur via a concerted pathway. The corresponding activation Gibbs free energy is 3.4 and 2.3 kcal mol^{-1} less stable than those computed for transition states **B**–**C** and **D**–**E**, respectively. In this line, the proposal of a step-wise mechanism in which hydride transfer might occur before the proton transfer during the AD cycle indicates disfavored kinetics, with an activation barrier of 59.8 kcal mol^{-1} relative to **A**.

Subsequently, the HA cycle has been investigated by DFT analysis (Figure 1 B). The first part of the HA process involves the dehydrogenation of glycolaldehyde to glyoxal by hydrogen transfer to the Mn and N centers, which also results in the hydrogenated catalytic species, **F′**. In this process, proton transfer exhibits a Gibbs free activation energy of 8.0 kcal mol^{-1}, **G**–**H**, whereas hydride transfer is carried out via the formation of complex **I**, 11.7 kcal mol^{-1}, also through a barrier-less process.

The second part of the HA process involves the endergonic interaction between the manganese species **F′** bearing a shuttled hydrogen molecule with the azadiene intermediate that resulted from a C–H alkylation reaction. This intermediate is formed by the addition of glyoxal with the enamine compound, a coupling that is exergonic by 8.2 kcal mol^{-1}. In more detail, hydride transfer from the Mn atom to the sp^2 carbon atom positioned β to the CHO group occurs via transition state **K**–**L** and a Gibbs free activation energy of 27.1 kcal mol^{-1} relative to **F′**. The proton transfer occurs through transition state **L**–**M** and a free energy barrier of 35.6 kcal mol^{-1} relative to **L**. This penalty represents the highest kinetic impediment of

the whole reaction in which the Mn^{I}–PNP catalytic species participates as partial cyclization of the substrate is seen in **L** by N→C(sp^2)HO bond formation. Finally, the released hydrogenated azadiene can undergo cyclization to the observed pyrrole derivative with a free energy gain of 29.1 kcal mol^{-1}.

In conclusion, we have reported a new base metal catalyzed heterocondensation cascade that occurs through an acceptorless dehydrogenation hydrogen autotransfer methodology. The reaction is catalyzed by a new homogeneous base metal catalyst based on an inexpensive and air-stable manganese complex bearing a PNP ligand. The great potential of our catalytic system was demonstrated by the synthesis of more than 35 different substituted pyrroles in good yields by using renewable substrates and only catalytic amounts of base. Importantly, water and hydrogen gas are the sole byproducts. Computational studies support an acceptorless dehydrogenation hydrogen autotransfer reaction mechanism in which the metal–ligand complex plays a dual role for the acceptorless dehydrogenation of ethylene glycol followed by non-typical hydrogen autotransfer process.

Acknowledgements

J.C.B. is thankful for the financial support of the German Federal Environmental Foundation (DBU). L.M.A. and L.C. acknowledge King Abdullah University of Science and Technology (KAUST) for support. We thank KAUST Supercomputing Laboratory for use of the supercomputer Shaheen II and providing the computational resources.

Conflict of interest

The authors declare no conflict of interest.

Keywords: acceptorless dehydrogenation · alcohols · base metals · heterocycles · hydrogen autotransfer

[1] a) L. Levi, T. J. J. Müller, *Chem. Soc. Rev.* **2016**, *45*, 2825 – 2846; b) B. H. Rotstein, S. Zaretsky, V. Rai, A. K. Yudin, *Chem. Rev.* **2014**, *114*, 8323 – 8359; c) A. Dömling, W. Wang, K. Wang, *Chem. Rev.* **2012**, *112*, 3083 – 3135; d) J. E. Biggs-Houck, A. Younai, J. T. Shaw, *Curr. Opin. Chem. Biol.* **2010**, *14*, 371 – 382; e) B. B. Touré, D. G. Hall, *Chem. Rev.* **2009**, *109*, 4439 – 4486; f) J. D. Sunderhaus, S. F. Martin, *Chem. Eur. J.* **2009**, *15*, 1300 – 1308.

[2] a) *Heterocyclic Chemistry, 5th ed.* (Eds.: J. A. Joule, K. Mills), Wiley, Chichester, **2010**; b) A. Hagfeldt, G. Boschloo, L. Sun, L. Kloo, H. Pettersson, *Chem. Rev.* **2010**, *110*, 6595 – 6663; c) V. Estévez, M. Villacampa, J. C. Menéndez, *Chem. Soc. Rev.* **2014**, *43*, 4633 – 4657; d) G. Chelucci, *Coord. Chem. Rev.* **2017**, *331*, 37 – 53.

[3] T. P. Vispute, H. Zhang, A. Sanna, R. Xiao, G. W. Huber, *Science* **2010**, *330*, 1222 – 1227.

[4] Selected reviews: a) A. Corma, J. Navas, M. J. Sabater, *Chem. Rev.* **2018**, *118*, 1410 – 1459; b) A. Nandakumar, S. P. Midya, V. G. Landge, E. Balaraman, *Angew. Chem. Int. Ed.* **2015**, *54*, 11022 – 11034; *Angew. Chem.* **2015**, *127*, 11174 – 11186; c) Y. Obora, *ACS Catal.* **2014**, *4*, 3972 – 3981.

[5] Selected reviews: a) R. H. Crabtree, *Chem. Rev.* **2017**, *117*, 9228 – 9246; b) F. Huang, Z. Liu, Z. Yu, *Angew. Chem. Int. Ed.* **2016**, *55*, 862 – 875; *Angew. Chem.* **2016**, *128*, 872 – 885; c) Q. Yang, Q. Wang, Z. Yu, *Chem. Soc. Rev.* **2015**, *44*, 2305 – 2329; d) C. Gunanathan, D. Milstein, *Science* **2013**, *341*, 249; e) J. Choi, A. H. R. MacArthur, M. Brookhart, A. S. Goldman, *Chem. Rev.* **2011**, *111*, 1761 – 1779; f) G. Guillena, D. J. Ramón, M. Yus, *Chem. Rev.* **2010**, *110*, 1611 – 1641.

[6] a) T. Yan, K. Barta, *ChemSusChem* **2016**, *9*, 2321 – 2325; for related heterocycles, see: b) K.-i. Fujita, T. Fujii, R. Yamaguchi, *Org. Lett.* **2004**, *6*, 3525 – 3528; c) M. H. S. A. Hamid, C. L. Allen, G. W. Lamb, A. C. Maxwell, H. C. Maytum, A. J. A. Watson, J. M. J. Williams, *J. Am. Chem. Soc.* **2009**, *131*, 1766 – 1774; d) T. Yan, B. L. Feringa, K. Barta, *Nat. Commun.* **2014**, *5*, 5602.

[7] a) N. D. Schley, G. E. Dobereiner, R. H. Crabtree, *Organometallics* **2011**, *30*, 4174 – 4179; b) S. Michlik, R. Kempe, *Nat. Chem.* **2013**, *5*, 140 – 144; c) D. Srimani, Y. Ben-David, D. Milstein, *Angew. Chem. Int. Ed.* **2013**, *52*, 4012 – 4015; *Angew. Chem.* **2013**, *125*, 4104 – 4107; d) K. Iida, T. Miura, J. Anda, S. Saito, *Org. Lett.* **2013**, *15*, 1436 – 1439; e) P. Daw, S. Chakraborty, J. A. Garg, Y. Ben-David, D. Milstein, *Angew. Chem. Int. Ed.* **2016**, *55*, 14373 – 14377; *Angew. Chem.* **2016**, *128*, 14585 – 14589; f) F. Kallmeier, B. Dudziec, T. Irrgang, R. Kempe, *Angew. Chem. Int. Ed.* **2017**, *56*, 7261 – 7265; *Angew. Chem.* **2017**, *129*, 7367 – 7371.

[8] a) M. Zhang, H. Neumann, M. Beller, *Angew. Chem. Int. Ed.* **2013**, *52*, 597 – 601; *Angew. Chem.* **2013**, *125*, 625 – 629; b) M. Zhang, X. Fang, H. Neumann, M. Beller, *J. Am. Chem. Soc.* **2013**, *135*, 11384 – 11388.

[9] a) R. M Bullock, *Catalysis without Precious Metals*, **2010**, Wiley-VCH, Weinheim; b) B. Plietker, *Iron Catalysis in Organic Chemistry: Reactions and Applications, 2nd ed.*, Wiley-VCH, Weinheim, **2008**.

[10] For recent reviews, see: a) N. Gorgas, K. Kirchner, *Acc. Chem. Res.* **2018**, *51*, 1558 – 1569; b) G. A. Filonenko, R. van Putten, E. J. M. Hensen, E. A. Pidko, *Chem. Soc. Rev.* **2018**, *47*, 1459 – 1483; c) F. Kallmeier, R. Kempe, *Angew. Chem. Int. Ed.* **2018**, *57*, 46 – 60; *Angew. Chem.* **2018**, *130*, 48 – 63; d) T. Zell, R. Langer, *ChemCatChem* **2018**, *10*, 1930 – 1940; e) B. Maji, M. K. Barman, *Synthesis* **2017**, *49*, 3377 – 3393; f) M. Garbe, K. Junge, M. Beller, *Eur. J. Org. Chem.* **2017**, 4344 – 4362; g) W. Liu, L. Ackermann, *ACS Catal.* **2016**, *6*, 3743 – 3752.

[11] Selected examples: a) A. Mukherjee, A. Nerush, G. Leitus, L. J. W. Shimon, Y. Ben-David, N. A. Espinosa Jalapa, D. Milstein, *J. Am. Chem. Soc.* **2016**, *138*, 4298 – 4301; b) S. Elangovan, C. Topf, S. Fischer, H. Jiao, A. Spannenberg, W. Baumann, R. Ludwig, K. Junge, M. Beller, *J. Am. Chem. Soc.* **2016**, *138*, 8809 – 8814; c) S. Elangovan, J. Neumann, J.-B. Sortais, K. Junge, C. Darcel, M. Beller, *Nat. Commun.* **2016**, *7*, 12641; d) M. Mastalir, M. Glatz, E. Pittenauer, G. Allmaier, K. Kirchner, *J. Am. Chem. Soc.* **2016**, *138*, 15543 – 15546; e) N. Deibl, R. Kempe, *Angew. Chem. Int. Ed.* **2017**, *56*, 1663 – 1666; *Angew. Chem.* **2017**, *129*, 1685 – 1688; f) P. Daw, A. Kumar, N. A. Espinosa-Jalapa, Y. Diskin-Posner, Y. Ben-David, D. Milstein, *ACS Catal.* **2018**, *8*, 7734 – 7741; g) K. Das, A. Mondal, D. Srimani, *J. Org. Chem.* **2018**, *83*, 9553 – 9560; h) K. Das, A. Mondal, D. Srimani, *Chem. Commun.* **2018**, *54*, 10582 – 10585.

[12] Examples from our group: a) A. Brzozowska, L. M. Azofra, V. Zubar, I. Atodiresei, L. Cavallo, M. Rueping, O. El-Sepelgy, *ACS Catal.* **2018**, *8*, 4103 – 4109; b) V. Zubar, Y. Lebedev, L. M. Azofra, L. Cavallo, O. El-Sepelgy, M. Rueping, *Angew. Chem. Int. Ed.* **2018**, *57*, 13439 – 13443; *Angew. Chem.* **2018**, *130*, 13627 – 13631; c) E. Matador, A. Brzozowska, O. El-Sepelgy, M. Rueping, *ChemSusChem* **2018**, *11*, https://doi.org/10.1002/cssc.201801660; for C–H activation see: d) C. Wang, B. Maity, L. Cavallo, M. Rueping, *Org. Lett.* **2018**, *20*, 3105 – 3108; e) C. Wang, M. Rueping, *ChemCatChem* **2018**, *10*, 2681 – 2685; f) C. Wang, A. Wang, M. Rueping, *Angew. Chem. Int. Ed.* **2017**, *56*, 9935 – 9938; *Angew. Chem.* **2017**, *129*, 10067 – 10070.

[13] For reviews, see: a) R. Khusnutdinova, D. Milstein, *Angew. Chem. Int. Ed.* **2015**, *54*, 12236 – 12273; *Angew. Chem.* **2015**, *127*, 12406 – 12445; b) O. R. Luca, R. H. Crabtree, *Chem. Soc. Rev.* **2013**, *42*, 1440 – 1459; c) V. Lyaskovskyy, B. de Bruin, *ACS Catal.* **2012**, *2*, 270 – 279.

[14] a) O. El-Sepelgy, N. Alandini, M. Rueping, *Angew. Chem. Int. Ed.* **2016**, *55*, 13602 – 13605; *Angew. Chem.* **2016**, *128*, 13800 – 13803; b) O. El-Sepelgy, A. Brzozowska, M. Rueping, *ChemSusChem* **2017**, *10*, 1664 – 1668; c) O. El-Sepelgy, A. Brzozowska, L. M. Azofra, Y. K. Jang, L. Cavallo, M. Rueping, *Angew. Chem. Int. Ed.* **2017**, *56*, 14863 – 14867; *Angew. Chem.* **2017**, *129*, 15059 – 15063; d) O. El-Sepelgy, A. Brzozowska, J. Sklyaruk, Y. K. Jang, V. Zubar, M. Rueping, *Org. Lett.* **2018**, *20*, 696 – 699.

[15] U. K. Das, Y. Ben-David, Y. Diskin Posner, D. Milstein, *Angew. Chem. Int. Ed.* **2018**, *57*, 2179 – 2182; *Angew. Chem.* **2018**, *130*, 2201 – 2204.

[16] A. Hantzsch, *Ber. Dtsch. Chem. Ges.* **1890**, *23*, 1474 – 1476.

[17] P. Dydio, D. Lichosyt, J. Jurczak, *Chem. Soc. Rev.* **2011**, *40*, 2971 – 2985.

[18] Gas phase enthalpies of formation at room temperature can be found at: a) NIST database: M. Frenkel, K. N. Marsh, R. C. Wilhoit, G. J. Kabo, G. N. Roganov, *Thermodynamics of Organic Compounds in the Gas State*, Thermodynamics Research Center, College Station, TX, **1994**; b) J. P. Porterfield, J. H. Baraban, T. P. Troy, M. Ahmed, M. C. McCarthy, K. M. Morgan, J. W. Daily, T. L. Nguyen, J. F. Stanton, G. B. Ellison, *J. Phys. Chem. A* **2016**, *120*, 2161 – 2172.

[19] Optimized geometries were located by using the PBE functional together with the SVP basis set for main group atoms and the TZVP basis set for Mn. Single-point energy refinement calculations were done at the M06/TZVP level. Solvent effects (1-butanol) were included through the polarizable continuum model (PCM) at both steps. All calculations have been performed through the facilities provided by the Gaussian 09 package. See the Supporting Information for full computational details.

[20] H. Li, M. B. Hall, *ACS Catal.* **2015**, *5*, 1895 – 1913.

Manuscript received: October 19, 2018
Revised manuscript received: November 6, 2018
Version of record online: January 2, 2019

Curriculum Vitae

Personal Data

Title	*Dr.*
First name	*Osama*
Name	*El-Sepelgy*
Current position	*Independent Junior Research Group Leader (Nachwuchsgruppenleiter)*
Current institution	*Leibniz Institute for Catalysis e.V., Rostock, Germany*
Scopus ID/ORCID	*35421840800 / 0000-0003-3131-4988*

Qualifications and Career

Stages	**Periods and Details**
Independent Junior Group Leader	***Since July 2021*** *Photoexcited base metal catalysis, open-shell transformations*
Visiting Researcher	**5/2021 – 6/2022** Institute of biotechnology, RWTH Aachen, Aachen *Development of asymmetric photobiocatalysis*
Subgroup leader	**1/2017-11/2019** Institute of Organic Chemistry, RWTH Aachen, Aachen *Development of manganese catalyzed de(hydrogenation)*
Postdoc	**8/2014- 12/2016** Institute of Organic Chemistry, RWTH Aachen, Aachen Supervisor: Prof. Magnus Rueping *Merger of iron catalysis and biocatalysis*
PhD (Internship abroad)	**10/2012 – 9/2013** Leipzig university, Leipzig Supervisor: Prof. Christoph Schneider *Asymmetric organocatalysis: Brønsted acid catalysis, o-quinomethide*
PhD *With highest honours*	**3/2010 - 2/2014** Jagiellonian University, Krakow, Poland Supervisor: Prof. Jacek Mlynarski *Asymmetric organocatalysis: biomimetic aldol reaction, amine catalysis*
MSc. in Organic Chemistry	**4/2007 - 2009** Mansoura University, Egypt *Thesis on heterocyclic synthesis*
BSc. in Chemistry *With honours "ranked first"*	**2001 - 2004** Mansoura University, Egypt

Supplementary Career Information

Activities in the Research System
Recent teaching activities

Period	details
WS 2024/25 WS 2023/24	**Bioorganic Chemistry**: MSc. biochemistry and microbiology (Mandatory), Rostock University
SS 2024	**Organic Chemistry V**: MSc. Chemistry (mandatory) Rostock University
SS 2024 SS 2023 SS 2022	**Catalysis I:** BSc. Chemistry, Rostock University
Since WS 23/24 *Visiting professorship*	**Photochemistry and Photocatalysis** (mandatory) University of Poitiers, France. MSc. Erasmus program (SuCat)

Recent talks (conferences and invited lectures)

-*Chemiedozententagung (3/2024),* Aachen, Germany.
-*GDCh-Wissenschaftsforum Chemie* (9/2023), Leipzig, Germany.
-7th Green and Sustainable Chemistry (5/2023), Dresden, Germany
-*Chemiedozententagung* (3/2023), Dresden, Germany
-6th International symposium on CH activation (6/2022), Göttingen, Germany
-*GDCh-Colloquium, Rostock University* (1/2021), Rostock, Germany.
-*Invited Lecture,* Johannes Gutenberg University Mainz (12/2019), Mainz, Germany
-*GDCh-Wissenschaftsforum Chemie* (9/2019), Aachen, Germany.
-*14th European Congress on Catalysis* (8/2019), Aachen, Germany.
-*2nd IMPRS RECHARGE Symposium*, MPI- Mülheim (5/2019), Mülheim an der Ruhr, Germany.
-*Invited Lecture, Leibniz institute for catalysis* (3/2019), Rostock, Germany.
-*22nd IUPAC International Conference on organic Synthesis* (9/2018), Florence, Italy.
-*7th International Conference on MCR and Related Chemistry* (8/2018), Düsseldorf, Germany.
-*28th International Conference on Organometallic Chemistry* (7/2018), Florence, Italy.

Research Grants

DFG individual grant (EL 1041/3-1) Principal investigator. 223.4K€ (2021-2025).
Title: *Sustainable Hydrocarbon Functionalization Enabled by Base-Metal Catalysis*.
Industrial funding, Rolfs Consulting und Verwaltungs-GmbH. 360 K€ (2024-2027)
Title: *Late-Stage Functionalization of Drug Molecules*

Visiting professorship, University of Poitiers, France since 2023

Erasmus Munds program of EU. MSc program of sustainable catalysis
One week/year of intensive teaching of photochemistry and photocatalysis

List of Publications

1. Zuo K, Zhu J, Akhtar F, Dam P, Azofra, LM, El-Sepelgy O.* Biomimetic Catalytic Remote Desaturation of Aliphatic Alcohols. *Org. Lett.* **2025**, *27*, 30-35.

2. Dam, P.; Zuo, K.; Azofra, L. M.; El-Sepelgy, O.* Biomimetic Photoexcited Cobaloxime Catalysis in Organic Synthesis. *Angew. Chem. Int. Ed.* **2024**, *63*, e202405775.

3. Elghobashy, M.; El-Sepelgy, O.* Catalytic Methylation Using Methanol as C1 Source. In *Dehydrogenation Reactions with 3d Metals*, Sundararaju, B. Ed.; Springer Nature Switzerland, **2024**; pp 173-197.

4. Wang, C.; Dam, P.; Elghobashy, M.; Brückner, A.; Rabeah, J.; Azofra, L. M.; El-Sepelgy, O.* Biomimetic Dehydroamination of Primary Amines. *ACS Catal.* **2023**, *13*, 14205-14212.

5. Wang, C.; Azofra, L. M.; Dam, P.; Espinoza-Suarez, E. J.; Do, H. T.; Rabeah, J.; Brückner, A.; El-Sepelgy, O.* Photoexcited cobalt catalysed endo-selective alkyl Heck reaction. *Chem. Commun.* **2023**, *59*, 3862-3865.

6. Wang, C.; Azofra, L. M.; Dam, P.; Sebek, M.; Steinfeldt, N.; Rabeah, J.; El-Sepelgy, O.* Catalytic Desaturation of Aliphatic Amides and Imides Enabled by Excited-State Base-Metal Catalysis. *ACS Catal.* **2022**, *12*, 8868-8876.

7. Wang, C.; El-Sepelgy, O.* Reductive depolymerization of plastics catalyzed with transition metal complexes. *Curr. Opin. Green Sustain. Chem* **2021**, *32*, 100547.

8. Azofra, L. M.; Tran, M. A.; Zubar, V.; Cavallo, L.; Rueping, M.; El-Sepelgy, O.* Conversion of racemic alcohols to optically pure amine precursors enabled by catalyst dynamic kinetic resolution: experiment and computation. *Chem. Commun.* **2020**, *56*, 9094-9097.

9. Sklyaruk, J.; Borghs, J. C.; El-Sepelgy, O.*; Rueping, M.* Catalytic C1 Alkylation with Methanol and Isotope-Labeled Methanol. *Angew. Chem. Int. Ed.* **2019**, *58*, 775-779.

10. Borghs, J. C.; Tran, M. A.; Sklyaruk, J.; Rueping, M.*; El-Sepelgy, O.* Sustainable Alkylation of Nitriles with Alcohols by Manganese Catalysis. *J. Org. Chem.* **2019**, *84*, 7927-7935.

11. Borghs, J. C.; Lebedev, Y.; Rueping, M.*; El-Sepelgy, O.* Sustainable Manganese-Catalyzed Solvent-Free Synthesis of Pyrroles from 1,4-Diols and Primary Amines. *Org. Lett.* **2019**, *21*, 70-74.

12. Borghs, J. C.; Azofra, L. M.; Biberger, T.; Linnenberg, O.; Cavallo, L.; Rueping, M.*; El-Sepelgy, O.* Manganese-Catalyzed Multicomponent Synthesis of Pyrroles through Acceptorless Dehydrogenation Hydrogen Autotransfer Catalysis: Experiment and Computation. *ChemSusChem* **2019**, *12*, 3083.

13. El-Sepelgy, O.*; Matador, E.; Brzozowska, A.; Rueping, M.* C-Alkylation of Secondary Alcohols by Primary Alcohols through Manganese-Catalyzed Double Hydrogen Autotransfer. *ChemSusChem* **2019**, *12*, 3099.

14. Brzozowska, A.; Azofra, L. M.; Zubar, V.; Atodiresei, I.; Cavallo, L.; Rueping, M.; El-Sepelgy, O.* Highly Chemo- and Stereoselective Transfer Semihydrogenation of Alkynes Catalyzed by a Stable, Well-Defined Manganese(II) Complex. *ACS Catal.* **2018**, *8*, 4103-4109.

15. Zubar, V.; Lebedev, Y.; Azofra, L. M.; Cavallo, L.; El-Sepelgy, O.*; Rueping, M.* Hydrogenation of CO2-Derived Carbonates and Polycarbonates to Methanol and Diols by Metal-Ligand Cooperative Manganese Catalysis. *Angew. Chem. Int. Ed.* **2018**, *57*, 13439-13443.

16. Jang, Y. K.; Krückel, T.; Rueping, M.*; El-Sepelgy, O.* Sustainable Alkylation of Unactivated Esters and Amides with Alcohols Enabled by Manganese Catalysis. *Org. Lett.* **2018**, 7779-7783.

17. El-Sepelgy, O.*; Brzozowska, A.; Sklyaruk, J.; Jang, Y. K.; Zubar, V.; Rueping, M.* Cooperative Metal-Ligand Catalyzed Intramolecular Hydroamination and Hydroalkoxylation of Allenes Using a Stable Iron Catalyst. *Org. Lett.* **2018**, *20*, 696-699.

18. El-Sepelgy, O.*; Brzozowska, A.; Rueping, M.* Asymmetric Chemoenzymatic Reductive Acylation of Ketones by a Combined Iron-Catalyzed Hydrogenation-Racemization and Enzymatic Resolution Cascade. *ChemSusChem* **2017**, *10*, 1664-1668.

19. El-Sepelgy, O.*; Brzozowska, A.; Azofra, L. M.; Jang, Y. K.; Cavallo, L.*; Rueping, M.* Experimental and Computational Study of an Unexpected Iron-Catalyzed Carboetherification by Cooperative Metal and Ligand Substrate Interaction and Proton Shuttling. *Angew. Chem. Int. Ed.* **2017**, *56*, 14863-14867.

20. El-Sepelgy, O.; Alandini, N.; Rueping, M.* Merging Iron Catalysis and BiocatalysisIron Carbonyl Complexes as Efficient Hydrogen Autotransfer Catalysts in Dynamic Kinetic Resolutions. *Angew. Chem. Int. Ed.* **2016**, *55*, 13602-13605.

21. Molenda, M. A.; Bas, S.; El-Sepelgy, O.; Stefaniak, M.; Mlynarski, J.* Chemistry of Pyruvate Enolates: anti-Selective Direct Aldol Reactions of Pyruvate Ester with Sugar Aldehydes Promoted by a Dinuclear Zinc Catalyst. *Adv. Synth. Catal.* **2015**, *357*, 2098-2104.

22. El-Sepelgy, O.; Haseloff, S.; Alamsetti, S. K.; Schneider, C.* Bronsted Acid Catalyzed, Conjugate Addition of beta-Dicarbonyls to In Situ Generated ortho-Quinone Methides-Enantioselective Synthesis of 4-Aryl-4H-Chromenes. *Angew. Chem. Int. Ed.* **2014**, *53*, 7923-7927.

23. El-Sepelgy, O.*; Mlynarski, J.* Biomimetic Direct Aldol Reaction of Pyruvate Esters with Chiral Aldehydes. *Adv. Synth. Catal.* **2013**, *355*, 281-286.

24. Woyciechowska, M., El-Sepelgy, O.; Młynarski, J.* Aldol reaction. In *Water in organic synthesis*, Kobayashi, S. Ed.; Georg Thieme Verlag KG., 2012; pp 353–384.

25. El-Sepelgy, O.; Schwarzer, D.; Oskwarek, P.; Mlynarski, J.* Direct Aldol Reaction of Pyruvic Derivatives: Catalytic Attempt To Synthesize Ulosonic Acids. *Eur. J. Org. Chem.* **2012**, 2724-2727.

26. Waly, M. A.*; El-Gogary, S. R.; El-Sepelgy, O. One-Pot New Synthetic Method for 3-Amino-2-Quinoxalinecarbonitrile. *Synth. Commun.* **2010**, *40*, 739-743.

27. El-Gogary, S. R.; Waly, M. A.*; Ibrahim, I. T.; El-Sepelgy, O. Synthesis and UV absorption of new conjugated quinoxaline 1,4-dioxide derivatives anticipated as tumor imaging and cytotoxic agents. *Monatsh. Chem* **2010**, *141*, 1253-1262.